MASSACHUSETTS INSTITUTE OF TECHNOLOGY

RADIATION LABORATORY SERIES

LOUIS N. RIDENOUR, *Editor-in-Chief*

COMPUTING MECHANISMS AND LINKAGES

MASSACHUSETTS INSTITUTE OF TECHNOLOGY

RADIATION LABORATORY SERIES

---

1. RADAR SYSTEM ENGINEERING—*Ridenour*
2. RADAR AIDS TO NAVIGATION—*Hall*
3. RADAR BEACONS—*Roberts*
4. LORAN—*Pierce, McKenzie, and Woodward*
5. PULSE GENERATORS—*Glasoe and Lebacqz*
6. MICROWAVE MAGNETRONS—*Collins*
7. KLYSTRONS AND MICROWAVE TRIODES—*Hamilton, Knipp, and Kuper*
8. PRINCIPLES OF MICROWAVE CIRCUITS—*Montgomery, Dicke, and Purcell*
9. MICROWAVE TRANSMISSION CIRCUITS—*Ragan*
10. WAVEGUIDE HANDBOOK—*Marcuvitz*
11. TECHNIQUE OF MICROWAVE MEASUREMENTS—*Montgomery*
12. MICROWAVE ANTENNA THEORY AND DESIGN—*Silver*
13. PROPAGATION OF SHORT RADIO WAVES—*Kerr*
14. MICROWAVE DUPLEXERS—*Smullin and Montgomery*
15. CRYSTAL RECTIFIERS—*Torrey and Whitmer*
16. MICROWAVE MIXERS—*Pound*
17. COMPONENTS HANDBOOK—*Blackburn*
18. VACUUM TUBE AMPLIFIERS—*Valley and Wallman*
19. WAVEFORMS—*Chance, Hughes, MacNichol, Sayre, and Williams*
20. ELECTRONIC TIME MEASUREMENTS—*Chance, Hulsizer, MacNichol, and Williams*
21. ELECTRONIC INSTRUMENTS—*Greenwood, Holdam, and MacRae*
22. CATHODE RAY TUBE DISPLAYS—*Soller, Starr, and Valley*
23. MICROWAVE RECEIVERS—*Van Voorhis*
24. THRESHOLD SIGNALS—*Lawson and Uhlenbeck*
25. THEORY OF SERVOMECHANISMS—*James, Nichols, and Phillips*
26. RADAR SCANNERS AND RADOMES—*Cady, Karelitz, and Tutner*
27. COMPUTING MECHANISMS AND LINKAGES—*Svoboda*
28. INDEX—*Linford*

COMPUTING MECHANISMS AND LINKAGES

By ANTONÍN SVOBODA

Edited by HUBERT M. JAMES

OFFICE OF SCIENTIFIC RESEARCH AND DEVELOPMENT
NATIONAL DEFENSE RESEARCH COMMITTEE

FIRST EDITION
THIRD IMPRESSION

NEW YORK AND LONDON
McGRAW-HILL BOOK COMPANY, INC.
1948

COMPUTING MECHANISMS AND LINKAGES

PRINTED IN THE UNITED STATES OF AMERICA

THE MAPLE PRESS COMPANY, YORK, PA.

Foreword

The tremendous research and development effort that went into the development of radar and related techniques during World War II resulted not only in hundreds of radar sets for military (and some for possible peacetime) use but also in a great body of information and new techniques in the electronics and high-frequency fields. Because this basic material may be of great value to science and engineering, it seemed most important to publish it as soon as security permitted.

The Radiation Laboratory of MIT, which operated under the supervision of the National Defense Research Committee, undertook the great task of preparing these volumes. The work described herein, however, is the collective result of work done at many laboratories, Army, Navy, university, and industrial, both in this country and in England, Canada, and other Dominions.

The Radiation Laboratory, once its proposals were approved and finances provided by the Office of Scientific Research and Development, chose Louis N. Ridenour as Editor-in-Chief to lead and direct the entire project. An editorial staff was then selected of those best qualified for this type of task. Finally the authors for the various volumes or chapters or sections were chosen from among those experts who were intimately familiar with the various fields, and who were able and willing to write the summaries of them. This entire staff agreed to remain at work at MIT for six months or more after the work of the Radiation Laboratory was complete. These volumes stand as a monument to this group.

These volumes serve as a memorial to the unnamed hundreds and thousands of other scientists, engineers, and others who actually carried on the research, development, and engineering work the results of which are herein described. There were so many involved in this work and they worked so closely together even though often in widely separated laboratories that it is impossible to name or even to know those who contributed to a particular idea or development. Only certain ones who wrote reports or articles have even been mentioned. But to all those who contributed in any way to this great cooperative development enterprise, both in this country and in England, these volumes are dedicated.

L. A. DuBridge.

Preface

THE work on linkage computers described in this volume was carried out under the pressure of war. War gives little opportunity for the advancement of abstract knowledge; all efforts must be concentrated on meeting immediate needs. In developing techniques for the design of linkage computers, the author has therefore been forced to concentrate on finding practical methods for the design of computers rather than on developing a unified and systematic analysis of the subject. The war has thus given to this work a special character that it might not otherwise have had.

The impulse to the development of the methods presented in this volume for the mathematical design of linkage computers grew out of a collaboration of the author with his friend, Dr. Vladimir Vand. That collaboration was begun in France in 1940, and was brought to a premature end by the progress of the war. Though these ideas and methods have largely been developed by the author since that time, he wishes to emphasize that credit for the initiation of the work is shared by Dr. Vand. It must be mentioned also that the techniques described in this book were for the most part developed before the author became associated with the Radiation Laboratory.

The author wishes to express sincere gratitude to Dr. H. M. James, the editor of this volume, who gave the book its present form, contributing many examples and many improvements to the methods. (Secs.: 6·7, 6·8, 6·15, 8·6.)

The book would never have been completed in such a short time without the assistance of Miss Constance D. Boyd, who read the manuscripts, and Miss Elizabeth J. Campbell, Mrs. Kathryn G. Fowler, Miss Virginia Driscoll, and Miss Patrica J. Boland, who calculated the tables and drew nomograms. The author also wishes to thank Dr. I. Maddaus, Jr., for bibliographical research.

A. SVOBODA.

PRAHA, CZECHOSLOVAKIA,
June, 1946.

Contents

CHAPTER 1

INTRODUCTION

1·1. Types of Computing Mechanisms.—Computing mechanisms may be divided into two distinct types: arithmetical computing machines, familiar to the layman through their common use in business offices, and continuously acting computing mechanisms and linkages that range in complexity from simple cams and levers to enormously complex devices for the direction of naval and antiaircraft gunfire.

The arithmetical computing machines accept inputs in numerical form, usually on a keyboard, and with these numbers perform the simple arithmetical operations of addition, subtraction, multiplication, and division—usually by the iteration of addition and subtraction in counting devices. The results are finally presented to the operator, again in numerical form. In their simplest forms these machines have the virtue of applicability in a wide variety of computations, including those requiring very high accuracy. By elaboration of these devices, as by the introduction of punched-tape control, their possibilities for automatic operation can be greatly increased. Characteristic of their operation, however, is their production of numerical results by calculations in discrete steps, involving delays which are always appreciable and may be very large if the required calculation is of complex form.

Continuously acting computing mechanisms are less flexible and have less potential accuracy, but their applicability to the instantaneous or to the continuous solution of specific problems—even quite complex ones—makes them of great practical importance. They may serve as mere indicators of the solutions of a problem, and require further action by human agency for the completion of their function (speedometer, slide rule); or they may themselves produce a mechanical action functionally related to other mechanical actions (mechanical governors, automatic gunsight).

Continuously acting computers fall into two main classes: function generators and differential-equation solvers. Function generators produce mechanical actions—usually displacements or shaft rotations—that are definite functions of many independent variables, themselves introduced into the mechanism as mechanical actions. Simple examples of such mechanisms are gear differentials, two- and three-dimensional cams, slide multipliers and dividers, linkage computers, and mechanized nomograms. Computers of the second class generate solutions of some definite

differential or integrodifferential equation—often an equation that involves functions continuously determined by variable external circumstances. Elementary devices of this type are the integrators, component solvers, speedometers, and planimeters.

From these elementary devices one can build up complicated mechanisms that perform elaborate calculations. We may mention their application in gunsights, bombsights, automatic pilots (for airplanes, submarines, ships, and torpedoes), compensators for gyroscopic compasses, tide predictors, and other robots of varied types.

The present volume will deal only with the problem of designing continuously acting computing mechanisms.

1·2. Survey of the Problem of Computer Design.—There is no set rule or law for the guidance of a designer of complex mechanical computers. He must weigh against each other many diverse factors in the problem: the accuracy required; the cost, weight, volume, and shape of the computer; its inertia and delay in action; the forces required to operate it; its resistance to shock, wear, and changes in weather conditions. He must consider how long it will take to design the computer, how easily it can be built, how easily it can be operated by a crew, whether suitable sources of power will be available, and so on. The complexity of the theoretical and practical problems is so great that two designers working on a given problem will never arrive at precisely the same solution.

For practical reasons, a designer should be asked to find a computer that meets certain specified tolerances, rather than the best possible computer for a given use. He should know what will be the maximum tolerated error of the computer, the maximum cost, weight, and volume occupied, the maximum number of operators in the crew, the maximum number of servomechanisms allowed, and so on. Tolerances provide a convenient means for controlling the development of the computer, and—if established in a practical way—they permit some freedom of choice by the designer.

Choice of Approach to the Design Problem.—The type of computer to be built is sometimes indicated in the specifications. If not, the first task of the designer is to decide whether the computer is to be mechanical, electrical, optical, or a combination of these. At the same time that this important decision is made, the designer must weigh in his mind the path that his thinking will follow. There are two principal methods for designing a computer: the constructive method and the analytic.

The constructive method makes use of a small-scale model of the real system with which the computer is to deal. For example, a constructive antiaircraft fire-control computer might determine the elements of the lead triangle by maintaining within itself and measuring the elements of a small model of this triangle.

In using the analytic method, the designer concentrates on the analytic relations between the variables involved. A relation between variables, such as

$$z = xy + \frac{x}{y}, \tag{1}$$

can be given mechanical expression in terms of displacements or shaft rotations, without regard to the nature of the quantity represented by the variables x, y, and z. For example, one may possess two devices that generate output displacements xy and x/y, respectively, given input displacements x and y. Combining these with a third device for adding their output displacements, one can then produce a computer that, given input displacements x and y, generates a final output displacement z having continuously the value specified by Eq. (1). The computer is then a "mechanization" of Eq. (1), rather than a model of any special system involving variables x, y, and z thus related.

Computers designed by analytic methods consist of units ("cells") that mechanize fairly simple relations, so connected as to provide a mechanization of a more complex equation or system of equations. For any given problem a great variety of designs is possible. This variety arises in part from the possible choice among mechanical cells mechanizing a given elementary relation, and in part from the variety of ways in which the relation between a given set of variables can be given analytic expression. Thus, each of the equations

$$z = \frac{x}{y}(y^2 + 1), \tag{2a}$$

$$z = x\left(y + \frac{1}{y}\right), \tag{2b}$$

$$zy = x(y^2 + 1), \tag{2c}$$

[all equivalent to Eq. (1)] suggests a different method of connecting mechanical cells into a complete computer. This flexibility in analytic design methods makes it possible to arrive at designs that are in general more satisfactory mechanically than those obtained by constructive methods.

In the present volume we shall be concerned entirely with mechanical computers designed by the analytic method.

Block Diagram of the Computer.—To each formulation of the problem in analytic terms there corresponds a block diagram of the computer. In this diagram each analytic relation between variables is represented by a square or similar symbol, from which emerge lines representing the variables involved; a line representing a variable common to two relations will connect the corresponding squares in the diagram. In mechanical terms, each square then represents an elementary computer that estab-

lishes a specified relation between the variables, and the connecting lines represent the necessary connections between these elementary computers. By examination of block diagrams the designer will be able to see the principal virtues of each computing scheme: the complexity of the system, the working range of variables, the accuracy required of individual components, and so on. On this basis he can make at least a tentative selection of the block diagram to be used.

Selection of Components for the Computer.—Knowing the accuracy and mechanical properties required of each computing element, the designer can select the elementary computers from which the complete device is to be built.

As an example of the diverse factors to be borne in mind, let us suppose that it is required to provide a mechanical motion proportional to the product of two variables, X_1 and X_2. A slide multiplier of average size will allow an error of from 0.1 per cent to 0.5 per cent of the whole range of the variable; this error will depend on the quality of the construction —on the backlash and the elasticity of the system. A linkage multiplier will have an error of some 0.3 per cent due to its structure, practically no error from backlash, and a slight error due to elasticity of the system if the unit is well designed; the space required by a linkage multiplier is small, but its error cannot be reduced by increasing its size. If these devices do not promise sufficient accuracy, the designer must use multipliers based on other principles. It is possible to perform multiplication by use of two of the precision squaring devices illustrated in Fig. 1·23, by connecting these in the way suggested by the equation

$$X_1X_2 = \tfrac{1}{4}(X_1 + X_2)^2 - \tfrac{1}{4}(X_1 - X_2)^2. \tag{3}$$

The error of such a multiplier may be as low as 0.01 per cent, but the system has an appreciable inertia. About the same accuracy is attainable by a multiplier based on the differential formula for multiplication,

$$d(X_1X_2) = X_1\,dX_2 + X_2\,dX_1; \tag{4}$$

this employs two integrators, and is commonly used when two quantities are to be multiplied in a differential analyzer. This scheme is useful only when it is possible to allow a slow change in a constant added to the product X_1X_2—a change which will result from slippage in the integrators, negligible for a single multiplication but accumulating with repetition of the operation.

From this discussion it should be evident that there is no "best" multiplier. Similarly, other components of a computer must be selected with due regard for their special characteristics and the demands to be made upon them.

Mathematical Design of the System.—From the block diagram one should proceed to the mechanical design of a system through an inter-

mediate step—that of establishing the "mathematical design" of the system. The mathematical design ignores the dimensions not essential to the nature of the computation to be carried out—diameters of shafts, dimensions of ball bearings, dimensions of the frame—but specifies the dimensions of levers measured between pivots and joints, the size of friction wheels, tentative gear diameters and gear ratios. The properties of this design should be studied carefully, because this usually leads to a change in some detail of the design, and sometimes even to choice of a new block diagram.

Final Steps in the Design.—From the mathematical design of the system one can proceed to the design of a working model. The elements of this model should be accessible rather than massed together, inexpensive, and quick to manufacture. If the performance of the working model is found to be satisfactory, the first model can be designed. Here the ingenuity of the designer must be used to the maximum. The parts of the mechanism must be arranged compactly to decrease space requirements, weight, and the effects of elasticity and thermal expansion, but they should not be massed in such a way that assembly is difficult, or repair or servicing impossible. Sometimes division of the whole computer into several independent parts is advisable. Finally, the computer can be built and tested against specifications.

1·3. Organization of the Present Volume.—It is not possible to discuss in one volume all elements of the problem of computer design. This book will deal principally with bar-linkage computers—specifically, with the mathematical design of elements for such computers. Bar linkages are mechanically very satisfactory, and computers built from them have many important virtues, but the mathematical design of these systems is relatively difficult and is not widely understood. There are few standard bar-linkage elements for computers; it is usually necessary to design the components of the computer, and not merely to organize standard elements into a complex assembly. It is hoped that the design methods to be described here will lead to their more general use.

Bar linkages can be used in combination with the standard computing mechanisms. For this reason, and for the contrast with the bar linkages which are to be discussed later, this volume begins with a brief survey of some more or less standard elements of mechanical computers. Chapter 2 is devoted to a general discussion of bar linkages. Chapter 3 establishes terminology and describes graphical procedures of which extensive use will be made. Chapters 4, 5, and 6 discuss, in order of their increasing complexity, bar linkages with one degree of freedom—generators of functions of one independent variable. Chapter 7 indicates some mathematical methods of importance in bar-linkage design. Finally, Chaps. 8, 9, and 10 develop methods for the design of bar-linkage gener-

ators of functions of two independent variables—a field in which bar linkages have very striking advantages.

ELEMENTARY COMPUTING MECHANISMS

The remainder of this chapter will give a brief survey of elementary computing mechanisms, or "cells," of more or less standard type. Discussion of bar-linkage cells will be deferred to Chap. 2.

1·4. Additive Cells.—"Additive" or "linear" cells establish linear relations between mechanical motions of the cell, usually shaft rotations or slide displacements. If these are described by parameters X_1, X_2, X_3, the cell will compute

$$X_3 = Q \cdot X_1 + Q' \cdot X_2 + C. \tag{5}$$

Here Q, Q', and C are constants depending on the design of the cell and the choice of the zero positions from which X_1, X_2, and X_3 are measured. By

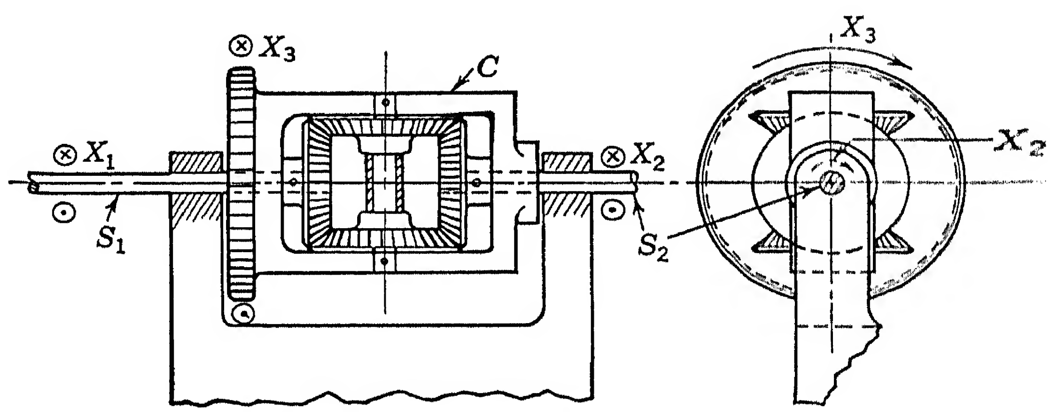

FIG. 1·1.—Bevel-gear differential.

proper choice of the zero positions, C can always be made to vanish; in what follows it will be assumed that this has been done.

The *bevel-gear differential* (Fig. 1·1) is a well-known linear cell for which all three parameters are rotations. The parameter X_1 is the rotation of the shaft S_1 from a predetermined zero position, $X_1 = 0$; the positive direction of rotation is indicated by symbols representing the head and tail of an arrow with this direction. The parameter X_2 is the rotation of the shaft S_2 from a similar zero position; X_3 is the rotation from its zero position of the cage C carrying the planetary bevel gears G. The zero positions are not indicated in the figure.

The equation of the bevel-gear differential is

$$X_3 = 0.5X_1 + 0.5X_2. \tag{6}$$

To derive this it is convenient to consider the value of X_2 corresponding to given values of X_1 and X_3. Let us consider the differential to be originally in the position $X_1 = X_2 = X_3 = 0$. The parameters X_1 and X_3 can then be given their assigned values in two steps, the first a rotation of both the

shaft S_1 and the cage C through the angle X_3, and the second a rotation of the shaft S_1 through an additional angle $X_1 - X_3$. In the first step the differential moves as a unit; the shaft S_2 is rotated through the angle X_3. In the second step, the cage is stationary and the movement of the shaft S_1 is transmitted to the shaft S_2 with its sense of rotation reversed; the rotation through angle $X_1 - X_3$ of the shaft S_1 causes rotation through $X_3 - X_1$ of the shaft S_2. The total rotation of the shaft S_2 is then $X_2 = X_3 + (X_3 - X_1)$, from which Eq. (2) follows immediately. It is, of course, essential that all rotations be taken as positive in the same sense.

It is remarkable that Eq. (6) is independent of the ratio of the bevel gearing of the differential; the essential characteristic of this type of

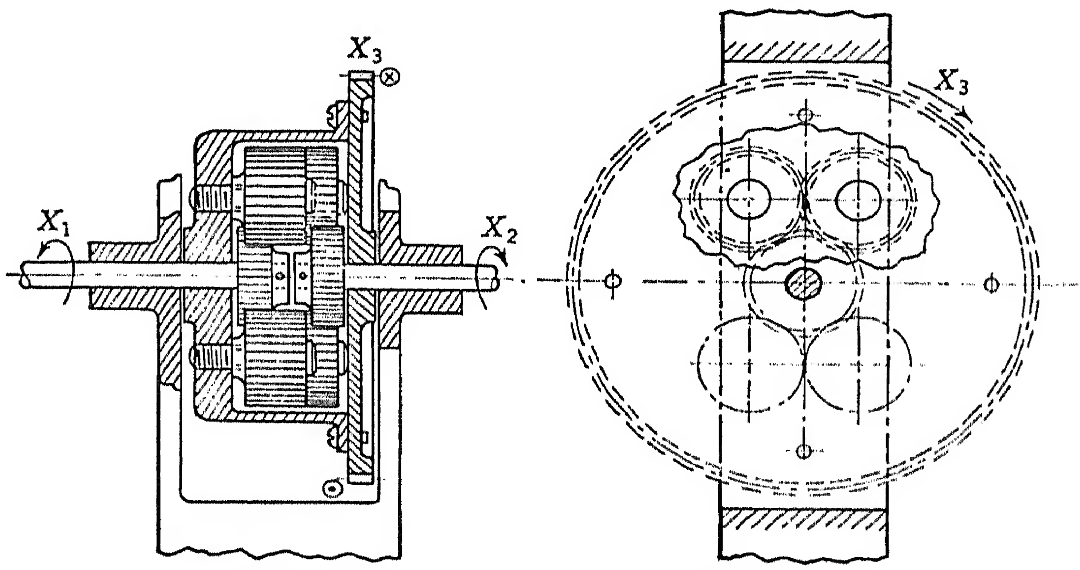

FIG. 1·2.—Cylindrical-gear differential.

differential is that the gearing of the cage transmits the relative motion of the shaft S_1 to the shaft S_2 in the ratio 1 to 1, but with reversed sense. It is not necessary to use bevel gears in the cage to obtain this result; cylindrical gears can accomplish the same purpose. A *cylindrical-gear differential* is shown in Fig. 1·2. This differential is equivalent to the common bevel-gear differential, except in its mechanical features. It is flatter, and easier to construct in large numbers, but there is one more gear mesh than in the common type; there may be more backlash and more friction. It should be noted, however, that bevel gears are subject to axial as well as radial forces in their bearings, and that these may also increase friction.

The *spur-gear differential* shown in Fig. 1·3 has only two gear meshes, and is quite flat. The planetary gears G in their cage C do not invert the motion of the shaft S_1 when transmitting it to the shaft S_3, but can be made to transmit it at a ratio different from 1. The equation of this

differential is

$$X_3 = QX_1 + (1 - Q)X_2. \tag{7}$$

To prove this relation we can use the same method as before. Let us begin by considering the differential in the zero position,

$$X_1 = X_2 = X_3 = 0.$$

We wish to find the value of X_3 corresponding to given X_1 and X_2. We introduce the angles X_1 and X_2 in two steps, first turning both the shaft

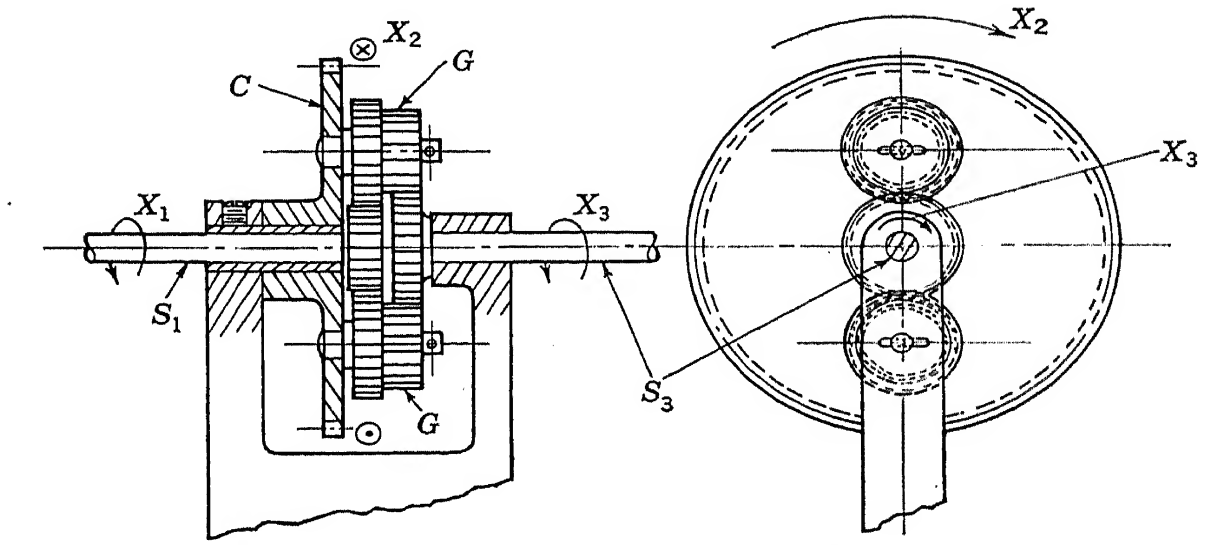

FIG. 1·3.—Spur-gear differential.

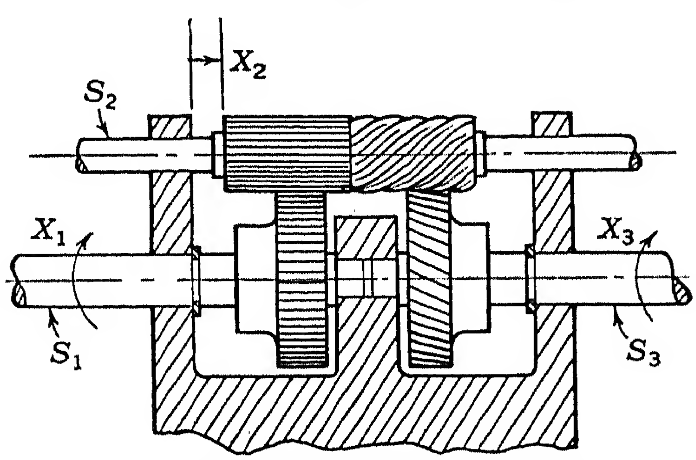

FIG. 1·4.—Differential with axially displaced spiral gear.

S_1 and the cage C through the angle X_2, and then the shaft S_1 through an additional $X_1 - X_2$. In the first step the differential is turned as a rigid body; the shaft S_2 is also turned through the angle X_2. In the second step the shaft S_3 is turned through $Q(X_1 - X_2)$; its total motion is $X_3 = X_2 + Q(X_1 - X_2)$, in agreement with Eq. (7).

If we make $Q = Q' = 0.5$ by proper choice of the gear ratios, we can obtain a differential equivalent to the bevel-gear differential. The fact that the free choice of Q gives to this differential a larger field of applicability does not necessarily mean that this differential should be preferred

to those with $Q = 0.5$; it is convenient to use differentials with $Q = 0.5$ as prefabricated standard elements.

A *differential with axially displaced spiral gear* is shown in Fig. 1·4. The parameter X_2, which measures the axial displacement of the spiral gear and the pin P_2, is variable only within finite limits. The mechanical structure of this differential is, however, much simpler than that of the differentials already mentioned, for which all parameters can change without limitation. The equation of this differential is

$$X_3 = X_1 \pm \frac{2\pi n}{m} X_2, \tag{8}$$

where n is the number of threads per inch along the axis of the spiral gear on the shaft S_2 and m is the number of teeth on the gear with which it

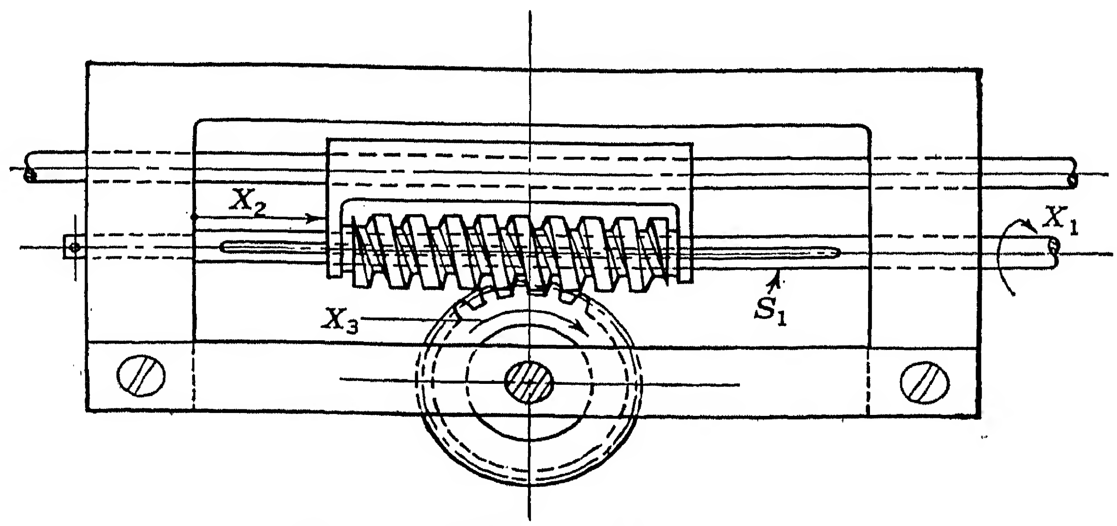

FIG. 1·5.—Differential worm gearing.

meshes. The helical angle of the gears should be at least 45° for smooth action and small backlash.

The *differential worm gearing* shown in Fig. 1·5 is used for the same purpose as the preceding differential, especially if the range of values of X_2 corresponds to a large fraction of a revolution of the shaft S_1 or even to several revolutions of this shaft. The equation of this differential is

$$X_3 = \pm \frac{m}{t} X_1 + \frac{1}{R} X_2 \qquad \text{(radians)}, \tag{9}$$

where t is the number of teeth of the worm gear, m is the multiplicity of the threads of the worm, and R is the radius of the worm gear.

The sign in Eqs. (8) and (9) depends on the sense of the threads of the spiral or worm gear.

The *screw differential* shown in Fig. 1·6 combines an axial translation X_1 of a screw with a translation X_2 of the nut N with respect to the screw;

$$X_3 = X_1 + X_2. \tag{10}$$

To obtain the first translation, the pin P on which the screw turns is displaced by X_1. The rotation of the screw comes from the gear G, which meshes with a cylindrical rack C and slides along it. The real input

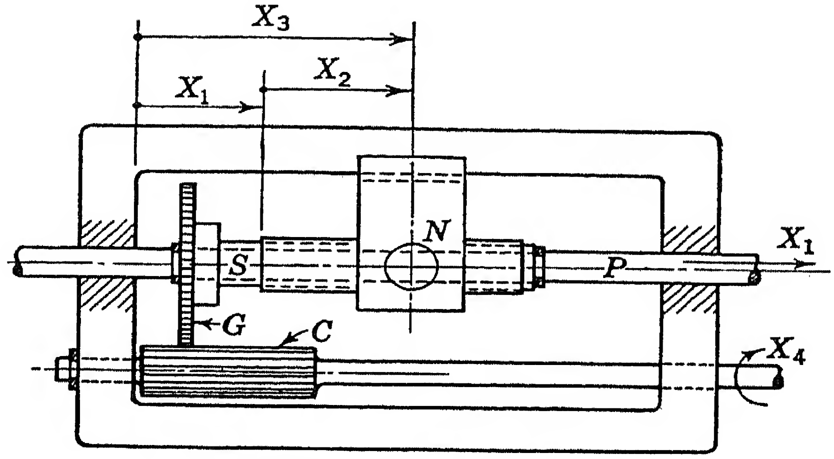

FIG. 1·6.—Screw differential.

parameter of the differential is not X_2, but the angle X_4 through which the rack is turned. The equation of the differential is then

$$X_3 = X_1 \pm kX_4. \tag{11}$$

The sign depends on the sense of the screw; k is a constant determined by the gear ratio, the number of threads per inch on the screw, and their multiplicity. All three parameters of this differential have constructive limits.

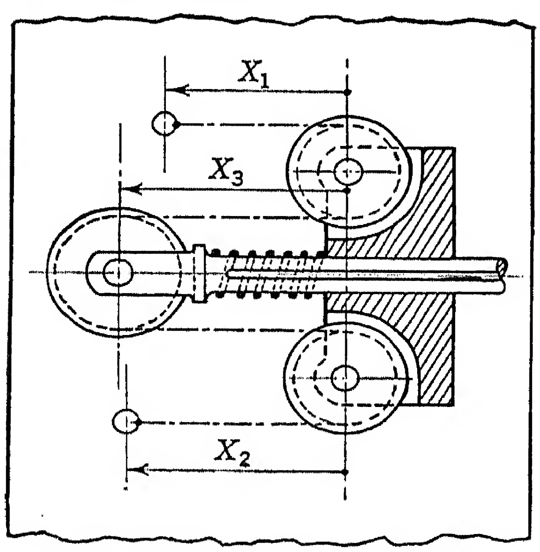

FIG. 1·7.—Belt differential.

The *belt differential* (Fig. 1·7) makes use of the inextensibility of a belting on several pulleys. In practice, chains, strings, and special cables are used as belts. The equation of the belt differential is

$$X_3 = C - 0.5X_1 - 0.5X_2, \tag{12}$$

where C is a constant depending on the choice of zero points of the parameters.

The tension in the belt must not fall below zero at any time; if it does, the belt will sag and the equation of the differential will not hold. To obtain positive action in the direction of increasing X_3, it is necessary to preload the belt by putting a load on the output pulley—for instance, by a spring that can exert a force large enough to produce the desired action. The maximum driving force required for this differential will then be about twice the force necessary to operate it without preloading.

The *loop-belt differential* (Fig. 1·8) has the belting in the form of a loop with length independent of the position of the pulleys. The belt can then

be preloaded (turnbuckle B) without adding to the driving force of the differential, except by the increased friction in the bearings.

Belt differentials are sometimes used to add a large number of parameters; they are easily combined in batteries, as indicated schematically in Fig. 1·9. In such an arrangement the parameter X_7 may have so large a range that it is impractical to use a slide as the output terminal. It is better practice to use a drum (dashed line in Fig. 1·9) on which the belt is wound on and at the same time wound off. To prevent slippage, the belt should make many turns on the drum and be fastened to it; a chain on chain sprockets may also be used as the belt.

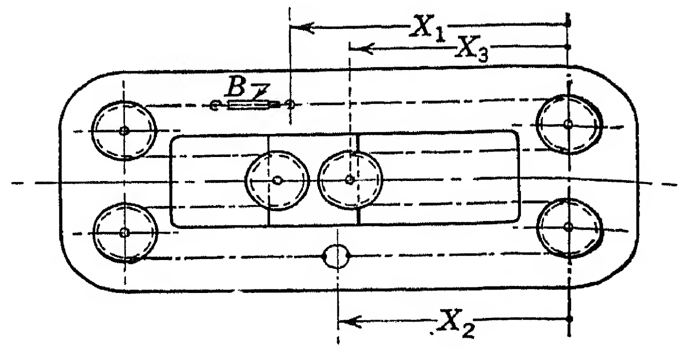

FIG. 1·8.—Loop-belt differential.

The above enumeration does not exhaust the possibilities for linear mechanical cells; there are many variants the use of which may be dictated by special circumstances.

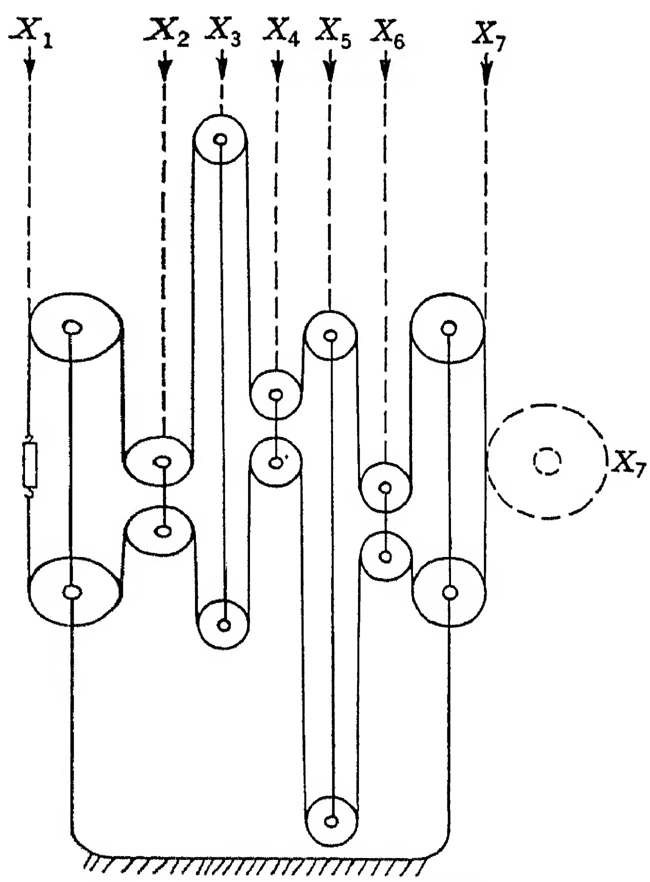

FIG. 1·9.—Loop-belt differential for the evaluation of

$$X_7 = C - X_1 - 2X_2 + 2X_3 - 2X_4 + 2X_5 - 2X_6.$$

As a rule, when a differential is used in a computing mechanism, two of its members (the input terminals) are moved by external forces; this results in movement of a third member (the output terminal) which is in turn required to furnish an appreciable force. If differentials were frictionless, any two of their three terminals could be used as input terminals. In reality, only a few of the differentials described here have complete interchangeability of the terminals. For instance, with the screw differential (Fig. 1·6) it is impossible to have X_4 as the output parameter if the helical angle of the screw is so low that self-locking of the nut on the screw occurs; it is possible to use X_1 as an output parameter, and, of course, also X_3. With the differential worm gearing of Fig. 1·5, X_1 is an impracticable output parameter.

1·5. Multipliers.—Multipliers are computers that establish between three parameters a relation

$$RX_3 = X_1 \cdot X_2, \tag{13}$$

where R is a constant that depends on the type of multiplier and on its dimensions.

The action of the *slide multiplier* shown in Fig. 1·10 is based on the proportionality of the sides of two similar triangles. These are triangles with horizontal bases, and vertices at the central pin shown in the figure:

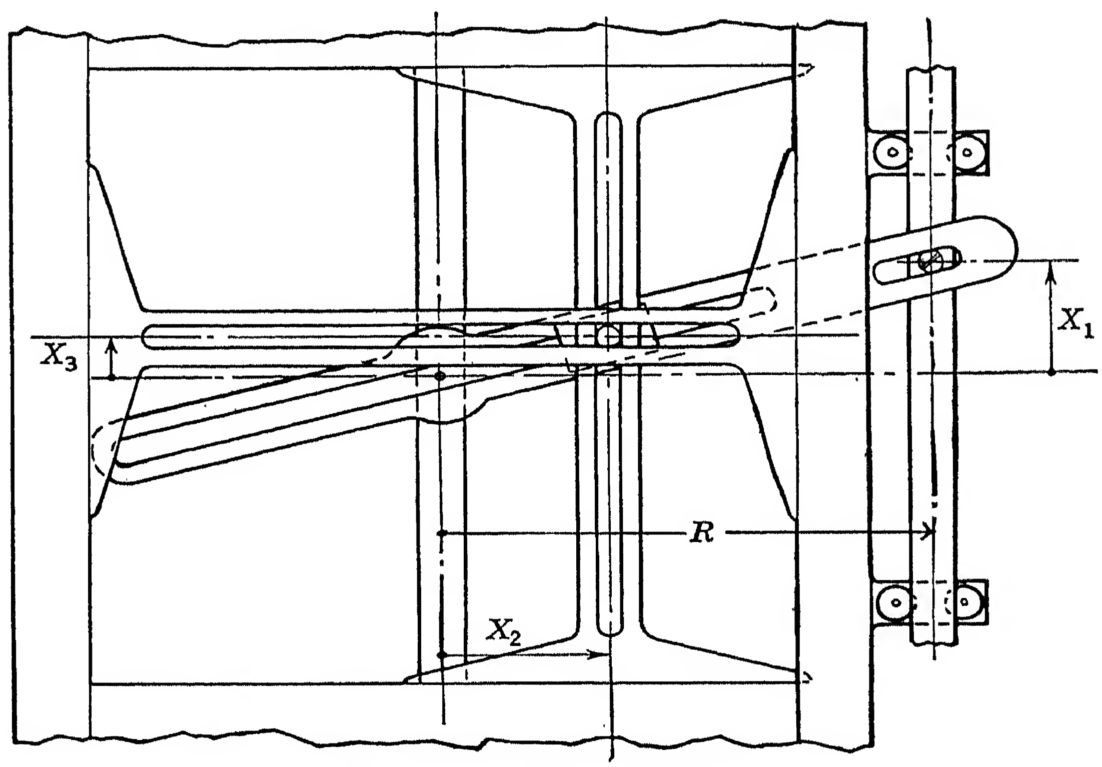

FIG. 1·10.—Slide multiplier.

the first has a base of length R and altitude X_1, the second a base of length X_2 and altitude X_3. Thus

$$\frac{R}{X_1} = \frac{X_2}{X_3}, \tag{14a}$$

or

$$RX_3 = X_1X_2. \tag{14b}$$

The figure gives a schematic rather than a practical design; the lengths of the sliding surfaces as shown are not great enough to prevent self-locking in all possible positions of the mechanism. These lengths determine the space requirements for multipliers of this type; they must be relatively large in two directions. It is difficult to make this type of multiplier precise. The pins in slots, as shown in the figure, are mechanically inadequate, and roller slides on rails must be used. One can not achieve the same end by increasing the dimensions of the multiplier because the

elasticity of parts comes into play, not only when the parts are operating in a computer, but also when they are being machined.

The slide multiplier shown in Fig. 1·11 saves space in one direction. There are fewer sliding contacts, and the slides are easier to construct.

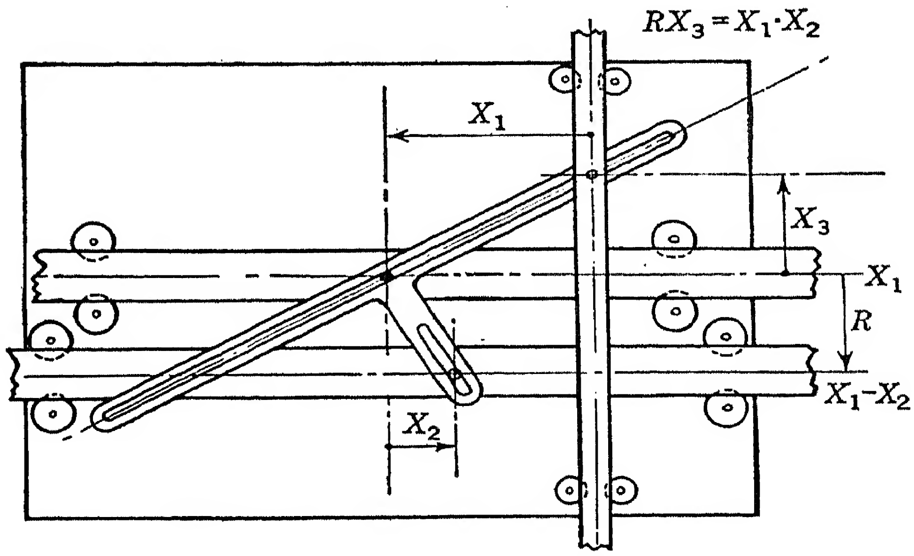

FIG. 1·11.—Slide multiplier with inputs X_1, $X_1 - X_2$.

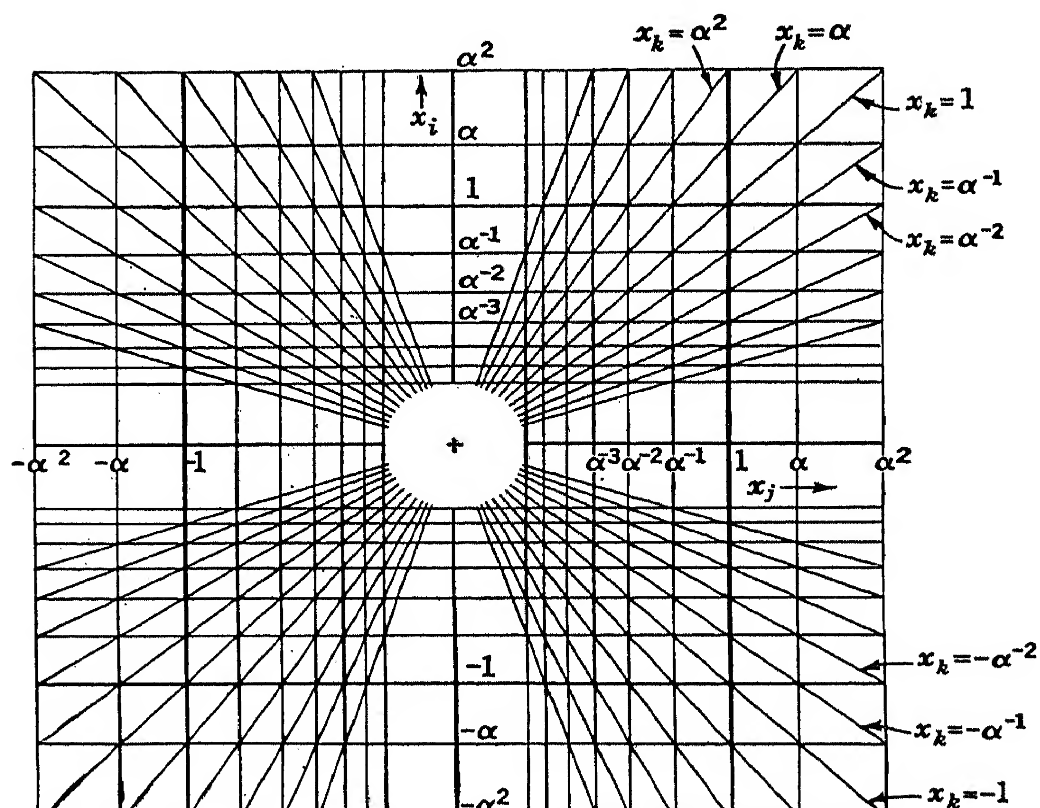

FIG. 1·12.—Intersection nomogram for multiplication $x_i = x_j \cdot x_k$.

This device cannot multiply X_1 and X_2 directly to compute $RX_3 = X_1X_2$; the input terminals must be given translations of X_1 and $X_1 - X_2$. The difference is easy to obtain if the parameters are generated as shaft revolutions before entering the multiplier; screws can then be used instead

of the slides shown in the figure, and the required difference can be formed by a gear differential.

Nomographic Multipliers.—A multiplier that is structurally related to a nomogram for multiplication will be called a "nomographic multiplier." Such multipliers can be derived from intersection or alignment nomograms; the examples to be given here are related to intersection nomograms.

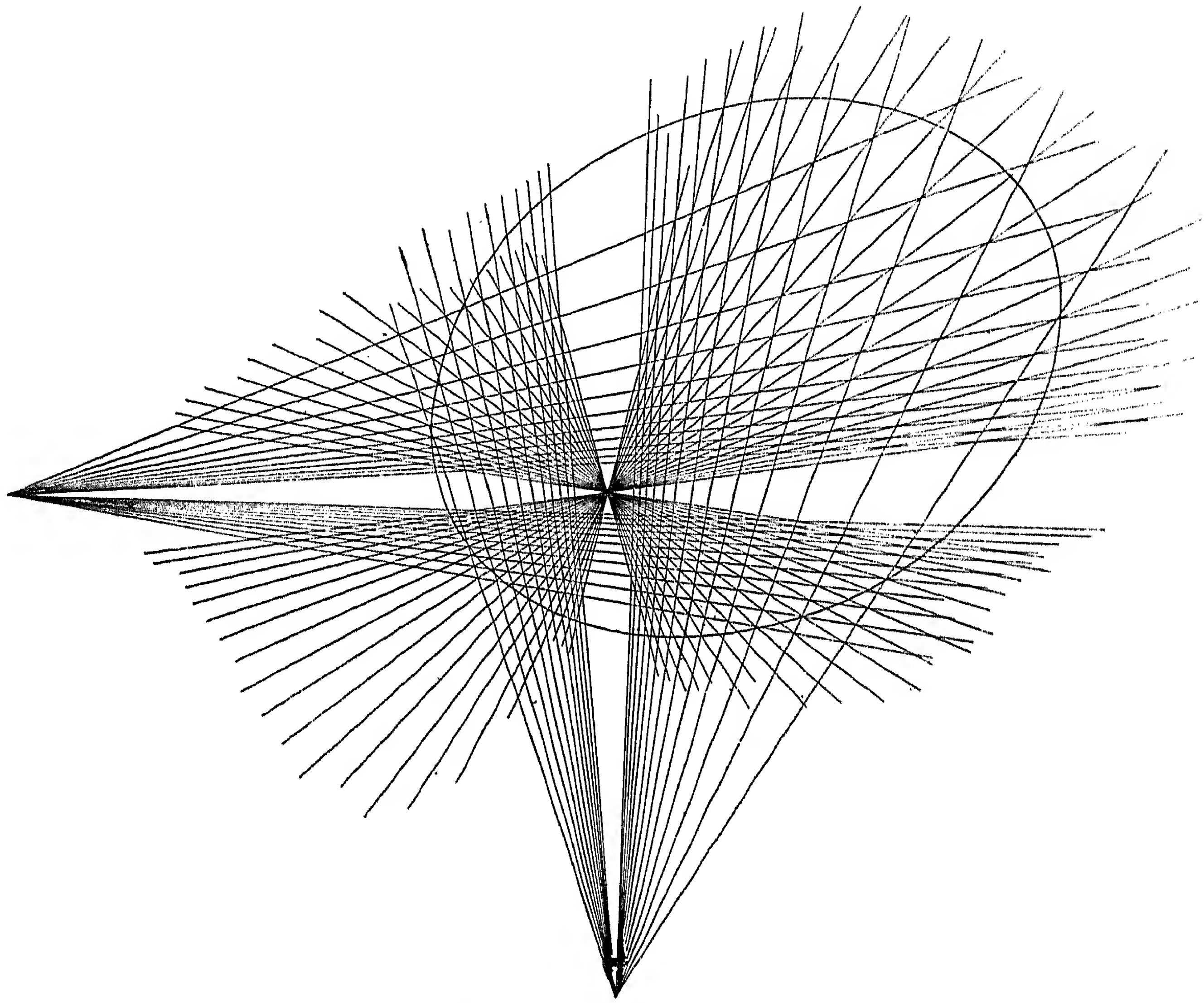

FIG. 1·13.—An intersection nomogram for multiplication, obtained from the nomogram in Fig. 1·12 by a projective transformation.

Figure 1·12 shows an intersection nomogram for multiplication in an unusual form, the full significance of which will be made clear in the latter part of this book. This represents the formula

$$x_i = x_j x_k. \tag{15}$$

It consists of three families of lines, of constant x_i, x_j, and x_k, respectively; through each point of the nomogram passes a line of each family, corresponding to values of x_i, x_j, and x_k which satisfy Eq. (15). (The lines in this particular figure are drawn for values of the x's that are powers of 1.25; this is not of immediate importance for our discussion.) The multi-

plier of Fig. 1·10 is structurally related to this nomogram. The rotating slide can be brought to positions corresponding to the radial lines in the nomogram; the horizontal and vertical slots correspond structurally to the horizontal and vertical lines on the nomogram, and the pin that connects all slides mechanically assures a triple intersection of these lines. The values of x_i, x_j, and x_k corresponding to the positions of the three slides must then satisfy Eq. (15); to complete the multiplier it is only necessary to provide scales from which these values can be read, or, as is done in Fig. 1·10, to provide mechanical connections such that terminal displacements are proportional to these quantities.

By a projective transformation of the nomogram in Fig. 1·12 one can obtain the nomogram in Fig. 1·13, where lines of constant values of the

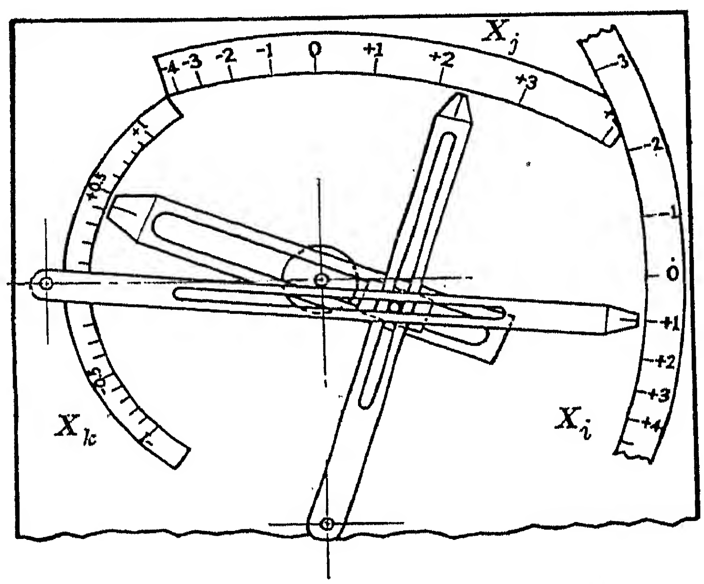

FIG. 1·14.—Nomographic multiplier.

variables x_i, x_j, and x_k form three families of radial lines intersecting in three centers. The obvious mechanical analogue of this nomogram for multiplication is shown in Fig. 1·14. It consists of three slides that rotate about centers corresponding to the centers of the radial lines in Fig. 1·13; these slides are bound together by a pin, which establishes the triple intersections found in the nomogram, and the corresponding values of x_i, x_j, and x_k are read on circular scales. It will be noted that the scale divisions are not uniform. Such nonuniform scales are of more general use than one might expect. Often one will have to deal with variables generated with nonuniform scales by some other computer; by proper choice of the projective transformation one can then hope to produce a multiplier of this type with similarly deformed scales.

1·6. Resolvers.—The *resolver* is a special type of multiplier. It generates a parameter X_3, and usually also another parameter X_4, as a product of a parameter X_1 and a trigonometric function—the sine or

cosine—of a parameter X_2. The equations are

$$X_3 = X_1 \sin X_2, \tag{16a}$$
$$X_4 = X_1 \cos X_2. \tag{16b}$$

The name of this device is derived from its action as a resolver of a vector displacement into its rectangular components.

A simplified design of a resolver is shown in Fig. 1·15. In the plan view, Fig. 1·15*a*, we see the materialization of a vector by a screw: the axis of the screw points in the direction of the vector, at an angle X_2 to a zero line; the length X_1 of the vector is established as the distance from the pivot O on which the whole screw is rotated to a pin T on the nut of the screw.

To obtain the components of the vector, slides are sometimes used, as in the case of the multiplier in Fig. 1·10. In Fig. 1·15 there is suggested a solution that gives much better precision and saves space. Perpendicular shafts pass through the block B that carries the pin P. These shafts are carried by rollers on rails; their parallelism to given lines is well assured by gears that mesh with racks fastened to the frame. For convenience of construction the axes of the shafts do not intersect with each other and with the axis of the pin T. This introduces a constant term e into the displacement of the shafts—that is, it causes a displacement e in the effective zero positions of X_3 and X_4.

It is of interest to note how the parameter X_1 is controlled from the input shaft S_1 (Fig. 1·15*b*.). While the screw is rotated through the angle X_2 on the shaft S_2, it is necessary to control the value of X_1 by a gear G that rotates freely on this shaft. If such a gear is turned through an angle proportional to X_1—is held fixed when X_1 is constant—the screw will spin on its axis whenever X_2 is changed; the length of the vector will be affected by change in X_2, and will not represent the desired value of X_1. It is thus necessary to keep the screw without spin with respect to S_2 when only X_2 is changed—to keep the gear G moving along with the shaft S_2 whenever X_1 is fixed. This is accomplished by the so-called "compensating differential," D. As is shown in the figure, the planetary gear of this bevel-gear differential is geared to the shaft S_2 in the ratio 1 to 1; the differential thus receives an input $-X_2$. When the input shaft S_6 is rotated through X_6, the output shaft S_5 is rotated through an angle

$$X_5 = -X_6 - 2X_2. \tag{17}$$

By gearing the gear G to the shaft S_5 in the ratio 2 to 1, the angle turned by G can be made to be

$$X_G = -0.5X_5 = 0.5X_6 + X_2.$$

Then if S_6 is stationary, X_G changes equally with X_2, and the screw is not spun; X_1 remains constant. If the shaft S_6 is turned, the gear G turns

with respect to the shaft S_2 through an equal angle. The change in X_1 is then proportional to the rotation of the shaft S_6: $X_6 = QX_1$, the constant Q depending on gear ratios and the threading of the screw.

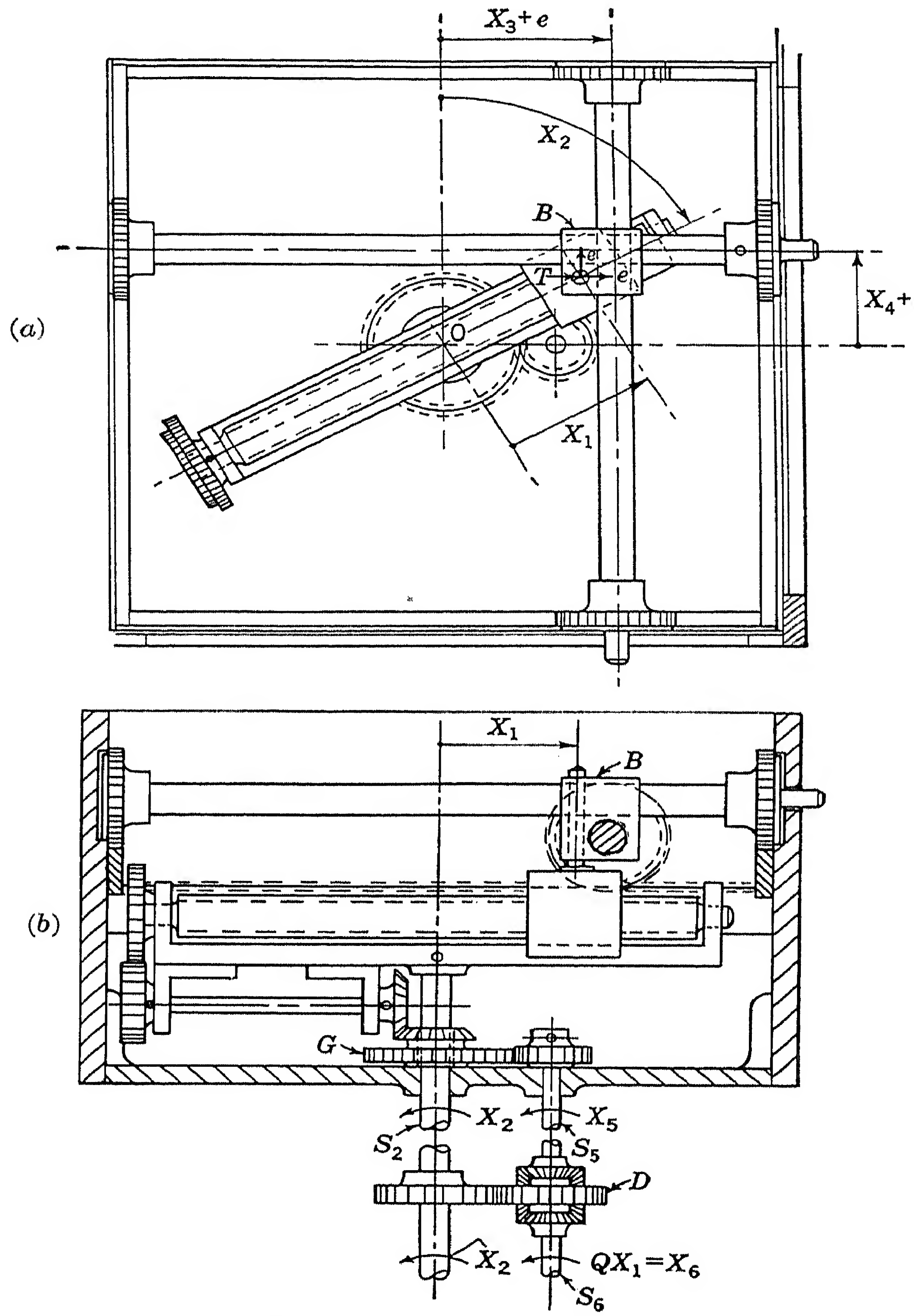

FIG. 1·15.—Resolver. (*a*) Plan view. (*b*) Elevation. The teeth of the racks are omitted from the figures.

The design in Fig. 1·15 is so oversimplified that the resolver is sure to be lacking in precision. In particular, the flexibility of the structure supporting the screw is excessive: shaft S_2 is easily bent and easily twisted.

This can be remedied by placing the screw subassembly on a circular plate with a large ball bearing on its circumference, and using a driving shaft of reasonable diameter.

A better construction (but one that is not always usable) is presented in Fig. 1·16. In the plan view, Fig. 1·16a, we observe the main difference between the subassembly of the screw in Fig. 1·15 and the present design.

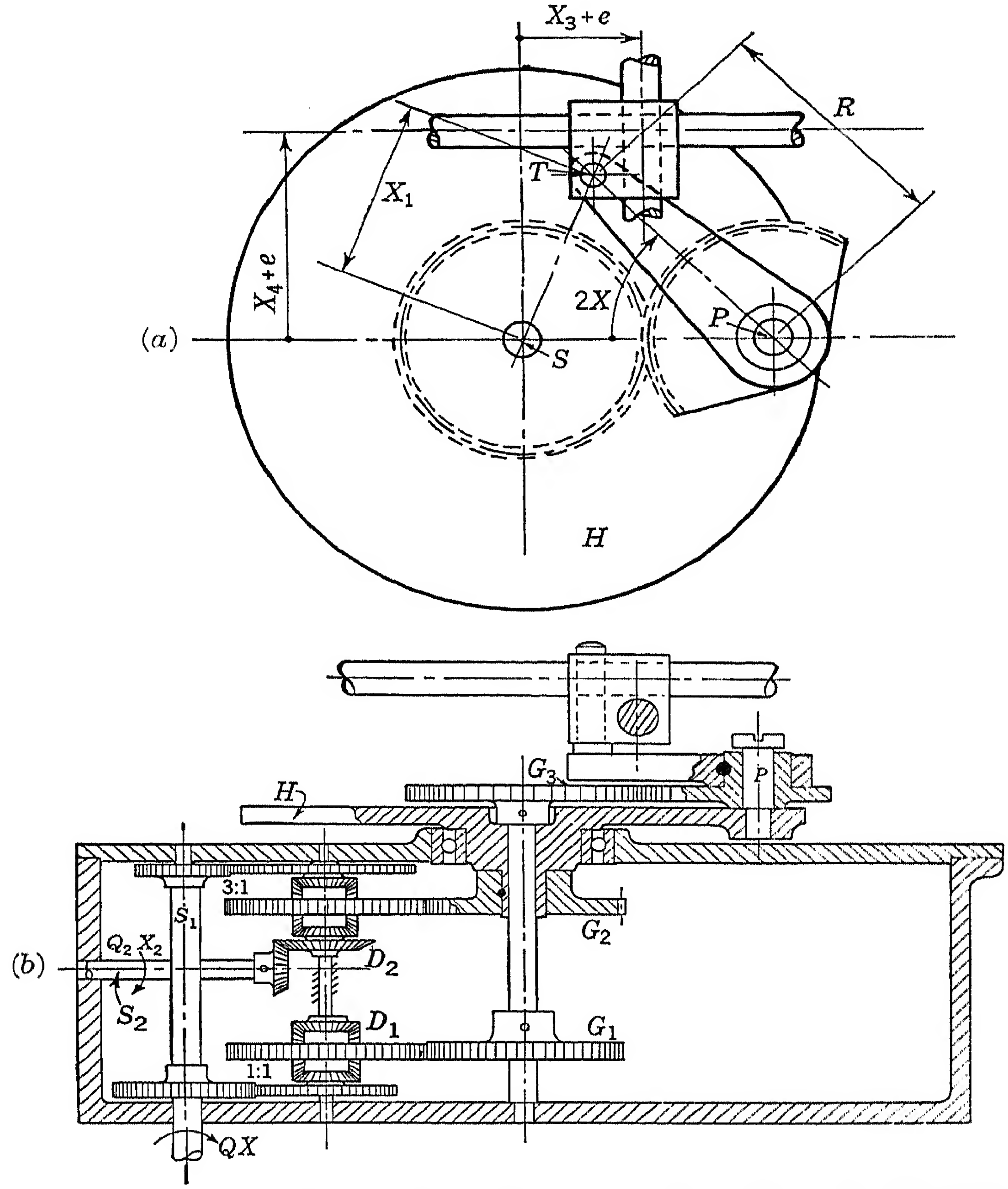

FIG. 1·16.—Alternative resolver design. (a) Plan view. (b) Elevation.

In Fig. 1·16a the pin T is carried on an arm of radius R that rotates on a pivot P. This pivot is placed at a distance R from the center S of the circular plate H to which it is fastened. By rotating the arm PT, the vector ST can be changed in length. Its direction would be changed at the same time if it were not for a compensating rotation of the plate H. Since the triangle SPT is isosceles the angle of rotation of ST to be com-

pensated for is exactly half of the angle of rotation of the arm PT. To introduce this compensation a differential is used; to change the direction of the vector ST in a desired manner, the table H is rotated through a second differential. The two differentials, D_1 and D_2, are shown in Fig. 1·16b. Their function may be understood in this way. To change the direction of the vector ST we must rotate the whole subassembly of the plate H as a unit; we must turn the gears G_1 and G_2 by the same amounts. These gears are geared to the cages of the planetary gears of the differentials D_1, D_2, at the same ratio (1 to 1 in the figure); these also must be turned equally. That is accomplished by turning the shaft S_2 and by keeping the shaft S_1 stationary. To change the length of the vector ST without turning it we have to turn the arm clockwise, for example, in the plan view, and the plate H counterclockwise by half the amount. This is accomplished by turning the shaft S_1. This shaft is geared to the input of the differential D_1 at the ratio 1 to 1 and to the input of the differential D_2 at the ratio 3 to 1; when the shaft S_1 rotates, the gear G_1 turns three times faster than the gear G_2. To see that this gives a compensating rotation of the plate through an angle $-X$ when the arm PT rotates through $2X$ relative to the plate H, we observe that if the gear G_1 were fixed, a rotation of G_2 and the plate H through $-X$ would rotate the arm with respect to the plate also by $-X$. To bring it to the correct position, $+2X$, it must then be rotated through an angle of $+3X$ with respect to the plate. To accomplish this the gear G_1 must be rotated through an angle $-3X$, since the direction of rotation is reversed in the gear G_3. Thus G_1 must turn in the same direction as G_2, but three times as fast.

1·7. Cams.—A cam is a mechanism that establishes a functional relation between parameters X_1 and X_2:

$$X_2 = F(X_1). \tag{18}$$

If X_1 is the input parameter, X_2 the output parameter, it is necessary in practice that $F(X_1)$ be a single-valued, continuous function with derivatives which do not exceed certain limits.

Plane cams exist in two principal variants, shown in Figs. 1·17 and 1·18. In the first the cam has the form of a disk shaped along a general curve. Contact with this cam is made by a roller on an arm; the contact is assured by tension of a spring. A cam of this type is easy to build and has negligible backlash, but the force on the arm is rather small in one of the two senses of motion—not larger than the force of the spring. In the second variant there is a slot milled into a flat surface rotating on a pivot; contact is made by a roller carried on a slide, as shown in Fig. 1·18. The second form does not permit use of as steep a spiral as does the first, since self-locking is more likely to occur.

The *cylindrical cam* shown in Fig. 1·19 has a slot milled into the surface of a cylinder; a small roller carried by a slide passes along the slot when the cam is turned on its axis through the input angle X_1. The form of the slot is so chosen that the motion of the slide, described by the output parameter X_2, has the desired character.

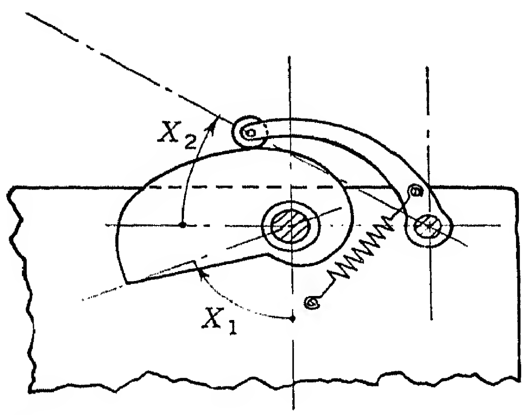

Fig. 1·17.—Plane cam with spring contact.

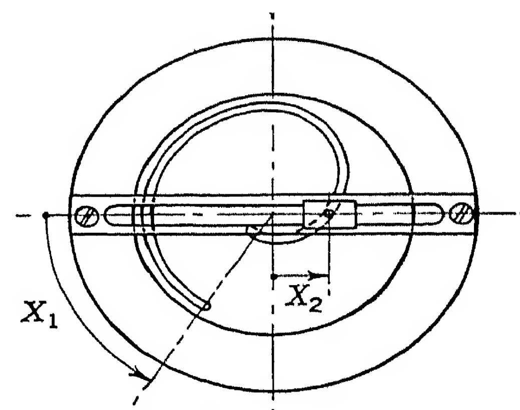

Fig. 1·18.—Plane cam with groove contact.

One variant of *pin gearing*, as shown in Fig. 1·20, has a gear with a special type of tooth meshing with a milled curved rack. (The milling tool has a cutting shape identical with the shape of the teeth of the gear.) Another form of pin gear (Fig. 1·21) has pins of special shape inserted in a plate; these mesh with a specially formed gear. In both variants the gear is keyed on a shaft, with freedom for lateral motion; this motion

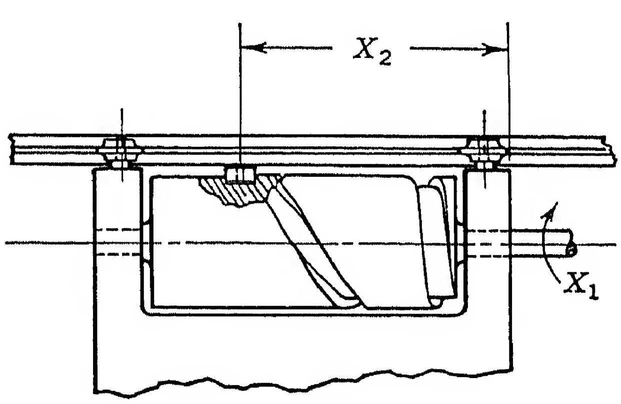

Fig. 1·19.—Cylindrical cam with groove contact.

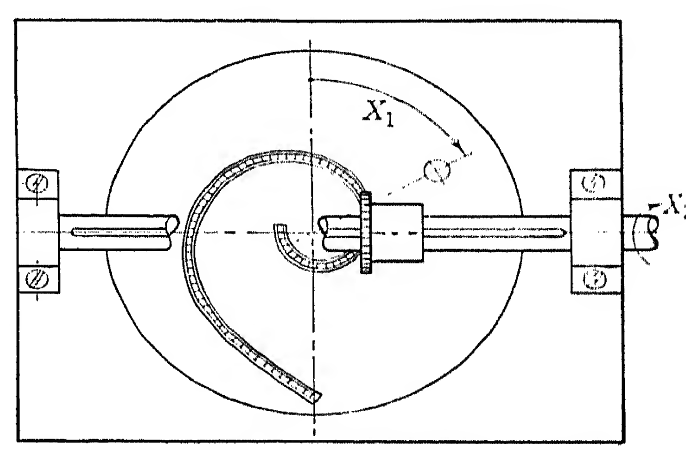

Fig. 1·20.—Pin gearing with pins on gear.

of the gear is assured by the action of the curved rack on the pins on the gear, or by a special cam constructed for this purpose.

The *belt cam* shown in Fig. 1·22 is a noncircular pulley or drum on which is wound a belt, or string, or some other kind of belting. If the number of revolutions of such a cam is to be greater than one, the string is wound in a spiral; the shape of this spiral should assure a smooth tangential winding of the string on the cams. Cams of this type can allow

very large travels of the belt and shaft, but they are mechanically less desirable than pin gears. They are not so safe in operation, and rather

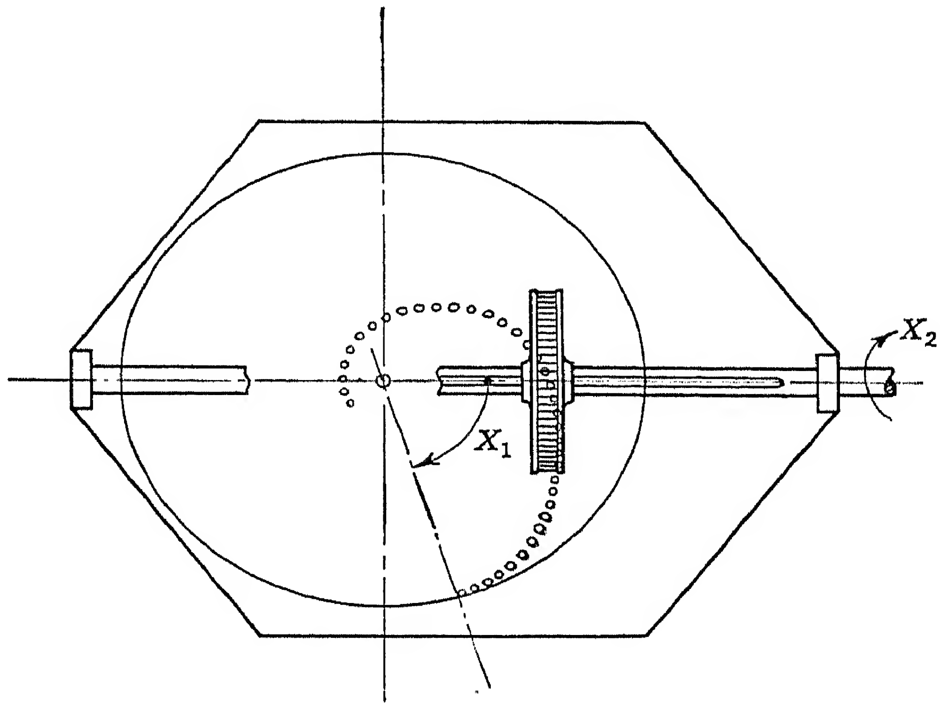

FIG. 1·21.—Pin-gearing with pins on the disk.

delicate, especially in the compensated form in which equal lengths of string are simultaneously wound off and wound on.

An example of a *compensated belt cam* is the squaring cam shown in Fig. 1·23. In this, two strings are wound partly on a cylinder, partly on a cone. The winding on the cone is in the form of a spiral with equally spaced threads; the form of the winding is assured by a groove. One string begins on the left side of the drum and, after a number of turns, passes on to the cone and continues in the groove to the tapered right end of the cone. The second string begins on the right side of the cylinder and after several turns to the left passes also onto the cone, where it continues through the groove to the left, to end at the larger end of the cone. The element of rotation dX_1 of the cone produces a motion of the string equal to R_1dX_1, where R_1 is the average radius of the cone at the points where the string meets and leaves the cone. The corresponding rotation of the drum is therefore $dX_2 = (-R_1dX_1)/R_2$,

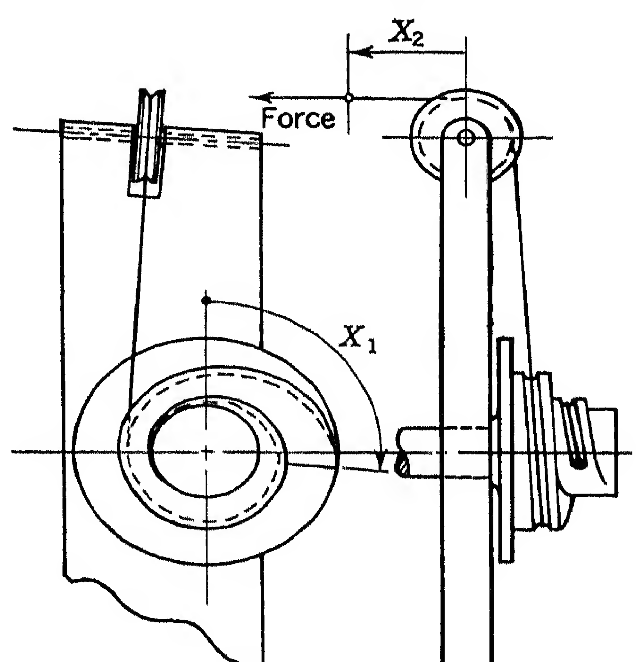

FIG. 1·22.—Belt cam.

where R_2 is the radius of the drum. The radius R_1 is proportional to the angle X_1 measured from a properly chosen zero position of the shaft S_1. (This zero position is, of course, not practically attainable, since it would correspond to zero radius of the cone at the point of contact.) We have then

$$-dX_2 = \frac{kX_1dX_1}{R_2}, \tag{19a}$$

$$X_2 = -\frac{k}{2R_2}X_1^2, \tag{19b}$$

if the zero point for X_2 is properly chosen. Here k is the increment of the radius R_1 per radian rotation of the shaft S_1.

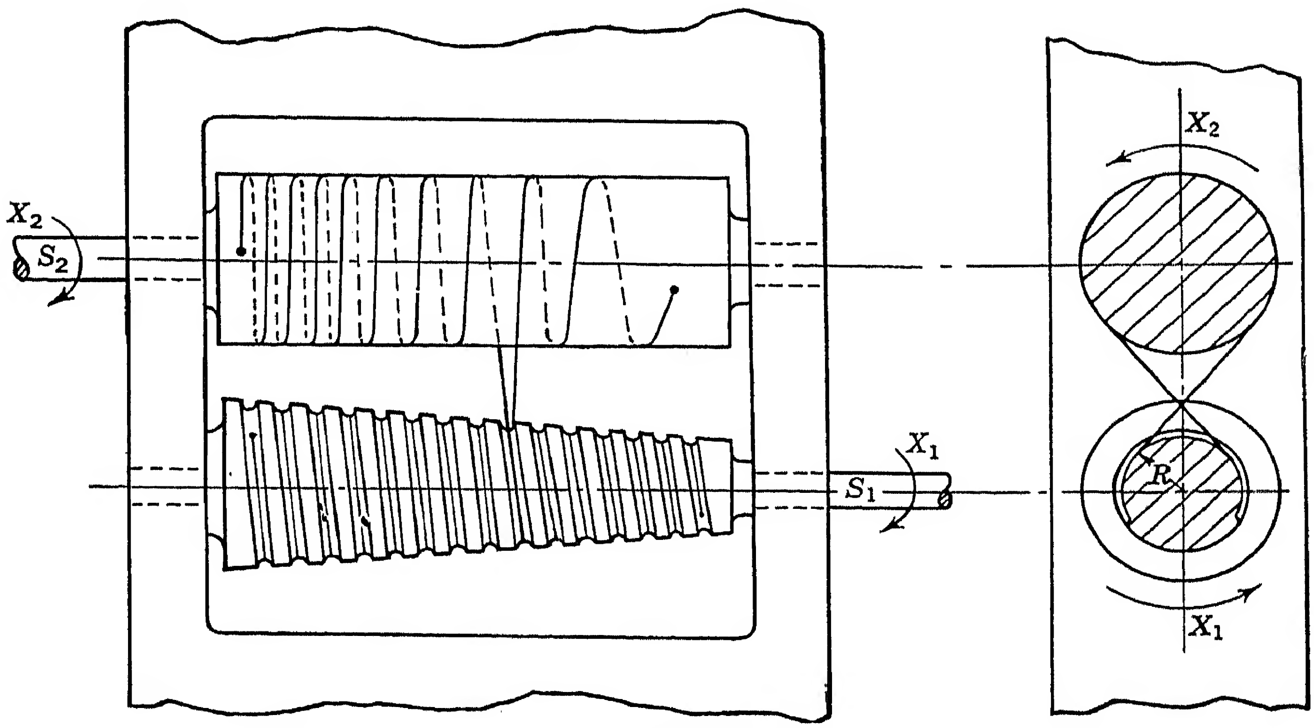

FIG. 1·23.—Compensated squaring cam.

This squaring cam does not by itself operate down to $X_1 = 0$. It can, however, be used in a range including zero if it is combined with a differential. With

$$X_1 = X_3 + C, \tag{20}$$

Eq. (19) becomes

$$X_2 = KX_3^2 + 2KCX_3 + KC^2. \tag{21}$$

Introducing the new parameter

$$X_4 = X_2 - 2KCX_1 + KC^2, \tag{22}$$

we have

$$X_4 = KX_3^2; \tag{23}$$

this holds even if X_3 is zero or negative. The larger the negative values of X_3 to be reached the larger must be the positive constant C. The

precision of a cam of this type can be made very high; the error may be less than 0.02 per cent of the total travel of the output shaft S_2. The relatively great inertia and bulk of the device (especially when it is combined with a differential for squaring negative numbers), limits its use to cases where precision is essential.

Three-dimensional cams or "camoids," such as that shown in Fig. 1·24, are bodies of general form with two degrees of freedom—for instance, a translation of X_1 and a rotation X_2—in contact with another body with one degree of freedom, for instance, a translation X_3. The parameter X_3 will then be a function of two independent parameters, X_1 and X_2:

$$X_3 = F(X_1, X_2). \tag{24}$$

The body in contact is called the "follower"; it may be a ball on a slide, as shown in the figure, or an arm rotating on a pin parallel to the main axis of the camoid and touching the surface of the cam. Camoids are valuable in that they can generate any well-behaved function of two independent variables. They are, however, expensive to build with enough precision, have considerable friction, and take too much space. Bar linkages are always to be preferred to camoids when it is possible to design such a linkage.

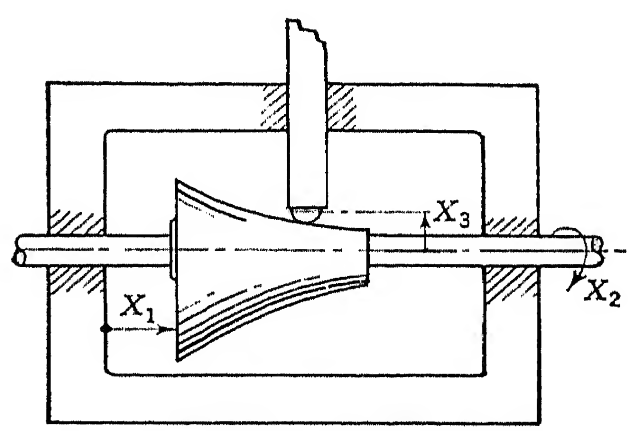

FIG. 1·24.—Three-dimensional cam.

1·8. Integrators.—Integrators are computers that have an output parameter, X_3, and two input parameters, X_1 and X_2, functionally related by

$$X_3 - X_{30} = \int_{X_{20}}^{X_2} F(X_1)dX_2. \tag{25}$$

The simplest form of integrator gives

$$X_3 - X_{30} = \int_{X_{20}}^{X_2} KX_1dX_2. \tag{26}$$

The parameters X_1, X_2, of an integrator can be varied at will; they can, for instance, be given functions of time t. The value of the integral, as a function of t, will depend on the form of these functions, and not merely on the instantaneous values of X_1 and X_2. Thus, unlike a function generator, an integrator does not establish a fixed relation between the instantaneous values of the parameters involved.

The equations of integrators are conveniently written in differential form; Eq. (26) becomes then

$$dX_3 = KX_1dX_2. \tag{27}$$

This is particularly convenient in schematic diagrams of complete computing systems.

A common type of integrator is the *friction-wheel integrator* shown in Fig. 1·25. The output parameter X_3 is generated by a friction wheel in contact with a plane disk, the rotation of which is described by the parameter X_2. Since the motion of the friction wheel depends on friction between the disk and the wheel, a normal force must act to maintain the

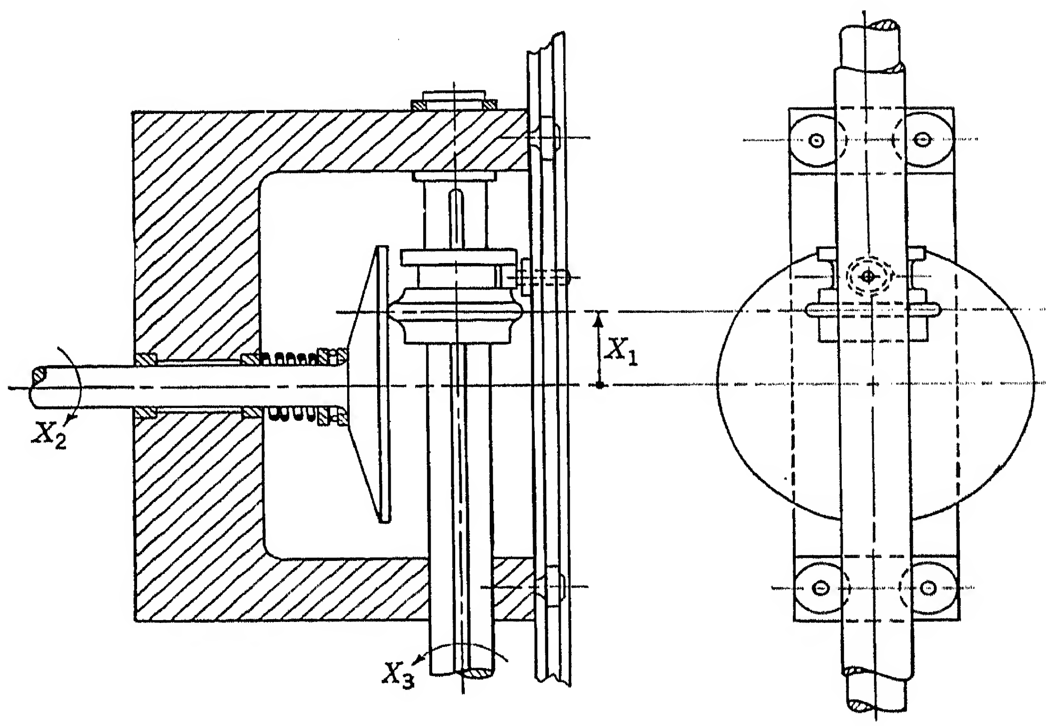

FIG. 1·25.—Friction-wheel integrator.

frictional force at an adequate level; for this reason the disk is pressed against the wheel by a spring. The friction wheel is transportable along its axis; the distance from the axis of the disk to the point of contact is the parameter X_1. In precision integrators the friction wheel is carried by a fixed shaft and the rotating disk is moved with respect to the frame by the amount X_1. The equation of the integrator in the figure is

$$dX_3 = \frac{1}{r} X_1dX_2, \tag{28}$$

where r is the radius of the friction wheel.

The *double-ball integrator* of Fig. 1·26 has the same equation as the friction-wheel integrator; the difference between these two designs is constructive only. The friction wheel is replaced by two balls carried in a small cylindrical container, as shown in the figure, or in a special con-

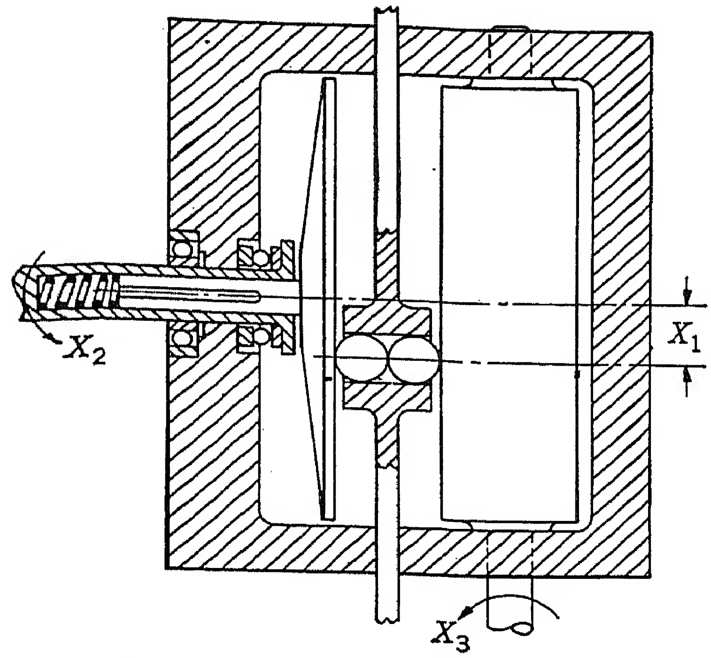

FIG. 1·26.—Double-ball integrator.

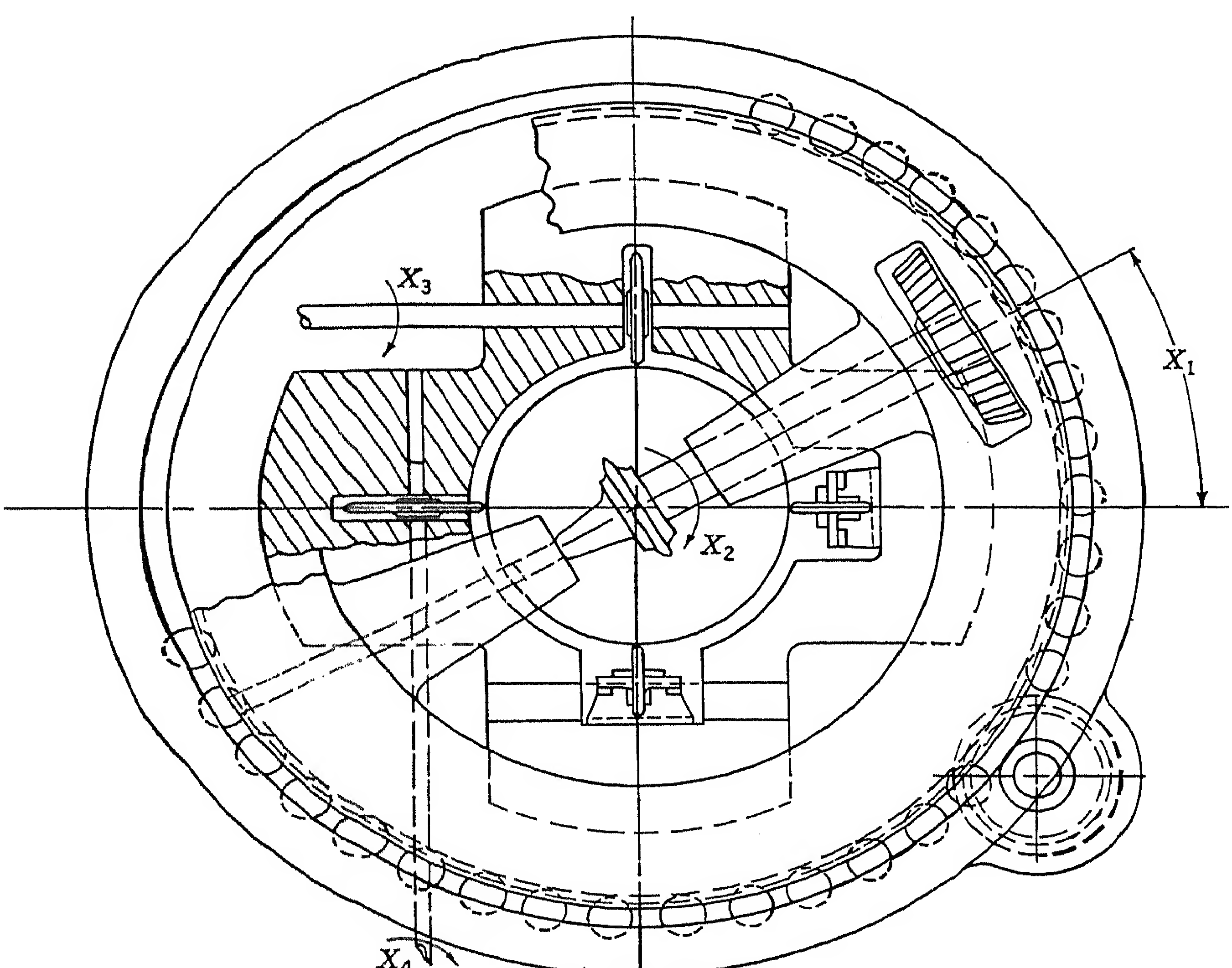

FIG. 1·27.—Plan view of component solver.

tainer with roller guides for the balls, to reduce friction. These balls transfer the motion of the disk (X_1dX_2) to a drum of radius r, which rotates through an angle dX_3 given by Eq. (28). The balls are easily transportable, rolling along the drum, with which they are in contact under constant pressure. This design is useful when one requires an efficient compact computer but does not need the maximum accuracy possible with mechanical integrators. The main source of error is the lack of absolutely sharp definition of the distance from the axis of the plate to the point of contact of the plate with the balls. Any lateral freedom of the lower ball impairs the precision of the results.

The *component solver* shown in Fig. 1·27 is a good example of an integrator of the more general type. A large ball of glass or steel is held between four rollers placed in a square, with axes in the same plane, and two rollers with axes parallel to that plane; the points of contact are at the corners of a regular octahedron. (Figure 1·27 shows only five of the six rollers.) The first four rollers have fixed axes, but the other two have axes that are always parallel, but may assume any direction in the horizontal plane. The rotation of these latter axes in the horizontal plane, measured from a certain zero position, is the input parameter X_1; the rotation of these rollers on their shafts is the second input parameter X_2; the rotation of any one of the four rollers on fixed axes may be taken as an output parameter. Since rollers on parallel axes rotate through equal angles, there are two different output parameters, X_3 and X_4. If all rollers have the same diameter, the equations of the component solver are

$$dX_3 = \cos X_1 dX_2, \tag{29a}$$
$$dX_4 = \sin X_1 dX_2. \tag{29b}$$

Thus the component solver is described by Eq. (25), but not by Eq. (26).

CHAPTER 2

BAR-LINKAGE COMPUTERS

2·1. Introduction.—A bar linkage is, in the classical sense of the word, a system of rigid bars pivoted to each other and to a fixed base. In this volume the term "bar linkage" will denote any mechanism consisting of rigid bodies moving in a plane and pivoted to each other, to a fixed base, or to slides. Consideration will be limited to essentially plane mechanisms because these are mechanically the easiest to construct. The inclusion in bar linkages of rigid bodies of arbitrary form is not an essential extension of the term, since any rigid body can be replaced by a corresponding system of rigid bars. Similarly, the admission of slides is not a real extension, since bar linkages—in the classical sense—can be designed to apply the same constraints.

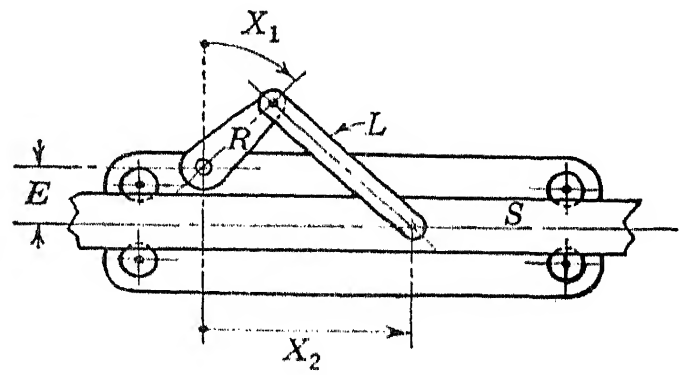

FIG. 2·1.—Bar linkage: a nonideal harmonic transformer.

A *link* in a bar linkage is a body connected to two other bodies by pivots. A *lever* is a body connected to three other bodies by pivots. A *crank* is a body pivoted to the fixed base, and to one or more other bodies of the linkage. Figure 2·1 shows a bar linkage that consists of a crank R, a link L, and a slide S.

Bar linkages are very satisfactory devices from a mechanical point of view. Pivots and slides are easily constructed and have small backlash, small friction, and good resistance to wear.

As computing mechanisms, bar linkages can perform all the functions of the elementary function generators discussed in Chap. 1. They cannot, however, be used to establish relations between differentials; they cannot perform the functions of integrators. As function generators it is characteristic of bar linkages that they do not, generally speaking, perform their intended operations with mathematical accuracy; on the other hand, they can generate in a simple and direct way, and with good approximation, functions that can be generated only by complicated combinations of the classical computing elements.

There are few standard bar-linkage function generators; one must usually design a bar linkage for any given purpose. Methods for designing such linkages from the mathematical point of view are the main sub-

ject of this book. The problem is to find a bar linkage that will generate a given function. It must be noted immediately that in general this can be accomplished exactly only by a linkage with an infinite number of elements; mechanisms with a finite number of elements cannot generate the complete field of functions. From a practical point of view, however, even the simpler bar linkages offer enough flexibility to permit solution of the design problem with an acceptably small error. The approach to the problem must be synthetic and approximative, not analytic and exact.

The mechanical design of bar linkages cannot be discussed in this volume. It is of course possible to treat analytically the properties of a given linkage: its motion, the distribution of velocities of its parts, accelerations, inertia, forces. In this respect the theory of linkages has been well developed, even in elementary texts; the kinematics of bar linkages have been treated especially thoroughly. It is of course necessary that the designer of linkages have knowledge of the practical properties of these devices, even when he is primarily interested in their mathematical design. In the present volume there will be some comment on the mechanical features of bar linkages, but only enough to give the designer the necessary base for reasoning when the design procedure is started.

2·2. Historical Notes.—Engineers and mathematicians have in the past considered bar linkages primarily as curve tracers—that is, as devices serving to constrain a point of the linkage to move along a given curve. The classical problem in the field has been that of finding a bar linkage that will constrain a point to move along a straight line. This problem was considered by Watt in designing his steam engine. Watt found a sufficiently accurate solution of the problem, and it was the cost and space required that caused the use of a slide in his original design. Bar linkages are now extensively used in mechanical design because of their small frictional losses and high efficiency in transmitting power—efficiency greater than that of any gear or cam. The usefulness of bar linkages to the mechanical engineer can be illustrated by a locomotive: its transmission contains the famous parallelogram linkage, and the valve motions are controlled by bar linkages of some complexity. A designer of linkage multipliers will

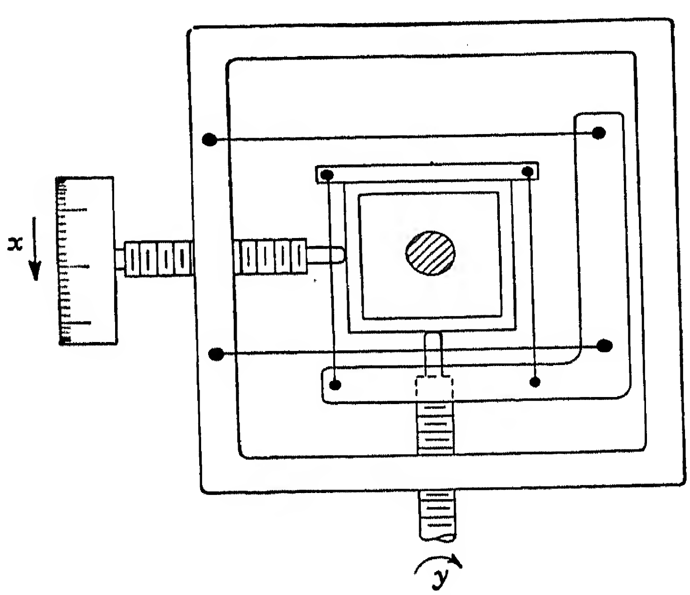

FIG. 2·2.—Bar linkages in a microscope plate holder.

recognize among these structures elements that he is accustomed to use in his own work.

Bar linkages are used in heavy construction as counterweight linkages and for the transmission of spring action. They also serve as elements of fine instruments. The parallelogram linkage used to assure pure translational motion of a slide being examined by a microscope is illustrated in Fig. 2·2. Springs are omitted from the diagram. The field of the microscope is indicated at the center of the plate.

The problem of producing an exact straight-line motion by a bar linkage was first solved by Peaucellier.[1] This was accomplished by application of the Peaucellier inversor to the conversion of the circular motion of a crank into a rectilinear motion. The Peaucellier inversor is illustrated in Fig. 2·3. It consists of a jointed quadrilateral with four sides of equal lengths B, to the opposite vertices of which there are jointed two other bars of equal lengths A; these latter bars are themselves joined at their other ends. Three joints of this structure necessarily lie on the same straight line, and the distances X_1 and X_2 between these joints vary inversely with each other. It will be noted that X_1 is the sum of the lengths of the bases of two right triangles of altitude T and hypotenuses A and B respectively, whereas X_2 is the difference of these base lengths. We have then

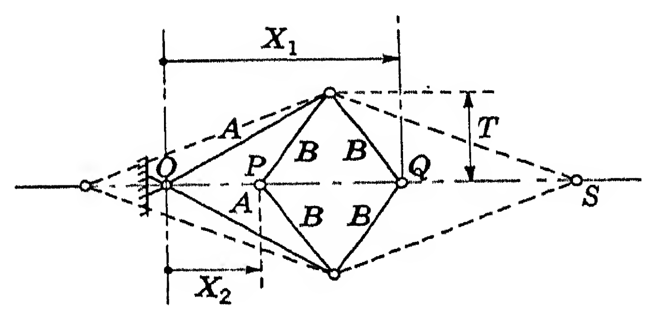

FIG. 2·3.—Six-bar Peaucellier inversor. The solid lines illustrate the case $B < A$, the dashed lines the case $B > A$.

$$X_1 = \sqrt{A^2 - T^2} + \sqrt{B^2 - T^2}, \tag{1a}$$
$$X_2 = \sqrt{A^2 - T^2} - \sqrt{B^2 - T^2}. \tag{1b}$$

In these equations A, B, T, and the square roots are necessarily positive. On multiplying together Eqs. (1a) and (1b) we obtain

$$X_1X_2 = A^2 - B^2, \tag{2a}$$

or

$$X_2 = \frac{A^2 - B^2}{X_1}. \tag{2b}$$

There are two variants of this inversor, with A greater than B or with B greater than A. If B is greater than A (dashed lines in Fig. 2·3), X_2 is always negative; there is no possibility of having X_1 equal X_2. If A is greater than B (solid lines in Fig. 2·3), it is possible to have

$$X_1 = X_2 = (A^2 - B^2)^{1/2}.$$

[1] A concise summary of work in this field, by R. L. Hippisley, will be found under *Linkages*, in the Encyclopedia Britannica, 14th ed.

At this point the mechanism exhibits an undesirable singularity; the joints P and Q of Fig. 2·3 become coincident, and self-locking of the device may occur. These two forms of the Peaucellier inversor also differ in their useful ranges. These are

$$\sqrt{A^2 - B^2} < X_1 < A + B, \qquad \text{if } A > B, \tag{3a}$$
$$B - A < X_1 < A + B, \qquad \text{if } A < B. \tag{3b}$$

The freedom from self-locking and the greater range make it desirable to have B greater than A. Figure 2·4 shows the Peaucellier inversor in a form suitable for use as a computer.

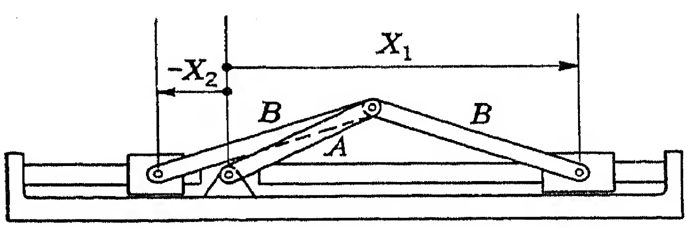

FIG. 2·4.—Three-bar Peaucellier inversor.

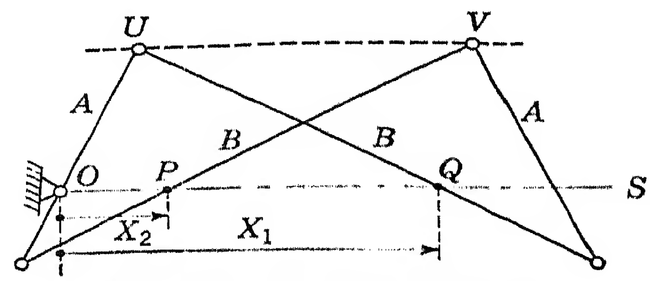

FIG. 2·5.—The Hart inversor.

Another inversor has been devised by Hart.[1]

The Hart inversor (Fig. 2·5) is essentially a bar-linkage parallelogram with one pair of bars reflected in a line through opposite vertices. Let any line OS be drawn parallel to a line UV through alternate vertices of the quadrilateral. It can be shown that this will intersect adjacent bars of the linkage at points O, P, Q, that remain collinear as the linkage is deformed; furthermore, the distances $X_1 = \overline{OQ}$ and $X_2 = \overline{OP}$ will vary inversely with each other.

There have been described linkages for the tracing of conic sections, the Cassinian oval, the lemniscate, the limaçon of Pascal, the cardioid, and the trisectrix; indeed it is theoretically possible to describe any plane curve of the nth degree in Cartesian coordinates x and y by a bar linkage.[2] Linkages for the solution of algebraic equations have also been devised.[3]

[1] H. Hart, "On Certain Conversions of Motion," *Messenger of Mathematics*, **4**, 82 (1875).

[2] A. Cayley, "On the Mechanical Description of a Cubic Curve," *Proc. Math. Soc., Lond.*, **4**, 175 (1872). G. H. Dawson, "The Mechanical Description of Equipotential Lines," *Proc. Math. Soc., Lond.*, **6**, 115 (1874). H. Hart, "On Certain Conversions of Motion," *Messenger of Mathematics*, **4**, 82 and 116 (1875); "On the Mechanical Description of the Limaçon and the Parallel Motion Deduced Therefrom," *Messenger of Mathematics*, **5**, 35 (1876); "On Some Cases of Parallel Motion," *Proc. Math. Soc., Lond.*, **8**, 286 (1876–1877). A. B. Kempe, "On a General Method of Describing Plane Curves of the nth Degree by Linkwork," *Proc. Math. Soc., Lond.*, **7**, 213 (1875); "On Some New Linkages," *Messenger of Mathematics*, **4**, 121 (1875). W. H. Laverty, "Extension of Peaucellier's Theorem," *Proc. Math. Soc., Lond.*, **6**, 84 (1874).

[3] A. G. Greenhill, "Mechanical Solution of a Cubic by a Quadrilateral Linkage," *Messenger of Mathematics*, **5**, 162 (1876). A. B. Kempe, "On the Solution of Equations by Mechanical Means," *Messenger of Mathematics*, **2**, 51 (1873).

Analytical studies[1] have been made of the "three-bar motion" of a point C rigidly attached to the central link AB of a three-bar linkage (Fig. 2·6). Three-bar motion is very useful in the design of complex computers, and will be discussed in Sec. 10·4.

To complete this survey of the bar-linkage literature in English, it will suffice to mention the papers of Emch and Hippisley on closed linkages.[2]

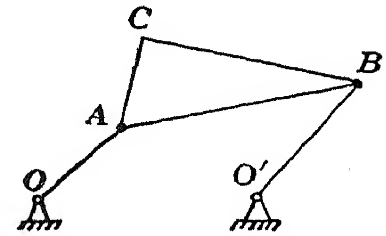

FIG. 2·6.—Three-bar linkage with point C rigidly attached to the central bar.

2·3. The Problem of Bar-linkage–computer Design.—It is only recently that much attention has been paid to the problem of using bar linkages in computing mechanisms. The literature in the field is especially restricted. The author knows of only one published work that employs the synthetic approach to bar-linkage computer design[3]—and this in a more restricted field than that of the present volume.

The basic ideas in the synthetic approach to bar-linkage design are simple, but quite different from the ideas behind the classical types of computers. Bar linkages can be characterized by a large number of dimensional constants, and the field of functions that they can generate is correspondingly large—though not indefinitely so. Given a well-behaved function of one independent variable, one should be able to select from the field of functions generated by bar linkages with one degree of freedom at least one function that differs from the given function by a relatively small amount. The characteristic problem of bar-linkage design is thus that of selecting from a family of curves too numerous and varied for effective cataloguing one that agrees with a given function within specified tolerances.

The presence of a residual error sets bar linkages apart from other computing mechanisms. The error of a computer of classical type arises from its construction as an actual physical mechanism, with unavoidable imperfections. It is possible to reduce the error to within almost any limits by sufficiently careful design—as, for instance, by enlarging the

[1] A. Cayley, "On Three-bar Motion," *Proc. Math. Soc., Lond.*, **7**, 136 (1875). R. L. Hippisley, "A New Method of Describing a Three-bar Curve," *Proc. Math. Soc., Lond.*, **15**, 136 (1918). W. W. Johnson, "On Three-bar Motion," *Messenger of Mathematics*, **5**, 50 (1876). S. Roberts, "On Three-bar Motion in Plane Space," *Proc. Math. Soc., Lond.*, **7**, 14 (1875).

[2] A. Emch, "Illustration of the Elliptic Integral of the First Kind by a Certain Link-work," *Annals of Mathematics*, Series **2**, **1**, 81 (1899–1900). R. L. Hippisley, "Closed Linkages," *Proc. Math. Soc., Lond.*, **11**, 29 (1912–1913); "Closed Linkages and Poristic Polygons," *Proc. Math. Soc., Lond.*, **13**, 199 (1914–1915).

[3] Z. Sh. Blokh and E. B. Karpin, "Practical Methods of Designing Flat Four-sided Mechanisms," Izdatelstvo Akademie nauk SSSR, Moscow, Leningrad (1943). E. B. Karpin, "Atlas of Nomograms," Izdatelstvo Akademie nauk SSSR, Moscow, Leningrad (1943).

whole computer. In bar linkages there is usually a residual error that cannot be eliminated by any care in construction, an error that is evident in the mathematical design of the device, as well as in the finished product. This error will be called "structural error" because it depends only on the structure of the computer, and not on its size or other mechanical properties. Reduction of structural error requires a change in the structure of the computer—usually the addition of parts. The great number of adjustable dimensional constants gives greater flexibility and extends the field of functions that the linkage can generate; from this larger field of functions one can then select a better approximation to the given function.

The fact that bar linkages can be used to generate functions of a large class has been known for many years, and has been used (instinctively, rather than with a full development of the theory) by designers of mechanisms. The field of functions that can be generated by some simple bar linkages has been analytically described. This, however, represents only the easier half of the problem; what one needs is to describe the field of functions that can *almost* be generated by a given type of linkage. The first attempts to solve this problem for one independent variable have been tabular or graphical. For very simple structures it is possible to devise graphs that allow one to determine whether a given function can be generated approximately by such a structure, and what structural error is inevitable. These methods are practicable if the linkage can be specified by means of only two dimensional parameters—that is, if the field of functions depends upon only two adjustable parameters. Such graphical methods are difficult or are necessarily incomplete if the field of functions depends upon three adjustable parameters. Such a procedure can hardly be attempted when four or more dimensional parameters are involved.

The design methods presented in this book are in many cases based on a graphical factorization of the given function into functions suitable for mechanization by simple linkages; the elements of the mechanism designed in this way can then be assembled into the desired complete linkage. By such methods it is possible to design linkages having a great many adjustable parameters, but the solution obtained cannot be claimed to be the best possible. Usually it is easy to apply these methods to find bar linkages that have errors everywhere within reasonable tolerances. This is ordinarily sufficient for practical purposes.

2·4. Characteristics of Bar-linkage Computers.—The special properties of bar-linkage computers may be summarized as follows.

Advantages.

1. Bar linkages occupy less space than classical types of computers.
2. They have negligible friction.

3. They have small inertia.
4. They have great stability in performance.
5. Their complexity does not necessarily increase with the complexity of the analytical formulation of the problem.
6. They are easy to combine into complex systems.
7. They are relatively cheap.

Disadvantages.

1. Bar linkages usually possess a structural error.
2. The field of mechanizable functions is somewhat restricted.
3. The complexity of the linkage increases with decreasing tolerances.
4. Linkage computers are relatively difficult to design. The difficulty of the design procedure increases with increasing complexity and decreasing tolerances.
5. The travel of the mechanism is usually limited to a few inches. Backlash error and elasticity error must be reduced by careful construction: the use of ball bearings is essential, and rigidity of the structure perpendicular to the plane of motion must be assured. The design should be such that mechanical errors are less than the assigned tolerances for structural error.

Bar linkages can attain extensive use as elements of computers only as efficient methods of design are established. The complexity and difficulty of the design procedure depends largely on the nature of the given function. It is usually easy to design a linkage with a structural error that does not exceed 0.3 per cent of the whole range of motion of the computer. It becomes relatively laborious to reduce the structural error below 0.1 per cent. If the tolerances are below 0.1 per cent—as a typical value—alternatives to the use of a bar linkage should be explored.

Bar linkages can advantageously be combined with cams when the tolerated error is small and a bar linkage alone would be excessively complex. For instance, if a given function of one independent variable were to be mechanized with an error of not more than 0.01 per cent, it might be desirable to mechanize this function by a simple bar linkage with an error of, for example, 1 per cent, and to use a cam to introduce the required correction term. Since this corrective term represents only 1 per cent of the whole motion of the linkage, it need not be generated with very high precision; for instance, if the working displacement of the cam is to be 1 in., it can be fabricated with a tolerance as rough as 0.01 in.

It is a feature of bar-linkage computers that they can be used to generate functions of two independent variables in a very direct and mechanically simple way. Methods for the design of linkages generating functions of three independent variables are not now available when it is

not possible to reduce the problem to the mechanization of functions of one or two independent variables; there is, however, some hope that practically useful methods can be found.

Bar-linkage computers have great advantages when feedback is to be used in the design of complex computers. In computers of the classical type, feedback motion must be a small fraction of the total output motion. Linkage computers can, however, operate very close to the critical feedback—that is, the degree of feedback at which the position of the mechanism becomes indeterminate.

2·5. Bar Linkages with One Degree of Freedom.—Bar linkages with one degree of freedom serve the same purpose as cams; they may be called "linkage cams." The parallelogram linkage of Fig. 2·2 and the linkage inversors have motions expressed accurately by very simple formulas, but they are not generally useful in the mechanization of given functions. For this purpose, the following bar linkages are much more interesting.

The *harmonic transformer*, shown in Fig. 2·1, establishes a relation between an angular parameter X_1 and a translational parameter X_2. It is convenient to disregard variations in the form of this relation due to changes in scale of the mechanism—to consider as equivalent two geometrically similar mechanisms. The field of functions

$$X_2 = F(X_1) \tag{4}$$

generated by the harmonic transformer then depends upon two ratios of dimensions: L/R and E/R, the ratios to the crank length of the link length and the displacement of the crank pivot from the center line of the slide. As L is increased from its minimum value, the plot of X_2 against X_1 changes (in a typical case) from an isolated point to a closed curve, then to a sinusoid, and finally, in the limit as L approaches infinity, to a pure sinusoid. From a practical point of view, the pure sinusoidal form is reached for links short enough for practical use. In the limiting case, $L = \infty$, the equation of the harmonic transformer is

$$X_2 = R \sin X_1 + C. \tag{5}$$

Such a harmonic transformer will be called "ideal."

Only rarely is the complete range of motion of a harmonic transformer used. When the range of the parameter X_1 is limited to $X_{1m} < X_1 < X_{1M}$ and the functions defined within these restricted limits are taken as elements of a new functional field, there is obtained a four-dimensional functional field depending on X_{1m} and X_{1M} as well as on L/R and E/R. Methods for the design of harmonic transformers will be discussed in Chap. 4.

The *three-bar linkage* shown in Fig. 2·7 consists of two cranks pivoted to a frame and joined at their free ends by a connecting link. As a computer, this serves to "compute" the parameter X_2 as a function of the parameter X_1. The linkage itself is described by four lengths: A_1, B_1, A_2, B_2. The field of functions generated by this type of linkage is only three-dimensional, because two geometrically similar mechanisms estab-

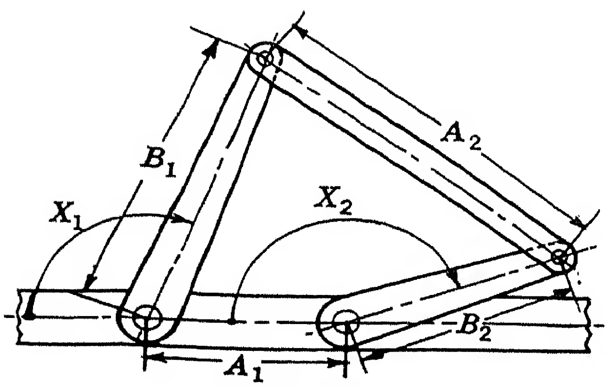

FIG. 2·7.—Three-bar linkage.

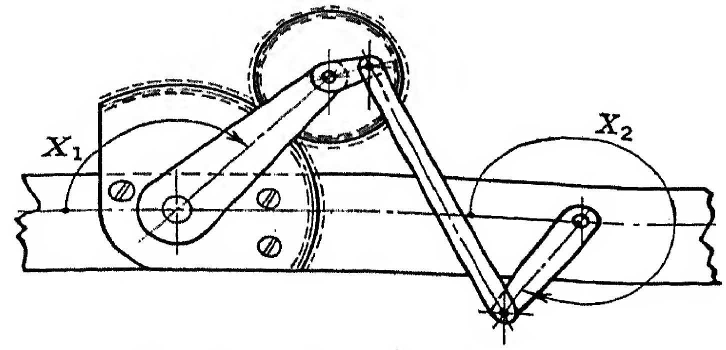

FIG. 2·8.—Three-bar linkage modified by eccentric linkage.

lish the same relation between X_1 and X_2. The field of functions thus depends on three ratios—for example, B_1/A_1, A_2/A_1, and B_2/A_1. Usually only a part of the possible motion of the mechanism is used. Limits of motion can be assigned for X_1 or X_2, though, of course, not independently for the two parameters; for instance, one may fix $X_{1m} < X_1 < X_{1M}$. This increases the number of independent parameters by two; the field of functions generated by a three-bar linkage operating within fixed limits

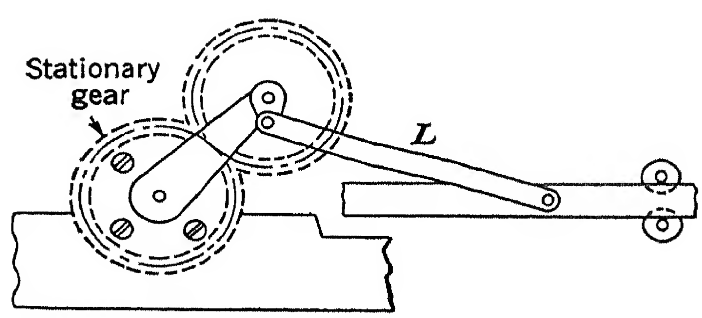

FIG. 2·9.—Harmonic transformer modified by eccentric linkage.

is five-dimensional. In Chap. 5 we shall see how to design a three-bar linkage for the approximate generation of a given function.

The *eccentric linkage* is not a bar linkage, but is so conveniently used in connection with bar linkages that it should be mentioned here. Figure 2·8 shows a three-bar linkage modified by the insertion of an eccentric linkage. One crank of the three-bar linkage carries a planetary gear that meshes with a gear fixed to the frame. The central link is then pivoted eccentrically to the planetary gear, rather than to the crank itself. Linkages of this type will be discussed in Sec. 7·9, where their importance will

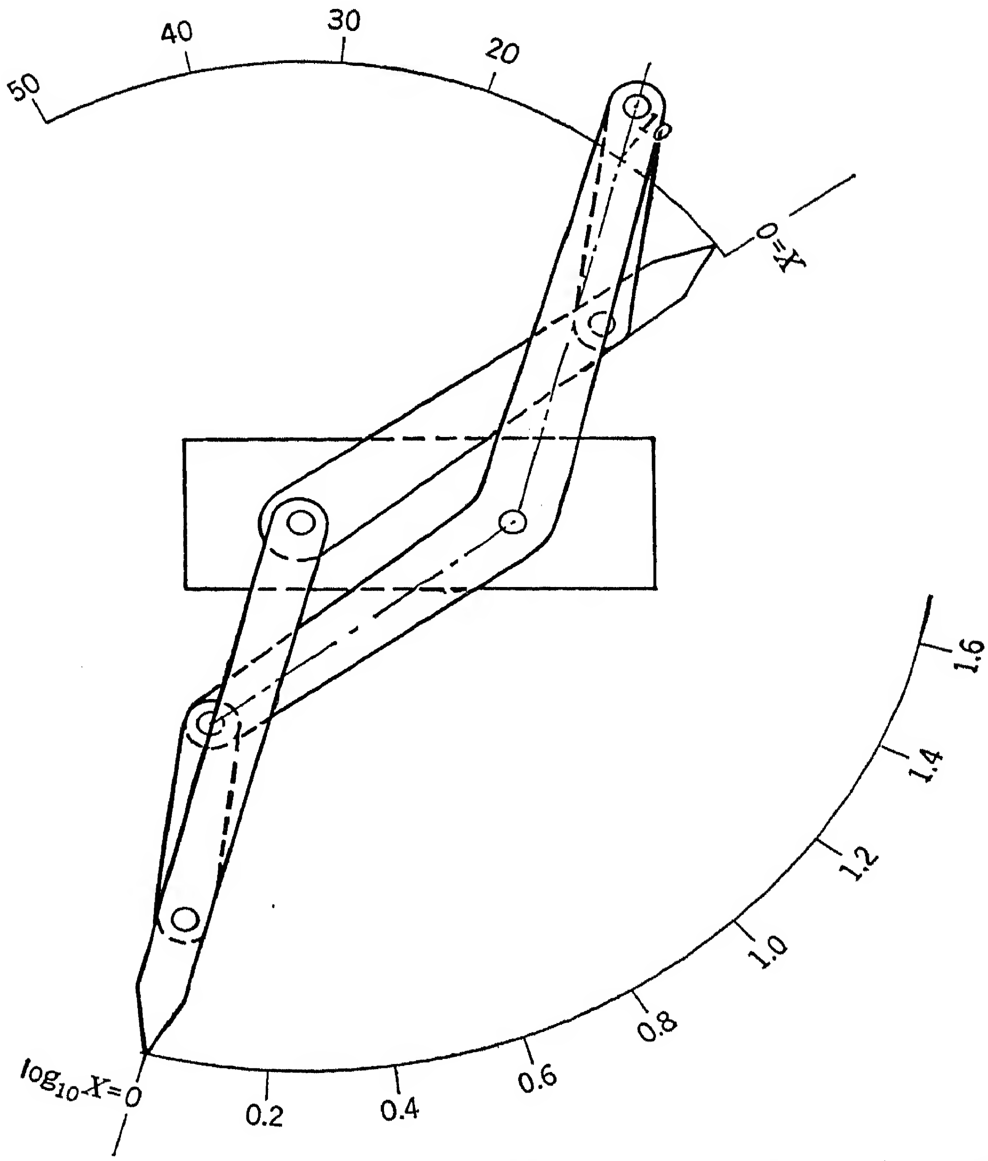

FIG. 2·10.—Double three-bar linkage generating the logarithmic function.

be explained. Another important application of the eccentric linkage is in the modification of harmonic transformers, as illustrated in Fig. 2·9. It is possible to choose the constants of the eccentric linkage in such a way that the linkage output is an almost perfect s i n u s o i d, even though the length of the link L is relatively small.

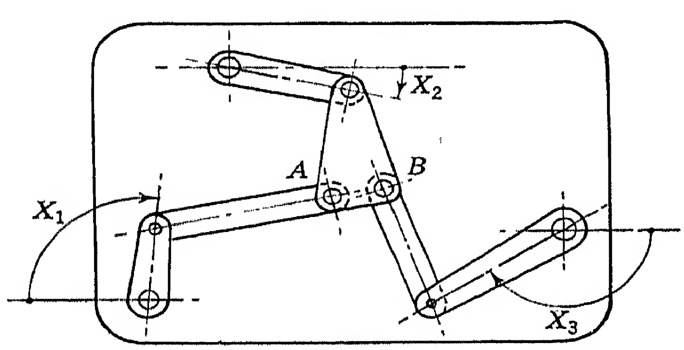

FIG. 2·11.—Bar linkage with two degrees of freedom.

Combinations of these linkages to be discussed in this book are the double harmonic transformer (Sec. 4·9 and following), harmonic transformers in series with three-bar linkages (Sec. 8·1 and following), and the double three-bar linkage (Sec. 8·8). Figure 2·10 shows a double three-bar linkage that generates the logarithmic function through the range indicated in the figure.

2·6. Bar Linkages with Two Degrees of Freedom.—Bar linkages with two degrees of freedom can be used in the generation of almost any well-behaved function

$$X_3 = F(X_1, X_2) \tag{6}$$

of two independent variables. They provide a mechanically satisfactory substitute for three-dimensional cams, which have many disadvantages and are to be avoided if possible. Figure 2·11 shows a linkage with two degrees of freedom, which consists of three cranks connected by two links and a lever. The lever will degenerate into a simple link if the pivots A and B are superposed; the resulting structure of three links jointed at a single pivot will be called a "star linkage." Its properties are discussed in Chap. 9.

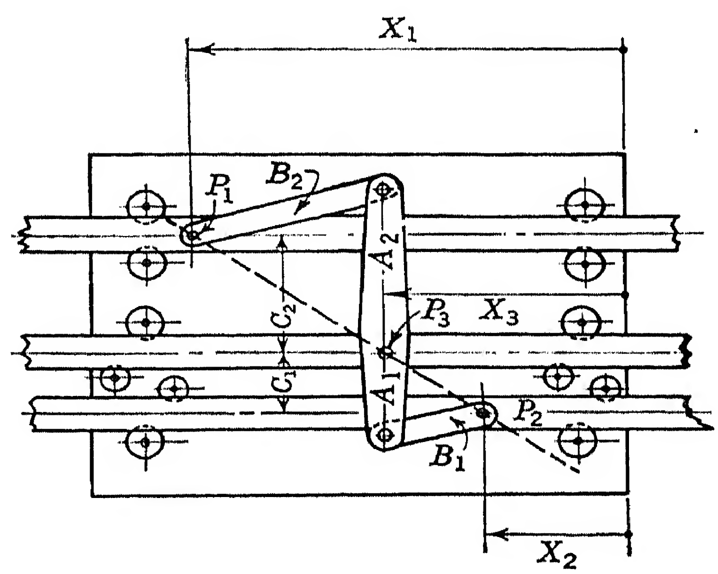

FIG. 2·12.—Bar-linkage adder.

The *bar-linkage adder* shown in Fig. 2·12 consists of essentially the same parts as the linkage of Fig. 2·11, except that slides are used instead of cranks to constrain the links. The dimensions obey the simple relation

$$\frac{A_1}{A_2} = \frac{B_1}{B_2} = \frac{C_1}{C_2}. \tag{7}$$

It is easy to show that when this proportionality holds, the three pivots P_1, P_2, and P_3 lie on a straight line. This device can, therefore, be used to mechanize any alignment nomogram that consists of three parallel straight lines; in particular, it can be used to mechanize the well-known nomogram for addition. If X_1, X_2, and X_3 are three parameters measured along these lines in the same direction from a common zero line, then

$$(A_1 + A_2)X_3 = A_1X_1 + A_2X_2. \tag{8}$$

This bar linkage is free from structural error.

In contrast to the adders, *bar-linkage multipliers* do not perform the operation of multiplication exactly, but with a small error; the equation of such a multiplier is

$$RX_3 = X_1X_2 + \delta, \tag{9}$$

where δ, the error of the multiplier, is a function of the two independent parameters X_1 and X_2. The design of multipliers will be discussed in Chap. 9; a much simplified explanation of the principle will be given here.

Figure 2·13 shows the essential elements of one type of multiplier. Three bars of equal lengths, $R_1 = R_2 = R_3 = 1$, are pivoted together. The first is pivoted also to the frame at the point O, the third to a slide with center line passing through O. If the joints A_1 and A_2 are placed at distances X_1 and X_2 from the center line of the slide, the distance $OS = D$ will be exactly

$$D = \sqrt{1 - X_1^2} - \sqrt{1 - (X_2 - X_1)^2} + \sqrt{1 - X_2^2}. \tag{10}$$

Expanding in series the terms on the right, one obtains

$$X_3 = 1 - D = X_1X_2 + \tfrac{1}{2}X_1X_2^3 - \tfrac{3}{4}X_1^2X_2^2 + \tfrac{1}{2}X_1^3X_2 + \cdots, \tag{11}$$

where X_3 is the displacement of the pivot S from the position S_0 which it occupies when $X_1 = X_2 = 0$ and the three links are coincident. It is evident that X_3 is equal to the product X_1X_2 to the approximation in which the terms of fourth and higher degrees can be neglected in comparison with the term of the second degree. For sufficiently small values of X_1 and X_2 this mechanism is thus a multiplier for these parameters.

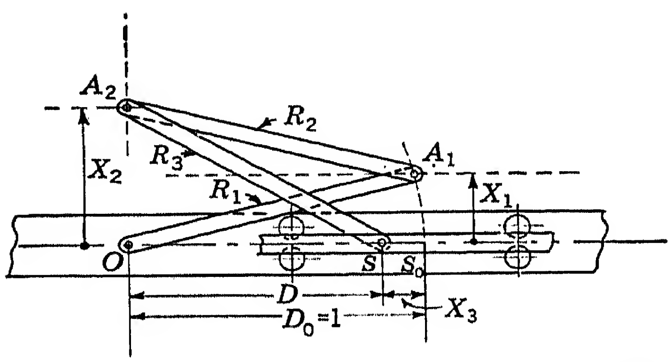

FIG. 2·13.—Elements of a bar-linkage multiplier.

Such a multiplier is not practical, however, because of its small range of motion. If the error in the multiplication is to be kept below 1 per cent, it is necessary to keep $X_1, X_2 \leqq 0.2$. [If $X_1 = X_2 = 0.2$, then

$$X_3 = (0.2)^2 + \tfrac{1}{4}(0.2)^4 + \cdots,$$

and the fractional error is almost exactly one per cent.] Under these conditions, however, one has $X_3 = 0.04$, an impracticably small range of motion.

There are in principle two ways to improve this multiplier. With either method it is necessary to make the structure more complicated—to add new adjustable parameters. One possible arrangement is indicated in Fig. 2·14. Here the parameter X_2 is a displacement of a slide (of adjustable position) that controls the position of the joint A_2 through a link of adjustable length L_2; X_3 becomes an angular parameter, the angle turned by a crank with adjustable length and pivot position.

With the first method, the output parameter X_3 is expressed in terms of X_1 and X_2, in the form of a series with coefficients which depend on the adjustable dimensions of the mechanism. These dimensions can then be so chosen as to cause the terms of the fourth degree in X_1 and X_2

to vanish. In this way, the multiplier can be made more accurate for small values of X_1 and X_2, and the domain of useful accuracy substantially increased. Toward the limits of this domain, however, the inaccuracy of the multiplier will increase very rapidly.

The second method for improving the multiplier—that followed in this book—can be indicated only very roughly at this point. It involves comparison of the ideal product and the function actually generated by the multiplier over the entire range of motion, and adjustment of the dimensional constants of the system in such a way that the error of the mechanism is brought within specified tolerances everywhere within this domain. To see in principle how this can be done, let us consider the mechanism of Fig. 2·13. Let X_3 and X_1 be given a series of values that have the fixed ratio

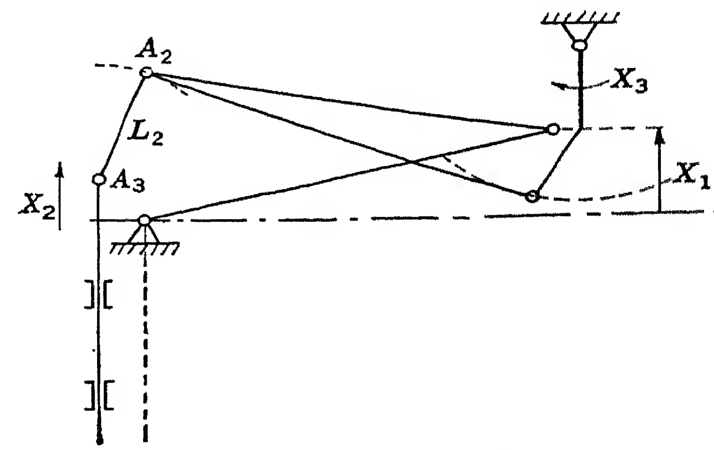

FIG. 2·14.—Modified bar-linkage multiplier.

$$\frac{X_3}{X_1} = X_2'. \tag{12}$$

If this linkage were an exact multiplier, the pivot A_2 would indicate always the same value of X_2; it would move along a straight line at constant distance X_2' from the line of the slide. Actually, the pivot A_2 will describe a curve that is tangent to this straight line for small values of X_1 and X_3, but will diverge from it as these parameters increase. To each value of X_2 there will correspond another curve; the curves of constant X_2 form a family, each of which can be labeled with the associated value of this parameter. Now we can make this multiplier exact if we can introduce a constraint which, for any specified value of X_2, will hold the pivot A_2 on the corresponding curve of this family. For example, if these curves were all circles with the same radius L_2 and centers lying on a straight line, it would be possible to use the type of constraint illustrated in Fig. 2·14. The X_2-slide could then be used to bring the pivot A_3 to the center of the circle corresponding to an assigned value of X_2, and the pivot A_2 would stay on that circle, as required. Actually, the curves of constant X_2 will not form such a family of identical circles. It will, however, be possible to approximate them by such circles in a way which will split the error and bring it within tolerances held fairly uniformly over the whole domain of action. Unlike the multipliers designed by the first method, a multiplier thus designed will not have unnecessarily small errors in one part of the domain and excessively large errors in another part.

This concept of multiplier design must be very greatly extended before it can lead to the design of satisfactory computers. A powerful guide in beginning the work is provided by the idea of nomographic multipliers, already discussed in Sec. 1·5. It is possible to design *approximate* intersection nomograms for multiplication that have as their mechanical analogues bar linkages with two degrees of freedom. For instance, Fig. 8·14 shows a nomogram for multiplication obtained by topological transformation of the nomogram of Fig. 1·12; it consists of two families of identical circles and a third family of curves that can be very closely approximated by a family of identical circles. This nomogram corresponds to the bar-linkage multiplier illustrated in Fig. 8·15, which, on improvement of its mechanical features, takes on the form shown in Fig. 8·16. The design techniques to be described in Chaps. 8 and 9 make it possible to design multipliers with large domain of action and good uniformity of performance through this domain.

Multipliers can be used to perform the inverse operation of division; that is, they can be used to evaluate $X_2 = X_3/X_1$. It is, of course, not possible to divide by zero; when a multiplier is used in this way X_1 will never pass through zero. It is therefore useless to attempt to reduce to zero the error of such a multiplier for values of X_1 very near to zero; it is also undesirable to attempt to reduce the errors of the device for negative values of X_1 when only positive values can be introduced. For this reason three types of multiplier may be distinguished.

1. Full-range multipliers, for which both input parameters can change signs.
2. Half-range multipliers, for which only one parameter can change signs.
3. Quarter-range multipliers, for which neither input parameter can change signs.

Dividers may be divided into two types.

1. The plus-minus type, for which the numerator may change sign.
2. The single-sign type, for which all parameters have fixed signs.

An example of a practical full-range linkage multiplier is shown in Fig. 8·16; a half-range multiplier is shown in Fig. 9·15.

2·7. Complex Bar-linkage Computers.—The elementary linkage cells already described may be combined to form complex computers. Since simple linkages can add, multiply, and generate functions of one and two independent variables, bar-linkage computers can solve any problem that can be expressed in a system of equations involving only these operations. The field of application of bar-linkage computers is quite large; they

are especially useful if the computer must be light, as when it is to be carried in aircraft or guided missiles.

An important feature of bar-linkage computers is the ease with which the cells can be assembled into a compact unit. It is natural to spread the parts of the computer out in a plane, to produce a rather flat mechanism with its parts easily accessible. The connections between cells are provided by shafts or connecting bars.

There is a simple trick that makes the connection of linkage cells even easier, and the structure of some cells less complex. The simplification of linkage adders is a characteristic example of this trick. The bar-linkage adder shown in Fig. 2·12 has no structural error. Any deviation from the principle of this design is likely to lead to a structural error; it is, however, possible to change the principle in such a way that the structural error is negligibly small. For instance, if the links B_1 and B_2 are very long, their lengths can be chosen at will without appreciably affecting the accuracy of the addition. Figure 2·15 shows such an approximate adder; its equation is

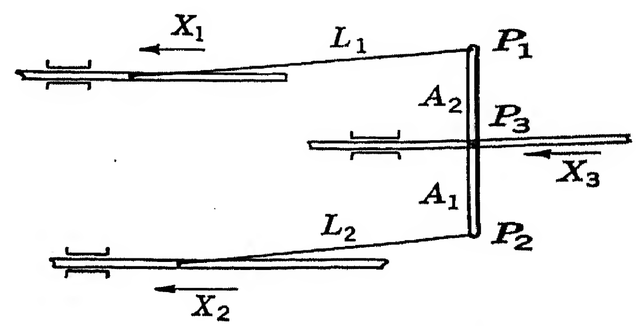

FIG. 2·15.—Bar-linkage adder (approximate).

$$(A_1 + A_2)X_3 \approx A_1X_1 + A_2X_2. \tag{13}$$

The links L_1 and L_2 must be so long that they lie nearly parallel to the lines of the slide, but they need not be exactly parallel to each other. The action of this device depends upon the essential constancy of the projection of the lengths of these bars along the line of the slides. Let X_1', X_2', and X_3' be defined as the distances of the pivots P_1, P_2, and P_3 from some zero line perpendicular to the line of the slides. One then has, exactly,

$$(A_1 + A_2)X_3' = A_1X_1' + A_2X_2'. \tag{14}$$

Now let θ_1 be the angle between the bar L_1 and the line of the slides. Then

$$X_1 = X_1' + L_1 \cos \theta_1 + C, \tag{15a}$$
$$= X_1' - L_1(1 - \cos \theta_1) + (C + L_1). \tag{15b}$$

Except for an additive constant (which can be reduced to zero by proper choice of the zero point), X_1' and X_1 differ only by the variable term $L_1(1 - \cos \theta_1)$. As L_1 is increased, θ_1 decreases with $1/L_1$, $(1 - \cos \theta_1)$ decreases with $1/L_1^2$, and $L_1(1 - \cos \theta_1)$ decreases with $1/L_1$. Thus, by making L_1 large and properly choosing the zero point, one can make X_1 and X_1' differ by a negligibly small term. In the same way X_2 can be made negligibly different from X_2'; X_3 and X_3' are identical. Equation

(13) follows as an approximation to Eq. (14). If θ_1 is kept less that 0.035 radians (about 2°) the difference between X_1 and X_1' will be about $0.0006\,L_1$. Thus if the bars deviate from parallelism with the slides by no more than $\pm 2°$ during operation of the adder, the resulting error in the output will not exceed 0.06 per cent of the total length of the bars.

If the lengths of the bars in approximate adders are great enough, it is even immaterial whether the slides move along straight lines; the essential

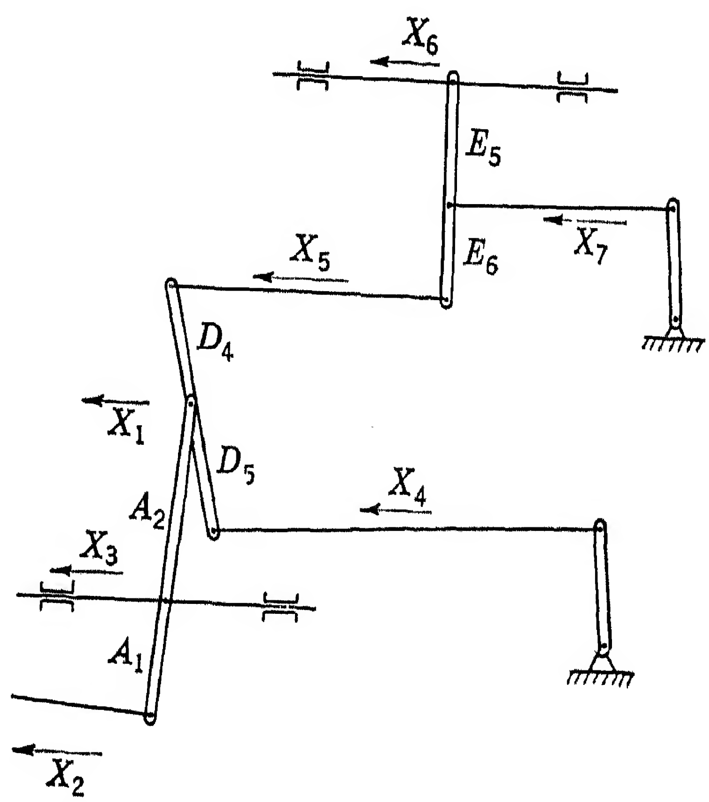

FIG. 2·16.—Combination of approximate adders.

thing is that the parameters be measured as distances from a zero line. It is, therefore, possible to connect adding cells through long connecting bars, and to omit some of the slides that would appear in the standard construction. Fig. 2·16 shows a combination of three adding cells that will solve (approximately) the equations

$$\left.\begin{aligned}(A_1 + A_2)X_3 &= A_1X_1 + A_2X_2,\\ (D_4 + D_5)X_1 &= D_4X_4 + D_5X_5,\\ (E_5 + E_6)X_7 &= E_5X_5 + E_6X_6.\end{aligned}\right\} \tag{16}$$

CHAPTER 3

BASIC CONCEPTS AND TERMINOLOGY

The present chapter will define the terminology to be employed in discussing bar-linkage design and introduce some concepts with wide application in the field. Of particular importance are the concepts of "homogeneous parameters" and "homogeneous variables," and a graphical calculus used in discussing the action of computing mechanisms in series.

3·1. Definitions. *Ideal Functional Mechanism.*—Any mechanism can be used as a computer if it establishes definite geometrical relations between its parts—that is, if it is sufficiently rigid and free from backlash,

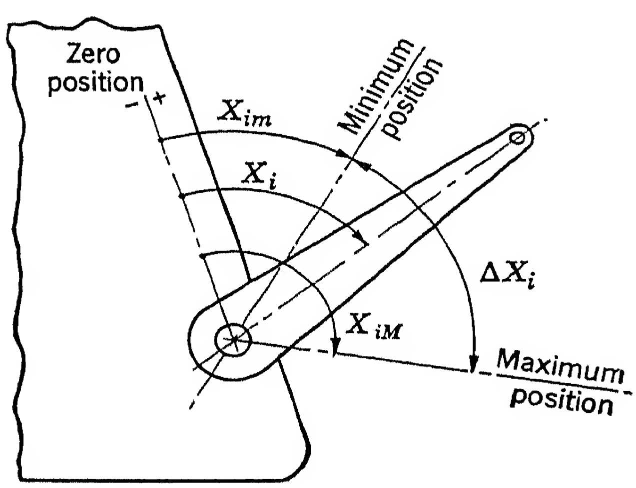

FIG. 3·1.—Crank terminal.

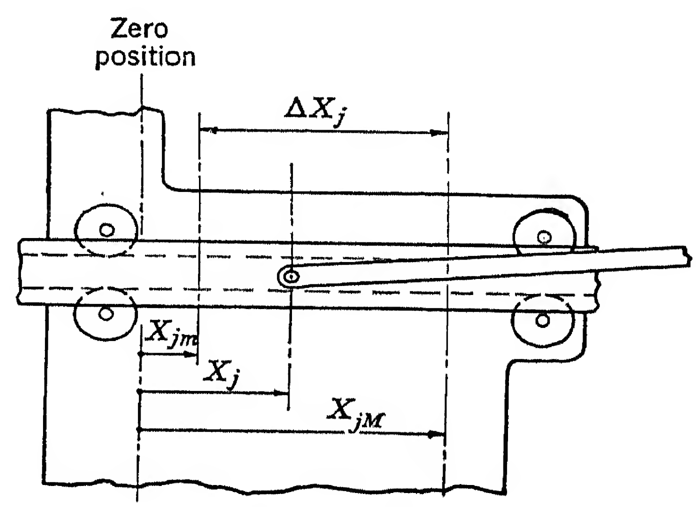

FIG. 3·2.—Slide terminal.

slippage, or mechanical play. In the following discussion we shall be concerned only with such *ideal functional mechanisms.*

Terminals.—The *terminals* of a computing mechanism are those elements that, by their motions, represent the variables involved in the computation. The motion of all terminals is usually specified with respect to some common frame of reference. If the position of a terminal is controlled in order to fix the configuration of the mechanism, it may be called an "input terminal"; if its position is used in controlling a second mechanism, or is simply observed, it may be called an "output terminal." A terminal may be suitable for use only as an input terminal, or only as an output terminal, or in either way, according to the nature of the mechanism.

Terminals that are mechanically practical are of two kinds:

1. Crank or rotating-shaft terminals (Fig. 3·1), which represent a variable by their angular motion.
2. Slide terminals (Fig. 3·2), which represent a variable by a linear motion.

Parameters.—A parameter is a geometrical quantity that specifies the position of a terminal. With a crank terminal, it is usually the angular position of the terminal with respect to some specified zero position; with a slide terminal, it is usually the distance of the slide from a zero position. Parameters may be defined in other ways— for instance, as the distance of a slide terminal from some movable element of the mechanism—but such parameters are less generally useful than those just mentioned.

An *input parameter* describes the position of an input terminal, an *output parameter* that of an output terminal.

Linkage Computers.—A linkage computer establishes between its parameters, $X_1, X_2, \ldots X_s$, definite relations of the form

$$F_r(X_1, X_2, \cdots X_s) = 0, \qquad r = 1, 2, \cdots, \tag{1}$$

which involve only these parameters and the dimensional constants of the mechanism. With more general types of mechanisms these equations of motion may also involve derivatives of the parameters. Such mechanisms are useful in the solution of differential equations, but they will be excluded from our future considerations; we shall be concerned only with linkage computers, which generate fixed functional relations between the parameters.

To describe the configuration of linkage computers with n degrees of freedom, one must in general specify the values of n input parameters, $X_1, X_2, \ldots X_n$. The values of any number of output parameters can then be expressed explicitly in terms of these n parameters:

$$X_{n+r} = G_r\,(X_1, X_2, \cdots X_n), \qquad r = 1, 2, \cdots m. \tag{2}$$

Domain.—The parameters of a computing mechanism cannot, in general, assume all values. The limitations may arise from the geometrical nature of the mechanism (a linear dimension will never change without limit) or from the way in which it is employed. To each possible set of values of the input parameters $X_1, \ldots X_n$, there corresponds a point $(X_1, X_2, \ldots X_n)$ in n-dimensional space; to all sets of values that may arise during a specific application of the mechanism, there corresponds a domain in n-dimensional space, which will be referred to as the "domain" of the parameters. It must be emphasized that the domain of the parameters is not necessarily determined by the structure of the mechanism, but by the task set for it.

In the most general case, the domain of the input parameters may be of arbitrary form—except, of course, that it must be simply connected, since all parameters must change continuously. In such cases the values possible for any one parameter may depend on the values assigned to other parameters. A mechanism will be said to be a "regular mechanism" when each input parameter can vary independently of all others, between definite upper and lower limits,

$$X_{im} \leqq X_i \leqq X_{iM}, \qquad i = 1, 2, \cdots n, \tag{3}$$

which define the domain of the parameter. With angular parameters, neither of these limits is necessarily finite: it is possible to have $X_{im} = -\infty$, or $X_{iM} = +\infty$.

The output parameters of a regular mechanism will vary between definite (though not necessarily finite) limits as the input parameters take on all possible values. These limits serve to define a domain for each output parameter. Although the input parameters vary independently through their respective domains, this is not always true of the output parameters.

Travel.—The range of motion of a terminal is called its "travel." This is

$$\Delta X_i = X_{iM} - X_{im}, \tag{4}$$

both for input and output terminals.

Variables.—The term "variable" will denote the variables of the problem which the computing mechanism is designed to solve. A variable will be associated with each terminal of a mechanism, an *input variable* with an input terminal, an *output variable* with an output terminal. To each value of a variable there will correspond a definite configuration of the terminal; each variable, then, will be functionally related to a parameter of the mechanism:

$$x_i = \phi_i(X_i). \qquad i = 1, 2, \cdots. \tag{5}$$

It is important to keep in mind the distinction between parameters, which are geometrical quantities measured in standard units, and the variables of the problem, which are only functionally related to the parameters. In this book, variables will be denoted by lower-case letters, parameters by capitals.

Scales.—The value of the variable corresponding to a given configuration of a terminal can be read from a scale associated with that terminal. The calibration of this scale is determined by the form of the functional relation between x_i and X_i. If x_i is a linear function of X_i the scale will be *even*—that is, evenly spaced calibrations will correspond to evenly spaced values of x_i. Such a scale may also be referred to as "linear,"

in reference to the form of the functional relation represented. (This term does not describe the geometrical form of the scale, which may be circular.) A *linear terminal* is a terminal with which there is associated a linear scale.

Range of a Variable.—As a parameter changes between its limits, X_{im} and X_{iM}, the associated variable will also change within fixed, but not necessarily finite, limits:

$$x_{im} \leqq x_i \leqq x_{iM}. \tag{6}$$

In the case of a regular mechanism, this may be referred to as the "domain" of the variable; its *range* is

$$\Delta x_i = x_{iM} - x_{im}. \tag{7}$$

Mechanization of a Function.—An ideal functional mechanism establishes definite relations between its parameters:

$$F_r(X_1, X_2, \cdot \cdot \cdot) = 0, \qquad r = 1, 2, \cdot \cdot \cdot . \tag{8}$$

It may be said to provide "a mechanization" of these functional relations within the given domain of the independent parameters.

Such a mechanism, together with its associated scales, similarly provides a mechanization of functional relations,

$$f_r(x_1, x_2, \cdot \cdot \cdot) = 0, \qquad r = 1, 2, \cdot \cdot \cdot , \tag{9}$$

between the variables x_i, within a given domain of the independent variables. The forms of these relations may be derived by eliminating the values of the parameters X_i between Eq. (8), which characterizes the mechanism, and Eq. (5), which characterizes the scales.

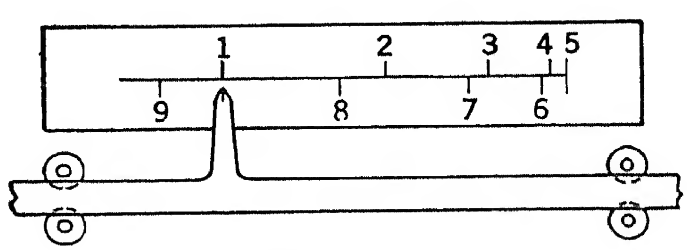

FIG. 3·3.—Input scale.

If the output variables are to be single-valued functions of the input variables, the input parameters must be single-valued functions of the input variables, and the output variables must be single-valued functions of the output parameters; it is not, however, necessary that the inverse relations be single-valued. Thus an input scale may have the form shown in Fig. 3·3, and an output scale that shown in Fig. 3·4, but not the reverse.

Linear Mechanization.—A mechanization of a relation between variables will be termed a "linear mechanization" if all scales are linear.

A nonlinear mechanization of a given function may be useful when input variables are set by hand, and only a reading of the output variables is required. When a computing mechanism is to be part of a more complex device, it is usually necessary that the terminals have mechanical motion proportional to the change in the associated variable—that is, a linear mechanization of the function is needed. For instance, if one has only to compute the superelevation angle for an antiaircraft gun it may be quite satisfactory to read this on an unevenly divided scale. If, however, one wishes to use the computer to control directly the sight on a gun, then a linear mechanization of the superelevation function will be required.

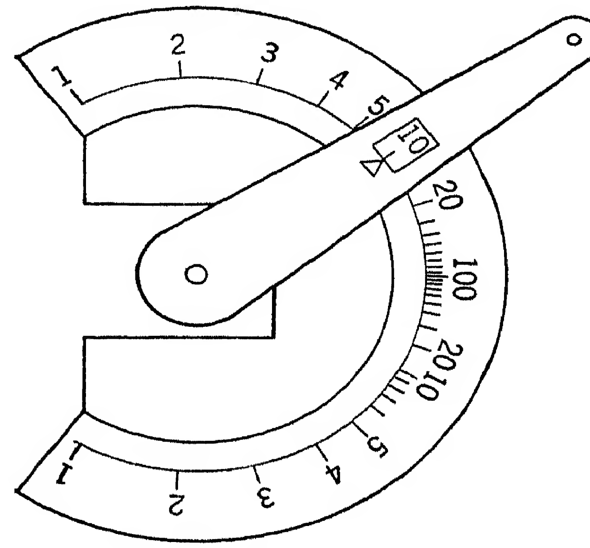

FIG. 3·4.—Output scale.

It is a trivial matter to design a nonlinear mechanization of a function of one independent variable. One requires only a single pointer, serving both as input and output terminal, to indicate corresponding values of input and output variables as parallel scales (Fig. 3·5). For this reason the term mechanization as applied to functions of a single independent variable will always denote *linear* mechanization; a distinction will be made between linear and nonlinear mechanization only in the case of linkages of two or more degrees of freedom.

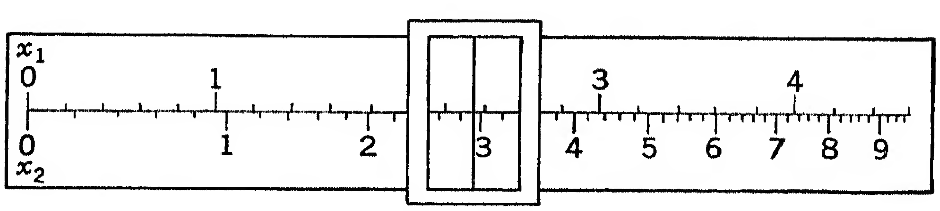

FIG. 3·5.—Nonlinear mechanization of a function of one independent variable.

3·2. Homogeneous Parameters and Variables.—Homogeneous variables and parameters are very useful tools in the design of individual computing linkages, and also in the drawing up of schematic diagrams for complex computers. They are defined only for variables and parameters which vary within finite limits.

Associated with each variable x_i having a finite range Δx_i is a *homogeneous variable* defined by

$$h_i = \frac{x_i - x_{im}}{x_{iM} - x_{im}}. \tag{10}$$

As x_i varies from its lower to its upper bound, h_i varies linearly with it, from 0 to 1. The inverse form of Eq. (10) may be written

$$x_i = x_{im} + h_i \Delta x_i. \tag{11}$$

Another homogeneous variable, "complementary to h_1," is defined by

$$\bar{h}_i = \frac{x_{iM} - x_i}{x_{iM} - x_{im}}, \tag{12}$$

or by

$$h_i + \bar{h}_i \equiv 1. \tag{13}$$

In the same way, there are associated with each parameter X_i, having a finite travel ΔX_i, two complementary homogeneous parameters,

$$H_i = \frac{X_i - X_{im}}{X_{iM} - X_{im}}, \tag{14}$$

$$\bar{H}_i = 1 - H_i, \tag{15}$$

which change linearly with X_i between bounds 0 and 1:

$$X_i = X_{im} + H_i \Delta X_i = X_{iM} - \bar{H}_i \Delta X_i. \tag{16}$$

In a linear mechanization, the homogeneous variables and parameters are very simply related. The quantities X_i and x_i are connected by a linear relation,

$$X_i - X_i^{(0)} = k_i(x_i - x_i^{(0)}). \tag{17}$$

If k_i is positive, the minimum values of X_i and x_i occur together, as do the maximum values:

$$X_{im} - X_i^{(0)} = k_i(x_{im} - x_i^{(0)}), \tag{18a}$$

$$(k_i > 1)$$

$$X_{iM} - X_i^{(0)} = k_i(x_{iM} - x_i^{(0)}). \tag{18b}$$

It follows by introduction of these relations into Eqs. (10) and (14) that

$$H_i \equiv h_i. \qquad (k_i > 1). \tag{19}$$

If k_i is negative, the maximum value of X_i occurs together with the minimum value of x_i, and conversely:

$$X_{im} - X_i^{(0)} = k_i(x_{iM} - x_i^{(0)}), \tag{20a}$$

$$(k_i < 1)$$

$$X_{iM} - X_i^{(0)} = k_i(x_{im} - x_i^{(0)}); \tag{20b}$$

then

$$H_i \equiv \bar{h}_i = 1 - h_i. \qquad (k_i < 1). \tag{21}$$

Equation (19) will be referred to as the "direct" identification of H_i with h_i. It implies that X_i and x_i are linearly dependent on each other,

changing in the same sense between minimum and maximum values which they attain simultaneously; the scale of x_i is even, and increases in the direction of increasing X_i. Equation (21) will be termed the "complementary identification" of H_i and h_i; it implies that the scale of x_i is even, and increases in the direction of decreasing X_i.

In terms of homogeneous variables, the problem of linearly mechanizing a given function takes on a particularly simple form. For instance, if the given function involves a single independent variable, it may be expressed in terms of a homogeneous input variable h_1 and a homogeneous output variable h_2:

$$h_2 = f(h_1). \tag{22}$$

A linkage with one degree of freedom, operating in a specified domain of the input parameter,

$$X_{im} \leqq X_i \leqq X_{iM}, \tag{23}$$

will generate a relation between homogeneous input and output parameters, H_1 and H_2, respectively:

$$H_2 = F(H_1). \tag{24}$$

It is then required to find a mechanism and domain of operation such that Eq. (24) can be transformed into the given Eq. (22) by direct or complementary identification of H_1 with h_1, with H_2 with h_2.

The usefulness of homogeneous parameters and variables will be abundantly illustrated in the chapters to follow.

3·3. An Operator Formalism.—It is often necessary to combine mechanisms in series, in such a way that the output parameter of the first becomes the input parameter of the second, and so on. The first mechanism determines an output parameter X_2 as a function of the input parameter X_1:

$$X_2 = \phi_1(X_1). \tag{25a}$$

The second mechanism determines an output parameter X_3 in terms of X_2,

$$X_3 = \phi_2(X_2); \tag{25b}$$

the third determines an output parameter X_4 in terms of X_3,

$$X_4 = \phi_3(X_3); \tag{25c}$$

and so on. The final output parameter, for example, X_4, is then determined as a function of X_1:

$$X_4 = \phi_3\{\phi_2[\phi_1(X_1)]\}. \tag{26}$$

The conventional notation of Eqs. (25) and (26) is fully explicit, but sometimes cumbersome. For many purposes the author finds it more convenient and more suggestive to use the following operator notation.

Equation (25a) implies that the value of X_2 can be obtained by carrying out an operation (of character specified by the definition of ϕ_1) on the value of X_1. As an alternative notation we shall write

$$X_2 = (X_2|X_1) \cdot X_1, \tag{27a}$$

where $(X_2|X_1)$ denotes an operator converting the parameter X_1 into the parameter X_2. Similarly, Eqs. (25b) and (25c) become

$$X_3 = (X_3|X_2) \cdot X_2, \tag{27b}$$
$$X_4 = (X_4|X_3) \cdot X_3. \tag{27c}$$

In this notation Eq. (26) becomes

$$X_4 = (X_4|X_3) \cdot (X_3|X_2) \cdot (X_2|X_1) \cdot X_1. \tag{28}$$

This form shows clearly the successive operations carried out upon X_1 to produce X_4. It will be noted, however, that the operators are distinguished from each other only by specification of the parameters involved; it is not possible to change the argument of a given function, as in the conventional functional notation.

The over-all effect of Eqs. (27) is to define X_4 as a function of X_1:

$$X_4 = (X_4|X_1) \cdot X_1. \tag{29}$$

On comparing Eqs. (28) and (29) we obtain the operator equation

$$(X_4|X_3) \cdot (X_3|X_2) \cdot (X_2|X_1) = (X_4|X_1). \tag{30}$$

The form of this equation calls our attention to a possible manipulation of these functional operators. In a meaningful product of operators, each internal parameter will occur twice in neighboring positions in adjacent operators. One can, without changing the significance of the operator, strike out such duplicated symbols and condense the notation thus:

$$(X_4|X_3) \cdot (X_3|X_2) \cdot (X_2|X_1) \rightarrow (X_4|X_3) \cdot (X_3|X_1) \rightarrow (X_4|X_1), \tag{31a}$$

or

$$(X_4|X_3) \cdot (X_3|X_2) \cdot (X_2|X_1) \rightarrow (X_4|X_2) \cdot (X_2|X_1). \tag{31b}$$

Conversely, one can describe the structure of an operator in more detail, with consequent expansion of the notation:

$$(X_4|X_1) \rightarrow (X_4|X_3) \cdot (X_3|X_1) \rightarrow (X_4|X_3) \cdot (X_3|X_2) \cdot (X_2|X_1). \tag{32}$$

The inverse operator to $(X_2|X_1)$ will be $(X_1|X_2)$. Thus

$$X_1 = (X_1|X_2) \cdot X_2, \tag{33}$$
$$(X_1|X_2) \cdot (X_2|X_1) \equiv 1. \tag{34}$$

Both sides of an operator equation can be multiplied by the same operator. This must be done in such a way that the resulting operators have meaning: the multiplied operators must have neighboring symbols in

common. Thus one can multiply both sides of Eq. (30) from the left by the operator $(X_2|X_4)$, to obtain

$$(X_2|X_4) \cdot (X_4|X_3) \cdot (X_3|X_2) \cdot (X_2|X_1) = (X_2|X_4) \cdot (X_4|X_1), \quad (35)$$

which may be condensed to

$$(X_2|X_3) \cdot (X_3|X_1) = (X_2|X_4) \cdot (X_4|X_1). \quad (36)$$

Multiplication of Eq. (30) by $(X_2|X_4)$ from the right is not defined, but multiplication from the right by, for example, $(X_1|X_3)$ is defined.

This operator formalism can be applied to variables as well as to parameters. An input scale, which determines a parameter X_i as a function of a variable x_i, can be represented by an operator $(X_i|x_i)$; an output scale would be represented by an operator $(x_k|X_k)$.

3·4. Graphical Representation of Operators.—The operator $(X_k|X_i)$, like the function $\phi_i(X_i)$, is conveniently represented by a plot of X_k against X_i. This representation is most uniform and most useful when homogeneous parameters or variables are used. A plot of H_k against H_i always lies in a unit square (Fig. 3·6); it can be used in the graphical construction of curves representing products of the operator $(H_k|H_i)$ with other operators, and in the solution of other types of operator equations, in a way which will now be explained.

Given the analytic form of the relations symbolized by

$$H_k = (H_k|H_i) \cdot H_i, \quad (37a)$$
$$H_s = (H_s|H_k) \cdot H_k, \quad (37b)$$

one can determine the form of the relation

$$H_s = (H_s|H_i) \cdot H_i \quad (37c)$$

by eliminating the parameter H_k. In the same way, one can determine the graphical representation of the product operator

$$(H_s|H_i) = (H_s|H_k) \cdot (H_k|H_i) \quad (38)$$

by graphical elimination of the parameter H_k from plots of $(H_s|H_k)$ and $(H_k|H_i)$. Figure 3·7 illustrates the required construction. The operators $(H_k|H_i)$ and $(H_s|H_k)$ are represented, in the standard way, by plotting the first parameter vertically against the second horizontally. In the representation of $(H_k|H_i)$, H_k is thus plotted vertically, but in the representation of $(H_s|H_k)$ it is plotted horizontally. The parameter H_i is plotted horizontally in the first case, and H_s vertically in the second; it is in this way that they are to be plotted in the standard representation of the product operator $(H_s|H_i)$, which we must now construct. On the main diagonal of the square, the line $(0, 0) \rightarrow (1, 1)$, we select a point A;

this will represent, by its equal horizontal and vertical coordinates, a particular value of the parameter H_k. A horizontal line through A will intersect the curve $(H_k|H_i)$ at a point B; the horizontal coordinate of B is a value of H_i corresponding to the chosen H_k. A vertical line through A will intersect the curve $(H_s|H_k)$ at a point C; the vertical coordinate of C is the value of H_s corresponding to the chosen H_k. The point D, constructed by completing the rectangle $ABDC$, then has the horizontal coordinate H_i and the vertical coordinate H_s corresponding to the same

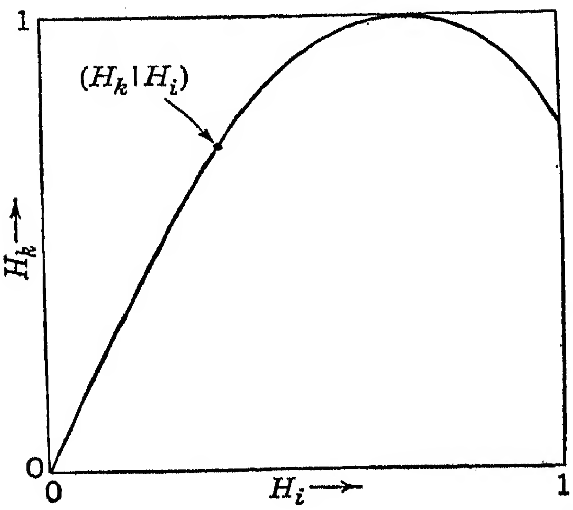

FIG. 3·6.—Graphical representation of a typical operator $(H_k|H_i)$.

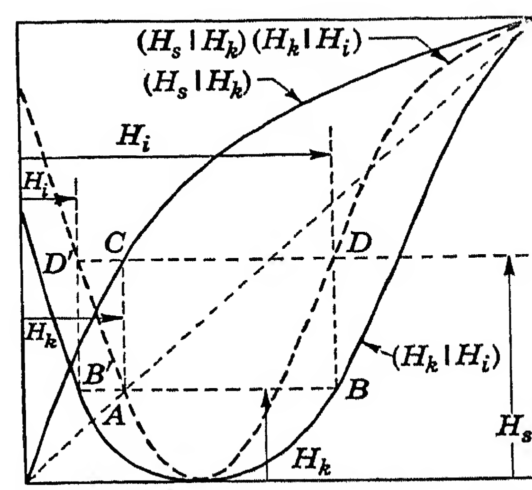

FIG. 3·7.—Construction of a product of operators.

value of H_k; it is a point on the curve of the product operator $(H_s|H_i)$. It will be noted that the horizontal line through A intersects the curve $(H_k|H_i)$ at a second point, B', to which corresponds a second value of H_i compatible with the same values of H_k and H_s. The point D' determined by constructing the rectangle $AB'D'C$ is thus a second point on the curve $(H_s|H_i)$. By carrying out this construction for a sufficient number of points A, one can determine enough points D, D', on the curve $(H_s|H_i)$ to permit its construction with any desired accuracy.

The slopes of the factor and product curves are simply related. The analytic relation

$$\frac{dH_s}{dH_i} = \frac{dH_s}{dH_k} \cdot \frac{dH_k}{dH_i} \tag{39}$$

becomes, in the notation of Fig. 3·7,

$$[\text{Slope of } (H_s|H_i) \text{ at } D] = [\text{Slope of } (H_s|H_k) \text{ at } C] \times [\text{Slope of } (H_k|H_i) \text{ at } B]. \tag{40}$$

If the factor curves intersect at a point A on the main diagonal, the rectangle $ABDC$ reduces to a single point; the product curve passes through this same point, with a slope equal to the slopes of the factor curves. An important special case is that in which both factor functions are con-

tinuous and monotonically increasing in the range of definition. The factor curves then intersect at the points (0, 0) and (1, 1), at the ends of the main diagonal; the terminal slopes of the product curve are equal to the products of the corresponding terminal slopes of the factor curves.

It is sometimes desirable to construct the product $(H_s|H_k) \cdot (H_k|H_i)$, using, instead of a plot of $(H_s|H_k)$, a plot of its inverse, $(H_k|H_s)$. The required construction is shown in Fig. 3·8. A horizontal line through a point A, corresponding to an arbitrarily chosen value of H_k, will intersect the curve $(H_k|H_s)$ at a point C with horizontal coordinate H_s, and the curve $(H_k|H_i)$ at a point B with horizontal coordinate H_i. A vertical line through C will intersect the main diagonal at a point D with vertical coordinate H_s. Finally, by completing the rectangle $CDEB$, one can

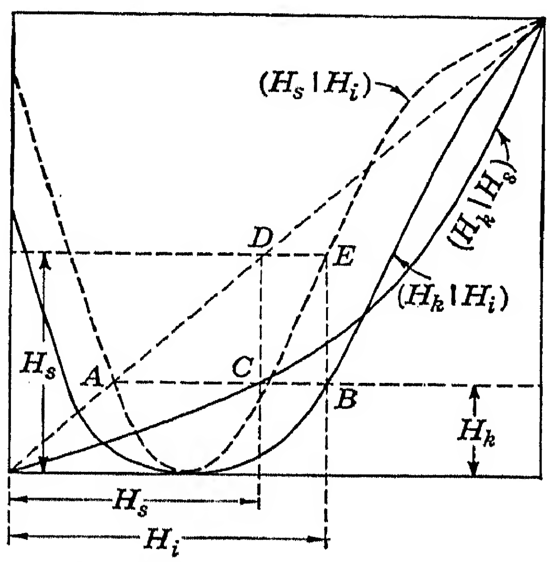

FIG. 3·8.—Construction of the product $(H_s|H_k) \cdot (H_k|H_i)$, using plot of $(H_k|H_s)$.

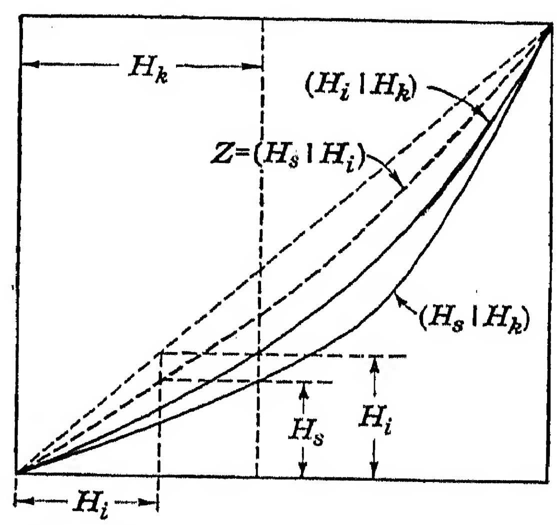

FIG. 3·9.—Graphical solution of $Z \cdot (H_i|H_k) = (H_s|H_k)$.

determine the point E, with vertical and horizontal coordinates H_s and H_i, respectively; this point, then, lies on the required curve $(H_s|H_i)$.

This construction is essentially a solution of the operator equation

$$(H_k|H_s) \cdot (H_s|H_i) = (H_k|H_i), \tag{41}$$

the first and third of these operators being known. Otherwise stated, it is a graphical solution of the operator equation

$$(H_k|H_s) \cdot Y = (H_k|H_i) \tag{42}$$

for the unknown operator Y, which is obviously the desired $(H_s|H_i)$. It will be noted that the construction of Fig. 3·8 is that required for the multiplication of $(H_k|H_s)$ and $(H_s|H_i)$ to produce $(H_k|H_i)$, according to the method first explained.

Another operator equation often encountered is

$$Z \cdot (H_i|H_k) = (H_s|H_k). \tag{43}$$

The construction for Z is sketched in Fig. 3·9 in the case of monotone operators $(H_i|H_k)$ and $(H_s|H_k)$.

3·5. The Square and Square-root Operators.—It is sometimes desirable to connect in series two identical linkages with equal input and output travels. The first linkage carries out the transformation

$$H_k = (H_k|H_i) \cdot H_i, \tag{44a}$$

the second linkage, the transformation

$$H_s = (H_s|H_k) \cdot H_k, \tag{44b}$$

where the operators $(H_k|H_i)$ and $(H_s|H_k)$ are identical in form, though not, of course, in the arguments. Then

$$(H_s|H_i) = (H_s|H_k) \cdot (H_k|H_i) \tag{45}$$

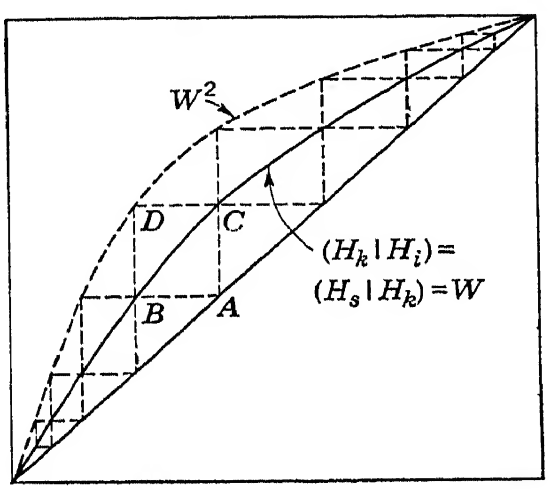

FIG. 3·10.—Squaring an operator.

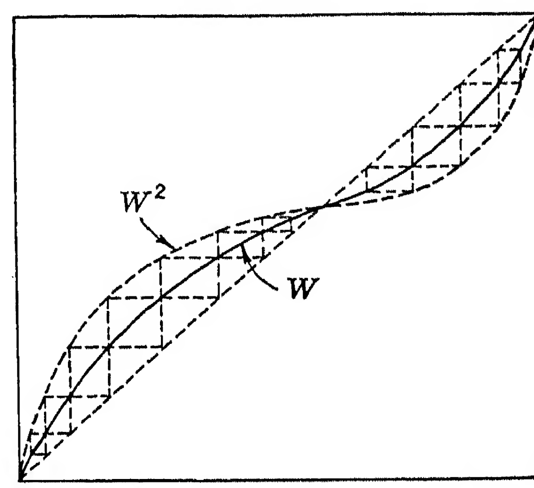

FIG. 3·11.—Squaring an operator W represented by a curve which crosses the main diagonal.

is essentially the square of the operator

$$W \equiv (H_s|H_k) \equiv (H_k|H_i); \tag{46}$$

Eq. (45) may be written as

$$(H_s|H_i) = W \cdot W = W^2. \tag{47}$$

The construction for the operator W^2 is illustrated in Figs. 3·10 and 3·11. In principle, it is the same as the construction of Fig. 3·7; differences in appearance arise from the fact that, since the functions are identical, the points B and C lie on the same curve, instead of on two different ones.

The curve representing W^2 lies beyond the W-curve, away from the main diagonal. Where the W-curve crosses the main diagonal, the W^2-curve also crosses it, with a slope equal to the square of the slope of the W-curve; terminal slopes are related in the same way when the terminal points are (0, 0) or (1, 1). Thus the variations in slope of the W^2-curve, and its curvature, are greater than those of the W-curve.

The difficulty in designing a linkage to generate a given function tends to increase with the curvature of the function. It is often impossible to use a linkage of given type to mechanize a given functional operator $(H_s|H_i) = W^2$ with large curvature, but quite feasible to mechanize the less strongly curved square-root operator W. If it is possible to solve Eq. (47) for the operator W, and to mechanize this by a linkage with equal input and output travels, it is then possible to mechanize the given function by two such linkages in series. This technique will be discussed in Chap. 6; we shall here consider only the graphical method for solving for the square-root operator W, when W^2 increases monotonically.

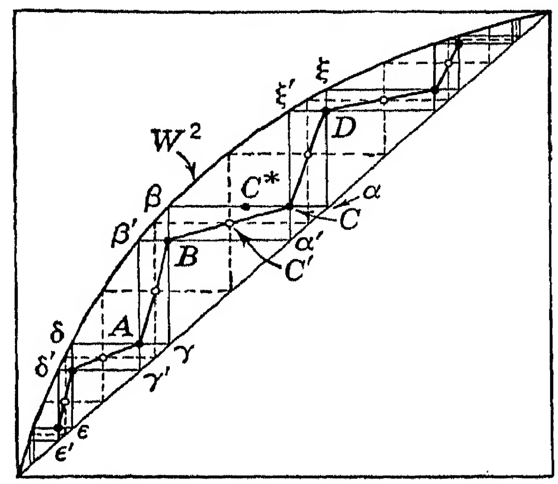

FIG. 3·12.—Construction of a square-root operator.

The general nature of the problem of solving for W can be understood by inspection of Fig. 3·10. One needs to fill out the region between the main diagonal and the W^2-curve by a system of rectangles with horizontal and vertical sides, such that one corner of each rectangle lies on the main diagonal, the opposite corner lies on the W^2-curve, and the other two corners fall on a continuous curve, the W-curve. This can always be done, and in an infinite number of ways; the square-root operator is not unique, but has the multiplicity of the curves that can be drawn between two given points.

A square-root operator can be constructed in the following way. Between the main diagonal and the W^2-curve, let a point C be chosen, quite arbitrarily (Fig. 3·12). Beginning at the point C, construct the horizontal line $\alpha\beta$, the vertical line $\beta\gamma$, the horizontal line $\gamma\delta$, and so on; these form a step structure with vertexes alternately on the main diagonal and the W^2-curve, extending through the region between these lines. A second step structure passing through C is formed by the vertical line $\xi'\alpha'$, the horizontal line $\alpha'\beta'$, the vertical line $\beta'\gamma'$, and so on. These two step structures define a series of rectangles with opposite vertexes on the main diagonal and the W^2-curve. The other vertexes define a sequence of points, . . . , A, B, C, D, . . . , such that a W-curve which passes through any point of the sequence, say C, must pass also through all the others. This sequence of points will have a point of condensation where the W^2-curve crosses the main diagonal, and cannot be extended through such a point. In Fig. 3·12 the points of condensation are the terminal points (0, 0) and (1, 1); in a case like that of Fig. 3·11, independent sequences must be defined in regions separated by points of condensation.

Let us choose to construct a square-root operator, W, which passes through the sequence of points, . . . , A, B, C, D, . . . , indicated by solid circles in Fig. 3·12. We can also require that it pass through any other similarly constructed series of points, . . . , A', B', C', D', . . . , such as that indicated in Fig. 3·12 by small circles. We can, in fact, completely define W by requiring that it pass between points B and C in an arbitrarily chosen continuous curve. Corresponding to the points of this curve, the above construction will define sequences of points that connect A to B, C and D, and so on; these points define a continuous W-curve extending from one condensation point to the next. The reader will find it easy to prove that if W is to be single-valued everywhere, it must increase monotonically between B and C.

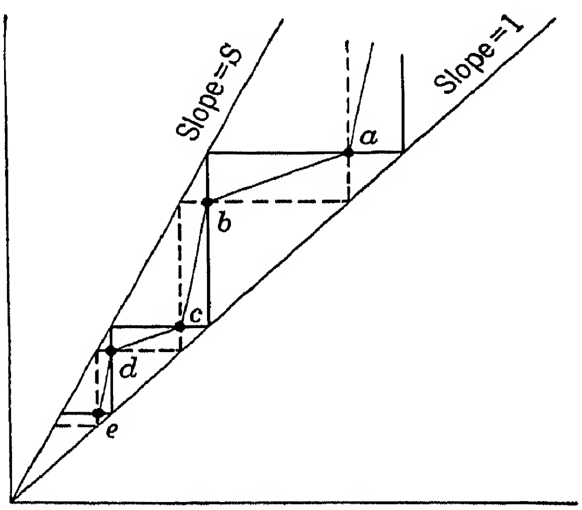

FIG. 3·13.—Construction of a squareroot operator near a point of condensation.

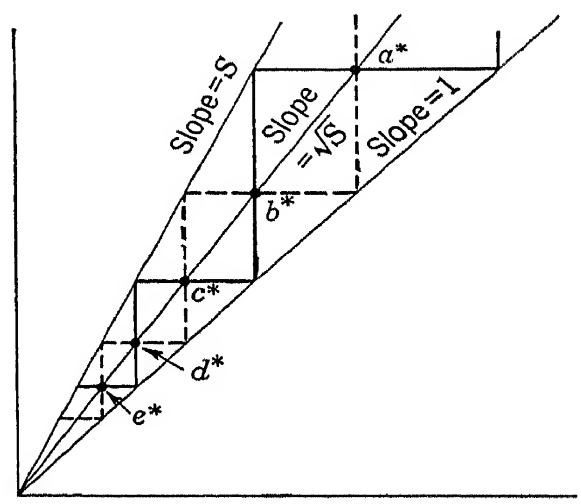

FIG. 3.14.—Square-root-operator curve having a derivative at a point of condensation.

The square-root operators thus defined do not, in general, have derivatives at the limiting points of condensation. In Fig. 3·12 it is evident that the W-curve oscillates more and more rapidly as the origin is approached, and it is hardly to be expected that a derivative will exist at that point. Figure 3·13 represents the part of Fig. 3·12 very near the origin, in a neighborhood in which the W^2-curve can be replaced by a straight line with finite slope $S \neq 1$. The points a, b, c, d, e, fall in the same sequence as the points A, B, C, D, of Fig. 3·12. No attempt is made to represent the forms of the intervening curve segments, which are replaced by straight lines. The step structure shown dashed is the continuation of the structure $\alpha\beta\gamma\delta\epsilon$ . . . of Fig. 3·12; it will be unchanged if the point C is shifted horizontally, say to C^*. The other step structure is the continuation of $\alpha'\beta'\gamma'\delta'$ . . . , and it will be changed by a horizontal shift of C. It is easy to show that the segments ab, cd, ef, . . . , are parallel, as are the segments bc, de, fg, ... The segments ab and cd are in general not parallel to each other; the average slopes in successive

segments of the W-curve remain constant and different as the origin is approached, and no derivative exists at the origin.

As we have already noted, a shift of the point C of Fig. 3·12 to the left will modify one of the step structures, defining a new sequence of points a^*, b^*, c^*, . . . , corresponding to the new point C^*. By proper choice of C^* the new sequence of points can be brought to lie on a straight line through the origin, as shown in Fig. 3·14. Only through this particular sequence of points can one pass a W-curve having a derivative at the origin; the limiting slope of that curve must be the slope of the line $a^*b^*c^*$ . . . , wh ch is easily shown to be $\sqrt{S}$. This geometric argument thus leads to the already stated conclusion that the slope of the W-curve at a point of condensation must (if it exists) be equal to the square root of the slope of the W^2-curve.

The argument of the preceding paragraph also leads to the conclusion that on any given horizontal line there is one and only one point C^* that lies on a W-curve with derivative at the origin. It is evident, then, that the condition that the W-curve shall have a derivative at the origin (or any other point of condensation where the W^2-curve intersects the main diagonal with a finite difference of slope) is sufficient to determine uniquely the form of the W-curve as far as the next adjacent point of condensation. Since an independently determinable section of the W-curve usually lies between two such points of condensation, the condition that it have a derivative everywhere places on it two conditions, which may or may not be consistent. Thus for any given monotonic W^2-curve there can exist, at most, one W-curve with a derivative everywhere; there may exist none at all.

If the W-curve is to be mechanized exactly, it is obviously necessary that it have a derivative everywhere. For an approximate mechanization it is only necessary that the W-curve oscillate with sufficiently small amplitude about a mechanizable curve with a derivative everywhere. In either case, the analysis just outlined forms a practical basis for the determination of W-curve. Trying in turn several points C, one can quickly find a point C^* such that the slopes of the segments $\alpha^*\beta^*$, $\beta^*\gamma^*$, . . . approach equality as one of the two limiting points of condensation is approached. The corresponding slopes may then oscillate near the other point of condensation, at which this W-curve will have no derivative. It is, however, usually possible to choose C^* so that the oscillations of the W-curve are negligibly small near both points of condensation. By interpolation one can then determine a smooth approximate W-curve suitable for mechanization.

CHAPTER 4

HARMONIC TRANSFORMER LINKAGES

We turn now to the problem of designing a bar linkage for the mechanization of a given functional relation between two variables. The devices used will be discussed in the order of their increasing flexibility and the increasing complexity of the design procedure required: in Chap. 4, harmonic transformers and double harmonic transformers; in Chap. 5, three-bar linkages; in Chap. 6, three-bar linkages in combination with harmonic transformers or other three-bar linkages. Full examples of the design techniques will be provided by detailed discussions of the problem of mechanizing the tangent and logarithmic functions.

THE HARMONIC TRANSFORMER

4·1. Definition and Geometry of the Harmonic Transformer.—An *ideal harmonic transformer* is a mechanical cell for which input and output parameters X_i and X_k are related by

$$X_k = R \sin X_i, \tag{1}$$

R being an arbitrary constant. Such a relationship can be obtained with simple mechanisms modeling a right triangle, such as are sketched in Fig.

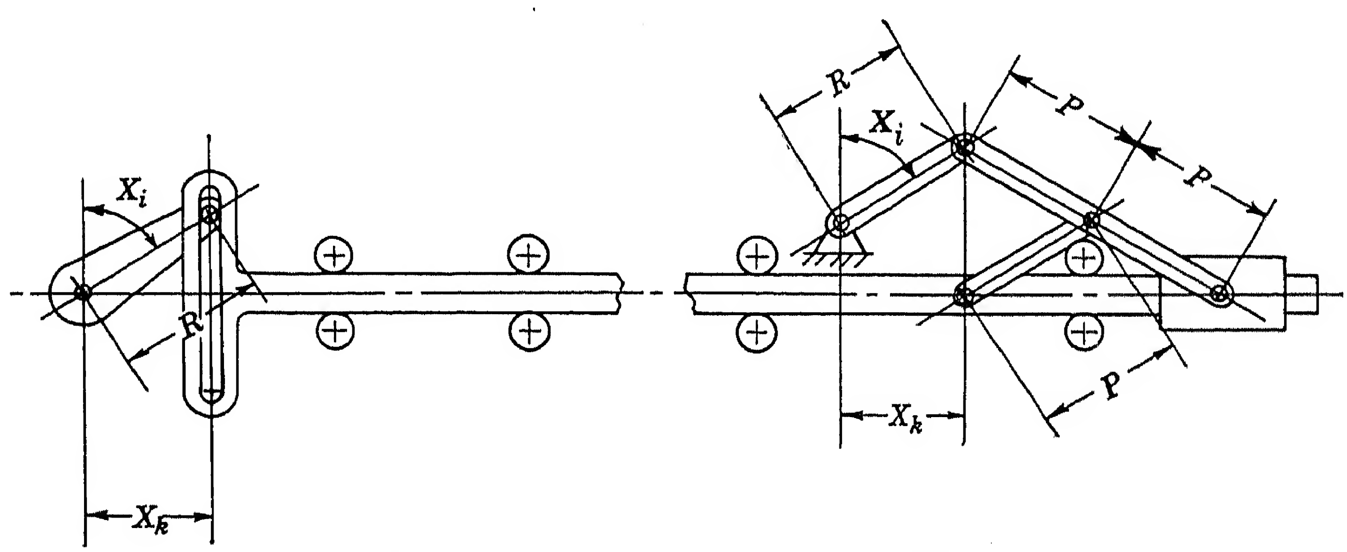

FIG. 4·1.—Ideal harmonic transformers.

4·1. These harmonic transformers are called "ideal" because they generate the sine or arc-sine functions accurately; unfortunately, they are somewhat unsatisfactory mechanically, and are therefore used only exceptionally in practical work. It is usually preferable to employ *nonideal harmonic transformers*, such as those shown in Figs. 4·2 and 4·3,

which give only an approximately sinusoidal relation between input and output parameters.

The mechanism shown in Fig. 4·2 is an ordinary crank-link system with unsymmetrically placed slide. The deviation of the output parameter from its "ideal" value depends upon the angle ϵ between the link L and the line of the slide. Representing the output parameter by X'_k, one has

$$X'_k = R \sin X_i - L(1 - \cos \epsilon). \tag{2}$$

This may be written as

$$X'_k = X_k + \delta X_k, \tag{3}$$

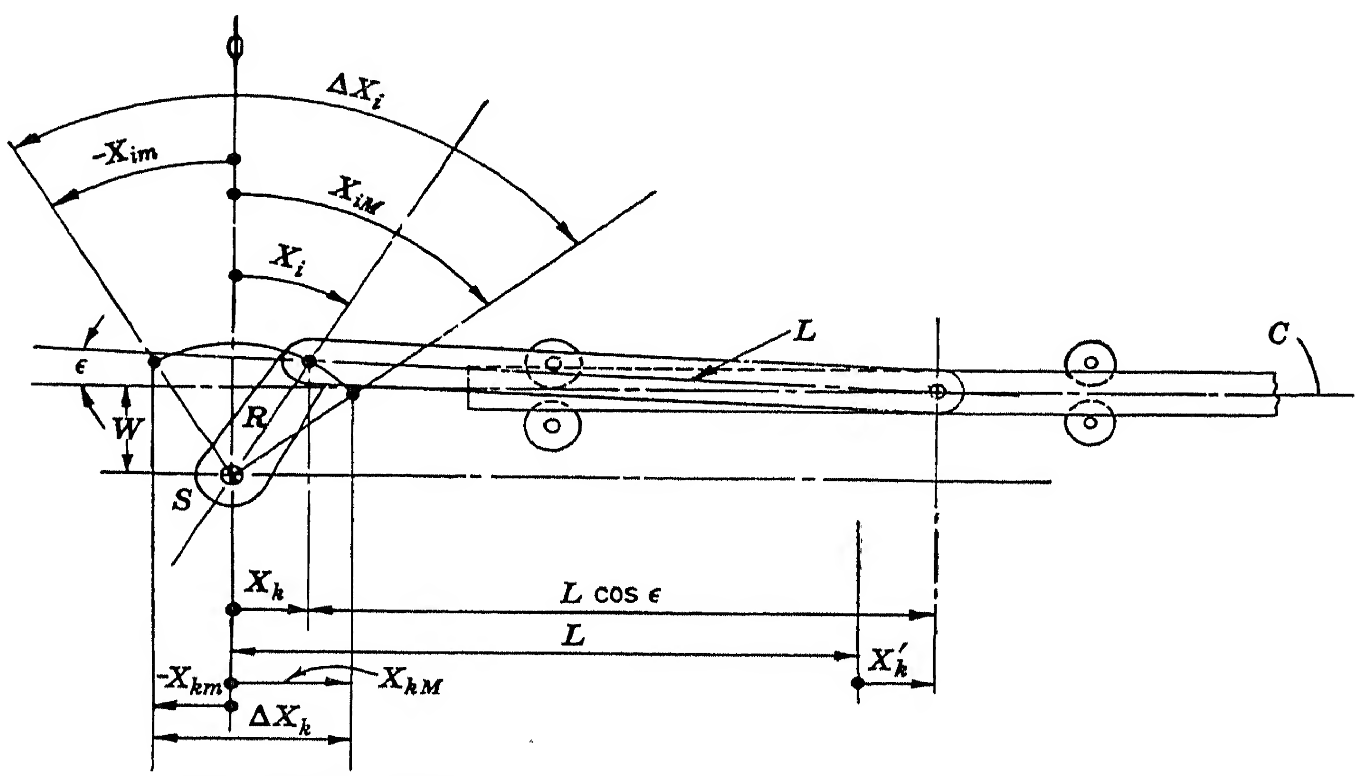

FIG. 4·2.—Crank-link system as a nonideal harmonic transformer.

where δX_k is the structural error of the mechanism as compared with the ideal harmonic transformer:

$$\delta X_k = -L(1 - \cos \epsilon). \tag{4}$$

In the mechanism of Fig. 4·2, ϵ is variable, being given by

$$L \sin \epsilon = R \cos X_i - W. \tag{5}$$

In Fig. 4·2 the slide displacement W has been so chosen as to keep ϵ, and hence δX_k, small as the crank turns through its limited operating angle. As will be discussed in detail later, it may be desirable to make a different choice of W in order to obtain a desired nonvanishing form for δX_k.

Figure 4·3 represents a harmonic transformer connected to another linkage such that the pivot P may be found anywhere within the shaded area. Equations (2), (3), and (4) hold in this case, but ϵ and the structural-error function δX_k now depend not only on X_i, but also on the position of the pivot P within the possible boundary.

An ideal harmonic transformer generates a section of sine or arc-sine curve, the form of which can be fixed by specification of the angular limits of the rotation of the crank, X_{im} and X_{iM}. The nonideal harmonic transformer requires four parameters for its specification—for instance, X_{im}, X_{iM}, L/R, and W/R. The presence of these additional parameters per-

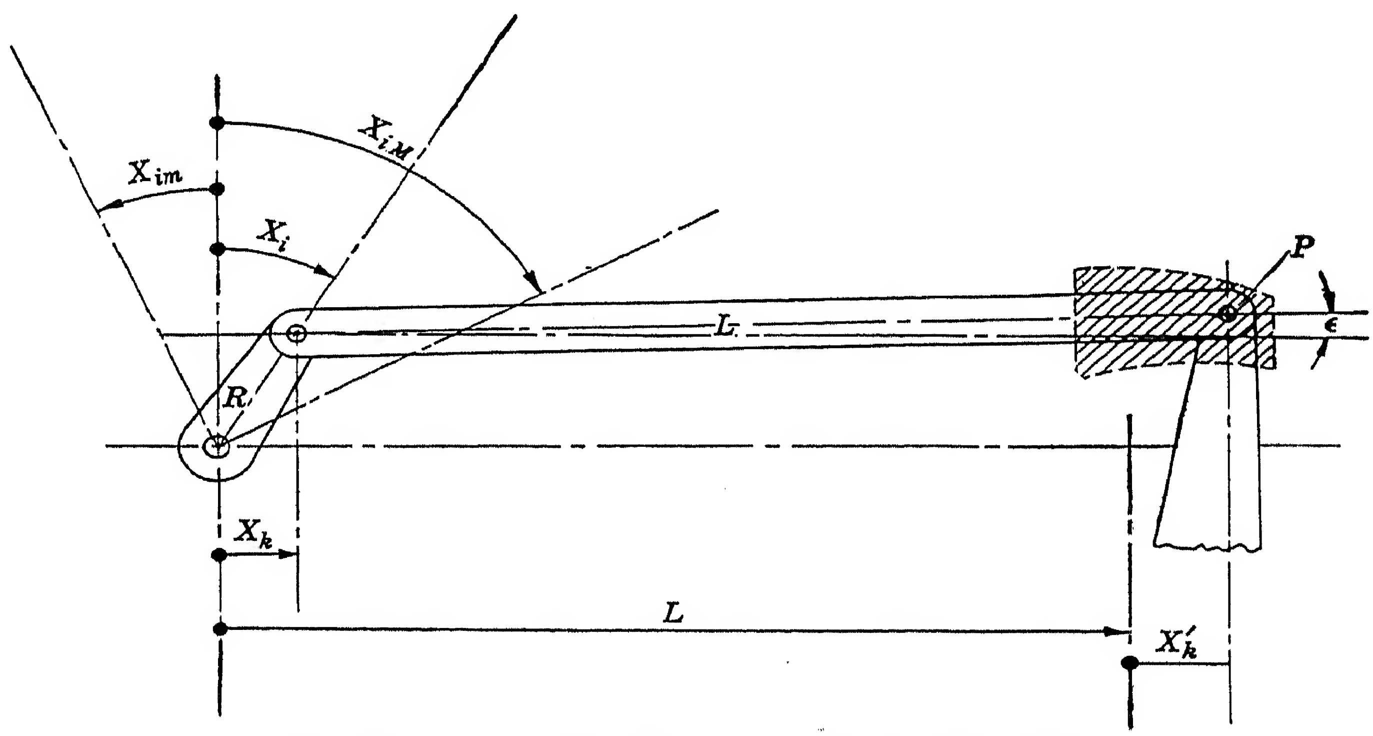

FIG. 4·3.—A nonideal transformer without fixed slide.

mits a considerable extension of the field of mechanizable functions—an extension which becomes striking if ϵ is permitted to assume large values. In most practical work ϵ and δX_k are kept fairly small; δX_k then appears either as an error arising from the use of a nonideal design, or as a small correction to the sinusoidal form, by which one makes the mechanized function correspond more closely to a given, not exactly sinusoidal, function.

In working out the mathematical design of a system that includes a nonideal harmonic transformer, it is usually desirable to carry through the first calculation as though the transformer were ideal. The error arising from use of the nonideal design can then be corrected in the final stages of the work (if this is required by very rigid tolerances), or so chosen as to minimize the over-all error of the system.

4·2. Mechanization of a Function by a Harmonic Transformer.—In the harmonic transformer one parameter is a rotation, the other a translation. Either of these may be taken as the input parameter. If the crank R is the input terminal, the limits of the input parameter X_i may be chosen at will; the crank can describe any angle or make any number of revolutions. The mechanized function will always be a sinusoid or a part of a sinusoid between chosen limits (Fig. 4·4). If the slide is the input terminal, the range of the input parameter X_k must be limited to keep the mechanism far enough from the self-locking positions. The mechanized function is then a portion of an arcsinusoid (Fig. 4·5) within which the slope does not exceed some maximum value determined by mechanical considerations.

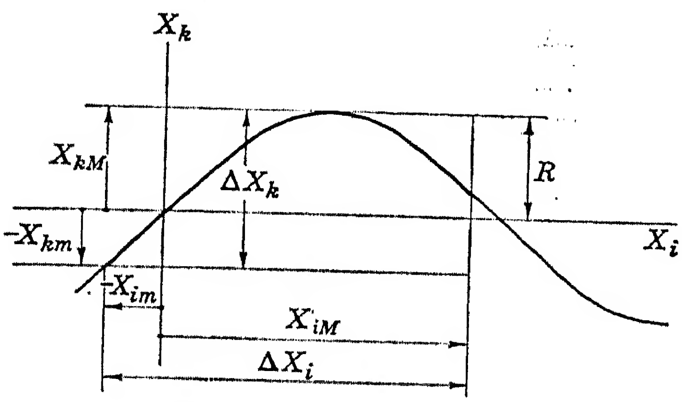

FIG. 4·4.—Sinusoid generated by an ideal harmonic transformer.

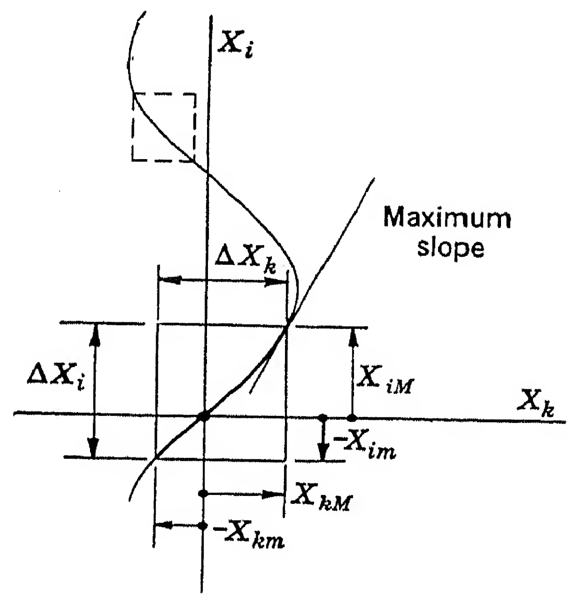

FIG. 4·5.—Arcsinusoid generated by an ideal harmonic transformer.

The simplest problem in ideal-harmonic-transformer design is that of mechanizing a harmonic relation, analytically expressed, between variables x_i and x_k:

$$x_k - x_{k_0} = r \sin (x_i - x_{i_0}), \qquad r > 0, \tag{6a}$$

or

$$x_i - x_{i_0} = \sin^{-1} \left(\frac{x_k - x_{k_0}}{r} \right), \tag{6b}$$

given specified limits for the input variables. To determine the constant R of the harmonic transformer and the required relation of the variables x_i, x_k, to the parameters X_i, X_k, one need only compare Eqs. (1) and (6):

$$\frac{x_k - x_{k_0}}{r} = \frac{X_k}{R}, \qquad x_i - x_{i_0} = X_i. \tag{7}$$

The value of R, chosen at will, determines the scale factor K_k of the parameter X_k:

$$K_k = \frac{x_k - x_{k_0}}{X_k - X_{k_0}} = \frac{x_k - x_{k_0}}{X_k} = \frac{r}{R} \tag{8}$$

$[X_{k_0} = 0$, by Eq. (7)]. The scale factor for X_i is unity. These constants being fixed, the harmonic transformer is determined. The range of parameter values for which it must operate is determined by the limited range of the input and output variables, $x_{im} \leqq x_i \leqq x_{iM}$, $x_{km} \leqq x_k \leqq x_{kM}$:

$$X_{im} = x_{im} - x_{i_0}, \qquad X_{iM} = x_{iM} - x_{i_0}, \tag{9}$$

$$X_{km} = \frac{x_{km} - x_{k_0}}{K_k}, \qquad X_{kM} = \frac{x_{kM} - x_{k_0}}{K_k}. \tag{10}$$

A less trivial problem is that of mechanizing a function that has a generally sinusoidal character, but is given only in tabulated form. One possible method in such a case is to fit the given function as well as possible (for example, using the method of least squares) by the analytic expressions of Eq. (6), and then to proceed as just explained. A quicker way, making use of homogeneous variables and parameters, will now be presented.

4·3. The Ideal Harmonic Transformer in Homogeneous Parameters. Before expressing the equation of an ideal harmonic transformer in homogeneous parameters, we must define the parameters more precisely.

The position of the crank R (Fig. 4·2) is described by the parameter X_i, the rotation of the crank clockwise from a zero position perpendicular to the center line C of the slide. The other parameter, X_k, is defined as the normal projection of the arm R onto the center line of the slide. The crank R in the zero position is pictured as directed upwards, and X_k is taken as positive toward the right from the point S.

The homogeneous parameters θ_i, H_k, are related to the parameters X_i, X_k, by

$$\theta_i = \frac{X_i - X_{im}}{\Delta X_i}, \qquad H_k = \frac{X_k - X_{km}}{\Delta X_k}. \tag{11}$$

(The symbol θ_i is chosen to represent one homogeneous parameter, instead of H_i, to emphasize the fact that in this case one is concerned with a rotation.) From these definitions it follows that both homogeneous parameters increase in the same sense as the original parameters: θ_i increases always clockwise, H_k increases to the right.

The connection between ordinary and homogeneous parameters in a harmonic transformer is illustrated in Fig. 4·6. The arc of the angle of travel ΔX_i, scaled evenly clockwise from 0 to 1, permits direct reading of θ_i. The projection of that arc on a straight line perpendicular to the zero line SO, scaled evenly from 0 to 1, from left to right, permits direct reading of H_k. Any line parallel to OS passes through corresponding values of θ_i and H_k. The correlation of values of H_k to those of θ_i is unique so long as $\Delta X_i < 360°$; the converse correlation may be double-valued in some cases, as is illustrated by Figs. 4·6(*b*) and 4·6(*c*).

From the definition of homogeneous parameters and from Eq. (11) it is evident that, always,

$$H_k = \frac{\sin (X_{im} + \theta_i \Delta X_i) - (\sin X_i)_{\min}}{(\sin X_i)_{\max} - (\sin X_i)_{\min}} \tag{12}$$

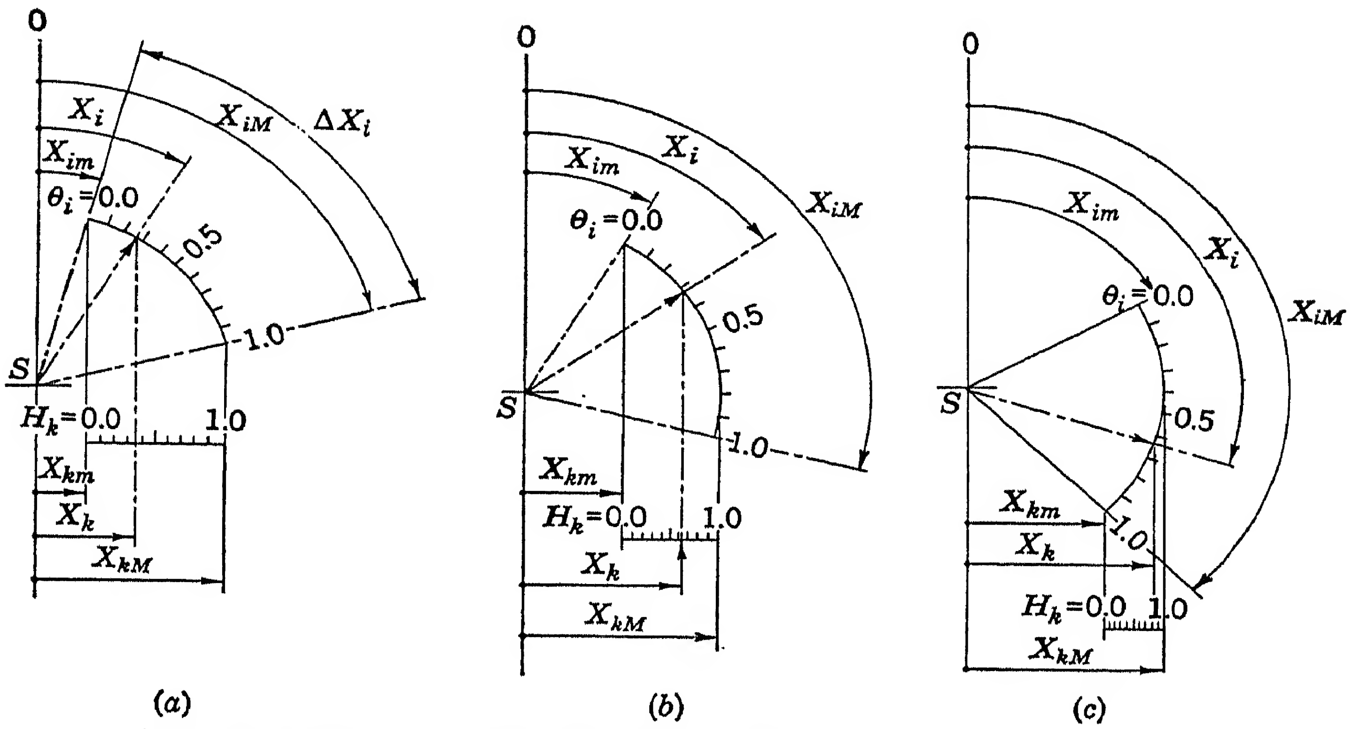

FIG. 4·6.—Ideal harmonic transformer with homogeneous parameters. (a) $(\sin X_i)_{\max} = \sin X_{iM}$. (b) $(\sin X_i)_{\max} = 1$. (c) $(\sin X_i)_{\min} = \sin X_{iM}$.

Special forms of this relation, applicable in cases of the types illustrated in Figs. 4·6(a), 4·6(b), 4·6(c), respectively, are as follows:

$$H_k = \frac{\sin (X_{im} + \theta \, \Delta X_i) - \sin X_{im}}{\sin X_{iM} - \sin X_{im}} \tag{13a}$$

$$H_k = \frac{\sin (X_{im} + \theta_i \Delta X_i) - \sin X_{im}}{1 - \sin X_{im}} \tag{13b}$$

$$H_k = \frac{\sin (X_{im} + \theta_i \Delta X_i) - \sin X_{iM}}{1 - \sin X_{iM}}. \tag{13c}$$

4·4. Tables of Harmonic-transformer Functions.—The use of harmonic transformers as parts of complex linkages is so extensive and the design problem is so greatly simplified by the use of homogeneous parameters that it is very convenient to have available a fairly complete table of the functions appearing in Eq. (13). Table A·1 gives H_k for $\theta_i = 0.0$, 0.1, 0.2, · · · 0.9, 1.0, and for $\Delta X_i = 40°$, 50°, · · · 140°. Smaller values of ΔX_i are of little interest, since with small angular travel the errors due to mechanical play become relatively important, and other devices can serve as well for mechanization of the corresponding nearly linear functions $H_k(\theta_i)$. Two facing pages are required for each value of

ΔX_i. Columns of values of H_k are grouped in pairs in a way intended to facilitate the calculation of structural error functions, as discussed in Sec. 4·5. The first of these columns has the corresponding values of X_{im} and X_{iM} indicated at the top, and is tabulated with θ_i (indicated to the left) increasing downward. The second column has the values of X_{im} and X_{iM} indicated at the bottom, and is tabulated with θ_i (indicated at the right) increasing upward. The associated columns correspond to harmonic transformers with $X_{im} \leqq X_i \leqq X_{iM}$ and with

$$(90° - X_{iM}) \leqq X_i \leqq (90° - X_{im}),$$

respectively; the significance of this and of other features of the table which are not of importance at this point will be explained in Sec. 4·5.

Table A·2 gives θ_i for $H_k = 0.0, 0.1, 0.2, \cdots 0.9, 1.0$, and for the same ΔX_i as Table A·1. The arrangement is simple and should require no explanation here. Only single-valued relationships between H_k and θ_i are tabulated, since the table is intended for use when H_k is the input variable; all regions that include a point with infinite $d\theta_i/dH_k$ may be excluded.

In using Tables A·1 and A·2 to mechanize a tabulated function with a pronounced sinusoidal character, the function should first be expressed in homogeneous variables. We shall call the homogeneous input variable h_r, the homogeneous output variable h_s, in order to avoid any commitment as to which is to be the angular parameter in the mechanization.

Next, there should be tabulated in a column the values of the output variable h_s, for $h_r = 0.0, 0.1, 0.2, \cdots 1.0$, making such interpolations as may be necessary.

It remains only to compare this column of numbers with those in Tables A·1 and A·2. One can easily find which of these columns gives the best fit to the given set of numbers; each column, it is important to note, may be read either up or down. This determines the best values of X_{im} and X_{iM} for the harmonic transformer, to within 10°; by interpolation one may fix these values even more precisely. The remainder of the design process is then trivial.

If the best fit is found in Table A·1, the output variable h_s is being identified with H_k; the output terminal of the mechanization will be the slide, the input terminal the crank. If the best fit is found in Table A·2, the reverse is true.

Suppose that the best fit is found in Table A·1, and that, in reading the corresponding columns, h_r and θ_i increase together. Then one has $h_r = \theta_i$, $h_s = H_k$. Knowing X_{im} and X_{iM}, one can construct scales of θ_i and H_k as described in the preceding section; these are the required scales of h_r and h_s, which one can recalibrate in terms of the original variables, if this should be desired.

If the best fit is found in Table A·1, but correspondence of the columns requires that they be read in such directions that h_r decreases as θ_i increases, then $1 - h_r = \theta_i$, $h_s = H_k$. The h_r-scale thus differs from the θ_i-scale only in that h_r increases to the left instead of the right; the rest of the construction is as before.

If the best fit is found in Table A·2, one has $h_s = \theta_i$, $h_r = H_k$, if h_s and θ_i increase together, and otherwise $1 - h_s = \theta_i$, $h_r = H_k$.

In the operational language introduced in Chap. 3 this process may be described as follows: A functional operator $(h_s|h_r)$ is given, and there is sought a functional operator $(H_k|\theta_i)$ or $(\theta_i|H_k)$ of a harmonic transformer which transforms into the given operator $(h_s|h_r)$ when the pair of variables (h_r, h_s) is transformed into the pair of parameters (θ_i, H_k) or (H_k, θ_i) through a direct or complementary identification.

When the tables are employed it is useful to make graphs of operators and sketches of mechanisms in order to prevent mistakes. It is recommended that the H_k-scale run always from left to right, that the zero line for X_i be directed upward, and that the scale for θ_i increase clockwise, as in Fig. 4·6.

Example: Use an ideal harmonic transformer to mechanize the relation

$$x_2 = \tan x_1 \tag{14}$$

with the range of the input variable x_1 from 0° to 50°. The homogeneous variables are

$$h_r = \frac{x_1}{50°}, \qquad h_s = \frac{x_2}{\tan 50°}. \tag{15}$$

Table 4·1 gives the relation of h_s to h_r in tabular form.

TABLE 4·1.—$x_2 = \tan x_1$, $0 \leq x_1 \leq 50°$, IN HOMOGENEOUS VARIABLES

h_r	h_s
0.0	0.0000
0.1	0.0734
0.2	0.1480
0.3	0.2248
0.4	0.3054
0.5	0.3913
0.6	0.4844
0.7	0.5875
0.8	0.7041
0.9	0.8391
1.0	1.0000

In seeking a corresponding column in the tables, we need examine only those which show no maximum. In such cases the first and last values are always 0 and 1; every such column matches the given column at the two ends.

Consider first Table A·1. Fixing on a value of ΔX_i, we seek a column that gives a match at the middle as well as at the ends; for example, with $\Delta X_i = 70°$ the best match is obtained for $X_{im} = -70°$, $X_{iM} = 0°$. However, this column contains values that are too small at small θ_i, too large at large θ_i. Repeating this process for smaller ΔX_i, one obtains a better over-all fit, but the improvement is slight; one must either use very small values of ΔX_i or tolerate errors of over 2 per cent of the total range.

Next we examine Table A·2. Again the best match is obtained for relatively small ΔX_i—a consequence of the nearly linear character of the tangent function in the given range. Here, however, a much better match is possible. Comparing with the given h_s the values of θ_i shown in Table A·2 for $X_{im} = 30°$, $X_{iM} = 70°$ and for $X_{im} = 35°$, $X_{iM} = 75°$, one finds the differences shown in Table 4·2.

TABLE 4·2.—VALUES OF h_s-θ_i

H_k	$X_{im} = 30°$ $X_{iM} = 70°$	$X_{im} = 35°$ $X_{iM} = 75°$	$X_{im} = 31.5°$ $X_{iM} = 71.5°$
0.0	0.0000	0.0000	0.0000
0.1	−0.0004	0.0036	0.0008
0.2	−0.0023	0.0056	0.0001
0.3	−0.0050	0.0065	−0.0015
0.4	−0.0076	0.0072	−0.0032
0.5	−0.0097	0.0080	−0.0044
0.6	−0.0106	0.0095	−0.0046
0.7	−0.0095	0.0120	−0.0030
0.8	−0.0060	0.0152	0.0003
0.9	−0.0009	0.0160	0.0042
1.0	0.0000	0.0000	0.0000

Linear interpolation between these columns shows that with $X_{im} = 31.5°$, $X_{iM} = 71.5°$ the difference between h_s and θ_i remains less than 0.005; an ideal harmonic transformer with these constants would have a structural error everywhere less than 0.5 per cent of the travel.

Figure 4·7 shows the harmonic transformer thus designed, with functional scales for $h_s = H_k$ and $h_r = \theta_i$. The travel, ΔX_k, can be given any desired value by proper choice of R:

$$\Delta X_k = R(\sin 71.5° - \sin 31.5°) = 0.4258R. \tag{16}$$

It is interesting to note that in this example the angular variable x_1 of Eq. (14) has been mechanized as a slide displacement, the linear variable x_2 as an angular displacement, whereas in a constructive computer the reverse would be the case.

In this design procedure we have treated the harmonic transformer as ideal. To construct it as nonideal would introduce an additional structural error, δX_k, described by Eq. (4)—an error that can be made sufficiently small by making the link L very long and by so placing the center line of the slide as to reduce the maximum value of the angle ϵ as much as possible. In general it is better to make positive use of the term δX_k, so choosing the design constants that δX_k tends to cancel out the structural error δh_k of the ideal-harmonic-transformer component of the mechanism. In the present case this may seem hardly worth the trouble, as the fit obtained with the ideal transformer is very good. However, it is to be

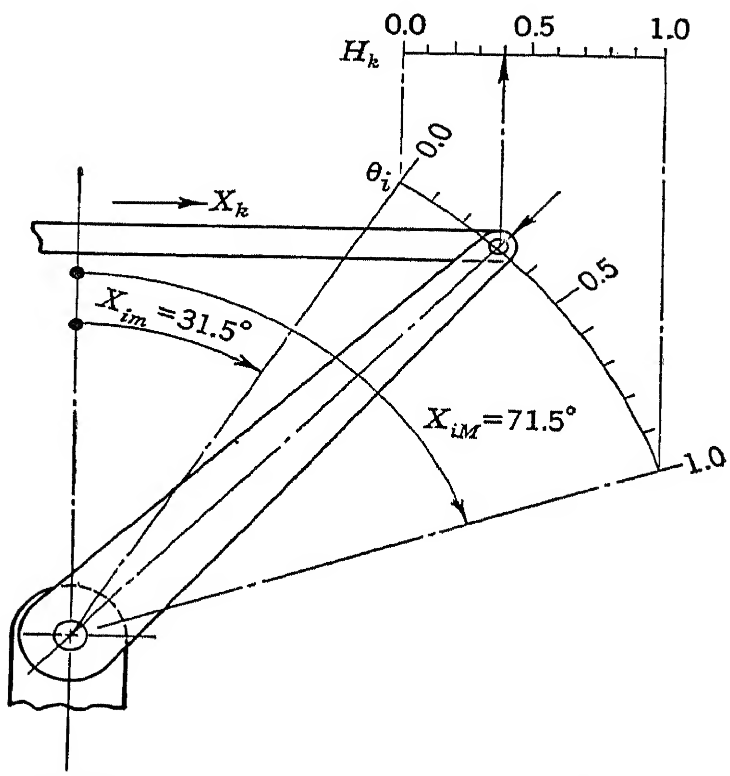

FIG. 4·7.—Harmonic transformer mechanizing $X_2 = \tan X_1$, $0° < X_1 < 50°$. A better design is shown in Fig. 4·12.

noted that this design is unsatisfactory in that the angular travel ΔX_i is rather small. In practice, it would be better to employ a nonideal transformer with large angular travel, keeping the total structural error small by judicious choice of L and the slide position (Fig. 4·12). The required design technique is discussed in the next sections.

4·5. Total Structural Error of a Nonideal Harmonic Transformer.—In finding a harmonic transformer to mechanize a given relation,

$$h_k = (h_k|h_i) \cdot h_i, \tag{17}$$

one begins, as already described, by finding an ideal harmonic transformer that gives an approximate fit. Then if θ_i is identified with h_i, H_k can also be identified with h_k, except for the small structural error δh_k:

$$H_k = h_k + \delta h_k. \tag{18}$$

If the transformer to be used is nonideal, its output parameter will be not H_k but H'_k. Representing by δH_k the change in output arising from the nonideal character of the transformer, we write

$$H'_k = H_k + \delta H_k. \tag{19}$$

The complete mechanism then has a structural-error function

$$\delta h'_k = H'_k - h_k = \delta H_k + \delta h_k; \tag{20}$$

it is this error that should be reduced to tolerable limits over the whole range of operation.

A nonideal harmonic transformer has been sketched in Fig. 4·2. Of the four design constants, X_{im} and X_{iM} characterize the ideal-harmonic-transformer component and determine the form of δh_k; L/R and W/R affect only the form of δH_k. It is of course impossible in general to make $\delta h'_k$ vanish identically by any choice of these parameters. Ideally, one would manipulate all four parameters in order to make $\delta h'_k$ everywhere satisfactorily small, without regard to the resulting magnitude of δH_k and δh_k. An easier technique is to make δh_k as small as possible by choice of X_{im} and X_{iM}, and then to choose L/R and W/R so as to minimize $\delta h'_k$; however, one can often arrive at more satisfactory designs, and even appreciably reduce the over-all error, by some other choice of X_{im} and X_{iM}.

4·6. Calculation of the Structural-error Function δH_k of a Nonideal Harmonic Transformer.—In designing harmonic transformers it is important to have a quick, efficient way to compute the structural-error function δH_k. Use of Eq. (4) is neither quick nor well adapted for work with homogeneous parameters; better methods to be described here and in Sec. 4·7 depend upon reference to Table A·1. The discussion will be illustrated by Fig. 4·8, which shows a harmonic transformer with alternative positions for the link L, extending from the crank toward the left or toward the right. Here, and throughout the discussion that follows, the unit of length, in which all dimensions are stated, is taken to be the length of the H_k-scale; thus, $\Delta X_k = 1$. As before, we consider the harmonic transformer in its basic position, with θ_i increasing clockwise, the zero for X_i vertically upward, and scales H_k increasing from left to right.

The change from the ideal harmonic transformer (scale H_k) to the nonideal one (scale H'_k) will be traced through two steps.

First, the H_k-scale may be shifted bodily to the right or left by a distance L. On this scale, shown in Fig. 4·8 above the slide, the reading opposite the pointer will be H_k, modified by an error

$$DH_k = \pm|L|(1 - \cos\epsilon). \tag{21}$$

The sign of this error depends only on whether the crank extends to the right or to the left. Taking L as positive when the link extends toward the left, negative when it extends toward the right, one has always

$$DH_k = L\,(1 - \cos \epsilon). \tag{22}$$

As H_k changes from zero to one, $H_k + DH_k$ changes between limits which are in general not zero and one:

$$(H_k + DH_k)_{\min} \leqq H_k + DH_k \leqq (H_k + DH_k)_{\max}; \tag{23}$$

thus $H_k + DH_k$ is not in general a homogeneous parameter.

As the second step, the $H_k + DH_k$-scale is replaced by the homogenized H'_k scale, shown in Fig. 4·8 below the slide:

$$H'_k = \frac{H_k + DH_k - (H_k + DH_k)_{\min}}{(H_k + DH_k)_{\max} - (H_k + DH_k)_{\min}}. \tag{24}$$

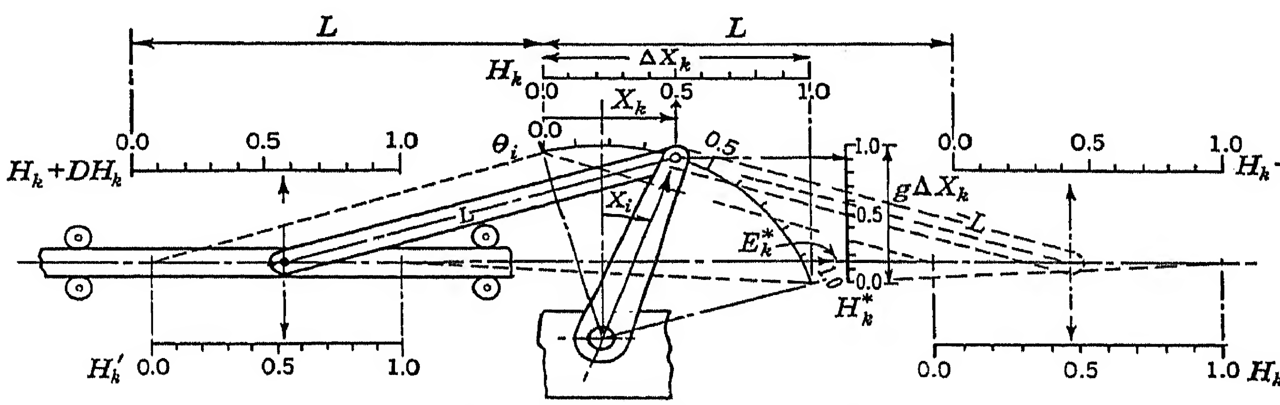

FIG. 4·8.—Notation used in harmonic transformer design.

When DH_k is reasonably small the maximum value of $H_k + DH_k$ will occur at essentially the same θ_i as the maximum of H_k—that is, when $H_k = 1$. One can then write

$$(H_k + DH_k)_{\max} \approx 1 + (DH_k)_1, \tag{25}$$

and similarly

$$(H_k + DH_k)_{\min} \approx (DH_k)_0, \tag{26}$$

$(DH_k)_0$ and $(DH_k)_1$ being the values of DH_k for H_k equal to 0 and 1 respectively. As an approximation good enough for all preliminary calculations one has then

$$H'_k \approx \frac{H_k + DH_k - (DH_k)_0}{1 + (DH_k)_1 - (DH_k)_0}. \tag{27}$$

To compute DH_k, we observe that if Y_k is the distance above the slide center line of the pivot between L and R, then

$$\sin \epsilon = \frac{Y_k}{L} \tag{28}$$

and

$$DH_k = L\left[1 - \left(1 - \frac{Y_k^2}{L^2}\right)^{1/2}\right]. \tag{29}$$

When ϵ is small

$$DH_k \approx \frac{Y_k^2}{2L}. \tag{30}$$

The quantity Y_k is conveniently found as a function of θ_i by use of Table A·1, by taking advantage of the special relationship of associated columns of that table. The relationship of the corresponding harmonic trans-

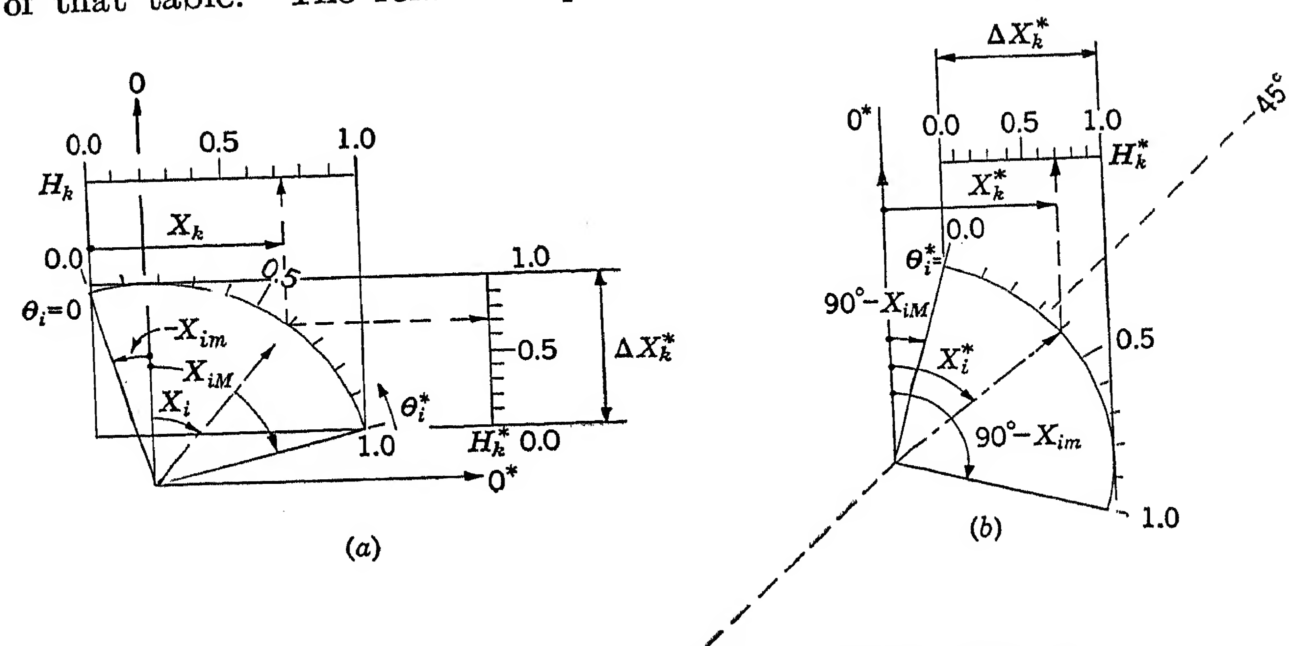

FIG. 4·9.—Harmonic transformers associated in Table A·1.

formers is illustrated in Fig. 4·9. The first transformer (parameters X_i, X_k; θ_i, H_k) operates through the range

$$X_{im} \leqq X_i \leqq X_{iM}$$

($X_{im} = -15°$, $X_{iM} = 75°$ in Fig. 4·9*a*). The second transformer (parameters X_i^*, X_k^*; θ_i^*, H_k^*) operates through the range

$$X_{im}^* = 90° - X_{iM} \leqq X_i^* \leqq X_{iM}^* = 90° - X_{im}$$

($X_{im}^* = 15°$, $X_{iM}^* = 105°$ in Fig. 4·9*b*). Now it will be observed that if Fig. 4·9*b* is reflected in the line $X_i^* = 45°$ and superimposed on Fig. 4·9*a*, the angular scales will then coincide, but with $\theta_i^* = 1 - \theta_i$. The H_k^*-scale, however, becomes a vertical scale, as compared with the horizontal H_k-scale. The entries in a section of Table A·1 may then be interpreted as follows: For a harmonic transformer with limits on X_i as given at the *top*, the four entries in each row, from *left to right*, correspond to (1) θ_i for some index point P on the angular scale, (2) H_k, which measures the horizontal displacement of that point to the right of a vertical

reference line, (3) H_k^*, which measures the displacement of the same point upward from a horizontal reference line (though in different units, since the H_k^*-scale is not in general of unit length), and (4) $\theta_i^* = 1 - \theta_i$. If the limits on X_i are those given at the *bottom* of the section, the entries in each row have the same meaning if they are taken in order from *right to left*.

The quantity $H_k(= X_k)$ measures the actual distance of the point P from the vertical reference line, since the H_k-scale is one unit long by definition. The length of the vertical scale is

$$g = \frac{(\cos X_i)_{\max} - (\cos X_i)_{\min}}{(\sin X_i)_{\max} - (\sin X_i)_{\min}}; \tag{31}$$

hence the actual distance of the point P from the horizontal reference line is

$$X_k^* = gH_k^*. \tag{32}$$

Values of g are given in Table A·1, in the same line with those of X_{im} and X_{iM} and in the same column with the values of H_k^*.

Returning now to the computation of Y_k, we define E_k^* as the value on the H_k^*-scale at the point where the slide center line intersects it. In Fig. 4·8, E_k^* lies on the calibrated part of the scale. This is not necessarily so; E_k^* is a parameter in the design which may be assigned negative values, or values greater than one. In any case

$$Y_k = g(H_k^* - E_k^*). \tag{33}$$

It is convenient to specify a nonideal harmonic transformer by giving X_{im}, X_{iM}, E_k^*, and L. Calculation of its structural-error function for a series of values of θ_i or H_k then requires reading from Table A·1 the corresponding values of H_k^*, followed by computation of Y_k' by Eq. (33), DH_k by Eq. (29) or (30) (according to the accuracy required), H_k' by Eq. (27), and finally δH_k by Eq. (19). An illustrative calculation will be found in Table 4·5. This procedure is quick and easy if E_k^* and L are known, but when it is desired to determine the approximate form of δH_k for a considerable series of values of E_k^* and L, or to find required values of E_k^* and L, the method to be described in the next section is to be preferred.

4·7. A Study of the Structural-error Function δH_k.—For a general investigation of the structural-error function δH_k or for a preliminary (and usually final) choice of E_k^* and L in the process of designing a nonideal harmonic transformer, it is sufficiently accurate to use Eq. (30) in computing DH_k, and to assume that

$$|DH_k - (DH_k)_0| \ll 1. \tag{34}$$

To this approximation δH_k has a simple dependence on E_k^* and L which facilitates its computation for a series of values of these parameters, or,

conversely, the finding of values of E_k^* and L which give δH_k a desired form and magnitude.

Expanding H_k', as given by Eq. (27), in powers of the small quantity $(DH_k)_1 - (DH_k)_0$, and neglecting terms of the second order of smallness, one finds

$$H_k' \approx H_k + [DH_k - (DH_k)_0] + H_k[(DH_k)_0 - (DH_k)_1] \tag{35}$$

and

$$\delta H_k \approx [DH_k - (DH_k)_0] + H_k[(DH_k)_0 - (DH_k)_1]. \tag{36}$$

This approximation to δH_k, like the function itself, vanishes when $H_k = 0$ or 1.

By Eqs. (30) and (33),

$$DH_k \approx \frac{g^2}{2L}(H_k^* - E_k^*)^2. \tag{37}$$

When this is introduced into Eq. (36) the quadratic terms in E_k^* cancel, and one finds

$$\delta H_k \approx \frac{g^2}{2L}[f_1(\theta_i) + E_k^* f_2(\theta_i)], \tag{38}$$

where $f_1(\theta_i)$ and $f_2(\theta_i)$ depend only on the parameters X_{im} and X_{iM} of the harmonic transformer. With $(H_k^*)_0$ and $(H_k^*)_1$ the values of H_k^* when H_k has the values 0 and 1, respectively,

$$f_1(\theta_i) = H_k^{*2} - (H_k^*)_0^2 + H_k[(H_k^*)_0^2 - (H_k^*)_1^2], \tag{39}$$
$$f_2(\theta_i) = -2\{H_k^* - (H_k^*)_0 + H_k[(H_k^*)_0 - (H_k^*)_1]\}. \tag{40}$$

Knowing the form of $f_1(\theta_i)$ and $f_2(\theta_i)$, one can easily compute δH_k for a large series of values of L and E_k^*.

To this approximation the magnitude of the structural-error function varies inversely with L, but its form is determined entirely by E_k^*. The possible range in forms is easily investigated by computing δH_k for some value of E_k^*—for example, for $E_k^* = 0$, in which case one has simply the first term of Eq. (38)—and then adding to this the function $f_2(\theta_i)$ in different proportions.

Although $f_2(\theta_i)$ is easily computed by Eq. (40), it is worth while to take note of its simple analytic form. As functions of X_i, one has

$$H_k = \frac{\sin X_i - (\sin X_i)_{\min}}{(\sin X_i)_{\max} - (\sin X_i)_{\min}}, \tag{41}$$

$$H_k^* = \frac{\cos X_i - (\cos X_i)_{\min}}{(\cos X_i)_{\max} - (\cos X_i)_{\min}}. \tag{42}$$

Let X_a and X_b be the values of X_i for which $\sin X_i$ has its minimum and its maximum values, respectively. (These are not necessarily X_{im} and X_{iM}, nor are they always the angles at which $\cos X_i$ has its minimum or

maximum values.) Then on combining Eqs. (40), (41), (42), one finds, after some trigonometric manipulation, that

$$f_2 = -\frac{2\sec\left(\frac{X_a + X_b}{2}\right)}{(\cos X_i)_{\max} - (\cos X_i)_{\min}} \times \left[\cos\left(X_i - \frac{X_a + X_b}{2}\right) - \cos\left(\frac{X_b - X_a}{2}\right)\right]; \qquad (43)$$

f_2 is thus symmetric about the value of θ_i corresponding to $X_i = \dfrac{X_a + X_b}{2}$, midway between the values of θ_i for which $H_k = 0$ and $H_k = 1$; it is of the form of a sinusoid minus a constant, and vanishes for $H_k = 0$ and

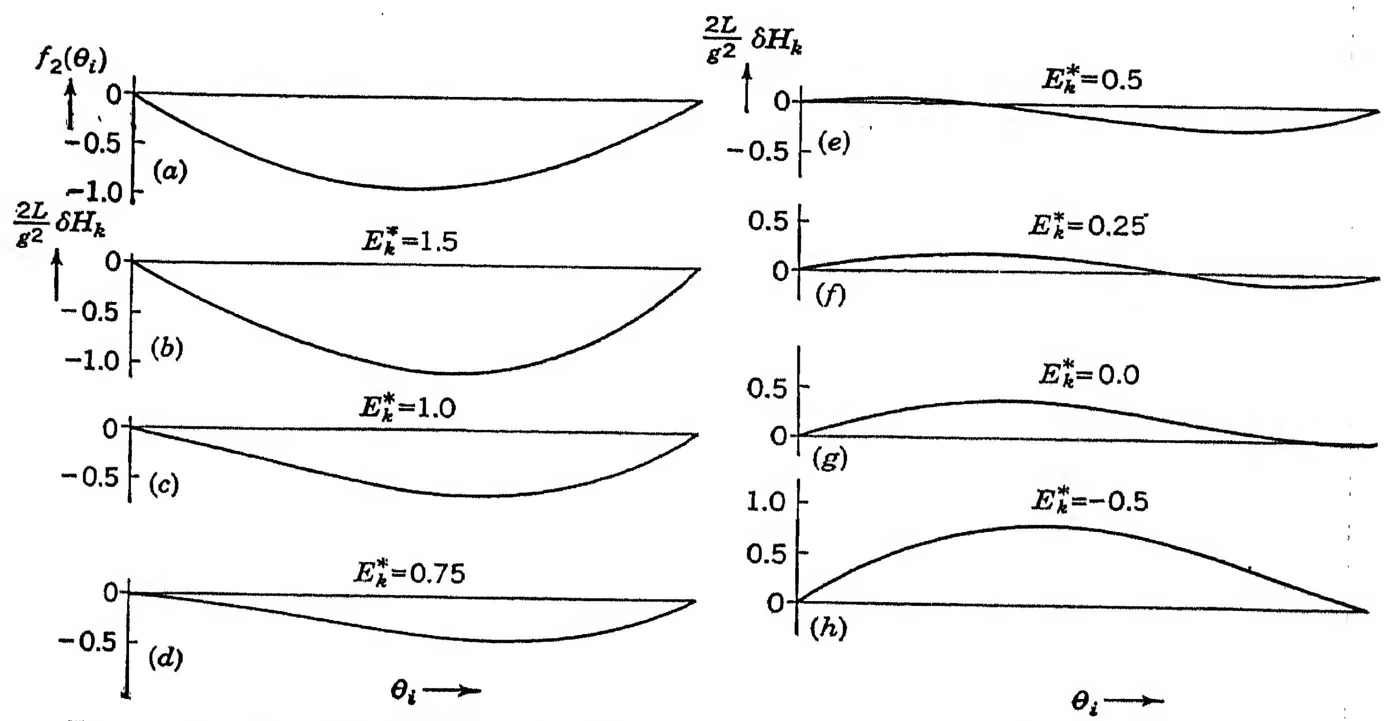

FIG. 4·10.—Structural-error functions for nonideal harmonic transformers. The functions shown are (a) $f_2(\theta_i)$, and (b) to (h) $(2L/g^2)\,\delta H_k$ for a series of values of E_k^*, when $X_{im} = -15°$, $X_{iM} = 75°$.

$H_k = 1$. Its general form is thus easily sketched without reference to Table A·1. When H_k increases monotonically with θ_i, $f_2(\theta_i)$ is symmetrical about $\theta_i = \frac{1}{2}$*, a fact which makes computation even simpler.

To illustrate the change in form of δH_k with changing E_k^* let us consider the special case of a harmonic transformer for which $-15° < X_i < 75°$. The variation of H_k with θ_i for this transformer is shown by the middle curve of Fig. 4·11. Figure 4·10 shows the form of $f_2(\theta_i)$, and of

$$\frac{2L}{g^2} \cdot \delta H_k = f_1(\theta_i) + E_k^* f_2(\theta_i) \qquad (44)$$

for a series of values of E_k^*. When E_k^* is less than -0.5 or greater than 1.5, δH_k has nearly the same form as $f_2(\theta_i)$, which is symmetrical about

$\theta_i = 0.5$. To produce a desired form of H'_k that differs from the given H_k by a symmetrical correction δH_k, one would thus choose $E_k < -0.5$ or $E_k > 1.5$; to raise the H_k curves in the center one would use a positive L (link to the left) in the first case and a negative L in the second, whereas to depress the curve in the center these orientations of the link would be reversed. To lift or depress the H_k-curves for small θ_i, with little change for θ_i near 1, $E^*_k = 0$ is an appropriate choice; to make a change near $\theta_i = 1$ but not near $\theta_i = 0$, one should take $E^*_k \approx 0.75$. With E^*_k ranging from 0.25 to 0.5 it is possible to depress one side of the curve while raising the other, and so on. These observations of course apply only to the particular harmonic transformer here considered; similar sketches would need to be made as the basis for a discussion of other cases.

The magnitude of δH_k is directly controlled by the choice of L. It will be noted however, that when $(2L/g^2)\delta H_k$ is small, as for $E^*_k \approx 0.5$, a particularly small value of L may be required in order to give δH_k a desired magnitude. In general, it is relatively difficult to depress one side of the curve $H_k(\theta_i)$ while raising the other, and one may find that an impractically small value of L is required to produce a desired effect. On the other hand, if one desires merely to reduce δH_k below some established tolerance one can with advantage make $E^*_k \approx 0.5$, since conveniently small values of L are then acceptable.

The magnitude of δH_k in typical cases is illustrated by Fig. 4·11, in which δH_k is given for three values of

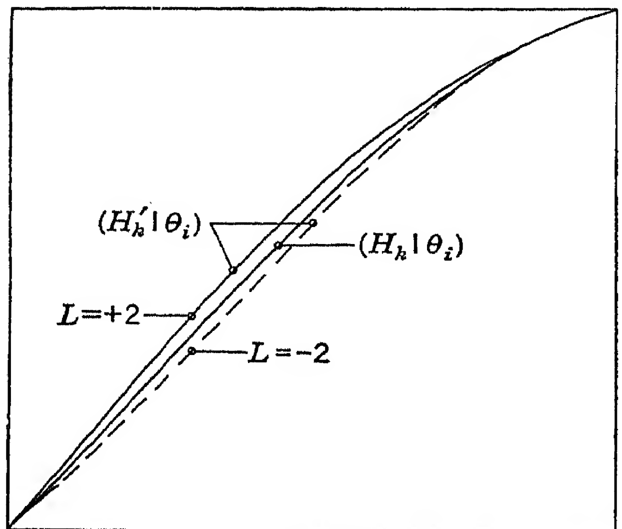

(a) $E^*_k=0.0$

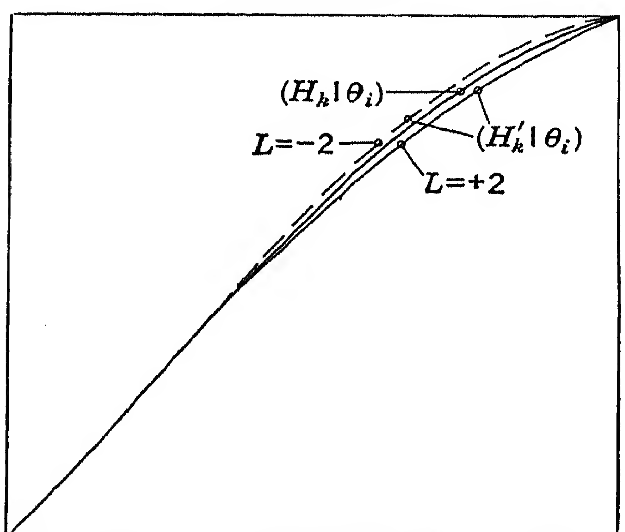

(b) $E^*_k=0.5$

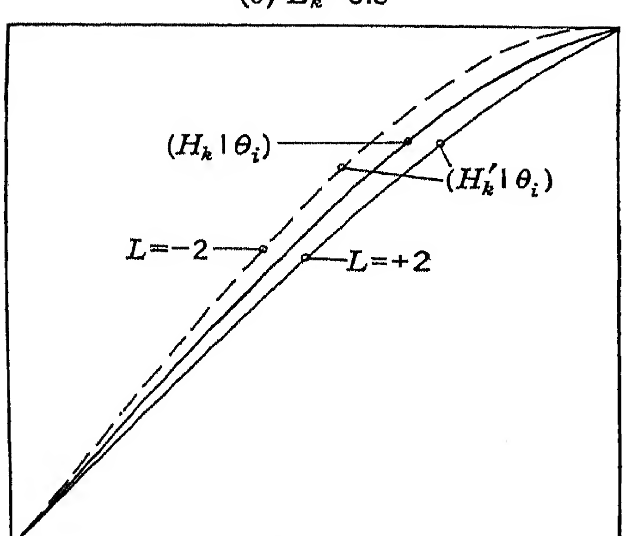

(c) $E^*_k=1.0$

FIG. 4·11.—$H_k(\theta_i)$ for nonideal harmonic transformers. $X_{im} = -15°$, $X_{iM} = 75°$, $L \pm 2$, $E_k{}^*$ as indicated.

$E_k^*(0.0, 0.5, \text{and } 1.0)$ with $L = \pm 2$. The difference between the exact calculations on which these graphs are based and approximate calculations using the results of Fig. 4·10 would not be evident to the eye. It is to be emphasized, however, that final calculations should be made using the exact formulas in all cases in which ϵ approaches 45° (a value which, for mechanical reasons, ought never to be much exceeded).

4·8. A Method for the Design of Nonideal Harmonic Transformers.—The experienced designer of nonideal harmonic transformers will find it possible to guess satisfactorily the required values of E_k^* and L, guided only by visual comparison of the H_k-curves with the desired form of H_k', and perhaps a few exploratory computations. On the other hand, a simple and straightforward design procedure can be based on the results of the preceding section. To illustrate this, we return to the problem (Sec. 4·4) of using a harmonic transformer to mechanize the relation $x_2 = \tan x_1$, for $0° < x_1 < 50°$. Here, however, we shall add the requirement that the angular travel of the transformer shall be twice as great as that previously used: $\Delta X_i = 80°$.

Despite the imposition of this additional condition, it remains true that it is best to mechanize x_1 as a linear displacement, x_2 as an angular displacement: the best fit for Table 4·1 is to be found in Table A·2, rather than in Table A·1. Since Table A·1 is to be used in the determination of E_k^* and L it is convenient to retabulate the relation of the homogeneous variables h_r and h_s for equally spaced values of the variable h_s, which is to be identified with θ_i. The result is shown in the first two columns of Table 4·3. The best fit for the relation thus expressed is to be found in Table A·1, for $X_{im} = -5°$, $X_{iM} = 75°$—the same values, of course, for which one finds in Table A·2 the best fit to Table 4·1. The fit could be improved somewhat by interpolation in the tables, the best value of X_{im} lying between $-10°$ and $-5°$. We shall not bother with this interpola-

TABLE 4·3.—COMPUTATIONS IN DESIGNING A HARMONIC TRANSFORMER

$h_s = \theta_i$	h_r	H_k	$h_r - H_k$	f_1	f_2	$(\delta H_k)_{\text{approx.}}$	$(\epsilon)_{\text{approx.}}$	$(\epsilon)_{\text{exact}}$
0.0	0.0000	0.0000	0.0000	0.0000	0.0000	0.0000	0.0000	0.0000
0.1	0.1359	0.1325	0.0034	0.1378	−0.2701	0.0048	0.0014	0.0018
0.2	0.2683	0.2640	0.0043	0.2225	−0.4858	0.0051	0.0008	0.0010
0.3	0.3934	0.3919	0.0015	0.2565	−0.6433	0.0015	0.0000	0.0000
0.4	0.5097	0.5139	−0.0042	0.2465	−0.7387	−0.0049	−0.0007	−0.0012
0.5	0.6158	0.6274	−0.0116	0.2027	−0.7708	−0.0127	−0.0011	−0.0018
0.6	0.7115	0.7304	−0.0189	0.1396	−0.7387	−0.0197	−0.0008	−0.0018
0.7	0.7967	0.8207	−0.0240	0.0724	−0.6433	−0.0240	0.0000	−0.0010
0.8	0.8726	0.8967	−0.0241	0.0173	−0.4858	−0.0233	0.0008	−0.0002
0.9	0.9401	0.9569	−0.0168	−0.0110	−0.2701	−0.0158	0.0010	0.0002
1.0	1.0000	1.0000	0.0000	0.0000	0.0000	0.0000	0.0000	0.0000

tion, but shall choose $X_{im} = -5°$, $X_{iM} = 75°$, and throw the entire burden of correcting our design on the choice of E_k^* and L. The values of H_k read from Table A·1 are shown in Column 3 of Table 4·3. The desired value of δH_k is then $h_r - H_k$, shown in Column 4 of this table.

As the next step, $f_1(\theta_i)$ and $f_2(\theta_i)$ are computed (Columns 5 and 6). By Eq. (38) we can express δH_k in terms of these functions:

$$\delta H_k = af_1(\theta_i) + bf_2(\theta_i), \tag{45}$$

where

$$a = \frac{g^2}{2L} \tag{46}$$

and

$$b = \frac{g^2 E_k^*}{2L}. \tag{47}$$

Our problem is then to make a linear combination of Columns 5 and 6 that will approximate Column 4 as well as possible. It is a simple matter to find the best fit in the sense of least rms error, but an even simpler method will suffice: we shall fit δH_k to $h_r - H_k$ exactly at two chosen points. In applying such a method some discretion is necessary as a poor choice of these points may lead to a bad over-all fit. We choose to make the fit exact at $\theta_i = 0.3$ and at $\theta_i = 0.7$, assuring a proper height for the principal maximum in δH_k and a change in sign near the correct value of θ_i. The error in the mechanization will then vanish for four nearly equally spaced values of θ_i: 0.0, 0.3, 0.7, 1.0. We require then

$$\left.\begin{aligned} 0.2565a - 0.6433b &= 0.0015, \\ 0.0724a - 0.6433b &= -0.0240. \end{aligned}\right\} \tag{48}$$

Hence

$$a = 0.1385, \qquad b = 0.0529. \tag{49}$$

By Eqs. (46) and (47),

$$\begin{aligned} E_k^* &= \frac{b}{a} = 0.382, \\ L &= \frac{g^2}{2a} = 1.788. \end{aligned} \tag{50}$$

The corresponding values of δH_k (as computed by this approximate method) appear in Column 7 of Table 4·3, and values of

$$\epsilon = \delta H_k - (h_r - H_k),$$

the residual error in the mechanization, in Column 8. The maximum error in the mathematical design thus appears to be about 0.1 per cent of the total travel. The maximum value of sin ϵ for this design is

$$(\sin \epsilon)_{\max} = \frac{g(1 - 0.382)}{1.788} = 0.243, \tag{51}$$

a sufficiently small value to assure good accuracy of the approximate formulas employed. Exact calculation of the total design error in the mechanization (last column of Table 4·3) shows that it nowhere exceeds 0.2 per cent, a highly satisfactory result. The device itself is sketched in Fig. 4·12.

If excessively large values of ϵ occur in a design thus determined, the exact values of δH_k will not be in satisfactory agreement with $h_r - H_k$. A further correction in δH_k is then necessary. This may be added to the original values of $h_r - H_k$, and the process of determining E_k^* and L carried through as before. The quantities δH_k, computed with the resulting constants by the exact formula, should now show better agreement with the desired values (the original $h_r - H_k$). Repetition of this process will usually lead to a satisfactory design, except when excessively large values

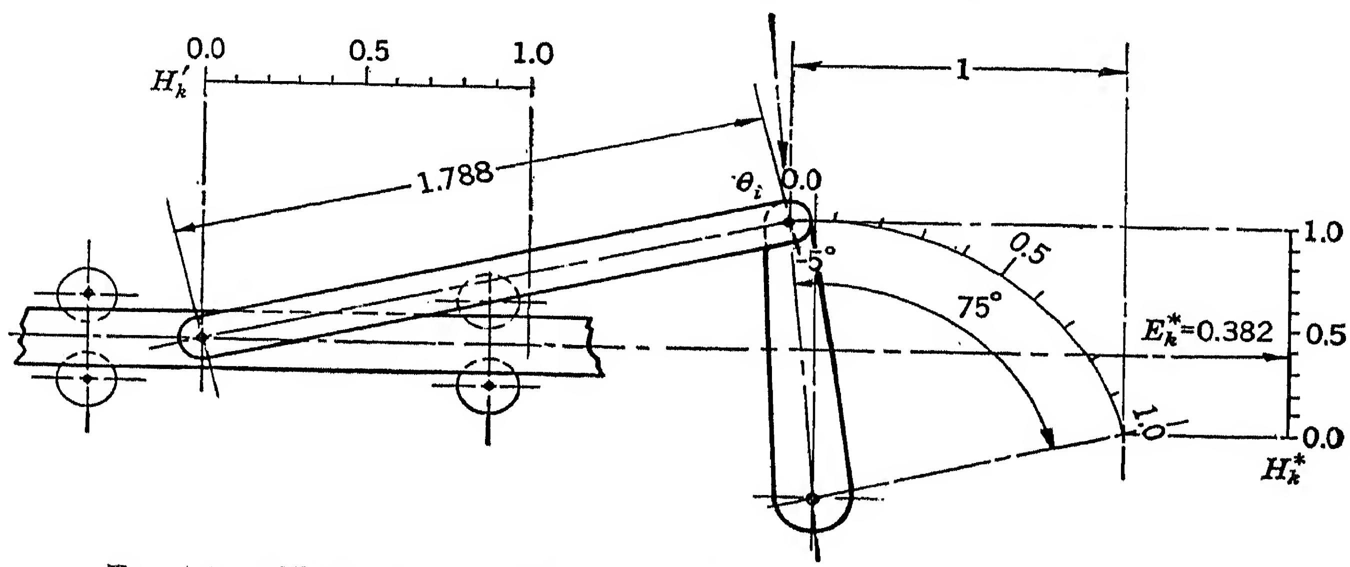

FIG. 4·12.—Harmonic transformer mechanizing $x_2 = \tan x_1$, $0° < x_1 < 50°$.

of ϵ are called for. In such cases another choice of X_{im} and X_{iM} may help, or another type of linkage may be required.

HARMONIC TRANSFORMERS IN SERIES

4·9. Two Ideal Harmonic Transformers in Series.—With a single harmonic transformer one can mechanize only a relatively narrow field of functions. These devices have also a mechanical disadvantage in that one terminal rotates or is rotated by a shaft, while the other pushes or is pushed by a slide; usually one desires that all cells in a computer have terminal motions of the same type.

As a first step in the extension of the field of mechanical functions we consider the combination of two ideal harmonic transformers into an "ideal double harmonic transformer," as shown in Fig. 4·13. This mechanical cell has satisfactory mechanical properties, with both terminals moving in straight lines. The field of functions that it can generate can be described by three independent parameters—for instance, by

ΔX_i, X_{im}, X_{jm}, where ΔX_i is the range of angular motion common to both arms of the rotating member, and X_{im} and X_{jm} are the minimum values for the angular parameters X_i and X_j, which describe the orientation of the two arms. Although a considerable variety in form of the generated function is obtainable by proper choice of these parameters, the ideal double harmonic transformer is best suited to the mechanization of monotonic functions with a mild change in curvature (as in Fig. 4·14) and functions of roughly sinusoidal character (as in Fig. 4·16).

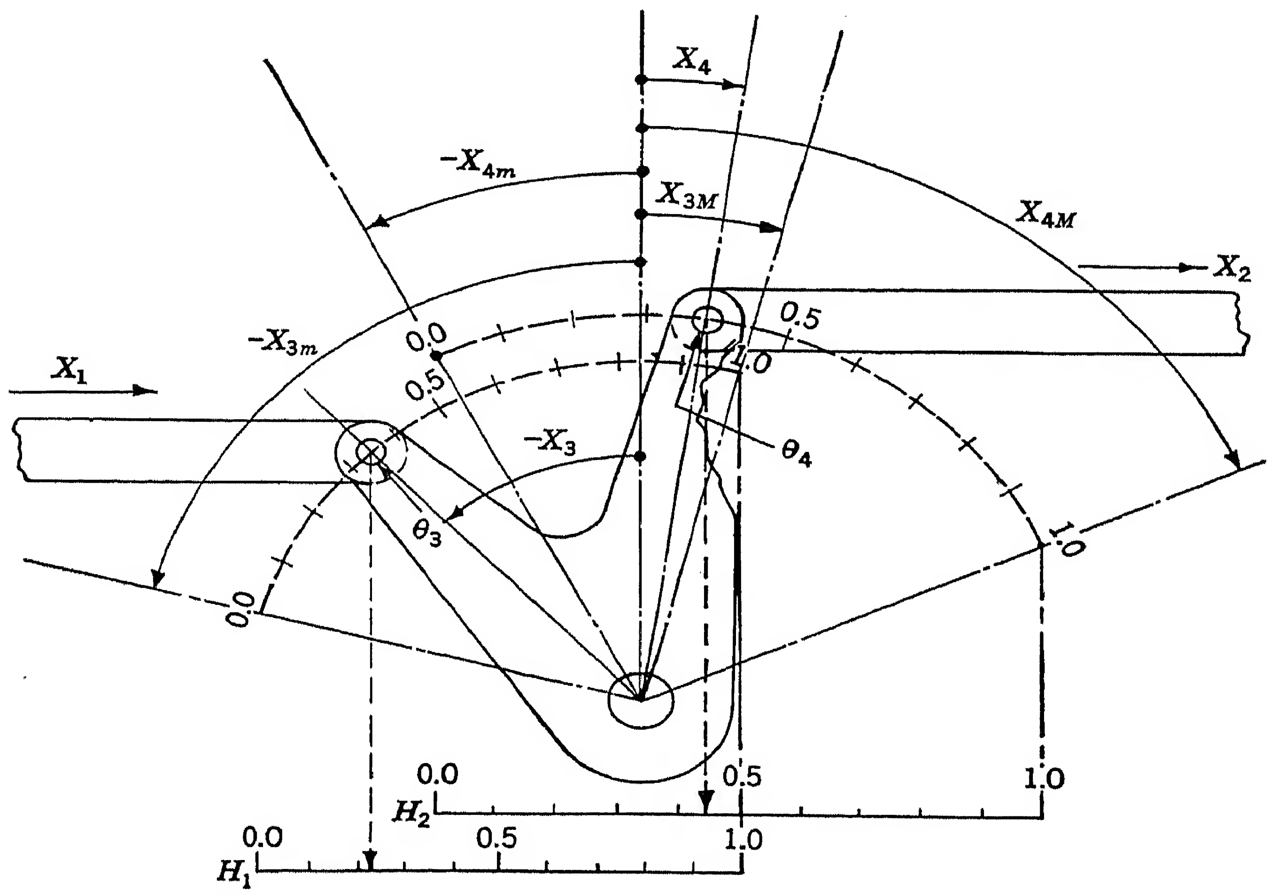

FIG. 4·13.—Ideal double harmonic transformer.

Mechanically, the action of the double harmonic transformer may be thus described: The input parameter X_1 is transformed into a rotary output parameter X_3 by the first harmonic transformer; this rotation is imparted to a second harmonic transformer, for which it serves as a rotary input parameter, X_4; X_4 is transformed by the second harmonic transformer into the final output parameter X_2. Symbolically, in terms of the corresponding homogeneous variables,

$$\theta_3 = (\theta_3|H_1) \cdot H_1, \tag{52}$$

$$\theta_4 = (\theta_4|\theta_3) \cdot \theta_3 = \theta_3, \tag{53}$$

$$H_2 = (H_2|\theta_4) \cdot \theta_4, \tag{54}$$

or, combining these relations,

$$H_2 = (H_2|\theta_4) \cdot (\theta_4|\theta_3) \cdot (\theta_3|H_1) \cdot H_1 = (H_2|\theta_3) \cdot (\theta_3|H_1) \cdot H_1. \tag{55}$$

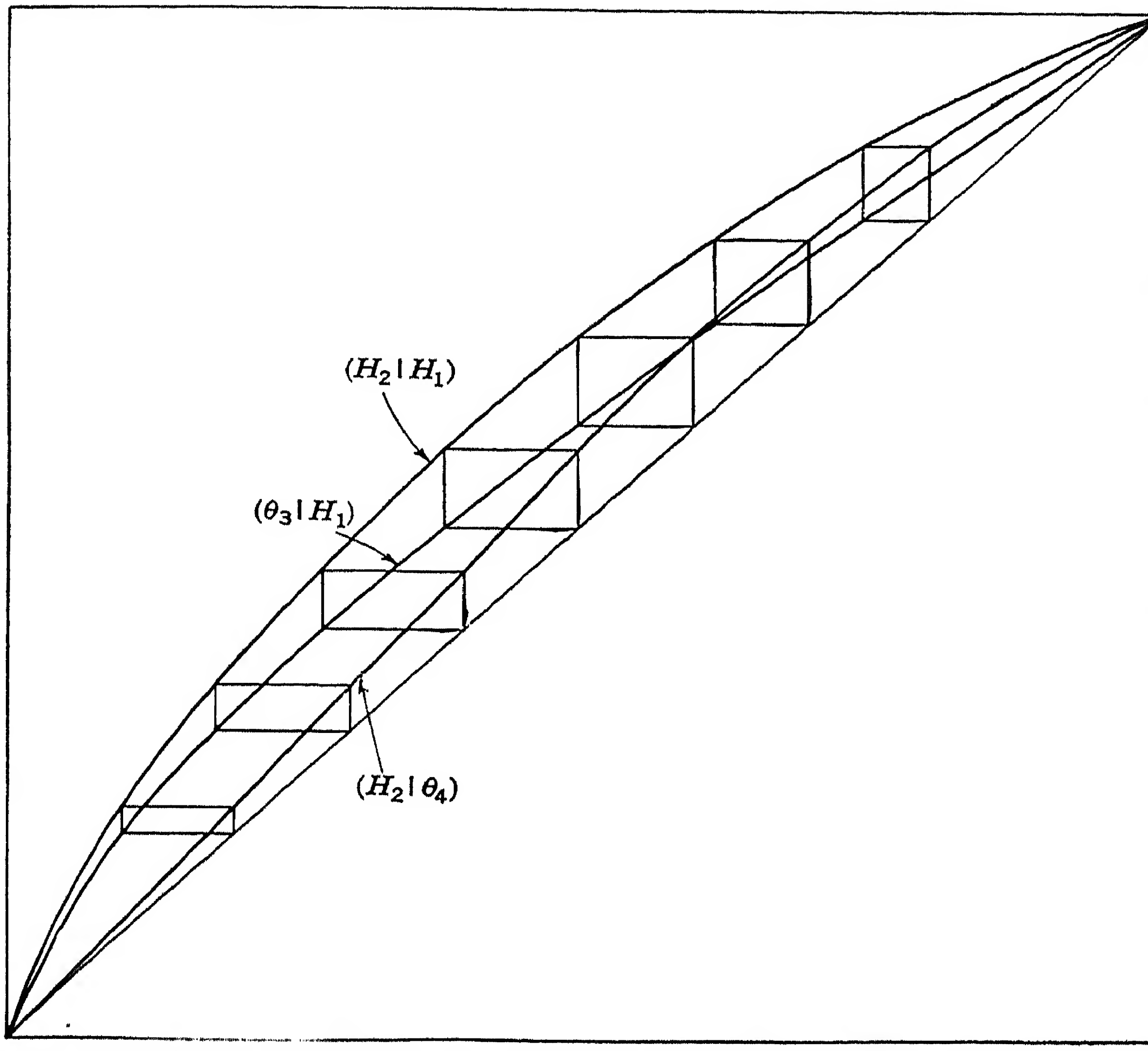

FIG. 4·14.—Graphical construction of the function generated by a double harmonic transformer (Fig. 4·13).

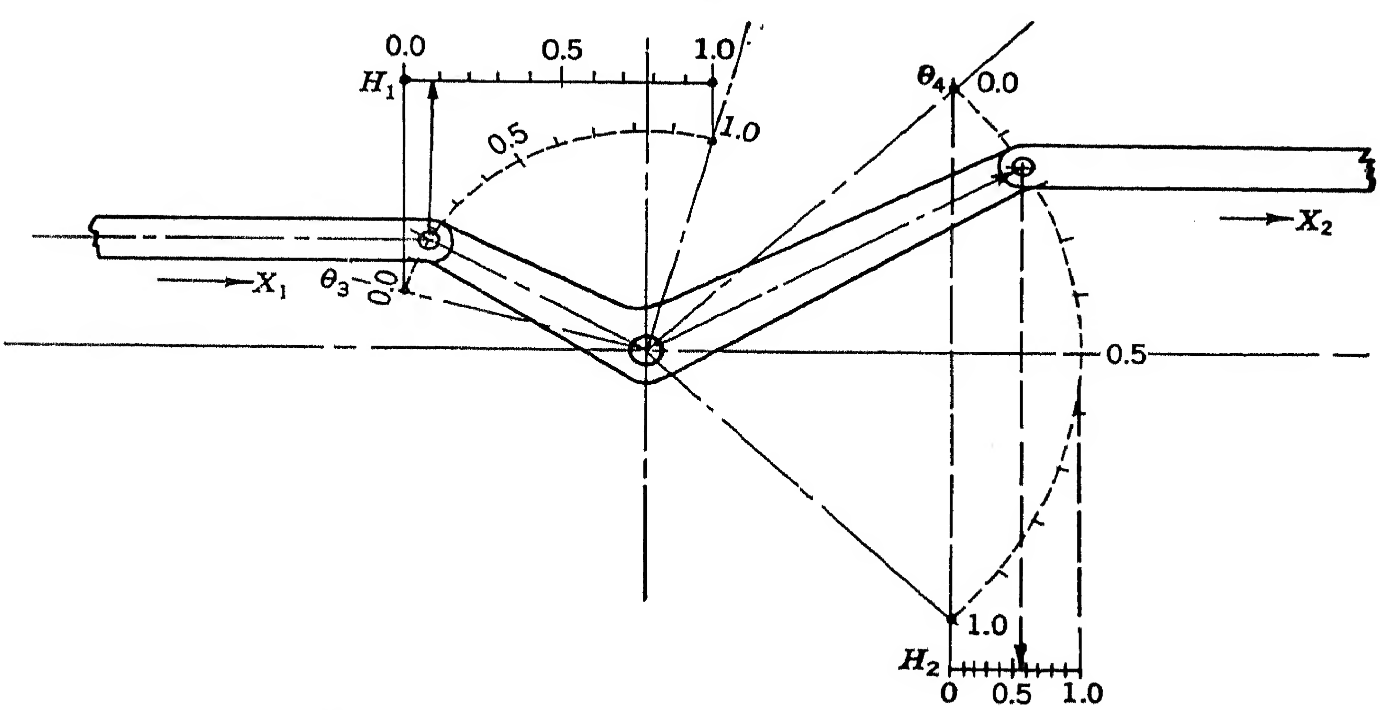

FIG. 4·15.—Ideal double harmonic transformer.

From this symbolic equation it is evident that one can find the operator for a double harmonic transformer,

$$(H_2|H_1) = (H_2|\theta_3) \cdot (\theta_3|H_1) \tag{56}$$

by the graphical multiplication of operators for the component harmonic transformers, as explained in Chap. 3. The operator $(\theta_3|H_1)$ may be obtained from Table A·2, the operator $(H_2|\theta_3)$ from Table A·1; they must of course correspond to the same value of ΔX_2.

As an example we take a double harmonic transformer (Fig. 4·13) for which $-75° \leqq X_3 \leqq 15°$; $-25° \leqq X_4 \leqq 65°$; $\Delta X_3 = \Delta X_4 = 90°$. We find in Tables A·1 and A·2 the following relations:

H_1	θ_3	θ_4	H_2
0.0	0.0000	0.0	0.0000
0.1	0.1942	0.1	0.1106
0.2	0.3207	0.2	0.2263
0.3	0.4249	0.3	0.3443
0.4	0.5175	0.4	0.4616
0.5	0.6033	0.5	0.5754
0.6	0.6849	0.6	0.6828
0.7	0.7641	0.7	0.7813
0.8	0.8422	0.8	0.8684
0.9	0.9204	0.9	0.9419
1.0	1.0000	1.0	1.0000

Figure 4·14 shows graphs of these two operators, and the geometric construction required for their multiplication as required by Eq. (56). The graphical representation of the product $(H_2|H_1)$ is an almost circular arc, quite different from the functions mechanizable by a single harmonic transformer.

Another typical example of two harmonic transformers in series is shown in Fig. 4·15. The travels are $\Delta X_3 = \Delta X_4 = 90°$, with

$$-75° \leqq X_1 \leqq 15°, \qquad 45° \leqq X_2 \leqq 135°.$$

The operator $(\theta_3|H_1)$ is the one used in the preceding example, and the operator $(H_2|\theta_4)$ will be found in Table A·1. These operators are plotted and their graphical multiplication indicated in Fig. 4·16. The resulting operator is represented by a deformed sinusoid with its maximum displaced to the left.

4·10. Mechanization of a Given Function by an Ideal Double Harmonic Transformer.—As the first step in mechanizing a functional relation by an ideal double harmonic transformer, it should, as usual, be expressed in homogeneous variables:

$$h_2 = (h_2|h_1) \cdot h_1, \tag{57}$$

with h_1 the input variable, h_2 the output variable. One then desires to find ideal-harmonic-transformer operators $(H_2|\theta_4)$ and $(\theta_3|H_1)$ which

correspond to the same value of ΔX_1 and which make

$$(H_2|H_1) = (H_2|\theta_3) \cdot (\theta_3|H_1) \tag{56}$$

approximate as well as possible to the given operator $(h_2|h_1)$. It is necessary for mechanical reasons, which apply whenever the slide terminal of a harmonic transformer is used as the input, that $(\theta_3|H_1)$ not

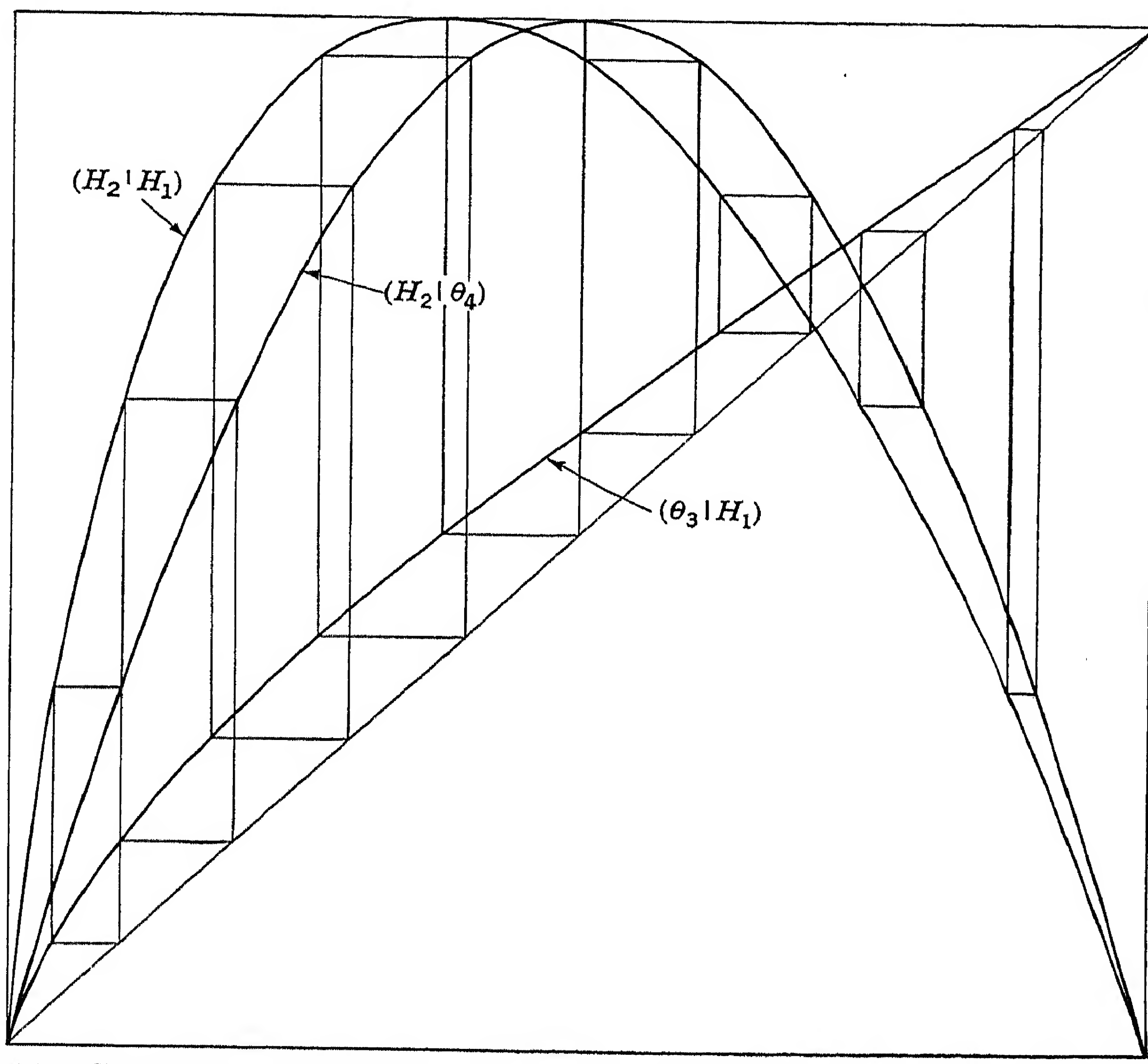

FIG. 4·16.—Graphical construction of the function generated by a double harmonic transformer (Fig. 4·15).

involve an infinity in $\dfrac{d\theta_3}{dH_1}$; we need consider only those cases for which Table A·2 is constructed, with $-90° < X_{im}, X_{iM} < 90°$.

Solution of this problem falls into two steps:

1. A preliminary solution of the problem, by which an appropriate value of ΔX_i is fixed upon and a preliminary choice of X_{3m} and X_{4m} is made.
2. Improvement of the choice of X_{3m} and X_{4m} by a process of successive approximations.

To gain a preliminary estimate of an appropriate value of ΔX_i one may fit the given curve very roughly by a section of sinusoid (by reference to Tables A·1 and A·2, or even by a visual estimate); the angular range of this section of sinusoid will be approximately the desired value of ΔX_i. The roughness of the approximation will be evident from inspection of Figs. 4·14 and 4·16, in both of which the curves correspond to $\Delta X_i = 90°$. However, the nature of the calculations required in computing double-harmonic-transformer functions is such that it is desirable to begin an attempt to fit a given function by fixing on a value ΔX_i, even when the choice must be made quite arbitrarily. By adjusting the parameters X_{3m} and X_{4m} one can then, in principle, obtain the best fit of the mechanized function to the given function consistent with the chosen ΔX_i; by repeating this for a series of values of ΔX_i one could at length determine the best value of this parameter and the best possible fit to the given function. In practice, it is not necessary to find the best fit carefully for each ΔX_i. In the preliminary calculations it is sufficient to use a simple and easily applied method of fit in choosing X_{3m} and X_{4m}, to establish an equally simple criterion for the accuracy of the over-all fit thus obtained, and to choose the best ΔX_i in the sense of this criterion. When a value of ΔX_i has been established in this way, it then becomes worth while to use more careful methods, described in Sec. 4·13, in the further adjustment of X_{3m} and X_{4m}.

We shall consider separately the quite different methods of getting a preliminary fit to monotonic functions (Sec. 4·11) and to functions with maxima and minima (Sec. 4·12).

4·11. Preliminary Fit to a Monotonic Function.—A monotonic function will in general be fitted by a monotonic function; the range of X_4 will not include either $+90°$ or $-90°$. In this case one has automatically a fit of the generated function to the given function at both ends of the range of variables. In addition, for any given ΔX_i the values of X_{3m} and X_{4m} can be so chosen that the generated function will (1) agree with the given function at any chosen pair of interior points, or (2) have the same slopes as the given function at the two ends of the range of the input variable, or (3) have the same ratios between the slopes at any three points in the range of the input variables. The first of these methods of fitting would in many cases be the most satisfactory; however, it is the most difficult to apply and will not be considered further. The second method has somewhat wider utility than the third and will be made the basis of our further discussion.

When X_{3m} and X_{4m} are so chosen that the generated function not only fits the given function at the end points but has the same slope as well, a satisfactory fit is assured throughout a more or less broad region near both ends of the range of variables. The fit will then be good everywhere

if the given function is well adapted to mechanization by an ideal harmonic transformer with the chosen value of ΔX_i. If the chosen value of ΔX_i is not appropriate, the central portion of the generated function, having been subject to no control during this simplified fitting process, may show marked differences from the given function. As an indication of the over-all accuracy of fit attained in this process, and of the appropriateness of the chosen value of ΔX_i, it is natural to take the difference between the generated and the given functions at the midpoint of the curve, $H_1 = \frac{1}{2}$; ΔX_i should then be so chosen as to minimize this difference.

The following steps can thus be used in obtaining a preliminary fit to a monotonic function:

1. Choose a value of ΔX_i, arbitrarily if there is no guide.
2. Choose X_{3m} and X_{4m} (by a method to be described below) such that the slope of the generated function has the proper values for $H_1 = 0$ and $H_1 = 1$.
3. With these values of the parameters, find the value of H_2 when $H_1 = \frac{1}{2}$. (θ_3 can be read from Table A·2, since ΔX_3 and X_{3m} are known; using this value of θ_3 to enter the column of Table A·1 that corresponds to the known values of ΔX_4 and X_{4m}, interpolate to find the required value of H_2.)
4. The difference d between this and the desired value of H_2 is taken as a measure of the over-all error in the fit.
5. Repeat the preceding steps for several other values of ΔX_i, until the trend of d as a function of ΔX_i is established.
6. Choose as the value of ΔX_i to be used in further calculations the one which minimizes $|d|$.

It remains to describe a quick and easy method for finding those values of X_{3m} and X_{4m} for which the generated function has specified terminal slopes:

$$\left(\frac{dH_2}{dH_1}\right)_{H_1=0} = S_0; \qquad \left(\frac{dH_2}{dH_1}\right)_{H_1=1} = S_1. \tag{58}$$

We note that

$$\frac{dH_2}{dH_1} = \frac{dH_2}{d\theta_3} \cdot \frac{d\theta_3}{dH_1} = \frac{\dfrac{dH_2}{d\theta_3}}{\dfrac{dH_1}{d\theta_3}}. \tag{59}$$

For mechanical reasons the input transformer must be such that

$$\theta_3 = \theta_4 = 0$$

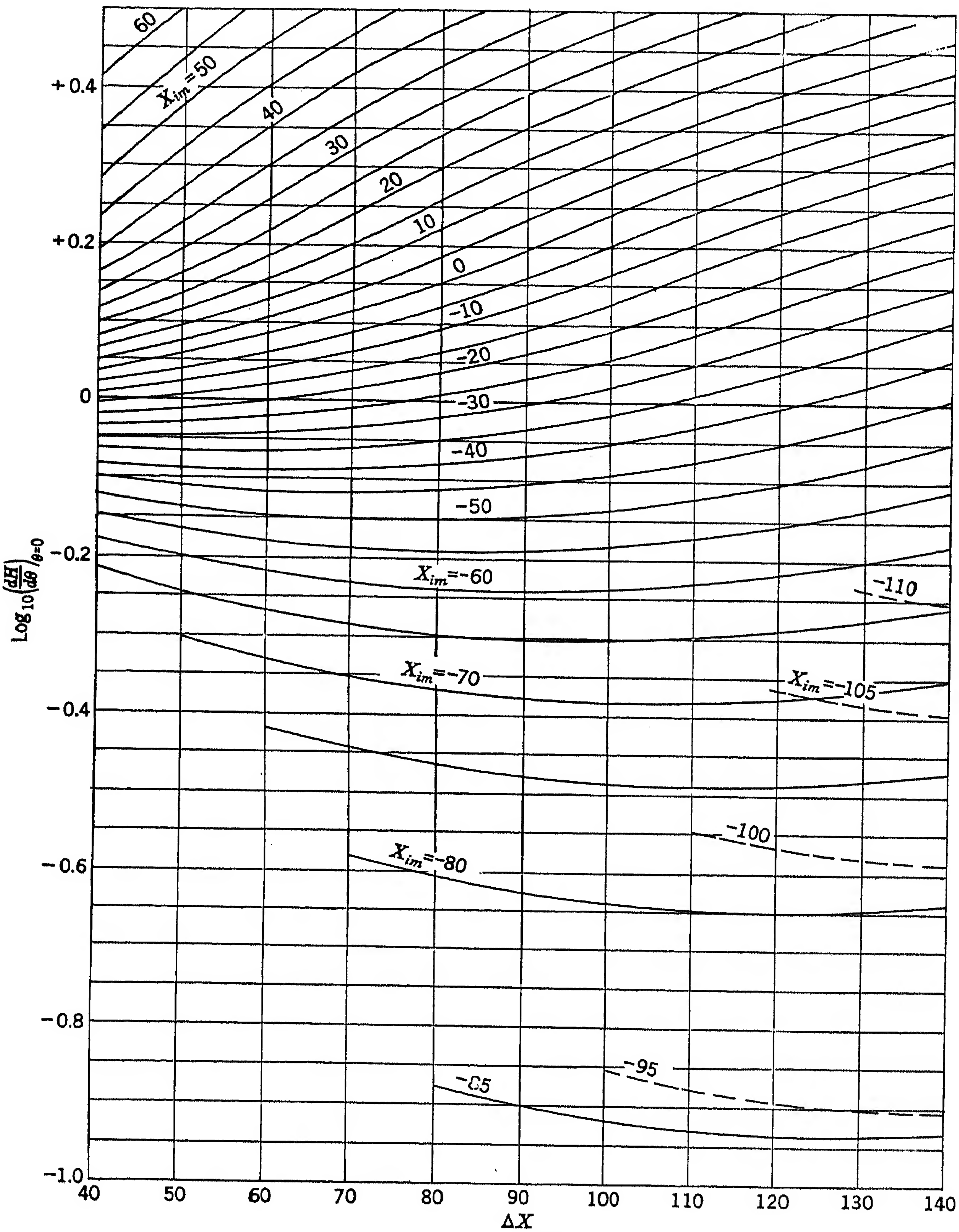

FIG. 4·17.—Logarithm of the initial slope, $\left(\frac{dH}{d\theta}\right)_{\theta=0}$, of ideal-harmonic-transformer functions, plotted against angular travel for a series of values of X_{im}. Dashed lines indicate that the initial slope is negative.

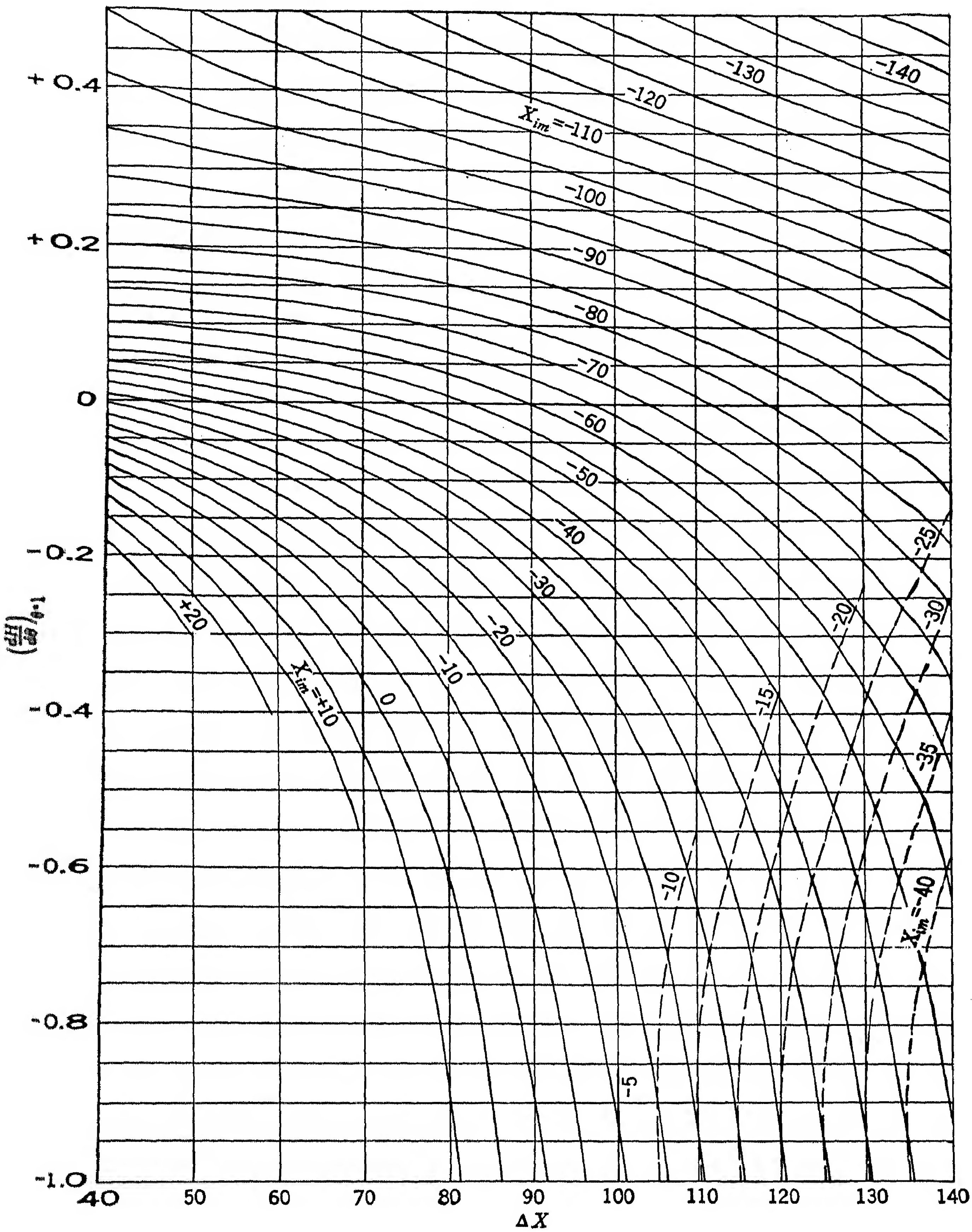

FIG. 4·18.—Logarithm of the final slope, $\left(\frac{dH}{d\theta}\right)_{\theta=1}$, of ideal-harmonic-transformer functions, plotted against angular travel for a series of values of X_{im}. Dashed lines indicate that the final slope is negative.

when $H_1 = 0$, and $\theta_3 = \theta_4 = 1$ when $H_1 = 1$. Thus

$$S_0 = \left(\frac{dH_2}{dH_1}\right)_{H_1=0} = \frac{\left(\dfrac{dH_2}{d\theta_3}\right)_{\theta_3=0}}{\left(\dfrac{dH_1}{d\theta_3}\right)_{\theta_3=0}} \tag{60}$$

and

$$S_1 = \left(\frac{dH_2}{dH_1}\right)_{H_1=1} = \frac{\left(\dfrac{dH_2}{d\theta_3}\right)_{\theta_3=1}}{\left(\dfrac{dH_1}{d\theta_3}\right)_{\theta_3=1}}. \tag{61}$$

In other words, each terminal slope of the graph of the double-harmonic-transformer operator $(H_2|H_1)$ is equal to the corresponding terminal slope for the output operator $(H_2|\theta_3)$ divided by that for the input operator $(H_1|\theta_3)$. Our problem is thus, in effect, to pick out of the part of Table A·1 that corresponds to a given value of ΔX_i two columns such that the ratio of their initial slopes is S_0 and the ratio of their final slopes is S_1.

Consider now Fig. 4·17, which shows the variation with ΔX_i of the quantity

$$\log_{10}\left(\frac{dH}{d\theta}\right)_{\theta=0} = \log_{10}\left(\frac{\cos X_{im}}{(\sin X_i)_{\max} - (\sin X_i)_{\min}}\right), \tag{62}$$

for a series of values of X_{im}. On this chart the distance along the vertical line $\Delta X = \Delta X_i$ from the curve $X_{im} = X_{3m}$ to the curve $X_{im} = X_{4m}$ (counted as positive upward, negative downward) is

$$\log_{10} S_0 = \log_{10}\left(\frac{dH_2}{d\theta_3}\right)_{\theta_3=0} - \log_{10}\left(\frac{dH_1}{d\theta_3}\right)_{\theta_3=0}, \tag{63}$$

the logarithm of the initial slope $\left(\dfrac{dH_2}{dH_1}\right)_{H_1=0}$ for an ideal double harmonic transformer characterized by the parameters ΔX_i, X_{3m}, X_{4m}. Conversely, if we draw a line of length $\log_{10} S_0$ on a strip of paper and move this, always in a vertical position, over Fig. 4·17, its ends will continually indicate the paramaters ΔX_i, X_{3m}, and X_{4m} for an ideal double harmonic transformer with initial slope $\left(\dfrac{dH_2}{dH_1}\right)_{H_1=0}$ equal to the chosen value of S_0.

Fig. 4·18 presents in a similar manner values of

$$\log_{10}\left(\frac{dH}{d\theta}\right)_{\theta=1} = \log_{10}\left[\frac{\cos X_M}{(\sin X)_{\max} - (\sin X)_{\min}}\right]. \tag{64}$$

It is obvious that if we draw a line of length $\log_{10} S_1$ on a strip of paper and move it, always in a vertical position, over Fig. 4·18, its ends will

continually indicate the parameters ΔX_i, X_{3m}, and X_{4m} for an ideal double harmonic transformer with terminal slope $\left(\frac{dH_2}{dH_1}\right)_{H_1=1}$ equal to the chosen value of S_1.

In order to determine the parameters of an ideal double harmonic transformer for which the initial and terminal slopes have values S_0 and S_1 respectively, one may proceed as follows. (Attention will be restricted to cases in which S_0 and S_1 are both positive; a case in which both slopes are negative can be reduced to this case by replacing X_{4m} by $X_{4m} + 180°$.) At the edge of a strip of paper draw an arrow of length $|\log_{10} S_0|$ (using the scale at the left of Fig. 4·17) and place it on Fig. 4·17, directing it upward if $\log_{10} S_0$ is positive and downward if this is negative. Similarly construct an arrow of length $|\log_{10} S_1|$ and place it on Fig. 4·18, directing it upward or downward according as $\log_{10} S_1$ is positive or negative. If these arrows are placed on vertical lines corresponding to the same $\Delta X = \Delta X_i$, with the heads of both arrows on curves corresponding to the same $X_m = X_{4m}$ and the tails on curves corresponding to the same $X_m = X_{3m}$, then these values of ΔX_i, X_{3m}, and X_{4m} give simultaneously the desired initial and final slopes. Such positions for the arrows can be found quickly, for any specified ΔX_i, by placing the tails of the arrows successively at several values of X_{3m}, until a value is found for which the heads of the arrows also lie at the same X_{4m}.

Example: As our principal example of double-harmonic-transformer design we shall take the problem of mechanizing the relation

$$x_2 = \tan x_1, \tag{65}$$

previously considered, over the larger range $0° \leqq x_1 \leqq 70°$,

$$0 \leqq x_2 \leqq 2.7475.$$

On introduction of homogeneous variables

$$h_1 = \frac{x_1}{70°}, \qquad h_2 = \frac{x_2}{2.7475}, \tag{66}$$

this relation becomes

$$2.7475h_2 = \tan (h_1 \cdot 70°) \tag{67}$$

This is tabulated for uniformly spaced values of h_1 in Table 4·4. The slope of the curve in homogeneous variables is

$$\frac{dh_2}{dh_1} = 0.4447 \sec^2 x_1, \tag{68}$$

and the terminal slopes are 0.445 and 3.802.

For a preliminary fit we try $\Delta X_i = 90°$. We place on the corresponding line in Fig. 4·17 an arrow of length $|\log_{10} 0.445|$, and on that line in

TABLE 4·4.—$x_2 = \tan x_1$, $0 = x_1 \leqq 70°$, IN HOMOGENEOUS VARIABLES

h_1	h_2
0.0	0.0000
0.1	0.0447
0.2	0.0907
0.3	0.1397
0.4	0.1935
0.5	0.2549
0.6	0.3277
0.7	0.4187
0.8	0.5396
0.9	0.7143
1.0	1.0000

Fig. 4·18 an arrow of length $\log_{10} 3.802$. We note that if $X_{3m} = 10°$, correct initial slope requires $X_{4m} = -58°$ (Fig. 4·17), and correct final slope requires $X_{4m} = -52°$ (Fig. 4·18); if $X_{3m} = -15°$, correct initial slope requires $X_{4m} = -62°$, correct final slope requires $X_{4m} = -75°$. Interpolating to zero difference of the values of X_{4m}, we have a set of constants assuring correct terminal slopes:

$$\Delta X_i = 90°, \qquad X_{3m} = -12°, \qquad X_{4m} = -59°.$$

Assuming these constants, we now compute H_2 for $H_1 = \frac{1}{2}$. First we center attention on the input harmonic transformer and determine $\theta_3 = \theta_4$: in Table A·2, $\Delta X_i = 90°$, we interpolate between columns for $X_{im} = -15°$ and $X_{im} = -10°$; for $H = \frac{1}{2}$, $X_{im} = -12°$ we find

$$\theta_i = 0.385 = \theta_3 = \theta_4.$$

Turning attention to the second transformer, we can now determine H_2: interpolating between columns of Table A·1 for $\Delta X_i = 90°$, $X_{im} = -60°$ and $X_{im} = -55°$, we find that $H = 0.325$ when $X_{im} = -59°$ and $\theta_i = 0.385$. The desired value of H_2, read from Table 4·4, is 0.255; the curve thus fitted lies too high in the center by $d = 0.070$.

Next we try $\Delta X_i = 70°$. Moving the arrows to the corresponding lines of Figs. 4·17 and 4·18, we find that correct terminal slopes are obtained by using

$$\Delta X_i = 70°, \qquad X_{3m} = 8°, \qquad X_{4m} = -56°.$$

With these constants, if $H_1 = \frac{1}{2}$, then $\theta_3 = 0.371$, $H_2 = 0.308$, $d = 0.053$.

Trial of still smaller values of ΔX_i shows that d can be decreased only slightly below this value; an exact fit of terminal slopes will always lead to a generated curve too high in the middle. The "best" value of ΔX_i, in this sense, is a little smaller than is mechanically desirable, and not much can be gained by adopting precisely this value instead of a larger and more convenient one. In the further discussion of this problem we shall therefore fix $\Delta X_i = 90°$.

4·12. Preliminary Fit to a Nonmonotonic Function.—Nonmonotonic functions that can be generated by an ideal double harmonic transformer possess only a single maximum or minimum. Expressed in homogeneous variables, they fall into four types illustrated in Fig. 4·19:

(a) $H_2 = 0$ when $H_1 = 0$.
(b) $H_2 = 0$ when $H_1 = 1$.
(c) $H_2 = 1$ when $H_1 = 0$.
(d) $H_2 = 1$ when $H_1 = 1$.

As with monotonic functions, it is possible to find, for any given ΔX_i, values of X_{3m} and X_{4m} that make the terminal slopes of the generated function equal to those of a given nonmonotonic function. However, a fit of the value of the generated function to that of the given function is assured at only one end of the range of H_1: for $H_1 = 0$ with types (a) and

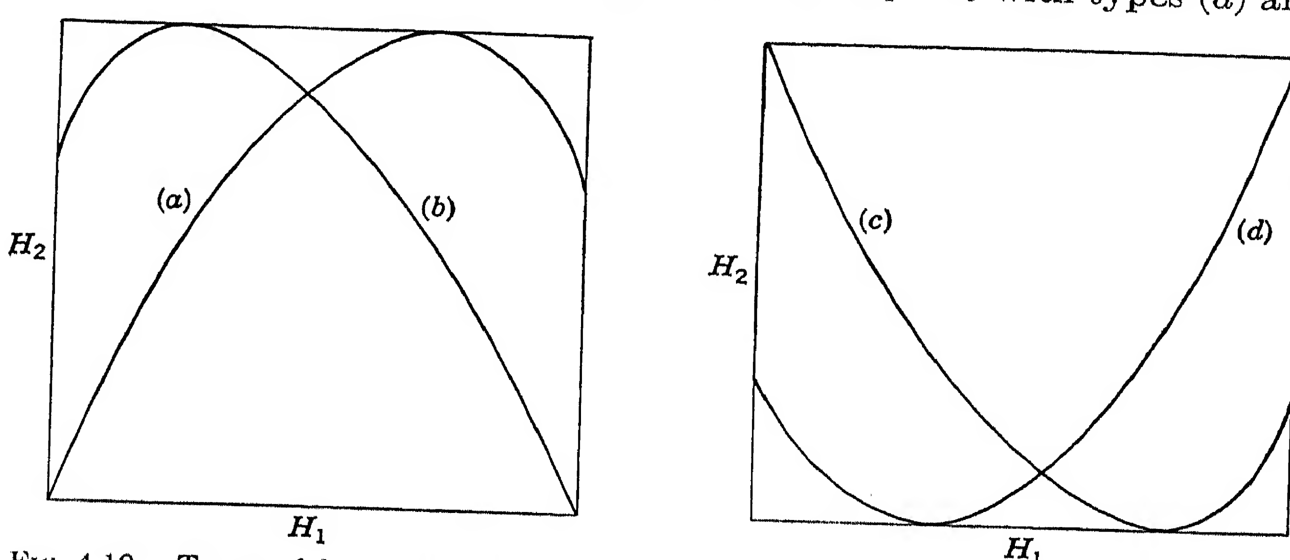

FIG. 4·19.—Types of functions mechanizable by an ideal double harmonic transformer.

(c), and for $H_1 = 1$ with types (b) and (d). Agreement of the slopes at the other end of the range of H_1 thus does not assure tangency of the given and the generated functions, and the fit may be very unsatisfactory. For this reason it is not advisable to make a preliminary fit to a given nonmonotonic function by the method of Sec. 4·11. It is usually best to choose a value of X_{4m} such that a fit in the value of the function is secured at the end where this is not otherwise assured, and then make the maximum or minimum in H_2 occur for the proper value of H_1; as an indication of the accuracy of the over-all fit one can take the difference between the given and generated functions at a chosen point between the maximum or minimum and the more remote end of the range of H_1.

The procedure for securing a preliminary fit to a nonmonotonic function is then as follows:

1. Choose a value of ΔX_i, arbitrarily if necessary.

2. Referring to Table A·1, choose X_{4m} such that H_2 has the desired value when $\theta_3 = H_1 = 1$, for types (*a*) or (*c*), or when $\theta_3 = H_1 = 0$, for types (*b*) or (*d*).
3. From the same column of Table A·1 read the value of θ_3 for which $H_2 = 1$ [types (*a*) or (*b*)] or the value of θ_3 for which $H_2 = 0$ [types (*c*) or (*d*)].
4. From the given function, determine the value of H_1 for which $H_2 = 1$ [types (*a*) or (*b*)] or the value of H_1 for which $H_2 = 0$ [types (*c*) or (*d*)].
5. By reference to Table A·1 or A·2, for the same ΔX_i, find the value of X_{3m} for which the value of θ_3 determined in Step (3) corresponds to the value of H_1 determined in Step (4).
6. For these values of ΔX_i, X_{3m}, and X_{4m}, determine the difference d between the generated function and the given function at the chosen test value of H_1.
7. Repeat the preceding steps for several other values of ΔX_i, until the trend of d as a function of ΔX_i is established.
8. Choose as the value of ΔX_i for use in further calculations that which minimizes $|d|$.

Example: As an example, we take the problem of making a preliminary fit to the curve $(H_2|H_1)$ of Fig. 4·16—a case in which we happen to know that an exact fit can be obtained. The curve is of a borderline type, belonging to types (*a*) and (*b*). For the purposes of the preliminary fitting we desire

$$\begin{aligned} H_2 &= 0 && \text{when } H_1 = 0, \\ H_2 &= 0 && \text{when } H_1 = 1, \\ H_2 &= 1 && \text{when } H_1 = 0.38. \end{aligned}$$

For test purposes, we shall compare the generated function with the given function when $H_1 = 0.70$ (desired value, $H_2 = 0.710$).

First, choose $\Delta X_i = 70°$. In Table A·1 we find that $H_2 = 0$ for both $\theta_3 = 0$ and $\theta_3 = 1$ if $X_{4m} = 55°$; from the same column we see that $H_2 = 1$ for $\theta_3 = 0.5$. The desired X_{3m} must then make $\theta_3 = 0.5$ correspond to $H_1 = 0.38$. From Table A·1 it is evident that

$$-75° < X_{3m} < -70°;$$

interpolating, we obtain $X_{3m} = -72°$.

To test the over-all fit given by $\Delta X_i = 0.70$, $X_{3m} = -72°$, $X_{4m} = 55°$, we compute H_2 for $H_1 = 0.70$. Interpolating in Table A·2 (since H_1 has a value appearing there) between columns corresponding to $X_{3m} = -70°$ and $X_{3m} = -75°$, we find $\theta_3 = 0.771$. Returning to Table A·1,

$$X_{4m} = 55°,$$

we obtain by linear interpolation $H_2 = 0.692$ for $\theta_3 = 0.771$. Linear interpolation, however, is here obviously inadequate; quadratic interpolation yields $H_2 = 0.700$, $d \approx -0.010$.

Repeating the process with $\Delta X_i = 90°$ we find that little interpolation is necessary. To make $H_2 = 0$ for $\theta_3 = 0$ and for $\theta_3 = 1$ requires $X_{4m} = 45°$; the maximum comes for $\theta_3 = 0.5$, $H_1 = 0.38$; hence

$$X_{3m} = -75°.$$

Computing H_2 for $H_1 = 0.7$, we obtain essentially the graphically determined value, 0.710, and $d \approx 0$.

Although $\Delta X_i = 90°$ is the best value, it is evident that the fit is not very sensitive to the choice of ΔX_i.

4·13. Improvement of the Fit by a Method of Successive Approximations.—A satisfactory fit of the generated to the given function is not assured by the simple and rather arbitrary methods just described; these should be depended upon only in choosing a value of ΔX_i. The final adjustment of X_{3m} and X_{4m}, to obtain the best over-all fit possible with the chosen ΔX_i, is most satisfactorily accomplished by a graphical method of successive approximations which gives a complete view of the fit at each stage of the process. Convergence of the successive approximations on the final result can be speeded up by exercise of the superior judgment of an experienced designer, but a satisfactory result is assured even for a beginner.

The problem to be solved is that of finding ideal harmonic transformer operators $(H_2|\theta_3)$ and $(\theta_3|H_1)$, both corresponding to the chosen ΔX_i, which make the approximate relation

$$(H_2|\theta_3) \cdot (\theta_3|H_1) = (H_2|H_1) \approx (h_2|h_1) \tag{69}$$

as nearly exact as possible over the entire range of variables. This will be done by alternately improving the choice of the two harmonic-transformer operators—that is, the choice of the parameters X_{4m} and X_{3m}, respectively.

Let the harmonic-transformer operators chosen after S stages in the approximation be $(H_2|\theta_3)_S$ and $(\theta_3|H_1)_S$. Then

$$(H_2|\theta_3)_S \cdot (\theta_3|H_1)_S \approx (h_2|h_1). \tag{70}$$

Let it be desired to replace $(H_2|\theta_3)_S$ by an operator $(H_2|\theta_3)_{S+1}$, which will make the approximation of Eq. (70) more exact. Let the operator Z_S be defined by

$$(h_2|h_1) \cdot (H_1|\theta_3)_S = Z_S. \tag{71}$$

Then

$$Z_S \approx (H_2|\theta_3)_S, \tag{72}$$

as may be shown by multiplying Eq. (70) from the right by the operator $(H_1|\theta_3)_S$. If this approximation were exact, Eq. (70) would necessarily be exact; if this approximation is improved, that of Eq. (70) will be improved. Now Z_S can be computed with sufficient accuracy by graphical methods. If it is possible to find an ideal-harmonic-transformer operator $(H_2|\theta_3)_{S+1}$ which gives a better fit to Z_S than does $(H_2|\theta_3)_S$, then this is the desired improved operator; the approximation in the relation

$$(H_2|\theta_3)_{S+1} \cdot (\theta_3|H_1)_S \approx (h_2|h_1) \tag{73}$$

is better than that in Eq. (70).

Next one will wish to replace $(\theta_3|H_1)_S$ by an improved operator $(\theta_3|H_1)_{S+1}$. Let the operator Y_{S+1} be defined by

$$(h_2|h_1) \cdot Y_{S+1} = (H_2|\theta_3)_{S+1}. \tag{74}$$

By Eq. (73)

$$(H_1|\theta_3)_S \approx Y_{S+1}. \tag{75}$$

An improved operator $(H_1|\theta_3)_{S+1}$ would make this approximation more exact; one can therefore determine it by computing Y_{S+1} by graphical means and finding the ideal harmonic transformer function that best fits this function. The approximation in writing

$$(H_2|\theta_3)_{S+1} \cdot (\theta_3|H_1)_{S+1} \approx (h_2|h_1) \tag{76}$$

is then even better than that in Eq. (73).

It is now possible to make a further improvement in $(H_2|\theta_3)$, computing Z_{S+1} by Eq. (71) and fitting $(H_2|\theta_3)_{S+2}$ to this as exactly as possible. The operator $(\theta_3|H_1)$ can then be improved again, and the process repeated until the improvement obtained does not repay the effort expended. It is of course possible that a satisfactory fit can not be given by any ideal double harmonic transformer; it will then be necessary to make use of methods to be described later in this chapter.

Example: We return to the Example of Sec. 4·11, the mechanization of the tangent function from 0° to 70°. We there fixed on the value $\Delta X_i = 90°$ and found approximate values of X_{3m} and X_{4m}. Rounding off these values to those appearing in Table A·1, we might take

$$(H_2|\theta_3) \sim X_{4m} = -60° \tag{77}$$
$$(\theta_3|H_1) \sim X_{3m} = -5°. \tag{78}$$

These values, especially the second, are good. In order to provide a better illustration of the method of successive approximations we shall deliberately select a poorer value, $X_{3m} = -15°$, with which to start the computations.

Figure 4·20 shows a graph of the given function $(h_2|h_1)$, points on the graph of $(H_1|\theta_3)_1 \sim -15° \leqq X_3 \leqq 75°$, as read from Table A·1, and

the construction needed to determine corresponding points on the graph of Z_1, which has been drawn in as a continuous curve. A good over-all fit to Z_1 can not be found in Table A·1 ($\Delta X_i = 90°$!), but a reasonable fit at the lower end is obtained by taking $X_{4m} = -70°$, as shown in the same figure. Therefore, as the basis for the next step in the computation we make $(H_2|\theta_3)_2$ correspond to $X_{4m} = -70°$.

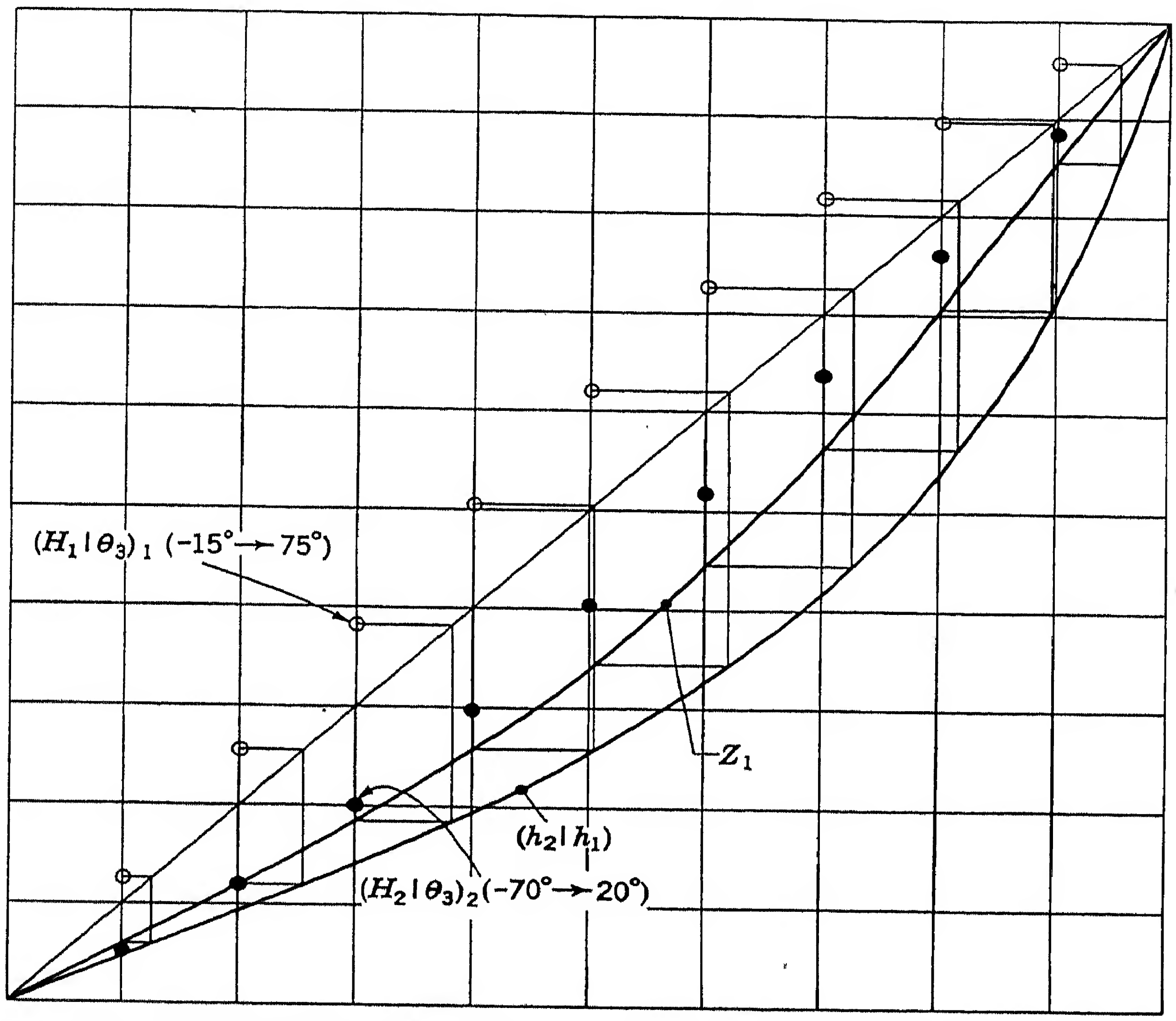

FIG. 4·20.—Mechanization of $x_2 = \tan x_1$. First step in the method of successive approximations: construction of the operator Z_1 and approximate fitting of this by $(H_2|\theta_3)_1 \sim \Delta X_i = 90°$, $X_{im} = -70°$.

Next, Fig. 4·21 shows the construction used in determining Y_2. (In practice this would be carried out on the same graph as the construction for Z_1, but for the sake of clarity a new figure is used here.) The operator $(H_1|\theta_3)_2$ can be made to fit this fairly well by taking $X_{3m} = -5°$.

Repetition of this process will lead to little further improvement. It can be seen in Fig. 4·23 that Z_2 is perhaps best fitted by the value of X_{4m}, $-70°$, arrived at in Fig. 4·20. It would be of little value to reduce the error further by interpolation in the tables; the solution would in any case apply only to an ideal double harmonic transformer, which could be realized only by using undesirably complex mechanisms or

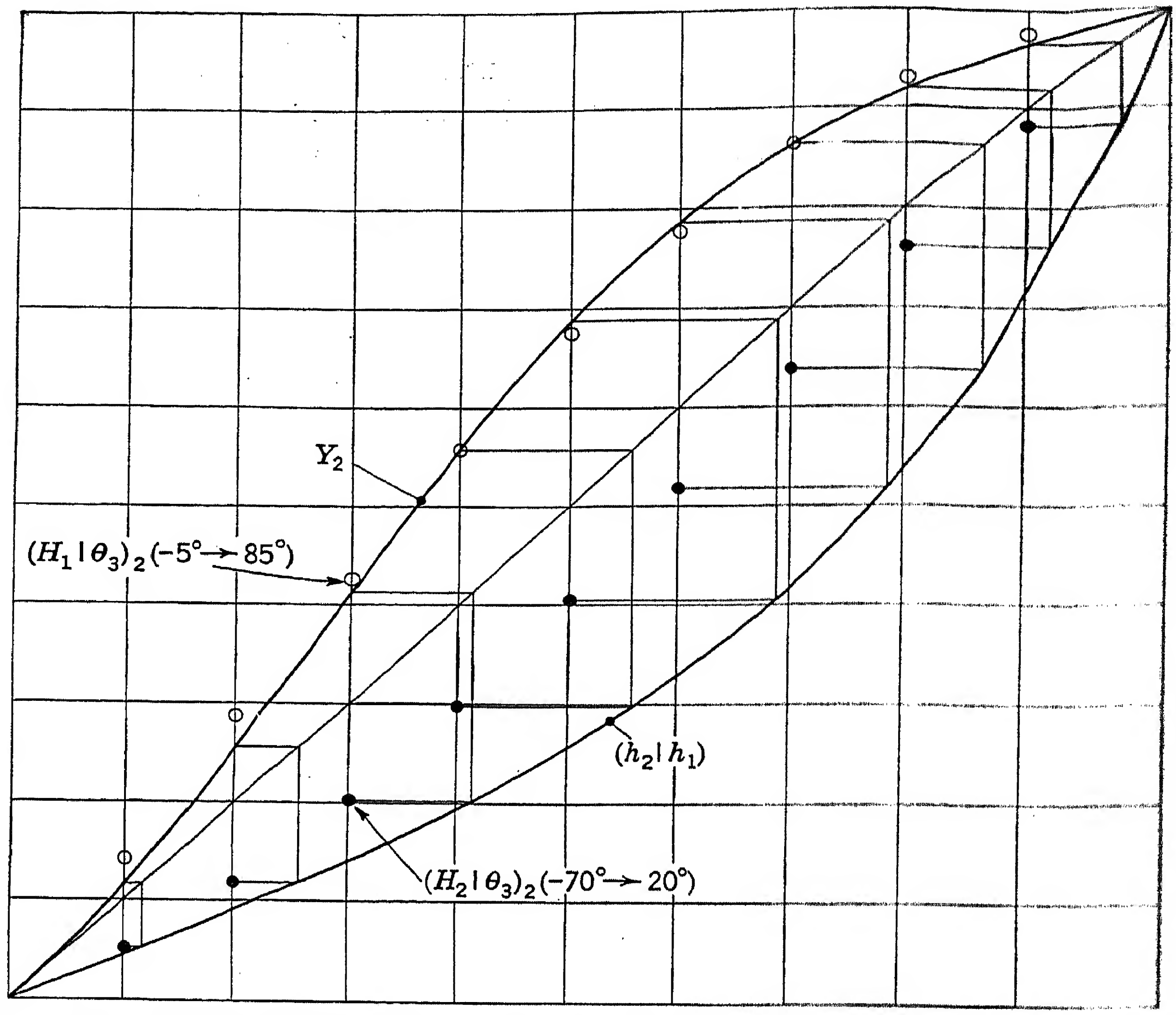

FIG. 4·21.—Mechanization of $x_2 = \tan x_1$. Second step in method of successive approximations: construction of the operator Y_2 and approximate fitting of this by

$$(H_1|\theta_3)_2 \sim \Delta X_i = 90°,\ X_{im} = -5°.$$

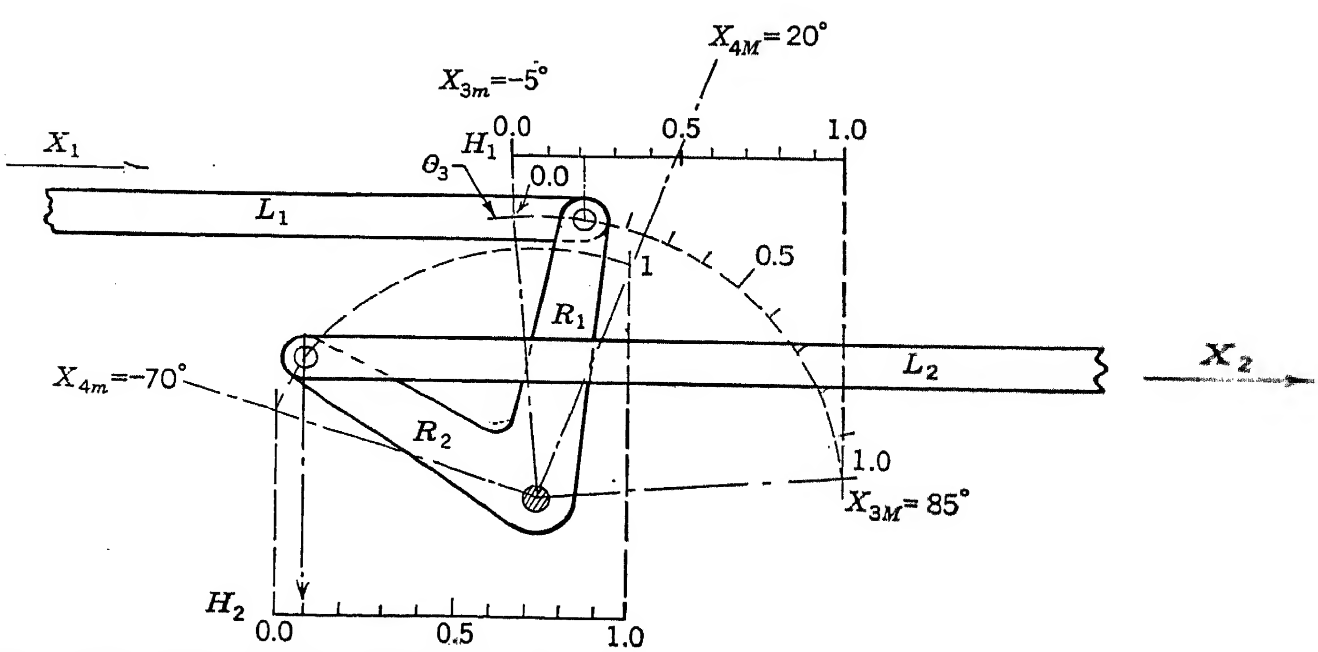

FIG. 4·22.—Ideal double harmonic transformer approximately mechanizing $x_2 = \tan x_1$.

nonideal double harmonic transformers with very long links. It is better to design the transformer as nonideal, further reducing the error by adjustment of link lengths and slide positions, as explained in Sec. 4·13.

Figure 4·22 shows the ideal double harmonic transformer corresponding to the present stage of solution of the problem. The cell has been normalized by making

$$R_1[(\sin X_1)_{\max} - (\sin X_1)_{\min}] = R_2[(\sin X_2)_{\max} - (\sin X_2)_{\min}]. \quad (79)$$

4·14. Nonideal Double Harmonic Transformers.—The field of mechanizable functions is very substantially extended if nonideal harmonic transformers are coupled instead of ideal ones. (A typical nonideal double harmonic transformer is shown in Fig. 4·26.) Instead of three independent parameters, there are seven to be adjusted: $\Delta X_3 = \Delta X_4$, X_{3m}, X_{4m}, L_1, L_2, E_1^*. and E_2^*. Here, as before, the lengths L_1 and L_2 of the links are to be measured in terms of the horizontal travels ΔX_1 and ΔX_2, respectively. E_1^* is the reading on the H_1^*-scale where it is intercepted by the center line of the X_1' slide, and E_2^* is the reading on the H_2^*-scale where this is intercepted by the center line of the X_2' slide. The Peaucellier inversor shown in Fig. 2·4 is a special case of the nonideal double harmonic transformer, with $X_{3m} = X_{4m}$, $L_1 = L_2$, and $E_1^* = E_2^* = 0$; it is thus evident that such devices can serve for the mechanization of functions that are not even roughly of sinusoidal form.

To determine the function generated by a given nonideal double harmonic transformer one can apply the method described in Sec. 4·8, obtaining the operator $(H_2|H_1)$ as the product of operators $(H_2|\theta_3)$ and $(\theta_3|H_1)$, which describe the component nonideal harmonic transformers.

In the converse problem of mechanizing a given function by a nonideal double harmonic transformer it is not feasible to vary all seven of the available parameters simultaneously. One should begin as though the double harmonic transformer were to be ideal, carrying out an approximate fit (Secs. 4·11 and 4·12) to determine a value of ΔX_i, which is held constant thereafter, and then improving the choices of X_{3m} and X_{4m} (Sec. 4·13) until this ceases to be profitable. At this point it becomes necessary to begin the adjustment of L_1, L_2, E_1^*, E_2^*. Since the device may be regarded as two nonideal harmonic transformers in series, the problem to be solved is still formally the same as that considered in Sec. 4·13—that of making the approximation in

$$(H_2|\theta_3) \cdot (\theta_3|H_1) = (H_2|H_1) \approx (h_2|h_1) \quad (69)$$

as nearly exact as possible—and the method of solution by successive approximations is the same. Here, however, each of the component transformers is characterized not by one, but by three constants, (X_{3m},

E_1^*, L_1) or (X_{4m}, E_2^*, L_2), which must be chosen at each stage of the process —for instance, by the methods of Secs. 4·4 and 4·8.

Example: We continue the example of Sec. 4·13, that of mechanizing the tangent function from 0° to 70°. Figure 4·23 shows the construction of Z_2, to fit which we shall now adjust the three constants characterizing $(H_2|\theta_3)$: X_{4m}, E_2^*, and L_2. As already noted, the best fit obtainable with

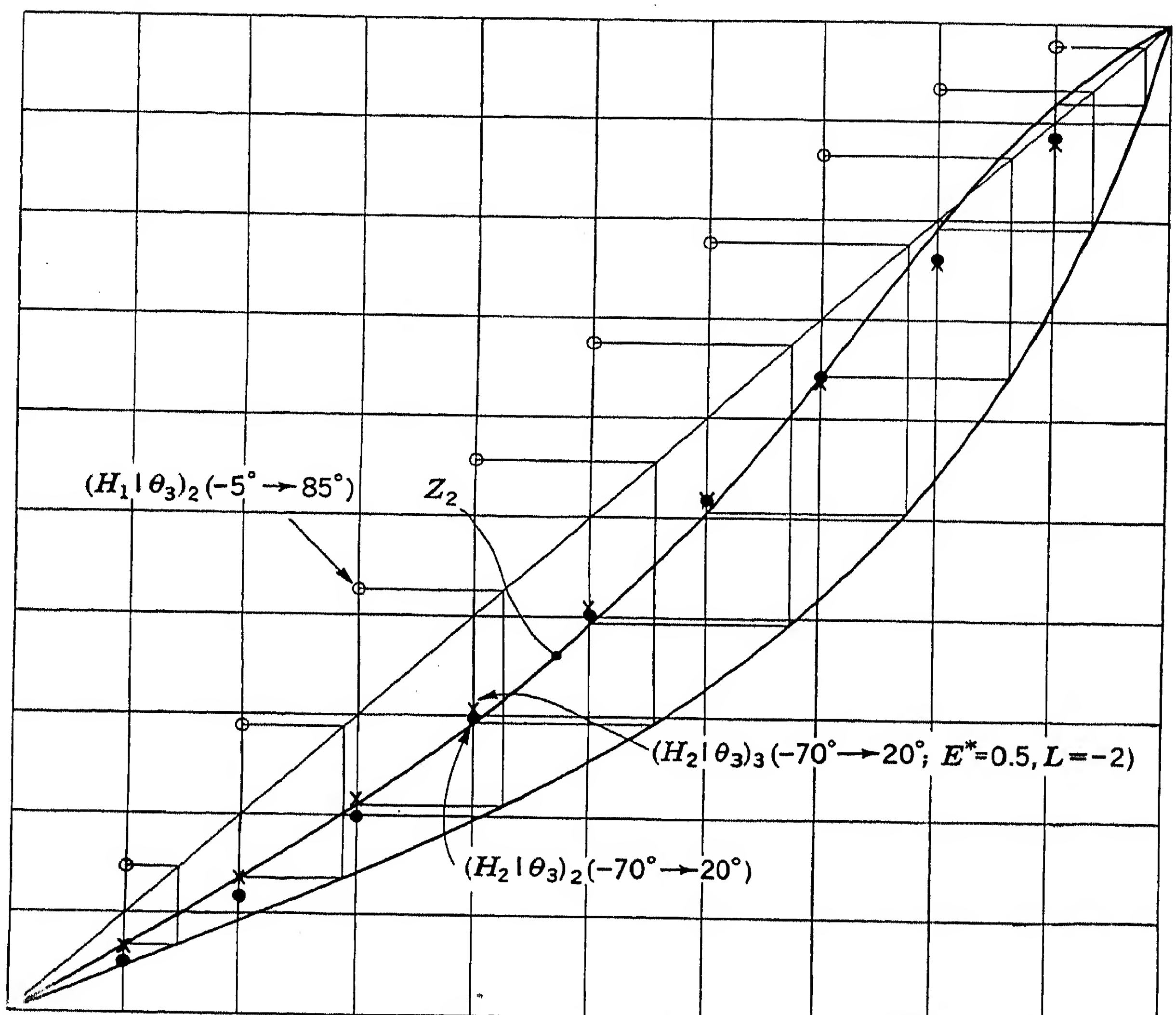

FIG. 4·23.—Mechanization of $x_2 = \tan x_1$. Third step in method of successive approximations: construction of the operator Z_2 and approximate fitting of this by

$$(H_2|\theta_3)_2 \sim \Delta X_i = 90°,\ X_{im} = -70°,\ (\ .\ .\ .\ ),$$

and by $(H_2|\theta_3)_3 \sim \Delta X_i = 90°,\ X_{im} = -70°,\ E^* = 0.5,\ L = -2$ (crosses).

an ideal-harmonic-transformer operator is given by $X_{4m} = -70°$, $X_{4m} = 20°$; the residual error then changes sign twice, tending to be large near the ends of the range of variables. Now the limits of X_4 here are roughly the same as those of the example of Sec. 4·8 (−15°, 75°) except for a change in sign, and the geometrical situations differ only as mirror images if one replaces a link to the left by a link to the right, and vice versa. Correspondingly, one easily sees, the structural error functions δH_k applicable here differ from those of Fig. 4·10 in replacement of

θ_i by $1 - \theta_i$, that is, reflection of the curves in a vertical line. Thus it is evident that it is not possible, by any choice of E_2^* and L_2, to obtain a structural-error function that changes sign twice, such as is needed to give a good fit to Z_2 over the whole range of variables. We shall therefore concentrate our attention on improving the fit for low values of θ, raising the curve in this region, and attempting only to keep the change small elsewhere. Inspection of Fig. 4·10 then shows (the differences of

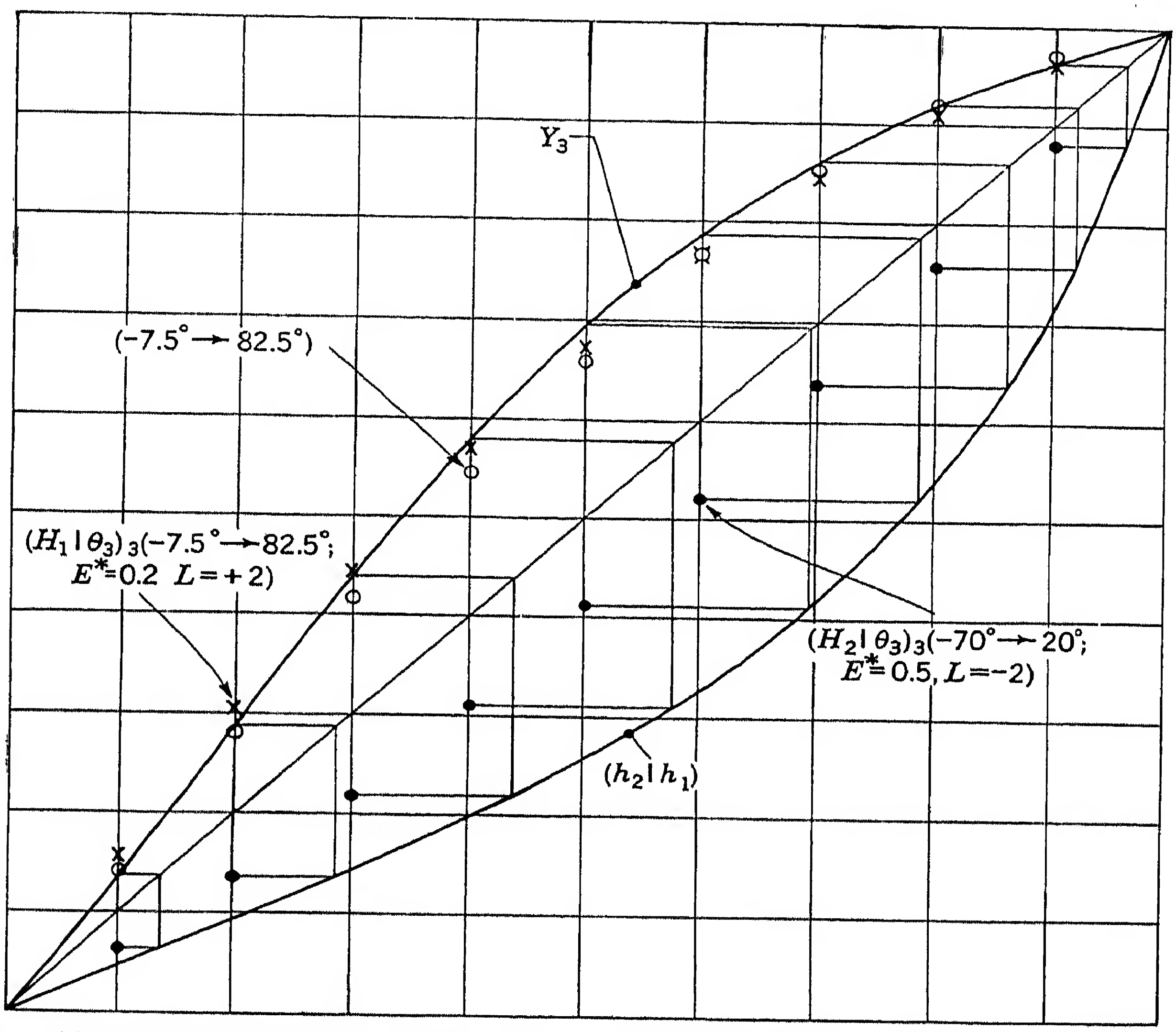

FIG. 4·24.—Mechanization of $x_2 = \tan x_1$. Fourth step in the method of successive approximations: construction of the operator Y_3, and approximate fitting of this by an ideal-harmonic-transformer function with $\Delta X_i = 90°$, $X_{im} = -7.5°$ (circles) and by $(H_1|\theta_3)_3 \sim \Delta X_i = 90°$, $X_{im} = -7.5°$, $E^* = 0.2$, $L = 2$ (crosses).

the present from the former case being borne in mind) that $E_2^* = \frac{1}{2}$ is an appropriate value, and that L should be negative, the link to the right. Rough consideration of the magnitudes involved leads to choice of $L = -2$. The resulting fit, as shown in Fig. 4·23, is quite satisfactory for low values of θ.

The process of successive approximations is continued in Fig. 4·24 with the graphical construction of Y_3. We have now to fit $(H_1|\theta_3)_3$ to this by choosing X_{3m}, E_1^*, L_1. Inspection of Table A·1 shows that with

$X_{3m} = -5°$ one has a bad fit at the left, and with $X_{3m} = -10°$ the curve is much too low in the middle. In such a case it is desirable to interpolate. We choose $X_{3m} = -7.5°$. The values of the corresponding function are found with sufficient accuracy for our graphical method by a linear interpolation in Table A·1; the resulting values are plotted in Fig. 4·24 as a series of points in small circles. In further improving the fit one will wish to raise the central part of the curve, to depress the

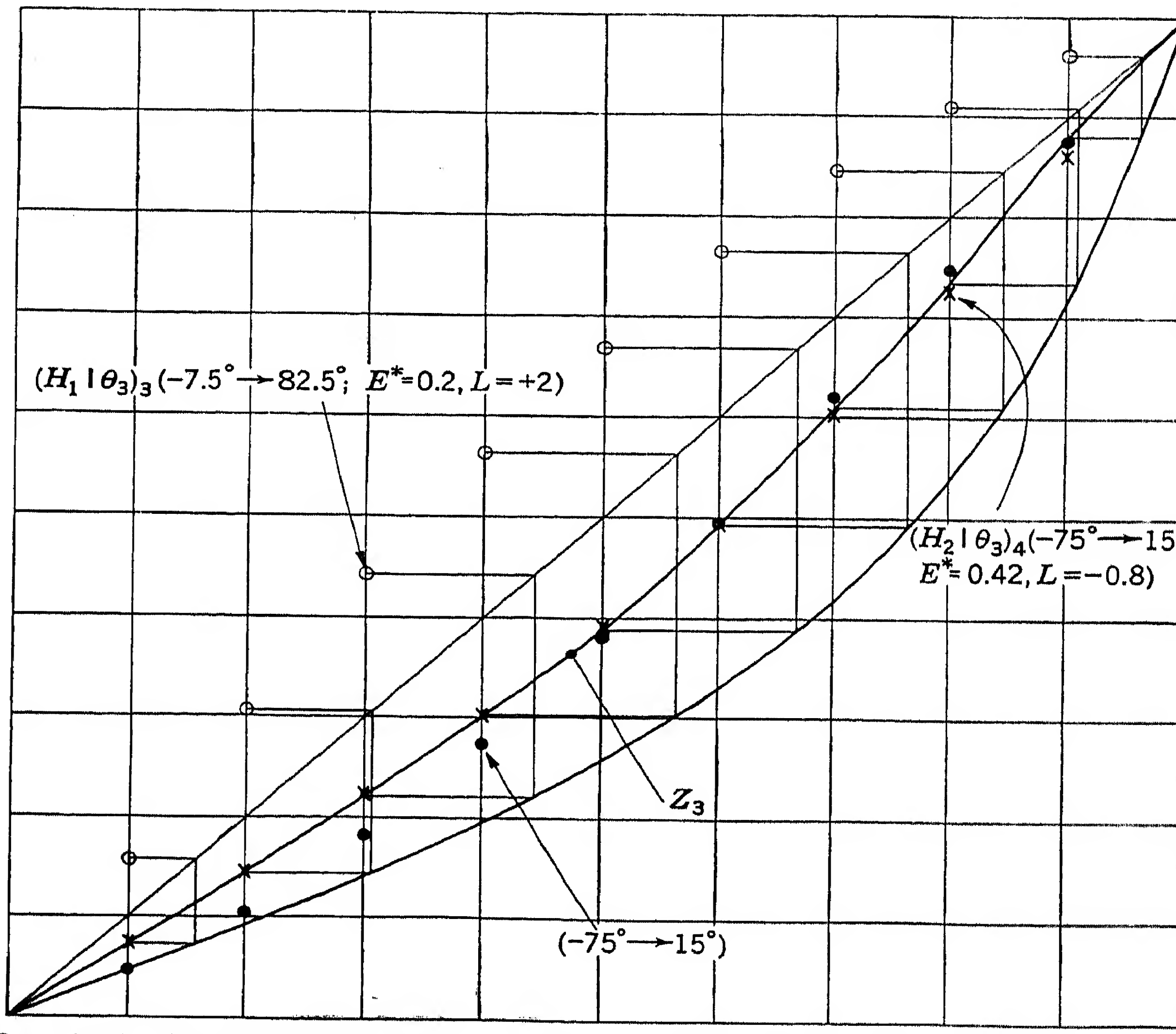

FIG. 4·25.—Mechanization of $x_2 = \tan x_1$. Fifth step in the method of successive approximations: construction of the operator Z_3, and approximate fitting of this by $(H_2|\theta_3)_4$: $\Delta X_i = 90°$, $X_{im} = -75°$, $E^* = 0.42$, $L = -0.8$.

extreme upper end, and to leave the lower and unchanged. The values of X_{3m} and X_{3M} are sufficiently like those of Fig. 4·10 for this to be used as a guide; it is again evident that no choice of constants can accomplish everything that is desired. We choose therefore to allow a considerable error at the lower end of the curve, leaving this to be corrected (as before) by our choice of E_2^* and L_2; we concentrate on improving the fit at the upper end, and, secondarily, that in the central region. Inspection of Fig. 4·10 leads to choice of $E_1^* = 0.2$ and $L = +2$. Computation of the structural-error function then leads to the corrected points of Fig. 4·24,

indicated by crosses. It is evident that a value of E_1^* nearer to zero would have been preferable, as giving a depression of the curve over a less extended region. However, it is hardly worth while at this stage of the computation to make a more careful choice of constants, and we accept the resulting function as $(H_1|\theta_3)_3$.

The next stage of the calculation, the determination of $(H_2|\theta_3)_4$, is shown in Fig. 4·25. When Z_3 is constructed it is found that a better fit can be obtained at the upper end by taking $X_{3m} = -75°$ than by taking $X_{3m} = -70°$. The error functions shown in Fig. 4·10 then apply exactly, with the substitution $\theta_i \rightarrow 1 - \theta_i$. Since preliminary fits have been made in all parts of the range of θ_i, it is now worth while to make a careful adjustment of the constants E_2^* and L_2, as by the methods of Sec. 4·8. With $E_2^* = 0.42$, $L_2 = -0.8$, one finds exactly computed points that give an excellent fit except at the extreme upper end of the curve. This is very satisfactory, as it is in this last region that the fit is being controlled by choice of E_1^* and L_1.

The final graphical stage of the solution, the determination of $(H_1|\theta_3)_4$, is not illustrated by a figure. It leads to the choice of $X_{3m} = -7.5°$, $E_1^* = 0.2$, $L_1 = +1.8$, with an excellent over-all fit. This is as far as the fit can be carried by these graphical methods; further refinements are best obtained by the methods discussed in Chap. 7.

We have thus arrived at the following choice of constants:

$$X_{3m} = -7.5°, \qquad X_{3M} = 82.5°, \qquad E_1^* = 0.2, \qquad L_1 = 1.8, \tag{80a}$$
$$X_{4m} = -75°, \qquad X_{4M} = 15°, \qquad E_2^* = 0.42, \qquad L_2 = -0.8. \tag{80b}$$

Calculation of the resultant total structural error is illustrated in Table 4·5, which consists of three sections. The first shows the calculation, by the method described in Sec. 4·6, of values of the homogeneous input parameter H_1' for a series of values of θ_3. The second shows the calculation of values of the homogeneous output parameter H_2' for the same series of values of θ_3. In the third section there are shown corresponding values of

$$x_1 = H_1' \cdot 70°, \tag{81}$$

the generated tangent function

$$x_{2g} = H_2' \tan 70°, \tag{82}$$

the ideal tangent function $x_2 = \tan x_1$, and the ideal generated homogeneous variable h_2. The error in the generated function, $\delta h_2 = H_2' - h_2$, is found to be less than 0.8 per cent of the total variation of the output variable.

The linkage corresponding to these constants is drawn in Fig. 4·26. Reduction of the linkage to the normalized form shown here requires a

TABLE 4·5.—COMPUTATION OF THE TOTAL STRUCTURAL ERROR (LINKAGE OF FIG. 4·26)

	θ_3	H_1	$H_1^* - E_1^*$	$\sin \epsilon_1 = \frac{g_1}{L_1} \times (H_1^* - E_1^*)$	$1 - \cos \epsilon_1$	$DH_1 = L_1 \times (1 - \cos \epsilon_1)$	$H_1 + DH_1 - (DH_1)_0$	H_1
$(H_2\|\theta_3)_4$	0.0	0.0000	0.7887	0.3396	0.0594	0.1069	0.0000	0.0000
	0.1	0.1398	0.7986	0.3438	0.0610	0.1098	0.1427	0.1586
	0.2	0.2791	0.7801	0.3358	0.0581	0.1046	0.2768	0.3076
	0.3	0.4143	0.7337	0.3159	0.0512	0.00 2	0.3996	0.4441
	0.4	0.5421	0.6605	0.2844	0.0413	0.0743	0.5095	0.5662
	0.5	0.6586	0.5624	0.2421	0.0297	0.0535	0.6052	0.6726
	0.6	0.7633	0.4418	0.1902	0.0183	0.0329	0.6893	0.7661
$g_1 = 0.7749$	0.7	0.8513	0.3016	0.1298	0.0085	0.0153	0.7597	0.8443
	0.8	0.9211	0.1453	0.0626	0.0020	0.0036	0.8178	0.9089
$\frac{g_1}{L_1} = 0.4305$	0.9	0.9711	−0.0233	0.0100	0.0000	0.0000	0.8642	0.9605
	1.0	1.0000	−0.2000	0.0861	0.0037	0.0067	0.8998	1.0000

	θ_3	H_2	$H_2^* - E_2^*$	$\sin \epsilon_2$	$1 - \cos \epsilon_2$	DH_2	$H_2 + DH_2 - (DH_2)_0$	H_2'
$(H_2\|\theta_3)_4$	0.0	0.0000	−0.4200	−0.3178	0.0518	0.0414	0.0000	0.0000
	0.1	0.0428	−0.2204	−0.1667	0.0140	0.0112	0.0730	0.0750
	0.2	0.1038	−0.0344	−0.0260	0.0003	0.0002	0.1450	0.1490
	0.3	0.1819	0.1336	0.1011	0.0051	0.0041	0.2192	0.2252
$g_2 = 0.6052$	0.4	0.2748	0.2793	0.2113	0.0226	0.0181	0.2981	0.3063
	0.5	0.3804	0.3992	0.3020	0.0467	0.0374	0.3844	0.3950
	0.6	0.4961	0.4904	0.3710	0.0714	0.0571	0.4804	0.4936
	0.7	0.6189	0.5505	0.4164	0.0908	0.0726	0.5877	0.6039
$\frac{g_2}{L_2} = 0.7564$	0.8	0.7459	0.5782	0.4374	0.1007	0.0806	0.7067	0.7262
	0.9	0.8740	0.5726	0.4331	0.0986	0.0789	0.8365	0.8595
	1.0	1.0000	0.5340	0.4040	0.0852	0.0682	0.9732	1.0000

θ_3	x_1, degrees	x_{2a}	$\tan x_1$	h_2	δh_2
0.0	0.00	0.0000	0.0000	0.0000	0.0000
0.1	11.10	0.2061	0.1962	0.0714	0.0036
0.2	21.53	0.4094	0.3945	0.1436	0.0054
0.3	31.09	0.6187	0.6030	0.2195	0.0057
0.4	39.63	0.8416	0.8282	0.3014	0.0049
0.5	47.08	1.0853	1.0754	0.3914	0.0036
0.6	53.63	1.3562	1.3579	0.4942	−0.0006
0.7	59.10	1.6592	1.6709	0.6081	−0.0042
0.8	63.62	1.9952	2.0163	0.7339	−0.0077
0.9	67.24	2.3615	2.3836	0.8675	−0.0080
1.0	70.00	2.7475	2.7475	1.0000	0.0000

slightly different calculation from that in the case of ideal double harmonic transformers (Eq. 79). Perhaps the simplest method is to choose arbitrary values of R_1 and R_2, and to compute the corresponding travels $\Delta X_1'$ and $\Delta X_2'$ from the geometry of the linkage. Since these travels are proportional to the R's, and are to be equal in the normalized cell, one has as the ratio of the normalized arm lengths

$$\frac{R_{1n}}{R_{2n}} = \frac{R_1}{R_2}\frac{\Delta X_2'}{\Delta X_1'}. \tag{83}$$

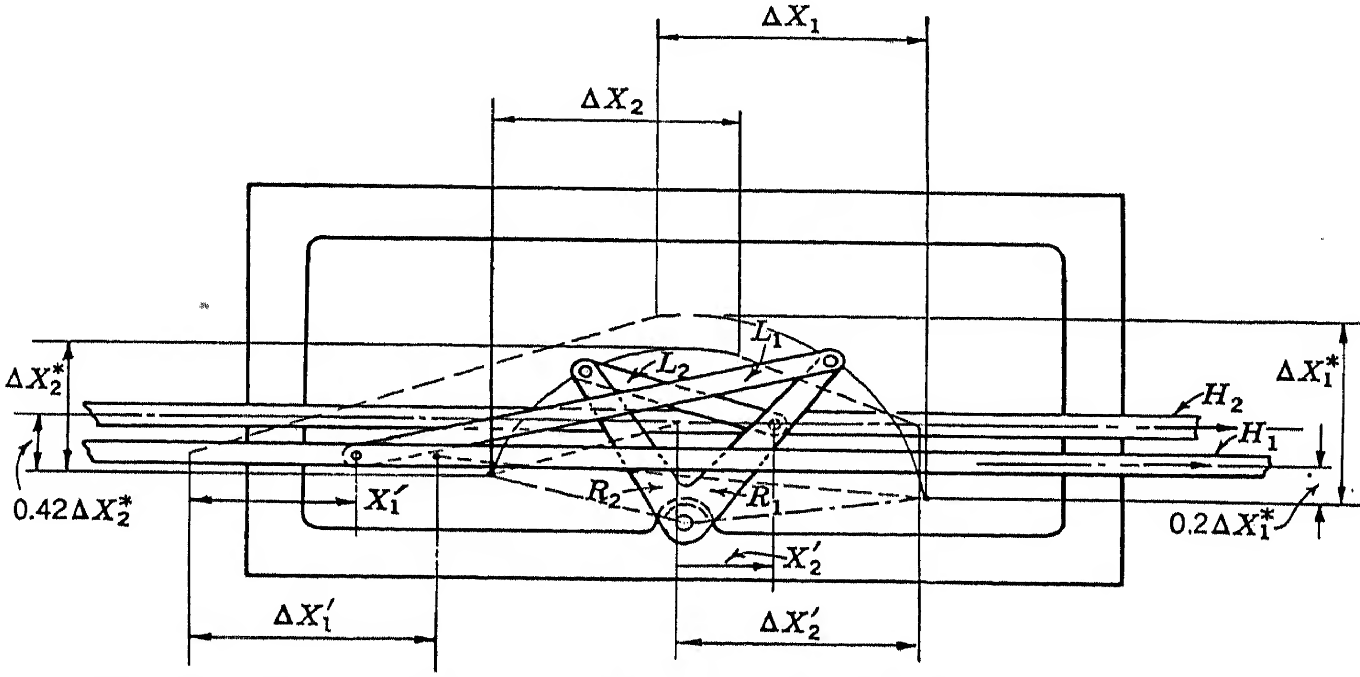

FIG. 4·26.—Nonideal double harmonic transformer generating, approximately, $x_2 = \tan x_1$, $0 < x_1 < 70°$. Values of the constants are given in Eq. (80).

4·15. Alternative Method for Double-harmonic-transformer Design The graphical method described in Sec. 4·14 has the advantage that it permits readjustment of the constants X_{3m} and X_{4m} at all stages of the design process. The alternative method to be described in the present section is useful when values of ΔX_3, X_{3m}, and X_{4m} can be considered as fixed; it is essentially an extension of the method of Sec. 4·8, which permits simultaneous adjustment of the constants L_1, L_2, E_1^*, E_2^*, of the two harmonic transformers.

Let us assume that a given relation

$$h_2 = (h_2|h_1) \cdot h_1 \tag{84}$$

has been mechanized approximately by an ideal double harmonic transformer that generates the relation

$$H_2 = (H_2|H_1) \cdot H_1 \tag{85}$$

between its input and output parameters. This relation we can express parametrically in terms of the angle θ_3:

$$\left.\begin{aligned} H_1 &= H_1(\theta_3), \\ H_2 &= H_2(\theta_3). \end{aligned}\right\} \tag{86}$$

Without changing the constants ΔX_3, X_{3m}, X_{4m} of this linkage, let the ideal harmonic transformers be replaced by nonideal ones. The input and output parameters will then be H_1' and H_2', differing from H_1 and H_2 by the structural-error functions δH_1 and δH_2:

$$\left.\begin{aligned} H_1'(\theta_3) &= H_1(\theta_3) + \delta H_1(\theta_3), \\ H_2'(\theta_3) &= H_2(\theta_3) + \delta H_2(\theta_3). \end{aligned}\right\} \tag{87}$$

The resulting nonideal double harmonic transformer will then generate a relation

$$H_2' = (H_2'|H_1') \cdot H_1'. \tag{88}$$

Our problem is to assign to the constants L_1, L_2, E_1^*, E_2^*, values such that Eq. (88) will approximate as closely as possible to the given relation, Eq. (84), when H_1' takes over the role of H_1, H_2' that of H_2.

It was shown in Sec. 4·8 that when δH_1 and δH_2 are small one can write

$$\delta H_1 = af_1(\theta_3) + bf_2(\theta_3), \tag{89a}$$
$$\delta H_2 = cf_3(\theta_3) + df_4(\theta_3), \tag{89b}$$

where

$$\left.\begin{aligned} a &= \frac{g_1^2}{2L_1}, \qquad & b &= \frac{g_1^2E_1^*}{2L_1}, \\ c &= \frac{g_2^2}{2L_2}, \qquad & d &= \frac{g_2^2E_2^*}{2L_2}. \end{aligned}\right\} \tag{90}$$

The functions $f_1(\theta_3)$ and $f_2(\theta_3)$ can be computed using Eqs. (39) and (40), with H_k replaced by $H_1(\theta_3)$; $f_3(\theta_3)$ and $f_4(\theta_3)$ are also computed by Eqs. (39) and (40), respectively, with H_k replaced by $H_2(\theta_3)$.

Let it be desired to choose the constants a, b, c, d, in such a way that the linkage generates the desired relation exactly for some fixed value of θ_3:

$$h_1(\theta_3) = H_1(\theta_3) + af_1(\theta_3) + bf_2(\theta_3), \tag{91a}$$
$$h_2(\theta_3) = H_2(\theta_3) + cf_3(\theta_3) + df_4(\theta_3). \tag{91b}$$

Equation (84) specifies which values of h_1 and h_2 must correspond to each other, but there is nothing to prescribe which pair of values (h_1, h_2) must correspond to any given value of θ_3. We could, for instance, pick this pair arbitrarily and still satisfy Eqs. (91) by properly choosing the disposable constants. However, we do know that if Eqs. (91) are to be accurate δH_1 and δH_2 must be small; $h_1(\theta_3)$ must be nearly equal to

$H_1(\theta_3)$, $h_2(\theta_3)$ nearly equal to $H_2(\theta_3)$. We therefore place on our choice of the pair of values (h_1, h_2) only the condition that

$$h_1(\theta_3) = H_1(\theta_3) + \Delta h_1, \tag{92}$$

where Δh_1 is small. The corresponding value of $h_2(\theta_3)$ is easily computed. Let

$$h_2 = h_2^{(0)}(\theta_3) \qquad \text{when } h_1 = H_1(\theta_3). \tag{93}$$

Then

$$h_2(\theta_3) = h_2^{(0)}(\theta_3) + \left(\frac{dh_2}{dh_1}\right)_{h_1=H_1(\theta_3)} \cdot \Delta h_1, \tag{94}$$

to terms of the first order in the small quantity Δh_1. Combining Eqs. (91,) (92), and (94), we find that the conditions to be satisfied are

$$af_1(\theta_3) + bf_2(\theta_3) = \Delta h_1, \tag{95a}$$

$$cf_3(\theta_3) + df_4(\theta_3) = h_2^{(0)}(\theta_3) - H_2(\theta_3) + \frac{dh_2}{dh_1} \cdot \Delta h_1. \tag{95b}$$

Eliminating Δh_1 from these equations, we have

$$-a\left(\frac{dh_2}{dh_1}\right)_{\theta_3} f_1(\theta_3) - b\left(\frac{dh_2}{dh_1}\right)_{\theta_3} f_2(\theta_3) + cf_3(\theta_3) + df_4(\theta_3) = h_2^{(0)}(\theta_3) - H_2(\theta_3). \tag{96}$$

This is the only condition that must be satisfied by the constants a, b, c, d, so long as no attempt is made to control the value of the small quantity Δh_1.

Since one can satisfy simultaneously four conditions such as Eq. (96), it is possible to make the linkage generate the desired relation exactly at four chosen values of θ_3. One has to solve four simultaneous linear equations in the four unknowns a, b, c, d:

$$\left.\begin{aligned} -a\left(\frac{dh_2}{dh_1}\right)_{\theta_3^{(1)}} f_1(\theta_3^{(1)}) - b\left(\frac{dh_2}{dh_1}\right)_{\theta_3^{(1)}} f_2(\theta_3^{(1)}) + cf_3(\theta_3^{(1)}) + df_4(\theta_3^{(1)}) \\ = h_2^{(0)}(\theta_3^{(1)}) - H_2(\theta_3^{(1)}), \\ \cdots\cdots\cdots\cdots\cdots\cdots\cdots\cdots\cdots\cdots \\ -a\left(\frac{dh_2}{dh_1}\right)_{\theta_3^{(4)}} f_1(\theta_3^{(4)}) - b\left(\frac{dh_2}{dh_1}\right)_{\theta_3^{(4)}} f_2(\theta_3^{(4)}) + cf_3(\theta_3^{(4)}) + df_4(\theta_3^{(4)}) \\ = h_2^{(0)}(\theta_3^{(4)}) - H_2(\theta_3^{(4)}). \end{aligned}\right\} \tag{97}$$

The constants of the linkage can then be computed by Eqs. (90). This should be followed by exact calculation of the function generated by the linkage, as in the example of Sec. 4·14.

Example.—To illustrate this method we shall treat again the example considered in Sec. 4·14. Here, however, we shall accept as fixed the

constants arrived at in Sec. 4·13,

$$\Delta X_3 = 90°, \qquad X_{3m} = -5°, \qquad X_{4m} = -70°, \tag{98}$$

(cf. Fig. 4·22) and shall adjust only the constants L_1, L_2, E_1^*, E_2^*.

The function $H_2(H_1)$ generated by the linkage of Fig. 4·22 can be written down in parametric form by reference to Table A·1, the values of H_1 being found in the column $\Delta X_i = 90°$, $X_{im} = -5°$; the values of H_2, in the column $\Delta X_i = 90°$, $X_{im} = -70°$. These are shown in Table 4·6, together with the corresponding values of $h_2^{(0)}$ [computed by Eqs. (65) and (66) with h_1 set equal to H_1] and the over-all structural error. The structural-error function exceeds 3 per cent of the total travel; by choice of the four disposable constants we shall now attempt to reduce this error to zero for $\theta_3^{(i)} = 0.2$, 0.4, 0.6, and 0.8.

TABLE 4·6.—FUNCTION GENERATED BY LINKAGE OF FIG. 4·22

θ_3	H_1	H_2	$h_2^{(0)}$	$h_2^{(0)} - H_2$
0.0	0.0000	0.0000	0.0000	0.0000
0.1	0.1448	0.0508	0.0650	0.0142
0.2	0.2881	0.1183	0.1337	0.0154
0.3	0.4262	0.2010	0.2087	0.0077
0.4	0.5559	0.2969	0.2938	−0.0031
0.5	0.6738	0.4034	0.3926	−0.0108
0.6	0.7771	0.5181	0.5083	−0.0098
0.7	0.8632	0.6381	0.6413	0.0032
0.8	0.9301	0.7604	0.7843	0.0239
0.9	0.9761	0.8820	0.9159	0.0339
1.0	1.0000	1.0000	1.0000	0.0000

We have first to give explicit numerical form to Eqs. (97), which determine the constants a, b, c, d. Values of H_1^* and H_2^* are read from Table A·1, for the chosen values of θ_3; the f's are then computed as explained below Eq. (90). Values of $\dfrac{dh_2}{dh_1}$ can be computed by Eq. (68)

TABLE 4·7.—CONSTANTS REQUIRED IN DESIGN PROCEDURE

θ_3	H_1^*	$f_1(\theta_3)$	$f_2(\theta_3)$	H_2^*	$f_3(\theta_3)$	$f_4(\theta_3)$	$\dfrac{dh_2}{dh_1}$
0.0	0.9958	......	....	0.0000	......	....	......
0.2	0.9719	0.2587	−0.5260	0.4159	0.0754	−0.6169	0.5046
0.4	0.8435	0.2836	−0.8025	0.7402	0.3030	−0.9410	0.7344
0.6	0.6232	0.1736	−0.8025	0.9411	0.4582	−0.9410	1.3121
0.8	0.3326	0.0433	−0.5260	0.9991	0.3709	−0.6169	2.5094
1.0	0.0000	......	....	0.9083	......	....	......

with $x_1 = 70° \times H_1$. All these quantities appear in Table 4·7. By using also the last column of Table 4·6 we can easily determine all the constants of Eqs. (97):

$$\left.\begin{aligned} -0.1305a + 0.2654b + 0.0754c - 0.6169d &= 0.0154 \\ -0.2083a + 0.5894b + 0.3030c - 0.9410d &= -0.0031 \\ -0.2278a + 1.0530b + 0.4582c - 0.9410d &= -0.0098 \\ -0.1087a + 1.3199b + 0.3709c - 0.6169d &= 0.0239 \end{aligned}\right\}. \tag{99}$$

Solution of these equations yields

$$a = 0.1966, \qquad b = 0.0566, \qquad c = -0.1874, \qquad d = -0.0651. \tag{100}$$

Hence, by Eqs. (90),

$$L_1 = 1.806, \qquad L_2 = -0.703, \qquad E_1^* = 0.288, \qquad E_2^* = 0.347. \tag{101}$$

The constants specified by Eqs. (98) and (101) are not very different from those found in Sec. 4·14, and the linkage would closely resemble that of Fig. 4·26. The exact total structural error of the new linkage is given in Table 4·8: it is about a third of that of the first design. At first sight it may appear surprising that the error does not vanish for $\theta_3 = 0.2$, 0.4, 0.6, 0.8, since this was the condition applied in determining the constants of the linkage. It is to be remembered that the equations on which this method is based are approximations obtained by treating ϵ

TABLE 4·8.—TOTAL STRUCTURAL ERROR IN SECOND MECHANIZATION OF $x_2 = \tan x_1$, $0 < x_1 < 70°$

θ_3	$H_1' = h_1$	H_2'	h_2	δh_2
0.0	0.0000	0.0000	0.0000	0.0000
0.1	0.1589	0.0734	0.0715	0.0019
0.2	0.3074	0.1460	0.1435	0.0025
0.3	0.4429	0.2212	0.2187	0.0025
0.4	0.5643	0.3020	0.3001	0.0019
0.5	0.6709	0.3908	0.3899	0.0009
0.6	0.7628	0.4905	0.4901	0.0004
0.7	0.8409	0.6024	0.6026	−0.0002
0.8	0.9061	0.7268	0.7280	−0.0012
0.9	0.9589	0.8609	0.8624	−0.0015
1.0	1.0000	1.0000	1.0000	0.0000

as a small angle. The error computed by these formulas does vanish at the specified values of θ_3, but there are present other and larger errors due to the use of the small angle approximations, which are, essentially, those disclosed by the exact calculations on which Table 4·8 is based. We could make allowance for these errors, approximately, by repeating the calculation, taking as the constants on the right-hand side of Eqs.

(99) sums of corresponding entries in the last columns of Table 4·6 and 4·8. Such a refinement would be worth while only if the mechanism were to be constructed with exceptional care.

In Sec. 6·6 we shall meet a problem in which the straightforward application of this method leads to a less satisfactory result; the required modification of the method will be described there.

CHAPTER 5

THE THREE-BAR LINKAGE

5·1. Fundamental Equations for the Three-bar Linkage.—A three-bar linkage (Fig. 5·1) consists of two cranks, B_1, A_2, pivoted on a frame and connected through a link B_2. The symbols A_1, B_1, A_2, B_2 will be used to represent distances between the pivotal points within the corresponding mechanical parts: B_1 and A_2 are the lengths of arms of the cranks, B_2 is the length of the connecting link, and A_1 is the distance between pivots in the frame.

The three-bar linkage serves as a mechanical cell having one of the cranks as the input terminal, the other as the output terminal. The

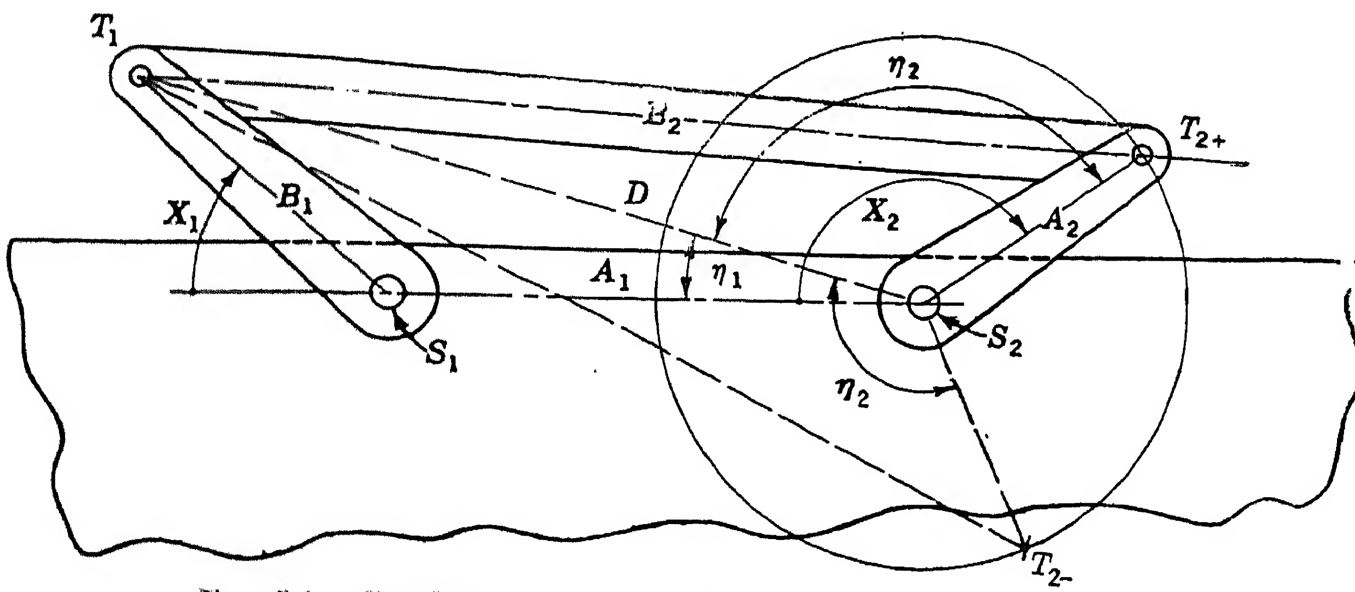

FIG. 5·1.—Symbols used in the discussion of three-bar linkages.

input and output parameters, X_1, X_2, are rotations of those cranks measured clockwise from a zero line passing through the pivotal points, S_1 and S_2, of the cranks; the zero position for each crank is that in which it points toward the left.

The functional relationship of the parameters X_1, X_2 follows from the geometry of the quadrilateral $S_1T_1T_2S_2$.

To find X_2 graphically for a given X_1 and dimensions A_1, B_1, A_2, B_2, one would first construct the zero line S_1S_2 and the line of the input crank, S_1T_1. The end T_2 of the output crank must lie on a circle of radius B_2 about T_1, and on a circle of radius A_2 about S_2. If these two circles intersect, a solution for X_2 exists; in general they will intersect in two points T_{2+}, T_{2-}, which are vertices of two congruent triangles, $T_1S_2T_{2+}$ and $T_1S_2T_{2-}$. Let η_1 be the principal value of the angle $S_1S_2T_1$, lying

between $-180°$ and $+180°$, and η_2 the principal value of the angle $T_1S_2T_{2+}$, lying between $0°$ and $+180°$. There are then two possible values of X_2:

$$X_{2+} = \eta_1 + \eta_2,$$
$$X_{2-} = \eta_1 - \eta_2. \tag{1}$$

In terms of the problem specified here, X_2 is thus a double-valued function of X_1; the functional relation $X_2 = (X_2|X_1) \cdot X_1$ has two branches, represented by the operators $(X_{2+}|X_1)$ and $(X_{2-}|X_1)$. If η_1 is not restricted to its principal value, X_2 is of course a highly multiple-valued function of X_1. Cases in which this multiple-valuedness is of significance in actual mechanical cells will appear later.

For numerical calculation of X_2 the following procedure is probably the best:

1. Compute the diagonal D of the quadrilateral using the cosine law:

$$D^2 = A_1^2 + B_1^2 + 2A_1B_1 \cos X_1. \tag{2}$$

2. Compute η_1 and η_2 by further applications of this law:

$$\cos \eta_1 = \frac{D^2 + A_1^2 - B_1^2}{2A_1D}, \qquad \text{with} \quad \sin \eta_1 \sin X_1 > 0, \tag{3}$$

$$\cos \eta_2 = \frac{D^2 + A_2^2 - B_2^2}{2A_2D}, \qquad \text{with } 0 < \eta_2 < 180°. \tag{4}$$

3. Find X_{2+}, X_{2-} by Eq. (1).

5·2. Classification of Three-bar Linkages.—Three-bar linkages are conveniently classified according to the inherent limitations on the range of the input parameter X_1. To find these limits, within which the function $X_2(X_1)$ is defined, we observe first that the diagonal D is a side of the triangle $S_1S_2T_1$ and as such is limited:

$$|A_1 - B_1| \leqq D \leqq A_1 + B_1. \tag{5}$$

Similarly, since D is a side of the triangle $T_1S_2T_{2+}$,

$$|A_2 - B_2| \leqq D \leqq A_2 + B_2. \tag{6}$$

These are the only limitations on D, and they imply the limitations on X_1 with which we are concerned.

Since Eqs. (5) and (6) apply simultaneously, they must be consistent; unless there is overlapping of the intervals set by them for D, it will not be possible to construct a cell with the given dimensions. When the two intervals overlap, D can take on any value within the range common to them. As is illustrated in Fig. 5·2, the intervals can overlap in four different ways, which form the first basis for our classification of these linkages:

$$\text{Class } a\text{: } |A_2 - B_2| < |A_1 - B_1| < A_1 + B_1 < A_2 + B_2, \tag{7}$$
$$\text{Class } b\text{: } |A_1 - B_1| < |A_2 - B_2| < A_1 + B_1 < A_2 + B_2, \tag{8}$$
$$\text{Class } c\text{: } |A_2 - B_2| < |A_1 - B_1| < A_2 + B_2 < A_1 + B_1, \tag{9}$$
$$\text{Class } d\text{: } |A_1 - B_1| < |A_2 - B_2| < A_2 + B_2 < A_1 + B_1. \tag{10}$$

In each case, D can take on all values between the two intermediate quantities of the corresponding line.

The linkages of Class a have an unlimited input, since Eq. (5) implies no limitation on X_1, and Eq. (6) is automatically satisfied. Linkages of the other three classes have a limited input range. With linkages of Class b, passage through the value $X_1 = 180°$ is impossible, since D cannot assume the corresponding value $|A_1 - B_1|$. With linkages of Class c, passage through $X_1 = 0°$ is excluded, since D cannot assume the corresponding value $A_1 + B_1$. Finally, with linkages of Class d, passages through $X_1 = 0$ and $X_1 = 180°$ are both impossible; D cannot attain values corresponding to either of these points. The range of the output variables can be discussed similarly.

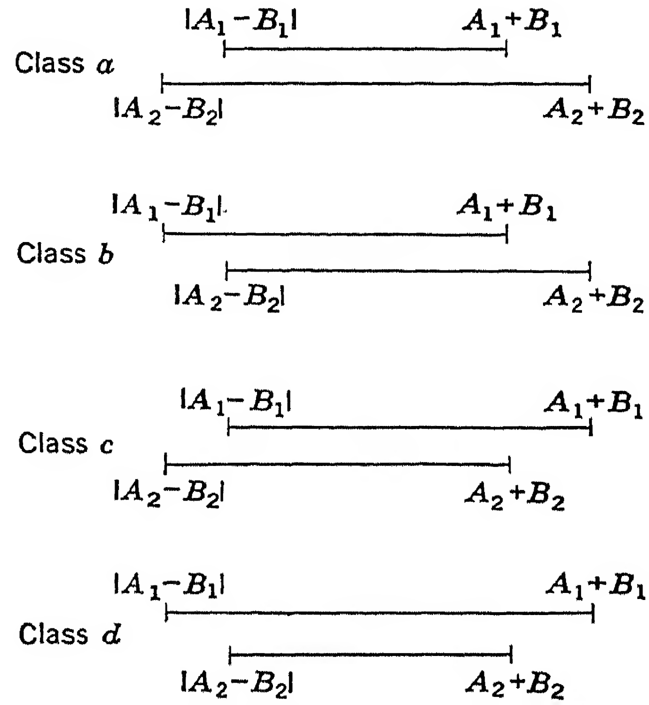

FIG. 5·2.—Classification of three-bar linkages.

From what has been said it is obvious that the four linkages with

1. $A_1 = p,\ B_1 = q,\ A_2 = r,\ B_2 = s$
2. $A_1 = q,\ B_1 = p,\ A_2 = r,\ B_2 = s$
3. $A_1 = p,\ B_1 = q,\ A_2 = s,\ B_2 = r$
4. $A_1 = q,\ B_1 = p,\ A_2 = s,\ B_2 = r$

belong to the same class. Now the relative magnitudes of A_1, A_2, B_1, B_2 form the basis of a further subclassification of three-bar linkages, the subclasses being given the numerical designation above if one takes always $p > q$, $r > s$. That is, Class a linkages are divided into four subclasses:

$$a1\text{: } A_1 > B_1, \qquad A_2 > B_2, \tag{11}$$
$$a2\text{: } A_1 < B_1, \qquad A_2 > B_2, \tag{12}$$
$$a3\text{: } A_1 > B_1, \qquad A_2 < B_2, \tag{13}$$
$$a4\text{: } A_1 < B_1, \qquad A_2 < B_2, \tag{14}$$

and the other classes are similarly divided into four subclasses.

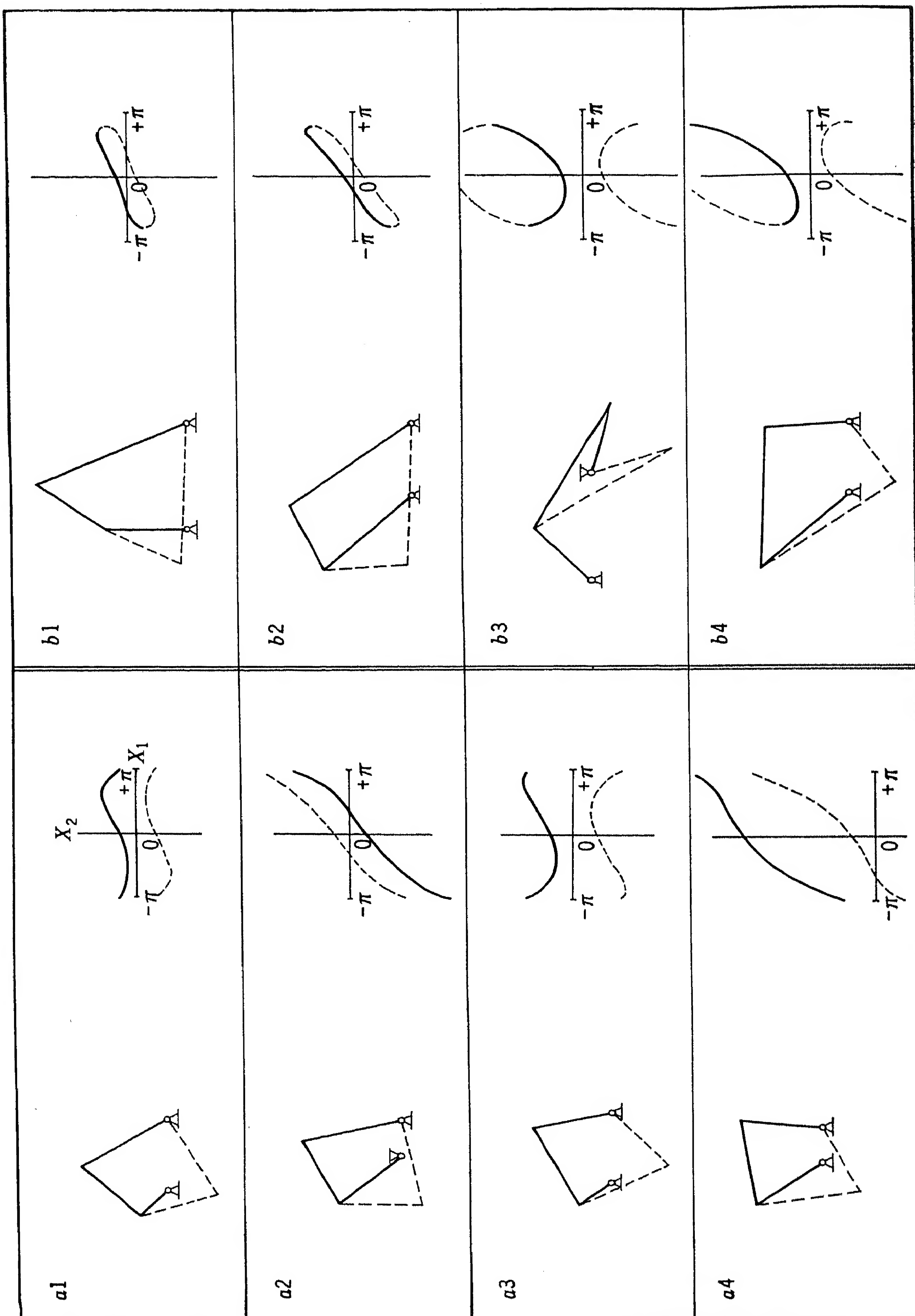
a1
a2
a3
a4
b1
b2
b3
b4
X_1
X_2
$+\pi$
0
$-\pi$

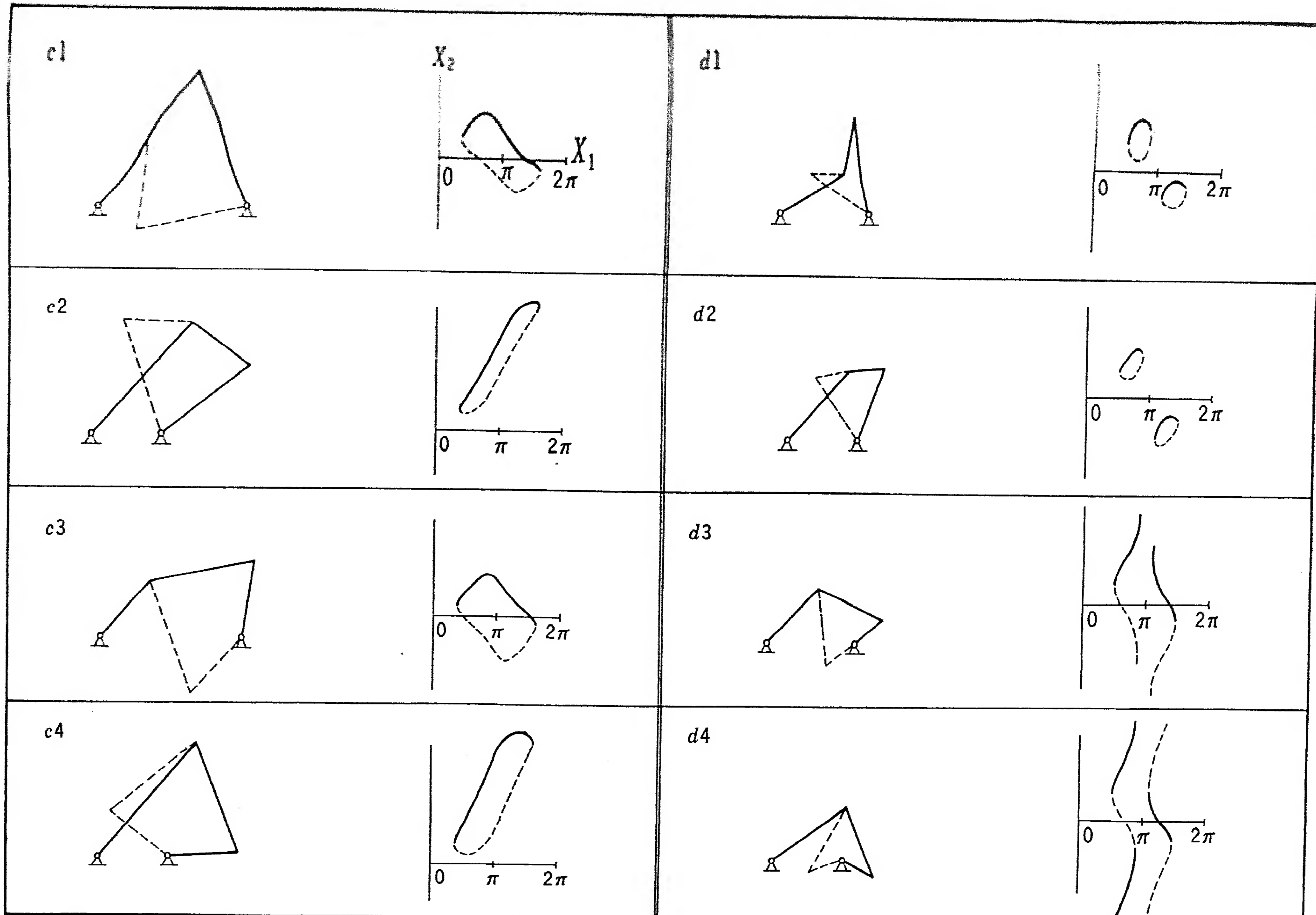

FIG. 5·3.—Types of functions generated by three-bar linkages. The positive branch is indicated by a continuous line, the negative branch by a dashed line. The vertical X_2-scale is the same as the horizontal X_1-scale.

Finally, in each subclass X_2 is a function with two branches, X_{2+} and X_{2-}, which we place in separate sub-subclasses of the subclass. Three-bar linkages are thus divided into $4 \times 4 \times 2 = 32$ sub-subclasses in all. A sub-subclass will be indicated by a symbol such as $c3^+$, which applies to the positive branch of a linkage for which

$$|A_2 - B_2| < |A_1 - B_1| < A_2 + B_2 < A_1 + B_1,$$
$$A_1 > B_1, \qquad A_2 < B_2.$$

The general forms of the functions generated by all these types of three-bar linkage are illustrated in Fig. 5·3. In each case the X_2 has been plotted as a function of X_1, for a three-bar linkage with dimensions illustrated in the adjoining sketch. A mechanical configuration and the generated curve are both shown for the positive branch by continuous lines, for the negative branch by dotted lines. The value of X_2 shown is not necessarily the principal value. In some cases the positive and negative branches join continuously, but always at a point of infinite slope near which the linkage is not operable. The reader should study this figure carefully, since one should not attempt to mechanize by this means functions that obviously are not included in the class of functions of the three-bar linkage.

5·3. Singular Cases of Three-bar Linkages.—Certain special three-bar linkages that belong to more than one of the classes defined above,

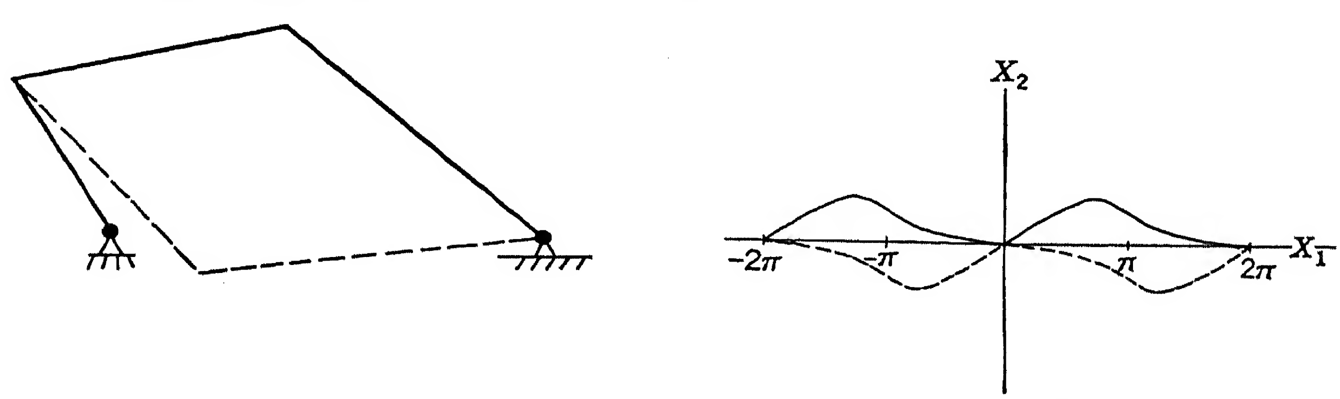

FIG. 5·4.—Three-bar linkage with $A_1 + B_1 = A_2 + B_2$.

as limiting cases, have special properties that entitle them to separate mention.

Case A: $$A_1 + B_1 = A_2 + B_2. \qquad (15)$$

A linkage of this type (Fig. 5·4) has a singular point for $X_1 = 0$. So long as the input variable is restricted to a range not including the point $X_1 = 0$, the configuration of the mechanism and the value of the output variable are uniquely determined. When $X_1 = 0$ the value of X_2 is still uniquely determined, but the mechanism has at this point an indeterminate motion, there being two possible finite values for dX_2/dX_1.

Thus, when the input parameter is allowed to pass through the value $X_1 = 0$, X_2 may or may not pass from the positive to the negative branch of the function, or conversely; the value of X_2 is no longer uniquely determined by the value of X_1, but may have either of two values, unless appropriate stops are introduced.

Case B:

$$|A_1 - B_1| = |A_2 - B_2|. \tag{16}$$

In this case (Fig. 5·5) a similar singularity exists for $X_1 = 180°$.

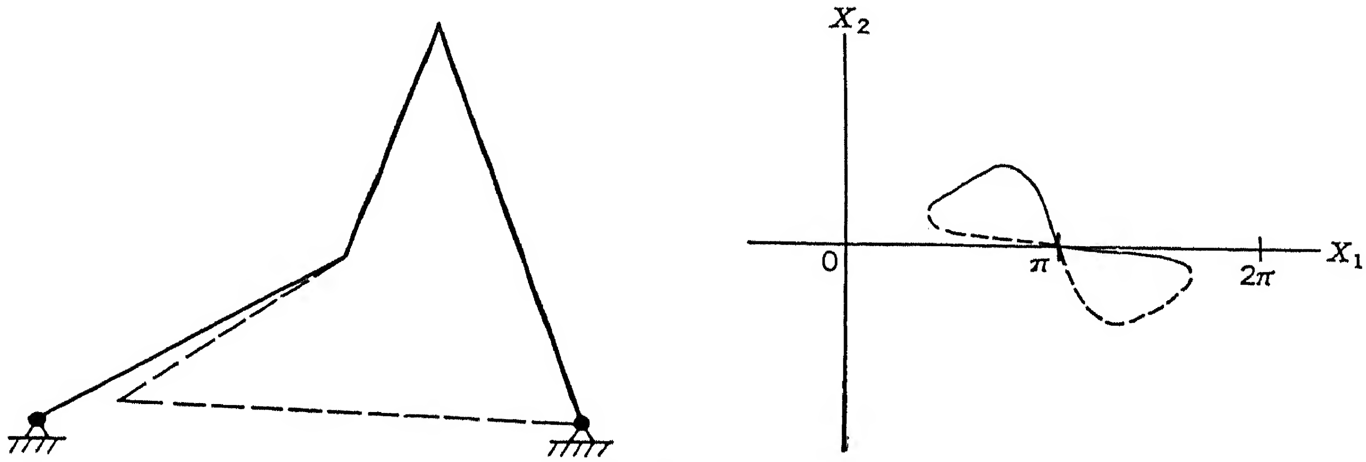

FIG. 5·5.—Three-bar linkage with $A_1 - B_1 = A_2 - B_2$.

Case C:

$$\left.\begin{aligned} A_1 + B_1 &= A_2 + B_2 \\ |A_1 - B_1| &= |A_2 - B_2| \end{aligned}\right\} \quad \text{simultaneously.} \tag{17}$$

In this case there are, of course, singular points for both $X_1 = 0$ and $X_1 = 180°$, as well as some other important features that should be mentioned.

The conditions in Eq. (17) can be satisfied in two ways:

$$C_1: \quad A_1 - B_1 = -(A_2 - B_2); \quad B_1 = A_2; \quad A_1 = B_2. \tag{18}$$
$$C_2: \quad A_1 - B_1 = A_2 - B_2; \quad A_1 = A_2; \quad B_1 = B_2. \tag{19}$$

The Case C_1, the parallelogram linkage (Fig. 5·6), is very well known. Its positive branch (for $0 < X_1 < 180°$) is used to transmit rotation from one shaft to another at the ratio 1 to 1, within limits set far enough from the points of singularity, at which backlash may become important. (A good range in practice is $30° < X_1 < 150°$, but larger ranges can be attained by increased care in manufacture.) The corresponding negative branch of the linkage function, shown dotted in Fig. 5·6, is rarely used; its curvature decreases as the length of the link B_2 is increased. It will be noted that the various positive and negative branches, differing by changes in X_1 and X_2 which are multiples of 2π, form a connected network through the whole of the X_1X_2-plane. If no stops are introduced the generated X_2 may or may not pass from a positive branch to a

negative branch, or vice versa, every time X_1 passes through a value that is a multiple of π. The value of X_2 is thus not uniquely determined by the value of X_1; it is not even restricted to one of two values, as in Cases A and B; it may take on an infinite number of values, which fall, of course, into two sequences with spacing 2π, corresponding to the positive and negative branches.

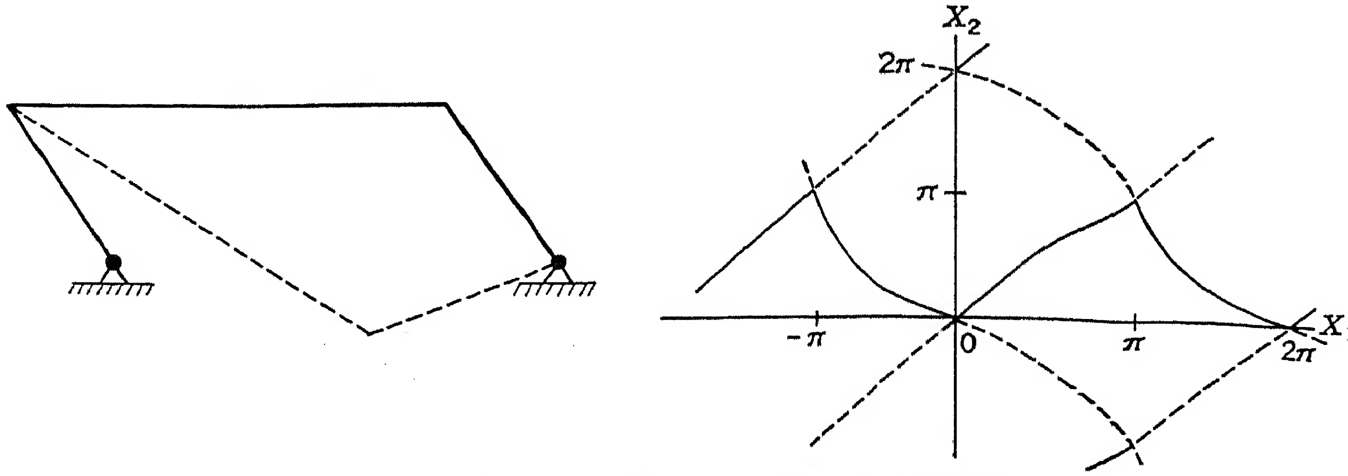

FIG. 5·6.—Three-bar linkage with $B_1 = A_2$, $A_1 = B_2$.

Linkages of Class C_2 (Fig. 5·7) are of special interest in that X_2 remains zero on part of the positive and negative branches, whatever the value of X_1; how this can happen will be evident from the geometry of the sketch. [The classification of branches as positive and negative is here quite formal; physically it would be more appropriate to think of the branches as (1) the straight line $X_2 = 0$, and (2) the oscillatory curve with continuous derivative.] If the generated X_2 is following the positive

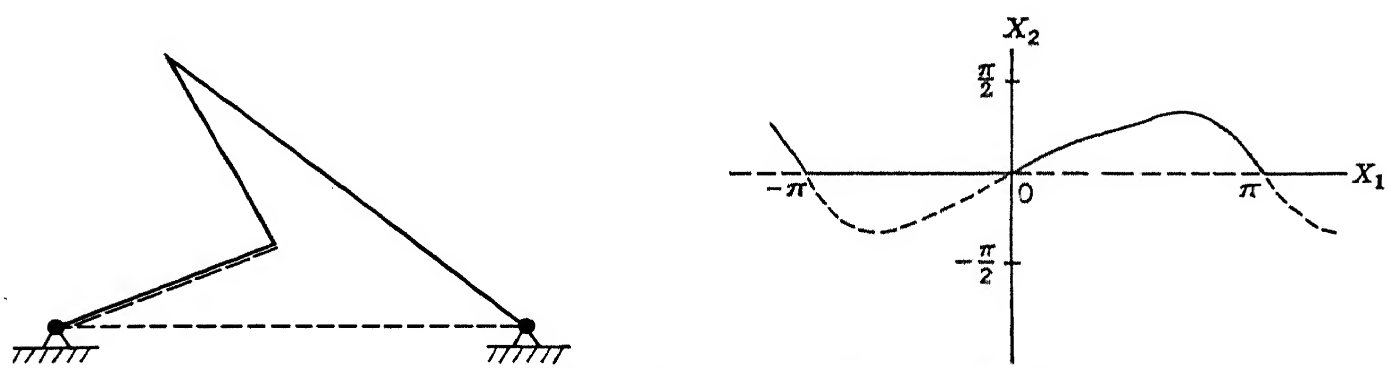

FIG. 5·7.—Three-bar linkage with $A_1 = A_2$, $B_1 = B_2$.

branch between $X_1 = 0$ and $X_1 = \pi$, and X_1 passes through the former point, then X_2 may continue to change at a uniform rate by passing over to the negative branch, or it may follow the positive branch and remain zero thereafter; this latter behavior can be assured by the introduction of stops. This type of linkage is therefore of value in mechanizing functions with a discontinuity in the derivative. Unfortunately, these cells cannot supply any appreciable effort near the point of singularity;

torques must be applied to both cranks in the directions of the desired motions.

In practical applications the author uses a still more special linkage, with $A_1 = B_1 = A_2 = B_2$ (Fig. 5·8). This is also a special case of the other singular classes, A, B, and C_1; it is interesting to observe how the diverse curves of Figs. 5·4 to 5·7 can pass over into the curves of Fig. 5·8 as a common limiting case. With this linkage three types of configura-

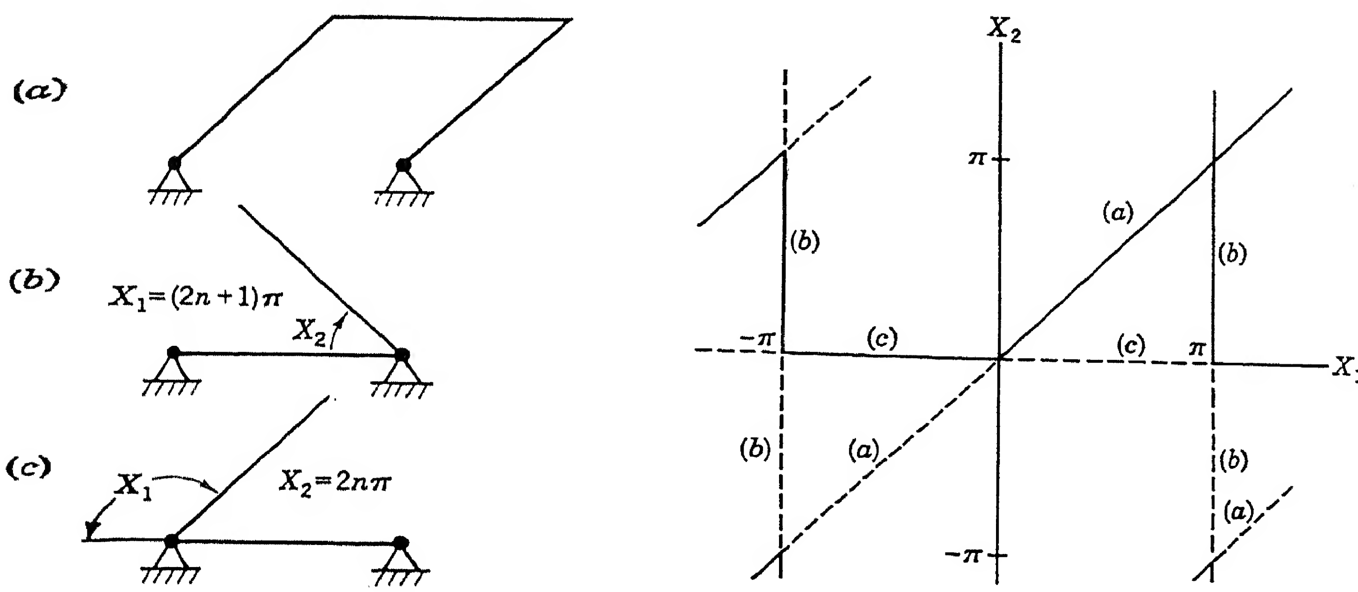

FIG. 5·8.—Three-bar linkage with $A_1 = B_1 = A_2 = B_2$.

tion are possible, represented by three sets of lines on the graph in Fig. 5·8:

a. The parallelogram linkage configuration, represented by the curves $X_2 = X_1 + 2\pi n$.

b. Configurations in which the input terminal is locked in a definite position, $X_1 = (2n + 1)\pi$, while the output terminal can assume any position.

c. Configurations in which the output terminal is locked in a definite position, $X_2 = 2\pi n$, while the input terminal can assume any position.

Of particular interest are the transitions between configurations of types (*b*) and (*c*), which can be assured by the use of stops. We shall now see how these can be used in generating a function with a discontinuous derivative.

Figure 5.9 shows a mechanical cell for which

$$
\begin{aligned}
X_k &= aX_i \qquad \text{when } X_i > 0,\\
X_k &= bX_i \qquad \text{when } X_i < 0,
\end{aligned}
\tag{20}
$$

with

$$a > 1 > b.$$

It consists of the linkage of Fig. 5·8, with added input and output terminals which are push-rods pivoted to the central link B_2. The input and output parameters, X_i and X_k, are displacements of these rods perpendicular to the line of the pivots S_1 and S_2 of the three-bar linkage. When $X_i = X_k = 0$, the linkage is in its critical position, with $X_1 = 180°$, $X_2 = 0°$; the two cranks then just touch stops C_1, C_2, which limit their motions to $X_1 \geqq 180°$, $X_2 \geqq 0$. If X_i is now increased by a push exerted on the X_i terminal, the crank A_2 will be held firmly by the stop C_2, while the crank B_1 and the link B_2 will rotate together about their collinear pivotal axes S_1 and T_2 into, for example, the configuration illustrated in Fig. 5·9. The parameter X_k will then increase more rapidly than X_i, in the ratio of the distances of the corresponding push-rod pivots from the axis of rotation:

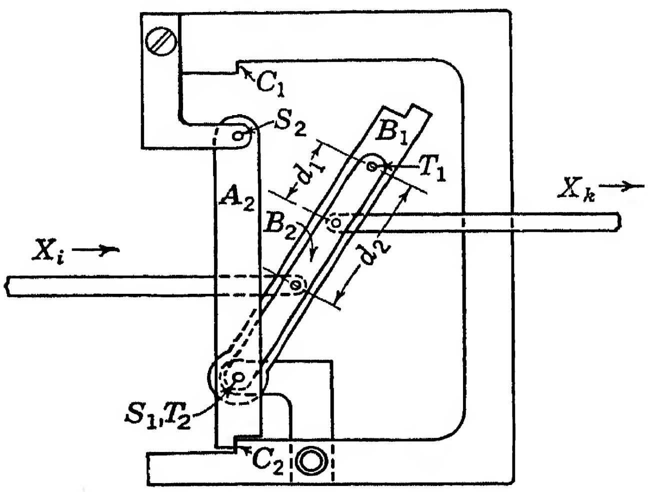

FIG. 5·9.—Mechanical cell generating a function with discontinuous derivative.

$$a = \frac{B_2 - d_1}{B_2 - d_2}. \tag{21}$$

If the direction of motion is reversed by a push exerted on the X_k terminal, A_2 will be held against the stop C_2 both by the linkage constraint and by the torque due to any resisting force at the X_i terminal, until the crank B_1 touches the stop C_1. At this point the situation changes abruptly: the crank B_1 can no longer rotate; the crank A_2 is no longer locked in position by the linkage constraint; a further push on the X_k terminal will cause the crank A_2 and the link B_2 to rotate together about their now collinear pivotal axes S_2 and T_1. Then X_i and X_k both become negative, the ratio of their values being

$$b = \frac{d_1}{d_2}. \tag{22}$$

The change in dX_2/dX_1 as the linkage is pushed through its critical position, in either direction, is quite abrupt; it is associated with a similarly sudden increase in the driving force necessary to overcome a resisting force at the other terminal, when the mechanical advantage is reduced by the change in fulcrum.

The desired discontinuity in the derivative is not so perfectly realized if the link is pulled rather than pushed through its critical position. When the configuration is that illustrated in Fig. 5·9, a pull exerted on the

X_i-terminal and a resisting pull on the X_k-terminal will produce a torque tending to move the arm A_2 away from its stop. This arm, however, is locked in position by the linkage constraint, and the locking will be effective until the critical position is approached, and mechanical play in the linkage becomes important. This will allow crank A_2 to begin to move away from stop C_2 before crank B_1 quite reaches stop C_1; the result is some rounding off of the otherwise abrupt transition from one slope to another, but there is no tendency for the mechanism to jam.

5·4. The Problem of Designing Three-bar Linkages.—We have now to consider the problem of determining the elements of a three-bar linkage that will mechanize a given function

$$x_2 = (x_2|x_1) \cdot x_1. \tag{23}$$

If this function is to fall within the class of linkage functions, it must be required to generate it only for a finite range Δx_1 of the input variable x_1, or, if the range of x_1 is infinite, x_2 must be a periodic function of x_1 with period Δx_1. In either case, restricting attention to the range Δx_1 of the input variable, one can write the relation in homogeneous form:

$$h_2 = (h_2|h_1) \cdot h_1. \tag{24}$$

To mechanize this relation we have to design a three-bar linkage described by

$$X_2 = (X_2|X_1) \cdot X_1, \qquad X_{1m} \leqq X_1 \leqq X_{1M}, \tag{25}$$

such that when homogeneous parameters H_1, H_2 are introduced, the corresponding relation

$$H_2 = (H_2|H_1) \cdot H_1 \tag{26}$$

becomes identical with Eq. (24) on direct or complementary identification of the pair of variables (h_1, h_2) with the pair $(H_1\ H_2)$. If the function to be generated is periodic, it is necessary, in addition, that

$$\Delta X_1 = X_{1M} - X_{1m} = 360°;$$

the infinite range of x_1 then corresponds to the infinite range of X_1, when passage to the next period of the generated function is permitted.

A three-bar linkage may be described by the constants $A_1\ B_1$, A_2, B_2, X_{1m}, X_{1M}, ΔX_1, X_{2m}, X_{2M}, ΔX_2; of these only five are independent. The form of the function $(X_2|X_1)$ is determined by three independent ratios of the sides of the quadrilateral; the angles X_1 and X_2 do not depend on the over-all scale of the mechanism. We shall choose the three side-ratios, B_1/A_1, B_2/A_2, A_1/A_2, as the independent constants that determine the form of $(X_2|X_1)$. Now, the field of functions $(X_2|X_1)$

of the three-bar linkage is three-dimensional, but each function $(X_2|X_1)$ can generate a whole field of functions $(H_2|H_1)$ that depend on the choice of additional constants: two constants (for example, X_{1m} and X_{1M}) in the case of a nonperiodic function, and one (for example, X_{2m}) in the case of periodic functions. The field of all functions $(H_2|H_1)$ of a three-bar linkage is therefore five-dimensional where nonperiodic functions are concerned, and four-dimensional with respect to periodic functions. We shall henceforth concentrate our attention on the more difficult case of nonperiodic functions.

In practical terms, the problem is that of approximating a given function $(h_2|h_1)$ as well as possible by a three-bar-linkage function $(H_2|H_1)$ characterized by five independent constants. It is very difficult to find the best fit by varying all five constants independently; one must begin by assigning fixed values to at least two of them, even when choice of these values must be made rather arbitrarily. Fortunately, in practice one has usually some indication of an appropriate value for one or more of these constants.

The way in which a linkage is used in the computer as a rule suggests an appropriate value for ΔX_1 and ΔX_2. In particular, in generating a monotonic function one can hardly have $\Delta X_1 > 180°$; on the other hand, ΔX_1 must not be chosen too small lest the linkage degenerate into what is essentially a harmonic transformer. It is thus evident that it will be useful to have a method for finding the best fit to the given function consistent with specified values of ΔX_1 and ΔX_2; the side-ratios (or their equivalent) will then be the adjustable parameters. The nomographic method, to be described immediately, is suited for this type of curve fitting. It should be used for all monotonic functions and is useful in many other cases.

When the given function is not monotonic, it is sometimes difficult to choose ΔX_1. The geometric method, to be described later in this chapter, is then useful. In applying this method, ΔX_2 and B_2/A_2 are fixed and the fit to the given function is obtained by adjustment of ΔX_1, B_1/A_1, and A_1/A_2.

THE NOMOGRAPHIC METHOD

The "nomographic method" here discussed is a method of curve fitting by three-bar linkages with given ΔX_1 and ΔX_2. It takes its name from the use made of an intersection nomogram, which appears as an insert in the back of this book. This nomogram, Fig. B·1, is also useful in many other types of calculations on three-bar linkages.

5·5. Analytic Basis of the Nomographic Method.—For analytic purposes it is convenient to specify the side-ratios of the quadrilateral through the three independent constants

$$b_1 = \ln\left(\frac{B_1}{A_1}\right), \tag{27}$$

$$b_2 = \ln\left(\frac{B_2}{A_2}\right), \tag{28}$$

$$a = \ln\left(\frac{A_1}{A_2}\right). \tag{29}$$

Correspondingly, we may specify the configuration of the quadrilateral in terms of the diagonal-to-side ratio, through one or the other of the new variable parameters

$$p_1 = \ln\left(\frac{D}{A_1}\right), \tag{30}$$

$$p_2 = \ln\left(\frac{D}{A_2}\right) = p_1 + a, \tag{31}$$

which will replace the input parameter X_1 in our discussion.

In terms of these new symbols the equations of Sec. 5·1 take on a less familiar but very useful form. Since

$$\frac{D}{A_1} = e^{p_1}, \qquad \frac{B_1}{A_1} = e^{b_1}, \qquad \frac{B_2}{A_2} = e^{b_2}, \qquad \frac{A_1}{A_2} = e^{a}, \tag{32}$$

one can rewrite Eq. (2) as

$$e^{2p_1} = 1 + e^{2b_1} + 2e^{b_1}\cos X_1, \tag{33}$$

or

$$e^{2p_1} = 2e^{b_1}\left(\frac{e^{b_1} + e^{-b_1}}{2} + \cos X_1\right). \tag{34}$$

Hence the relation between the variable parameters X_1 and p_1 is given by

$$\cos X_1 = \tfrac{1}{2}\, e^{2p_1 - b_1} - \cosh b_1, \tag{35}$$

or

$$p_1 = \tfrac{1}{2}\ln\left(2\cos X_1 + 2\cosh b_1\right) + \tfrac{1}{2}\, b_1. \tag{36}$$

By similar manipulations Eqs. (3) and (4) become, respectively,

$$\cos\eta_1 = \cosh p_1 - \tfrac{1}{2}e^{2b_1}e^{-p_1}, \tag{37}$$

$$\begin{aligned}\cos\eta_2 &= \cosh p_2 - \tfrac{1}{2}e^{2b_2}e^{-p_2}\\ &= \cosh(p_1 + a) - \tfrac{1}{2}e^{2b_2}e^{-(p_1+a)}.\end{aligned} \tag{38}$$

As before, $\sin\eta_1$ and $\sin X_1$ must have this same sign, while

$$0 \leqq \eta_2 \leqq 180°.$$

Then the output parameter is given by

$$X_{2+} = \eta_1 + \eta_2, \tag{39}$$

or by

$$X_{2-} = \eta_1 - \eta_2. \tag{40}$$

Equations (36) to (40) describe all three-bar-linkage functions $(X_2|X_1)$. The important feature of this formulation is the expression of η_1 and η_2 in terms of the same function of two independent variables,

$$G(p, b) = \cos^{-1} (\cosh p - \tfrac{1}{2}e^{2b-p}); \tag{41}$$

one has

$$\eta_1 = G(p_1, b_1) \tag{42}$$

and

$$\eta_2 = G(p_2, b_2) = G(p_1 + a, b_2). \tag{43}$$

This makes it possible to compute η_1 and η_2 by the same intersection nomogram, with other advantages that will become clear as the discussion proceeds.

5·6. The Nomographic Chart.—In three-bar-linkage calculations one repeatedly encounters the relations

$$\eta = G(p, b) = \cos^{-1} (\cosh p - \tfrac{1}{2}e^{2b-p}) \tag{44}$$

and

$$p = F(X,b) = \tfrac{1}{2} \ln (2 \cos X + 2 \cosh b) + \tfrac{1}{2}b, \tag{45}$$

where p stands for p_1 or $p_2 = p_1 + a$, b for b_1 or b_2, X for X_1, and η for η_1 or η_2. It may be required to solve these equations singly or simultaneously, with various choices of the unknown. For rapid calculations of this type the use of an intersection or grid nomogram is very convenient.

The intersection nomogram representing a given functional relation is not uniquely determined, but may be given an infinite variety of forms. In the present case it is desirable to take lines of constant p as vertical lines, lines of constant η as horizontal lines, and to plot on the (p, η)-plane curved lines of constant b and constant X (Fig. 5·10). It is at once evident that choice of *consistent* values of any two of the variables will determine a definite point on the chart—the intersection of the lines corresponding to the given values of these variables; corresponding values of the two other variables, as determined by Eqs. (44) and (45), can then be read off at the same point. Before illustrating this process, however, we must consider in more detail the structure and properties of the chart.

As shown in Fig. 5·10, the horizontal scale is uniform in p with the vertical lines spaced at intervals of 0.1 ln 10; they are labeled in terms of the variable

$$\mu p = \log_{10} \left(\frac{D}{A}\right), \tag{46}$$

for which the intervals are 0.1. The vertical scale is uniform in η, with lines of constant η shown in Fig. 5·10 at intervals of 30°, from $-180°$ to $+180°$.

On the grid thus established there have been plotted lines of constant b at intervals of 0.1 ln 10; they are labeled in terms of the variable

$$\mu b = \log_{10} \frac{B}{A}, \tag{47}$$

for which the intervals are 0.1. (The factor $\mu = 1/\ln 10$ is introduced in this way to facilitate computation with decimal logarithms.) The curve $b = 0$ is open, with the horizontal asymptotes $\eta = \pm 90°$. Curves

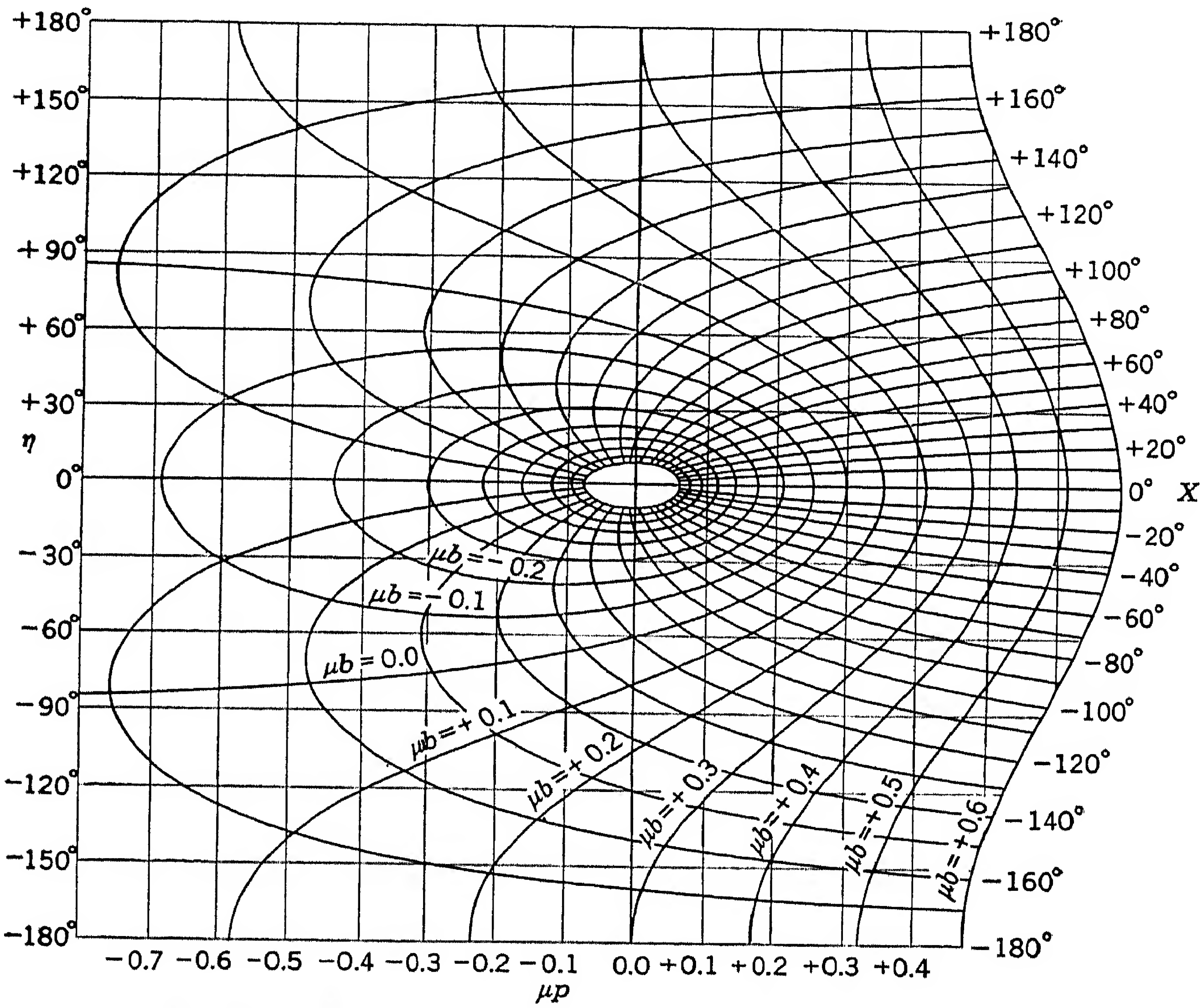

FIG. 5·10.—Intersection nomogram solving Eqs. (44) and (45).

of constant $b < 0$ are closed. Curves of constant $b > 0$ are open and periodic in η with period $\Delta\eta = 360°$; they have a pronounced sinusoidal character, being symmetric to reflection in the lines

$$\eta = \cdots -180°, 0°, 180°, \ldots$$

and centrally symmetric about the points where they cross the lines

$$\eta = \cdots -90°, +90°, \ldots .$$

For a more detailed discussion the reader is referred to Appendix B.

Lines of constant X have been plotted at intervals of 10°. All are open curves, and each has the same shape as a part of the curve $b = 0$. Indeed, the curves $X = X_0$ and $X = X_0 - 180°$, which join smoothly at $p = \eta = 0$ if $0 < X_0 < 180°$, together form a curve congruent with the curve $b = 0$. All have asymptotes parallel to the p-axis, but run to infinity toward the right ($p = +\infty$), instead of toward the left ($p = -\infty$) as does the curve $b = 0$. Again the reader is referred to Appendix B for a more complete discussion.

Since the parameters p and η have no limits, the nomogram extends in principle over the whole plane. It is periodic in η with period 360°; the part shown in Fig. 5·10 could be supplemented by the addition of similar figures above and below, extending indefinitely to positive and negative η. The chart could also be extended to larger and smaller p, but the added portions would be of less practical importance since very large or very small values of b are not much used.

In actual work one does not need the whole field covered by Fig. 5·10 but only its upper half, since the lower half is a mirror image. By suppressing the lower half, longer scales can be used in a given available space. This has been done in the preparation of Fig. B·1, which presents this nomogram on the largest scale possible in this book. This figure is quite adequate for a study of the method; in actual design work it is desirable to have it drawn on a scale twice as large and with a greater number of curves. Table B·1 of Appendix B presents the information needed for redrawing the nomogram—the coordinates $(\mu p, \eta)$ of the points of intersection of the curves $\mu b = 0, \pm 0.01, \pm 0.02, \cdots, \pm 0.5$, with the curves $X = 0, \pm 5°, \pm 10°, \cdots, \pm 180°$.

5·7. Calculation of the Function Generated by a Given Three-bar Linkage.—The intersection nomogram permits solution of Eqs. (36) to (40), which completely describe any three-bar linkage; it therefore suffices for the graphical construction of any three-bar-linkage function $(X_2|X_1)$. The procedure will be described in connection with its application to the special linkage sketched in Fig. 5·11, for which $\mu b_1 = -0.1$, $\mu b_2 = 0.3$, $\mu a = 0.3$. For this linkage $\dfrac{B_1}{A_1} = 0.795$, $\dfrac{B_2}{A_2} = 1.995$, $\dfrac{A_1}{A_2} = 1.995$; with B_2 taken as unity, the links have lengths $B_1 = 0.795$, $A_1 = 1.000$, $A_2 = 0.501$.

To determine the value of the output parameter X_2 corresponding to a given value of X_1—in the example, 140°, as illustrated in Fig. 5·11—we proceed as follows:

(1) Knowing X_1 and b_1, one can determine p_1 and η_1 by Eqs. (36) and (37). Instead, on the nomogram, Fig. 5·12, we follow the curve $X = X_1$ (=140°) until it intersects with the curve $\mu b = \mu b_1$ (= -0.1) at

the point $P^{(0)}$. At this point we can read off the corresponding values of μp_1 (= −0.191) and η_1 (= 52.5°).

(2) Knowing μp_1 and μa, one can compute $\mu(p_1 + a)$—in the example 0.109. Instead, on the nomogram we locate a point μa units to the right of $P^{(0)}$ (by the scale at the bottom of the figure) and through this construct the vertical line $\mu p = \mu(p_1 + a)$.

(3) Knowing $\mu(p_1 + a)$ and μb_2, one can compute η_2 by Eq. (38). Instead, on the nomogram we follow the vertical line $\mu p = \mu(p_1 + a)$ until it intersects the curve $\mu b = \mu b_2$ (= 0.3), as it does at the two points,

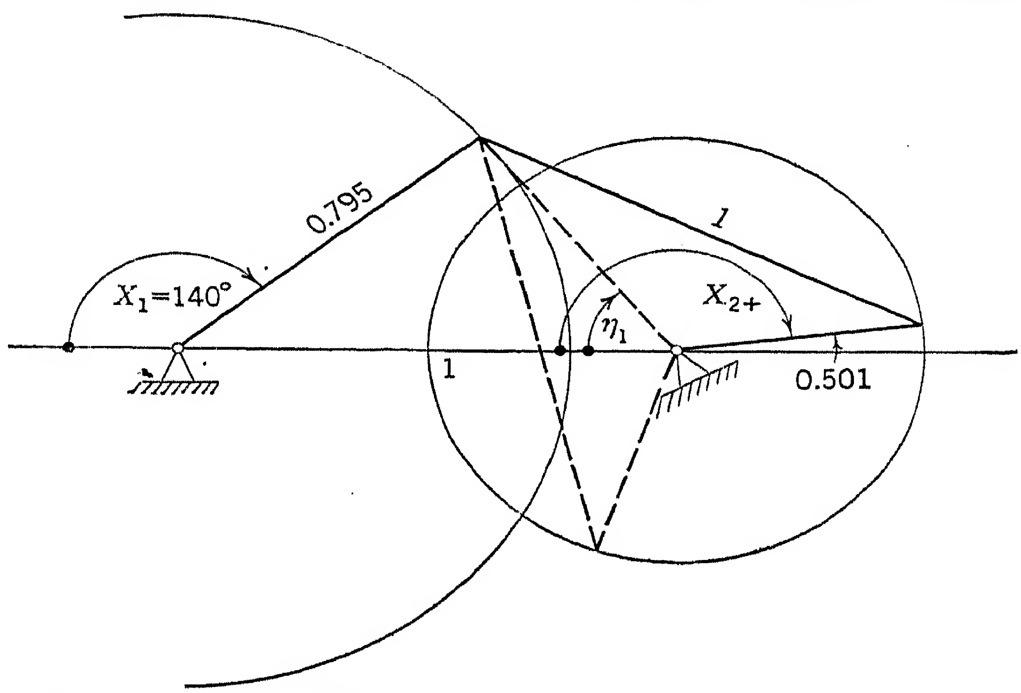

FIG. 5·11.—Three-bar linkage used in illustrative calculations.

$Q_+^{(0)}$ and $Q_-^{(0)}$, within the field of Fig. 5·12, and at an infinite sequence of points outside this field. It is at the point $Q_+^{(0)}$ that η lies between 0 and π, and it is, therefore, at this point that we can read off the value of η_2 (= 121°).

(4) Computation of X_2 is now simple:

$$X_{2+} = \eta_1 + \eta_2 = 52.5° + 121° = 173.5°,$$

and

$$X_{2-} = \eta_1 - \eta_2 = 52.5° - 121° = -68.5°.$$

These values can be checked on Fig. 5·11.

It will be noted that in Fig. 5·12 the value of η_1 is represented by a vertical line from the line $\eta = 0$ to the point $P^{(0)}$, and the value of η_2 is represented by a similar line to the point $Q_+^{(0)}$. Graphical methods for adding these lengths can be used to construct the value of X_{2+}. In the same way, the vertical line from $\eta = 0$ to the point $Q_-^{(0)}$ represents the (negative) quantity which must be added to η_1 to get X_{2-}; we call this η_{2-}, to distinguish it from the principal value, η_{2+}, and write

$$X_{2\pm} = \eta_1 + \eta_{2\pm}. \tag{48}$$

We shall often use this relation instead of Eqs. (39) and (40). The point $Q_+^{(0)}$ will then be regarded as corresponding to the positive branch of the solution for X_2, and $Q_-^{(0)}$ as corresponding to the negative branch.

By use of the nomogram we can get a graphic presentation of the entire course of the function generated by a given linkage. To picture

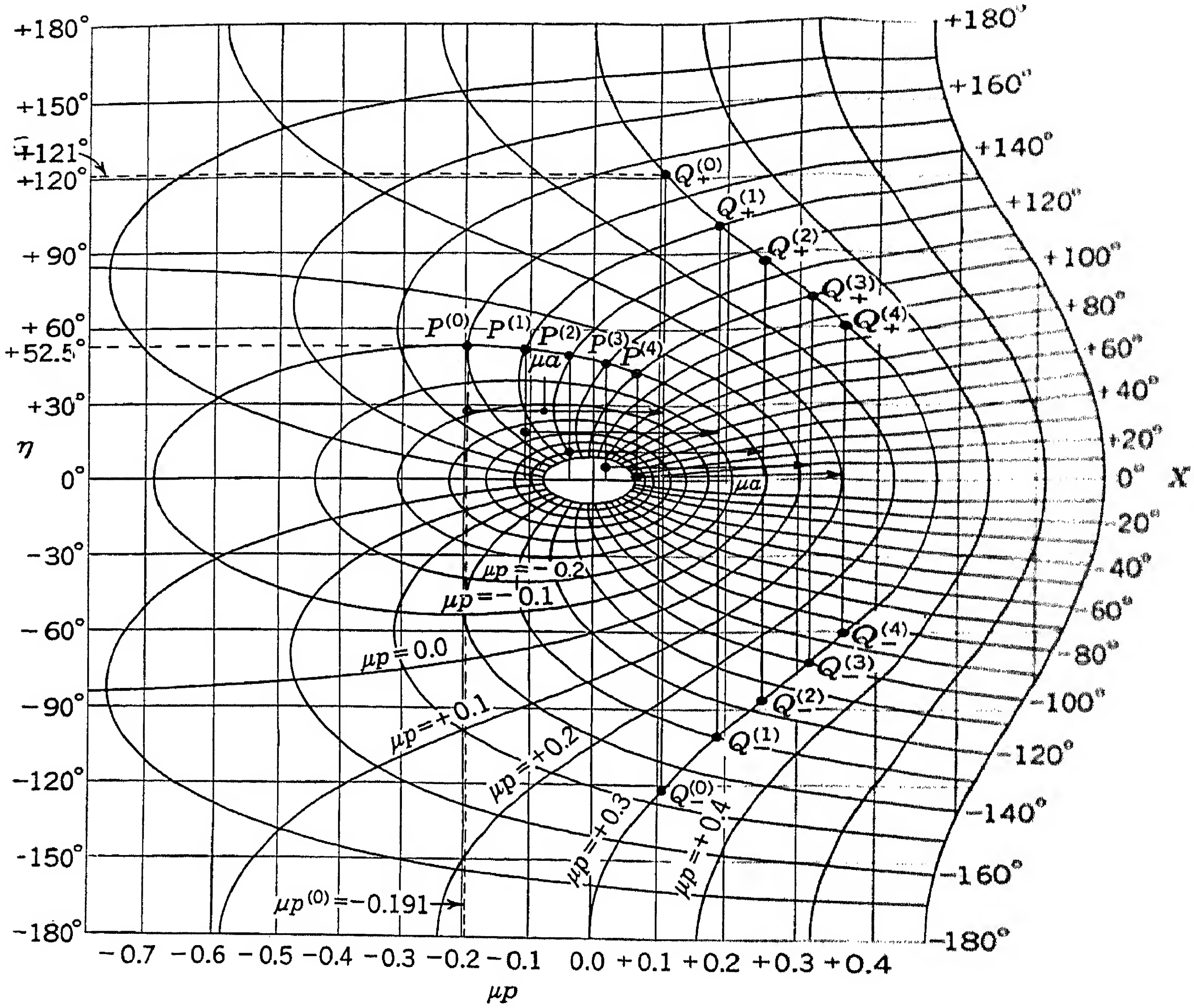

FIG. 5·12.—Calculation of the function generated by a given three-bar linkage.

the function $(X_2|X_1)$ we may wish to compute X_2 for a "spectrum of values of X_1":

$$X_1^{(0)}, X_1^{(1)}, X_1^{(2)}, \dots X_1^{(n)}.$$

(In Fig. 5·12, $X_1^{(r)} = 140° - r\cdot 10°$, $r = 0, 1, \cdots 4$.) Corresponding to this sequence of values, there is a sequence of points $P^{(0)}, P^{(1)}, \dots$, on the curve $\mu b = \mu b_1$, at which we can read off the spectra of values of μp_1 and of η_1:

$$\mu p_1^{(0)}, \mu p_1^{(1)}, \dots \mu p_1^{(n)};$$
$$\eta_1^{(0)}, \eta_1^{(1)}, \dots \eta_1^{(n)}.$$

Vertical lines from $\eta = 0$ to these points represent the spectrum of values of μp_1 by their horizontal spacing, the spectrum of values of η_1 by their lengths. On shifting each of these lines to the right by an amount μa we next obtain lines representing, by their horizontal spacing, the spectrum of the variable parameter $\mu p_2 = \mu(p_1 + a)$, which can assume the values

$$\mu(p_1^{(0)} + a),\ \mu(p_1^{(1)} + a),\ \cdot \cdot \cdot\ \mu(p_1^{(n)} + a).$$

Since this shift does not disturb the distribution of the lines, one can speak of the spectrum of values of μp_2 as congruent to the spectrum of values of μp_1. The spectral lines for μp_2, by their intersections with the curve $\mu b = \mu b_2$, define two sequences of points:

$$Q_+^{(0)},\ Q_+^{(1)},\ .\ .\ .\ Q_+^{(n)},$$

and

$$Q_-^{(0)},\ Q_-^{(1)},\ .\ .\ .\ Q_-^{(n)},$$

from which one may read off the spectral values of η_2:

$$\eta_{2\pm}^{(0)},\ \eta_{2\pm}^{(1)},\ .\ .\ .\ \eta_{2\pm}^{(n)}.$$

By terminating the spectral lines of μp_2 at the points $Q_\pm^{(r)}$, we can make them represent the spectral values of $\eta_{2\pm}^{(r)}$ by their upward and downward extensions, just as the spectral lines for μp_1 represent the values of η_1. There results a very clear picture of the way in which η_1 and $\eta_{2\pm}$ change together with X_1. Finally, the spectrum of values of the output variable,

$$X_{2\pm}^{(0)},\ X_{2\pm}^{(1)},\ .\ .\ .\ X_{2\pm}^{(n)},$$

can be obtained by adding corresponding spectral values of η_1 and $\eta_{2\pm}$.

5·8. Complete Representation of Three-bar-linkage Functions by the Nomogram.—It will soon become evident to the reader who attempts to use the nomogram that it is not possible to carry through for all X_1, and for given μb_1, μb_2, and μa, the calculation outlined in Sec. 5·7. This limitation corresponds to restrictions on X_1 inherent in the geometry of the linkage considered, and is not a shortcoming of the nomogram; that the nomogram gives a complete representation of the whole class of three-bar-linkage functions will be evident from the following discussion.

In the calculations discussed in Sec. 5·7 it is convenient, but not necessary, to select values of X_1 corresponding to lines appearing on the nomogram. We shall now consider a continuous spectrum $X_1^{(r)}$, which includes all values in the range $-\infty < X_1 < +\infty$. We shall call such a continuous and infinite spectrum of $X_1^{(r)}$ "the complete spectrum $X_1^{(r)}$." Corresponding to a continuous spectrum $X_1^{(r)}$ there will be a continuous spectrum $X_2^{(r)}$. The values of $X_2^{(r)}$, however, as computed by Eqs. (36) to (40), will not be real for the complete spectrum $X_1^{(r)}$ but only for certain "bands" of that spectrum. Real configurations of the linkage

correspond, of course, only to real values of $X_2^{(r)}$; thus, by observing the limiting values of $X_1^{(r)}$ and $X_2^{(r)}$ in the "bands" in which the solution is real, one might determine the limiting configurations of the linkage.

We now use the nomogram in studying the conditions for the existence of a real solution $X_2^{(r)}$ corresponding to a given value of $X_1^{(r)}$. We note first that, as $X_1^{(r)}$ goes through all values, μp_1 can go only through a limited range of values determined by the fixed value of μb_1. This corresponds to the limitation on the magnitude of the diagonal D, which has

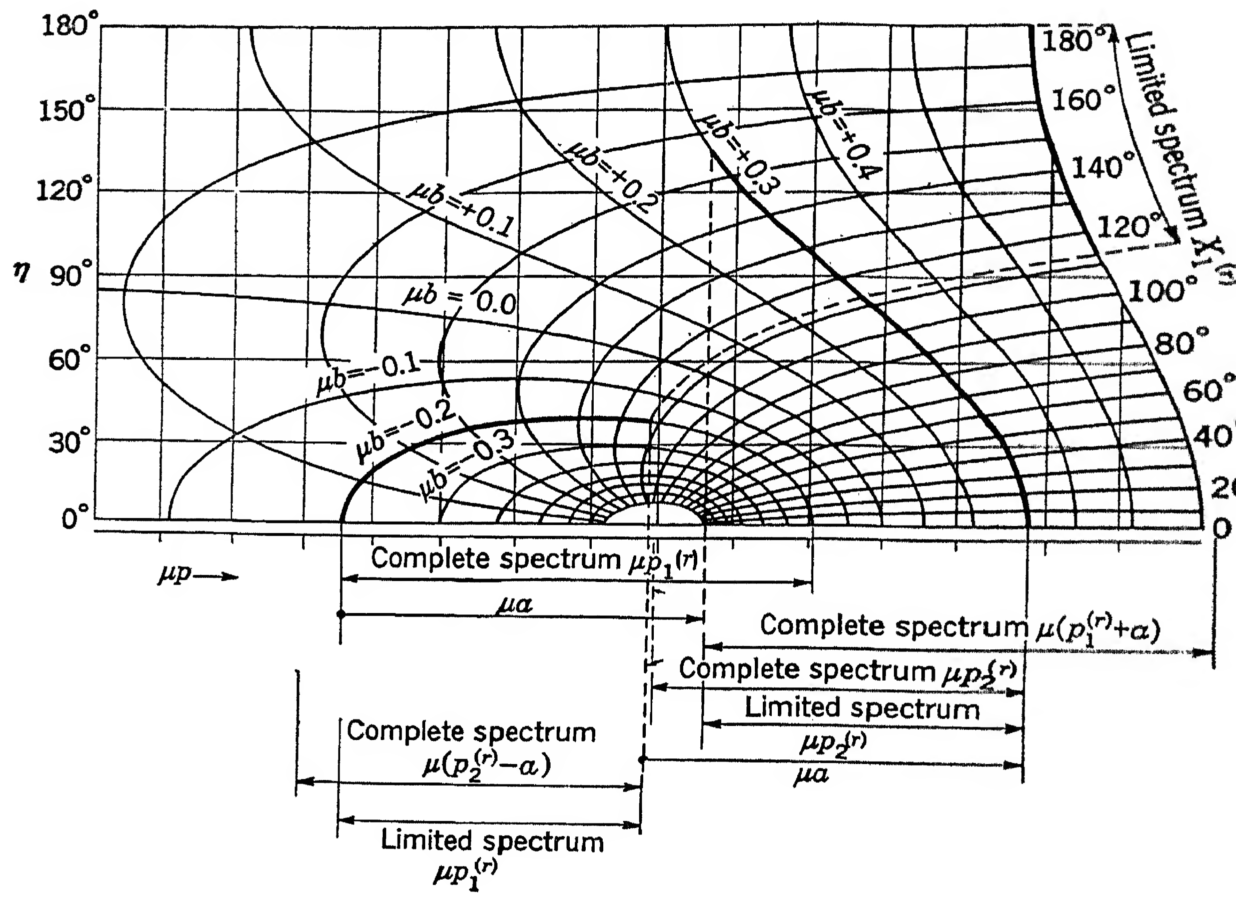

FIG. 5·13.—Range of operation of a three-bar linkage.

been expressed analytically in Eq. (5) and in our present notation can be rewritten as

$$\log_{10} |1 - 10^{\mu b_1}| \leqq \mu p_1 \leqq \log_{10} (1 + 10^{\mu b_1}). \tag{49}$$

The range of μp_1 is finite if $\mu b_1 \neq 0$, and extends to $-\infty$ when $\mu b_1 = 0$; we shall speak of the values in the range of μp_1 as making up "the complete spectrum $\mu p_1^{(r)}$." In Fig. 5·13, which applies to a linkage with

$$\mu b_1 = -0.2, \mu b_2 = 0.3, \mu a = 0.5,$$

it is clear that μp_1 can not be less than -0.432 (for $X_1 = 180°$), nor greater than 0.215 (for $X_1 = 0°$). We have, then, for the complete spectrum, $-0.432 \leqq \mu p_1^{(r)} \leqq 0.215$. By shifting the complete spectrum

$\mu p_1^{(r)}$ to the right by a distance μa, we obtain the complete spectrum $\mu(p_1^{(r)} + a)$. In our example

$$+0.068 \leqq \mu(p_1^{(r)} + a) \leqq 0.715.$$

In the same way it will be observed on the nomogram that there is a limited range of values of μp_2 consistent with the fixed value of μb_2. This corresponds to the restriction on D expressed analytically by Eq. (6), which in our present notation is

$$\log_{10} |1 - 10^{\mu b_2}| \leqq \mu p_2 \leqq \log_{10} (1 + 10^{\mu b_2}). \tag{50}$$

The values in this range make up the complete spectrum $\mu p_2^{(r)}$. In the case illustrated in Fig. 5·13, $-0.002 \leqq \mu p^{(r)} \leqq 0.476$.

In the nomographic computation of X_2 one has to identify μp_2 and $\mu(p_1 + a)$. This will be possible only for values of μp_2 which lie in the complete spectrum $\mu p_2^{(r)}$ and also in the complete spectrum $\mu(p_1^{(r)} + a)$; such values make up the "limited spectrum $\mu p_2^{(r)}$." By shifting the limited spectrum $\mu p_2^{(r)}$ to the left by an amount μa, we obtain finally the limited spectrum $\mu p_1^{(r)}$. The nomographic computation can be carried through for all values of μp_1 that lie within this limited spectrum; for the corresponding values of X_1, the limited spectrum $X_1^{(r)}$, one can compute real values of X_2. The range within which this calculation is possible corresponds exactly to the range within which both Eqs. (5) and (6) are satisfied, as illustrated in Fig. 5·2. Thus all physically possible configurations of the linkage, all real three-bar-linkage functions $(X_2|X_1)$, are covered by the nomogram.

The reader will find it instructive to apply the nomogram to the discussion of the parallelogram linkage.

5·9. Restatement of the Design Problem for the Nomographic Method.—The nomogram is conveniently used in three-bar-linkage design only when it is possible to preassign values for two of the design constants, ΔX_1 and ΔX_2. There remain three design constants—b_1, b_2, and a, or their equivalents—to be adjusted in the process of fitting the generated to the given function.

When the angular ranges of the input and output variables are thus specified, it becomes possible to express the given function in terms of angular variables φ_1 and φ_2, instead of the homogeneous variables h_1 and h_2:

$$\left.\begin{aligned} \varphi_1 &= \Delta X_1 h_1, \\ \varphi_2 &= \Delta X_2 h_2. \end{aligned}\right\} \tag{51}$$

In comparing the given function with the generated function, one will correspondingly express the latter in terms of the angular parameters X_1 and X_2:

$$\left.\begin{aligned} X_1 - X_{1m} &= \Delta X_1 H_1, \\ X_2 - X_{2m} &= \Delta X_2 H_2. \end{aligned}\right\} \tag{52}$$

The design problem can then be stated as follows. It is desired to find a three-bar linkage generating a function

$$X_2 = (X_2|X_1) \cdot X_1 \tag{25}$$

which can be identified with the given function

$$\varphi_2 = (\varphi_2|\varphi_1) \cdot \varphi_1 \tag{53}$$

on direct or complementary identification of H_1 with h_1, H_2 with h_2 (cf. Sec. 5·4). Direct identification in the two cases implies

$$\left.\begin{aligned} \varphi_1 &= X_1 - X_{1m}, \\ \varphi_2 &= X_2 - X_{2m}; \end{aligned}\right\} \tag{54}$$

complementary identification implies

$$\left.\begin{aligned} \Delta X_1 - \varphi_1 &= X_1 - X_{1m}, \\ \Delta X_2 - \varphi_2 &= X_2 - X_{2m}. \end{aligned}\right\} \tag{55}$$

The design problem is essentially the same if the identification is direct in both cases or complementary in both cases; if the identification is direct in one case and complementary in the other it does not matter in which case it is direct. It will be convenient to assume that it is always direct in the case of the output variable. The relations to be satisfied by the angular parameters are then

$$\left.\begin{aligned} \pm\varphi_1 &= X_1 - X_{1m} - \tfrac{1}{2}\Delta X_1 \pm \tfrac{1}{2}\Delta X_1, \\ \varphi_2 &= X_2 - X_{2m}, \end{aligned}\right\} \tag{56}$$

with the upper sign corresponding to direct identification.

It is important to note that the procedure to be described does not necessarily lead to a unique solution of the problem. There usually exist two quite different approximate solutions, with a positive and a negative value for b_1, respectively. During the design process the constants of both of these solutions should be determined sufficiently accurately to permit a rational choice between them. This point will be fully illustrated in later sections.

5·10. Survey of the Nomographic Method.—Fitting the generated to the given function by simultaneous and independent variations of the three remaining design constants is hardly practicable. We therefore (1) make a definite choice of b_1, and then find the best fit obtainable by independent variation of the other two design constants; (2) find a better value of b_1, as described in Sec. 5·13; (3) find the best fit obtainable by variation of the other design constants, using this improved value of b_1;

(4) find a better value of b_1; and so on, approaching the optimum choice of all three constants by successive approximations.

It would be quite natural to choose b_2 and a as the design constants to be adjusted in the first step of this procedure. However, to deal with these constants directly involves, in effect, the fitting of the given curve to a member of a two-parameter family of three-bar-linkage curves. It is preferable to choose X_{1m} and X_{2m} as the additional constants on which attention is concentrated, since it is then possible to work instead with two one-parameter families of curves, one easily constructed from the given function, the other appearing on the intersection nomogram. To make it clear how this can be done we shall consider three increasingly difficult problems. The discussion will be illustrated by Fig. 5·14.

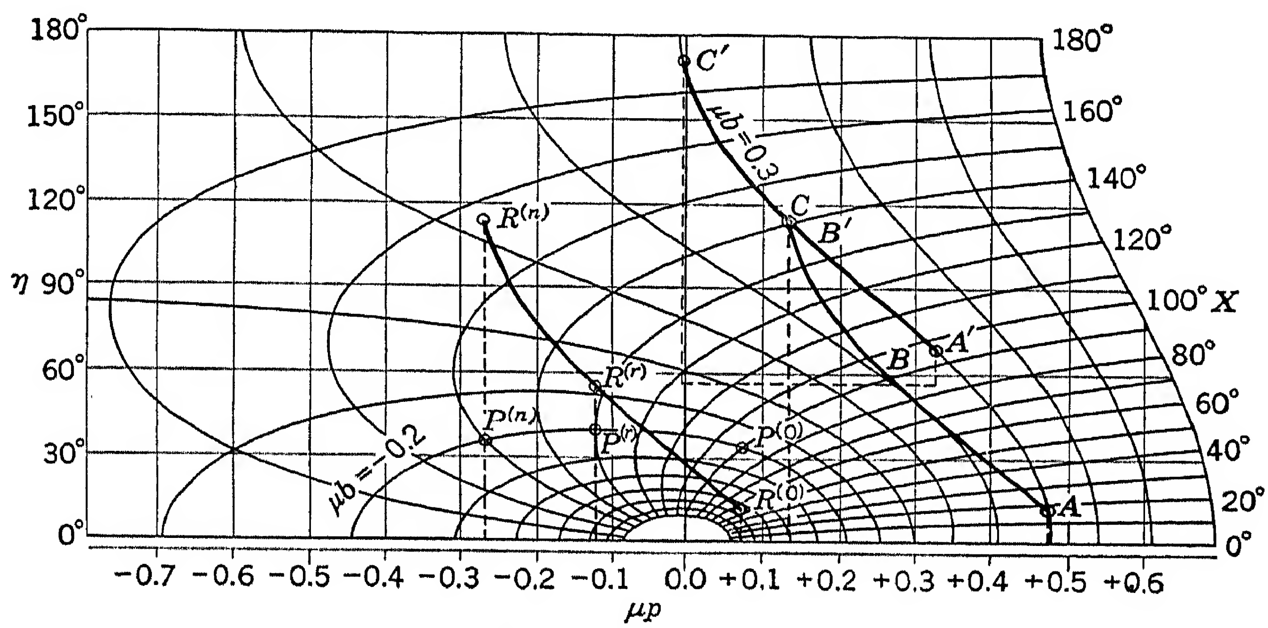

FIG. 5·14.—Curve fitting in Problems 1 and 2, Sec. 5·10.

Problem 1: *Determine whether or not a given function* $(\varphi_2|\varphi_1)$ *is generated by a linkage of specified constants* ΔX_1, ΔX_2, b_1, X_{1m}, X_{2m}.—Since ΔX_1, X_{1m}, and X_{2m} are known, it is possible to transform the given functional relation $(\varphi_2|\varphi_1)$ into a functional relation of the angles X_1 and X_2, $(X_2|X_1)$, by use of Eqs. (56), whether the identification is direct or complementary. The problem is then: Is this function $(X_2|X_1)$ really generated by a linkage characterized by the given constants?

Let $X_1^{(r)}$ be any value of X_1 in the specified range. On the nomogram we locate at the intersection of the lines $X = X_1^{(r)}$ and $\mu b = \mu b_1$ the point $P^{(r)}$; at this point we can read off the values of $\mu p_1^{(r)}$ and $\eta_1^{(r)}$ generated by the linkage. We do not yet know the generated values of $\eta_{2\pm}$ and X_2, but we do know the corresponding given value of X_2, $X_{2G}^{(r)}$, and can compute the "given" value of $\eta_{2\pm}$ using Eq. (48):

$$\eta_{2G}^{(r)} = X_{2G}^{(r)} - \eta_1^{(r)}. \tag{57}$$

On the vertical line through the point $P^{(r)}$ we erect a spectrum line of height $\eta_{2g}^{(r)}$, ending at point $R^{(r)}$. By moving this spectrum line to the right by an amount μa (still unknown) it can be brought into the position of the spectrum line $\mu p_2^{(r)}$. If the given value $\eta_{2g}^{(r)}$ is the one actually generated, this spectral line will then extend exactly to the curve $\mu b = \mu b_2$, (also unknown at the moment); the amount by which it falls short of that curve is the amount by which the generated value of $X_2^{(r)}$ exceeds the given $X_{2g}^{(r)}$. The complete spectrum of such lines, limited by the curve $R^{(0)} \ldots R^{(r)} \ldots R^{(n)}$, can be outlined quickly.

Let the curve $R^{(0)} \ldots R^{(r)} \ldots R^{(n)}$ be drawn on a transparent overlay. Suppose now that, by moving the overlay to the right by a distance μa, this curve can be made to coincide with some curve $\mu b = \mu b_2$. It will then follow that the given function is indeed generated by a linkage with the specified constants, ΔX_1, ΔX_2, b_1, X_{1m}, X_{2m}, and, furthermore, that this linkage is also characterized by the constants b_2 and a thus determined. For, in view of the methods of computation outlined in Sec. 5·7, it is clear that a linkage with the above values of b_1, b_2, and a will generate a spectrum of values of $\eta_{2\pm}$ which is just the spectrum of the "given" values, $\eta_{2g}^{(r)}$, and hence a spectrum of values of X_2 which is also the given spectrum $X_{2g}^{(r)}$, for $X_{1m} \leqq X \leqq X_{1m} + \Delta X_1$. The spectrum of X_1 is determined by the given constants X_{1m} and ΔX_1; the generated spectrum of X_2, which reproduces the given spectrum of X_2, must correspond to the constants X_{2m} and ΔX_2. Since the linkage that generates the given function is characterized by the five specified constants and by the derived b_2 and a, the truth of the statement follows.

As an example, shown in Fig. 5·14, we take a case in which the specified constants are $\Delta X_1 = 60°$, $\Delta X_2 = 105°$, $\mu b_1 = -0.2$, $X_{1m} = 90°$, $X_{2m} = 45°$. The given function $(\varphi_2|\varphi_1)$ has been assumed to increase monotonically from $\varphi_2 = 0°$ when $\varphi_1 = 0°$ to $\varphi_2 = 105°$ when $\varphi_1 = 60°$; by Eq. (56) (with the upper sign) X_2 then increases monotonically from $X_2 = 45°$ when $X_1 = 90°$ to $X_2 = 150°$ when $X_1 = 150°$. Taking $X_1^{(0)} = 45°$, we locate $P^{(0)}$ and read $\eta_1^{(0)} = 33°$; hence $\eta_{2g}^{(0)}$ is $45° - 33° = 12°$, corresponding to point $R^{(0)}$. With $X_1^{(n)} = 150°$, we locate $P^{(n)}$ and read $\eta_1^{(n)} = 36°$; hence $\eta_{2g}^{(n)} = 150° - 36° = 114°$, corresponding to point $R^{(n)}$. We shall assume that similar computations for intermediate X_1 serve to determine the curve $R^{(0)} \ldots R^{(r)} \ldots R^{(n)}$ as shown. If now this curve is moved to the right by an amount $\mu a \cong 0.4$, the end points can be brought to lie at points A and C on the same contour of constant μb: $\mu b_2 = 0.3$. The intermediate portions of the curve do not then lie on that contour, and it is evident that no other contour can give a fit. It follows that the given function can not be generated by a linkage with the specified constants. The difference between the given and the generated

functions is immediately evident. A linkage with $\mu a = 0.4$, $\mu b_2 = 0.3$ does give a fit at the very ends of the range of X_1 (points A and C), and thus at the ends of the range of X_2. This linkage has therefore the specified values of ΔX_1, ΔX_2, X_{1m}, and X_{2m}, as well as that of b_1; it is the specified linkage. It generates values of $\eta_{2\pm}$ given by the curve $AA'B'C$, instead of the "given" values of the curve ABC; the vertical separation between these curves is then the difference between the given and the generated values of X_2.

Problem 2: Determine whether or not a given function $(\varphi_2|\varphi_1)$ *can be generated by a linkage of specified constants* ΔX_1, ΔX_2, b_1, X_{1m}.—It is now possible to consider all values of X_{2m} in seeking a fit of the generated to the given curve, instead of only one value. Let the curve $R^{(0)} \ldots R^{(n)}$ be constructed as before, for an arbitrarily chosen value of X_{2m}—for example, X'_{2m}. If a fit can not be found for this among the curves of constant μb on the nomogram, one will desire to make a similar trial for another value of X_{2m} —for example,

$$X''_{2m} = X'_{2m} + \Delta. \tag{58}$$

By Eq. (56), this increase in X_{2m} will produce a uniform increase, by the same amount, in the "given" values X_{2g} and η_{2g}; the new curve $R^{(0)} \ldots R^{(n)}$ will be the old one raised by an amount Δ, and the fit will be sought as before. Of course, instead of redrawing the curve, one can simply shift upward by Δ the overlay on which the first curve was drawn. Thus by allowing all vertical shifts of the overlay in seeking a fit one treats X_{2m} as a disposable parameter.

The stated problem can then be solved as follows: On a transparent overlay draw a curve $R^{(0)} \ldots R^{(r)} \ldots R^{(n)}$, assuming $X_{2m} = X'_{2m}$. If, by translating the overlay to the right by an amount μa and upward by an amount Δ (as read on the scale of η), this curve can be made to coincide with some portion of the curve $\mu b = \mu b_2$, then the given function $(\varphi_2|\varphi_1)$ can be generated by a linkage with the specified constants ΔX_1, ΔX_2, b_1, and X_{1m}. Furthermore, that linkage will also be characterized by the constants b_2, a, and $X_{2m} = X'_{2m} + \Delta$, determined in this fitting process.

In the example of Fig. 5·14 a fit can be obtained by moving the overlay, prepared as previously described, upward by an amount $\Delta = 57°$, and to the right by $\mu a = 0.255$; curve $R^{(0)} \ldots R^{(n)}$ then lies on the curve $\mu b = \mu b_2 = 0.3$, extending from A' to C'. Thus the given curve is actually generated by a linkage with the constants

$$\Delta X_1 = 60°, \qquad \Delta X_2 = 105°, \qquad \mu b_1 = -0.2, \qquad X_{1m} = 90°,$$

and, as now determined, $\mu b_2 = 0.3$, $\mu a = 0.255$, $X_{2m} = 45° + 57° = 102°$. If the fit were not exact the difference between the generated and the

given functions could be read as the vertical separation of the curve $R^{(0)} \ldots R^{(n)}$ and the contour $\mu b = \mu b_2$.

Problem 3: *Determine whether or not a given function* $(\varphi_2|\varphi_1)$ *can be generated by a linkage of specified constants* ΔX_1, ΔX_2, b_1.—Both X_{1m} and X_{2m} are now to be treated as disposable constants; the problem is then essentially the same as that encountered in Step (1) of the design procedure described at the beginning of this section.

We have already seen how a fit can be sought for a given value of X_{1m}—for example, X'_{1m}—by a process that begins with the construction of a corresponding curve—for example, $R_0^{(0)} \ldots R_0^{(n)}$. To make the same test for another value of X_{1m}—for example X''_{1m}—one would similarly construct another curve, $R_r^{(0)} \ldots R_r^{(n)}$. Unfortunately, this is not of the same form as the first curve; the actual construction of this curve is not to be avoided, though it can be made relatively easy by methods to be described.

The problem is then to be solved as follows. On a transparent overlay, construct a family of curves $R^{(0)} \ldots R^{(n)}$ for sufficiently closely spaced values of X_{1m}, and for $X_{2m} = 0$; label each curve with the corresponding value of X_{1m}. Now suppose that, by translating the overlay to the right by an amount μa and upward by an amount X_{2m} (as read on the scale of η), the curve of this family labeled X_{1m} can be brought into coincidence with a part of the curve $\mu b = \mu b_2$ on the nomogram. Then the given function can be generated by a linkage with the given constants ΔX_1, ΔX_2, and b_1; this linkage would be characterized also by the constants X_{1m}, X_{2m}, μa, μb_2 thus determined.

The essential features of the nomographic method should now be evident to the reader. To find the three-bar linkage with given ΔX_1, ΔX_2, b_1, which most accurately generates a given function $(\varphi_2|\varphi_1)$, one constructs on an overlay a family of curves corresponding to $X_{2m} = 0$ and to various values of X_{1m}. Moving the overlay over the nomogram, one seeks the best possible fit of a curve of this family to a curve of the μb_2 family on the nomogram. The displacement of the overlay necessary to produce this fit determines X_{2m} and μa for the linkage; the choice of curves for this fit determines X_{1m} and μb_2. The error in the resultant mechanization is directly evident in the failure to obtain an exact fit between the overlay and nomogram curves, and is measured by their vertical separation. The steps involved in this process will be discussed in detail in Secs. 5·11 and 5·12. After the method of improving the choice of b_1 has been described in Sec. 5·13, the whole procedure will be fully illustrated in Sec. 5·14.

5·11. Adjustment of b_2 and a, for Fixed ΔX_1, ΔX_2, b_1.—We shall now describe in full detail a practical procedure for the construction of the

overlay mentioned in Sec. 5·10 and its use in determining the best values of b_2 and a.

Construction of the Overlay.

(1) Choose a spectrum of values of X_1,

$$X_1^{(s)} = s\delta, \tag{59}$$

which fills the entire range from 0 to 360° at intervals δ small compared to ΔX_1. One should choose δ as the difference in X between consecutive curves on the nomogram, or a multiple of this, so that there will be on the chart a curve corresponding to each value $X_1^{(s)}$. Usually $\delta = 10°$ is sufficiently small; $\delta = 5°$ is possible with the chart plotted from Table B·1.

(2) As the spectrum of values of φ_1, take

$$\varphi_1^{(r)} = r\delta, \tag{60}$$

with $r = 0, 1, \cdot \cdot \cdot n$. Since these values should fill the range ΔX_1, one must have $n\delta \approx \Delta X_1$.

(3) Compute the corresponding spectrum of φ_2:

$$\varphi_2^{(r)} = (\varphi_2|\varphi_1) \cdot \varphi_1^{(r)}. \tag{61}$$

Using the same scale as the η-scale of the nomogram, construct this spectrum as a series of tiny holes along a straight line on a strip of paper (see Fig. 5·15). On this strip mark the index r for each of the lines of the spectrum; indicate by an arrow the direction of increasing φ_2.

(4) Fasten over the nomogram the material on which the overlay is to be constructed—for instance, a piece of tracing paper. Copy onto the overlay all the points $P^{(s)}$ at which the contour $\mu b = \mu b_1$ is intersected by the lines $X = X_1^{(s)}$. (Figure 5·15 shows the complete contour.) Mark the points $P^{(s)}$ on the overlay with the subscript s. Also copy onto the overlay the lines $\eta = 0$, $p = 0$. This position of the overlay will be called its starting position.

(5) Draw on the overlay the vertical lines $\mu p = \mu p^{(s)}$ through all points $P^{(s)}$. These are the spectral lines for the variable μp. The overlay can now be separated from the nomogram.

(6) Place the strip of paper carrying the spectrum $\varphi_2^{(r)}$ on the overlay, along each line of the spectrum $\mu p^{(s)}$, making the arrow point downward and the first point $\varphi_2^{(0)}$ of this spectrum coincide with the point $P^{(s)}$. For each such position of the strip, mark on the line $\mu p = \mu p^{(s)}$ of the overlay the positions of the points $\varphi_2^{(r)}$ on the strip, labeling each with the corresponding value of r. These points we shall indicate as

$$P_1^{(s)}P_2^{(s)} \ . \ . \ . \ P_r^{(s)} \ . \ . \ . \ P_n^{(s)}.$$

(7) Starting at each point $P^{(s)}$ on the overlay, pass a curve successively through the points $P^{(s)}$, $P_1^{(s+1)}$, $P_2^{(s+2)}$, . . . $P_r^{(s+r)}$, . . . $P_n^{(s+n)}$.

This family of curves we shall call the plus family. It is unnecessary to use a French curve in this construction; it is sufficient to connect the points by hand with straight lines, in order to make clear the way in

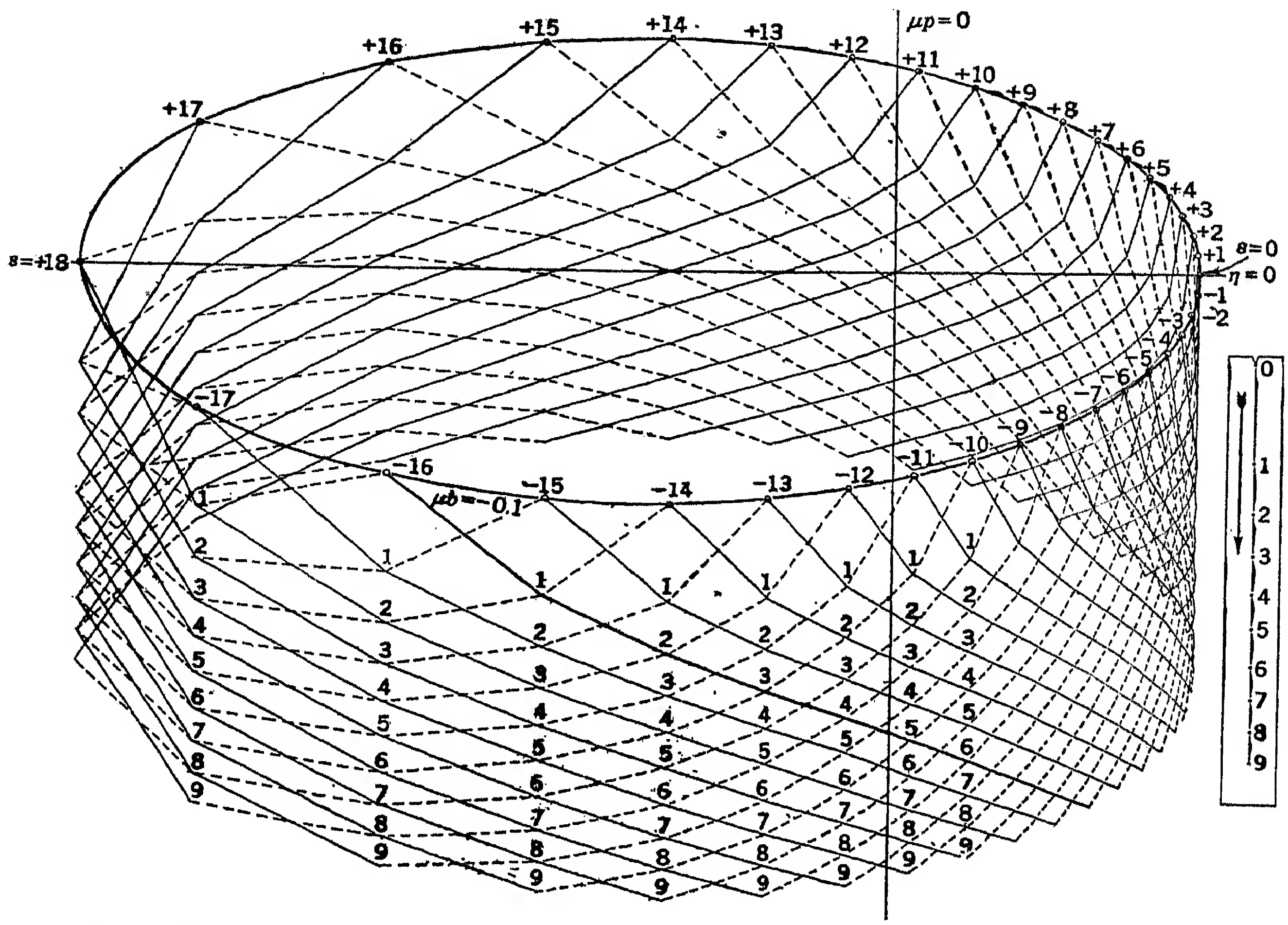

FIG. 5·15.—Scale and overlay for first application of the nomographic method.

which they are associated. The plus family of curves appears as continuous lines in Fig. 5·15.

(8) Again, starting with each point $P^{(s)}$ on the overlay, pass a curve successively through the points $P^{(s)}$, $P_1^{(s-1)}$, $P_2^{(s-2)}$, . . . $P_r^{(s-r)}$, . . . $P_n^{(s-n)}$. This family of curves (dashed lines in Fig. 5·15) we shall call the minus family.

This completes the construction of the overlay. As will appear from our later example, construction of the complete overlay is not always necessary.

We must now examine the significance of the curves thus drawn.

(1) The successive points $P^{(s)}$, $P^{(s+1)}$, . . . $P^{(s+n)}$, represent, by their distances from the lines $p = 0$ and $\eta = 0$, the values of μp and η_1 for a sequence of values of X_1: $X_1^{(s)}$, $X_1^{(s+1)}$, . . . By Eq. (54) these points also correspond to the sequence of values of φ_1: 0, $\varphi_1^{(1)}$ . . . $\varphi_1^{(n)}$, for the case

in which $X_{1m} = X_1^{(s)}$ and the identification of h_1 and H_1 is direct. In particular, $P^{(s+r)}$ represents the values of $\mu p^{(r)}$ and $\eta_1^{(r)}$ when $X_{1m} = X_1^{(s)}$.

(2) The separation of the points on the strip corresponding to $\varphi_2^{(0)}$ and $\varphi_2^{(r)}$ represents, on the same scale, the value of $\varphi_2^{(r)} - \varphi_2^{(0)} = \varphi_2^{(r)}$. By Eq. (54) this is also the value of $X_{2g}^{(r)}$ if $X_{2m} = 0$, and the identification of h_1 and H_1 is direct.

(3) The point $P_r^{(s+r)}$ thus corresponds to $\mu p = \mu p^{(r)}$ and has as its η coordinate [by Eq. (57)]

$$\eta_1^{(r)} - X_{2g}^{(r)} = -\eta_{2g}^{(r)},$$

for the case in which $X_{1m} = X_1^{(s)}$, $X_{2m} = 0$, and the identification of h_1 and H_1 is direct.

(4) We thus see that the curve of the plus family passed through the points $P^{(s)}$, $P_1^{(s+1)}$, . . . $P_r^{(s+r)}$, . . . $P_n^{(s+n)}$ on the overlay corresponds to the sequences of values

$$\begin{array}{rl} X_1: & X_1^{(s)},\ X_1^{(s+1)},\ \ldots\ X_1^{(s+r)},\ \ldots\ X_1^{(s+n)}, \\ \mu p: & \mu p^{(0)},\ \mu p^{(1)},\ \ldots\ \mu p^{(r)},\ \ldots\ \mu p^{(n)}, \\ \eta: & -\eta_{2g}^{(0)},\ -\eta_{2g}^{(1)},\ \ldots\ -\eta_{2g}^{(r)},\ \ldots\ -\eta_{2g}^{(n)}, \end{array}$$

for the case described under (3).

(5) The sign of η can be reversed by rotating the figure through 180° about the axis $\eta = 0$. Thus *if the overlay as constructed is turned face down by rotating it through* 180° *about the axis* $\eta = 0$, then the curve of the plus family labeled with an s gives the relation between η_{2g} and μp for the case in which $X_{1m} = X_1^{(s)}$, $X_{2m} = 0$, and the identification of h_1 and H_1 is direct.

(6) In the same way the reader will be able to show that, *with the overlay turned face down as above*, the curve of the minus family labeled with an s gives the relation between η_{2g} and μp for the case in which $X_{1M} = X_1^{(s)}$, $X_{2m} = 0$, and the identification of h_1 and H_1 is complementary.

Use of the Overlay.—With the overlay face down on the nomogram and the line $\eta = 0$ horizontal, a fit is sought between any curve on the overlay and a line $\mu b = \mu b_2$ of the nomogram. If a fit is found, the constants of the linkage are determined as follows:

(1) ΔX_1, ΔX_2, μb_1 have been previously chosen.

(2) μb_2 is read from the curve of the nomogram with which the fit is found.

(3) μa is the shift of the overlay to the right needed to establish the fit. It may be read at the intersection of the line $p = 0$ of the overlay with the μp-scale on the nomogram.

(4) X_{2m} is the shift of the overlay upward needed to establish the fit. It may be read at the intersection of the line $\eta = 0$ of the overlay with the η-scale of the nomogram.

(5) If the fit is established in the plus family of curves, one has $X_{1m} = s\delta$, s being read from the overlay curve with which the fit is made. The angles φ_1 and X_1 will increase together; this, of course, is *always* true of φ_2 and X_2.

(6) If the fit is established in the minus family of curves, one has $X_{1M} = s\delta$, $X_{1m} = s\delta - \Delta X_1$. The angle φ_1 will decrease as X_1 increases. The linkage and the associated scales are then completely determined.

The actually generated values of η_2 will not be $\eta_{2g}^{(r)}$, since these were computed on the assumption that $X_{2m} = 0$; instead, they will be

$$\eta_{2g}^{(r)} + X_{2m},$$

which can be read directly on the nomogram scale. If the fit is established on the upper half of the nomogram, η_2 is greater than zero and the generated function belongs to the positive branch; if the fit is established on the lower half of the nomogram one has to do with a negative branch.

Usually the fit obtained between the nomogram and overlay curves will be only approximate. The constants determined alone will then not all be mutually consistent, unless the approximate fit is so made that the error vanishes at the extreme values of X_1 and X_2. This is easily done when monotonic functions are being dealt with; in other cases one should remember that when five of the design constants have been fixed the others must be determined by appropriate calculations rather than read as above.

5·12. Alternative Methods for Overlay Construction.—Modifications of the above procedure are necessary when use is made of a nomogram like Fig. B·1, which includes only the range from $\eta = 0°$ to $\eta = 180°$. The missing portions of this chart can be constructed as mirror images of the part shown; or, more conveniently, the same effect can be obtained by appropriately turning the overlay.

For example: To construct the points $P^{(s)}$ on the overlay, copy the points $P^{(0)}$ to $P^{(18)}$ (assuming $\delta = 10°$) from the nomogram, and draw the reference lines. Then turn the overlay face down by rotating it about the line $\eta = 0$, and copy the same points onto the overlay. The points thus constructed are in fact $P^{(0)}$, $P^{(-1)}$, $P^{(-2)}$, . . . $P^{(-18)}$, and should be so labeled.

In the curve-fitting process described above, with the overlay face down, the lower part of the nomogram will be missing, and direct fitting to functions of the negative branch will not be possible. One can, however, turn the overlay again (so that it is now face up) and seek a fit on

the upper part of the nomogram. It must, of course, be remembered that readings made on the η-scale (for instance, readings of X_{2m}) must then be taken with a minus sign.

When $\mu b_1 > 0$, an overlay constructed as described above becomes excessively large; another modification in the overlay construction then becomes convenient. It will be noted that if the lower half of an overlay is turned about the line $\eta = 0$, the point $P_0^{(-s)}$ will be brought into coincidence with the point $P_0^{(s)}$, and the point $P_r^{(-s)}$ will lie as far above $P_0^{(s)}$ as $P_r^{(s)}$ lies below it. We shall speak of these points in their new position as the "transferred points"; they extend through the "transferred region" of the overlay. These transferred points can be constructed directly by the method described above with the one change that, in locating the transferred points $\bar{P}_0^{(-s)}$, $\bar{P}_1^{(-s)}$, . . . $\bar{P}_n^{(-s)}$, one places the point $\varphi_2^{(0)}$ of the spectrum strip on the point $P_0^{(s)}$ with the arrow directed *upward* before copying off the succession of points $\varphi_2^{(0)}$, $\varphi_2^{(1)}$, . . . $\varphi_2^{(n)}$.

In working with this transferred region one must remember that it is equivalent to a normal region turned face down. When fitting curves in a normal region, one turns the overlay face down and reads values directly from the η-scale of the nomogram; when fitting curves in the transferred region, one uses the overlay face up. The plus and minus families of curves in the transferred region are most readily identified by turning over the overlay.

5·13. Choice of Best Value of b_1 for Given ΔX_1, ΔX_2.—In the preceding sections we have seen how to find the elements of a three-bar linkage which gives an approximate mechanization of a given relation,

$$\varphi_2 = (\varphi_2|\varphi_1) \cdot \varphi_1, \tag{53}$$

when ΔX_1, ΔX_2, and μb_1 are specified in advance. We have now to consider the problem of finding an appropriate value for b_1 when only ΔX_1 and ΔX_2 are specified.

A method of trial and error is obviously applicable. One can carry through the above process for an arbitrarily chosen μb_1; if an acceptable fit is not found another value can be chosen for μb_1 and the process repeated, until a good fit is found or the useful range of μb_1 has been covered. Fortunately it is necessary to try only a relatively small number of values, such as $\mu b_1 = -0.5, -0.2, 0.0, 0.2, 0.5$, to determine roughly the value of μb_1 or to establish that the proposed type of mechanization is not appropriate.

Such a process of repeated trials can be abandoned as soon as even a poor approximate fit is found between the overlay and nomogram curves. Usually one finds at least a very rough fit with the first chosen value of μb_1, and can begin to apply a second method—one of successive approxi-

mations. Let the linkage that gives the first rough fit be characterized by the constants

$$\Delta X_1,\ \Delta X_2,\ \mu b_1^{(1)},\ \mu b_2^{(1)},\ \mu a^{(1)}, \tag{62}$$

of which the last two have been found by the process already described.

Now let us consider the problem of similarly mechanizing the inverted function

$$\varphi_1 = (\varphi_1|\varphi_2)\cdot\varphi_2, \tag{63}$$

with φ_2 playing the role of the input parameter, φ_1 the role of the ouput parameter. The parameters φ_1 and φ_2 will then be interchanged throughout the previous discussion, φ_1 varying with the angle X_2, φ_2 with the angle X_1. The linkage that mechanizes this relation will be the same as that which mechanizes the original relation, Eq. (54), except that input and output are interchanged. If Fig. 5·1 represents the linkage for Eq. (54), the linkage for Eq. (63) can be obtained from this by mirroring it in a vertical line, along with the associated scales for φ_1 and φ_2. This new linkage differs from the old in that B_1 and A_2 are interchanged, as are ΔX_1 and ΔX_2; X_{1m} is replaced by $180° - X_{2M}$, X_{2m} by $180° - X_{1M}$. As for the constants μb_1, μb_2, μa, we note that interchange of B_1 and A_2 carries

$$\mu a = \log_{10}\frac{A_1}{A_2} \tag{64}$$

into

$$\log_{10}\frac{A_1}{B_1} = -\log_{10}\frac{B_1}{A_1} = -\mu b_1, \tag{65}$$

and conversely, while

$$\mu b_2 = \log_{10}\frac{B_2}{A_2} \tag{66}$$

becomes

$$\log_{10}\left(\frac{B_2}{B_1}\right) = \log_{10}\left[\left(\frac{B_2}{A_2}\right)\left(\frac{A_2}{A_1}\right)\left(\frac{A_1}{B_1}\right)\right] = \mu b_2 - \mu a - \mu b_1. \tag{67}$$

Distinguishing the constants of the inverted linkage by a tilde, we may write

$$\begin{aligned}
\mu\tilde{a} &= -\mu b_1, &(68a)\\
\mu\tilde{b}_1 &= -\mu a, &(68b)\\
\mu\tilde{b}_2 &= \mu b_2 - \mu a - \mu b_1, &(68c)\\
\Delta\tilde{X}_1 &= \Delta X_2, &(68d)
\end{aligned}$$

and so on.

In attempting to mechanize Eq. (63) one might apply the nomographic

method as before, choosing arbitrarily a value of $\mu\tilde{b}_1$ and finding corresponding values of $\mu\tilde{b}_2$ and $\mu\tilde{a}$. However, $-\mu a^{(1)}$ is a known first approximation to the desired value of $\mu\tilde{b}_1$, and an appropriate choice for the fixed value of this quantity. We therefore take

$$\mu\tilde{b}_1^{(2)} = -\mu a^{(1)}, \tag{69}$$

and by the nomographic method determine the corresponding constants $\mu\tilde{b}_2^{(2)}$ $\mu\tilde{a}^{(2)}$ in the mechanization of the inverted problem. This mechanization of the relation between φ_1 and φ_2 must be at least as good as that described by the constants in Eq. (62), since it is chosen as the best of a family of linkages which includes the mirror image of that first linkage; usually it is much better. From these constants one can then obtain second approximations to the constants required for the direct problem:

$$\begin{aligned} \mu a^{(2)} &= -\mu\tilde{b}_1^{(2)} = \mu a^{(1)}, \\ \mu b_1^{(2)} &= -\mu\tilde{a}^{(2)}, \\ \mu b_2^{(2)} &= \mu\tilde{b}_2^{(2)} - \mu\tilde{a}^{(2)} - \mu\tilde{b}_1^{(2)}. \end{aligned} \tag{70}$$

The values of μb_1 and μb_2 have been improved; the value of μa was frozen in passing to the inverted problem, and is hence unchanged.

We can now return to a consideration of the problem as first formulated. It is obviously desirable to take $-\mu\tilde{a}^{(2)} = \mu b_2^{(2)}$ as the chosen value of μb_1; repetition of the curve-fitting process leads to a still better mechanization of the relation between φ_1 and φ_2, characterized by the constants

$$\mu b_1^{(3)}(= -\mu\tilde{a}^{(2)}),\ \mu b_2^{(3)},\ \mu a^{(3)}.$$

Thus by alternately considering the problem as formulated in Eqs. (53) and (63), and applying the methods of Secs. 5·11 and 5·12, one obtains successively better approximate solutions, which usually converge rapidly to a limit. The method is less laborious than might at first be supposed, since the constants to be expected in all solutions but the first are known approximately, and the complete overlay need not be constructed.

It will be found that if one obtains a fair fit with a given μb_1, one will obtain also a reasonably good fit with $-\mu b_1$. On application of the method of successive approximations, these two approximate solutions usually lead to two different solutions of the problem, which are equivalent neither with respect to the residual error, nor with respect to mechanical qualities. These two possibilities should receive separate consideration.

5·14. An Example of the Nomographic Method.—As a first example of the nomographic method, we shall apply it in attempting to mechanize the function presented in Table 5·1 in both direct and inverted forms.

TABLE 5·1.—GIVEN FUNCTIONS FOR THE EXAMPLE

$(\varphi_2\|\varphi_1)$		$(\varphi_1\|\varphi_2)$	
φ_2, degrees	φ_1, degrees	φ_1, degrees	φ_2, degrees
0.0	0	0.0	0
22.3	10	3.4	10
34.1	20	9.0	20
43.6	30	16.9	30
52.1	40	26.6	40
60.0	50	37.7	50
68.3	60	50.0	60
75.9	70	62.6	70
83.1	80	76.1	80
90.0	90	90.0	90

This tabulated function is in fact the one generated by a three-bar linkage with the following constants:

$$\left.\begin{array}{llll} X_{1m} = -170^\circ, & \Delta X_1 = 90^\circ, & X_{2m} = 160^\circ, & \Delta X_2 = 90^\circ, \\ \mu b_1 = 0, & \mu a = -0.286, & \mu b_2 = 0.0367, & \\ \dfrac{B_1}{A_1} = 1, & \dfrac{A_2}{A_1} = 1.932, & \dfrac{B_2}{A_1} = 2.102. & \end{array}\right\} \tag{71}$$

In applying the nomographic method we shall assume the ideal values for the angular travels,

$$\Delta X_1 = \Delta X_2 = 90^\circ, \tag{72}$$

but shall begin by choosing a value of μb_1 which is not the best:

$$\mu b_1^{(1)} = -0.1. \tag{73}$$

In this way we can make particularly evident the convergence toward the best constants that is usually afforded by the method of successive approximations. A second and quite different example, without this *ad hoc* character, will be found in Sec. 6·4.

Following the steps outlined in Sec. 5·11, we proceed thus:

(1), (2) In tabulating the given function, $\delta = 10^\circ$ has been chosen as sufficiently small compared to the ranges of X_1 and X_2; this will permit use of Fig. B·1 (folding insert in back of book) in applying the method. In mechanizing the function in the direct form the spectrum of values of φ_1 is 0°, 10°, . . . 90°. We have here $n = 9$.

(3) The values of $\varphi_2^{(r)}$ appear in the first column of Table 5·1. Using the η-scale of the nomogram, we transfer this spectrum of values to a strip

of paper, as illustrated in Fig. 5·15. The direction of increasing r is shown by an arrow.

(4) Tracing paper is used in making an overlay. This is taped to the nomographic chart, which should be made on cardboard, and 36 points, from $P^{(-18)}$ to $P^{(+18)}$, are constructed and marked with the proper value of s (Fig. 5·15). The reference lines are traced onto the overlay.

(5) The vertical lines of the spectrum $\mu p^{(s)}$ are omitted from Fig. 5·15 for the sake of clarity.

(6) Placing the zero point of the strip successively on each of the points $P^{(s)}$, with the arrow directed downwards, the 36 points $P_r^{(s)}$ are located and labeled with their r-values. (In first approximations one can sometimes skip half the values of r and half the values of s.)

(7), (8) The plus family of curves is now sketched (full lines in Fig. 5·15) through points with r-values successively increasing by 1 as s increases; curves of the minus family (dashed in Fig. 5·15) pass through points with r-values successively increasing by 1 as s decreases. The complete family of curves is shown in the figure. This is really unnecessary, since one can tell at a glance that some of them cannot lead to a fit. In particular, since $\varphi_2^{(s)}$ is a single-valued function of s, one could here omit the numerous curves that have infinities in their slopes.

The overlay is now turned about the horizontal reference line and translated over the nomogram until a fit is found—a quite satisfactory fit, as it happens, between the overlay curve $s = -16$ of the plus family and the curve $\mu b_2 = 0.075$ on the nomogram. Figure 5·16 shows, on the nomogram grid, the construction of the particular overlay curve for which the fit was obtained, and the position of fit on the chart (dotted curve at lower left). The fit has been made exact at the ends. The overlay curve then deviates downward from the nomogram curve; on a large chart it can be seen that the maximum error in η is a little more than one degree. The reference lines on the overlay are also shown in the position of fit.

The elements of the linkage are thus established:

$\mu b_1^{(1)} = -0.1$, as assumed.

$\mu b_2^{(1)} = 0.075$, read from the nomogram curve on which the fit was made.

$\mu a^{(1)} = -0.265$, read at the intersection of the vertical reference line with the μp-scale.

$X_{2m}^{(1)} = -202.5°$ or $+157.5°$, read at the intersection of the horizontal reference line with the η-scale. (When this reference line falls off the nomogram, as it would here, an auxiliary reference line on the overlay can be used.)

$X_{1m}^{(1)} = -160° = s\delta$, since the curve that gives the fit is of the plus family.

By Eq. (56) we have (using the upper signs in the first equation, since the fit was obtained with a curve of the plus family)

$$\begin{aligned} \varphi_1 &= X_1 + 160°, \\ \varphi_2 &= X_2 - 157.5°. \end{aligned} \tag{74}$$

These last equations represent the given function with errors visible as the vertical separation of the fitting curves in Fig. 5·16. Since the fit is exact

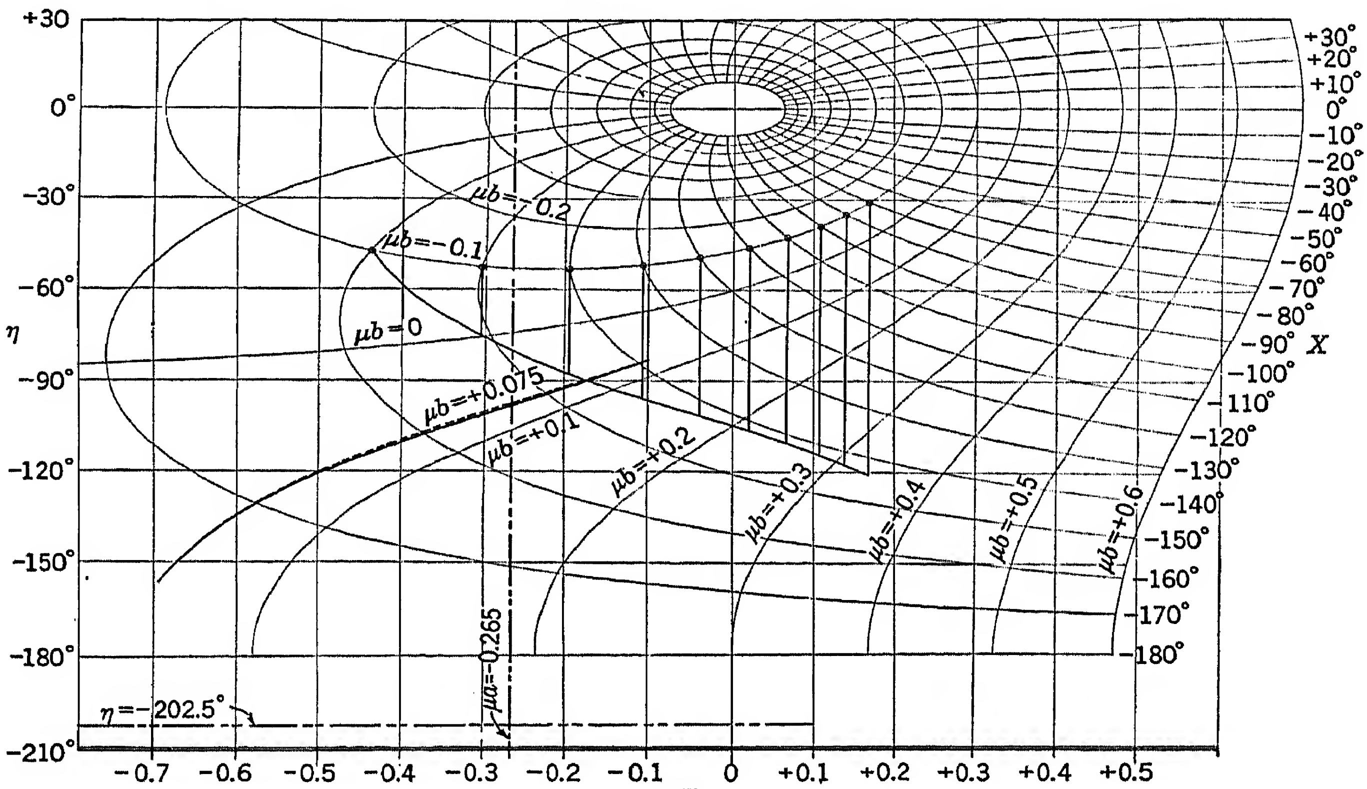

FIG. 5·16.—Construction of overlay line and position of fit in first application of the nomographic method. In the position of fit the overlay curve lies slightly below the contour $\mu b = 0.075$.

at the ends of the range of X_1, the travels of both input and output of the linkage as designed will have the required value, 90°. (It is not necessary to make the fit exact at the ends, except perhaps in the last stage of the design process. In earlier stages one can often accelerate convergence on the ideal constants by seeking a good fit on the average rather than an exact fit at any given points in the range.)

As a check it is useful to make a drawing of the linkage, showing the cranks in their extreme positions (Fig. 5·17). The distance $A_1^{(1)}$ between the crank pivots may be taken as the unit of length; the relative crank lengths are drawn in as

$$\left.\begin{aligned} \frac{B_1^{(1)}}{A_1^{(1)}} &= 10^{\mu b_1^{(1)}} = 10^{-0.1} = 0.794, \\ \frac{A_2^{(1)}}{A_1^{(1)}} &= 10^{-\mu a^{(1)}} = 10^{0.265} = 1.841. \end{aligned}\right\} \tag{75}$$

The constancy of the required length of the connecting link,

$$\frac{B_2^{(1)}}{A_1^{(1)}} = \frac{B_2^{(1)}}{A_2^{(1)}} \cdot \frac{A_2^{(1)}}{A_1^{(1)}} = 10^{\mu(b_2^{(1)} - a^{(1)})} = 10^{0.340} = 2.188, \tag{76}$$

provides a check on the quantities determined in the fitting process.

Of the constants thus determined for the linkage, b_1 has been held at a preassigned value, but the others have taken on values that are good approximations to those known to give an exact fit. Such behavior is of course essential if the method of successive approximations (Sec. 5·13) is to be effective. We now apply this method to the improvement of the linkage design.

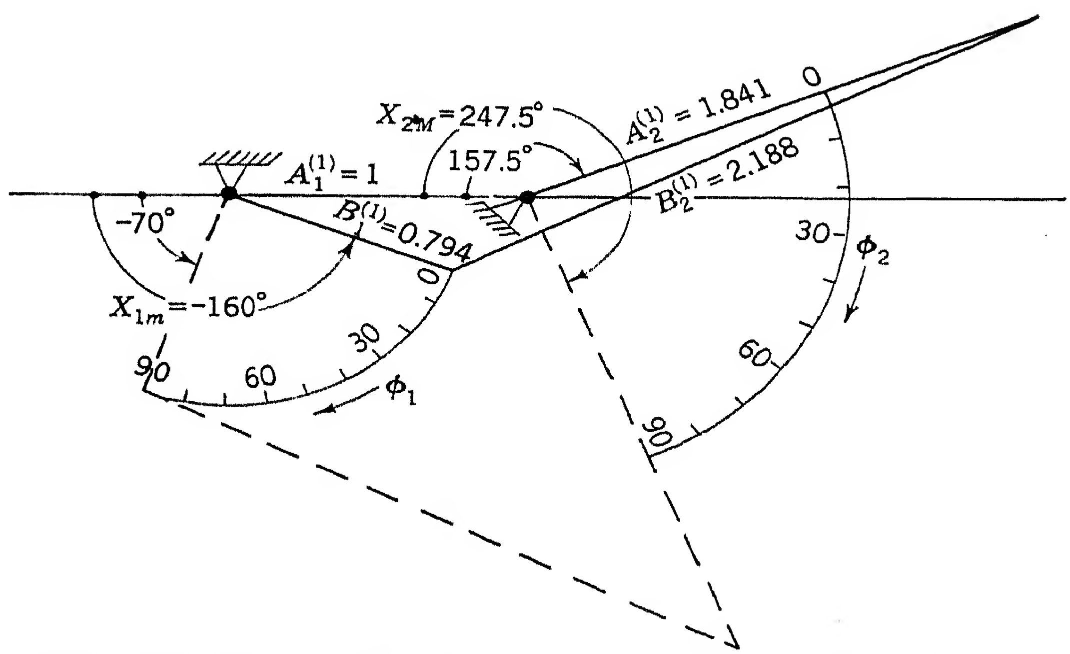

FIG. 5·17.—First approximate linkage for mechanization of the given function, Table 5·1.

The roles of φ_1 and φ_2 are to be interchanged throughout our next treatment of the problem. The inverted function has already been given in Columns 3 and 4 of Table 5·1. Now φ_2 is to be associated with the parameter X_1 of a new linkage; to remind us that this is a parameter of the inverted problem we shall distinguish it by a tilde: $\tilde{X}_1$. Similarly φ_1 is to be associated with the parameter $\tilde{X}_2$ in the new linkage.

According to Eq. (69) we should begin the process of mechanizing the inverted function by choosing $\mu\tilde{b}_1^{(2)} = 0.265$. To facilitate construction of the overlay we shall use an approximation to this:

$$\mu\tilde{b}_1^{(2)} = 0.25. \tag{77}$$

Such rounding off of values is generally useful in practical design work; we have here deliberately done it in such a way as to retard rather than accelerate the convergence of the method.

We know that the linkage to be designed will not be very different, in its dimensions and in the arrangement of the scales, from that of Fig.

5·17. It must, however, differ from that linkage by reflection in a vertical line, since the pivots are to be interchanged; and it may differ also by reflection in a horizontal line. One can determine whether or not this additional reflection is involved by examining the φ_1-scale, which, by the convention introduced in the discussion leading up to Eq. (56), must increase in the direction of increasing $\tilde{X}_2$. In the present case it is evident that the two linkages must differ also by a reflection in a horizontal line; the appearance of the new linkage will then be that of Fig. 5·17 turned upside down. One must accordingly expect $\tilde{X}_{1m} \approx -20°$, and on the overlay will need to construct only a few curves of the plus family with $s \approx -2$.

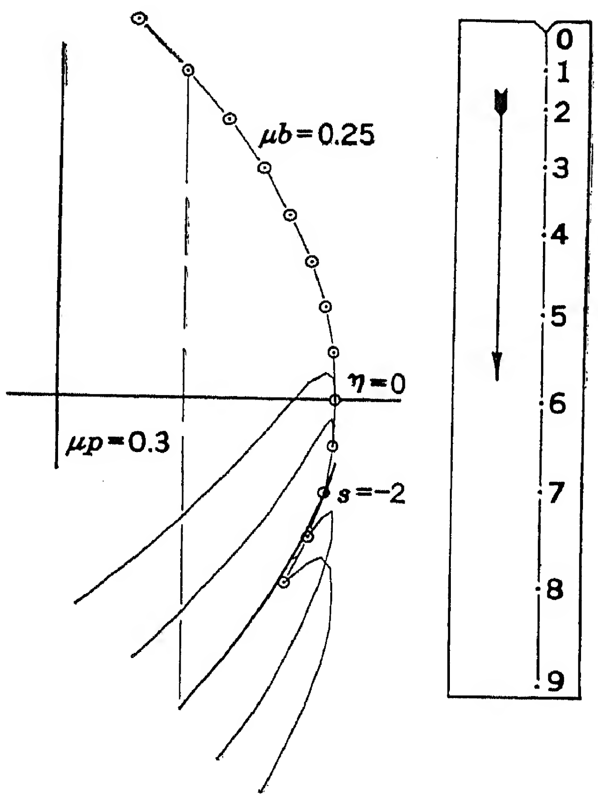

FIG. 5·18.—Scale and overlay for second application of the nomographic method.

Figure 5·18 shows the nomogram curve $\mu b = 0.25$ used in construction of the overlay, and the few lines of the plus family that need to be drawn. It is obvious that a good fit can not be obtained with curves for which η is not a single-valued function of p. The curve $s = -2$, for which we expect this fit, is, however, essentially single-valued. The retrograde portion of this curve closely overlaps the rest of it and is no bar to an accurate fit; its presence indicates only that η_2 may reverse its direction of change as the linkage operates.

When the overlay is turned about a horizontal line and moved over the nomogram a very accurate fit can be found between the overlay line $s = -2$ and the line $\mu b_2 = 0.275$ of the nomogram, in the position indicated in Fig. 5·19. Also shown are the usual horizontal reference line and the auxiliary reference line $\mu p = 0.3$, which appears also in Fig. 5·18. From the position of fit we read the following values of the constants:

$$\left.\begin{aligned} \mu\tilde{b}_1^{(2)} &= 0.25, \qquad \text{as assumed,} \\ \mu\tilde{b}_2^{(2)} &= 0.275, \\ \mu\tilde{a}^{(2)} &= 0.011, \\ \tilde{X}_{2m}^{(2)} &= 5° \\ X_{1m}^{(2)} &= -20°. \end{aligned}\right\} \tag{78}$$

Since the fit was obtained with a curve of the plus family, we have

$$\left.\begin{aligned} \varphi_2 &= \tilde{X}_1 + 20°, \\ \varphi_1 &= \tilde{X}_2 - 5°. \end{aligned}\right\} \tag{79}$$

To make more evident the change in constants due to this second calculation, we can rewrite the above results in terms of the constants of the uninverted linkage. Remembering that the two linkages differ, in this case, by reflections in both horizontal and vertical lines, we have

$$\tilde{X}_1 = X_2 - 180°, \qquad \tilde{X}_2 = X_1 - 180°, \tag{80a}$$
$$X_{1m} = \tilde{X}_{2m} \pm 180°, \qquad X_{2m} = \tilde{X}_{1m} \pm 180°. \tag{80b}$$

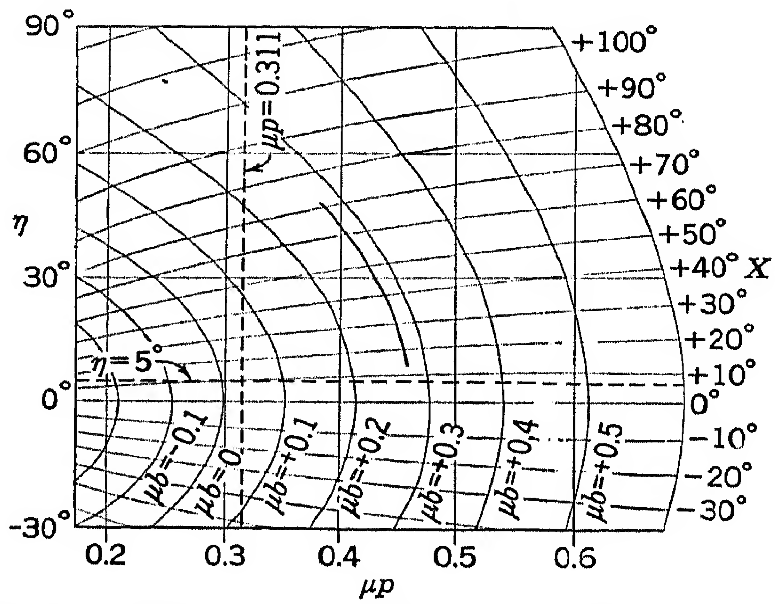

FIG. 5·19.—Position of fit in second application of the nomographic method.

By use of these relations and of Eqs. (68), we have

$$\left.\begin{array}{c} \mu b_1^{(2)} = -0.011, \\ \mu b_2^{(2)} = 0.014, \\ \mu a^{(2)} = -0.25, \\ X_{1m}^{(2)} = -175°, \\ X_{2m}^{(2)} = 160°, \\ \dfrac{B_1^{(2)}}{A_1^{(2)}} = 0.9975, \qquad \dfrac{A_2^{(2)}}{A_1^{(2)}} = 1.778, \qquad \dfrac{B_2^{(2)}}{A_1^{(2)}} = 1.837. \end{array}\right\} \tag{81}$$

These quantities represent distinct improvements over the first approximate values, except for $\mu a^{(2)}$ (which was rounded off in the wrong direction and not allowed to improve during the second fitting) and the ratios A_2/A_1 and B_2/A_1 (which depend upon μa_2). In particular, the value of μb_1 deviates from the ideal by only one-tenth as much as the value initially assumed. It is evident that a second application of the nomographic method to the mechanization of the given function in the direct form, with $\mu b_1 = -0.011$, would lead to values of the constants very near to the ideal.

THE GEOMETRIC METHOD FOR THREE-BAR LINKAGE DESIGN

We shall now discuss a geometric method for the design of three-bar linkages for which the input travel ΔX_1 is not fixed but may be treated as

a variable parameter. This is a less common problem than that solved by the nomographic method, in which both input and output travels are treated as fixed; nevertheless, the method is a necessary and frequently useful complement to the nomographic method.

The basic problem treated by the geometric method is that of finding the three-bar linkage with given values of ΔX_2 and B_2/A_2 which most accurately generates a given function. In essence, the method is one by which a rapid comparison can be made between the desired and the actual positions of the input crank, for a series of positions of the output crank, for any given linkage of a large family. This comparison is made so easy that it becomes a relatively simple matter to find that linkage of the given family which gives the best fit. This solution can be improved, if desired, by a method of successive approximations like that employed with the nomographic method: the values of B_2/B_1 and ΔX_1 determined by the first application of the procedure are treated as fixed, and the initially chosen values of B_2/A_2 and ΔX_2 improved by a second application of this procedure to the inverted function; then B_2/B_1 and ΔX_1 are readjusted, and so on. When this method is employed, no constant of the linkage is held at an arbitrarily frozen value.

5·15. Statement of the Problem for the Geometric Method.—The problem to be solved by the geometric method is that of mechanizing a given functional relation,

$$x_2 = (x_2|x_1) \cdot x_1, \qquad \begin{bmatrix} x_{1m} \leqq x_1 \leqq x_{1M} \\ x_{2m} \leqq x_2 \leqq x_{2M} \end{bmatrix}, \tag{82}$$

as accurately as possible by a three-bar linkage with given output travel ΔX_2 and given crank-link ratio B_2/A_2.

A linkage will generate a relation

$$X_2 = (X_2|X_1) \cdot X_1 \tag{83}$$

between its input and output parameters; it will constitute a mechanization of the given function if there exists a linear relation between the parameters X_1, X_2 and the variables x_1, x_2:

$$X_1 - X_1^{(0)} = k_1(x_1 - x_1^{(0)}), \tag{84a}$$
$$X_2 - X_2^{(0)} = k_2(x_2 - x_2^{(0)}). \tag{84b}$$

Here $X_1^{(0)}$ and $x_1^{(0)}$ are corresponding values of X_1 and x_1, $X_2^{(0)}$ and $x_2^{(0)}$ corresponding values of X_2 and x_2; $x_1^{(0)}$ and $x_2^{(0)}$ do not stand in any necessary relation to the limits of the interval of definition in Eq. (82).

In the problem at hand one knows both

$$\Delta X_2 = X_{2M} - X_{2m}, \tag{85}$$

and

$$\Delta x_2 = x_{2M} - x_{2m} \tag{86}$$

The magnitude of k_2 is thus determined:

$$|k_2| = \frac{\Delta X_2}{\Delta x_2}. \tag{87}$$

Also, it will be noted that a positive sign of k_2 implies direct identification of the homogeneous parameters h_2 and H_2 corresponding to x_2 and X_2; a negative sign implies complementary identification. As in Sec. 5·9 we can, without loss of generality in the design process, assume direct identification of h_2 and H_2, while admitting either direct or complementary identification of h_1 and H_1. Thus k_2 may be considered as completely known,

$$k_2 = \frac{\Delta X_2}{\Delta x_2}, \tag{88}$$

but k_1 is unknown both as to magnitude and sign. The fixed parameters of the problem are thus B_2/A_2 and k_2; attention will be focused, in the actual design process, on the adjustment of A_1/A_2, B_1/A_2, and k_1.

5·16. Solution of a Simplified Problem.—As in the case of the nomographic method, we first consider a simplified problem in which there are only two adjustable parameters. Here we shall treat B_2/A_2, k_2, and k_1 as fixed, and seek the best possible fit of the generated to the given function by adjusting A_1/A_2 and B_1/A_2. We reserve for Sec. 5·17 an explanation of the method for varying k_1.

To solve this problem we choose a spectrum of values of the variable x_1:

$$x_1^{(0)}, x_1^{(1)}, \ . \ . \ . \ , x_1^{(r)}, \ . \ . \ . \ , x_1^{(n)},$$

extending through the interval of definition of Eq. (82). Equation (82) then defines a corresponding spectrum of values of x_2:

$$x_2^{(0)}, x_2^{(1)}, \ . \ . \ . \ , x_2^{(r)}, \ . \ . \ . \ , x_2^{(n)}.$$

Since both k_1 and k_2 are known, Eq. (84) would define corresponding spectra of X_1 and X_2, if there were not present the unknown additive constants $X_1^{(0)}$ and $X_2^{(0)}$. Given values of these constants, one could compute $X_1^{(r)}$ and $X_2^{(r)}$, and make sketches showing, for each r, the corresponding positions of the input and output cranks, each in its correct relation to its own zero position. Now, even though $X_1^{(0)}$ and $X_2^{(0)}$ are unknown, one can still compute such quantities as

$$X_1^{(r+1)} - X_1^{(r)} = k_1(x_1^{(r+1)} - x_1^{(r)}), \tag{89a}$$

and

$$X_2^{(r+1)} - X_2^{(r)} = k_2(x_2^{(r+1)} - x_2^{(r)}). \tag{89b}$$

One can thus make a sketch showing the relative positions that the input crank must have for a sequence of values of r, and a sketch showing the

corresponding *relative* positions that the output crank must have, if the given function is to be generated. Figure 5·20 shows such a set of relative positions for the input crank, represented by the radial lines $B_1^{(r)}$ from the pivot point S_1. The orientation of this figure with respect to the zero position of X_1—or, to put it another way, the direction on this figure of the line $\overline{S_1S_2}$ between the crank pivots of the linkage—is unknown, since it depends on $X_1^{(0)}$. Similarly, Fig. 5·21 represents, by the radial lines $A_2^{(r)}$ from the pivot point S_2, the corresponding relative positions of the

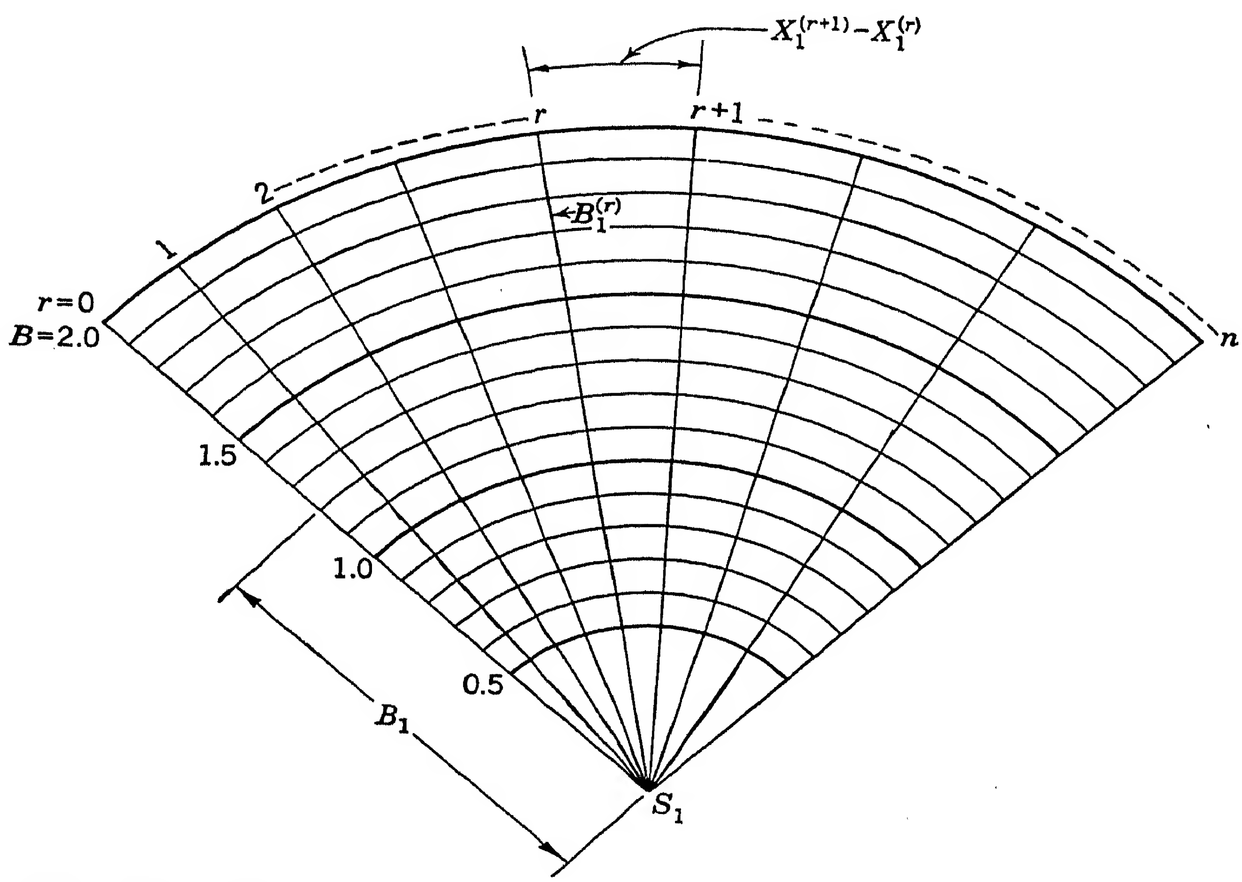

FIG. 5·20.—The radial lines represent a series of relative positions of the input crank of a three-bar linkage.

output crank; in this figure, too, the direction of the line $\overline{S_1S_2}$ between the pivots of the linkage cannot be specified, since it depends on $X_2^{(0)}$.

Figures 5 20 and 5·21 can be combined into a single figure representing a sequence of corresponding crank positions in the desired linkage, by placing them in proper relative positions. What the required relationship of these figures should be we do not yet know, but we do know enough about its characteristics to help us in finding it. For it is evident that (1) if the crank lengths A_2 and B_1 are laid out on the same scale, and (2) if the relative positions of the two figures are correct, and (3) if the given function can actually be generated by a linkage with the given B_2/A_2, k_1, and k_2, then the distances between the ends of the cranks, in all corresponding positions, must be constant, and indeed equal to B_2

on the chosen scale. By applying this idea one can determine the relative positions of Figs. 5·20 and 5·21 which correspond to that three-bar linkage (with the given constants) which most nearly generates the given function; from the combined figure one can then read off the constants of this linkage. To understand how this can be done we consider Figs. 5·20 and 5·21 in more detail.

The length A_2 of the output crank has been taken as the unit of length in both Figs. 5·20 and 5·21. In Fig. 5·21, the points $P^{(0)}$, . . . ,

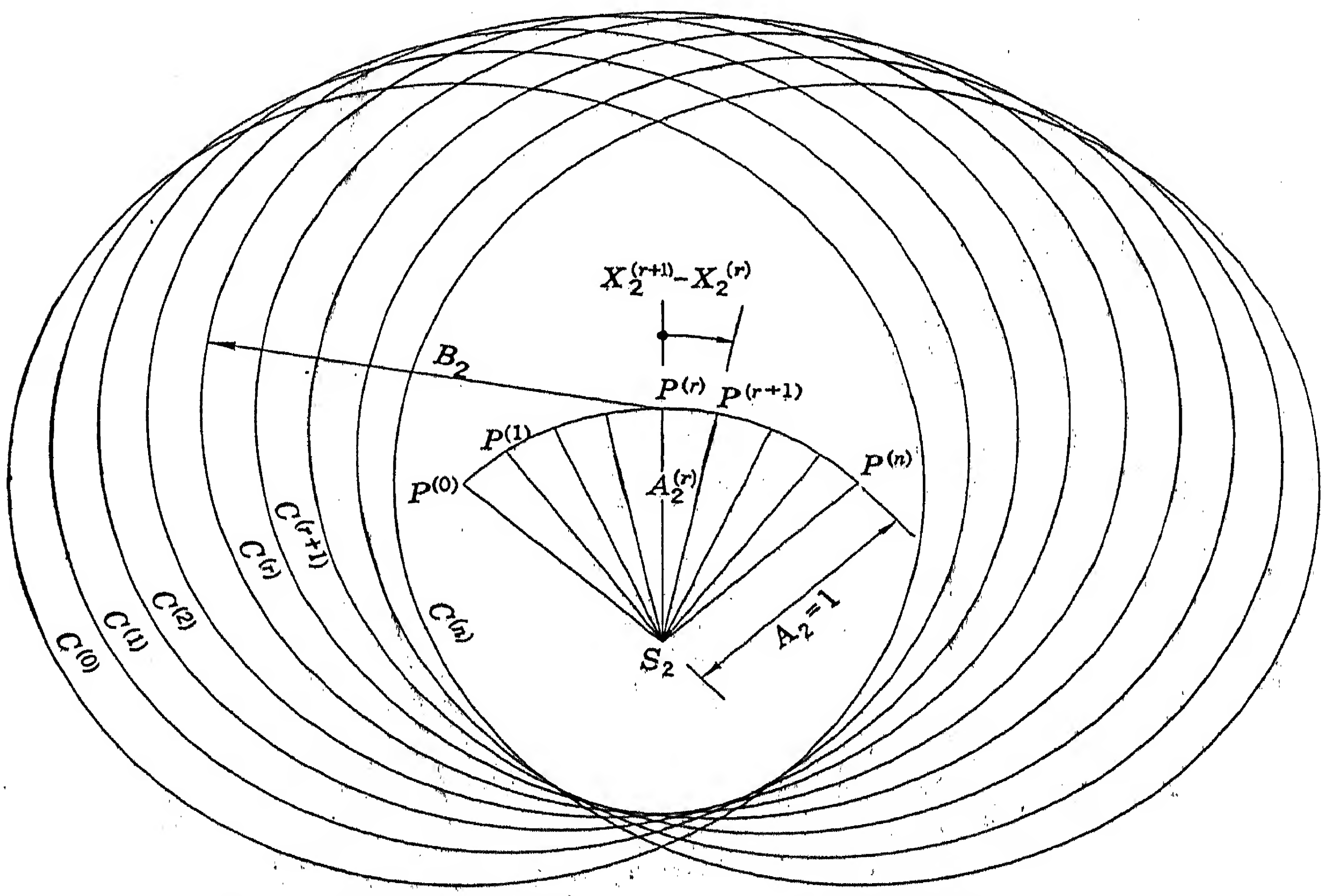

FIG. 5·21.—The radial lines represent a series of relative positions of the output crank of a three-bar linkage; the circles represent corresponding possible positions for the remote end of the connecting link.

$P^{(r)}$, . . . , $P^{(n)}$, represent a sequence of positions of the pivot T_2 between the output crank and the connecting link. In Fig. 5·20, one cannot construct corresponding definite positions for the pivot T_1 since the crank length B_1 is unknown; instead, there is shown a sequence of circles of different radii, each of which defines, by its intersections with the radial lines, corresponding positions $Q^{(0)}$, . . . , $Q^{(r)}$, . . . , $Q^{(n)}$, of this pivot when the input crank has the appropriate length.

In Fig. 5·21 there has been constructed about each point $P^{(r)}$ a circle $C^{(r)}$ having as its radius the known length B_2 of the link; the remote end of the link, the pivot T_1, must lie somewhere on this circle. If it is possible to generate the given function by a three-bar linkage with the

given constants, it must now be possible to place Fig. 5·21 on Fig. 5·20 in such a way that point $Q^{(0)}$ lies on the circle $C^{(0)}$, point $Q^{(1)}$ on circle $C^{(1)}$, and so on, as shown in Fig. 5·22. The value of A_1 in the required linkage will then be the length of $\overline{S_1S_2}$ on the common scale of the figures; the value of B_1 will be the radius of the circle on which the points $Q^{(0)}, \ldots, Q^{(r)}, \ldots, Q^{(n)}$ lie; and successive configurations of the linkage will be defined by the points $S_1, S_2, P^{(0)}, Q^{(0)}$; $S_1, S_2, P^{(1)}, Q^{(1)}$; etc.

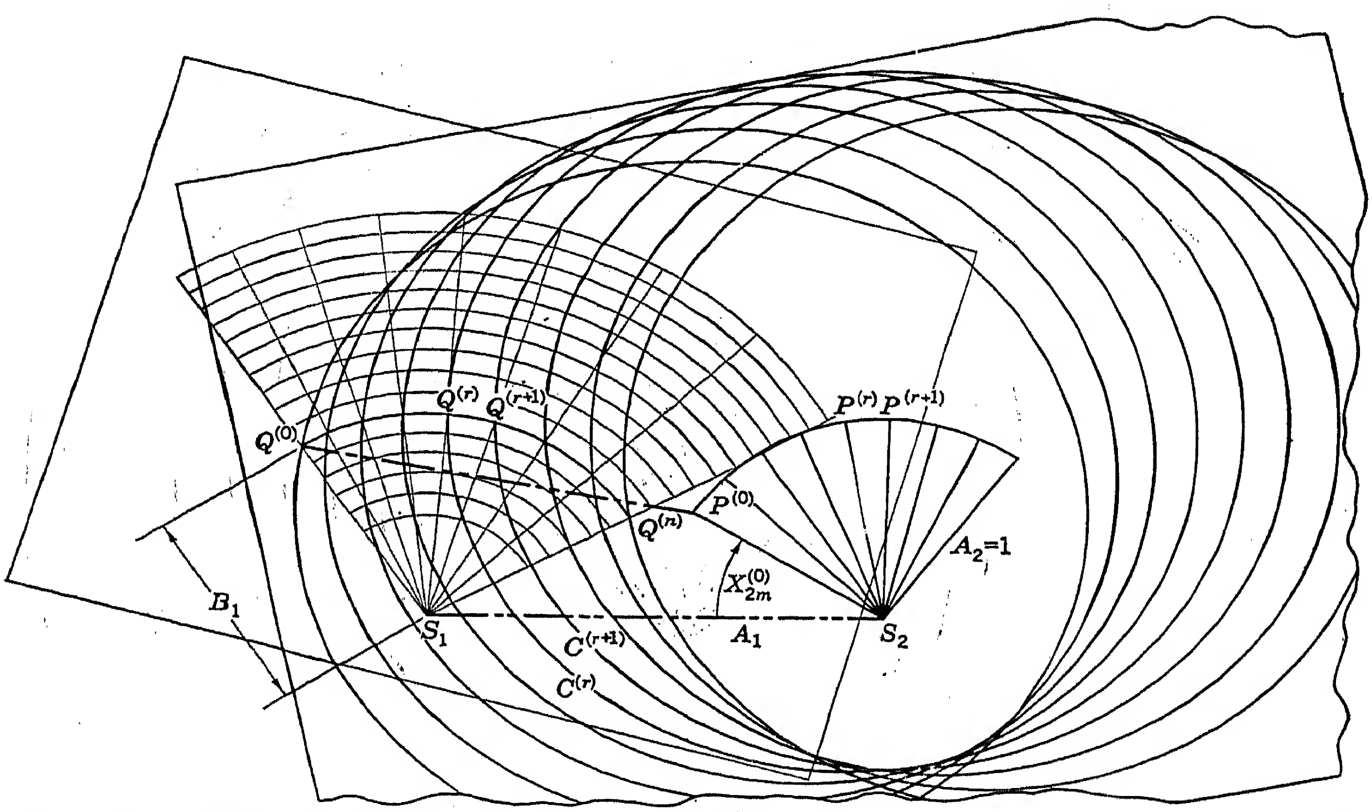

FIG. 5·22.—Relative positions of Figs. 5·20 and 5·21 corresponding to a three-bar linkage generating the given function.

In practical terms, the geometrical method of solving our restricted problem may be summarized thus:

1. Choose a spectrum of x_1.
2. Compute the spectral values of x_2, $X_1 - X_1^{(0)}$, $X_2 - X_2^{(0)}$.
3. Construct Fig. 5·21 as a chart, on a sufficiently large scale.
4. Construct Fig. 5·20 as a transparent overlay, on the same scale.
5. Move this overlay freely, using both translation and rotation, over the chart, seeking a position such that the circles $C^{(0)}, C^{(1)}, \ldots, C^{(n)}$ pass through the points $Q^{(0)}, Q^{(1)}, \ldots, Q^{(n)}$, on some circle of the overlay. (In making this fit it may be necessary to consider each overlay circle in turn.)
6. If a fit is found, the unknown constants of the link can be read off, A_1/A_2 as the distance $\overline{S_1S_2}$, B_1/A_2 as the distance $\overline{S_1Q^{(0)}}$, and X_{1m}, X_{2m} as the corresponding angles in the combined figure.

7. If only an approximate fit is found, the error in the input angle, for any given value of the generated output angle, can be read as the angle subtended at S_1 by the arc from the corresponding Q point (for example, $Q^{(r)}$) to the intersection of the corresponding C circle ($C^{(r)}$) with the arc $\overline{Q^{(0)}Q^{(n)}}$. Thus one should seek a position of the overlay which makes these errors as small as possible, and determine the constants of the linkage as above.

It will be evident to the reader that a change in sign of k_1 will leave Fig. 5·21 unchanged, but will produce the same effect on Fig. 5·20 as turning the overlay face down. A single overlay, used face up or face down, thus suffices for a given $|k_1|$.

5·17. Solution of the Basic Problem.—We now turn to the basic problem of the geometric method, that of obtaining the best fit of the generated to the given function by simultaneous variations of three parameters of the linkage, keeping fixed the values of B_2/A_2 and k_2. This can be accomplished without any essential complication of the procedure described in Sec. 5·16, by making a special choice of the spectrum of x_1. This has also the advantage that the overlay corresponding to Fig. 5·20 then has the same form for all problems and can be used again and again.

Let the spectrum of values $x_1^{(r)}$ be chosen as

$$x_1^{(r)} = x_1^{(0)} + \frac{g^r - 1}{g - 1} \cdot \delta, \qquad r = 0, 1, \cdots, n, \tag{90}$$

where δ and g are constants such that all values $x_1^{(r)}$ lie within the range of definition of Eq. (82). Equation (89a) then becomes

$$X_1^{(r+1)} - X_1^{(r)} = k_1\delta \frac{g^{r+1} - g^r}{g - 1} = k_1\delta g^r. \tag{91}$$

The separations of consecutive spectral values $X_1^{(r)}$, the angles between successive positions of the input crank, will then change in geometrical progression. Figure 5·20 has, in fact, been drawn for such a case.

So long as k_1 is unknown, one cannot construct an overlay like Fig. 5·20. To overcome this difficulty we construct an overlay, Fig. 5·23, on which appear radial lines $L^{(t)}$ with separations

$$Y^{(t+1)} - Y^{(t)} = \alpha g^t, \qquad t = 0, 1, 2, \cdots. \tag{92}$$

(In principle, the sequence of t's might start with other values than 0; such cases can be reduced to the above by changing the choice of α and renumbering the lines.) Let us consider the $n + 1$ lines of this system labeled $t = s, s + 1, \cdots, s + r, \cdots, s + n$, with separations

$$Y^{(s+r+1)} - Y^{(s+r)} = \alpha g^s \cdot g^r. \tag{93}$$

These will have the same separations as, and can be identified with, the lines $B_1^{(0)}$, $B_1^{(1)}$, . . . , $B_1^{(r)}$, . . . , $B^{(n)}$, provided

$$k_1\delta = \alpha g^s \tag{94}$$

or

$$k_1 = \frac{\alpha g^s}{\delta}. \tag{95}$$

Thus by identifying various lines $L^{(s)}$ of Fig. 5·23 as the line $B_1^{(0)}$, one can in effect assign to k_1 any value given by Eq. (95) for an integral s. The

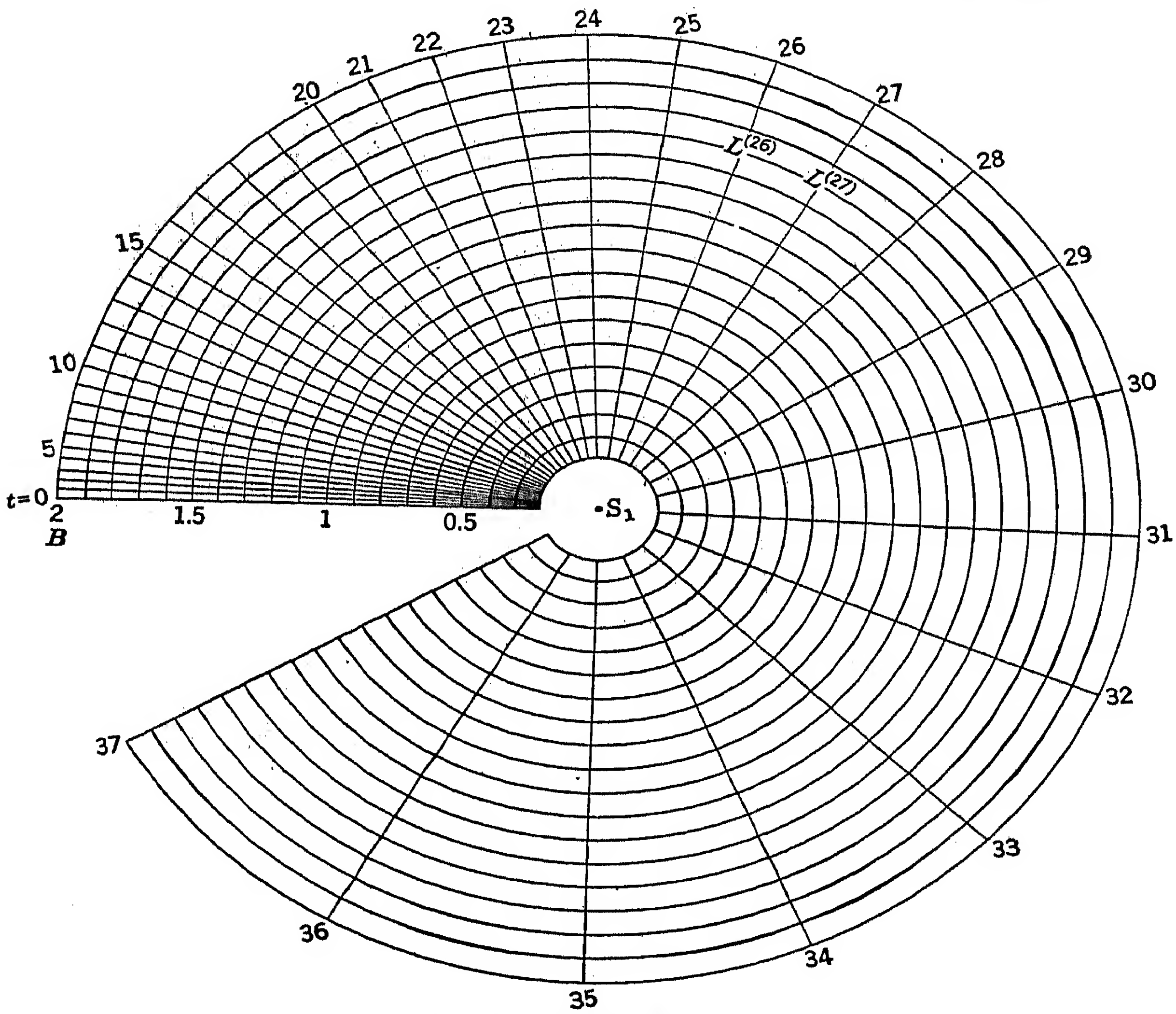

FIG. 5·23.—Overlay for the geometric method.

overlay is completed by the system of concentric circles which appears also in Fig. 5·20; it is used in the same way as that figure.

The procedure is then as follows:

(1) Choose a spectrum of values $x_1^{(r)}$, as given by Eq. (90). It is usually satisfactory to take $g = 1.1$; δ may be positive or negative and should be so chosen that n, defined by

$$\left|\frac{g^n - 1}{g - 1}\,\delta\right| \cong \Delta x_1, \tag{96}$$

lies in the range between 8 and 12. It is advantageous to choose the sign of δ, and the corresponding value of $x_1^{(0)}$, so as to make the spectrum of values $x_2^{(r)}$ as evenly spaced as possible. Thus in the case illustrated in Fig. 5·24a, in which dx_2/dx_1 decreases as x_1 increases, it is desirable to choose $x_1^{(0)}$ at the lower end of the range of x_1 and to make δ positive; when dx_2/dx_1 increases as x_1 increases, as in Fig. 5·24b, $x^{(0)}$ should lie at the upper end of the range of x_1 and δ should be negative.

(2) Compute the corresponding spectral values of x_2 and $X_2 - X_2^{(0)}$, using Eqs. (82) and (84b).

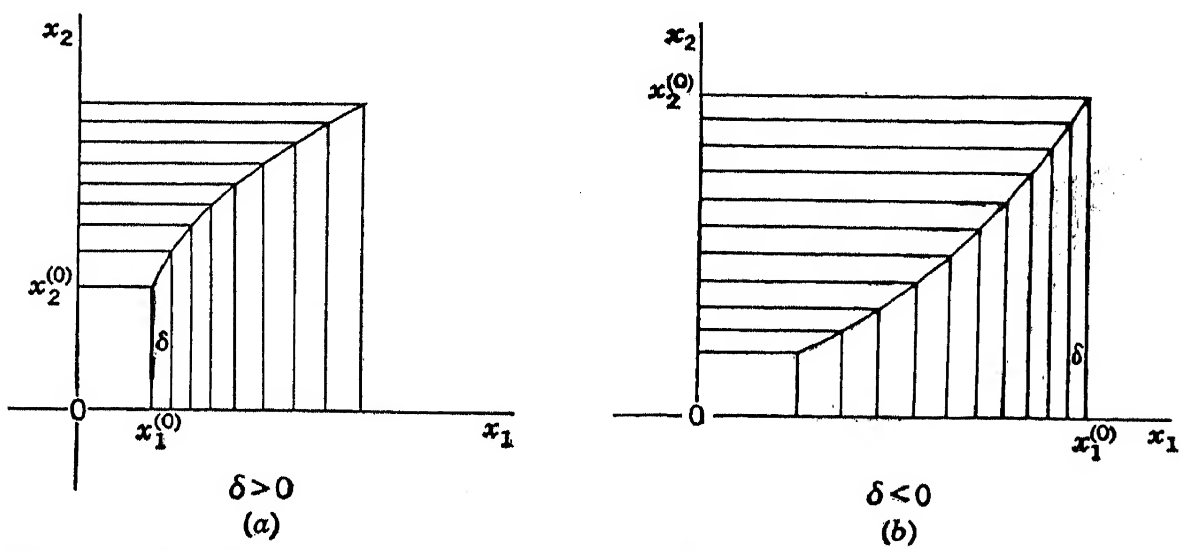

FIG. 5·24.—Choice of $x_1^{(0)}$ and δ to make the spectral values $x_2^{(r)}$ as evenly spaced as possible.

(3) Construct a transparent overlay similar to Fig. 5·23, with successive radial lines at angles

$$Y^{(t)} = \frac{\alpha}{g - 1} g^t \tag{97}$$

measured clockwise from the zero line. The value of g must be the same as that chosen in Step (1); α may be chosen arbitrarily but should be small. Figure 5·23 has been drawn with $g = 1.1$, $\alpha = 1°$. Label each radial line with the corresponding value of t.

(4) Using the spectral values of $X_2 - X_2^{(0)}$, construct a chart corresponding to Fig. 5·21. The length of the crank, A_2, should be one unit on the scale used in constructing the overlay. Lay down the successive crank positions, $A_2^{(r)}$, and about the end points $P^{(r)}$ construct circles $C^{(r)}$ with the known radius B_2.

(5) Place the overlay on this chart, face up, and seek a position for it such that the $(n + 1)$ circles, $C^{(0)}$, $C^{(1)}$, $C^{(n)}$, on the chart pass through $(n + 1)$ points $Q^{(s)}$, $Q^{(s+1)}$, . . . $Q^{(s+n)}$ on the overlay in which a circle of the concentric family, labeled B_1, intersects $n + 1$ consecutive radial lines, $L^{(s)}$, $L^{(s+1)}$, . . . $L^{(s+n)}$.

In seeking this fit one has to consider:

a. All possible positions on the chart of the point S_1 of the overlay.

b. All orientations of the overlay—i.e., all values of s.

c. All circles of the concentric family.

The problem is not as difficult as it might seem. Let the point S_1 of the overlay be placed in a fixed position on the chart. Each circle of the overlay will be intersected by the C circles in a sequence of points which will be unchanged by rotation of the overlay. Unless successive intervals between these points change in geometric progression, by a factor g, there is no possibility of obtaining a fit by turning the overlay. Thus, for each position of the overlay center S_1, a quick inspection of the spacings of the intersections of the two families of circles will suffice to determine whether there is any chance of a fit on any circle of the overlay. By a systematic survey of this type one can reject large areas of the chart as possible positions for S_1.

When a sequence of intersections has been found in which the intervals change in about the right way, it becomes worth while to turn the overlay until the radial lines in the region of intersection have similar spacings—for example, until an s is found such that circles $C^{(0)}$ and $C^{(n)}$ pass through the points $Q^{(s)}$ and $Q^{(s+n)}$, respectively. This configuration will correspond to a linkage in which the errors in the generated function would vanish at the ends of the range of x_1; the errors in the generated function in the intermediate range are evident, being measured by the angular distances on the overlay between the points $Q^{(s+r)}$ and the intersections of the circles $C^{(r)}$ with the B_1 overlay circle. With practice one rapidly develops a technique for improving this fit by smaller adjustments in the position of S_1, with corresponding rotations of the overlay.

(6) If an acceptable fit is not found with the overlay face up, turn the overlay face down, and repeat the process.

(7) When a fit has been found, the elements of the linkage can be read directly on the overlay scale; B_1/A_2 is the value of B for the overlay circle on which the fit is obtained, and A_1/A_2 is the value of B for the overlay circle that passes through the point S_2 on the chart. Limiting configurations of the linkage are evident from the arrangement, and values of X_{1m}, X_{2m}, and X_{1M} can be read.

Figure 5·22 actually represents an application of this method, since Fig. 5·21 is, in fact, the portion of Fig. 5·23 in which s changes from 22 to 30. A full example of the method is presented in Sec. 5·19.

5·18. Improvement of the Solution by Successive Approximations.—A first solution of the problem of mechanizing a given function can be improved by successive applications of the geometric method, in essentially the same way as with the nomographic method.

The first approximate solution will have been found with fixed values of the constants ΔX_2 and B_2/A_2. The first of these constants may be determined by other factors in the problem, but the choice of the second will have been to some degree an arbitrary one. If the choice of B_2/A_2 was very unfortunate, the fit obtained may be so bad that the process must be repeated with another value of this constant. In most cases one will find a reasonably good mechanization of the function—one which is at least sufficiently good to serve as a guide in finding a better one. In particular, note should be taken of the values found for the constants B_2/B_1 and ΔX_1 of this linkage.

Now let us consider the inverse of the function of Eq. (82),

$$x_1 = (x_1|x_2) \cdot x_2, \tag{98}$$

with x_2 treated as the input variable. Interchanging the roles of x_1 and x_2 in Secs. 5·16 and 5·17, one can apply the geometric method to the mechanization of this relation and thus obtain a second mechanization of the original relation. The inverted problem differs from the original in the interchange of B_1 and A_2, X_1 and $180° - X_2$ (cf. Sec. 5·13). Thus it is evident that appropriate choices for the fixed constants of the new problems are

$$\left.\begin{aligned} \frac{\tilde{B}_2^{(2)}}{\tilde{A}_2^{(2)}} &= \frac{B_2^{(1)}}{B_1^{(1)}}, \\ \Delta\tilde{X}_2^{(2)} &= \Delta X_1^{(1)}. \end{aligned}\right\} \tag{99}$$

If the conditions of the problem dictate a special choice of ΔX_2, one should treat $\Delta\tilde{X}_1^{(2)} = \Delta X_2^{(1)}$ also as a constant; the problem is then that discussed in Sec. 5·16. [It can, of course, be treated by the method of Sec. 5·17, with s restricted to a constant value determined by Eq. (94) or Eq. (95)]. In other cases one will treat $\Delta\tilde{X}_1$ as a variable parameter in the inverted problem. In any case the inverted function will be approximated by a linkage selected from a family which includes the mirror image of the original linkage; the fit, if properly made, must be at least as good as that found as a first approximation, and will usually be appreciably better.

A third approximation can then be found by returning to the consideration of the uninverted function and applying the geometric method with the fixed constants

$$\left.\begin{aligned} \frac{B_2^{(3)}}{A_2^{(3)}} &= \frac{\tilde{B}_2^{(2)}}{\tilde{B}_1^{(2)}}, \\ \Delta X_2^{(3)} &= \Delta\tilde{X}_1^{(2)}. \end{aligned}\right\} \tag{100}$$

As a rule this process converges toward a certain optimum solution of the problem. It is to be noted, however, that there may be several such

approximate solutions within the class of three-bar linkages; which of these is found will depend upon the initial choice of B_2/A_2 and ΔX_2. When one finds a mechanically unsatisfactory solution of the problem, it is usually profitable to start the process again with a different value of B_2/A_2.

In applying the geometric method it will be found that the values of ΔX_1 and ΔX_2 converge more rapidly to a limit than do the ratios of the sides of the quadrilateral. It is therefore suggested that this method be abandoned as soon as the values of ΔX_1 and ΔX_2 are sufficiently well determined, the calculation being completed by the nomographic method.

5·19. An Application of the Geometric Method: Mechanization of the Logarithmic Function.—We shall now apply the geometric method to the mechanization of the logarithmic function

$$x_2 = \log_{10} x_1 \tag{101}$$

in the range

$$1 < x_1 < 10, \qquad 0 < x_2 < 1. \tag{102}$$

In terms of the homogeneous variables

$$h_1 = \frac{x_1 - 1}{9}, \tag{103}$$

$$h_2 = x_2, \tag{104}$$

the relation to be mechanized becomes

$$h_2 = \log_{10} (9h_1 + 1). \tag{105}$$

Since the logarithmic function is of the type illustrated in Fig. 5·24*a*, we shall choose a positive δ. The spectrum of values of the homogeneous variable h_1 can then be written as

$$\left.\begin{aligned} h_1^{(0)} &= 0, \\ &\cdots\cdots\cdots\cdots \\ h_1^{(r)} &= \frac{g^r - 1}{g - 1} \cdot \delta, \\ &\cdots\cdots\cdots\cdots \\ h_1^{(n)} &= \frac{g^n - 1}{g - 1} \cdot \delta. \end{aligned}\right\} \tag{106}$$

We shall choose $g = 1.1$, $n = 10$. Solution of the last of Eqs. (106), with $h_1^{(n)} = 1$, gives

$$\delta = 0.0627. \tag{107}$$

The values of $h_1^{(r)}$ can then be computed by Eq. (106), and the corresponding values of $h_2^{(r)}$ by Eq. (105). The resulting values are shown in Table 5·2.

TABLE 5·2.—SPECTRAL VALUES FOR THE LOGARITHMIC RELATION

r	$h_1^{(r)}$	$h_2^{(r)}$
0	0.0000	0.0000
1	0.0627	0.1943
2	0.1318	0.3397
3	0.2077	0.4578
4	0.2912	0.5588
5	0.3830	0.6481
6	0.4841	0.7289
7	0.5952	0.8032
8	0.7175	0.8726
9	0.8520	0.9379
10	1.0000	1.0000

If we express this relation in the inverted form, treating x_2 or h_2 as the input variable, the function is of the type shown in Fig. 5·24*b*. In mechanizing this by the geometric method the spectral values of h_2 should be chosen with δ negative. Distinguishing by a tilde the spectral values required in this inverse mechanization, we have

$$\left.\begin{aligned}\tilde{h}_2^{(0)} &= 1\\ &\cdots\cdots\cdots\cdots\\ \tilde{h}_2^{(r)} &= 1 + \frac{g^{r-1}}{g-1}\,\delta,\\ &\cdots\cdots\cdots\cdots\\ \tilde{h}_2^{(n)} &= 1 + \frac{g^{n-1}}{g-1}\,\delta = 0.\end{aligned}\right\} \tag{108}$$

With $g = 1.1$, $n = 10$, as above, one finds, on solving the last of these equations, the same magnitude as before for δ:

$$\delta = -0.0627. \tag{109}$$

Thus

$$h_2^{(r)} = 1 - h_1^{(r)}; \tag{110}$$

the corresponding values of $\tilde{h}_1^{(r)}$, computed by Eq. 105), are shown in Table 5·3.

We begin mechanization of the relation in the direct form by choosing arbitrarily

$$\frac{B_2^{(1)}}{A_2^{(1)}} = 1.25; \qquad \Delta X_2^{(1)} = 100°. \tag{111}$$

The overlay required for the work is determined as soon as g and an arbitrary small angle α are chosen; with $\alpha = 1°$ it has the form shown in Fig. 5·23. The chart to be constructed depends, however, on the

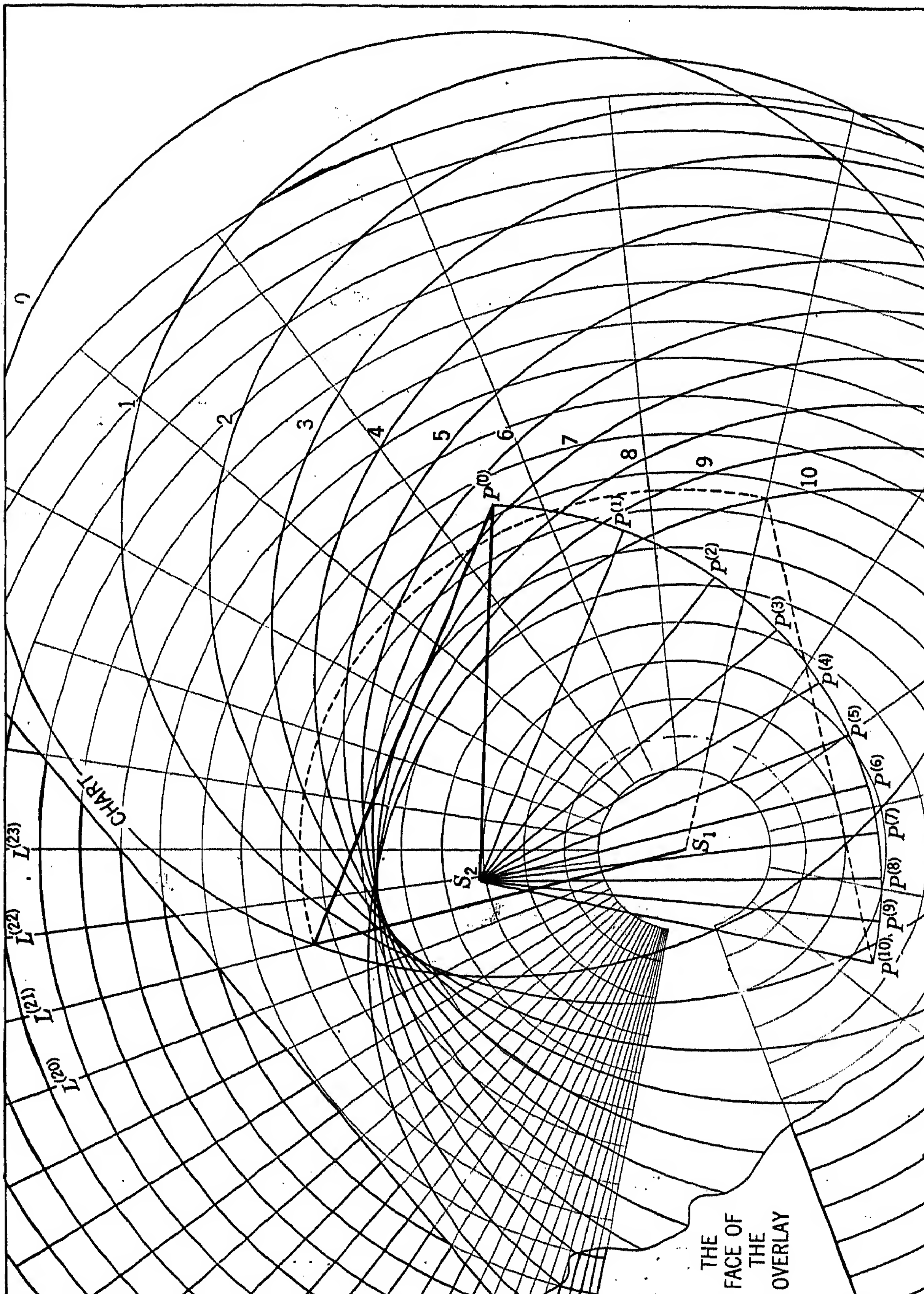

Fig. 5·25.—Relation of chart and overlay corresponding to the first trial mechanization of the logarithmic function. For the sake of clarity in the picture, the chart is shown as lying above the overlay instead of below it.

TABLE 5·3.—SPECTRAL VALUES FOR THE LOGARITHMIC RELATION IN INVERSE FORM

r	$\tilde{L}_2^{(r)}$	$\tilde{h}_1^{(r)}$	$55° \times \tilde{h}_1^{(r)}$, degrees
0	1.0000	1.0000	55.0
1	0.9373	0.8506	46.8
2	0.8682	0.7092	39.0
3	0.7923	0.5777	31.8
4	0.7088	0.4572	25.1
5	0.6170	0.3489	19.2
6	0.5159	0.2533	13.9
7	0.4048	0.1711	9.4
8	0.2825	0.1018	5.6
9	0.1480	0.0451	2.5
10	0.0000	0.0000	0.0

particular problem here considered. On this chart (cf. Fig. 5·25) the lines $A_2^{(r)}$ radiate from the point S_2, making angles $h_2^{(r)}\Delta X_2 = h_2^{(r)}100°$ with the zero line. The points $P^{(r)}$ lie on these lines at unit distance from S_2. About each of these is drawn a circle $C^{(r)}$ with radius

$$\frac{B_2}{A_2} = B_2 = 1.25.$$

This completes preparation of the equipment. The overlay is now placed face up on the chart, and it is found (as shown in Fig. 5·25) to be possible to make the circles $C^{(r)}$ pass, approximately, through the points $Q^{(0)} \cdots Q^{(10)}$ at which the interpolated circle $B = 0.95$ on the overlay (dashed circle in Fig. 5·25) intersects the radial lines $L^{(21)}$ to $L^{(31)}$. The fit, however, is rather poor at the points $Q^{(1)}$ $Q^{(8)}$, $Q^{(9)}$. In addition, the linkage would be mechanically unsatisfactory because of the small angles between the output crank and the link at small r, and between the input crank and the link at large r. (The extreme configurations are indicated by dashed and heavy solid lines in Fig. 5·25.) The fit could be improved by the method of Sec. 5·18, but the approximate solution thus found would probably have the same unsatisfactory mechanical characteristics. No satisfactory fit can be obtained by turning the overlay face down. We therefore repeat the process with another choice of B_2/A_2.

We now try

$$\frac{B_2^{(1)}}{A_2^{(1)}} = 1.8, \qquad \Delta X_2^{(1)} = 100°. \tag{112}$$

The overlay is unchanged, and the chart is changed only in that the circles $C^{(r)}$ have the larger radius $B_2 = 1.8$. The same chart can thus be used again, with the new circles drawn in ink of another color. A more satisfactory fit can now be obtained, this time with the overlay face

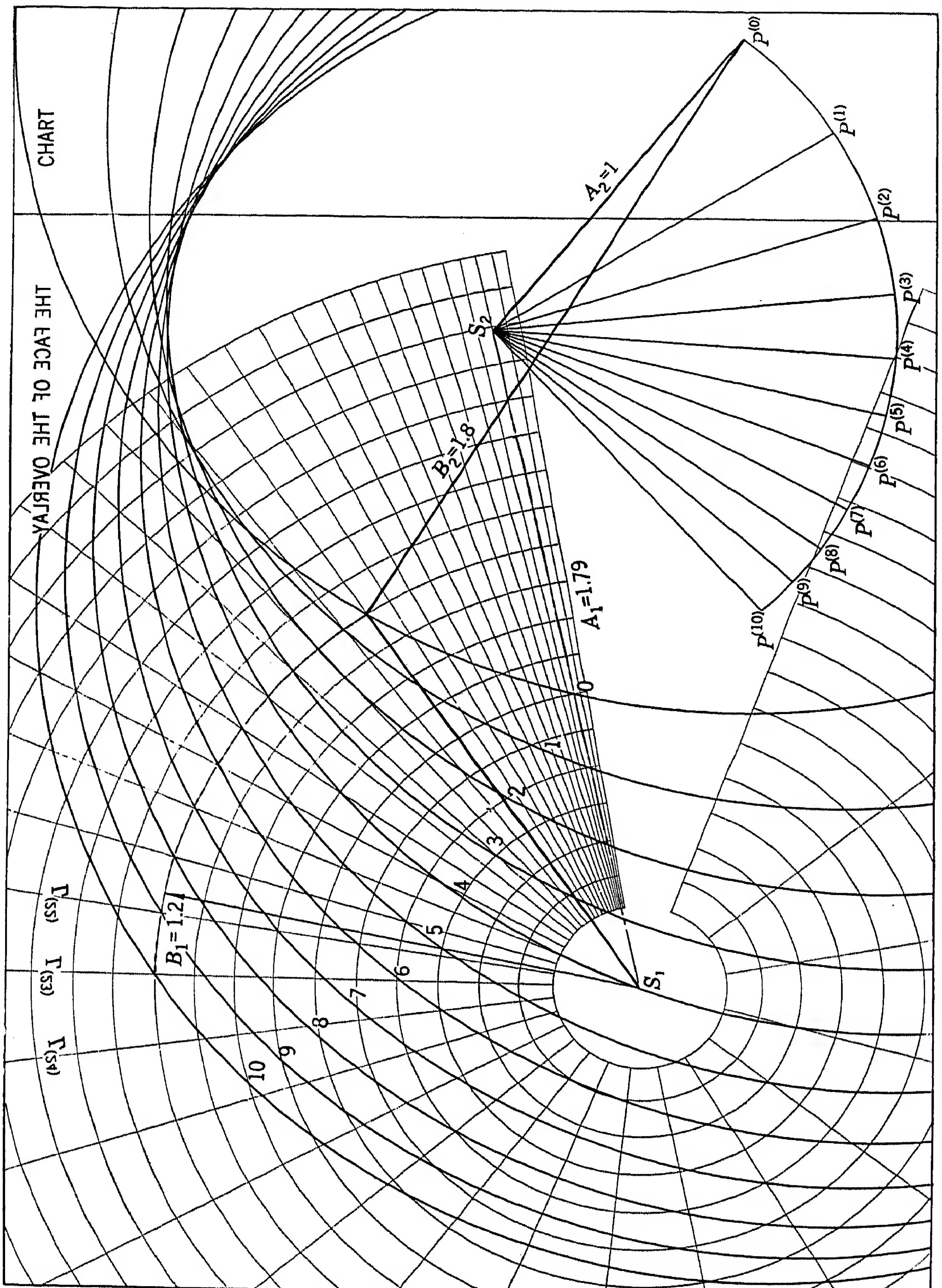

FIG. 5·26.—Relation of chart and overlay in the second attempt to mechanize the logarithmic function. The overlay is face down; for the sake of clarity in the picture, the chart is shown as lying above the overlay rather than below it.

down (Fig. 5·26); the circles $C^{(0)}$ to $C^{(10)}$ pass very nearly through the points $Q^{(0)}$ to $Q^{(10)}$, at which the overlay circle $B = 1.2$ intersects the radial lines $L^{(13)}$ to $L^{(23)}$. From this figure one reads the constants of the linkage:

$$\frac{B_2^{(1)}}{A_2^{(1)}} = 1.8; \qquad \frac{B_1^{(1)}}{A_2^{(1)}} = 1.2; \qquad \frac{A_1^{(1)}}{A_2^{(1)}} = 1.79. \tag{113}$$

Hence

$$\frac{B_2^{(1)}}{B_1^{(1)}} = 1.5. \tag{114}$$

The angle ΔX_1 can be measured on the overlay, but is even more easily obtained as the difference of tabulated values of $Y^{(t)}$:

$$\Delta X_1 = Y^{(s+n)} - Y^{(s)}. \tag{115}$$

These values are given, for the overlay Fig. 5·23, in Table 5·4. In the present case

$$\Delta X_1 = Y^{(23)} - Y^{(13)} = 89.54° - 34.52° = 55.02°. \tag{116}$$

TABLE 5·4.—$Y^{(t)}$, FOR $g = 1.1$, $\alpha = 1°$

t	$Y(t)$, degrees	t	$Y(t)$, degrees	t	$Y(t)$, degrees	t	$Y(t)$, degrees
0	10.00	10	25.94	20	67.27	30	174.49
1	11.00	11	28.53	21	74.00	31	191.94
2	12.10	12	31.38	22	81.40	32	211.14
3	13.31	13	34.52	23	89.54	33	232.25
4	14.64	14	37.97	24	98.50	34	255.48
5	16.11	15	41.77	25	108.35	35	281.02
6	17.72	16	45.96	26	119.18	36	309.13
7	19.49	17	50.54	27	131.10	37	340.04
8	21.44	18	55.60	28	144.21	38	374.04
9	23.58	19	61.16	29	158.63		

Although the linkage thus obtained is not mechanically satisfactory when r is small (x_1 and x_2 near their lower limits), we attempt to improve it by application of the geometric method to the inverted function, with

$$\frac{\tilde{B}_2^{(2)}}{\tilde{A}_2^{(2)}} = \frac{B_2^{(1)}}{B_1^{(1)}} = 1.5 \tag{117a}$$

and

$$\Delta\tilde{X}_2^{(2)} = \Delta X_1^{(1)} = 55°. \tag{117b}$$

A completely new chart must be constructed, with radial lines $A_2^{(r)}$ making angles $\tilde{h}_1^{(r)}\Delta\tilde{X}_2 = \tilde{h}_1^{(r)}\cdot 55°$ with the zero line; the required values will be found in Table 5·3. (It must be remembered that in this inverse problem $\tilde{h}_1$ and $\tilde{X}_2$ vary together, as do $\tilde{h}_2$ and $\tilde{X}_1$. In the procedure, $\tilde{h}_1^{(r)}$ now

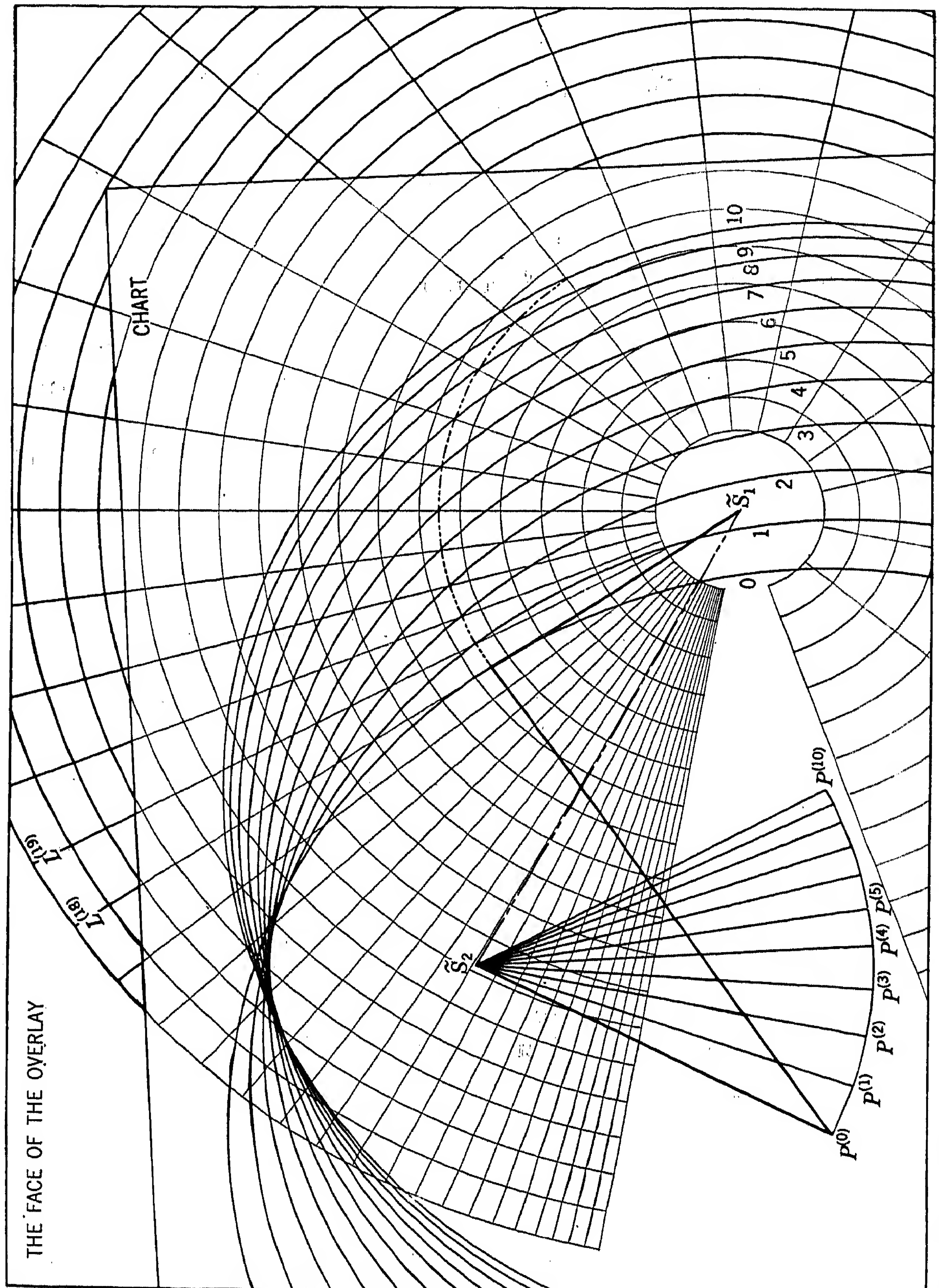

Fig. 5·27.—Relation of chart and overlay in mechanization of the logarithmic function in the inverted form. For the sake of clarity in the picture, the chart is shown as lying above the overlay rather than below it.

takes the place of $h_2^{(r)}$; the values of $\tilde{h}_2^{(r)}$ have been so chosen that the differences increase in geometrical progression and correspond to successive lines on the overlay.) The points $P^{(r)}$ are constructed at radius $\tilde{A}_2^{(2)} = 1$, and about these are drawn circles $C^{(r)}$ with radius $\tilde{B}_2^{(2)} = 1.5$ (Fig. 5·27). When the overlay is placed on this chart, face up, the circles $C^{(r)}$ can be made to pass very nearly through the points $Q^{(r)}$ at which the circle $B = 0.75$ intersects the radial lines $L^{(18)}$ to $L^{(28)}$; on a larger scale it can be seen that the fit is perhaps a little better than that obtained in the preceding step, but the accuracy obtained in both cases is about the best that can be expected of the geometric method. One reads from the figure

$$\frac{\tilde{B}_2^{(2)}}{\tilde{A}_2^{(2)}} = 1.5, \qquad \frac{\tilde{B}_1^{(2)}}{\tilde{A}_2^{(2)}} = 0.75, \qquad \frac{\tilde{A}_1^{(2)}}{\tilde{A}_2^{(2)}} = 1.39; \tag{118a}$$

hence

$$\frac{\tilde{B}_2^{(2)}}{\tilde{B}_1^{(2)}} = 2.0. \tag{118b}$$

The input angular range is

$$\Delta\tilde{X}_1^{(2)} = Y^{(28)} - Y^{(18)} = 88.61°. \tag{119}$$

In terms of the constants of the uninverted problem the above results become

$$\left.\begin{aligned} \frac{B_2^{(2)}}{B_1^{(2)}} = 1.5, \qquad \frac{A_2^{(2)}}{B_1^{(2)}} &= 0.75, \qquad \frac{A_1^{(2)}}{B_1^{(2)}} = 1.39, \\ \frac{B_2^{(2)}}{A_2^{(2)}} &= 2.0. \end{aligned}\right\} \tag{120}$$

and

$$\Delta X_2^{(2)} = 88.61°. \tag{121}$$

The values of $B_2^{(2)}/A_2^{(2)}$ and $\Delta X_2^{(2)}$ are not very different from those of Eq. (112), with which we started; it is evident that the solution is not far from the best one—or, at least, the best one with approximately these constants. It is therefore reasonable to fix on definite travels,

$$\Delta X_1 = 55°, \qquad \Delta X_2 = 90°, \tag{122}$$

as sufficiently close to the best values, and to determine a final design using the nomographic method.

The reader will find it a useful exercise to carry through this step, using the procedure of Sec. 5·11.

We have, by Eq. (51),

$$\begin{aligned} \varphi_1 &= h_1 \cdot 55°, \\ \varphi_2 &= h_2 \cdot 90°. \end{aligned} \tag{123}$$

TABLE 5·5.—SPECTRAL VALUES OF THE PARAMETERS

r	$\varphi_1^{(r)}$, degrees	$h_1^{(r)}$	$h_2^{(r)}$	$\varphi_2^{(r)}$, degrees
0	0	0.0000	0.0000	0.0
1	10	0.1818	0.4209	37.9
2	20	0.3636	0.6306	56.8
3	30	0.5454	0.7715	69.4
4	40	0.7272	0.8777	79.0
5	50	0.9090	0.9627	86.7
6	60	1.0908	1.0341	93.1

To make it possible to use Fig. B·1, we choose $\delta = 10°$, though, in view of the small value of ΔX_1, it would be better to use $\delta = 5°$. The spectral

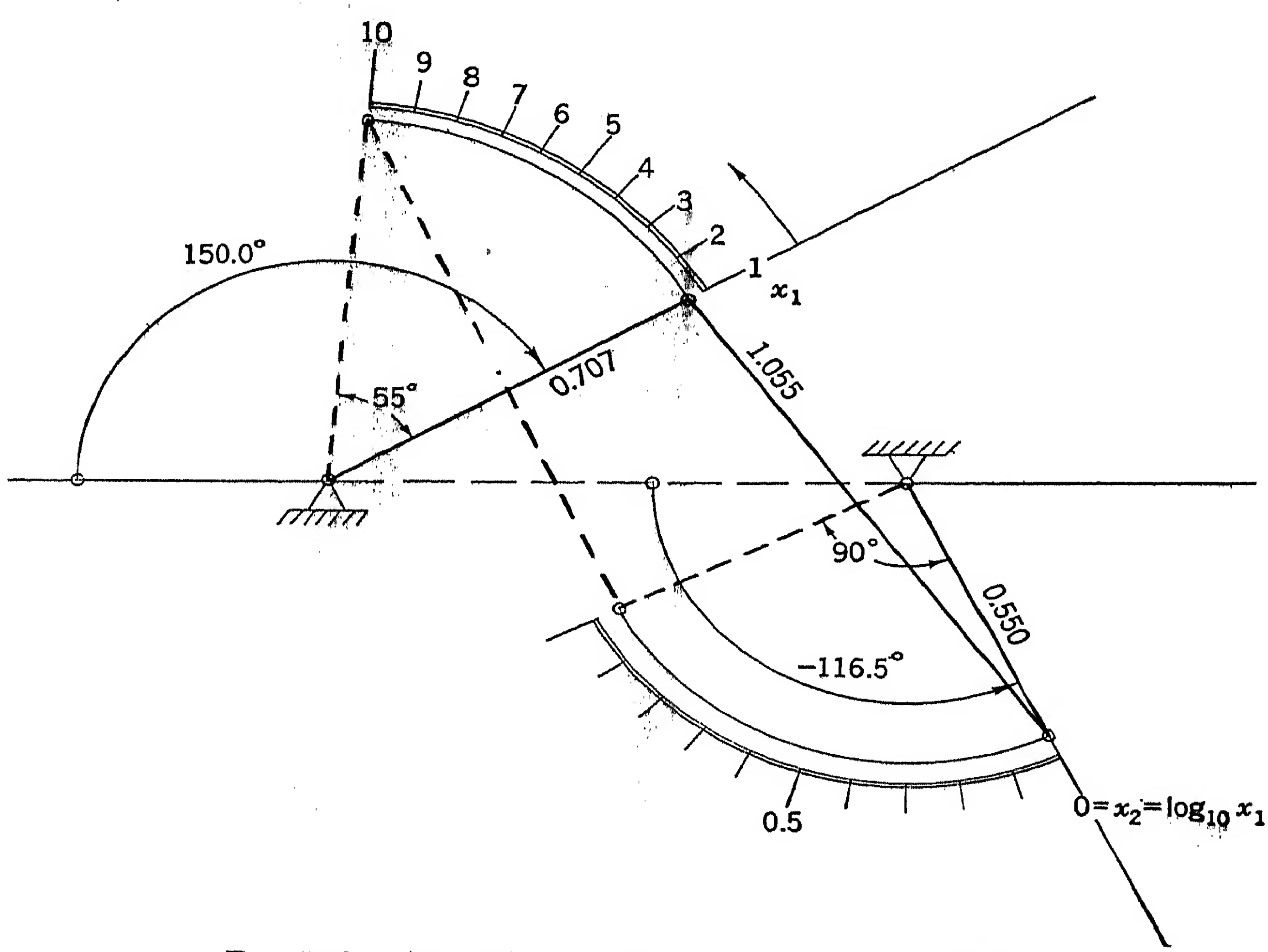

FIG. 5·28.—Approximate mechanization of $x_2 = \log_{10} x_1$.

values $\varphi_1^{(r)}$ and $\varphi_2^{(r)}$, computed with the aid of Eq. 105, appear in Table 5·5. The choice of μb_1 suggested by the last application of the geometric method [Eq. (120)] is

$$\mu b_1 = \log_{10}\left(\frac{B_1^{(2)}}{A_1^{(2)}}\right) = -\log_{10}(1.39) = -0.143 \approx -0.15. \tag{124}$$

Only a few lines need be drawn on the overlay. Picturing the mirrored form of Fig. 5·27 with S_1 to the left of S_2, one sees that the scales of φ_2 and X_2 increase together, whereas φ_1 and X_1 increase in opposite senses; the fit is to be expected with an overlay curve of the minus family, probably with $s = 15$, since $X_{1M} \approx 150°$.

Choosing

$$\mu b_1 = -0.15,$$

we find

$$\left.\begin{aligned} \mu b_2 &= 0.283, \\ \mu a &= 0.260, \\ X_{1M} &= s\delta = 150°, \\ X_{2m} &= -116.5°. \end{aligned}\right\} \tag{125}$$

Hence

$$\frac{B_1}{A_1} = 0.707, \qquad \frac{B_2}{A_2} = 1.919, \qquad \frac{A_1}{A_2} = 1.820,$$

and finally

$$\frac{B_2}{A_1} = 1.055, \qquad \frac{A_2}{A_1} = 0.550. \tag{126}$$

The linkage is sketched in Fig. 5·28. It will be discussed further in a later example (Sec. 7·8).

CHAPTER 6

LINKAGE COMBINATIONS WITH ONE DEGREE OF FREEDOM

It is only rarely that one can mechanize a given function with high accuracy by a harmonic transformer or a three-bar linkage. Usually a more complex linkage must be employed in order to gain the flexibility required in fitting the given function with sufficient accuracy. Instead of devising entirely new structures it is better to combine the elementary linkages; the double harmonic transformer discussed in Chap. 4 is such a combination. Other useful combinations are the double three-bar linkage—analogous in structure to the double harmonic transformer—and combinations of single or double three-bar linkages with one or two harmonic transformers. Choice of the proper combination should of course be determined by the type of function presented for mechanization. Techniques for the design of such linkages will be indicated in the present chapter.

COMBINATION OF TWO HARMONIC TRANSFORMERS WITH A THREE-BAR LINKAGE

6·1. Statement of the Problem.—The combination of two harmonic transformers with a three-bar linkage, as sketched in Figs. 6·1 and 6·2, is particularly useful when it is desirable to use slide terminals at both input and output. (In these figures both harmonic transformers are indicated as ideal; in practice both will usually be constructed as nonideal.) The input link and the crank R_1S_1 constitute a harmonic transformer that transforms the homogeneous input parameter H_1 into the homogeneous angular parameter θ_1. The angular parameter corresponding to θ_1 will be called X_1 (Fig. 6·2); the constants of the harmonic transformer are then X_{1m}, ΔX_1. (It is important to remember that θ_1, not H_1, is the homogeneous parameter corresponding to X_1.) The crank T_1S_1, rigidly linked to R_1S_1, is described by an angular parameter X_3 and a homogeneous angular parameter θ_3, which will be identically equal to θ_1. The input harmonic transformer thus carries out the transformation:

$$\theta_3 = (\theta_3|H_1) \cdot H_1. \tag{1}$$

The cranks T_1S_1 and T_2S_2, with the link T_1T_2, form a three-bar linkage (constants X_{3m}, $\Delta X_3 = \Delta X_1$, X_{4m}, ΔX_4, etc.) that transforms the parameter θ_3 into another homogeneous angular parameter,

$$\theta_4 = (\theta_4|\theta_3) \cdot \theta_3, \tag{2}$$

associated with the angular parameter X_4. The crank R_2S_2, rigidly linked to T_2S_2, is described by the angular parameter X_2, or by the homogenous angular parameter θ_2, identically equal to θ_4. Finally, the crank R_2S_2 and the output link form a harmonic transformer (constants X_{2m}, $\Delta X_2 = \Delta X_4$), which transforms $\theta_4 \equiv \theta_2$ into the homogeneous output parameter

$$H_2 = (H_2|\theta_4) \cdot \theta_4. \tag{3}$$

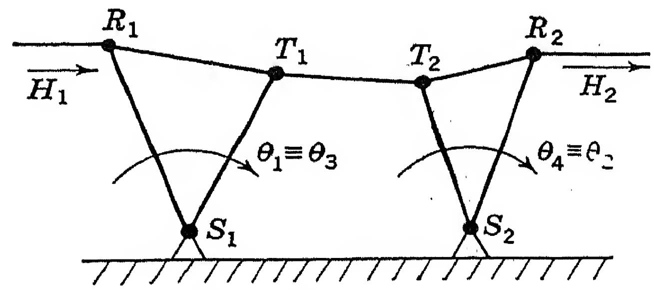

FIG. 6·1.—Three-bar linkage combined with two harmonic transformers.

It will be noted that the angles X_1 and X_2 describing the harmonic transformers cannot in general be measured from the same zero lines as the angles X_3 and X_4 describing the three-bar-linkage configuration, if the conventions of the preceding chapters are to be maintained. In the particular cases illustrated in Figs. 6·1 and 6·2, in which the input and output links of the transformers are parallel to the line of pivots of the three-bar linkage, the zero lines for X_1 and X_2 are perpendicular to those for X_3 and X_4.

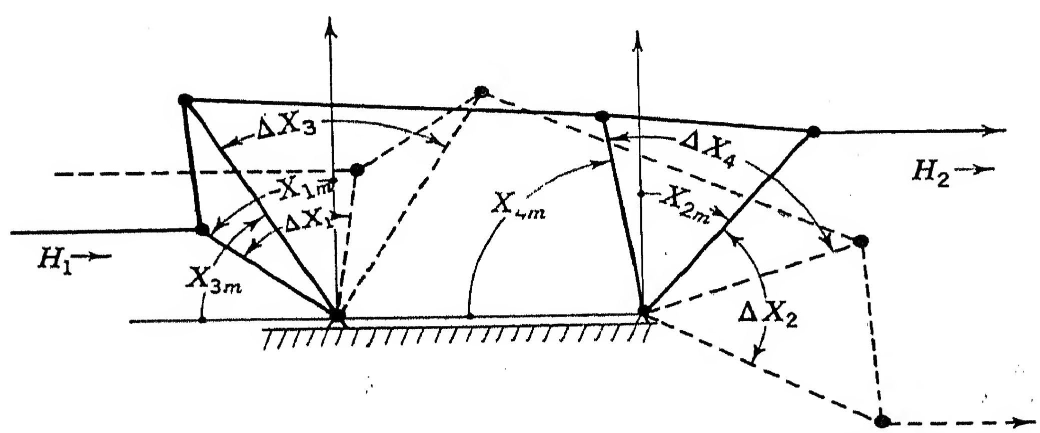

FIG. 6·2.—Combination of three-bar linkage with two harmonic transformers, sketched in its extreme positions.

The linkage as a whole carries out the transformation

$$H_2 = (H_2|H_1) \cdot H_1, \tag{4}$$

where

$$(H_2|H_1) = (H_2|\theta_4) \cdot (\theta_4|\theta_3) \cdot (\theta_3|H_1). \tag{5}$$

Given a functional relation in homogeneous form,

$$h_2 = (h_2|h_1) \cdot h_1, \tag{6}$$

one will wish to find harmonic-transformer functions, $(H_2|\theta_4)$ and $(\theta_3|H_1)$, and a three-bar-linkage function, $(\theta_4|\theta_3)$, such that the product operator $(H_2|H_1)$ will approximate as closely as possible to $(h_2|h_1)$, on direct or

complementary identification of the parameters (H_1, H_2) with the variables (h_1, h_2).

It would be very difficult to find the best approximation to $(h_2|h_1)$ within the twelve-parameter family of available functions. The technique to be described is intended only as a practically useful method for obtaining a good result in a reasonably short time. This involves a preliminary resolution of the desired operator $(H_2|H_1)$ into three factors: two harmonic transformer operators (usually ideal), and a third operator to be mechanized by the three-bar linkage. When the three-bar linkage has been designed, by the methods of Chap. 5, the harmonic transformers are redesigned, almost invariably as nonideal, in order to get a better fit to the given function. Finally, the over-all error is further reduced by small simultaneous variations of all constants of the linkage, by methods to be discussed in Chap. 7.

6·2. Factorization of the Given Function.—A rapid method for finding a satisfactory preliminary factorization of $(H_2|H_1)$ is essential to the success of this procedure. Let Eq. (5) be multiplied from the left by $(\theta_4|H_2)$, from the right by $(H_1|\theta_3)$. One obtains

$$(\theta_4|\theta_3) = (\theta_4|H_2) \cdot (H_2|H_1) \cdot (H_1|\theta_3). \tag{7}$$

Of the quantities on the right, $(H_2|H_1)$ has a prescribed form in the given problem, and the operators $(\theta_4|H_2)$ and $(H_1|\theta_3)$, though unknown, are of a relatively limited class—particularly when attention is restricted to the ideal-harmonic-transformer operators of Tables A·1 and A·2 in carrying out the preliminary factorization. More or less reasonable choices of the operators $(\theta_4|H_2)$ and $(H_1|\theta_3)$ can be based on consideration of the form of the given function. One can then quickly determine, by the graphical multiplication corresponding to Eq. (7), the required form of $(\theta_4|\theta_3)$. Inspection of this function will suffice to indicate whether it can be approximated by a three-bar-linkage function. If so, the constants of that linkage can be found by the methods of Chap. 5; if not, the problem must be reconsidered and another choice of harmonic-transformer functions tried. This process of trial and error is not excessively burdensome since each trial involves only reference to Tables A·1 and A·2 and a graphical construction. The speed with which it can be carried out depends, of course, on the judgment and experience of the designer, both in selecting the harmonic-transformer functions and in assessing the possibility of mechanizing the derived $(\theta_4|\theta_3)$ by a three-bar linkage. Some suggestions on the first of these matters are contained in the following paragraphs.

It is possible, though not usually desirable, to mechanize a given function approximately by a double harmonic transformer and to use an interposed three-bar linkage to make a small correction; it will rarely be

satisfactory to mechanize the given function approximately by a three-bar linkage and then attempt to convert to slide input and output by harmonic transformers that make only small changes in the form of the generated function. Instead, in mechanizing monotonic functions it is better to make all three components of the linkage combination contribute about equally to the curvature of the generated function. Perhaps the simplest way of accomplishing this is to focus attention on the terminal slopes of the factor functions, which become more and more different from 1 as the curvature increases. When all factor functions are monotonic one has

$$\left(\frac{dH_2}{dH_1}\right)_{H_1=0} = \left(\frac{dH_2}{d\theta_4}\right)_{\theta_4=0} \cdot \left(\frac{d\theta_4}{d\theta_3}\right)_{\theta_3=0} \cdot \left(\frac{d\theta_3}{dH_1}\right)_{H_1=0}, \tag{8a}$$

$$\left(\frac{dH_2}{dH_1}\right)_{H_1=1} = \left(\frac{dH_2}{d\theta_4}\right)_{\theta_4=1} \left(\frac{d\theta_4}{d\theta_3}\right)_{\theta_3=1} \left(\frac{d\theta_3}{dH_1}\right)_{H_1=1}; \tag{8b}$$

the terminal slopes of the generated function are products of the corresponding terminal slopes of the factor functions. For a first orientation, to make sure that no factor function need have excessive curvature, one can require that all factor functions have the same terminal slopes:

$$\left(\frac{dH_2}{d\theta_4}\right)_{\theta_4=0} \approx \left(\frac{d\theta_4}{d\theta_3}\right)_{\theta_3=0} \approx \left(\frac{d\theta_3}{dH_1}\right)_{H_1=0} \approx \left[\left(\frac{dH_2}{dH_1}\right)_{H_1=0}\right]^{1/3}, \tag{9a}$$

$$\left(\frac{dH_2}{d\theta_4}\right)_{\theta_4=1} \approx \left(\frac{d\theta_4}{d\theta_3}\right)_{\theta_3=1} \approx \left(\frac{d\theta_3}{dH_1}\right)_{H_1=1} \approx \left[\left(\frac{dH_2}{dH_1}\right)_{H_1=1}\right]^{1/3}. \tag{9b}$$

Specification of both terminal slopes is sufficient to fix the ideal-harmonic-transformer functions completely; they may be identified by reference to Figs. 4·17 and 4·18. By use of Eq. (7) one can then determine the corresponding required form of $(\theta_4|\theta_3)$, for examination as to the possibility of mechanizing it by a three-bar linkage. It is to be remembered that this linkage must be one of specified angular travels ΔX_3 and ΔX_4, these being fixed as the angular travels of the input and output harmonic transformers, respectively.

If there exists no ideal-harmonic-transformer function with the specified terminal slopes, or if the angular travels $\Delta X_1 = \Delta X_3$ and $\Delta X_2 = \Delta X_4$ are unsatisfactory, one can lighten the restrictions on the terminal slopes by requiring only that

$$\left(\frac{dH_2}{d\theta_4}\right)_{\theta_4=0} \left(\frac{d\theta_3}{dH_1}\right)_{H_1=0} \approx \left[\left(\frac{dH_2}{dH_1}\right)_{H_1=0}\right]^{2/3}, \tag{10a}$$

$$\left(\frac{dH_2}{d\theta_4}\right)_{\theta_4=1} \left(\frac{d\theta_3}{dH_1}\right)_{H_1=1} \approx \left[\left(\frac{dH_2}{dH_1}\right)_{H_1=1}\right]^{2/3}. \tag{10b}$$

In addition, any convenient angular travels ΔX_1 and ΔX_2 can be specified and the constants of the two ideal harmonic transformers then deter-

mined by use of Figs. 4·17 and 4·18. (An example is provided in Sec. 6·3.) The required three-bar-linkage function, found as before, will again have terminal slopes given by Eqs. (9).

When the given function has one maximum or minimum, at least one of the three factor functions must also have a maximum or minimum. Only one of Eqs. (8*a*) and (8*b*) can then be valid, and a different procedure must be employed. It is usually best to choose the output-harmonic-transformer function as nonmonotonic—that is, to attempt to mechanize the function by a linkage of the sort illustrated in Fig. 6·2. The constants of this transformer should be such that the function to be generated by the other two elements of the combination,

$$(\theta_4|H_1) = (\theta_4|\theta_3) \cdot (\theta_3|H_1) = (\theta_4|H_2) \cdot (H_2|H_1), \tag{11}$$

is monotonic and as smoothly curved as possible.

The function $(\theta_4|H_1)$ will be monotonic only if the harmonic-transformer function $(H_2|\theta_4)$ has the same values as the given function $(H_2|H_1)$ at the ends of the range of variables (Fig. 6·3). This requirement fixes the form of $(H_2|\theta_4)$, and hence $(\theta_4|H_1)$, for any given ΔX_2; it remains to choose the value of this constant. This should be done with some attention to mechanical suitability but primarily so as to assure that $(\theta_4|H_1)$ is a smoothly curved function, as in Fig. 6·3; it is more important to avoid points of inflection in $(\theta_4|H_1)$ than to make its curvature small. When $(H_2|\theta_4)$ has been determined and the corresponding function $(\theta_4|H_1)$ has been obtained by graphical construction (Sec. 3·4), it remains to resolve this latter function into the product on one harmonic-transformer function and a three-bar-linkage function, as expressed in the first part of Eq. (11).

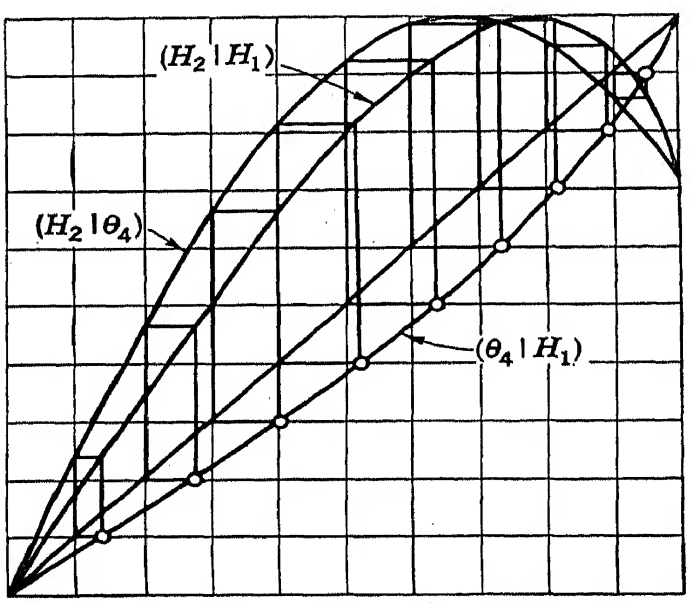

FIG. 6·3.—Resolution of a given function $(H_2|H_1)$ into an output-harmonic-transformer function $(H_2|\theta_4)$ and a monotonic function $(\theta_4|H_1)$.

As when resolving a given function into three factors, it may here be desirable to choose the harmonic-transformer factor by reference to its terminal slopes, fixing

$$\left(\frac{d\theta_3}{dH_1}\right)_{H_1=0} \approx \left[\left(\frac{d\theta_4}{dH_1}\right)_{H_1=0}\right]^{1/2}, \tag{12a}$$

$$\left(\frac{d\theta_3}{dH_1}\right)_{H_1=1} \approx \left[\left(\frac{d\theta_4}{dH_1}\right)_{H_1=1}\right]^{1/2}. \tag{12b}$$

This will determine the constants of the second harmonic transformer, and it will remain only to work out the required form of the three-bar-linkage function by a second graphical construction. In some cases it will not be possible to satisfy both of these conditions; one can then, for instance, satisfy one or the other, and in addition fix ΔX_1.

It is to be emphasized that the preceding paragraphs do not contain a prescription that assures immediate success, and are intended only to be suggestive. A satisfactory resolution of the function may be found only after several trials, in which the designer must be guided by his imagination and experience.

Sections 6·3 and 6·4 will carry an example through the stages of factorization of the given function and mechanization of the three-bar-linkage factor, to the point where there is obtained a first approximate mechanization of the given function by a combination of a three-bar linkage and two ideal harmonic transformers. In Sec. 6·5 we shall then return to a general discussion of the next stage of the design procedure—improvement of the fit by introduction of nonideal harmonic transformers.

6·3. Example: Factoring the Given Function.—To illustrate the details of the method we shall consider again the problem of mechanizing the tangent function, but through a wider range of variables than was attempted in Chap. 4:

$$x_2 = \tan x_1, \qquad 0 < x_1 < 80°. \tag{13}$$

As usual, we introduce homogeneous variables,

$$h_1 = \frac{x_1}{80°}, \tag{14a}$$

$$h_2 = \frac{x_2}{5.6713}. \tag{14b}$$

TABLE 6·1.—$x_2 = \tan x_1$, $0 \leqq x_1 \leqq 80°$, IN HOMOGENEOUS VARIABLES

h_1	h_2
0.0	0.0000
0.1	0.0248
0.2	0.0506
0.3	0.0785
0.4	0.1102
0.5	0.1480
0.6	0.1958
0.7	0.2614
0.8	0.3615
0.9	0.5427
0.95	0.7072
1.0	1.0000

Equation (13) then becomes

$$h_2 = 0.17632 \tan (h_1 \cdot 80°) = (h_2|h_1) \cdot h_1. \tag{15}$$

This function is tabulated in Table 6·1 and plotted, as the desired $(H_2|H_1)$, in Fig. 6·4. The terminal slopes, obtained by differentiating Eq. (15), are

$$\left(\frac{dh_1}{dh_2}\right)_{h_2=0} = 0.246, \qquad \left(\frac{dh_1}{dh_2}\right)_{h_2=1} = 8.165. \tag{16}$$

We first consider the possibility of applying Eqs. (9) in factoring this monotonic function. This would require

$$\left(\frac{dH_2}{d\theta_4}\right)_{C_4=0} = \left(\frac{d\theta_3}{dH_1}\right)_{H_1=0} = (0.246)^{1/2} = 0.627, \tag{17a}$$

$$\left(\frac{dH_2}{d\theta_4}\right)_{\theta_4=1} = \left(\frac{d\theta_3}{dH_1}\right)_{H_1=1} = (8.165)^{1/2} = 2.013. \tag{17b}$$

Inspection of Figs. 4·17 and 4·18 shows that there exist no ideal-harmonic-transformer functions with the required terminal slopes; it is necessary to use the lighter conditions of Eqs. (10), which become

$$\frac{\left(\dfrac{dH_2}{d\theta_4}\right)_{\theta_4=0}}{\left(\dfrac{dH_1}{d\theta_3}\right)_{\theta_3=0}} = (0.627)^2 = 0.393, \tag{18a}$$

$$\frac{\left(\dfrac{dH_2}{d\theta_4}\right)_{\theta_4=1}}{\left(\dfrac{dH_1}{d\theta_3}\right)_{\theta_3=1}} = (2.013)^2 = 4.057. \tag{18b}$$

In addition, values can be assigned to ΔX_1 and ΔX_2. If one requires that $\Delta X_1 = \Delta X_2$, the problem becomes identical with that discussed in Sec. 4·11. Applying the method of solution described there, one finds, for example, the following sets of constants that satisfy Eqs. (18):

1. $\Delta X_1 = \Delta X_2 = 90°$, $X_{1m} = -7.5°$, $X_{2m} = -67.5°$.
2. $\Delta X_1 = \Delta X_2 = 100°$, $X_{1m} = -17.5°$, $X_{2m} = -70°$.

Other sets of constants with $\Delta X_1 = \Delta X_2$ are easily found by the same method; a slight and obvious modification of the method is required if one wishes to have $\Delta X_1 \neq \Delta X_2$. For a first trial we shall choose $\Delta X_1 = \Delta X_2 = 100°$, these values being both mechanically satisfactory and especially convenient for the computations to be made. Then the harmonic-transformer functions to be used are

$$(H_1|\theta_3): \quad -17.5° \leqq X_1 \leqq 82.5°,$$
$$(H_2|\theta_4): \quad -70° \leqq X_2 \leqq 30°.$$

These functions are plotted in Fig. 6·4, the first as a set of encircled points, the second as a continuous curve.

The desired form of the three-bar-linkage function can now be computed by application of Eq. (7), or some equivalent equation. As is

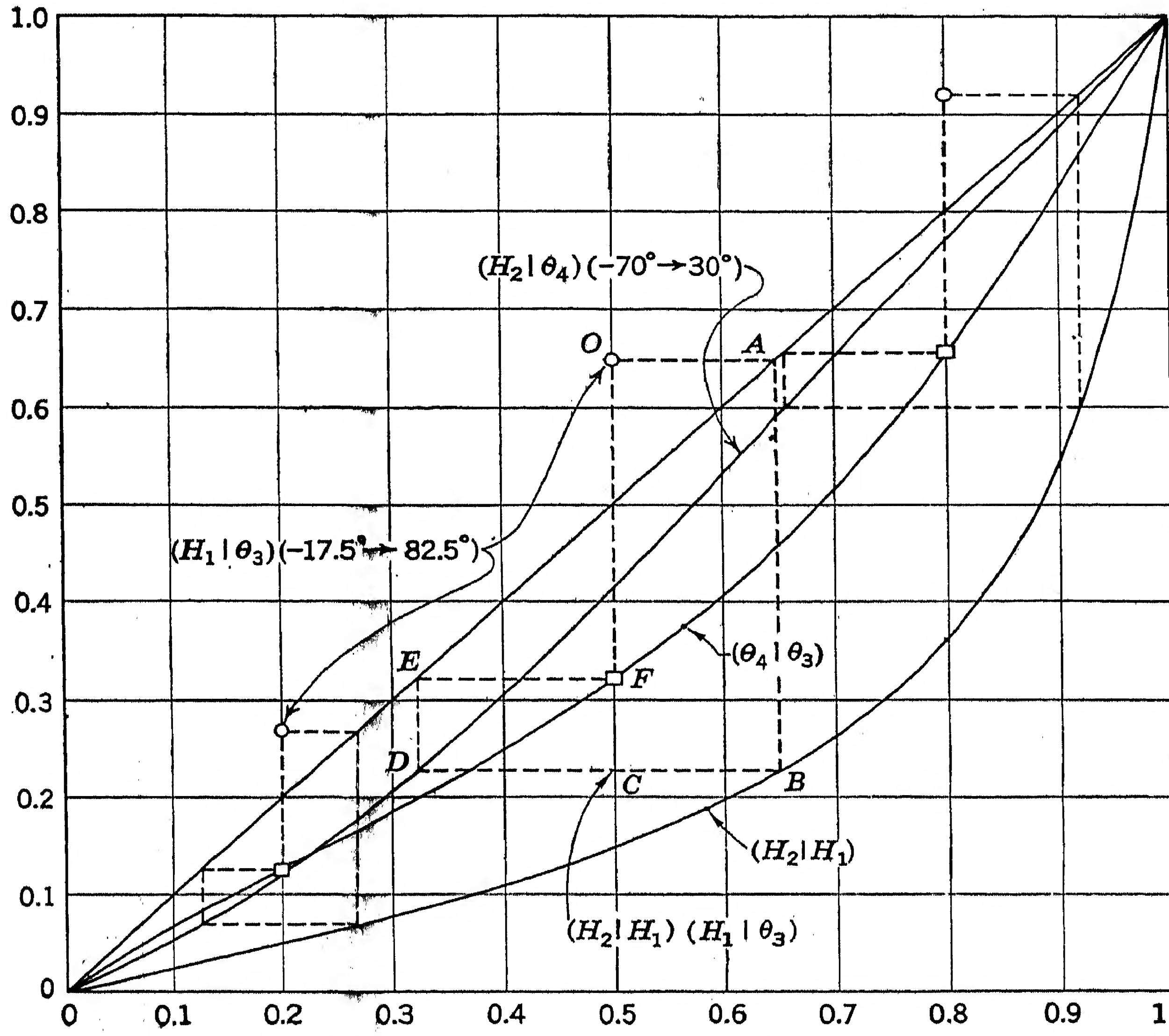

FIG. 6·4.—Resolution of the tangent function, $(H_2|H_1)$, into a product of harmonic-transformer functions, $(H_2|\theta_4)$ and $(\theta_3|H_1)$, and a function $(\theta_4|\theta_3)$ that is to be mechanized by a three-bar linkage.

usually desirable, in Fig. 6·4 we have plotted all functions with the θ-scale horizontal. (Systematic use of this convention helps to prevent mistakes and makes easier the change to nonideal transformers.) To make use of these plots in a graphical construction for $(\theta_4|\theta_3)$ we must, in effect, solve an equation that involves harmonic transformer functions only in the form $(H|\theta)$. This we can obtain by multiplying Eq. (7) from the left by $(H_2|\theta_4)$:

$$(H_2|\theta_4) \cdot (\theta_4|\theta_3) = (H_2|H_1) \cdot (H_1|\theta_3). \tag{19}$$

The product on the right can be formed by graphical multiplication of known operators, as in Fig. 6·4, where construction of the rectangle $O \to A \to B \to C$ leads to location of the point C on the (unplotted) curve representing this product. A corresponding point F on the curve of $(\theta_4|\theta_3)$ is then found by graphical solution of Eq. (19), through construction of the rectangle $C \to D \to E \to F$. It is, of course, unnecessary to locate point C. The complete construction for the point F of the function $(\theta_4|\theta_3)$, corresponding to the point O of the function $(H_1|\theta_3)$, then involves (1) construction of a vertical line through the point O, and (2) location of the point F by construction of the lines $O \to A \to B \to D \to E \to F$.

The complete curve $(\theta_4|\theta_3)$ shown in Fig. 6·4 is quickly determined by repeated application of this construction. It appears to be a function that can be mechanized by a three-bar linkage. We therefore tentatively accept the resolution of the given function as satisfactory, and turn, in Sec. 6·4, to the problem of designing the corresponding three-bar-linkage component.

6·4. Example: Design of the Three-bar-linkage Component.—We have now to consider the problem of mechanizing a function, given graphically in Fig. 6·4, by a three-bar linkage with fixed angular travels,

$$\Delta X_3 = \Delta X_4 = 100°. \tag{20}$$

Since both angular travels are fixed, the nomographic method must be used in determining the other constants of the linkage. Although this method has been illustrated in Sec. 5·14, it may be desirable to show all stages of the procedure also in the present case, which differs from the earlier example in that the method of successive approximations described in Sec. 5·13 converges very slowly. This example will also serve to illustrate the fact that a given function can often be mechanized by several quite different linkages, among which one must make a choice on the basis of mechanical suitability.

The function to be generated by the three-bar linkage, as read from a carefully constructed chart, is given in Table 6·2 in both the direct and the inverted form. The variables used are not the homogeneous variables θ_3 and θ_4, but the angular variables [cf. Eq. (5·51)],

$$\varphi_1 = \Delta X_3 \theta_3, \tag{21a}$$
$$\varphi_2 = \Delta X_4 \theta_4. \tag{21b}$$

(It is to be remembered that in this example X_3 will replace the X_1 of Secs. 5·7 to 5·13, and X_4 will replace X_2.)

We begin by taking

$$\mu b_1^{(1)} = -0.2, \tag{22}$$

the usual first choice of the author.

TABLE 6·2.—GIVEN FUNCTION FOR THE EXAMPLE

$(\varphi_2 \vert \varphi_1)$		$(\varphi_1 \vert \varphi_2)$	
φ_2, degrees	φ_1, degrees	φ_1, degrees	φ_2, degrees
0.0	0.0	0.0	0.0
6.7	10.0	15.5	10.0
12.6	20.0	32.4	20.0
18.5	30.0	47.3	30.0
24.7	40.0	59.2	40.0
32.1	50.0	68.9	50.0
40.7	60.0	76.4	60.0
51.3	70.0	82.8	70.0
65.5	80.0	88.6	80.0
82.5	90.0	94.3	90.0
100.0	100.0	100.0	100.0

Choosing $\delta = 10°$, $n = 100°/10° = 10$, we find the values of $\varphi_2^{(r)}$ and $\varphi_1^{(r)}$ in Columns 1 and 2 of Table 6·2. Construction of the overlay follows precisely the steps described in Sec. 5·14 and need not be explained here. On turning the overlay face down on the nomographic chart, a satisfactory fit is found between the curve $s = -8$ of the minus family on the overlay, and the curve $\mu b_2 = 0.075$ supplied by interpolation on the nomogram. Figure 6·5 shows on the nomogram grid the construction of the particular overlay curve for which the fit was obtained, and the position of fit on the chart. The fit is exact at the ends, very good for the larger values of μp and the smaller values of X_3, and somewhat less satisfactory for the larger values of X_3. The reference lines of the turned overlay are also shown in the position of fit.

The elements of the linkage are thus established:

$\mu b_1^{(1)} = -0.2$, as assumed.
$\mu b_2^{(1)} = 0.075$.
$\mu a^{(1)} = 0.207$, read at the intersection of the vertical reference line with the μp-scale.
$X_{4m}^{(1)} = -7.2°$, read at the intersection of the horizontal reference line with the η-scale.
$X_{3M}^{(1)} = -80°$. ($s\delta = X_{3M}$, not X_{3m}, because the curve that gives a fit is of the minus family.)

$$X_{3m}^{(1)} = X_{3M}^{(1)} - \Delta X_3^{(1)} = -180°.$$

By Eq. (5·56) we have (using the lower signs in the first equation because the fit was obtained with a curve of the minus family)

$$\varphi_1 = -X_3 - 80°, \tag{23a}$$
$$\varphi_2 = X_4 + 7.2°. \tag{23b}$$

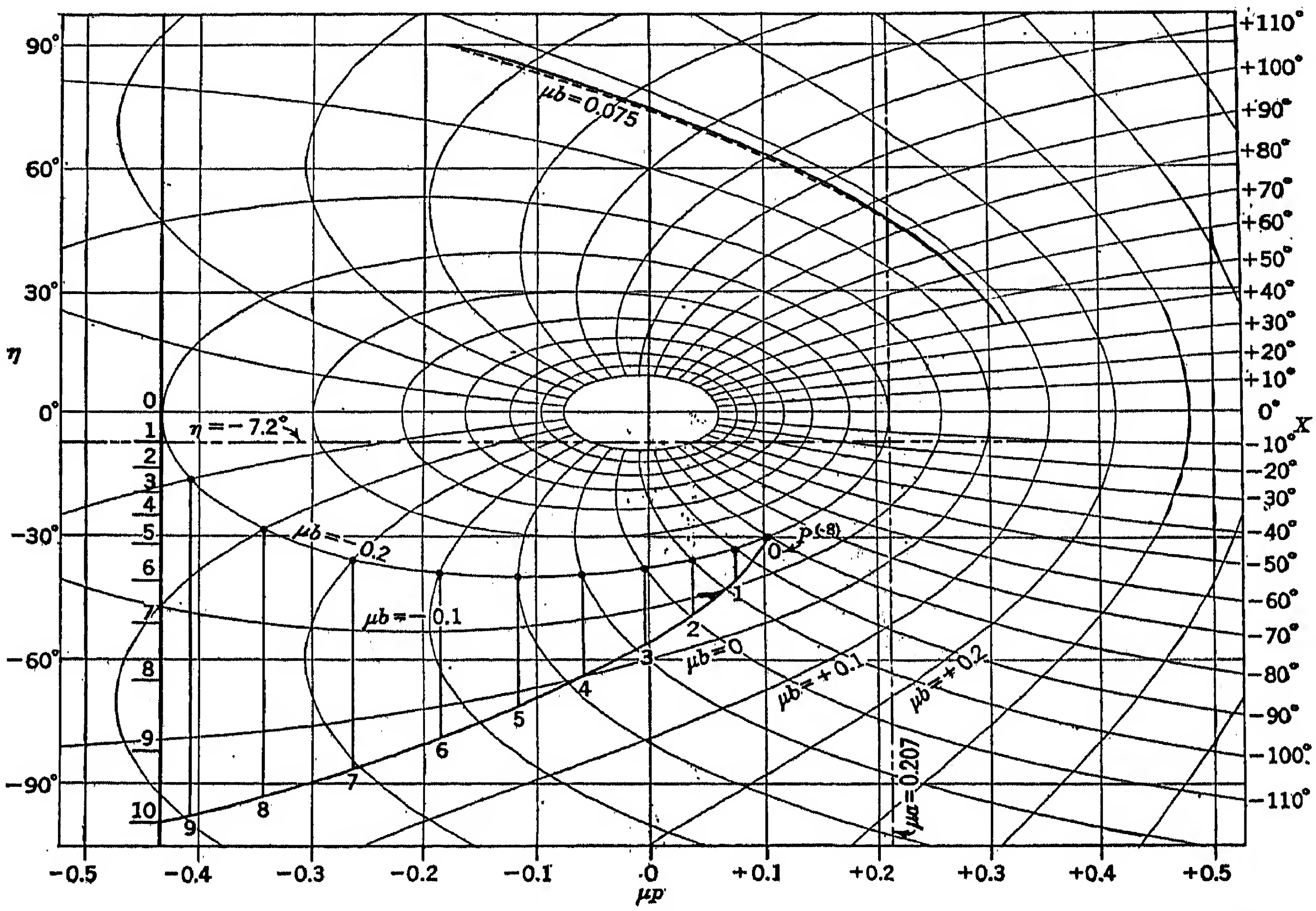

FIG. 6·5.—Mechanization of the tangent function: First application of the nomographic method. The dashed line is the interpolated contour $\mu b = 0.075$.

Equations (23) are only as exact as the fit obtained. Since the fit is exact at the ends of the range of X_3, the input and output travels of the linkage as designed will have the required value, 100°. The φ_1- and θ_3-scales will increase with decreasing X_3, and φ_2, θ_4, and X_4 will increase together.

As a check, the linkage is drawn as in Fig. 6·6, which shows the cranks in their extreme positions. The distance $A_1^{(1)}$ between the crank pivots is taken as the unit of length; the relative crank lengths are drawn in as

$$\frac{B_1^{(1)}}{A_1^{(1)}} = 10^{\mu b_1} = 10^{-0.2} = 0.630, \tag{24a}$$
$$\frac{A_2^{(1)}}{A_1^{(1)}} = 10^{-\mu a} = 10^{-0.207} = 0.620. \tag{24b}$$

The constancy of the required length of the connecting link,

$$\frac{B_2^{(1)}}{A_1^{(1)}} = \left(\frac{B_2^{(1)}}{A_2^{(1)}}\right)\left(\frac{A_2^{(1)}}{A_1^{(1)}}\right) = 10^{\mu(b_2-a)} = 10^{-0.132} = 0.736, \tag{25}$$

provided a check on the quantities determined in the fitting process.

The fit obtained with this first value of μb_1 is so good that one cannot expect it to be changed greatly by further calculations. Nevertheless, we now attempt to improve it by the process of successive approximations, interchanging the roles of φ_1 and φ_2. The inverted function (Sec. 5·13) has already been given in Columns 3 and 4 of Table 6·2. We begin the process of mechanizing this by taking

$$\mu\tilde{b}_1^{(2)} = -0.2 \approx -\mu a^{(1)}, \tag{26}$$

the approximation being close enough for the purpose at hand.

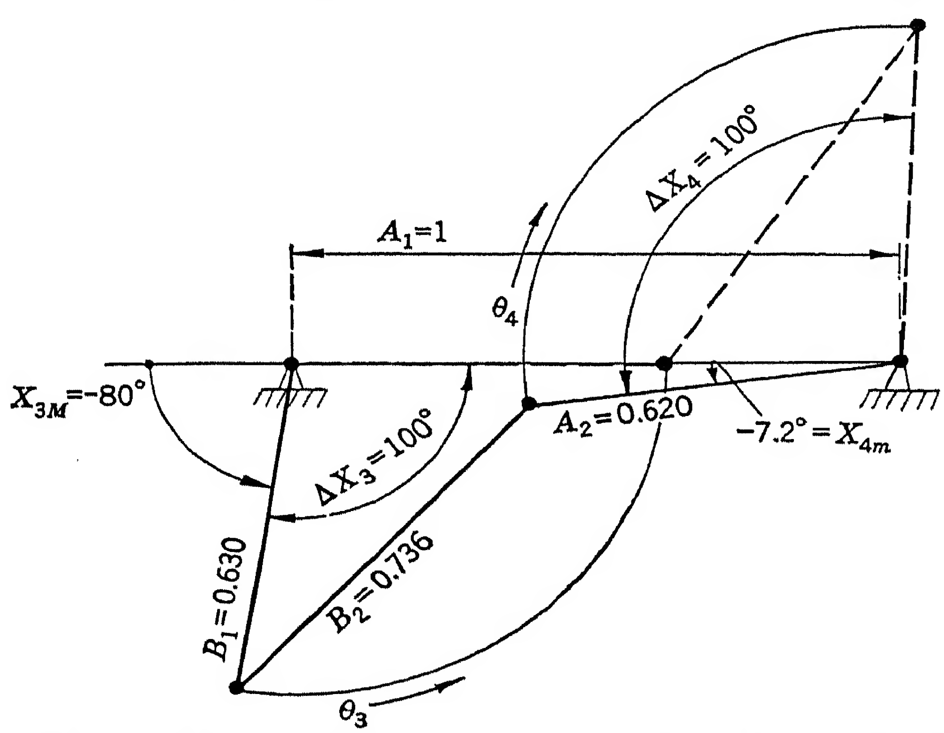

FIG. 6·6.—Mechanization of the tangent function: First three-bar-linkage design.

We know that the linkage to be designed will not be very different from that of Fig. 6·6 reflected in a vertical line. For the inverted problem we must then have $\tilde{X}_{1M} \approx -170°$, $s \approx -17$. (The fit will again be found in the minus family of curves.) Thus only a few lines need be drawn on the overlay.

Figure 6·7 shows the construction of the overlay line for which the best fit is obtained ($s = -17$ in the minus family, as predicted), and the position of fit with the turned overlay. This overlay line is peculiar in that it abruptly reverses its trend at the point $P_1^{(-18)}$, with the result that $P_0^{-(17)}$ and $P_2^{(-19)}$ fall together; this, however, is not an indication of any

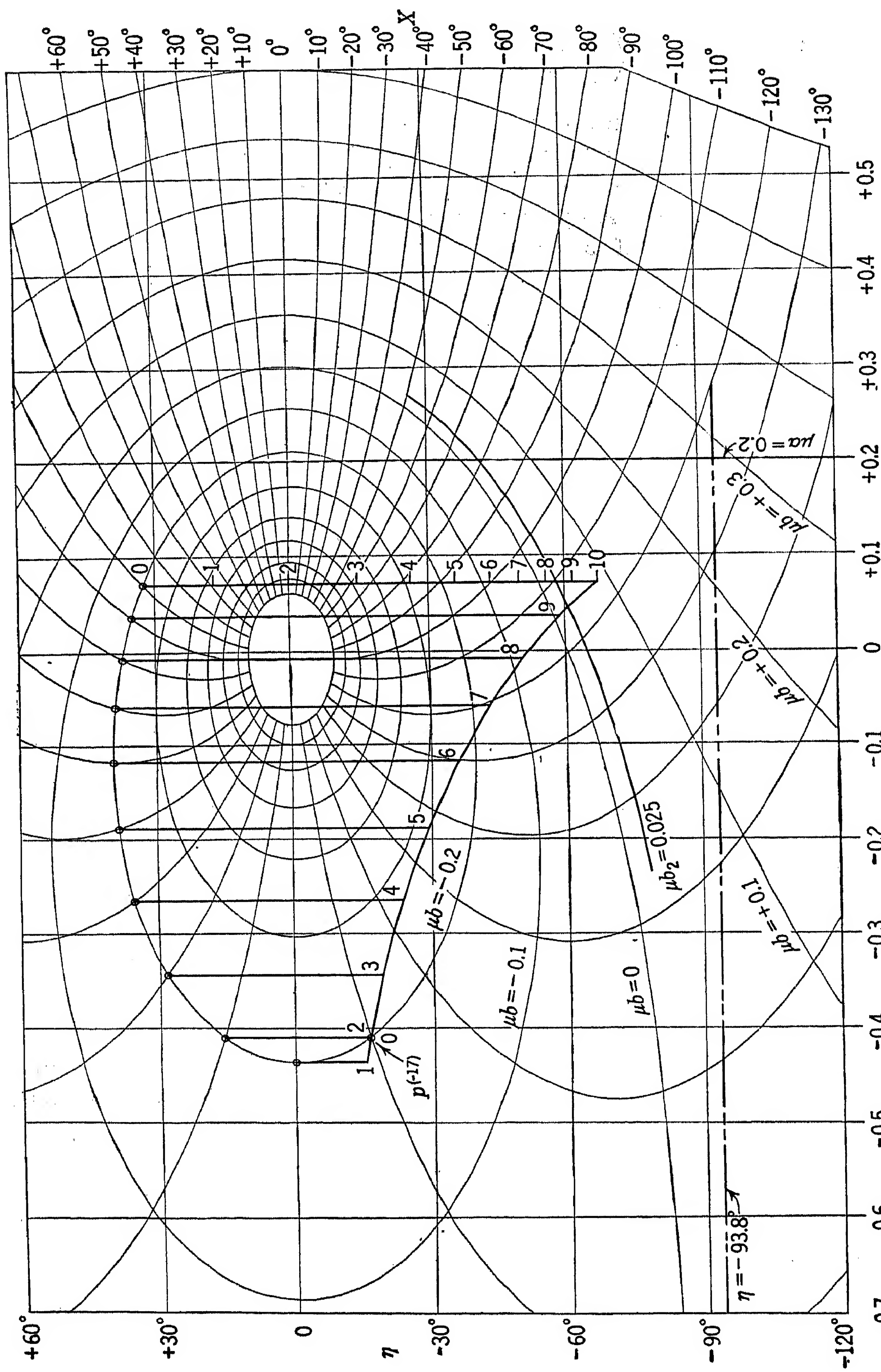

Fig. 6·7.—Mechanization of the tangent function: Second application of the nomographic method.

peculiarity in the linkage. From the position of fit we read the following values for the constants:

$$\left.\begin{aligned}
\mu\tilde{b}_1^{(2)} &= -0.2, \text{ as assumed,}\\
\mu\tilde{b}_2^{(2)} &= 0.025,\\
\mu\tilde{a}^{(2)} &= 0.200,\\
\tilde{X}_{4m} &= -93.8°,\\
\tilde{X}_{3M} &= -170°,\\
\tilde{X}_{3m} &= -270°,\\
\frac{\tilde{B}_1^{(2)}}{\tilde{A}_1^{(2)}} &= 10^{-0.2} = 0.630\\
\frac{\tilde{A}_2^{(2)}}{\tilde{A}_1^{(2)}} &= 10^{-0.2} = 0.630,\\
\frac{\tilde{B}_2^{(2)}}{\tilde{A}_1^{(2)}} &= 10^{-0.175} = 0.668.
\end{aligned}\right\} \tag{27}$$

Since φ_1 and φ_2 have interchanged in this problem, Eq. (5·56) becomes

$$\begin{aligned}
\varphi_2 &= -\tilde{X}_3 - 170°\\
\varphi_1 &= \tilde{X}_4 + 93.8°.
\end{aligned} \tag{28}$$

When the fitting process is carried out on a large scale it can be seen that these constants give a fit good to within 1°.

To make more evident the change in constants due to this second calculation, we rewrite the above results, using Eqs. (5·68) and the obvious relations

$$A_2^{(2)} = \tilde{B}_1^{(2)}, \qquad B_1^{(2)} = \tilde{A}_2^{(2)}, \qquad A_1^{(2)} = \tilde{A}_1^{(2)}, \qquad B_2^{(2)} = \tilde{B}_2^{(2)}. \tag{29}$$

One finds

$$\left.\begin{aligned}
\mu b_1^{(2)} &= -0.2,\\
\mu b_2^{(2)} &= 0.025,\\
\mu a^{(2)} &= 0.2,\\
\frac{B_1^{(2)}}{A_1^{(2)}} &= 0.630,\\
\frac{A_2^{(2)}}{A_1^{(2)}} &= 0.630,\\
\frac{B_2^{(2)}}{A_1^{(2)}} &= 0.668.
\end{aligned}\right\} \tag{30}$$

To throw Eq. (28) into a form comparable to Eq. (23), one must also remember that $\tilde{X}_3$ in the inverted problem corresponds to $\pm 180° - X_4$ in the direct problem, and $\tilde{X}_4$ corresponds to $\pm 180° - X_3$. We have then

$$\varphi_1 = -X_3 - 86.2°, \tag{31a}$$
$$\varphi_2 = X_4 + 10.0°. \tag{31b}$$

Figure 6·8 shows the mirror image of the linkage described by Eqs. (27) and (28)—that is, the linkage described by Eqs. (30) and (31). Direct comparison can then be made with the linkage of Fig. 6·6, with respect to which this is supposed to be an improvement. The scales of X_3 and $\tilde{X}_3$ in these figures are mirror images, as are those of X_4 and $\tilde{X}_4$, but the scales of θ_3 and θ_4, which alone are of real interest, are almost the same.

It will be observed that our consideration of the inverted problem has led us back to the initially assumed value of μb_1; indeed, all constants of the linkage are essentially the same in the second approximation as they

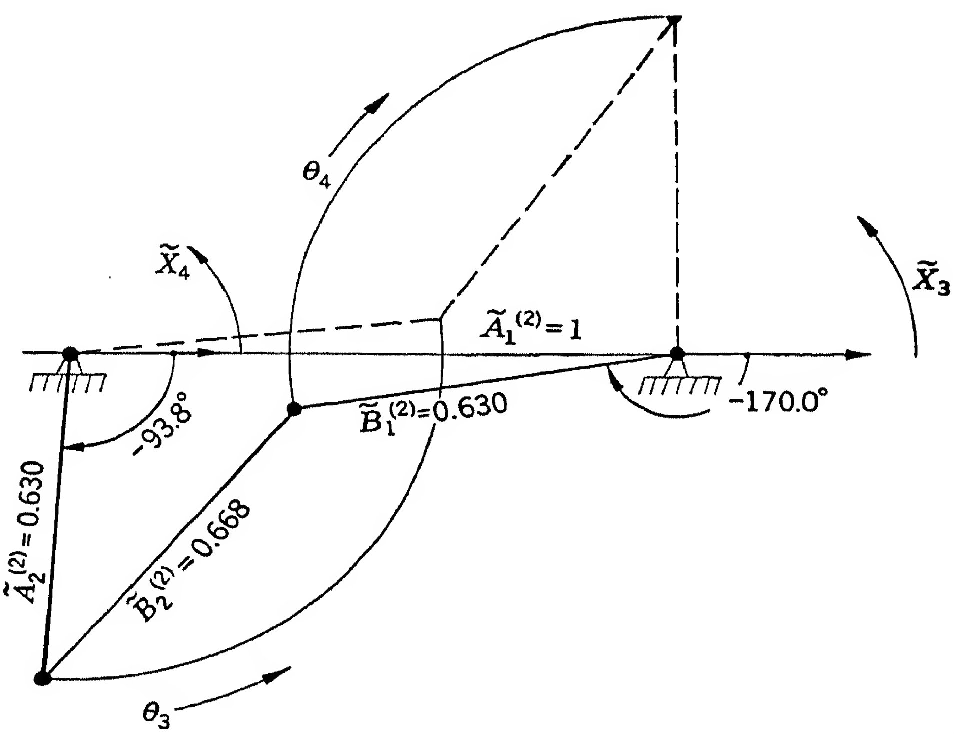

FIG. 6·8.—Mechanization of the tangent function: Second three-bar-linkage design.

were in the first. This, together with the good fit obtained, might lead one to suppose that the initial choice of μb_1 was unusually fortunate, that another choice would have been decidedly worse, and that the method of successive approximations would have led to convergence on the value $\mu b_1 = -0.2$. This, however, would be incorrect: we have here a case in which a good fit does not depend upon a particular choice of μb_1, and the method of successive approximations converges very slowly, if at all. For example, if we had chosen $\mu b_1^{(1)} = -0.3$ we would have found a good fit for $\mu a^{(1)} = 0.314$. Passing to the inverse problem, we would have assumed $\mu \tilde{b}_1^{(2)} = -\mu a^{(1)} = -0.314$ and then found $\mu b_1^{(2)} = -\mu \tilde{a}^{(2)} \approx -0.3$, very closely indeed.

Convergence to a definite value of μb_1 is here so slow as to be undetectable in a graphical method, and is not of any practical importance for obtaining a good fit. It will, however, be observed that there is one constant which is the same in all these linkages:

$$\mu b_1 + \mu a \approx 0.01, \tag{32a}$$

or

$$\log_{10}\left(\frac{B_1}{A_2}\right) \approx 0.01. \tag{32b}$$

It is evident that to obtain a good fit to our given function one must have the crank lengths very nearly equal. Any adjustment of parameters

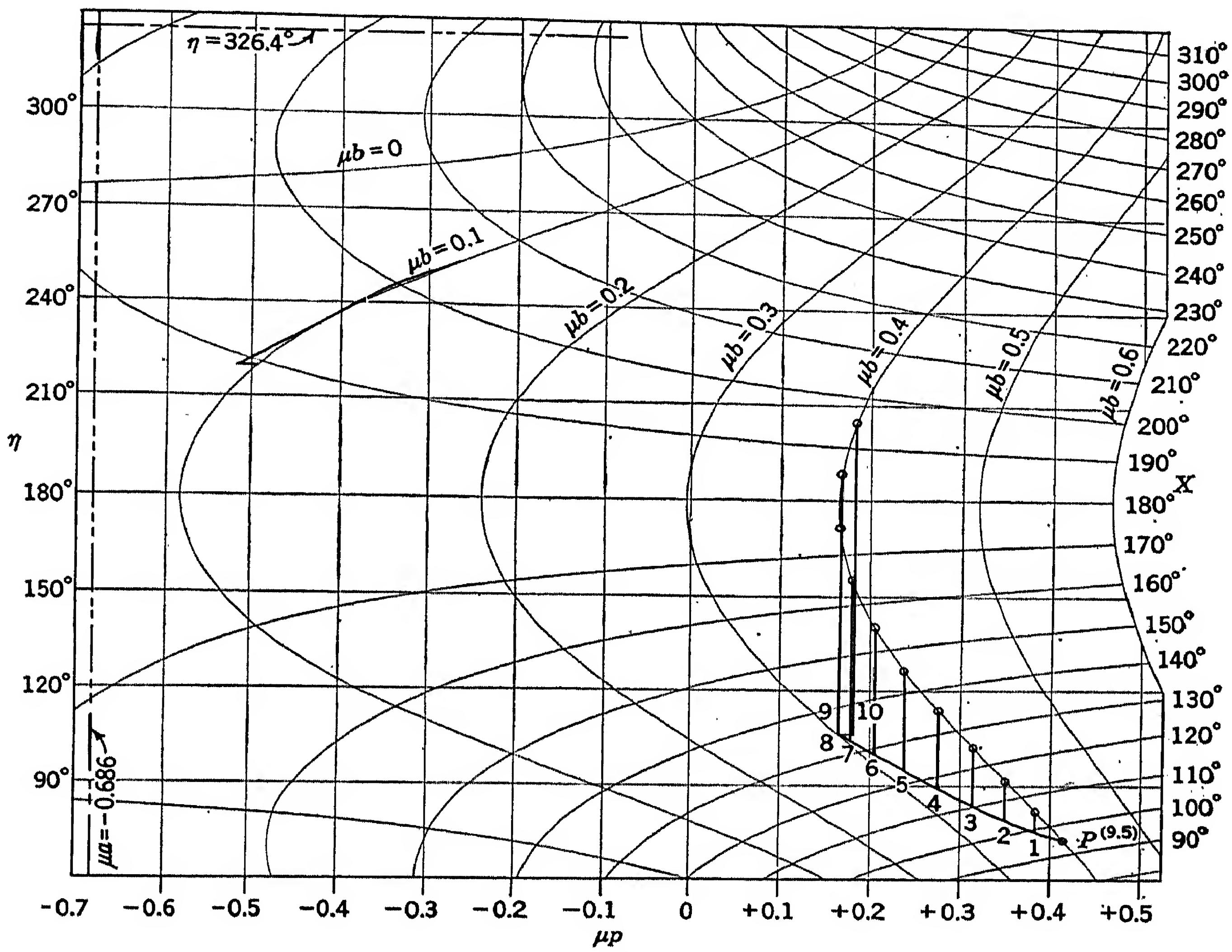

FIG. 6·9.—Mechanization of the tangent function: Third approximation of the nomographic method.

which tends to disturb this relation—for instance, change of a when b_1 is fixed—will lead to very little improvement in the over-all fit, even though it might result in a marked improvement in some other constant of the linkage. The ideal method for adjusting constants in this problem would be one in which $b_1 + a$ could be treated as fixed and the other constants varied. This is, however, a matter of rather academic interest as the fit already obtained is quite satisfactory.

This same given function can be mechanized by other radically different linkages. As noted at the end of Sec. 5·13, before accepting any design one should seek a solution of the problem with μb_1 of the opposite sign—in this case positive. Trial of $\mu b_1^{(1)} = 0.2$ leads to so poor a fit

that it is uncertain what value of μa is really best. In such a case it is desirable to try another value of $\mu b_1^{(1)}$. We take $\mu b_1^{(1)} = 0.4$. The curves of the plus family labeled $s = 9$ and $s = 10$ then give the best fit, but an intermediate overlay curve, $s = 9.5$, is appreciably better. Figure 6·9

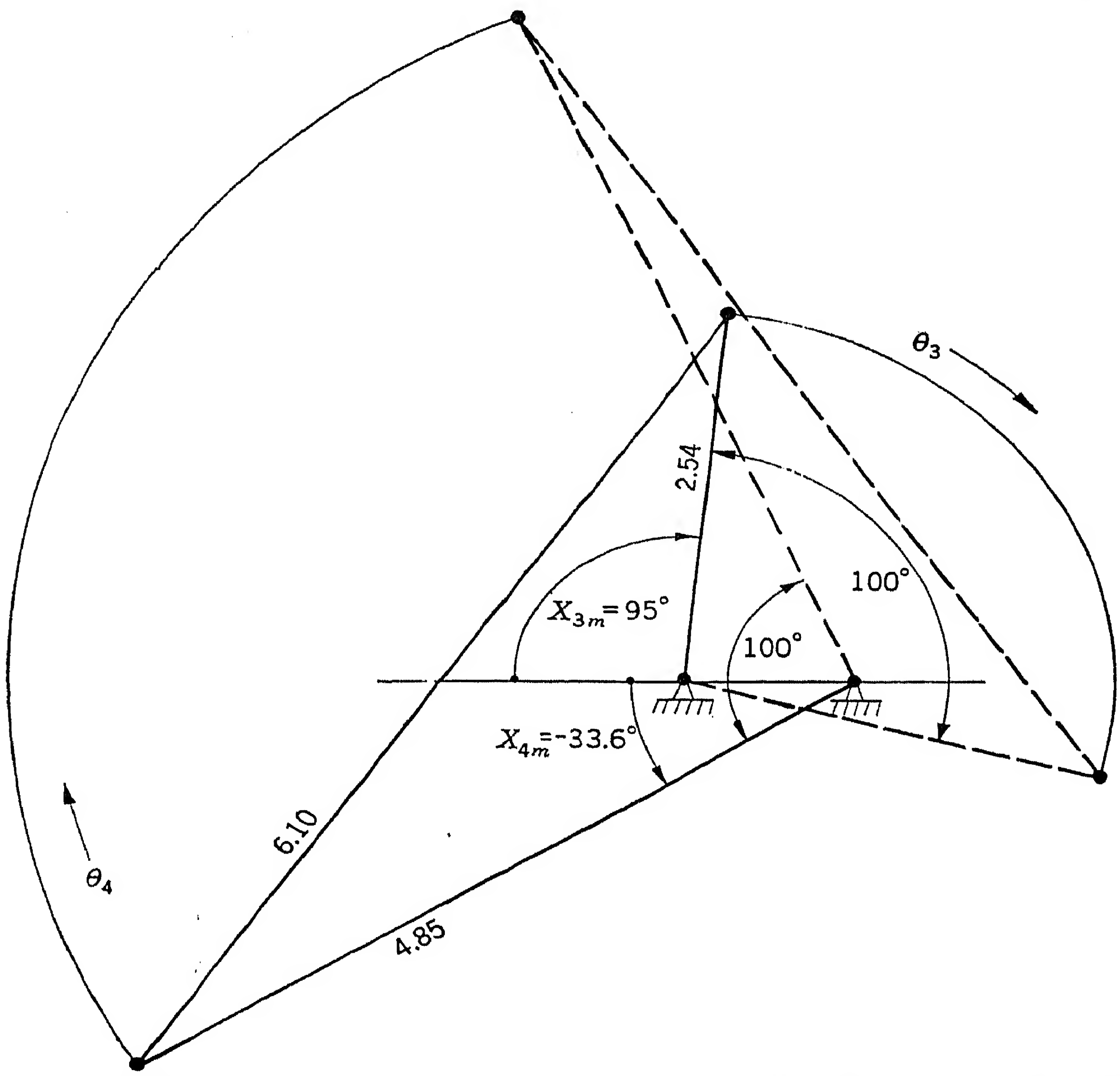

FIG. 6·10.—Mechanization of the tangent linkage: Third three-bar-linkage design.

shows the construction of this curve and the fit obtained on the contour $\mu b = 0.1$. The constants of the linkage are

$$\left.\begin{aligned}
\mu b_1^{(1)} &= 0.4,\\
\mu b_2^{(1)} &= 0.1,\\
\mu a^{(1)} &= -0.686,\\
X_{4m} &= 326.4^\circ \text{ or } -33.6^\circ,\\
X_{3m} &= 95^\circ,\\
\frac{B_1^{(1)}}{A_1^{(1)}} &= 2.54,\\
\frac{A_2^{(1)}}{A_1^{(1)}} &= 4.85,\\
\frac{B_2^{(1)}}{A_1^{(1)}} &= 6.10.
\end{aligned}\right\} \tag{33}$$

Here $X_{3m} = s\delta$, since the fit is found in the plus family. This linkage is sketched in Fig. 6·10. By Eq. (5·56), using the upper signs, we find

$$\varphi_1 = X_3 - 95°, \tag{34a}$$
$$\varphi_2 = X_4 + 33.6°. \tag{34b}$$

The directions of increasing θ_3 and θ_4 are then those indicated in the sketch.

In applying the method of successive approximations one would normally take $\mu\tilde{b}_1^{(2)} = -\mu a^{(1)} = 0.686$. Instead, in order to keep within the range of the nomogram, we shall take $\mu\tilde{b}_1^{(2)} = 0.6$. The linkage generating the inverted function must differ from that of Fig. 6·10 by reflection in a vertical line, and also in horizontal line, in order that the scale of the output quantity may increase clockwise (cf. Sec. 5·14). The fit is to be expected again in the plus family of overlay curves, for

$$\tilde{X}_{3m} \approx -150°,$$

or $p \approx -15$. It is in fact with this curve that the best fit is found, on the contour $\mu b = 0.3$. This fit is shown in Fig. 6·11, which makes use of the extension of the nomogram into the range $\eta > 180°$. The constants of the linkage as thus determined are

$$\left.\begin{aligned}
\mu\tilde{b}_1^{(2)} &= 0.6,\\
\mu\tilde{b}_2^{(2)} &= 0.3,\\
\mu\tilde{a}^{(2)} &= -0.435,\\
\tilde{X}_{4m} &= 279.8°,\\
\tilde{X}_{3m} &= 150°,\\
\frac{\tilde{B}_1^{(2)}}{\tilde{A}_1^{(2)}} &= 3.98,\\
\frac{\tilde{A}_2^{(2)}}{\tilde{A}_1^{(2)}} &= 2.72,\\
\frac{\tilde{B}_2^{(2)}}{\tilde{A}_1^{(2)}} &= 5.43.
\end{aligned}\right\} \tag{35}$$

The form of this linkage, after reflection in vertical and horizontal lines, is shown in Fig. 6·12, for comparison with Fig. 6·10. By Eq. (5·56),

$$\varphi_2 = \tilde{X}_3 - 150°, \tag{36a}$$
$$\varphi_1 = \tilde{X}_4 - 279.8°. \tag{36b}$$

The scales for θ_3 and θ_4, as associated with the reflected linkage, then have the senses indicated in the sketch. The linkage of Fig. 6·12 provides an excellent fit to the given function, and there is no reason to proceed to a third approximation, with $\mu b_1^{(3)} = -\mu\tilde{a}^{(2)} = 0.435$.

We have thus mechanized the given function by three-bar linkages

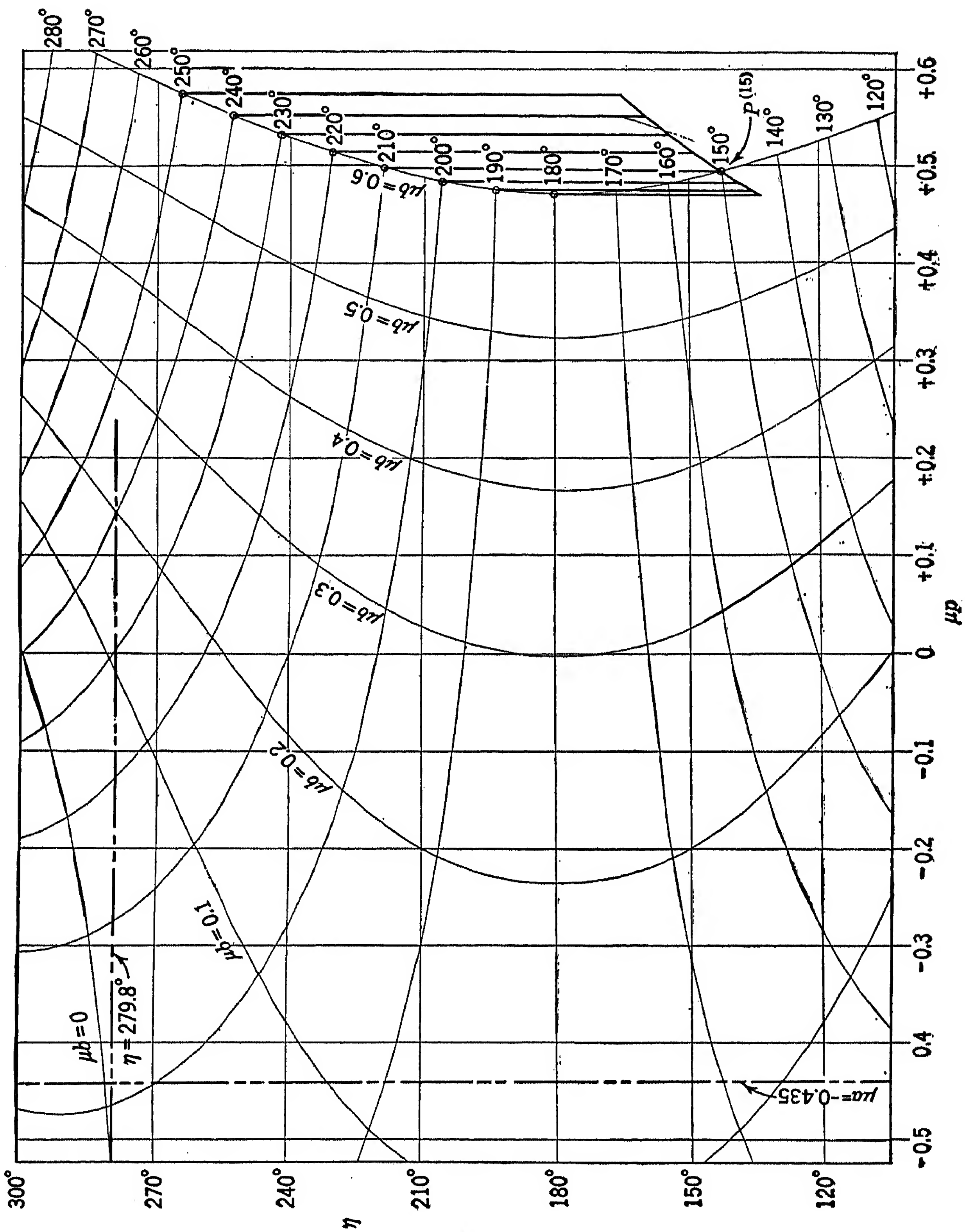

FIG. 6·11.—Mechanization of the tangent function; Fourth application of the nomographic method.

with $\mu b_2 < 0$ and $\mu b_2 > 0$, respectively. Ideally, either of these linkages might be used. Mechanically, the second linkage is much less satisfactory than the first, both as regards space required and the magnitude of backlash error (acute angles between the cranks and the connecting links will tend to magnify backlash). In our further discussion of this example we shall therefore use the linkage of Fig. 6·8, with constants given by Eqs. (30) and (31). Direct calculation, by the methods of

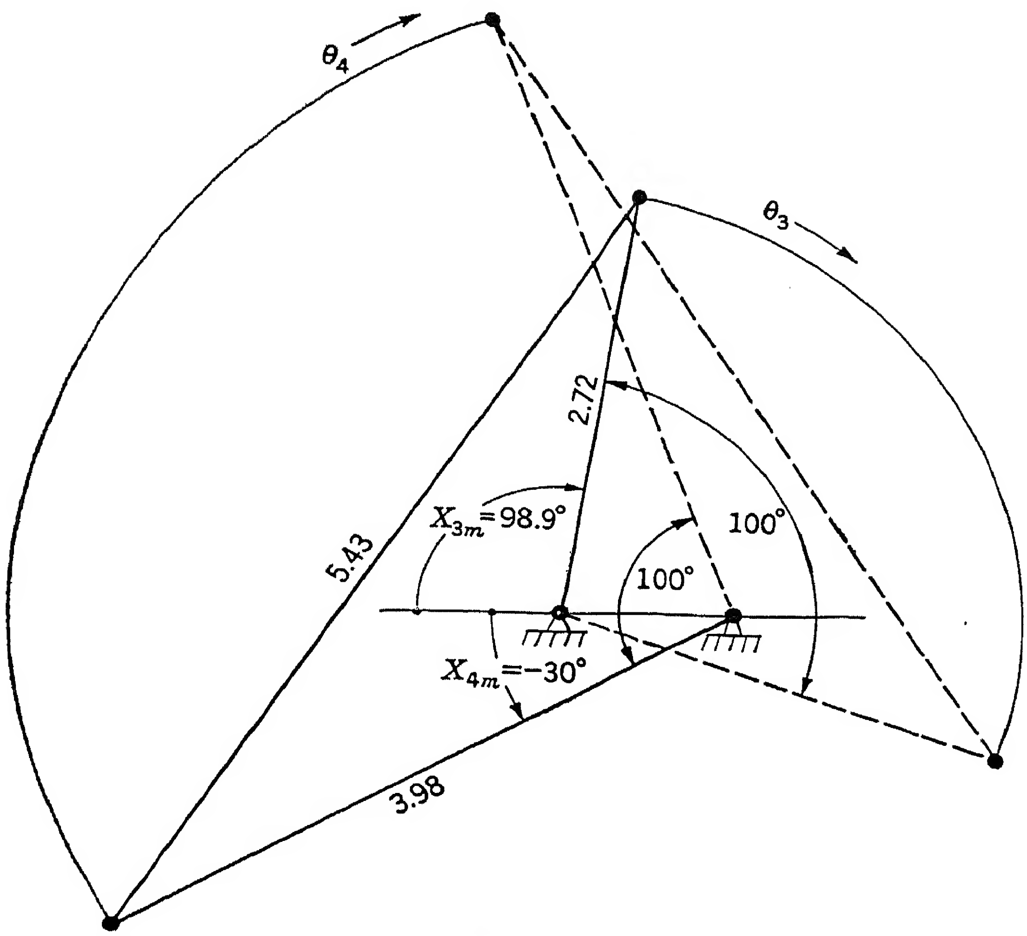

FIG. 6·12.—Mechanization of the tangent linkage: Fourth three-bar-linkage design.

Sec. 5·1, shows that this linkage generates the relation between θ_3 and θ_4 given in Table 6·3 (cf. Table 6·2).

TABLE 6·3.—$(\theta_4|\theta_3)$ AS GENERATED BY THREE-BAR LINKAGE

$\theta_3^{(r)}$	$\varphi_1^{(r)}$, degrees	$X_3^{(r)}$, degrees	$X_4^{(r)}$, degrees	$\varphi_2^{(r)}$ degrees	$\theta_4^{(r)}$ gen.	$\theta_4^{(r)}$ given
0.0	0	− 86.2	−10.10	−0.10	0.0000	0.000
0.1	10	− 96.2	− 2.80	7.20	0.0737	0.067
0.2	20	−106.2	3.08	13.08	0.1331	0.126
0.3	30	−116.2	8.71	18.71	0.1900	0.185
0.4	40	−126.2	14.66	24.66	0.2501	0.247
0.5	50	−136.2	21.48	31.48	0.3190	0.321
0.6	60	−146.2	29.88	39.88	0.4038	0.407
0.7	70	−156.2	40.80	50.80	0.5141	0.513
0.8	80	−166.2	55.17	65.17	0.6592	0.655
0.9	90	−176.2	72.56	82.56	0.8349	0.825
1.0	100	−186.2	88.90	98.90	1.0000	1.0000

With the constants as given the fit is not exact at one end of the curve, and ΔX_4 does not have exactly the desired value of 100°. This discrepancy could be removed by readjustment of the constants but will be corrected

later in an easier way. The generated $\theta_4^{(r)}$ in Column 6 of Table 6·3 is the homogeneous variable corresponding to the generated $\varphi_2^{(r)}$, rather than that given by Eq. (21*b*). The error in this quantity nowhere exceeds 1 per cent of the total travel.

We have thus arrived at a first approximate mechanization of the tangent function, Eq. (13), by a combination of two ideal harmonic transformers and a three-bar linkage, with the constants

$$\left.\begin{aligned} X_{1m} &= -17.5^\circ & \Delta X_1 &= \Delta X_3 = 100^\circ, \\ X_{2m} &= -70^\circ, & \Delta X_2 &= \Delta X_4 = 99^\circ, \\ X_{3m} &= -186.2^\circ, & X_{4m} &= -10.1^\circ, \\ \frac{B_1}{A_1} = 0.630, \quad & \frac{A_2}{A_1} = 0.630, & \frac{B_2}{A_1} &= 0.668. \end{aligned}\right\} \tag{37}$$

The error in this mechanization is most easily determined by extending Table 6·3 to either side. Using the harmonic-transformer constants of Eq. (37), one can compute the values of H_1 and H_2 associated with the tabulated values of θ_3 and θ_4; these can be compared with values of h_1 and h_2 computed by Eq. (15). The resulting values appear in Table 6·4.

TABLE 6·4.—$(H_2|H_1)$ AS GENERATED BY FIRST APPROXIMATE LINKAGE

$h_1 = H_1$	θ_3	θ_4	H_2	$h_2^{(0)}$	$h_2^{(0)} - H_2$
0.0000	0.0	0.0000	0.0000	0.0000	0.0000
0.1317	0.1	0.0737	0.0358	0.0328	−0.0030
0.2665	0.2	0.1331	0.0721	0.0688	−0.0033
0.4002	0.3	0.1900	0.1127	0.1103	−0.0024
0.5288	0.4	0.2501	0.1612	0.1604	−0.0008
0.6485	0.5	0.3190	0.2234	0.2247	+0.0013
0.7555	0.6	0.4038	0.3085	0.3108	+0.0023
0.8467	0.7	0.5141	0.4300	0.4306	+0.0006
0.9191	0.8	0.6592	0.6017	0.5965	−0.0052
0.9708	0.9	0.8349	0.8136	0.8064	−0.0072
1.0000	1.0	1.0000	1.0000	1.0000	0.0000

The over-all error thus remains less than 1 per cent of the total travel.

6·5. Redesign of the Terminal Harmonic Transformers.—The methods described in Sec. 6·2 will lead one to a preliminary mechanization of the given function by a combination of a three-bar linkage and two ideal harmonic transformers. Accepting the three-bar-linkage constants as fixed, one can then improve the accuracy of the device, and at the same time bring it into a more satisfactory mechanical form, by redesigning the terminal harmonic transformers as nonideal. The problem of designing the two terminal harmonic transformers differs but little from that of designing a double harmonic transformer and can be solved by the same methods. (Cf. Secs. 4·13 to 4·15.)

Graphical Method Of Successive Approximations.—The problem is to choose operators $(\theta_3|H_1)$ and $(H_2|\theta_4)$, each characterized by three disposable constants X_m, L, E^*, which give the product operator

$$(H_2|H_1) = (H_2|\theta_4) \cdot (\theta_4|\theta_3) \cdot (\theta_3|H_1) \tag{38}$$

as nearly as possible a specified form. We first try to make $(H_2|H_1)$ identical in form with $(h_1|h_2)$ by changing only one of the transformer operators—for example, $(H_2|\theta_4)$—and assigning to $(\theta_3|H_1)$ its first approximate form, $(\theta_3|H_1)_1$. The required form of $(H_2|\theta_4)$ can be determined by solution of

$$(h_2|h_1) = (H_2|\theta_4) \cdot (\theta_4|\theta_3) \cdot (\theta_3|H_1)_1, \tag{39}$$

by the graphical construction illustrated in Fig. 6·13 (which applies to the example discussed in Secs. 6·3 and 6·4). A judiciously chosen approximation to this will be $(H_2|\theta_4)_2$. The form of $(\theta_3|H_1)$ required, in conjunction with this form of $(H_2|\theta_4)$, to make the mechanization exact, can then be determined by graphical solution of

$$(h_2|h_1) = (H_2|\theta_4)_2 \cdot (\theta_4|\theta_3) \cdot (\theta_3|H_1); \tag{40}$$

$(\theta_3|H_1)_2$ is determined as a suitable approximation to this. Next, $(H_2|\theta_4)$ is readjusted, and so on until the fit can no longer be improved or until the limits of applicability of the graphical method are reached.

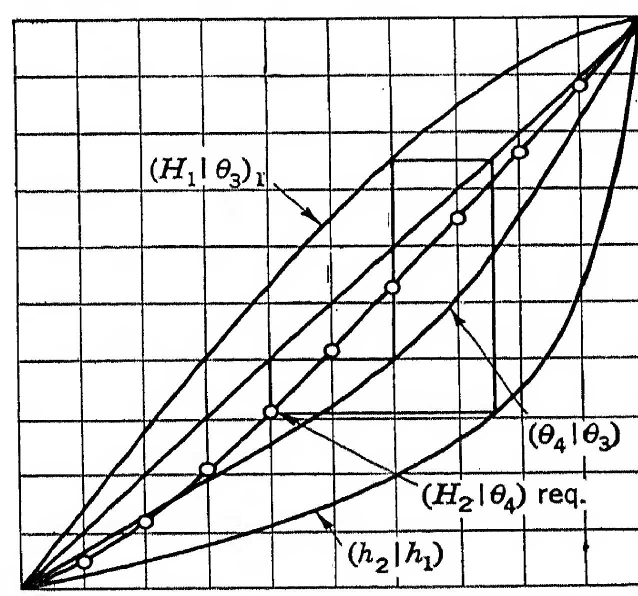

FIG. 6·13.—Graphical construction of the required form of $(H_2|\theta_4)$.

Numerical Method.—The numerical method for the design of nonideal double harmonic transformers (Sec. 4·15) can be applied to the present problem without essential change. In particular, Eqs. (4.89) to (4.97) are valid here also, provided only that $H_2(\theta_3)$ is taken to mean the value of H_2 corresponding to the specified value of θ_3; alternatively, we may consider $H_2(\theta_3)$ to be an abbreviation for $H_2[\theta_4(\theta_3)]$, where $H_2(\theta_4)$ is defined by Eq. (4·12) and the functional relation $\theta_4(\theta_3)$ is determined by the three-bar linkage under consideration. The method will be fully illustrated in the next section.

6·6. Example: Redesign of the Terminal Harmonic Transformers.—In continuing the example of Secs. 6·3 and 6·4 we apply numerical methods to the redesign of the terminal harmonic transformers. This example is of special interest in showing that straightforward application of the

method of Sec. 4·15 does not always lead to a satisfactory result; the modification required in the present case will be described.

We shall keep fixed all constants of the linkage specified in Eq. (37) and shall adjust only the constants L_1, L_2, E_1^*, E_2^*, which characterize the input and output links.

We shall first of all attempt to make the error in the mechanization vanish for $\theta_3 = 0.2, 0.4, 0.6, 0.8$. In Table 6·5 will be found the quantities needed to give explicit numerical form to Eqs. (4·97). Values of θ_3 and θ_4 will be found in Table 6·4. Values of H_1^* can be found from Table A·1 by an interpolation between corresponding entries in the columns $\Delta X_i = 100°$, $X_{im} = -20°$, and $\Delta X_i = 100°$, $X_{im} = -15°$. To obtain values of H_2^* would require interpolation in both ΔX_i and θ_4; it is advisable to make a direct calculation by Eq. (4·42). The values of H_1^* and H_2^* in Table 6·5 have been thus obtained. The f's have been computed from the H's and H^*'s, and the values of dh_2/dh_1 have been computed as

$$\left(\frac{dh_2}{dh_1}\right)_{h_1=H_1} = \frac{4\pi}{9 \tan 80°} \cdot \sec^2 (80° \cdot H_1). \tag{41}$$

TABLE 6·5.—CONSTANTS REQUIRED IN DESIGN PROCEDURE

θ_3	H_1^*	$f_1(\theta_3)$	$f_2(\theta_3)$	H_2^*	$f_3(\theta_3)$	$f_4(\theta_3)$	$\frac{dh_2}{dh_1}$
0.0	0.9468	0.0000	0.0000	0.0000	0.0000	0.0000	0.0000
0.2	0.9989	0.3403	−0.6087	0.3120	0.0501	−0.5073	0.2837
0.4	0.9124	0.4101	−0.9325	0.5505	0.1974	−0.8400	0.4501
0.6	0.6978	0.2678	−0.9325	0.7962	0.4318	−1.0930	1.0115
0.8	0.3809	0.0726	−0.6087	0.9848	0.5757	−0.9956	3.0622
0.9	0.1957	0.0121	−0.3361	0.9630	0.3944	−0.6090	5.399
1.0	0.0000	0.0000	0.0000	0.8094	0.0000	0.0000	

Equations (4·97) become, for $\theta_3 = 0.2, 0.4, 0.6, 0.8, 0.9$, respectively,

$$-0.0965a + 0.1727b + 0.0501c - 0.5073d = -0.0033, \tag{42a}$$
$$-0.1846a + 0.4197b + 0.1974c - 0.8400d = -0.0008, \tag{42b}$$
$$-0.2709a + 0.9432b + 0.4318c - 1.0930d = 0.0023, \tag{42c}$$
$$-0.2223a + 1.8640b + 0.5757c - 0.9956d = -0.0052, \tag{42d}$$
$$-0.0653a + 1.8146b + 0.3944c - 0.6090d = -0.0072. \tag{42e}$$

Attempting to reduce the error to zero at the first four values of θ_3, we solve simultaneously the first four of these equations, and obtain

$$a = 0.0246, \qquad b = -0.0206, \qquad c = 0.0702, \qquad d = 0.0017. \tag{43}$$

Equation (4·31) gives

$$g_1 = 0.6751, \qquad g_2 = 0.4627. \tag{44}$$

By Eqs. (4·46) and (4·47) we have then

$$L_1 = \frac{0.2279}{a}, \qquad L_2 = \frac{0.1070}{c}, \qquad E_1^* = \frac{b}{a}, \qquad E_2^* = \frac{d}{c} \tag{45}$$

or

$$L_1 = 9.264, \qquad L_2 = 1.525, \qquad E_1^* = -0.837, \qquad E_2^* = 0.024. \tag{46}$$

Calculation, by the methods of Table 4·5, of values of H_1', H_2', and of $h_2^{(0)\prime}$ (the value of h_2 corresponding to $h_1 = H_1'$), yields the results shown in Table 6·6. The over-all error, $h_2'^{(0)} - H_2'$, of this mechanization is actually larger than that with which we started, rather than zero at the chosen values of θ_3. This is evidently due to excessively large errors in the approximate linear equations used in the design procedure. In order

TABLE 6·6.—PERFORMANCE OF THE LINKAGE [EQ. (45)]

θ_3	H_1	H_1'	H_2	H_2'	$h_2^{(0)}$	$h_2^{(0)\prime}$	$h_2^{(0)\prime} - H_2'$
0.2	0.2665	0.2889	0.0721	0.0746	0.0688	0.0753	0.0007
0.4	0.5288	0.5602	0.1612	0.1732	0.1604	0.1752	0.0020
0.6	0.7555	0.7831	0.3085	0.3362	0.3108	0.3409	0.0047
0.8	0.9191	0.9344	0.6017	0.6398	0.5965	0.6469	0.0071
0.9	0.9708	0.9785	0.8136	0.8630	0.8064	0.8499	0.0100

to make a small correction in the over-all generated function we have been forced, by its peculiar form, to use harmonic transformers that deviate strongly from the ideal form; $h_2^{(0)} - h_2^{(0)\prime}$ and $H_2 - H_2'$ are large. According to our approximate equations, these large corrections should nearly cancel, leaving an over-all correction of much smaller magnitude and of the desired form. Unfortunately, in computing these large corrections with the linear equations we have made errors that do not tend to cancel out—errors that, in their aggregate, are even larger than the difference that it was desired to compute. Accordingly, the expected accuracy in the correction has not been realized.

Difficulties of this type can sometimes be avoided by very slight modifications in the conditions imposed. In the present case, for instance, one need admit only a very small error at $\theta_3 = 0.4$ in order to use harmonic transformers that are more accurately described by the linear equations; the linkage thus designed has a performance much closer to one's expectations, and correspondingly more satisfactory.

We desire to make a positive correction at $\theta_3 = 0.2$, a negative one at $\theta_3 = 0.6$. It is evident, then, that the correction made will tend to be small at $\theta_3 = 0.4$, whether or not special care is taken with this point. We shall therefore release this point from direct control, and shall solve the first, third, and fourth of Eqs. (42) for the constants a, c, d, in terms of

the constant b. (The choice of the constant b for this special treatment is quite arbitrary.) One finds

$$a = -0.226\,847 - 11.400\,571\,b, \tag{47a}$$
$$c = -0.015\,059 - 3.980\,738\,b, \tag{47b}$$
$$d = 0.048\,170 + 2.115\,946\,b. \tag{47c}$$

The error to be expected at $\theta_3 = 0.4$ is 0.0008 plus the quantity on the left-hand side of Eq. (42*b*):

$$\delta_{0.4} = -0.00076 - 0.03895\,b. \tag{48}$$

As one would expect, $\delta_{0.4}$ is quite insensitive to the choice of b; we can choose this constant with the idea of getting a good mechanical design, well described by the linear equations. We desire, then, that L_1 and L_2 shall not be either very large or very small, and that E_1^* and E_2^* shall lie between zero and one. It follows that a and c should be of the order of magnitude of 0.1, that b should have the same sign as a, and that d should have the same sign as c. We can give L_1 and L_2 roughly equal magnitudes, and obtain the desired sign relations, by setting $b = -0.0135$:

$$\begin{aligned} &a = -0.07294, \quad b = -0.0135, \quad c = 0.03868, \quad d = 0.01960, \\ &L_1 = -3.1245, \quad L_2 = 2.7676, \quad E_1^* = 0.185, \quad E_2^* = 0.507. \end{aligned} \tag{49}$$

The expected value of $\delta_{0.4}$ is then -0.0002. The actual performance of the linkage is shown in Table 6·7.

TABLE 6·7.—PERFORMANCE OF THE LINKAGE [EQ. (49)]

θ_3	H_1'	H_2'	$h_2^{(0)\prime} - H_2'$
0.0	0.0000	0.0000	0.0000
0.1	0.1217	0.0302	0.0001
0.2	0.2504	0.0640	0.0003
0.3	0.3819	0.1036	0.0005
0.4	0.5120	0.1523	0.0008
0.5	0.6361	0.2159	0.0010
0.6	0.7489	0.3037	0.0006
0.7	0.8457	0.4293	−0.0003
0.8	0.9219	0.6045	0.0005
0.9	0.9743	0.8170	0.0086
1.0	1.0000	1.0000	0.0000

The errors due to use of the approximate equations are small, and the performance of the linkage is satisfactory at the points controlled. Unfortunately, the error increases rapidly for $\theta_3 > 0.8$, and the design can not be considered acceptable. It is evident that in the design process more attention must be paid to the error for $\theta_3 = 0.9$.

An attempt to control the error at $\theta_3 = 0.9$ instead of $\theta_3 = 0.8$, by using Eq. (42e) instead of Eq. (42d), leads to similar results: one can actually make the error at $\theta_3 = 0.9$ very small, but the error at $\theta_3 = 0.8$ takes on a large negative value. An attempt to make the error vanish for both $\theta_3 = 0.8$ and $\theta_3 = 0.9$, by solving simultaneously Eqs. (42a), (42c), (42d), and (42e), leads to calculation of the constants

$$L_1 = 1.030, \qquad L_2 = 0.771, \qquad E_1^* = -0.171, \qquad E_2^* = -0.250. \tag{50}$$

These values are such that the linear equations can not be expected to be accurate; the linkage will not give the expected good performance even at $\theta_3 = 0.8$ and $\theta_3 = 0.9$.

The case here encountered is in fact one in which adjustment of the constants L_1, L_2, E_1^*, E_2^* can not bring the over-all error within very strict tolerances, such as ± 0.001. Readjustment of X_{1m} and X_{2m}, or even a new resolution of the given function and redesign of the three-bar-linkage component, would be required if such accuracy were demanded. On the other hand, a tolerance of ± 0.0025 can be met without such redesign, by a somewhat different approach.

Our problem is to correct the error appearing in the last column of Table 6·4 by making the proper linear combination of four correction functions: $-\left(\frac{dh_2}{dh_1}\right)_{\theta_3} f_1(\theta_3)$, $-\left(\frac{dh_2}{dh_1}\right)_{\theta_3} f_2(\theta_3)$, $f_3(\theta_3)$, and $f_4(\theta_3)$. We have been dealing with special values of these functions as coefficients in Eqs. (42). These are reproduced, with the error to be corrected, in Table 6·8. What is required is that we make linear combinations of

TABLE 6·8.—ERROR CORRECTION FUNCTIONS

θ_3	$-\frac{dh_2}{dh_1}\cdot f_1$	$-\frac{dh_2}{dh_1}\cdot f_2$	f_3	f_4	$h_2^{(0)} - H_2$	F_1	F_2
0.2	−0.0965	0.1727	0.0501	−0.5073	−0.0033	−0.0469	−0.1503
0.4	−0.1846	0.4197	0.1974	−0.8400	−0.0008	−0.0641	−0.1344
0.6	−0.2709	0.9432	0.4318	−1.0930	0.0023	0.0000	0.0000
0.8	−0.2223	1.8640	0.5757	−0.9956	−0.0052	0.3130	0.1824
0.9	−0.0653	1.8146	0.3944	−0.6090	−0.0072	0.4559	0.1538

entries in Columns 2 to 5, inclusive, with coefficients a, b, c, d, such that the sums approximate as well as possible to the corresponding entries in Column 6. Examination of Table 6·8 will make it clear that our difficulties have arisen from the attempt to make a positive correction in the center of the range and a negative correction at both ends, whereas not one of the error-correction functions changes sign. The error at $\theta_3 = 0.6$ can be tolerated; let us therefore make no correction at this point and attempt only to reduce the errors at the ends of the range. We shall in fact design

the input and output transformers so that neither changes the generated function at $\theta_3 = 0.6$, taking

$$\frac{b}{a} = E_1^* = 0.2872, \qquad \frac{d}{c} = E_2^* = 0.3950. \tag{51}$$

The form of the correction made in each terminal transformer (F_1 and F_2 in Table 6·8) is thus fixed; it remains to determine the constants a and c with which these should be added.

Next, let the (approximate) error at $\theta_3 = 0.2$ be required to vanish:

$$-0.0469a - 0.1503c = -0.0033. \tag{52}$$

The errors at $\theta_3 = 0.8$ and $\theta_3 = 0.9$ will then be

$$\delta_{0.8} = -0.0052 - 0.3130a - 0.1824c = -0.0092 - 0.2561a, \tag{53a}$$
$$\delta_{0.9} = -0.0072 - 0.4559a - 0.1538c = -0.0106 - 0.4079a. \tag{53b}$$

It is evident that for best results one must use a negative a, and allow a negative error at $\theta_3 = 0.8$, a positive one at $\theta_3 = 0.9$. An appropriate choice is

$$a = -0.0306, \qquad c = 0.0315. \tag{54}$$

We thus find as constants for the linkage

$$L_1 = -7.438, \qquad L_2 = 3.398, \qquad E_1^* = 0.2872, \qquad E_2^* = 0.3950. \tag{55}$$

The performance of this linkage is shown in Table 6·9; it is about the best that can be attained by adjustment of these four constants.

TABLE 6·9.—PERFORMANCE OF THE LINKAGE [EQ. (55)]

θ_3	H_1'	H_2'	$h_2^{(0)\prime} - H_2'$
0.0	0.0000	0.0000	0.0000
0.1	0.1285	0.0324	−0.0004
0.2	0.2615	0.0674	0.0000
0.3	0.3948	0.1077	0.0007
0.4	0.5244	0.1570	0.0015
0.5	0.6461	0.2209	0.0023
0.6	0.7555	0.3085	0.0023
0.7	0.8487	0.4334	0.0008
0.8	0.9222	0.6075	−0.0015
0.9	0.9734	0.8185	0.0021
1.0	1.0000	1.0000	0.0000

6·7. Example: Assembly of the Linkage Combination.—The final step in the mathematical design of a linkage combination is to coordinate properly its component parts. Careful attention must be paid to sign conventions and to the varying zero lines from which angles are measured in the several types of components.

It is safest to begin by sketching the component linkages in their basic positions. With each component there should be indicated the scales for the output parameters. In our example the linkages and scales are fully characterized as follows:

Input harmonic transformer:

$$X_{1m} = -17.5°, \qquad L_1 - 7.438,$$
$$\Delta X_1 = 100°, \qquad E_1^* = 0.287,$$
$$\theta_2 \text{ increases with } X_1.$$

Three-bar linkage:

$$X_{3m} = -186.2°, \qquad \frac{B_1}{A_1} = 0.630,$$
$$\Delta X_3 = 100°, \qquad \frac{A_2}{A_1} = 0.630,$$
$$X_{4m} = -10.1°, \qquad \frac{B_2}{A_1} = 0.668,$$
$$\Delta X_4 = 99°,$$
$$100° \cdot \theta_3 = 86.2° - X_3,$$
$$99° \cdot \theta_4 = 10.1° + X_4.$$

Output harmonic transformer:

$$X_{2m} = -70°, \qquad L_2 = 3.398,$$
$$\Delta X_2 = 99°, \qquad E_2^* = 0.395,$$
$$\theta_4 \text{ increases with } X_2.$$

These linkages are sketched in Fig. 6·14; scales of H_1, H_2, θ_3, and θ_4 are shown. There is an adjustable scale constant in the design of each component. The scale constants of the harmonic transformers (a and c, respectively) can be adjusted to control the travels at the input and output terminals; choice of the scale constant of the three-bar linkage (b) is subject only to considerations of mechanical convenience.

In the linkage combination the readings on the θ_3-scales of the input harmonic transformer and the three-bar linkage must always be the same. We have designed the two θ_2-scales to cover the same angular range, but the sign conventions have forced us to allow the θ_3-scale of the three-bar linkage to increase counterclockwise, whereas that of the transformer increases clockwise. These components might, for instance, be connected by the gearing indicated in Fig. 6·14. On the other hand, the θ_4-scales of the three-bar linkage and the output transformer increase

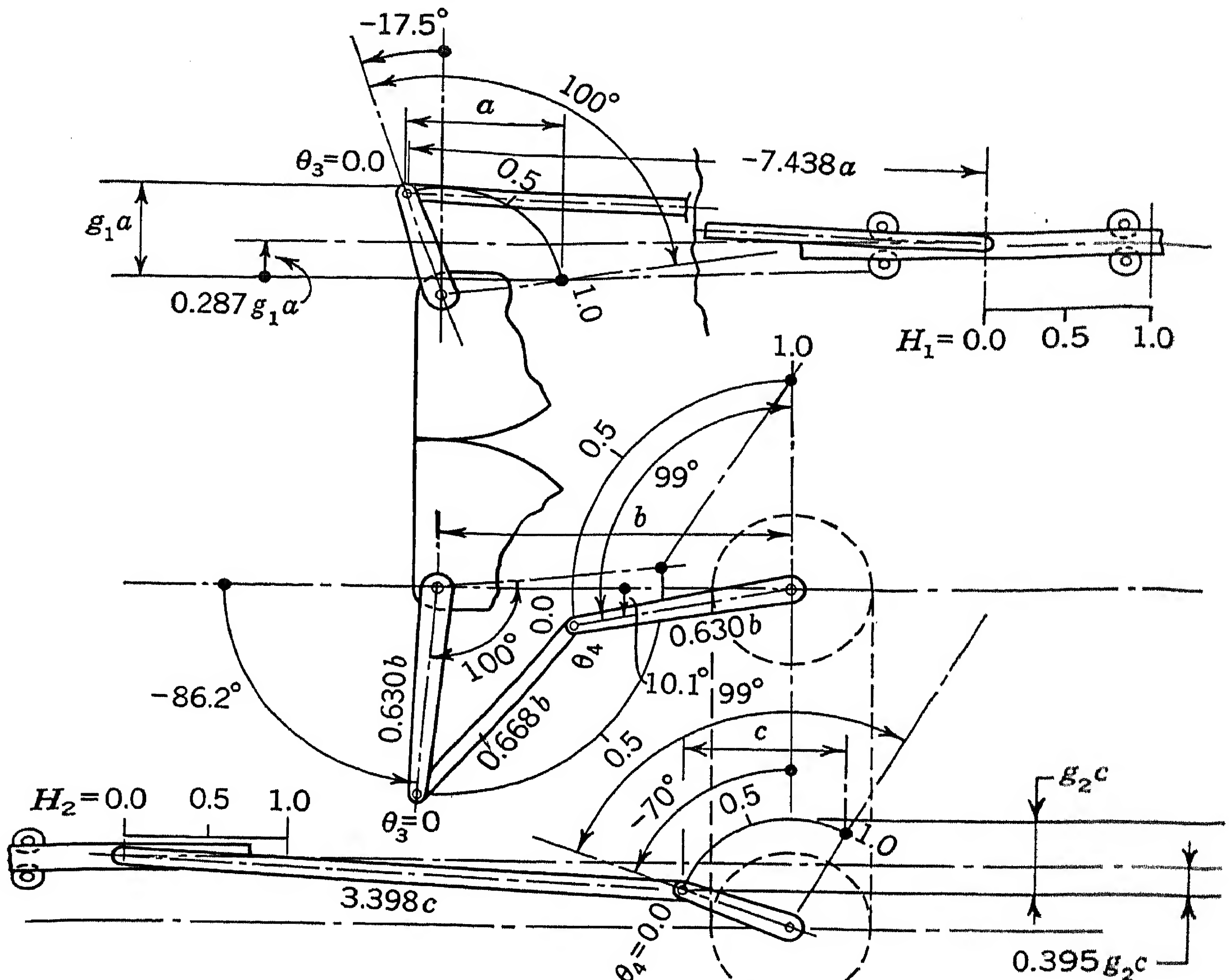

FIG. 6·14.—Components of the tangent linkage.

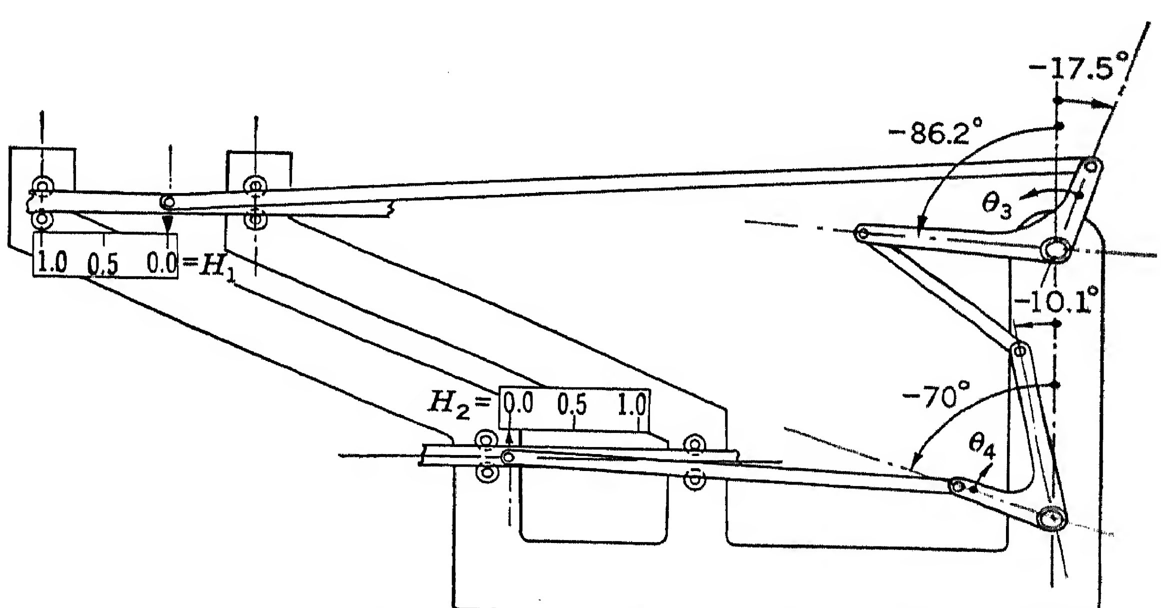

FIG. 6·15.—Completed linkage mechanizing $x_2 = \tan x_1$, $0 < x_1 < 80°$.

in the same sense; one possible method of connecting these components is indicated in Fig. 6·14. This completes the preliminary representation of the linkage combination.

Finally, one must convert the preliminary representation into a practical design without changing the essential relations of the components. One possible arrangement of this tangent linkage is shown in Fig. 6·15. The three-bar-linkage component is rotated through 90° from its position in Fig. 6·14, largely to gain clarity in the representation. The output crank of the three-bar linkage and the crank of the output transformer are made to rotate together as arms of the same bell crank. In order to use the same type of connection between the input transformer and the three-bar linkage, we must reverse the sense of rotation of one or the other of these cranks. This can be done by reflecting the input transformer and its associated scales in a vertical line. The two cranks can then be joined into a bell crank, and the linkage appears as in Fig. 6·15.

THREE-BAR LINKAGES IN SERIES

It is not desirable to use harmonic transformers in a computer in which all variables are represented by shaft rotations since the linear motion of the input or output slides must then be transformed into a rotary motion by a rack and pinion; it is much better to take the rotary motion directly from a rotating terminal. This remains true even when the angular travel must later be increased since this can be accomplished by gears that permit a more compact design than the rack and pinion.

For such computers a single three-bar linkage is ideal, except that it does not permit generation of a sufficiently large class of functions to cover all practical cases. Systems of two or more three-bar linkages provide greater flexibility, together with the same satisfactory mechanical characteristics.

6·8. The Double Three-bar Linkage.—In a double three-bar linkage, such as that sketched in Fig. 6·16, the homogeneous input parameter θ_1 is transformed into an intermediate parameter θ_3 by the first three-bar linkage; this serves as the input to the second three-bar linkage, which generates the output parameter θ_2. In the operator symbolism,

$$(\theta_2|\theta_1) = (\theta_2|\theta_3) \cdot (\theta_3|\theta_1). \tag{56}$$

The three-bar-linkage operators are each characterized by five constants, $(\Delta X_1, \Delta X_3, b_{11}, b_{21}, a_1)$ and $(\Delta X_3, \Delta X_2, b_{12}, b_{22}, a_2)$, respectively. Since the linkages must have a common value of the constant ΔX_3, the number of disposable constants in the combination is nine. The design problem is to choose operators $(\theta_2|\theta_3)$ and $(\theta_3|\theta_1)$ such that their product $(\theta_2|\theta_1)$ approximates as closely as possible to the given function

$$h_2 = (h_2|h_1) \cdot h_1 \tag{57}$$

on direct or complementary identification of the variables θ_1, θ_2 with the variables h_1, h_2.

Formally this problem resembles closely that of designing a double harmonic transformer, and the general approach to it is the same. For instance, one can apply the method of successive approximations described in Sec. 4·13. In each stage of the procedure one must then fit a three-bar-linkage function of specified ΔX_3 to a known function by an application of the nomographic or geometric method. Aside from this increase in manipulative difficulties, the principal difference between this problem and the earlier one lies in the first step, in which one must make an initial

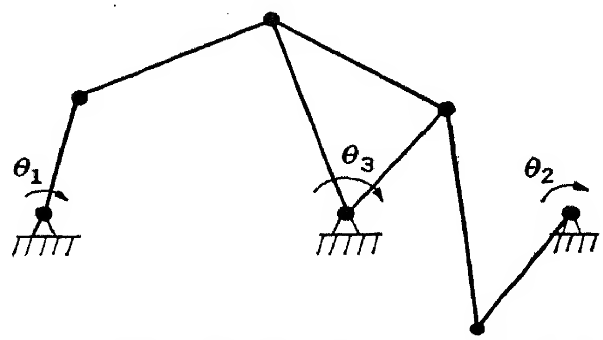

FIG. 6·16.—Double three-bar linkage.

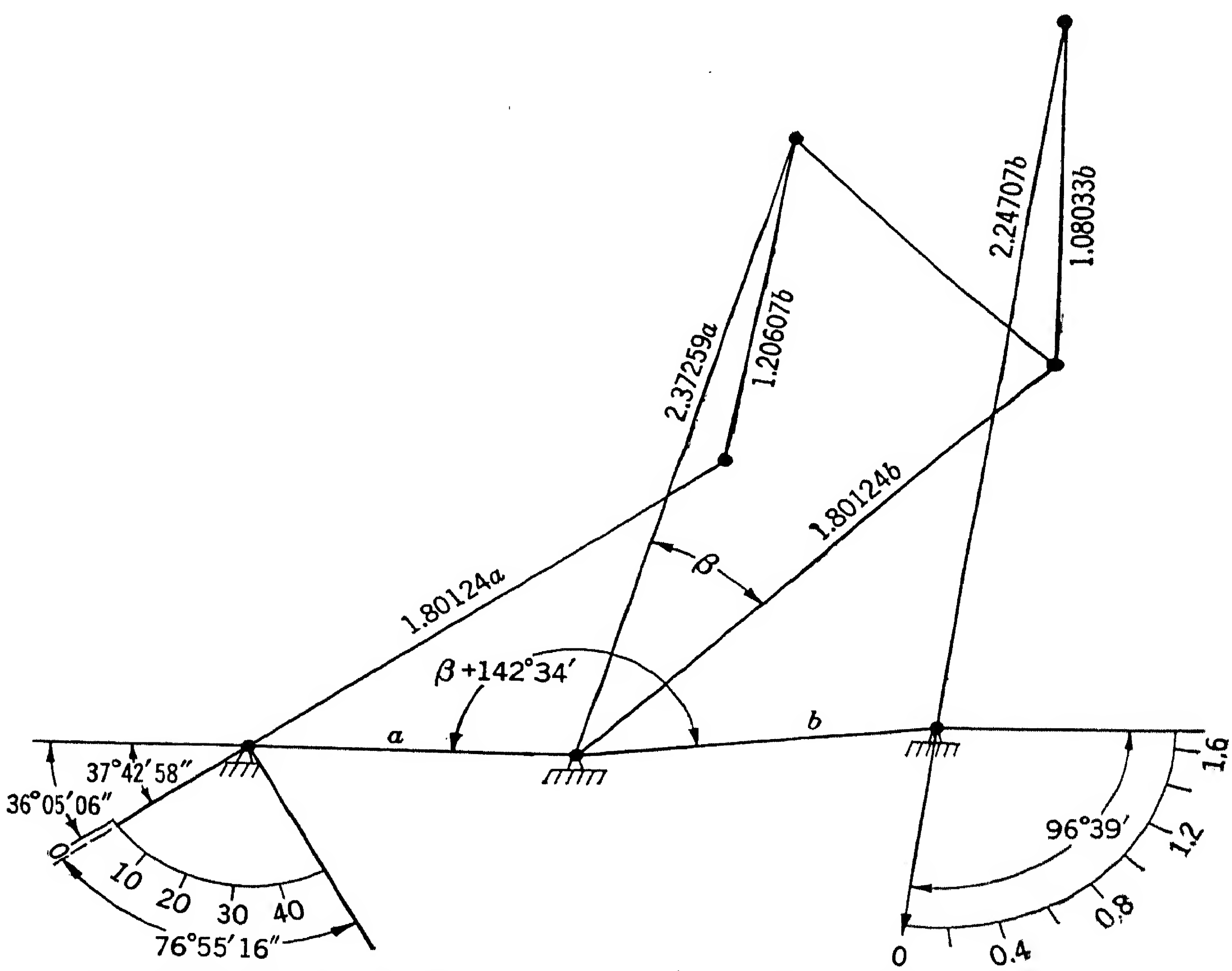

FIG. 6·17.—Constants of a double three-bar linkage mechanizing the logarithmic relation for $1 < x < 50$.

choice of one of the factor operators. It is to be noted that this choice fixes a value of ΔX_3 which will be used throughout the design procedure.

One can begin by using an operator $(\theta_1|\theta_3)$, for example, which by itself gives a rough fit to the given operator; the second factor will then serve to make relatively small corrections. This procedure leads to the design of combinations of quite different linkages, such as that illustrated in Fig. 6·16.

A generally sounder procedure is to try to find a combination of more or less similar linkages which will make roughly equal contributions to the curvature of the generated function (cf. Fig. 6·17). An appropriate begin-

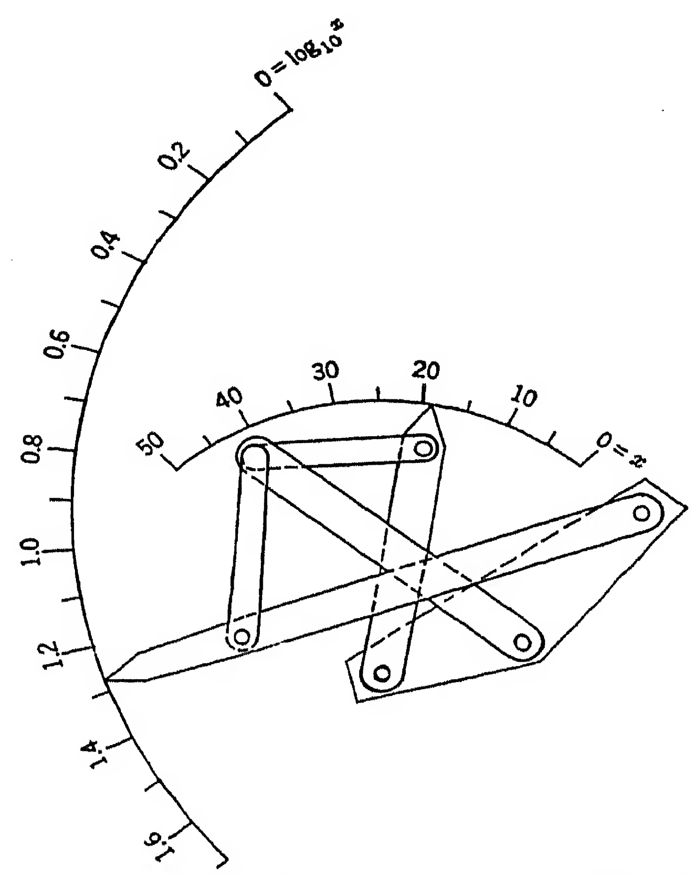

FIG. 6·18.—A possible physical form for the logarithmic linkage.

ning is then made by factoring the given operator into the product of two identical operators W:

$$(h_2|h_1) = W \cdot W = W^2. \tag{58}$$

The operator W, called "the square-root operator," has been discussed in Chap. 3, where it has been shown that it is not uniquely determined. If any one of the square-root operators can be mechanized by a three-bar linkage *with equal input and output travels*, then two of these linkages in series will generate the given function. If only an approximate mechanization of W can be found, the corresponding operator can at least serve as a first approximation to $(\theta_3|\theta_1)$, with which to begin application of the method of successive approximations.

An example of a linkage obtained by use of the square-root operator W is provided by a patented linkage[1] mechanizing the relation

$$x_2 = \log_{10} x_1, \qquad 1 \leqq x_1 \leqq 50, \tag{59}$$

with an error everywhere less than 0.003 of the output travel. In designing this, a three-bar linkage was used to mechanize, with good approximation, that one of the square-root operators W which has derivatives at the ends of the domain. Two such linkages in series gave a mechanization of the given function which was sufficiently good to permit immediate application of the methods of Chap. 7 in a final adjustment of the constants of the linkage combination. The final linkage is shown schematically in Fig. 6·17; the component linkages have similar, but not identical, constants. The angle β of the combination can be chosen at will. Figure 2·10 shows the linkage obtained on setting $\beta = -142° 34'$. A mechanically preferable form is that shown in Fig. 6·18, in which the two linkages share the intermediate crank:

$$\beta = 0 \qquad \text{and} \qquad 2.37259a = 1.80124b.$$

[1] A. Svoboda, U.S. Patent 2340350, Feb. 1, 1944.

CHAPTER 7

FINAL ADJUSTMENT OF LINKAGE CONSTANTS

7·1. Roles of Graphical and Numerical Methods in Linkage Design.—The preceding chapters have been concerned with methods for linkage design that are largely graphical, rather than numerical. Graphical methods are easily applied, and have the important virtue of making evident the character of the over-all fit to the given function, not merely the fit at a selected set of points. Their accuracy, however, is limited; when high accuracy is required, the final adjustment of linkage constants must be carried out by numerical methods because these alone permit sufficiently careful adjustment of the constants and sufficiently accurate evaluation of the performance of the linkage.

Numerical methods, on the other hand, tend to be excessively complex, except when they relate to changes in linkage constants so small that one can assume that the error function depends linearly on each of these changes. Graphical methods are thus very important in making it possible to find, quickly and easily, a linkage with constants which need to be changed only a little to bring its structural errors within the specified tolerances of the problem; it is only at this point that numerical methods become effective and convenient.

In general, then, graphical methods are desirable for the first stages of linkage design, which must yield a linkage with small error over the whole range of travel. The error can then be further reduced by numerical methods; often it can be made to vanish at several selected points. This was, for instance, the method employed in Secs. 4·7 and 4·15.

The present chapter will provide a general discussion, for linkages with one degree of freedom, of the problem of making final adjustments of all disposable constants of a linkage. It will be a basic assumption that the structural error at any point is nearly a linear function of each of the variations of constants to be considered. Thus the discussion will in most, but not all, cases apply only to small changes of the constants. Sometimes these methods are convenient even when an improved basic outline of the system is to be obtained by a substantial change in some constant. Such may be the case when the graphical method has been so applied that it does not establish a near optimum design within a whole class of linkages—for instance, when a combination of a three-bar linkage and harmonic transformers has been designed with frozen angular travels,

and one must consider the possibility of making fairly large changes in these travels.

The chapter will conclude with a discussion of a quite different method of reducing structural errors, which is particularly useful after the usual numerical methods have been applied: the introduction of small corrections by the eccentric linkage.

7·2. Gauging Parameters.—Let us consider the problem of checking the performance of a linkage designed to mechanize a given relation between variables x_1 and x_2:

$$x_2 = (x_2|x_1) \cdot x_1. \tag{1}$$

The linkage will generate a relation between an input parameter X_1 and an output parameter X_2:

$$X_2 = (X_2|X_1) \cdot X_1. \tag{2}$$

The form of the operator $(X_2|X_1)$ will depend upon dimensional constants of the linkage, the precise nature of which we need not specify. We denote these by $g_0, g_1, g_2, \ldots g_{n-4}$. At the input terminal there will be a linear scale which relates the values of the input variable and the input parameter:

$$X_1 = X_1^{(0)} + k_1(x_1 - x_1^{(0)}), \tag{3}$$

$X_1^{(0)}$ and $x_1^{(0)}$ being corresponding values of these quantities. At the output terminal there will be a similar scale relating the output parameter to the actually generated (not the ideal) values of the output variable. Denoting by x_{2a} these actual output values of the mechanism, we have

$$X_2 = X_2^{(0)} + k_2(x_{2a} - x_{2a}^{(0)}), \tag{4}$$

$X_2^{(0)}$ and $X_{2a}^{(0)}$ again being corresponding values. The linkage and scales together generate a relation between x_1 and x_{2a}, which depends on the constants of the linkage and on the four additional constants, k_1, $X_1^{(0)}$, k_2, and $X_2^{(0)}$, which characterize the terminal scales. These latter constants we denote also by g_{n-3}, g_{n-2}, g_{n-1}, and g_n. We have then

$$x_{2a} = F(x_1, g_0, g_1, \cdots g_n), \tag{5}$$

a function of the input variable and $n + 1$ constants of the mechanism.

Perhaps the most obvious way to study the structural error of the mechanism is to compare the desired and the actually generated values of the output variable for a spectrum of values of the input variable,

$$x_1^{(0)}, x_1^{(1)}, \ldots x_1^{(r)}.$$

The corresponding spectrum of values of x_2 is determined by Eq. (1):

$$x_2^{(s)} = (x_2|x_1) \cdot x_1^{(s)}; \qquad s = 0, 1, \cdots r. \tag{6}$$

Similarly, Eqs. (2), (3), and (4) determine spectra of values of X_1, X_2, and x_{2a}. In particular,

$$x_{2a}^{(s)} = F(x_1^{(s)}, g_0, g_1, \cdots g_n); \qquad s = 0, 1, \cdots r. \tag{7}$$

The structural error, δx_2, of the mechanism has the spectrum

$$\delta x_2^{(s)} = x_{2a}^{(s)} - x_2^{(s)}; \qquad s = 0, 1, \cdots r. \tag{8}$$

The corrections which one would like to make in the output of the mechanism are the negative of these quantities.

In such a test a comparison of the ideal and the actually generated values of x_2 is used as a gauge of the precision of the linkage; we shall say that x_2 is used as the gauging parameter.

It is not at all necessary to use x_2 in the gauging process. In most cases this is not even desirable; it is better to use as a gauging parameter one of the dimensional constants of the linkage, $g_0, g_1 \ldots g_s$. Let us solve Eq. (7) for this gauging parameter, for instance g_0:

$$g_0 = G(x_1^{(s)}, x_{2a}^{(s)}, g_1, g_2, \cdots g_n). \tag{9}$$

If we substitute on the right any corresponding values of x_1 and x_{2a}, we shall compute always the same value of g_0—the actual value of this constant in the linkage considered. If, however, we use ideal values of x_2, $x_2^{(s)}$, instead of the actually generated values, $x_{2a}^{(s)}$, g_0 will not in general have a constant value, but instead a spectrum of values,

$$g_0^{(s)} = G(x_1^{(s)}, x_2^{(s)}, g_1, g_2, \cdots g_n); \qquad s = 0, 1, 2, \cdots r. \tag{10}$$

The difference between the actual value g_0 of the constant and the value $g_0^{(s)}$ which it would need to have to make the linkage exact at the point s we shall call the gauging error,

$$\delta g_0^{(s)} = g_0 - g_0^{(s)}, \qquad s = 0, 1, \cdots r. \tag{11}$$

Such quantities are useful as gauges of the precision of linkages, although they do not give directly the error at the output. A wisely chosen gauging parameter is usually simpler to calculate and easier to interpret (at least as regards desirable changes in the constants) than is the error at the output; in particular, if $\delta g_0^{(s)}$ is independent of s it is only necessary to reduce g_0 by this amount to make the linkage exact. That the proof of perfect performance of the linkage is reduced to demonstration of the constancy of the results of a series of computations is also of value for the avoidance of computational errors.

7·3. Use of the Gauging Parameter in Adjusting Linkage Constants.—In the preceding chapters we have seen how to design linkages with small gauging errors. It may still be desirable to improve these linkages by making small variations in the dimensional constants $g_0, g_1, g_2, \cdots g_n$.

A perfect linkage will be obtained if values of $g_1, \cdots g_n$, can be found such that $g_0^{(s)}$ as computed by Eq. (10) is the same for all possible sets of values $(x_1^{(s)}, x_2^{(s)})$. In general, one can at best hope to make g_0 constant at a preassigned set of points equal in number to the independent constants of the linkage and thus to obtain a linkage which generates the given function exactly at these points.

If the dimensional constants are changed by amounts Δg_i, becoming

$$g_i' = g_i + \Delta g_i, \qquad i = 0, 1, \cdots n, \tag{12}$$

the gauging parameter will have the spectrum of values

$$g_0'^{(s)} = G(x_1^{(s)}, x_2^{(s)}, g_1', g_2', \cdots g_n'), \tag{13}$$

and the gauging error will become

$$\delta g_0'^{(s)} = g_0' - g_0'^{(s)}, \qquad s = 0, 1, \cdots p. \tag{14}$$

Expanding Eq. (13) in a Taylor's series, we may write

$$g_0'^{(s)} = g_0^{(s)} + \Delta g_0^{(s)} = g_0^{(s)} + \sum_{i=1}^{n} \frac{\partial g_0^{(s)}}{\partial g_i} \Delta g_i + \frac{1}{2!} \sum_{i=1}^{n} \sum_{j=1}^{n} \frac{\partial^2 g_0^{(s)}}{\partial g_i \partial g_j} \cdot \Delta g_i \Delta g_j + \cdots, \tag{15}$$

the partial derivatives being evaluated at $(x_1^{(s)}, x_2^{(s)}, g_1, g_2, \cdots g_n)$. The gauging error can thus be written as

$$\delta g_0'^{(s)} = g_0 + \Delta g_0 - g_0^{(s)} \\ \sum_{i=1}^{n} \frac{\partial g_0^{(s)}}{\partial g_i} \Delta g_i - \frac{1}{2} \sum_{i=1}^{n} \sum_{j=1}^{n} \frac{\partial^2 g_0^{(s)}}{\partial g_i \partial g_j} \Delta g_i \Delta g_k - \cdots \tag{16}$$

It is desired to reduce this to zero at a chosen set of $p + 1$ precision points: $s = 0, 1, 2, \cdots p$.

The general solution of this problem is prohibitively difficult, and it is necessary to make an approximation which will be valid only if the required changes in the constants are sufficiently small. Terms in Eq. (16) of higher than the first order in the small quantities Δg_i will be neglected. Let

$$G_i^{(s)} = \frac{\partial g_0^{(s)}}{\partial g_i}, \qquad G_0^{(s)} = -1. \tag{17}$$

Then, by use of Eq. (11) one can rewrite Eqs. (16) thus:

$$\sum_{i=0}^{n} G_i^{(s)} \Delta g_i = \delta g_0^{(s)}; \qquad s = 0, 1, \cdots p. \tag{18}$$

A set of Δg_i's which solve these equations will serve as corrections to the originally chosen g_i, as indicated in Eq. (12), under restrictions which must be discussed.

One can solve this system of linear equations for the Δg_i if the ranks of the matrix of coefficients $[G_i^{(s)}]$ and the augmented matrix ($[G_i^{(s)}]$ with the added column $\delta g_0^{(s)}$) are equal. In less precise but more direct terms, the equations will usually be soluble if and only if the number of independent constants characterizing the generated function is equal to or greater than the number of equations, $p + 1$. It would be natural to infer from this statement that the linkage can be made to generate a given function exactly at m arbitrarily chosen points whenever the generated function is characterized by m mathematically independent constants, $(m \leqq n + 1)$. In practice it will be found that this is not the case; the number of precision points which can be obtained depends upon the nature of the linkage and the given function, and on the way in which the precision points are chosen. Even when the linkage under consideration is well adapted to generation of the given function one must often be content to fix fewer than m precision points, or to use other methods of reducing the error.

This difference between the mathematical problem of solving Eqs. (18) and the practical problem of finding a linkage with $p + 1$ precision points arises from the fact that Eqs. (18) are mathematical approximations valid only for sufficiently small Δg_i. For practical purposes *one must not only solve Eqs. (18), but must solve them with Δg_i which are so small that the quadratic terms in Eqs.* (16) *are negligible.* We have seen in Sec. 6·6 (see Table 6·6) how different may be the expected and the actual performance of a linkage designed by using approximate linear equations very similar to Eqs. (18), when the Δg_i are so large that neglected terms are important.

Difficulties are most likely to arise in the straightforward application of Eqs. (18) when the restriction to small Δg_i has, for practical purposes, the effect of establishing a relation between mathematically independent parameters.

To simplify the discussion of this point we shall assume that the parameters $g_i (i = 0, 1, \cdots n)$ which occur in this equation are all independent of each other. One can then attempt to fix $n + 1$ precision points, determining the Δg_i by solving $n + 1$ of Eqs. (18). Because of the independence of the parameters, the determinant of the coefficients $G_i^{(s)}$ will not vanish; the solution for the Δg_i will be uniquely expressible as a fraction in which the numerator is the determinant $|G_i^{(s)}|$ with one column replaced by the column of coefficients $\delta g_0^{(s)}$, and the denominator is the determinant $|G_i^{(s)}|$ itself. The smaller the gauging errors $\delta g_0^{(s)}$ the smaller will be the Δg_i. However, even when the $\delta g_0^{(s)}$ are very small it may be

found that the Δg_i are large and that the linkage with constants given by Eq. (18) does not have the desired precision points, or even an improved performance. This happens most frequently when the determinant $|G_i^{(s)}|$, although not exactly zero (as it would be if there were an exact relation between the parameters), is very small. In such cases one can make large and properly related changes in the parameters which produce only a small net change in the generated function. For instance, as illustrated below, it may be possible to make large changes in two parameters, g_i and g_j, which will change the generated function very little if g_i/g_j is held constant. When one restricts attention to small changes in the parameters the generated function then depends, in effect, on a smaller number of parameters; in our example it would depend, not on g_i and g_j individually, but only on g_i/g_j. Thus the number of effectively independent parameters may be decreased by restricting considerations to small Δg_i, and with it the number of precision points which one can hope to establish.

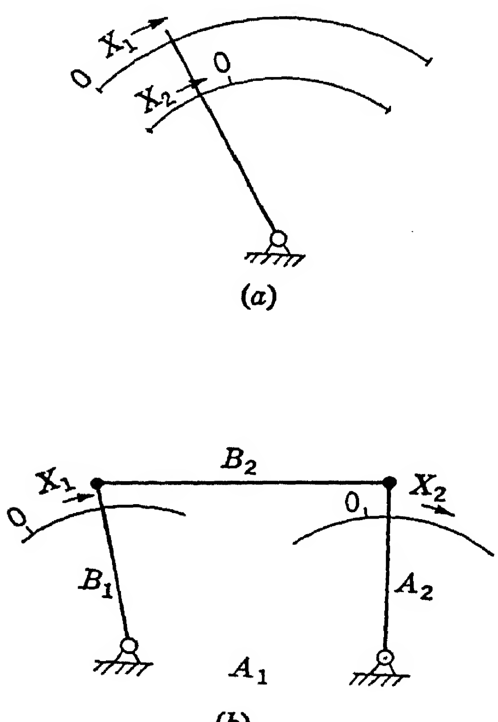

FIG. 7·1.—(*a*) Mechanization of a linear function. (*b*) Mechanization of an almost linear function.

An almost trivial example is illustrated by Fig. 7·1. A single pivoted arm (Fig. 7·1*a*) can be used in the generation of linear functions. The mechanism itself involves no adjustable constant. The input scale is characterized by the two parameters k_1 and $X_1^{(0)}$, the output scale by the two parameters k_2 and $X_2^{(0)}$. The generated linear function is characterized by only two independent constants; equal changes in $X_1^{(0)}$ and $X_2^{(0)}$ or proportional changes of all four variables do not produce any change in the generated function. In using such a device as a mechanization of an almost linear function one cannot in general reduce the error to zero at more than two preassigned points. Now consider the three-bar linkage in Fig. 7·1*b*. It is almost a parallelogram linkage, and generates an almost linear relation between x_1 and x_2—one which is characterized by seven mathematically independent parameters. The determinant $|G_i^{(s)}|$, with seven rows and columns, will not vanish; it will, however, be very small, and vanish as the parallelogram condition, $B_1 = A_2$, $B_2 = A_1$, is attained. It is obvious that equal changes of $X_1^{(0)}$ and $X_2^{(0)}$ will produce very small changes in the generated function, and that proportional changes of k_1, k_2, $X_1^{(0)}$ and $X_2^{(0)}$ will have a similarly small effect. Conversely, certain small changes in the generated function will be obtainable only by making such

large changes in these parameters that the linear theory will not apply. If we exclude large Δg_i from consideration there are in effect two fewer degrees of freedom than one might expect; an attempt to establish seven precision points will be likely to fail, although five should be obtainable if the initial fit is good. Such is usually the case with three-bar linkages, which will receive more detailed discussion in Sec. 7·7.

7·4. Small Variations of Dimensional Constants.—It is usually desirable to apply the approximate linear form of the gauging-parameter method, even when one must reduce the number of precision points in order to deal with small variations of the dimensional constants.

Let the number of independent dimensional constants be $n + 1$, and the number of specified precision points be k less than this. It is then possible to solve any $n + 1 - k$ independent equations from among Eqs. (18) for any $n + 1 - k$ of the Δg's, in terms of the other k of these quantities. For instance, solving for Δg_0, Δg_1, . . . Δg_{n-k}, in terms of Δg_{n-k+1}, . . . Δg_n, one obtains relations of the form

$$\left.\begin{aligned} \Delta g_0 &= C_{00} + C_{01}\Delta g_{n-k+1} + \cdots + C_{0k}\Delta g_n, \\ \Delta g_1 &= C_{10} + C_{11}\Delta g_{n-k+1} + \cdots + C_{1k}\Delta g_n, \\ &\cdots\cdots\cdots\cdots\cdots\cdots\cdots\cdots\cdots\cdots \\ \Delta g_{n-k} &= C_{n-k,0} + C_{n-k,1}\Delta g_{n-k+1} + \cdots + C_{n-k,k}\Delta g_n. \end{aligned}\right\} \tag{19}$$

Any set of *small* Δg's which satisfies Eqs. (19) will constitute a valid and practically useful solution of the given problem. Such a solution is not mathematically unique, but it will be effectively so if one is attempting to establish the maximum number of precision points subject to arbitrary choice.

7·5. Large Variations of Dimensional Constants.—By solution of Eqs. (18) one can determine a set of changes Δg_0, Δg_1, . . . Δg_n, in the dimensional constants which reduces to zero the first-order terms in the gauging error. Equations (16) become, exactly,

$$\delta g_0'^{(s)} = -\frac{1}{2}\sum_{i=1}^{n}\sum_{j=1}^{n}\frac{\partial^2 g_0^{(s)}}{\partial g_i \partial g_j}\Delta g_i \Delta g_j + \cdots, \qquad s = 0, 1, \cdots p. \tag{20}$$

When this gauging error is negligible we say that the Δg's are small; the problem has been solved in the first step. We turn now to the case in which $\delta g_0'^{(s)}$ is not negligible, but is adequately represented by the second-order terms written out in Eq. (20). In such cases the design problem is not satisfactorily solved by a first application of the method of Sec. 7·3, but it can often be solved by successive applications of the method, which produce successive improvements in the dimensional constants. We shall now see how the convergence of this process can be hastened.

Knowing the Δg's which solve Eqs. (18), and the gauging error $\delta g_0'^{(s)}$ after these corrections are made, one can easily compute also the gauging errors resulting when proportionally larger or smaller changes are made in the dimensional constants. Let a new set of corrected dimensional constants be given by

$$g_i''(\lambda) = g_i + \lambda\Delta g_i, \qquad i = 0, 1, \cdots p. \tag{21}$$

In the Taylor's series expansion for the gauging parameters, Eq. (15), the first-order terms are then changed by a factor λ, the second-order terms by a factor λ^2, and so on. The resulting gauging error is

$$\delta g_0''^{(s)} = g_0 - g_0^{(s)} + \lambda\Delta g_0 - \lambda\sum_{i=1}^{n} G_i^{(s)}\Delta g_i - \frac{1}{2}\lambda^2\sum_{i=1}^{n}\sum_{j=1}^{n}\frac{\partial^2 g_0^{(s)}}{\partial g_i\partial g_j}\Delta g_i\Delta g_j + \cdots, \tag{22}$$

or, by application of Eqs. (12), (18), and (20),

$$\delta g_0''^{(s)} = (1-\lambda)\delta g_0^{(s)} + \lambda^2\delta g_0'^{(s)}, \qquad s = 0, 1, \cdots p. \tag{23}$$

The validity of this expression of course depends on the possibility of neglecting higher-order terms in Eq. (20).

When $\lambda = 0$ the dimensional constants and gauging error have their uncorrected values. Increase in λ will reduce the gauging error $\delta g_0''^{(s)}$ so long as the quadratic term in Eq. (23) remains negligible. As λ approaches 1 the quadratic term will eventually (by our assumptions) become appreciable, and may even become very large. It is evident that one can obtain a smaller gauging error by applying a fraction of the correction indicated by the linear theory ($0 < \lambda < 1$) than by applying the whole correction ($\lambda = 1$). The more important the quadratic terms the smaller will this fraction be; it is, however, always possible to find some positive value of λ which gives a better set of constants than either $\lambda = 0$ or $\lambda = 1$.

In practice one begins with knowledge of $\delta g_0^{(s)}$, and computes the Δg's. As a check on the validity of the calculation one should then determine the values of $\delta g_0'^{(s)}$, usually by direct calculation [Eqs. (13) and (14)] rather than by use of Eqs. (20). If these quantities are not satisfactory small, one should make a smaller change in the g's; the appropriate value of λ can be determined by use of Eq. (23), λ being chosen to make the quantities $\delta g_0''^{(s)}$ as small as possible. The constants g_i'' computed by Eq. (21) will then serve as initial values for a second application of the method.

7·6. Method of Least Squares.—The designer's ultimate objective is to assure that the output error

$$\delta x_2 = x_{2a} - x_2 \tag{24}$$

shall be kept small throughout the domain of operation of the mechanism. One way to assure this is so to choose the dimensional constants of the mechanism, on which δx_2 depends, as to minimize the integrated squared error,

$$I(g_0, g_1, g_2, \cdots g_n) = \int (\delta x_2)^2 \, dx_2, \tag{25}$$

or the corresponding sum over a discrete spectrum of output values,

$$E\,(g_0, g_1, \cdots g_n) = \sum_r (\delta x_2^{(r)})^2. \tag{26}$$

Such conditions are most reasonable when accuracy is equally important for all values of the output variable, or all values of r. More generally, one should introduce a weighting function, $w(x_2)$ or $w(r)$, which increases with the importance of accuracy in the result at the corresponding x_2 or r. One will then so choose the g's as to minimize

$$I_w = \int [w(x_2)\; \delta x_2]^2 \, dx_2, \tag{27}$$

or

$$E_w = \sum_r [w(r)\; \delta x_2^{(r)}]^2, \tag{28}$$

subject to any other conditions which must be imposed on the dimensional constants.

Least-squares methods suitable for use in linkage problems have been developed by K. Levenburg.[1] It is, however, the opinion of the author that least-squares methods are relatively unrewarding. In particular, when the method depends on the use of an expansion in which only linear terms are retained there is always the danger that a result obtained after a large expenditure of labor may be invalidated by this approximation. In general the author prefers to set tolerances on the output error—tolerances which may vary with x_2 or r—and to apply the methods of the preceding sections to bring the actual structural errors within these tolerances.

7·7. Application of the Gauging-parameter Method to the Three-bar Linkage. *Formulation of the Equations.*—In applying the gauging-parameter method to three-bar linkage design we may choose the dimensional constants as follows:

[1] K. Levenburg, "A Method for the Solution of Certain Nonlinear Problems in Least Squares," *Quart. Appl. Math.*, **2**, 164 (1944).

$$\left.\begin{aligned} g_0 &= \left(\frac{B_2}{A_1}\right)^2, \\ g_1 &= \frac{B_1}{A_1}, \\ g_2 &= \frac{A_2}{A_1}, \\ g_3 &= X_1^{(0)}, \\ g_4 &= k_1, \\ g_5 &= X_2^{(0)}, \\ g_6 &= k_2. \end{aligned}\right\} \tag{29}$$

As gauging parameter we shall use g_0. In effect, we shall gauge the error of a design by computing the required length $B_2^{(s)}$ of the connecting bar as a function of the other dimensional constants and the variable pairs $(x_1^{(s)}, x_2^{(s)})$; we shall seek to make constant the related gauging parameter,

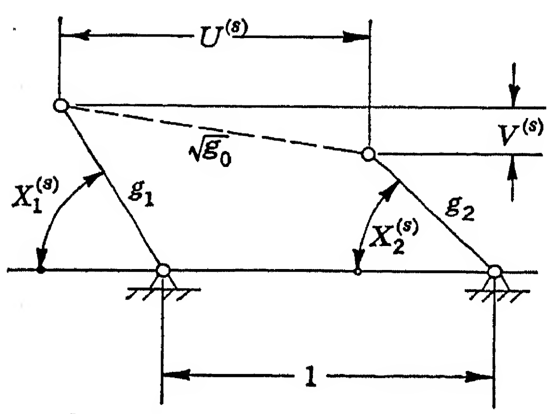

FIG. 7·2.—Three-bar linkage.

$$g_0^{(s)} = \left(\frac{B_2^{(s)}}{A_1}\right)^2. \tag{30}$$

A spectrum of values of x_1 can be chosen according to some arbitrary rule, symbolized by

$$x_1^{(s)} = (x_1^{(s)}|s) \cdot s. \tag{31}$$

The spectrum of x_2 is then determined:

$$x_2^{(s)} = (x_2|x_1) \cdot x_1^{(s)}. \tag{32}$$

Equations (3) and (4) become

$$X_1^{(s)} = g_3 + g_4(x_1^{(s)} - x_1^{(0)}) \tag{33}$$
$$X_2^{(s)} = g_5 + g_6(x_2^{(s)} - x_2^{(0)}). \tag{34}$$

Let the horizontal separation of the ends of the connecting bar, in terms of the unit A_1, be $U^{(s)}$, and the vertical separation, in the same units, be $V^{(s)}$. Then by the geometry of the linkage (Fig. 7·2) we have

$$U^{(s)} = 1 + g_1 \cos X_1^{(s)} - g_2 \cos X_2^{(s)}, \tag{35}$$
$$V^{(s)} = g_1 \sin X_1^{(s)} - g_2 \cos X_2^{(s)}, \tag{36}$$
$$g_0^{(s)} = (U^{(s)})^2 + (V^{(s)})^2. \tag{37}$$

An equation of the form of Eq. (9) could be obtained by eliminating from Eqs. (33) to (37) the quantities $X_1^{(s)}$, $X_2^{(s)}$, $U^{(s)}$, and $V^{(s)}$. This, however, is not necessary for our purposes.

The partial derivatives

$$G_i^{(s)} = \frac{\partial g_0^{(s)}}{\partial g_i} \tag{38}$$

will now be given in a form suitable for numerical calculation:

$$G_0^{(s)} = -1 = Q_0^{(s)} \tag{39}$$
$$\tfrac{1}{2} G_1^{(s)} = V^{(s)} \sin X_1^{(s)} + U^{(s)} \cos X_1^{(s)} = Q_1^{(s)} \tag{40}$$
$$-\tfrac{1}{2} G_2^{(s)} = V^{(s)} \sin X_2^{(s)} + U^{(s)} \cos X_2^{(s)} = Q_2^{(s)} \tag{41}$$
$$\frac{1}{2g_1} G_3^{(s)} = V^{(s)} \cos X_1^{(s)} - U^{(s)} \sin X_1^{(s)} = Q_3^{(s)} \tag{42}$$
$$\frac{1}{2g_1} G_4^{(s)} = \frac{1}{2g_1} G_3^{(s)}(x_1^{(s)} - x_1^{(0)}) = Q_4^{(s)} \tag{43}$$
$$-\frac{1}{2g_2} G_5^{(s)} = V^{(s)} \cos X_2^{(s)} - U^{(s)} \sin X_2^{(s)} = Q_5^{(s)} \tag{44}$$
$$-\frac{1}{2g_2} G_6^{(s)} = \left(-\frac{1}{2g_2} G_5^{(s)}\right) \cdot (x_2^{(s)} - x_2^{(0)}) = Q_6^{(s)}. \tag{45}$$

It is to be remembered that all angles are expressed in radians, and that g_3, g_4, g_5, and g_6 must be interpreted correspondingly.

One can use the quantities $Q_i^{(s)}$ directly in the solution of Eqs. (18). On introduction of the quantities

$$\Delta q_i = \frac{G_i^{(s)}}{Q_i^{(s)}} \cdot \Delta g_i, \qquad i = 0, 1, \cdots n, \tag{46}$$

which are simply constant multiples of the Δg's, Eqs. (18) become

$$\sum_{i=0}^{n} Q_i^{(s)} \Delta q_i = \delta g_0^{(s)}, \qquad s = 0, 1, \cdots p. \tag{47}$$

Having solved Eqs. (47) for the Δq's, one can compute the Δg's by Eqs. (46).

7·8. Application of the Gauging-parameter Method to the Three-bar Linkage. *An Example.*—As an example of the gauging-parameter method we shall check and improve the logarithmic linkage designed by the geometric method in Sec. 5·19. This was intended to generate the relation

$$x_2 = \log_{10} x_1 \tag{48}$$

in the domain $1 \leq x_1 \leq 10$. The design constants established in Sec. 5·19 will be taken as

$$\left.\begin{aligned}
g_0 &= \left(\frac{B_2}{A_1}\right)^2 = 1.05500^2 = 1.11303,\\
g_1 &= \frac{B_1}{A_1} = 0.70700,\\
g_2 &= \frac{A_2}{A_1} = 0.55000,\\
g_3 &= X_1^{(0)} = 2.61798\ (= 150.000°),\\
g_4 &= k_1 = -0.10666\ (= -55.000°/9),\\
g_5 &= X_2^{(0)} = -2.03330\ (= -116.500°),\\
g_6 &= k_2 = 1.57079\ (= 90.000°).
\end{aligned}\right\} \tag{49}$$

All constants are given to the fifth decimal place, or a thousandth of a degree, since this number of digits will be carried through the further calculations.

We have first to choose a suitable spectrum of values for x_1. A uniform distribution of values in this spectrum would yield a relatively

TABLE 7·1.—CALCULATION OF $\delta g_0^{(s)}$

s	$x_1^{(s)} - x_1^{(0)}$	$X_1^{(s)}$ degrees	$\sin X_1^{(s)}$	$\cos X_1^{(s)}$	$x_2^{(s)} - x_2^{(0)}$	$X_2^{(s)}$ degrees
0	0.00000	150.000	0.50000	−0.86603	0.0	−116.50
1	0.25892	148.418	0.52371	−0.85189	0.1	−107.50
2	0.58489	146.426	0.55306	−0.83317	0.2	− 98.50
3	0.99526	143.917	0.58901	−0.80817	0.3	− 89.50
4	1.51189	140.761	0.63256	−0.77451	0.4	− 80.50
5	2.16228	136.786	0.68472	−0.72880	0.5	− 71.50
6	2.98107	131.782	0.74568	−0.66630	0.6	− 62.50
7	4.01187	125.483	0.81428	−0.58046	0.7	− 53.50
8	5.30957	117.552	0.88659	−0.46255	0.8	− 44.50
9	6.94328	107.569	0.95336	−0.30185	0.9	− 35.50
10	9.00000	95.000	0.99619	−0.08716	1.0	− 26.50

s	$\sin X_2^{(s)}$	$\cos X_2^{(s)}$	$V^{(s)}$	$U^{(s)}$	$g_0^{(s)}$	$\delta g_0^{(s)}$
0	−0.89493	−0.44620	0.84571	0.63313	1.11608	−0.00303
1	−0.95372	−0.30071	0.89481	0.56310	1.11777	−0.00474
2	−0.98902	−0.14781	0.93497	0.49224	1.11647	−0.00344
3	−0.99996	0.00873	0.96641	0.42382	1.11357	−0.00054
4	−0.98629	0.16505	0.98968	0.36164	1.11025	0.00278
5	−0.94832	0.31730	1.00567	0.31022	1.10761	0.00542
6	−0.88701	0.46175	1.01505	0.27496	1.10593	0.00710
7	−0.80386	0.59482	1.01782	0.26246	1.10484	0.00819
8	−0.70091	0.71325	1.01232	0.28069	1.10358	0.00945
9	−0.58070	0.81412	0.99341	0.33883	1.10167	0.01136
10	−0.44620	0.89493	0.94972	0.44617	1.10104	0.01199

poor check in the range of small x_1, where fractional errors tend to be greatest. It is better to choose a uniform distribution of spectral values for x_2; we shall take

$$\left.\begin{aligned} x_2^{(s)} &= 0.1s \\ x_1^{(s)} &= 10^{0.1s} \end{aligned}\right\} s = 0, 1, 2, \cdots 10. \tag{50}$$

The calculation of the gauging error of this linkage is shown in Table 7·1. The gauging parameter $g_0^{(s)}$ is constant to within one per cent; the required length of the connecting bar, $\sqrt{g_0}$, is constant to within one-

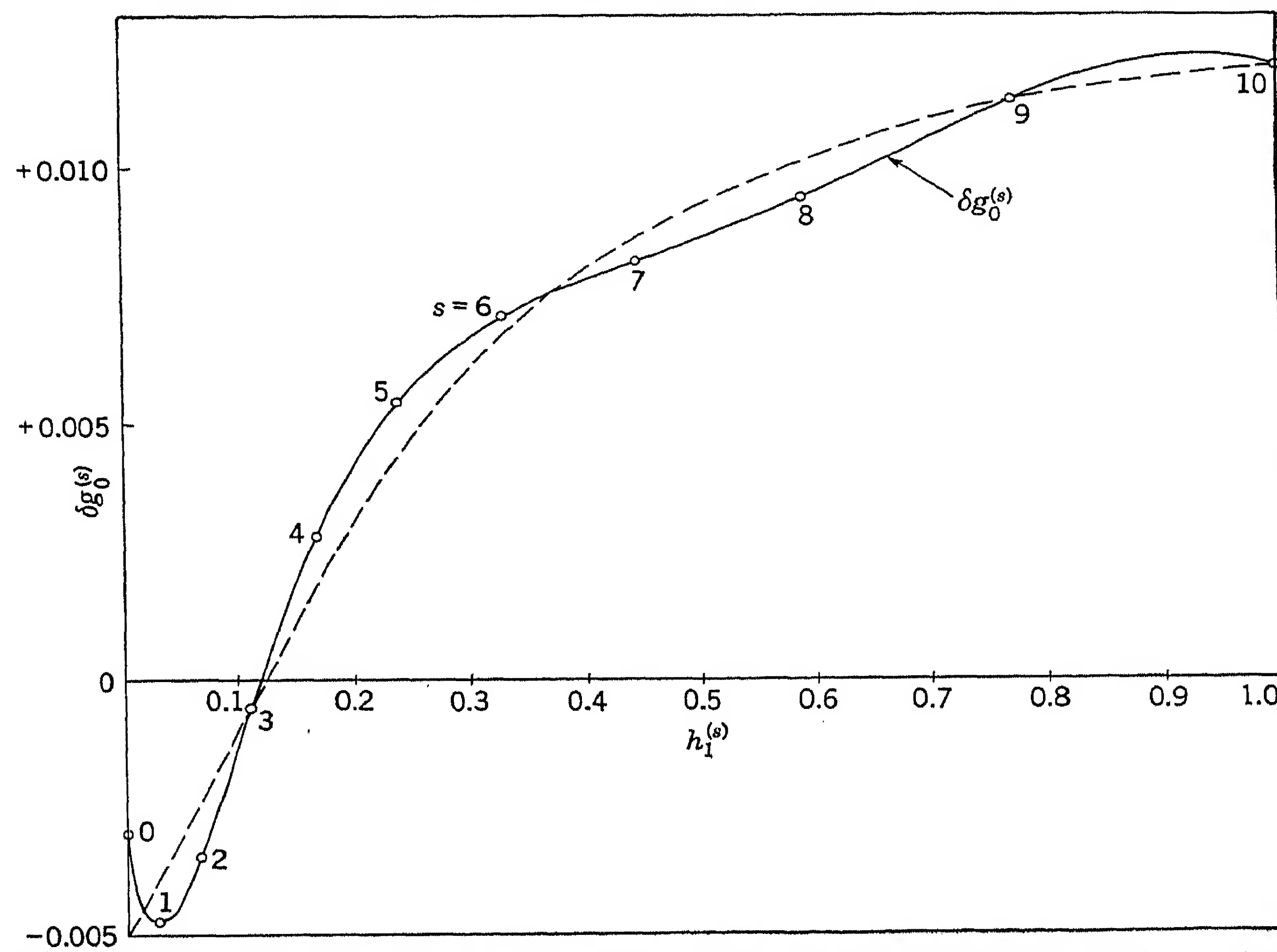

FIG. 7·3.—Gauging error in the first logarithmic linkage. Solid line, result of direct calculation. Dashed line, an approximation with slowly varying curvature.

half per cent. Figure 7·3 shows the gauging error $\delta g_0^{(s)}$ plotted against the homogeneous input variable $h_1^{(s)}$. The gauging error is not large, but it is evident that it can be made much smaller; this linkage has only one point of precision, whereas it should be possible to obtain five (Sec. 7·3).

We can proceed in the following way to make a reasonable choice of the points which are to be established as points of precision. Through the curve of $\delta g_0^{(s)}$ is drawn the dashed line of Fig. 7·3, which follows it closely but with minimum variation in curvature, intersecting it in five points. If we establish these points as points of precision, we will

be making a change in $\delta g_0^{(s)}$ which also has slowly varying curvature, and which must therefore approximate closely to the dashed curve; the residual gauging error should then be nearly equal to the vertical separation of the two curves in Fig. 7·3. For convenience, let us choose instead to establish points of precision at $s = 3$, 6, 9, and 10. The fifth point should lie between $s = 0$ and $s = 1$, and it would not be entirely satisfactory to take either of these as points of precision. Instead of taking $s = 0.5$ as the fifth point, we can obtain the same result by requiring that $s = 0$ shall be, not a point of precision, but a point where there is a predetermined error: $\delta g_0'^{(0)} = 0.0019$, as read from Fig. 7·3. That is, instead of solving Eqs. (18) or (47) with $\delta g_0^{(0)} = -0.0031$, which would make $s = 0$ a point of precision, we shall solve them with

$$\delta g_0^{(0)} = -0.0050.$$

We shall choose to solve Eq. (47). On calculation of the Q's by Eqs. (39) to (45), these equations take on the following form, for $s = 0$, 3, 6,9, 10, respectively:

$$\begin{aligned}
-1.00000\,\Delta q_0 &- 0.12545\,\Delta q_1 - 1.03935\,\Delta q_2 - 1.04898\,\Delta q_3 \\
&+ 0.00000\,\Delta q_4 + 0.18925\,\Delta q_5 + 0.00000\,\Delta q_6 = -0.00500, \\
-1.00000\,\Delta q_0 &+ 0.22671\,\Delta q_1 - 0.96267\,\Delta q_2 - 1.03066\,\Delta q_3 \\
&- 1.02577\,\Delta q_4 + 0.43224\,\Delta q_5 + 0.12967\,\Delta q_6 = -0.00054, \\
-1.00000\,\Delta q_0 &+ 0.57370\,\Delta q_1 - 0.77340\,\Delta q_2 - 0.88136\,\Delta q_3 \\
&- 2.62740\,\Delta q_4 + 0.71259\,\Delta q_5 + 0.42755\,\Delta q_6 = 0.00710, \\
-1.00000\,\Delta q_0 &+ 0.84480\,\Delta q_1 - 0.30102\,\Delta q_2 - 0.62289\,\Delta q_3 \\
&- 4.32490\,\Delta q_4 + 1.00551\,\Delta q_5 + 0.90496\,\Delta q_6 = 0.01136, \\
-1.00000\,\Delta q_0 &+ 0.90721\,\Delta q_1 - 0.02447\,\Delta q_2 - 0.52725\,\Delta q_3 \\
&- 4.74525\,\Delta q_4 + 1.04901\,\Delta q_5 + 1.04901\,\Delta q_6 = 0.01199.
\end{aligned} \tag{51}$$

Since there are here two fewer equations than there are variables, it is possible to fix two of the variables arbitrarily, subject only to the condition that all Δq's shall be small. On eliminating Δq_0, Δq_1, Δq_2, and Δq_3 from these equations we obtain

$$0.00294\,\Delta q_4 - 0.05528\,\Delta q_5 - 0.05390\,\Delta q_6 = 0.00229. \tag{52}$$

The coefficient of Δq_4 is small; Δq_4 can be chosen arbitrarily with little effect on the relation between Δq_5 and Δq_6. It is therefore reasonable to set

$$\Delta q_4 = 0. \tag{53}$$

We can then solve Eqs. (51) for each of the Δq's in terms of Δq_6, finding, for instance,

$$\begin{aligned}
\Delta q_3 &= 0.05486 - 0.85468\,\Delta q_6, \\
\Delta q_5 &= -0.04142 - 0.97503\,\Delta q_6.
\end{aligned} \tag{54}$$

If Δq_3 and Δq_5 are to be small, we must keep Δq_6 small, since its coefficients are large. The best value of Δq_6 is approximately zero; a positive value will increase the magnitude of Δq_5, a negative value that of Δq_3. We shall therefore choose

$$\Delta q_6 = 0, \tag{55}$$

and find in consequence

$$\left.\begin{aligned} \Delta q_0 &= -0.04512, \\ \Delta q_1 &= 0.04272, \\ \Delta q_2 &= -0.01985, \\ \Delta q_3 &= 0.05486, \\ \Delta q_5 &= -0.04142. \end{aligned}\right\} \tag{56}$$

By Eqs. (46),

$$\left.\begin{aligned} \Delta g_0 &= \Delta q_0 = -0.04512, \\ \Delta g_1 &= \tfrac{1}{2}\,\Delta q_1 = 0.02136, \\ \Delta g_2 &= -\tfrac{1}{2}\,\Delta q_2 = 0.00992, \\ \Delta g_3 &= \frac{1}{2g_1}\,\Delta q_3 = 0.03879, \\ \Delta g_4 &= +\frac{1}{2g_1}\,\Delta q_4 = 0, \\ \Delta g_5 &= -\frac{1}{2g_2}\,\Delta q_5 = 0.03765, \\ \Delta g_6 &= -\frac{1}{2g_2}\,\Delta q_6 = 0. \end{aligned}\right\} \tag{57}$$

Finally, by Eq. (12),

$$\left.\begin{aligned} g_0' &= 1.06791, \\ g_1' &= 0.72836, \\ g_2' &= 0.55992, \\ g_3' &= 2.65677\ (= 152.222^\circ), \\ g_4' &= -0.10666, \\ g_5' &= -1.99565\ (= -114.342^\circ), \\ g_6' &= 1.57079. \end{aligned}\right\} \tag{58}$$

To check the performance of the linkage with the new constants g_i', we compute the new gauging error $\delta g_0'^{(s)}$. This is shown in Table 7·2, together with the values

$$(\delta g_0'^{(s)})_{\text{exp}} = \delta g_0^{(s)} - \sum_{i=0}^{6} Q_i^{(s)}\,\Delta q_i \tag{59}$$

predicted by a theory in which only first-order terms in the δq's are retained. The difference between these two quantities, denoted by $\gamma^{(s)}$, represents the neglected quadratic and higher terms [Eq. (20)]. Figure 7·4 shows these quantities graphically, $\gamma^{(s)}$ appearing as the vertical separation of the full and dashed lines.

TABLE 7·2.—CALCULATION OF $\delta g_0'^{(s)}$

s	$X_1^{(s)}$	$\sin X_1^{(s)}$	$\cos X_1^{(s)}$	$X_2^{(s)}$	$\sin X_2^{(s)}$	$\cos X_2^{(s)}$
0	152.222	0.46605	−0.88476	−114.342	−0.91110	−0.41218
1	150.640	0.49030	−0.87156	−105.342	−0.96436	−0.26458
2	148.648	0.52029	−0.85399	− 96.342	−0.99388	−0.11046
3	146.139	0.55718	−0.83039	− 87.342	−0.99892	0.04637
4	142.983	0.60205	−0.79846	− 78.342	−0.97937	0.20207
5	139.008	0.65595	−0.75480	− 69.342	−0.93570	0.35279
6	134.004	0.71929	−0.69471	− 60.342	−0.86899	0.49482
7	127.705	0.79117	−0.61160	− 51.342	−0.78089	0.62467
8	119.774	0.86799	−0.49658	− 42.342	−0.67355	0.73914
9	109.791	0.94093	−0.33859	− 33.342	−0.54964	0.83540
10	97.222	0.99207	−0.12571	− 24.342	−0.41218	0.91110

s	$V^{(s)}$	$U^{(s)}$	$g_0'^{(s)}$	$\delta g_0'^{(s)}$	$(\delta g_0'^{(s)})$ exp.	$\gamma^{(s)}$
0	0.84960	0.58636	1.06564	0.00227	0.00197	0.00030
1	0.89708	0.51333	1.06826	−0.00035	−0.00059	0.00024
2	0.93545	0.43984	1.06852	−0.00061	−0.00041	−0.00020
3	0.96514	0.36921	1.06781	0.00010	0.00000	0.00010
4	0.98688	0.30529	1.06713	0.00078	0.00083	−0.00005
5	1.00168	0.25270	1.06722	0.00069	0.00083	−0.00014
6	1.01047	0.21694	1.06811	−0.00020	0.00000	−0.00020
7	1.01349	0.20477	1.06909	−0.00118	−0.00101	−0.00017
8	1.00934	0.22445	1.06915	−0.00124	−0.00118	−0.00006
9	0.99309	0.28563	1.06781	0.00010	0.00000	0.00010
10	0.95337	0.39829	1.06755	0.00036	0.00000	0.00036

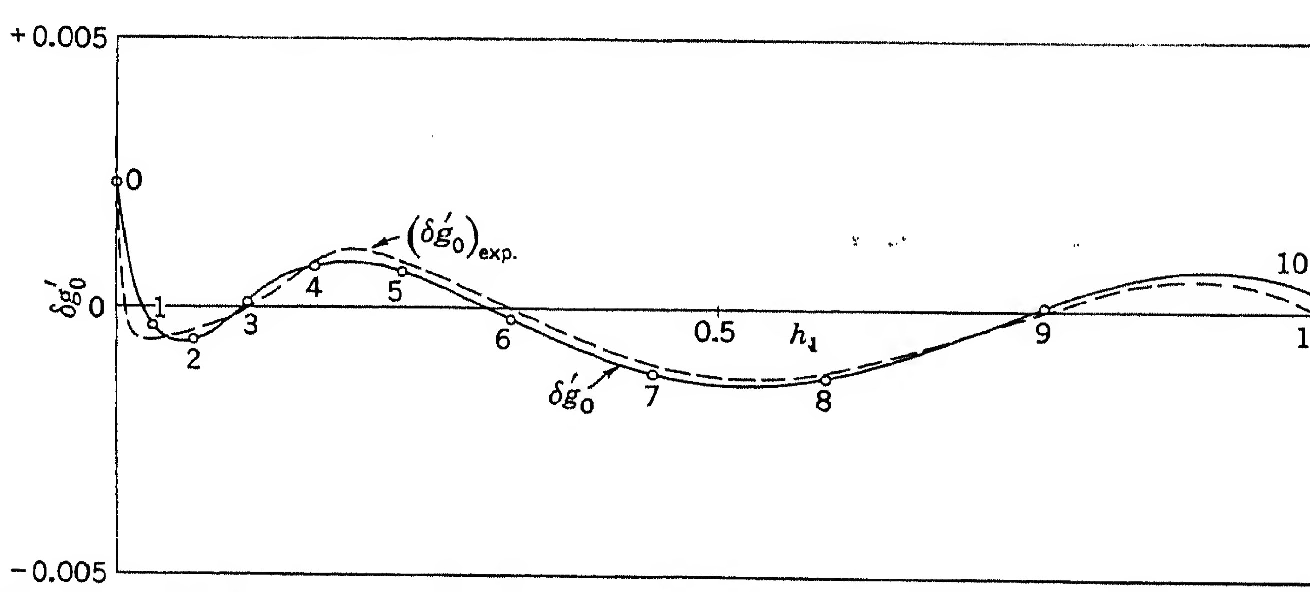

FIG. 7·4.—Gauging error in the first improved logarithmic linkage. Full line, result of exact computation. Dashed line, values expected on linear theory.

We have thus established precision points at positions shifted only slightly from those initially—and rather arbitrarily—selected. The result of this first calculation might very well be accepted as final. It is, on the other hand, easy enough to make a first-order correction for the effects of the quadratic and higher terms. We have only to replace $\delta g_0^{(s)}$ on the right-hand side of Eq. (51) by $\gamma^{(s)}$, and solve for new Δq's and Δg's to be added to those already obtained. As before, we choose arbitrarily $\Delta q_4 = \Delta q_6 = 0$. The second-order corrections to the g's are then found to be

$$\left.\begin{aligned} \Delta^2 g_0 &= 0.00246, \\ \Delta^2 g_1 &= -0.00170, \\ \Delta^2 g_2 &= -0.00130, \\ \Delta^2 g_3 &= -0.00292, \\ \Delta^2 g_4 &= 0.00000, \\ \Delta^2 g_5 &= -0.00328, \\ \Delta^2 g_6 &= 0.00000. \end{aligned}\right\} \tag{60}$$

The new and final constants of the linkage are

$$\left.\begin{aligned} g_0'' &= 1.07037, \\ g_1'' &= 0.72666, \\ g_2'' &= 0.55862, \\ g_3'' &= 2.65385\ (= 152.054°), \\ g_4'' &= -0.10666, \\ g_5'' &= -1.99893\ (= 114.530°), \\ g_6'' &= 1.57079. \end{aligned}\right\} \tag{61}$$

The final values of the gauging parameter and the gauging error are shown in Table 7·3, together with the resulting error in the homogeneous

TABLE 7·3.—CHARACTERISTICS OF THE SECOND IMPROVED LOGARITHMIC LINKAGE

s	$g_0''^{(s)}$	$\delta g_0''^{(s)}$	$-\dfrac{1}{2g_2Q_5^{(s)}}$	$\delta X_2''^{(s)}$, radians	$\delta X_2''^{(s)}$, degrees	δh_2
0	1.06846	0.00191	−4.7295	−0.00903	−0.517	−0.00574
1	1.07105	−0.00068	−3.3403	0.00227	0.130	0.00144
2	1.07123	−0.00086	−2.5673	0.00221	0.127	0.00141
3	1.07039	−0.00002	−2.0707	0.00004	0.002	0.00002
4	1.06958	0.00079	−1.7212	−0.00136	−0.078	−0.00087
5	1.06956	0.00081	−1.4594	−0.00118	−0.068	−0.00076
6	1.07035	0.00002	−1.2561	−0.00003	−0.002	−0.00002
7	1.07132	−0.00095	−1.0963	0.00104	0.060	0.00067
8	1.07149	−0.00112	−0.9742	0.00109	0.062	0.00069
9	1.07036	0.00001	−0.8902	−0.00001	0.000	0.00000
10	1.07042	−0.00005	−0.8532	0.00004	0.002	0.00002

output parameter, δh_2. To compute this we note that

$$\delta X_2^{\prime\prime(s)} \approx \left(\frac{\partial g_0^{(s)}}{\partial X_2^{(s)}}\right)^{-1} \delta g_0^{\prime\prime(s)}, \tag{62}$$

whence

$$\delta X_2^{\prime\prime(s)} = \frac{\delta g_0^{\prime\prime(s)}}{G_5^{(s)}} = -\frac{\delta g_0^{\prime\prime(s)}}{2Q_5^{(s)}}; \tag{63}$$

the conversion to terms of the homogeneous output variable is obvious. These results are also presented graphically in Fig. 7·5.

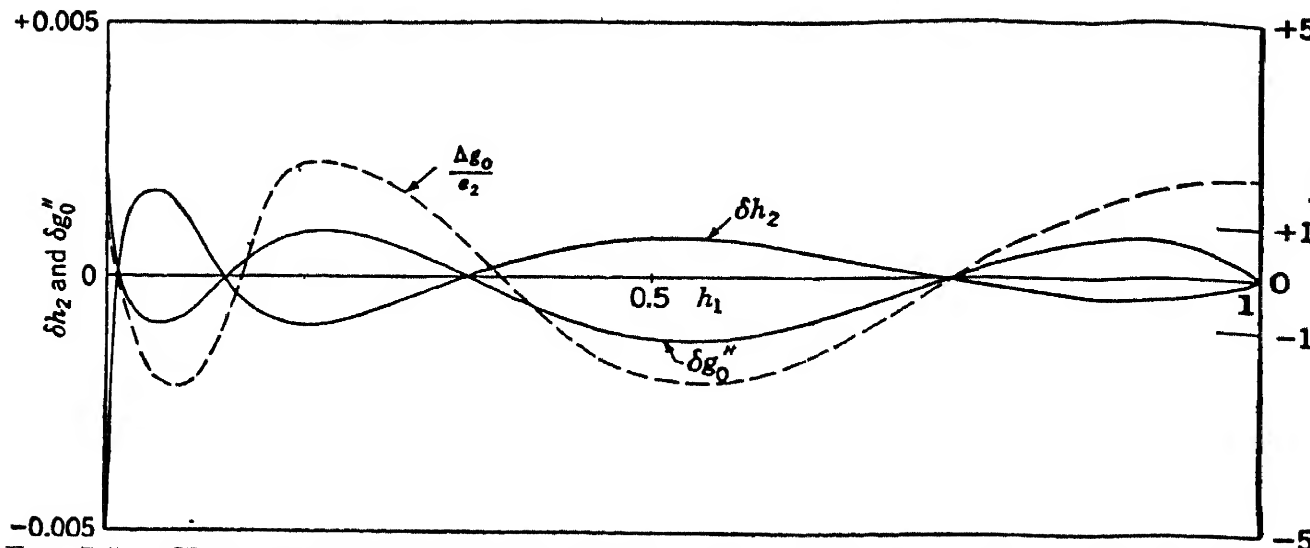

FIG. 7·5.—Characteristics of the second improved logarithmic linkage. The dashed line gives the form of a correction to be discussed in Sec. 7·9.

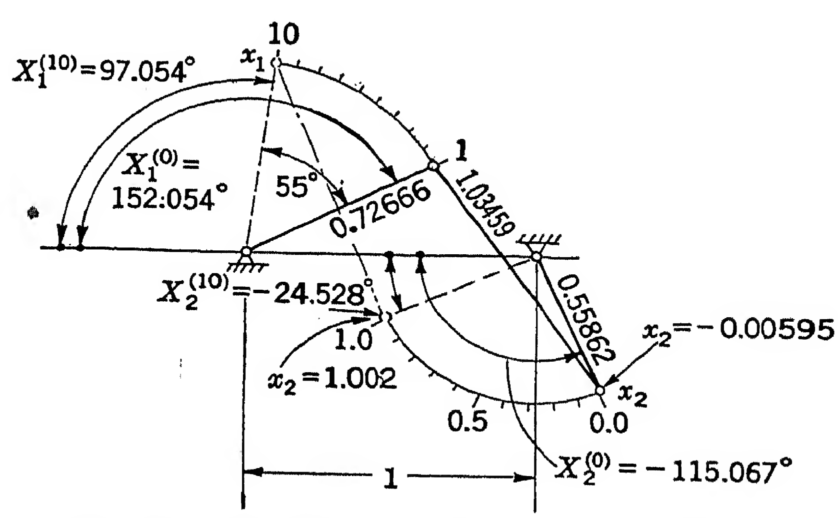

FIG. 7·6.—Second improved logarithmic linkage.

The linkage itself is outlined in Fig. 7·6. The constants g_0, g_1, and g_2 determine the lengths of the linkage arms, whereas g_3 and g_4 determine the nature of the input scale. The linkage is shown with the input arm at either end of this scale—that is, for $x_1 = 1$ and $x_1 = 10$. The output arm is shown in the corresponding positions required by the geometry of the linkage. Because of the structural error in the design, these posi-

tions do not coincide with the ends of the x_2 scale determined by g_5 and g_6; the scale readings are those shown in Fig. 7·6. (These have been determined by exact computation; hence one finds $x_2^{(0)} = h_2^{(0)} = -0.00595$ in Fig. 7·6, in contrast to the approximate value, -0.00574, in Table 7·3.)

7·9. The Eccentric Linkage as a Corrective Device.—When specified tolerances are very close it may not be possible to meet them by any choice of the parameters of such simple linkages as the three-bar linkage. Reduction of the structural error to tolerable limits then requires introduction of new adjustable parameters into the linkage. In many cases one can introduce small additional corrections by a superficial change

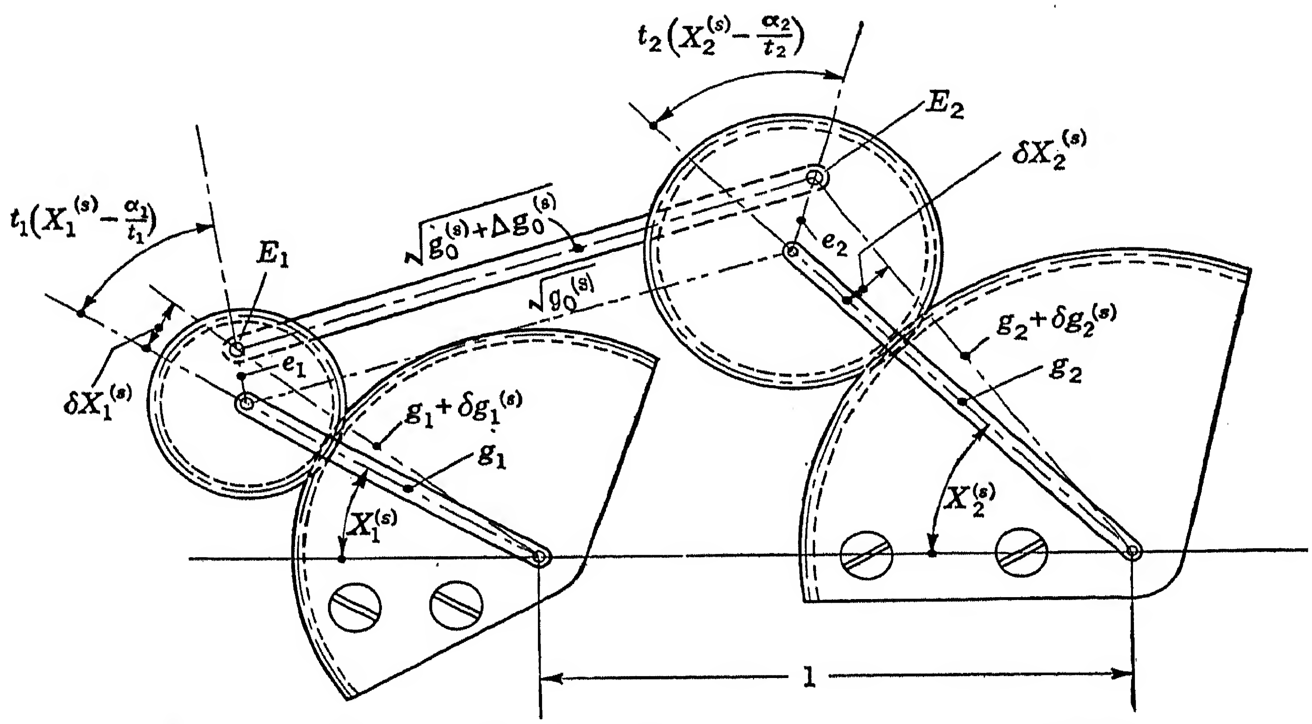

FIG. 7·7.—Three-bar linkage modified by a double eccentric linkage.

in the structure of the linkage. Replacement of an ideal harmonic transformer by a nonideal one is such a change; another is the introduction of eccentric linkages at the joints of three-bar linkages or harmonic transformers. These modifications in the structure are mechanically sound, and permit one to make use of all previous computations—an important economy in effort.

Figure 7·7 shows a three-bar linkage modified by the introduction of an eccentric linkage at either end of the connecting bar. The moving pivots of the input and output cranks carry planetary gears meshing with stationary gears. The connecting bar is not pivoted to the cranks, but to the eccentric pivots E_1 and E_2 on the planetary gears; the ends of the connecting link do not move with the pivots of the cranks, but about them in circles with radii e_1 and e_2—usually small. Thus the distance between the ends of the cranks is not a constant; in effect, g_0 can be made

to vary, as is required for more precise generation of the given functional relation.

Each eccentric linkage may be characterized by three constants: the tooth-ratio t of the stationary to the planetary gear, the eccentricity e of the planetary gear, and the angular position of the crank (denoted by $X_1 = \alpha/t$) for which the eccentric pivot lies on the center line of the crank, at a maximum distance from the frame pivot. The double eccentric linkage in Fig. 7·7 thus provides the designer with six additional parameters to adjust. Obviously, for greatest precision one should adjust all constants of the device simultaneously. Usually one can obtain very satisfactory results by accepting as fixed all constants determined in previous design work, varying only the constants of the eccentric linkages. Indeed it is often satisfactory to use only a single eccentric linkage, with consequent reduction to three in the number of constants to be adjusted.

To determine the constants of the eccentric linkage one can employ the gauging-parameter method in a somewhat modified form, valid so long as the eccentricity of the linkage is small.

In dealing with a modified three-bar linkage one can advantageously use the squared length of the connecting link, g_0, as the gauging parameter. Reference to Fig. 7·7 shows that introduction of the first eccentric linkage has the same effect on g_0 as a change $\delta g_1^{(s)}$ in the length of the input crank and a change $\delta X_1^{(s)}$ in its angular position, where

$$\delta g_1^{(s)} = e_1 \cos\,(t_1 X_1^{(s)} - \alpha_1), \tag{64a}$$

$$\delta X_1^{(s)} = \left(\frac{e_1}{g_1}\right) \sin\,(t_1 X_1^{(s)} - \alpha_1), \tag{64b}$$

to terms of the first order in the small quantity e_1. Similarly, introduction of the second eccentric linkage has the effect of changing g_2 and δX_2 by, respectively,

$$\delta g_2^{(s)} = e_2 \cos\,(t_2 X_2^{(s)} - \alpha_2), \tag{65a}$$

$$\delta X_2^{(s)} = \left(\frac{e_2}{g_2}\right) \sin\,(t_2 X_2^{(s)} - \alpha_2). \tag{65b}$$

The resulting change in the gauging parameter is

$$\Delta g_0^{(s)} = \frac{\partial g_0^{(s)}}{\partial g_1}\,\delta g_1^{(s)} + \frac{\partial g_0^{(s)}}{\partial X_1^{(s)}}\,\delta X_1^{(s)} + \frac{\partial g_0^{(s)}}{\partial g_2}\,\delta g_2^{(s)} + \frac{\partial X_0^{(s)}}{\partial X_2^{(s)}}\,\delta X_2^{(s)}, \tag{66}$$

or, by Eq. (38),

$$\Delta g_0^{(s)} = G_1^{(s)}\delta g_1^{(s)} + G_3^{(s)}\delta X_1^{(s)} + G_2^{(s)}\delta g_2^{(s)} + G_5^{(s)}\delta X_2^{(s)}. \tag{67}$$

It is thus the sum of four sinusoids multiplied by the slowly varying G's. Combining Eqs. (64), (65), and (67), one can write

$$\Delta g_0^{(s)} = e_1\left[(G_1^{(s)})^2 + \left(\frac{G_3^{(s)}}{g_1}\right)^2\right]^{\frac{1}{2}} \sin\left[t_1X_1^{(s)} - \alpha_1 + \tan^{-1}\left(\frac{g_1G_1^{(s)}}{G_3^{(s)}}\right)\right]$$
$$+ e_2\left[(G_2^{(s)})^2 + \left(\frac{G_5^{(s)}}{g_2}\right)^2\right]^{\frac{1}{2}} \sin\left[t_2X_2^{(s)} - \alpha_2 + \tan^{-1}\left(\frac{g_2G_2^{(s)}}{G_5^{(s)}}\right)\right]. \quad (68)$$

Here the contribution of each eccentric linkage to the gauging parameter is expressed as a sinusoid with adjustable frequency, amplitude, and phase constant, the second and third of these quantities being subject to slow variations of predetermined character. The difference in effect of eccentric linkages on the input and output cranks arises partly from differences in these variations, but principally from the fact that the argument of the sinusoid is in the first case a linear function of X_1, in the second case a linear function of X_2.

It is possible to use the additional flexibility provided by eccentric linkages to increase the number of precision points, if all constants of the device are adjusted simultaneously. When only the constants of the eccentric linkages are to be adjusted it is usually desirable to leave undisturbed the precision points already established. One can make $\Delta g_0^{(s)}$ vanish at five previously established precision points by adjustment of the five constants t_1, t_2, α_1, α_2, and e_2/e_1. Then $\Delta g_0^{(s)}$ will have the same zeros as the gauging error of the original three-bar linkage, and usually the same general form; by appropriate choice of the remaining constant, say e_1, one can give it roughly the same magnitude. The completed linkage will then have the same precision points as before, but smaller gauging errors. When a single eccentric linkage is to be used one can leave undisturbed only two precision points.

Example.—As an example, we shall further reduce the structural error of the logarithmic linkage of Fig. 7·6, using a single eccentric linkage. The design procedure is then extremely simple, but requires the exercise of some judgment if best results are to be obtained.

The error function of the original linkage, as shown in Fig. 7·6, has a generally sinusoidal character. The points of precision occur for

$$\begin{aligned} h_2^{(s)} &= 0.05,\ 0.3,\ 0.6,\ 0.9,\ 1.0, \\ h_1^{(s)} &= 0.0125,\ 0.1125,\ 0.3325,\ 0.772,\ 1.0. \end{aligned} \quad (69)$$

Except for the last, they are quite evenly spaced in X_2, but unevenly spaced in X_1; they have about the same distribution as the nulls in a sinusoid with argument linear in X_2. If a single eccentric linkage is to be used it should be placed on the output crank; it will then be possible to leave four, and not just two, of the points of precision essentially unchanged. We will have then, on introducing the Q's in place of the G's,

$$\Delta g_0^{(s)} = 2e_2[(Q_2^{(s)})^2 + (Q_5^{(s)})^2]^{\frac{1}{2}} \sin\left[t_2X_2^{(s)} - \alpha_2 + \tan^{-1}\left(\frac{Q_2^{(s)}}{Q_5^{(s)}}\right)\right]. \quad (70)$$

The nulls of this expression occur when

$$t_2X_2^{(s)} - \alpha_2 + \tan^{-1}\left(\frac{Q_2^{(s)}}{Q_5^{(s)}}\right) = n \cdot 180°. \tag{71}$$

Table 7·4 shows the values of $Q_2^{(s)}/Q_5^{(s)}$ at the previously established precision points, $s = 0.5, 3, 6, 9, 10$, and the values of $t_2X_2^{(s)} - \alpha_2$ required if these points are to be nulls of $\Delta g_0^{(s)}$; n has been assigned the values 0, 1, 2, 3, 4 at the successive nulls.

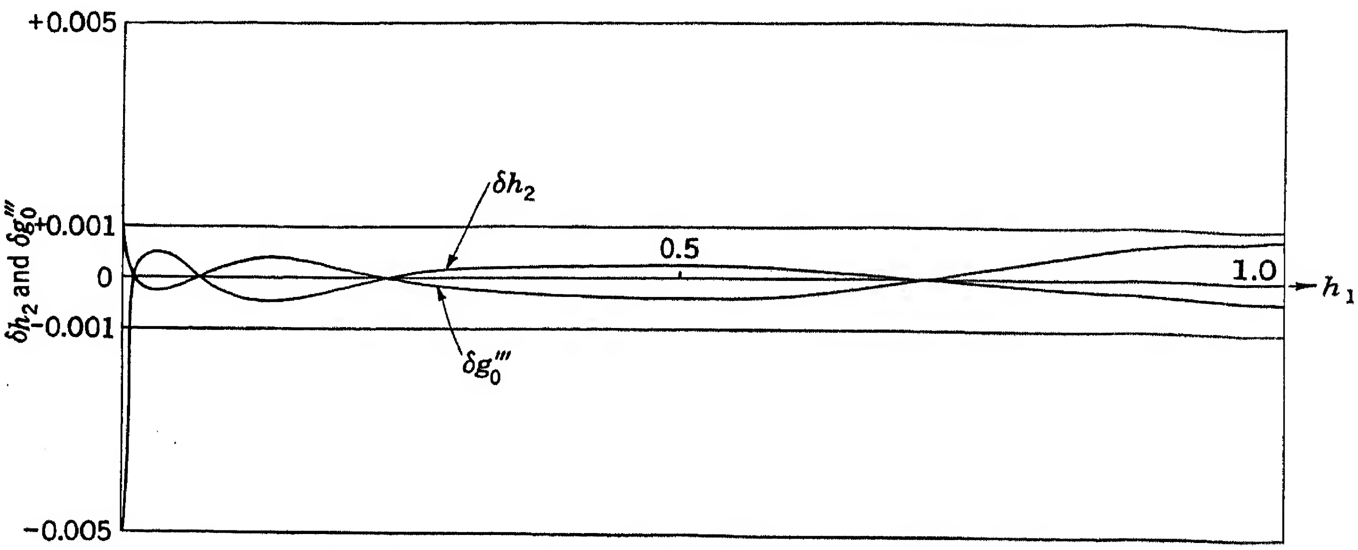

FIG. 7·8.—Structural error in the final logarithmic linkage.

TABLE 7·4.—VALUES OF $(t_2X_2^{(s)} - \alpha_2)$ REQUIRED FOR VANISHING OF $\Delta g_0^{(s)}$

s	$Q_2^{(s)}/Q_5^{(s)}$	$t_2X_2^{(s)} - \alpha_2$, degrees
0.5	−4.6543	77.9
3.0	−2.2272	245.8
6.0	−1.0853	407.3
9.0	−0.2994	556.7
10.0	−0.0233	721.3

Let us choose to retain the points $s = 0.5$ and $s = 9$ as points of precision. Taking the values of $X_2^{(s)}$ in Table 7·1 as sufficiently accurate, we then require

$$\left.\begin{aligned} t_2(-110°) - \alpha_2 &= 77.9°, \\ t_2(-33.5°) - \alpha_2 &= 556.7°, \end{aligned}\right\} \tag{72}$$

whence

$$\left.\begin{aligned} t_2 &= 6.26, \\ \alpha_2 &= -766.5°, \\ \frac{\alpha_2}{t_2} &= -122.4°. \end{aligned}\right\} \tag{73}$$

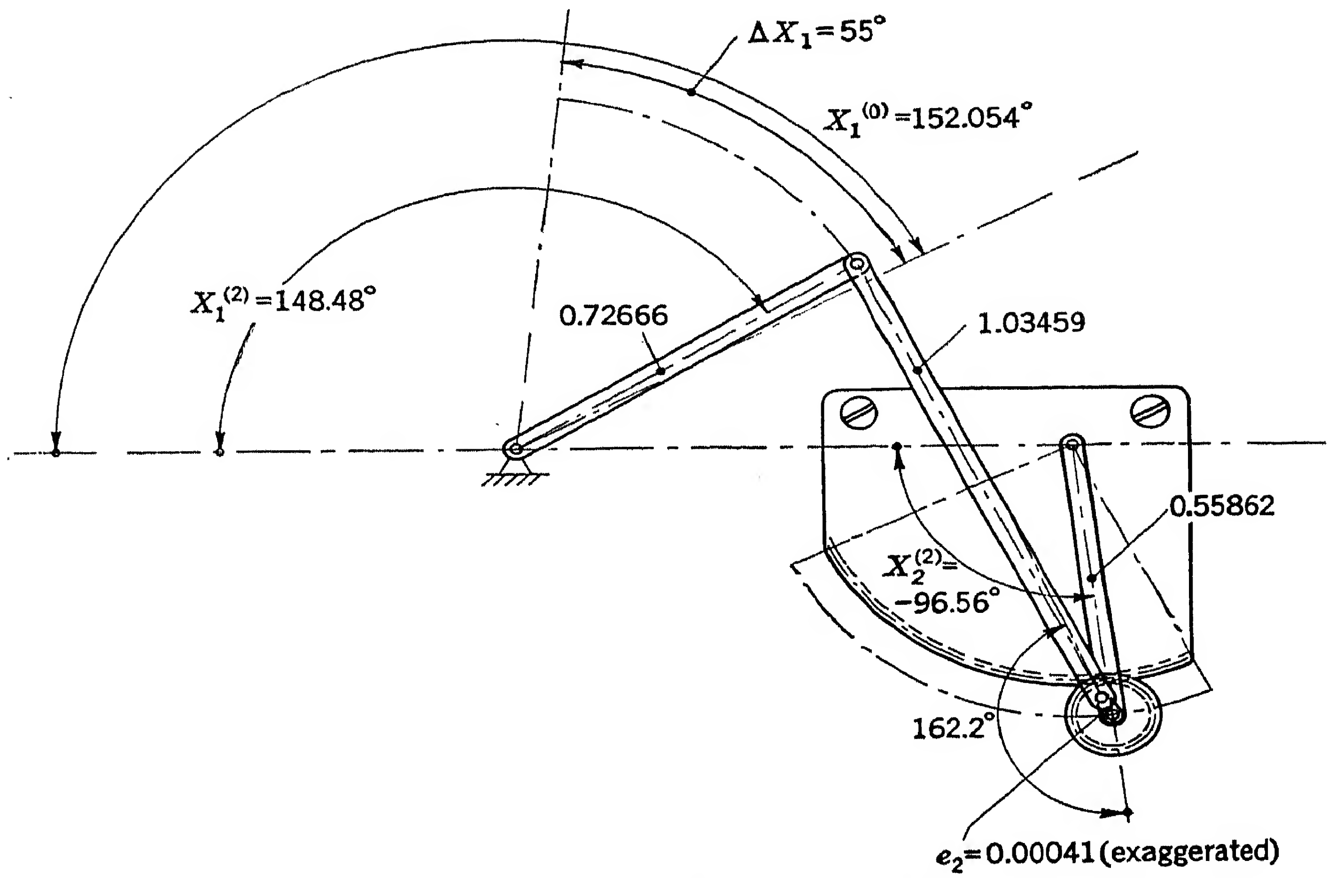

FIG. 7·9.—Final logarithmic linkage.

The corresponding values of $\Delta g_0^{(s)}/e_2$ are shown in Table 7·5, and are plotted (dashed curve) in Fig. 7·5. This curve has roughly the same form as the residual error $\delta g_0''^{(s)}$ of the linkage which is to be improved; inspection will show the $\Delta g_0^{(s)}$ gives about the best approximation to $\delta g_0''^{(s)}$ when

$$e_2 = 0.00041. \tag{74}$$

TABLE 7·5.—CALCULATION OF STRUCTURAL ERROR OF FINAL LOGARITHMIC LINKAGE

s	$\dfrac{\Delta g_0^{(s)}}{e_2}$	$\Delta g_0^{(s)}$	$\delta g_0'''^{(s)}$	δh_2
0	1.070	0.00042	0.00149	−0.00420
1	−1.066	−0.00042	−0.00026	0.00050
2	−2.113	−0.00084	−0.00002	0.00003
3	−0.975	−0.00039	0.00037	−0.00044
4	1.1845	0.00047	0.00032	−0.00032
5	2.0909	0.00084	−0.00003	0.00002
6	0.7207	0.00029	−0.00027	0.00019
7	−1.4760	−0.00059	−0.00036	0.00023
8	−1.9617	−0.00078	−0.00034	0.00019
9	−0.0107	−0.00004	0.00005	−0.00003
10	1.9882	0.00079	−0.00084	0.00041

The resulting values of $\Delta g_0^{(s)}$ and of the final gauging error

$$\delta g_0^{\prime\prime\prime(s)} = \delta g_0^{\prime\prime(s)} - \Delta g_0^{(s)} \tag{75}$$

are given in Table 7·5, together with the resulting error in the homogeneous output variable; the last two quantities are plotted in Fig. 7·8. The structural error remains less than 0.05 per cent except in the immediate neighborhood of $h_1 = h_2 = 0$, where it abruptly rises to 0.4 per cent.

The linkage is outlined in Fig. 7·9 in its configuration for $s = 2$, very near to one of its precision points.

CHAPTER 8

LINKAGES WITH TWO DEGREES OF FREEDOM

Functions of two independent variables are usually mechanized by three-dimensional cams (Fig. 1·24), which are expensive to manufacture, and rather bulky; they are, however, easy to design and have very wide application. Bar linkages with two degrees of freedom can also serve to mechanize functions of two independent variables. These linkages have the advantages of being flat and small, of giving smooth frictionless performance allowing appreciable feedback, and of being relatively inexpensive to manufacture in quantities. They are, on the other hand, relatively difficult to design, having always residual structural errors which must be brought within the specified tolerances. The mathematical design of these linkages will be treated in the remainder of this book. Basic concepts needed by the designer will be introduced in the present chapter. Succeeding chapters will show, partly by precept and partly by example, how to design linkage multipliers or dividers (Chap. 9) and linkage generators of more general functions of two independent variables (Chap. 10).

8·1. Analysis of the Design Problem.—Mechanisms with two degrees of freedom have at least one output parameter X_k functionally related to two input parameters X_i and X_j:

$$X_k = F(X_i, X_j). \tag{1}$$

If the domain of definition D of this relation is a rectangle,

$$X_{im} \leqq X_i \leqq X_{iM}, \qquad X_{jm} \leqq X_j \leqq X_{jM}, \tag{2}$$

the mechanism is said to be "regular."

To such a mechanism one may add functional scales that establish relations between the parameters X_i, X_j, X_k, and corresponding variables x_i, x_j, x_k, respectively. The mechanism will then serve to establish a functional relation

$$x_k = f(x_i, x_j) \tag{3}$$

between these variables; we may say that the device, mechanism plus scales, mechanizes Eq. (3). If this relation of the variables is to be single-valued, it is necessary that to definite values of the input variables there correspond definite values of the input parameters, and that to a definite value of the output parameter there corresponds a definite value

of the output variable. The scales must then establish relations of the form,

$$\left.\begin{aligned} X_i &= (X_i|x_i) \cdot x_i, \\ X_j &= (X_j|x_j) \cdot x_j, \\ x_k &= (x_k|X_k) \cdot X_k, \end{aligned}\right\} \tag{4}$$

where all three operators (but not necessarily their inverse operators) are single-valued. If Eqs. (4) are of linear form,

$$\left.\begin{aligned} X_i &= X_i^{(0)} + k_i(x_i - x_i^{(0)}), \\ X_j &= X_j^{(0)} + k_j(x_j - x_j^{(0)}), \\ x_k &= x_k^{(0)} + K_k(X_k - X_k^{(0)}), \end{aligned}\right\} \tag{5}$$

the device provides a "linear mechanization" of Eq. (3). When a mechanism is to be a component of a more complex computer, it is often, but not always, required to provide a linear mechanization of the relation between input and output variables.

Any mechanism generating a function F of two independent parameters may be represented schematically as in Fig. 8·1. This representation is sufficient in the case of three-dimensional cams, which can generate in one step, so to speak, any well-behaved function of two independent parameters. Simple bar linkages, on the other hand, can generate only a restricted class of functions; to mechanize a given relation between parameters one must usually build up a more complicated structure, a combination of one or more simple linkages of two degrees of freedom and several linkages of one degree of freedom. It is then necessary to consider the internal structure of the function generator F.

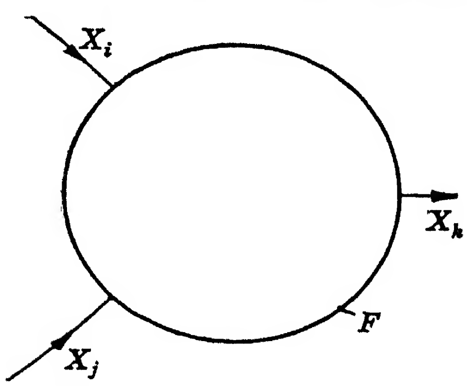

FIG. 8·1.—Schematic representation of mechanism generating a function X_k of two independent parameters, X_i and X_j.

Let G denote a simple bar linkage with two degrees of freedom, generating a function of two independent parameters,

$$Y_k = G(Y_i, Y_j), \tag{6}$$

of a restricted class. By combining such a linkage with three linkages having one degree of freedom, as shown schematically in Fig. 8·2, one can generate relations of a much wider class between parameters X_i, X_j, X_k. A more elaborate structure is that shown in Fig. 8·3, which consists of four linkages, each with two degrees of freedom, so connected as to make use of feedback. Theoretically, such structures make possible a further extension of the field of mechanizable functions. In practice it is usually sufficient to use the simpler structure of Fig. 8·2, to which we shall henceforth confine our attention.

We have then to consider structures consisting of a linkage with two degrees of freedom, which establishes a relation [Eq. (6)] between internal parameters Y_i, Y_j, Y_k, and three linkages of one degree of freedom, which relate the internal parameters to the corresponding external parameters X_i, X_j, X_k:

$$\left.\begin{aligned} Y_i &= (Y_i|X_i) \cdot X_i, \\ Y_j &= (Y_j|X_j) \cdot X_j, \\ X_k &= (X_k|Y_k) \cdot Y_k. \end{aligned}\right\} \tag{7}$$

Together, these establish a relation between the external parameters [Eq. (1)]; the functional scales, in turn, convert this into a relation [Eq. (3)] between variables x_i, x_j, x_k, which is to be made to approximate as closely as possible to some given relation, throughout a specified domain.

The linkage G, with two degrees of freedom, we shall call the "grid generator," for reasons which will become evident later. The linkages

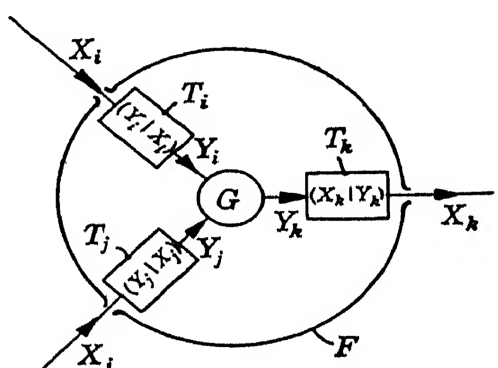

FIG. 8·2.—Combination of grid generator and transformer linkages.

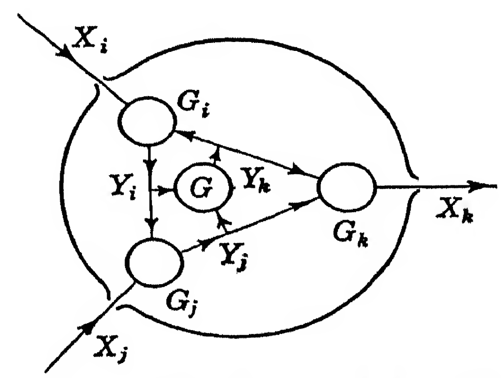

FIG. 8·3.—Feedback linkage with two degrees of freedom.

T_i, T_j, T_k, we shall call the "transformers," because they transform the internal parameters Y into the external parameters X. The division of a mechanism into a grid generator and transformers is to some extent arbitrary; the breakdown of a given functional relation [Eq. (1)] into a grid-generator relation [Eq. (6)] and transformer relations [Eq. (7)] is completely arbitrary. We shall therefore make use of the generalized term "grid generator for a given function" as denoting *any* linkage with two degrees of freedom which will serve as the linkage G in a mechanization of the given function.

Transformer linkages increase the field of linearly mechanizable functions, but not the field of functions mechanizable in the more general sense. A relation $x_k = f(x_i, x_j)$ mechanized by a grid generator [Eq. (6)], transformer linkages [Eq. (7)], and functional scales [Eq. (4)] can be mechanized also by associating the same grid generator directly with scales which establish relations

$$\left.\begin{aligned} Y_i &= (Y_i|X_i) \cdot (X_i|x_i) \cdot x_i = \phi_i(x_i), \\ Y_j &= (Y_j|X_j) \cdot (X_j|x_j) \cdot x_j = \phi_j(x_j), \\ x_k &= (x_k|X_k) \cdot (X_k|Y_k) \cdot Y_k = \phi_k(Y_k). \end{aligned}\right\} \tag{8}$$

Transformer linkages in a design thus serve only to change the form of the functional scales—usually to make them linear.

It is obvious that the choice of a grid generator is the central problem in the design of a linkage with two degrees of freedom. When a linear mechanization is desired, one can then proceed to design the transformer linkages by methods discussed in the preceding chapters; concerning this latter stage of the work, which offers no new theoretical problems, little more need be said. It is evident that a very simple grid generator may serve if the transformers are made sufficiently complex, whereas another choice of grid generator may make unnecessary the use of one or more transformers. It is important that the transformers not add too much to the complexity of the design; a good grid generator should be simple in structure, and also adapted to use with simple transformer linkages. For instance, we shall see that the common differential is a theoretically adequate grid generator for an important class of functions; its general use in linearly mechanizing these functions is, however, not to be recommended, since the required transformers tend to be excessively complex.

In practice one has available a relatively small number of types of linkage suitable for use as grid generators; the available grid-generator functions G belong to several restricted classes. Usually these will not include an exact grid-generator function for the given function; a structural error must be admitted in designing the grid generator. Structural errors must also be admitted in the design of the transformer linkages. Thus it is always important in designing such mechanisms to make a final adjustment of all available constants, in order to minimize the over-all structural error.

In summary, mechanization of a given function of two independent variables involves the following steps:

1. Choice of a suitable type of grid generator.
2. Selection of the constants of the grid generator.
3. Design of the transformer linkages.
4. Final adjustment of all constants of the mechanism.

The ideas to be developed in the remainder of this chapter are essential for the first of these steps; they also form a foundation for the procedures required in the second step, which will be described in later chapters.

8·2. Possible Grid Generators for a Given Function.—It is very easy to give a formal characterization of all functional relations which can be mechanized by use of a given grid generator. Combining Eqs. (6) and (8), we see that these are the relations which can be expressed as

$$x_k = f(x_i, x_j) = \phi_k\{G[\phi_i(x_i), \phi_j(x_j)]\}, \tag{9}$$

where G is the given grid-generator function and ϕ_i, ϕ_j, ϕ_k are arbitrary

single-valued functions of their arguments. Conversely, to mechanize a given functional relation

$$x_k = f(x_i, x_j) \tag{3}$$

one can employ a grid generator with parameters related by

$$Y_k = G(Y_i, Y_j) = \phi_k^{-1}\{f[\phi_i^{-1}(Y_i), \phi_j^{-1}(Y_j)]\}, \tag{10}$$

where ϕ_i^{-1}, ϕ_j^{-1}, ϕ_k^{-1} are the inverse of arbitrary single-valued functions ϕ_i, ϕ_j, ϕ_k.

The relations expressed in Eqs. (9) and (10) can also be expressed in terms of contour lines of the functions f and G. Let us plot contours of constant $Y_k = G(Y_i, Y_j)$ in the (Y_i, Y_j)-plane and label them with the cor-

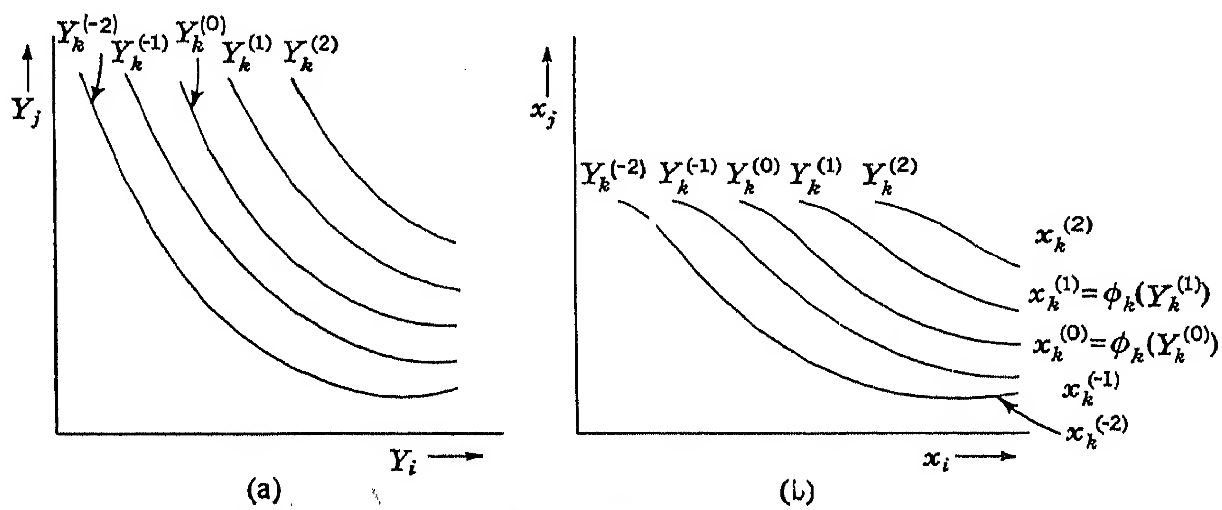

FIG. 8·4.—Topological transformation of contours.

responding values of Y_k (Fig. 8·4a). Next let us introduce a change in the independent variables, defined by the equations

$$\left.\begin{aligned} Y_i &= \phi_i(x_i), \\ Y_j &= \phi_j(x_j), \end{aligned}\right\} \tag{11}$$

where ϕ_i and ϕ_j are single-valued functions of these arguments. Replotting the contours of constant G in the (x_i, x_j)-plane (Fig. 8·4b), we obtain lines of constant $f(x_i, x_j)$, as defined by Eq. (9). If these contours are relabeled with values of x_k given by

$$x_k^{(r)} = \phi_k(Y_k^{(r)}), \tag{12}$$

they will represent the functional relation

$$x_k = f(x_i, x_j) \tag{13}$$

defined by Eq. (9), for a particular choice of the functions ϕ_i, ϕ_j, ϕ_k. It is thus clear that a given grid generator can be used in mechanizing a given function if the contours of constant $G(Y_i, Y_j)$ can be transformed into those of constant $f(x_i, x_j)$, or conversely, by any topological trans-

formation of the form of Eq. (11), with relabeling of the contours according to Eq. (12).

Formal relations such as Eqs. (9) and (10) are not of great value in practical design work. The graphic presentation of these relations by means of systems of contour lines is of more interest, but as an indication of a direction of development, rather than as a completed idea. What is really needed is a means of characterizing given functions, on the one hand, and available grid generators, on the other, which will make it clear at once whether or not a given grid generator can be used in mechanizing a given function. Even more valuable will be a means of characterizing a given function which will assist one in designing a new and satisfactory grid generator. In both respects the idea of "grid structure of a function" is of fundamental importance.

8·3. The Concept of Grid Structure.—The representation of a function of two independent variables by a grid structure is an extension of the familiar representation by a set of contours of constant value of the dependent variable. It will here be introduced in a specialized form, satisfactory for the classification of functions; in later sections it will be generalized and applied in design work.

Rectangular Grid Structure with Respect to a Center S and a Contour C.—We have now to construct the grid structure of a functional relation

$$x_k = f(x_i, x_j) \tag{14}$$

defined through a domain D in the (x_i, x_j)-plane.

Let S be a point in the domain D, associated with values of the variables which will be denoted by $x_i^{(0)}$, $x_j^{(0)}$, $x_k^{(0)}$; this is to serve as the "center" of the grid structure. Through S construct the contour B of constant x_k,

$$x_k^{(0)} = f(x_i, x_j). \tag{15}$$

(See Fig. 8·5.) Next choose an adjacent contour C, defined by

$$x_k = x_k^{(-1)}. \tag{16}$$

This, together with the point S, will fix the grid structure that is to be constructed.

Through S construct the vertical line $x_i = x_i^{(0)}$, intersecting the contour C at the point $(x_i^{(0)}, x_j^{(-1)}, x_k^{(-1)})$. Through this latter point construct the horizontal line $x_j = x_j^{(-1)}$, intersecting the contour B at the point $(x_i^{(1)}, x_j^{(-1)}, x_k^{(0)})$. Through this point, in turn, construct the vertical line $x_i = x_i^{(1)}$, intersecting the contour C at the point $(x_i^{(1)}, x_j^{(-2)}, x_k^{(-1)})$. Continuation of this process extends the steplike structure of lines between the two contours, both above and below S, and defines sequences of values of the two independent variables:

$$\ldots, x_i^{(-2)}, x_i^{(-1)}, x_i^{(0)}, x_i^{(1)}, x_i^{(2)}, \ldots,$$
$$\ldots, x_j^{(-2)}, x_j^{(-1)}, x_j^{(0)}, x_j^{(1)}, x_j^{(2)}, \ldots.$$

The rectangular grid of lines

$$x_i = x_i^{(r)} \tag{17}$$

and

$$x_j = x_j^{(s)} \tag{18}$$

will cover part, but not always all, of the domain D. This rectangular grid serves to define a system of contours

$$x_k = x_k^{(t)}, \tag{19}$$

which, together with this grid itself, will make up the "rectangular grid structure of the function, defined with respect to the center S and the contour C."

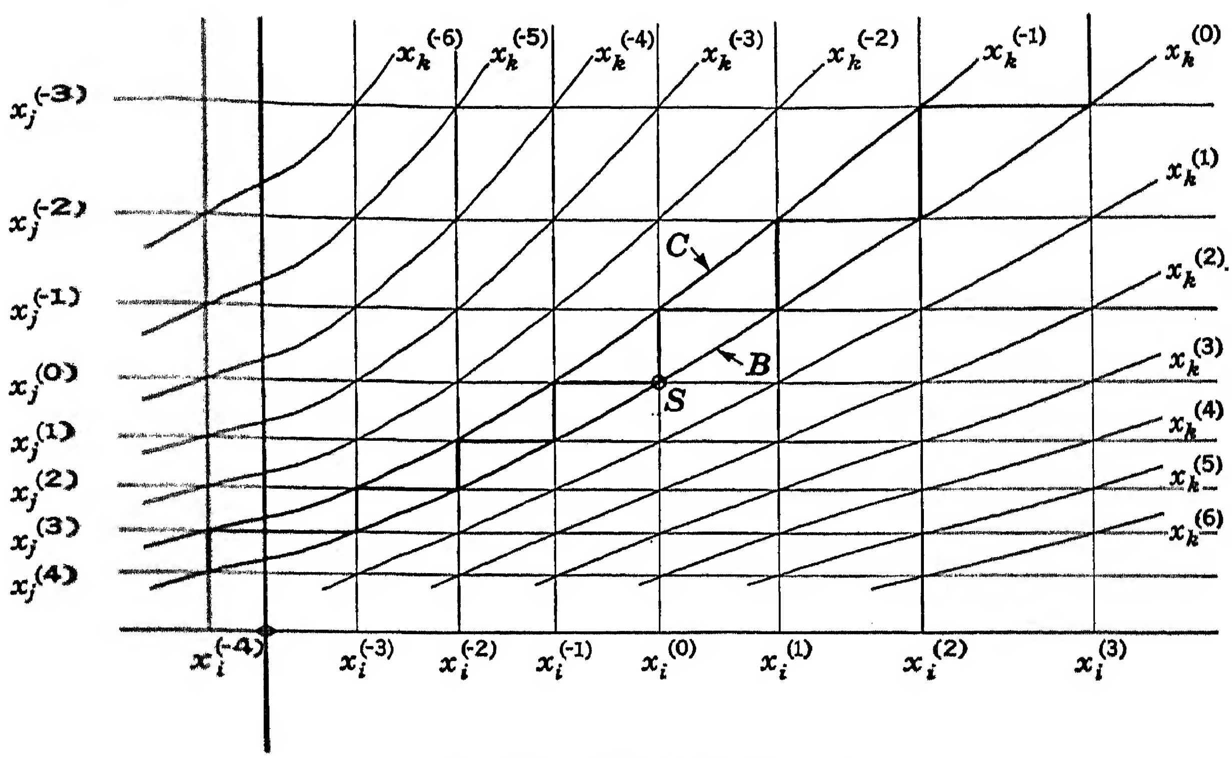

FIG. 8·5.—Ideal grid structure.

Ideal Grid Structure.—The rectangular grid has been so constructed, and its lines so numbered, that a single contour,

$$x_k = x_k^{(0)}, \tag{20a}$$

passes through all grid intersections for which

$$r + s = 0, \tag{20b}$$

and a single contour,

$$x_k = x_k^{(-1)}, \tag{21a}$$

passes through all grid intersections for which

$$r + s = -1. \tag{21b}$$

There is an important class of functions such that, no matter how the center S and the contour C are chosen, there will be a single contour,

$$x_k = x_k^{(t)}, \tag{19}$$

passing through all grid intersections for which

$$r + s = t, \tag{22}$$

t being any integer, positive or negative. Such a function will be said to have "ideal grid structure."

An ideal grid structure (defined with respect to a center S and a contour C) will consist of the rectangular grid specified above, plus all the contours of constant x_k which pass through the intersections of the grid. Such a grid structure will appear as shown in Fig. 8·5. This grid structure can also be described as consisting of three families of curves, given by Eqs. (17), (18), and (19), such that through every point of intersection there passes a curve of each family. This description will remain valid even when the concept of ideal grid structure is generalized.

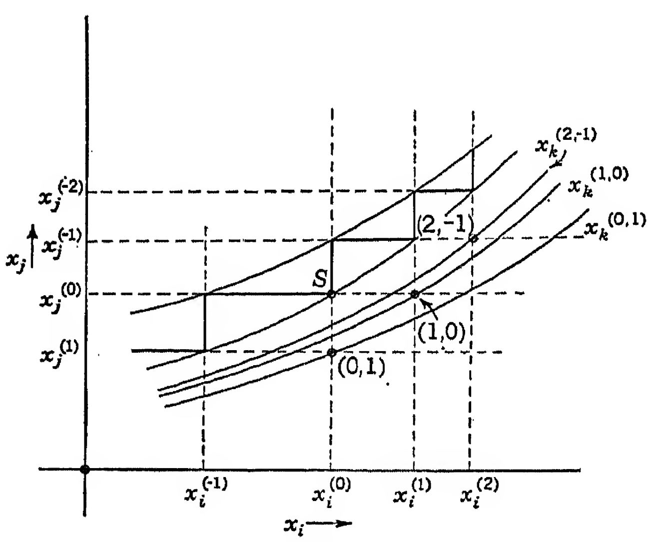

FIG. 8·6.—Nonideal grid structure.

Nonideal Grid Structure.—When different contours of constant x_k pass through grid intersections characterized by the same value of $(r + s)$, the grid structure will be said to be "nonideal." Figure 8·6 represents an extreme case of nonideal grid structure. When the grid structure is nonideal one cannot distinguish by the single index $(r + s)$ the contours of the family defined by the grid; one might instead label each curve with the two indices, r and s, of the corresponding grid intersection, as shown in Fig. 8·6.

It is not convenient to consider all these contours as belonging to the grid structure of the function, nor would this contribute to the clarity with which the grid structure represents the properties of the function. It is sufficient to include only one such contour for each value of $(r + s)$, labeling it with this quantity as the single index. The choice of the contours to be included is to some degree arbitrary. We shall consider a nonideal grid structure to consist of the rectangular grid defined in the usual way, plus the contours of constant x_k that pass through the grid intersections with $r = s = n$, plus intermediate contours that interpolate smoothly

between these and therefore pass near the intersections with

$$r = s + 1 = n$$

and $r + 1 = s = n$. (A precise method for choosing these intermediate contours will be indicated in Sec. 8·6.)

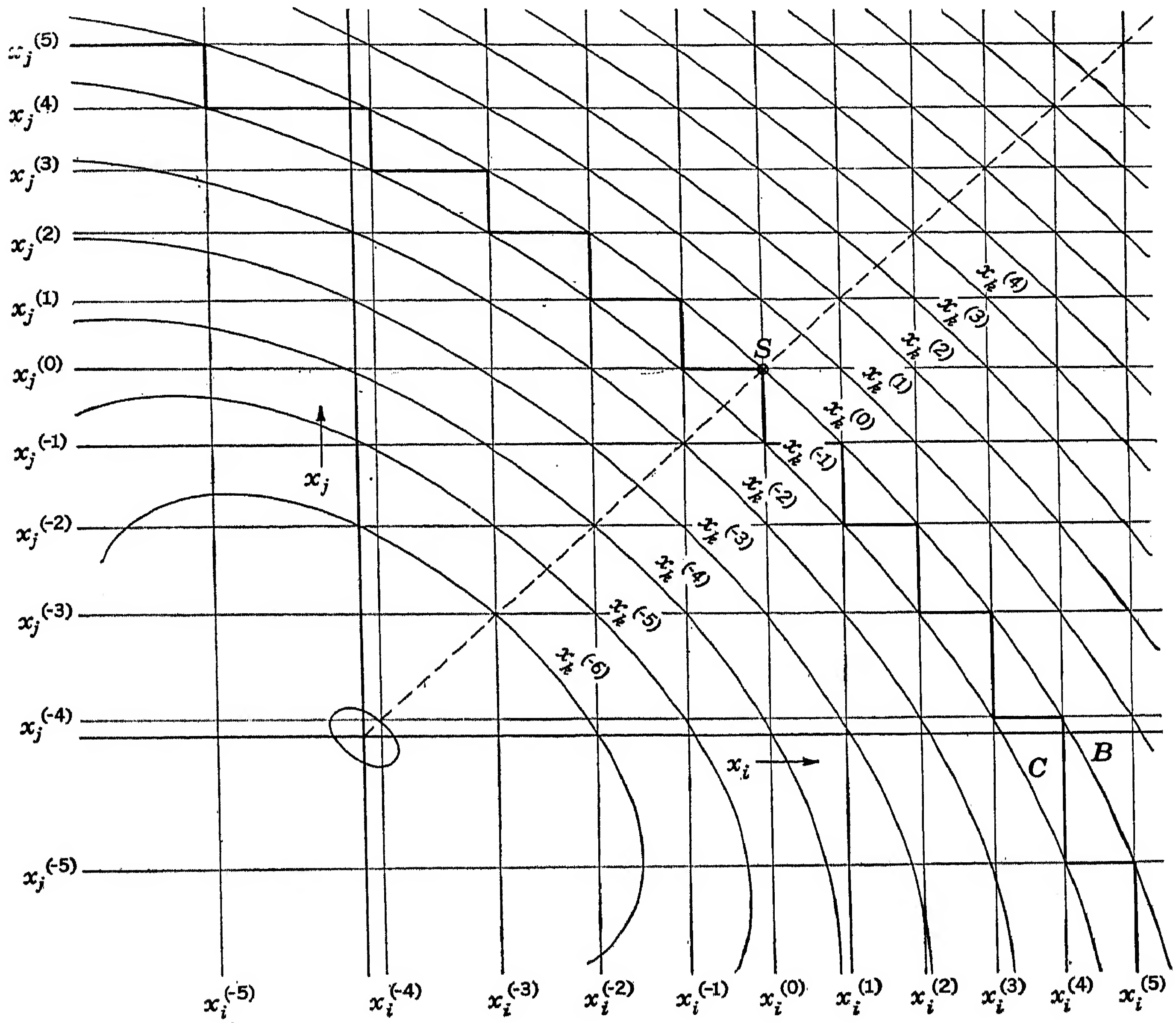

FIG. 8·7.—Grid structure of the function $x_k = \frac{1}{\sqrt{3}}(x_i^2 + x_ix_j + x_j^2)^{\frac{1}{2}}$

Figure 8·7 illustrates a typical nonideal grid structure, that of the function

$$x_k = \frac{1}{\sqrt{3}}(x_i^2 + x_ix_j + x_j^2)^{\frac{1}{2}}. \tag{23}$$

The point $x_i = x_j = x_k = 1$ has been chosen as the center S, and the contour C is that for which $x_k = 0.9 = x_k^{(-1)}$. The contours are symmetrical with respect to the dotted line in the figure, and so is the rec-

tangular grid. It will be observed that near the contours B and C, and near the line $r = s$, the contours pass very nearly through the grid intersections. Away from these lines the nonideal character of the grid structure becomes increasingly apparent, as the contours pass farther and farther from the grid intersections.

Grid Structure in the Neighborhood of a Center.—The greater the distance from the center S to the adjacent contour C of the grid structure, the more coarsely does the grid structure represent the properties of the function. In order to define for a function "the grid structure in the neighborhood of a center," one must allow the contour C to approach the center S, and concentrate attention on a very small region about the center which, nevertheless, contains a considerable number of grid lines.

One can expand in Taylor's series about the center S any well-behaved function:

$$x_k = f(x_i, x_j) = x_k^{(0)} + \left(\frac{\partial f}{\partial x_i}\right)_S (x_i - x_i^{(0)}) + \left(\frac{\partial f}{\partial x_j}\right)_S (x_j - x_j^{(0)})$$
$$+ \text{ terms of higher order in } (x_i - x_i^{(0)}) \text{ and } (x_j - x_j^{(0)}). \qquad (24)$$

In the immediate neighborhood of S the quadratic and higher terms in Eq. (24) can be neglected. To this approximation the contours of constant x_k are parallel straight lines, the grid consists of identical rectangles, and the grid structure is ideal. Thus one can say that the grid structure of any well-behaved function is ideal in the neighborhood of its center. The practical significance of this statement, which will be brought out more completely in later sections, is this: It is always easy to find a grid generator for a function if the domain of mechanization is sufficiently restricted; what is difficult is to find grid generators useful throughout extended domains.

8·4. Topological Transformation of Grid Structures.—It has been shown in Sec. 8·2 that the topological transformation

$$Y_i = \phi_i(x_i),$$
$$Y_j = \phi_j(x_j), \qquad (11)$$

carries contours of the function

$$Y_k = G(Y_i, Y_j) \qquad (6)$$

in the (Y_i, Y_j)-plane into contours of the function

$$x_k = f(x_i, x_j) \qquad (13)$$

in the (x_i, x_j)-plane. This transformation carries vertical straight lines in the (Y_i, Y_j)-plane into vertical straight lines in the (x_i, x_j)-plane, and horizontal straight lines into horizontal straight lines. Indeed, the reader will easily see that the idea of grid structure has been so defined

that if this transformation carries a center S_Y in the (Y_i, Y_j)-plane into a center S_x in the (x_i, x_j)-plane, and a contour C_Y into a contour C_x, then it carries the complete grid structure of the function $G(Y_i, Y_j)$, defined with respect to S_Y and C_Y, into the grid structure of the function $f(x_i, x_j)$, defined with respect to S_x and C_x. The values of the variables associated with the grid lines and contours will be transformed according to Eqs. (11) and (12), but the indices r, s, t, will be unchanged.

The main conclusion of Sec. 8·2 can therefore be restated in the following terms: A given grid generator can be used in the *exact* mechanization of a given function if, and only if, there exists a topological transformation, of the form of Eq. (11), that carries each grid structure of the function $G(Y_i, Y_j)$ into a corresponding grid structure of the given function $f(x_i, x_j)$. In practice, of course, all that need be shown is that some grid structure of the function $G(Y_i, Y_j)$, with sufficiently small meshes, can be thus transformed into a corresponding grid structure of the function $f(x_i, x_j)$, with errors within specified tolerances.

The topological transformation cannot change intersection properties of the lines of the grid structure; it must then transform an ideal grid structure into another ideal grid structure, a nonideal grid structure into another nonideal one. It follows that a given function with an ideal grid structure can be mechanized exactly only by a grid generator with ideal grid structure, a given function with nonideal grid structure only by a nonideal grid generator.

In Sec. 8·5 it will be shown that *all* functions with ideal grid structure can be mechanized by *any* grid generator with ideal grid structure, such as the common differential.

In the case of nonideal grid structures the situation is not so simple. There are many different ways in which a grid structure can be nonideal; it is in general possible to determine whether or not a given grid generator will serve in the mechanization of a given function only by making a detailed comparison of their respective grid-structure properties. In Sec. 8·6 there will be indicated the basic ideas of a systematic method for choosing from among a number of given types of grid generator the one which is most suitable for the mechanization of a given function. Unfortunately, this method cannot suffice for the design of nonideal grid generators until an extensive file of grid structures has been accumulated. In the present state of the art it is necessary to design a grid generator *ab initio* for each given function; the way in which this can be done, by a study of its grid structure, will be indicated in Sec. 8·7, and illustrated at length in Chap. 10.

8·5. The Significance of Ideal Grid Structure.—It will now be shown that if a functional relation

$$x_k = f(x_i, x_j) \tag{25}$$

has ideal grid structure, then there exists a topological transformation

$$\left.\begin{aligned} Y_i &= \phi_i(x_i), \\ Y_j &= \phi_j(x_j), \\ x_k &= \phi_k(Y_k), \end{aligned}\right\} \qquad \begin{aligned} &(26a)\\ &(26b)\\ &(26c)\end{aligned}$$

such that

$$Y_k = Y_i + Y_j. \tag{27}$$

In other words, if the functional relation Eq. (25) has ideal grid structure it can be expressed as

$$\phi_k^{-1}(x_k) = \phi_i(x_i) + \phi_j(x_j). \tag{28}$$

It will follow immediately that this function can be mechanized using a differential as grid generator, together with transformer linkages and scales which establish the relations of Eqs. (26).

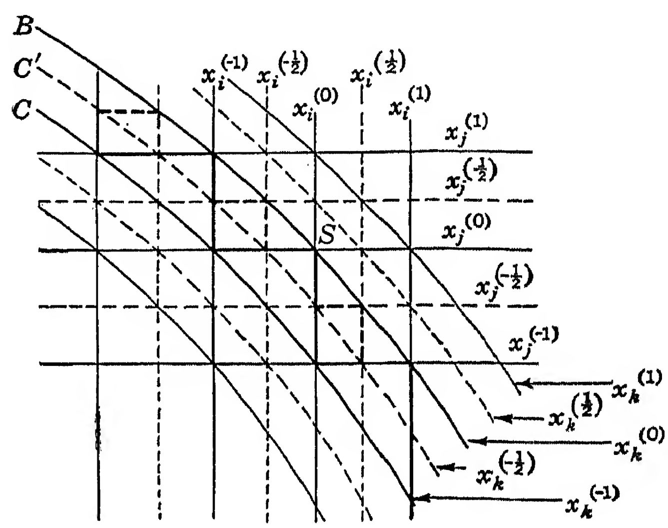

FIG. 8·8.—Subdivision of an ideal grid structure.

Let us consider the ideal grid structure defined with respect to a center S and a contour C, as shown by the solid lines of Fig. 8·8. Associated with each intersection in this grid structure are values of the indices r, s, and t, such that

$$r + s = t. \tag{29}$$

The index r is a single-valued function of the x_i-coordinate of the intersection, s is a single-valued function of x_j, and x_k is a single-valued function of t. In short, the indices r, s, t have all the characteristics which should be possessed by the parameters Y_i, Y_j, Y_k, respectively, except that they are defined only for a discrete sequence of values, instead of as continuous functions of x_i, x_j, x_k. We shall now show that the definition of the indices can be extended to apply to a continuum of values; the theorem above will then follow on identification of r, s, t with Y_i, Y_j, Y_k, respectively.

Let us consider the portion of Fig. 8·8 lying between the contours B and C, and between the lines $x_i^{(0)}$ and $x_i^{(1)}$. It is clearly possible to choose a contour C' such that a step structure constructed between the contours

B and C' passes from the center S to the point $(x_i^{(1)}, x_j^{(-1)}, x_k^{(0)})$ in two steps, instead of one. Now let us construct a grid structure with respect to the center S and the contour C' (solid and dashed lines of Fig. 8·8). It is clear from the method of construction that this new grid structure includes the contour C as its first contour beyond C'. It follows immediately that every line of the original grid appears in this new one; in addition, there is a new line interpolating between each pair of adjacent lines in the old grid. Instead of reassigning integral indices to all lines of the new grid, we shall retain the old indices for the old lines and assign half-integral indices to the intervening lines. All indices are just half as large as they would have been if the construction had been begun with the center S and the contour C'; Eq. (29) is still satisfied, but half-integral indices may occur in it as well as integral ones.

In the same way we can construct a new grid structure in which C' is the second contour (rather than the first) beyond S, and can assign to the lines of this structure quarter-integral indices which satisfy Eq. (29). Continuing to subdivide the original grid in this way, we can define grid-structure lines corresponding to arbitrary values of r, s, t, in a continuous range, throughout maintaining the validity of Eq. (29). These indices appear as functions of x_i, x_j, x_k, having the form of Eqs. (26); it is only necessary to identify r, s, t with Y_i, Y_j, Y_k, to complete the proof of the theorem.

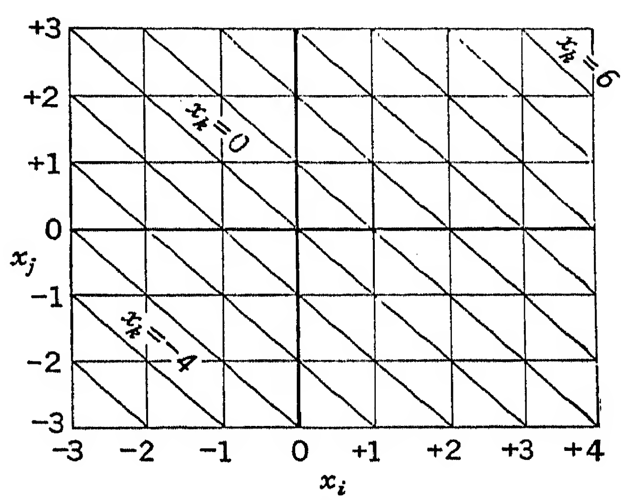

FIG. 8·9.—Grid structure of $x_i + x_j = x_k$.

As examples of functional relations with ideal grid structure we may take

$$x_k = x_i + x_j, \tag{30}$$

with grid structure shown in Fig. 8·9,

$$x_k^2 = x_i^2 + x_j^2, \tag{31}$$

with grid structure shown in Fig. 8·10, and

$$x_k = \frac{x_i}{x_j}, \tag{32}$$

or

$$\ln x_k = \ln x_i - \ln x_j, \tag{33}$$

with grid structure shown in Fig. 8·13.

An alternative statement of our result is the following: If a functional relation has ideal grid structure, it is always possible to apply a topo-

logical transformation of the form of Eqs. (26) that will transform this grid structure into the form shown in Fig. 8·9, within some domain of the variables. Possible limitations of the domain of this transformation will be evident on comparison of Figs. 8·9, 8·10, and 8·13. The grid structures of Figs. 8·9 and 8·10 correspond closely in the first quadrant, and the general form of the required transformation of horizontal and vertical

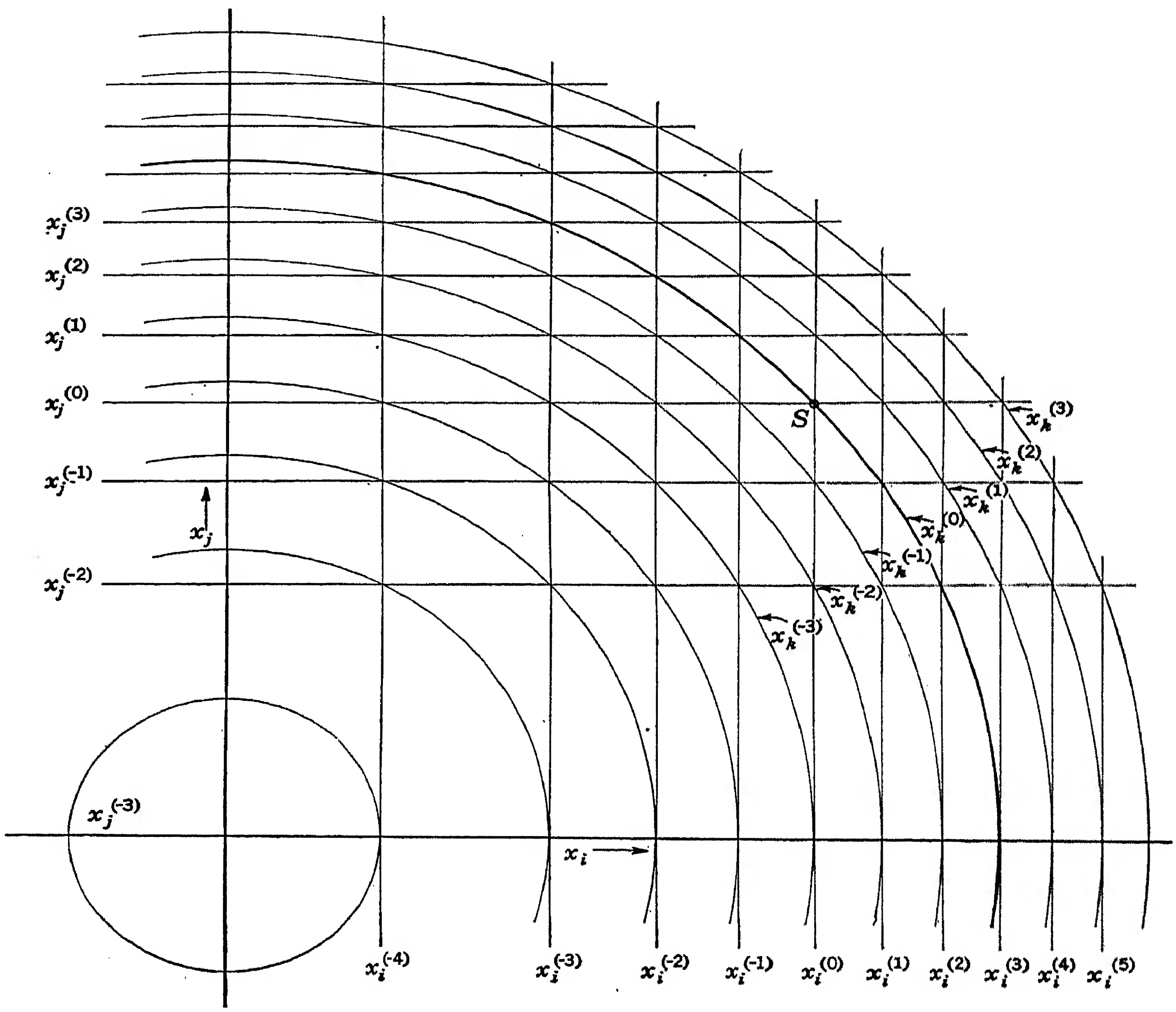

FIG. 8·10.—Grid structure of $x_i^2 + x_j^2 = x_k^2$.

coordinates is clear enough; on the other hand, it is also clear that a transformation which will serve to carry one grid structure into the other in the first quadrant will not have this effect in the second quadrant, or the fourth. This is due to the fact that the transformation Eq. (26a), as defined by the grid structure, ceases to be single-valued when the contour C is followed through a point of infinite slope; similarly, Eq. (26b) ceases to be single-valued when C is followed through a point of zero slope. Together, these limitations restrict the transformation from Fig. 8·9 to

Fig. 8·10 to corresponding quadrants. A very different example is provided by Eq. (33). The transformation equations

$$\begin{aligned} Y_i &= \ln x_i, \\ Y_j &= -\ln x_j, \\ Y_k &= \ln x_k, \end{aligned} \tag{34}$$

which transform Fig. 8·13 into Fig. 8·9, transform the first quadrant of Fig. 8·13 into the whole of Fig. 8·9; other transformations carry each of the other quadrants of Fig. 8·13 into the whole of Fig. 8·9.

We have now proved that any function with ideal grid structure can be mechanized using a differential as grid generator. This is by no means necessary, nor is it usually desirable. It is, in fact, possible to use any grid generator with ideal grid structure in mechanizing any given functional relation $x_k = f(x_i, x_j)$ with ideal grid structure; the choice should depend on the mechanical desirability of the device as a whole. In order to make contact with the analysis of Sec. 8·1, let us suppose that it is desired to establish between external parameters X_i, X_j, X_k, a given relation

$$X_k = F(X_i, X_j) \tag{35}$$

with ideal grid structure; this is a problem equivalent to that of finding a *linear* mechanization of a relation of the form of Eq. (35) between variables x_i, x_j, x_k. Let there be given a grid generator with ideal grid structure mechanizing the relation

$$Y_k = G(Y_i, Y_j) \tag{36}$$

between internal parameters Y_i, Y_j, Y_k. We have seen that this relation can also be mechanized using a differential as grid generator; Eq. (36) is equivalent to

$$Z_k = Z_i + Z_j, \tag{37}$$

$$\left.\begin{aligned} Z_i &= (Z_i|Y_i) \cdot Y_i, \\ Z_j &= (Z_j|Y_j) \cdot Y_j, \\ Y_k &= (Y_j|Z_k) \cdot Z_k, \end{aligned}\right\} \tag{38}$$

with the indicated transformer functions all single-valued. Conversely, the given grid generator, Eq. (36), can be used in mechanizing Eq. (37), as indicated in the inner circle of Fig. 8·11; the transformer functions required are the inverse of those in Eq. (38). We know also that the resulting differential can be used in mechanizing Eq. (35), in combination with transformer linkages generating the relations

$$\left.\begin{aligned} Z_i &= (Z_i|X_i) \cdot X_i, \\ Z_j &= (Z_j|X_j) \cdot X_j, \\ X_k &= (X_k|Z_k) \cdot Z_k, \end{aligned}\right\} \tag{39}$$

as shown in the outer circle of Fig. 8·11. It thus becomes obvious that the given grid generator can be used in mechanizing Eq. (35), by combining it with transformers mechanizing the operators

$$\left.\begin{aligned}(Y_i|X_i) &= (Y_i|Z_i)\cdot(Z_i|X_i),\\(Y_j|X_j) &= (Y_j|Z_j)\cdot(Z_j|X_j),\\(X_k|Y_k) &= (X_k|Z_k)\cdot(Z_k|Y_k).\end{aligned}\right\} \tag{40}$$

These transformers may be simpler in structure than those required with the simpler differential grid generator, and the domain of operation of the complete device may be more extensive. For example, it is certainly possible to build a multiplier with linear scales, using a differential

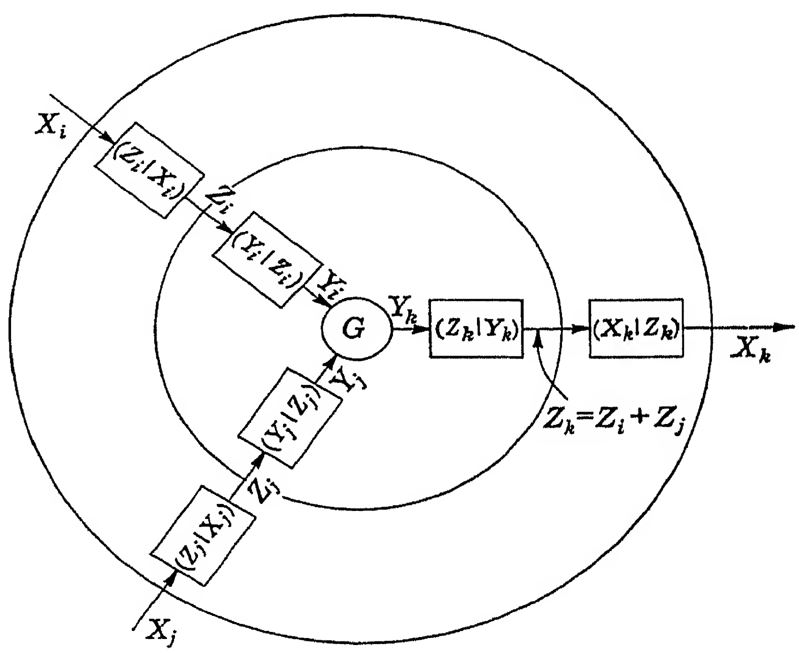

FIG. 8·11.—Mechanization of a given function with ideal grid structure by a given grid generator with ideal grid structure.

as grid generator, and logarithmic transformers [Eq. (34)] such as that illustrated in Fig. 7·9. The resulting mechanism would be unnecessarily complicated, and would be operable only in a domain in which none of the variables changes sign. It is much more satisfactory to use as grid generator a star linkage (Chap. 9). This can be so designed as to have an almost ideal grid structure, and, in combination with simple transformers, makes up a multiplier useful through a domain that includes both positive and negative values of x_i and x_j. It is thus evident that the problem of designing new grid generators with ideal grid structure is one of considerable practical importance; it will be the subject of Chap. 9.

8·6. Choice of a Nonideal Grid Generator.—The number of types of simple and mechanically satisfactory grid generators is rather limited, but the grid structures of these devices can be varied widely by changing design constants. It appears to be practicable to set up an atlas of grid

structures from which, by simple comparison with the grid structure of a given function, it would be possible to select a type of grid generator suitable for a mechanization of that function, and to determine approximately the required design constants. We may note here some characteristics of this problem, and some methods of simplifying it.

The grid structure of a given function may differ from the catalogued grid structure of a satisfactory grid generator for any or all of four reasons:

1. They may differ by a topological transformation, Eqs. (8), which is to be carried out by the transformer linkages.
2. The contours C of the grid structures may not correspond.
3. The centers S chosen for the grid structures may not correspond.
4. The catalogued grid structure may correspond to use of the wrong terminal as output terminal.

These four factors will be considered in turn.

Regularized Grid Structures.—In order to make possible direct comparison of the grid structures of given functions and given grid generators, it is desirable to reduce to a common form all grid structures which differ only by a topological transformation. This common form will be termed the "regularized grid structure." It is possible to mechanize a given function by a given grid generator if, and only if, their regularized grid structures are identical, or can be made so by proper choice of the elements mentioned in Items 2, 3, and 4 of the preceding paragraph.

In general terms, one may define a regularized grid structure as that obtained from any given grid structure by applying a topological transformation which converts the rectangular grid of the original structure into a square grid. More precisely, the transformation to be applied is that which maps into a square grid the very fine grid structure formed in the limit as the contour C approaches the center S. Let the given functional relation be

$$x_k = f(x_i, x_j). \tag{14}$$

The transformation to the plane of the new variables (z_i, z_j) can be defined in terms of line integrals in the (x_i, x_j)-plane, extending from the chosen center $S = (x_{i0}, x_{j0}, x_{k0})$ along the contour of constant x_k:

$$z_i = \phi_i(x_i) = \int_{x_{i0}}^{x_i} \left(\frac{\partial f}{\partial x_i}\right)_{x_k = x_{k0}} dx_i, \tag{41a}$$

$$z_j = \phi_j(x_j) = \int_{x_{j0}}^{x_j} \left(\frac{\partial f}{\partial x_j}\right)_{x_k = x_{k0}} dx_j. \tag{41b}$$

The variable z_k is then so defined, as a function of x_k, that Eq. (14) reduces to

$$z_k = z_i + z_j \tag{42}$$

along the line $z_i = z_j$ in the (z_i, z_j)-plane. Rewriting Eqs. (41) as

$$x_i = \phi_i^{-1}(z_i), \tag{43a}$$
$$x_j = \phi_j^{-1}(z_j), \tag{43b}$$

one may express the required relation as

$$x_k = f\left[\phi_i^{-1}\left(\frac{z_k}{2}\right), \phi_j^{-1}\left(\frac{z_k}{2}\right)\right]. \tag{44}$$

All functions with ideal grid structure have the same regularized grid structure—that illustrated in Fig. 8·9—except for possible differences in the spacing of the grid lines. For instance, if the given relation is

$$x_k = (x_i^2 + x_j^2)^{1/2} = f(x_i, x_j) \tag{45}$$

(cf. Fig. 8·10) one has

$$\left(\frac{\partial f}{\partial x_i}\right)_{x_k = x_{k0}} = \frac{x_i}{x_{k0}}, \qquad \left(\frac{\partial f}{\partial x_j}\right)_{x_k = x_{k0}} = \frac{x_j}{x_{k0}}. \tag{46}$$

Then

$$z_i = \frac{x_i^2 - x_{i0}^2}{2x_{k0}}, \tag{47a}$$
$$z_j = \frac{x_j^2 - x_{j0}^2}{2x_{k0}}. \tag{47b}$$

Thus

$$x_i = \phi^{-1}(z_i) = (x_{i0}^2 + 2x_{k0}z_i)^{1/2}, \tag{48a}$$
$$x_j = \phi^{-1}(z_j) = (x_{j0}^2 + 2x_{k0}z_j)^{1/2}, \tag{48b}$$

and Eq. (44) becomes

$$x_k = (x_{k0}^2 + 2x_{k0}z_k)^{1/2}, \tag{49a}$$

or

$$z_k = \frac{x_k^2 - x_{k0}^2}{2x_{k0}}. \tag{49b}$$

As with all functions having ideal grid structure, the z's thus defined satisfy Eq. (42) not only when $z_i = z_j$, but throughout the domain in which the transformation Eq. (41) is defined and single-valued; the regularized grid structure is that of Eq. (42).

Figure 8·12 shows a regularized nonideal grid structure, that of Eq. (23). It is, in fact, the regularized form of the grid structure shown in Fig. 8·7, and has been constructed graphically by reference to that figure, rather than by analytical working out of the transformation discussed above. We know that the rectangular grid of Fig. 8·7 would be reduced to an almost square grid by this transformation. In Fig. 8·12 this grid has been constructed as exactly square, with negligible error. The con-

tour lines in Fig. 8·12 must have the same relation to this square grid as the contour lines of Fig. 8·7 have to the rectangular grid; points of intersection are easily established by interpolation, and the contours passed through them. Such a construction is quite accurate enough for the purposes here contemplated if the mesh of the original grid structure is not too open.

The curves of the structure thus established must correspond to equally spaced values of z_i, z_j, z_k that satisfy Eq. (42) along the line $z_i = z_j$. One can determine the spacing constant α only by reference to the transformation equations; this, however, is a matter of scale which is of no practical importance.

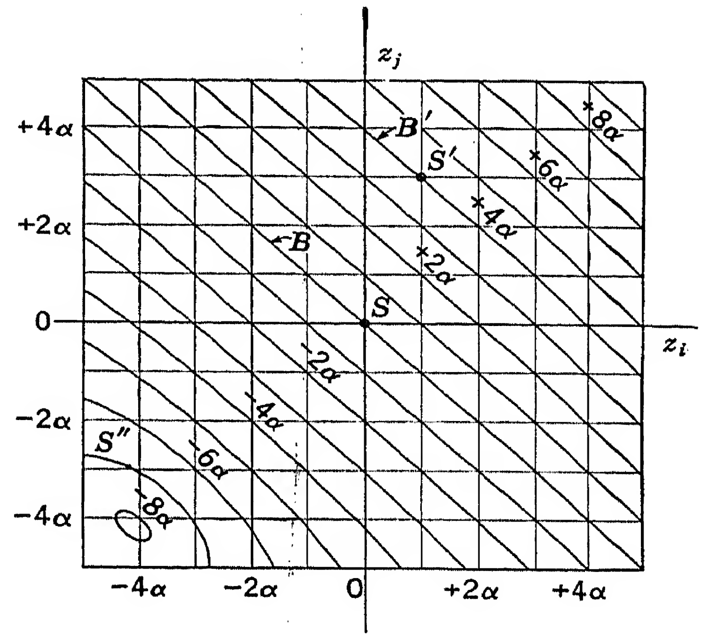

FIG. 8·12.—Regularized nonideal grid structure.

In a regularized grid structure the square grid contributes nothing to the characterization of the function; attention can be focused on the system of contours of constant z_k. The usefulness of the idea of regularized grid structure is largely due to this fact.

Effect of Change of Contour C.—The transformation to a regularized grid structure converts the functional relation

$$x_k = f(x_i, x_j) \tag{14}$$

into another,

$$z_k = g(z_i, z_j), \tag{50}$$

which defines a "regularized surface" in (z_i, z_j, z_k)-space. This surface is tangent to the plane $z_k = z_i + z_j$ all along the line $z_k = 0$, and intersects it all along the line $z_i = z_j$; its form is made obvious by the contour lines of the regularized grid structure. Change in the choice of the contour C changes the spacing of these contours, but not the form of the regularized surface that they describe. Thus, in comparing regularized grid structures of given function with those of given grid generators, one should compare surface to surface, not contour to contour. This can be done without knowledge of the spacing constant.

Effect of Change of the Center S.—Passage to the regularized grid structure always transforms the contour B through the chosen center S into the straight line $z_i + z_j = 0$ in the (z_i, z_j)-plane. When the grid structure is ideal, all contours of constant x_k are transformed into parallel straight lines; the appearance of the regularized grid structure does not

depend on S. When the grid structure is nonideal this is not precisely true. Adjacent contours are converted into lines which are only approximately straight, and the special characteristics of the nonideal structure become evident in the form of the more remote contours. Choice of the center S' on another contour B' (Fig. 8·12) would make that contour transform into a straight line, and introduce a corresponding curvature into the transformed contour B. If B' is very nearly a straight line in the original regularized grid structure, the change in form of B, and of the rest of the grid structure, will be small. It is thus evident that the chosen center of the grid structure in Fig. 8·12 could be changed within wide limits with little effect on the appearance of the regularized grid structure. On the other hand, a striking change would occur if S'' were chosen as the center.

It is usually sufficient, for practical purposes, to represent a given grid generator by a single regularized grid structure. The domain of usefulness of the grid generator will be limited by mechanical considerations, and it will be natural to choose S near the center of this domain. The domain of a given function to be mechanized will also be specified, and a center S' will be chosen near the center of this domain. If the grid generator is to be useful in mechanizing this particular function the centers S and S' must correspond at least roughly, and the difference between them will not cause large differences in the appearance of the regularized grid structures.

Effect of Choice of Output Terminal.—Given a mechanism suitable for use as a grid generator, one might choose any of the three terminals as the output terminal, and might associate the input parameters with the other terminals in two different ways. To each of the six possible ways of using this mechanism as a grid generator there corresponds a different grid structure. The appearance of the grid structure depends principally on which of the terminals is associated with the output parameter Y_k; interchange of the input terminals, in their association with Y_i and Y_j, merely produces a reflection of the grid structure in the diagonal line $Y_i = Y_j$.

In an atlas of grid structures one might then represent each mechanism by three regularized grid structures corresponding to the three choices of output terminal. Alternatively, one might present a single regularized grid structure. For each given functional relation it would then be necessary to construct three regularized grid structures, with x_i, x_j, and x_k, in turn, treated as the output variable. A match between one of these three structures and a catalogued structure (after a possible reflection in the diagonal) would then show that the catalogued mechanism could be used, and would indicate the way in which the parameter should be associated with its terminals.

8·7. Use of Grid Structures in Linkage Design.—The concept of grid structure is of fundamental importance as an aid in designing grid generators for special applications. For this purpose it becomes necessary to introduce the following generalization of the idea.

Generalized Grid Structures.—In the preceding discussion the grid structure of a functional relation

$$x_k = f(x_i, x_j) \tag{14}$$

has been defined as a system of lines in the (x_i, x_j)-plane: straight lines representing constant values of x_i and x_j, which form a rectangular grid, and a superimposed family of contours of constant x_k. Such a grid structure is a very special form of intersection nomogram representing the given relation.

Now it is not at all necessary to treat x_i and x_j as cartesian coordinates. Instead, one can take the plane of representation as the (z_i, z_j)-plane, and let x_i and x_j be any pair of curvilinear coordinates in this plane, given in terms of the cartesian coordinates z_i, z_j, by

$$\begin{aligned} x_i &= x_i(z_i, z_j), \\ x_j &= x_j(z_i, z_j). \end{aligned} \tag{51}$$

The construction of the grid structure then proceeds as before. Adjacent contours B and C of constant x_k are chosen, and between them, beginning at the center S, there is constructed a step structure consisting of portions of contours of constant x_i and x_j. These latter contours, extended through the plane, make up a curvilinear grid, instead of the rectangular one previously obtained. The complete grid structure consists of this grid, together with contours of constant x_k which pass through the grid intersections $r = s$, or interpolate smoothly between these contours.

The same grid structure can be obtained in a different way. Let Eqs. (51) define a topological transformation between the (x_i, x_j)-plane and the (z_i, z_j)-plane. This transformation will carry a center S_x in the first plane into a center S_z in the second, and a contour C_x in the first into a contour C_z in the second. It will also transform the entire grid structure defined in the (x_i, x_j)-plane, using S_x and C_x, into the grid structure defined in the (z_i, z_j)-plane, using S_z and C_z.

Such a topological transformation of the grid structure will, of course, affect none of its intersection properties; in particular, it will still serve as an intersection nomogram representing the given function. We shall, in fact, consider grid structures which differ only by a topological transformation of the form of Eq. (51) as equivalent representations of a functional relation.

Mechanical Realization of a Given Grid Structure.—The author's technique for mechanizing functions of two independent variables makes

important use of such topological transformations of grid structures. The basic idea is to transform the given grid structure into a form which suggests a satisfactory mechanical form for a grid generator. The technique employed in this transformation will be indicated in later chapters; here we shall merely take note of the way in which a given grid structure may suggest a corresponding mechanization of the function.

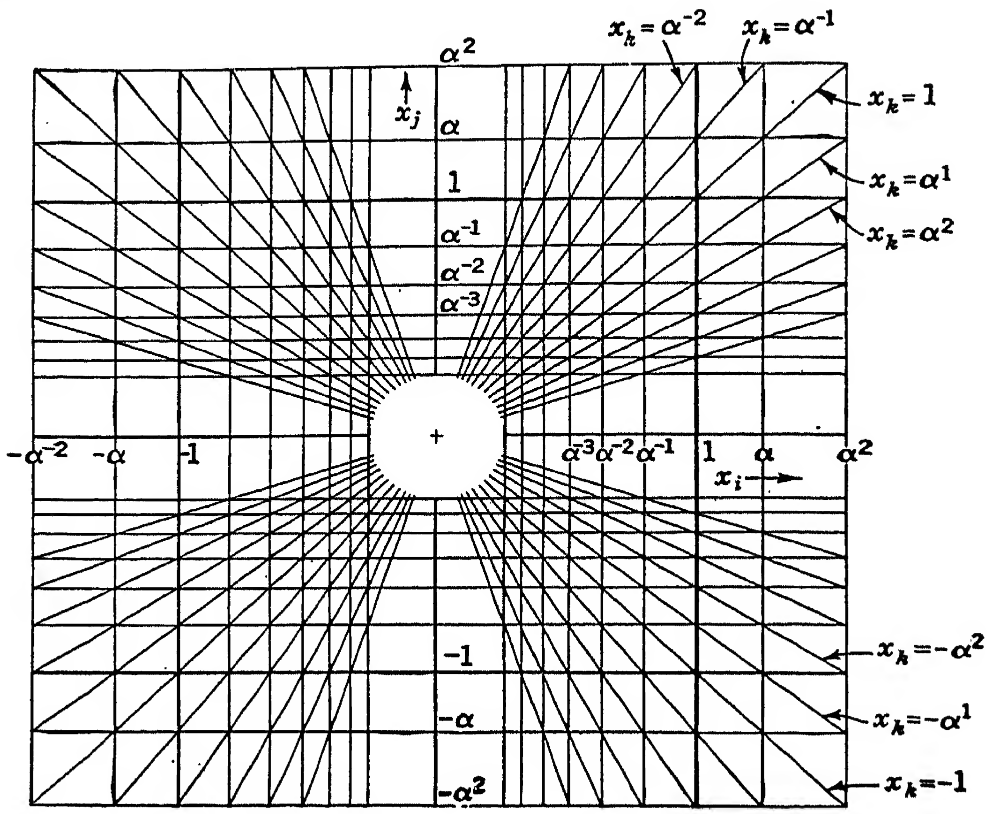

FIG. 8·13.—Grid structure of $x_k = x_i/x_j$ ($\alpha = 1.25$).

Consider, for example, the grid structure of the relation

$$x_k = \frac{x_i}{x_j} \tag{52}$$

as shown in Fig. 8·13. The spacings of the rectangular grid lines change in geometrical sequence; the fixed ratio is here 1.25. The contours of constant x_k are radial lines; the corresponding value of x_k for each line is the value of x_i at its intersection with the horizontal line $x_j = 1$. At each point of this figure one can read off corresponding values of x_i, x_j, and x_k which satisfy Eq. (52). Now, let there move over this figure a pin connected mechanically to three different scales. If these connections and scales are so arranged that one can read on the first scale the value of x_i at the position of the pin, on the second scale the value of x_j, and on the third scale the value of x_k, then the device as a whole becomes a mechanization of the given function. In the present case, the first scale should show the horizontal displacement of the pin from the origin, the second scale its vertical displacement; the reading of the third scale should be

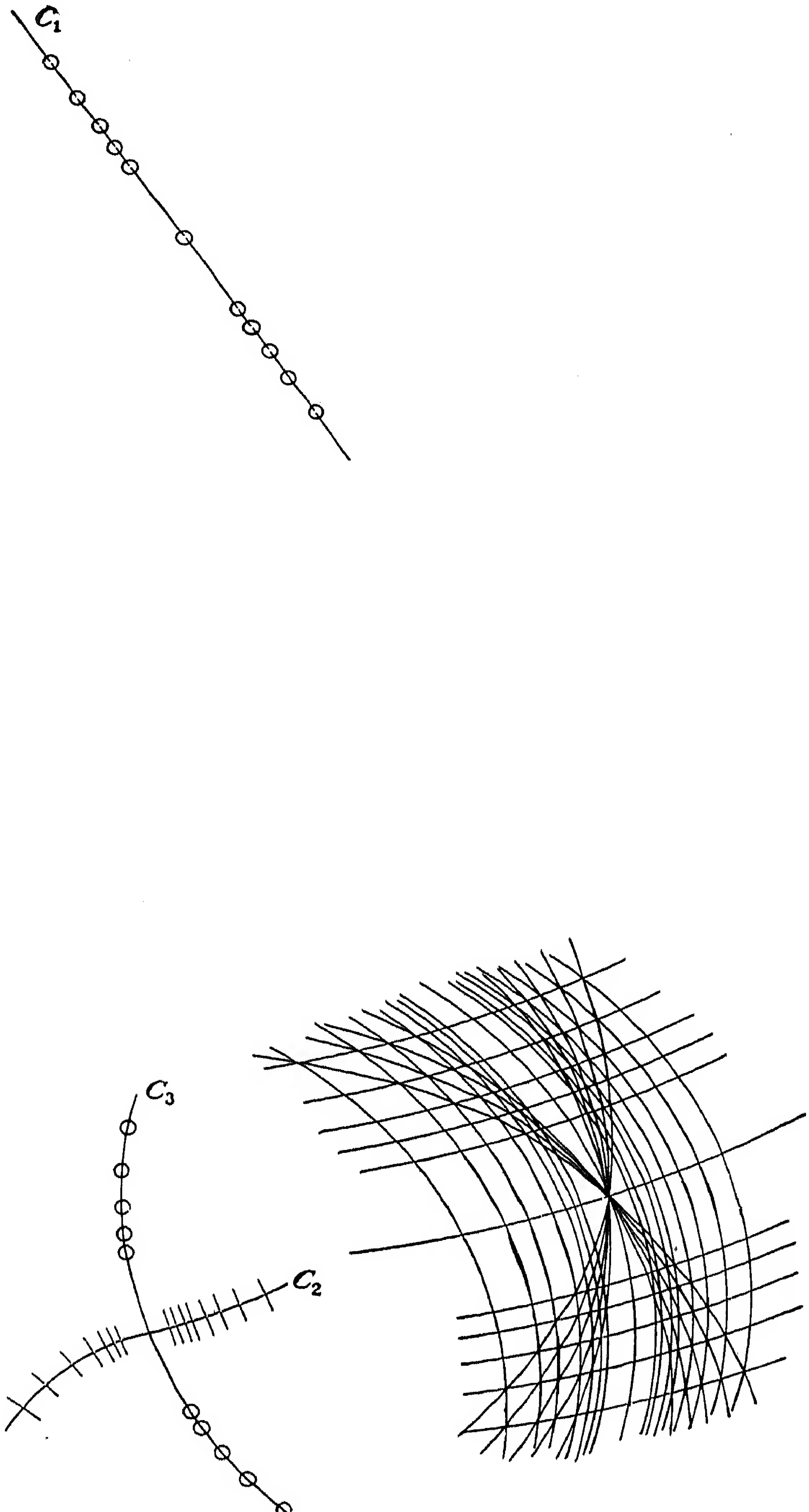

FIG. 8·14.—Transformed grid structure of $x_k = x_i/x_j$.

proportional to the horizontal displacement of the intersection of the radial line through the pin with a horizontal line. The divider (or multiplier) of Fig 1·10 accomplishes this in a very simple and obvious way; it is the natural mechanization of the grid structure of Fig. 1·12, which differs from Fig. 8 13 only by a reflection

A topological transformation of this grid structure will carry it into a form (Fig. 8·14) suggesting a very different type of mechanization. The horizontal lines of Fig. 8·13 are transformed into a family of circles, all of the same radius, L_1, with centers lying on a straight line C_1. The vertical lines of Fig. 8·13 are transformed into a second family of circles, all of the same radius, L_2, with centers lying on the curved line C_2. Finally, the radial lines of Fig. 8·13 are transformed into a third family of curves. These are very nearly, although not exactly, circles with the same radius, L_3; since the approximating circles intersect at a common point their centers must lie on another circle with radius L_3—curve C_3 in the figure.

On ignoring the small deviation from circular form of the curves of the third family, we are led directly to the mechanization shown in Fig. 8·15—an approximate divider or multiplier, but a quite accurate one. The joint P can be made to lie on a particular circle of the first family by placing it at one end of a bar PA_1 with length L_1, and fixing the joint A_1 in the center of this circle, on line C_1. Conversely, if the joint A_1 is constrained to lie on the line C_1—as by being pivoted to a slide—it will necessarily be always at the center of the x_j-circle on which P lies; a scale placed along C_1 can thus be calibrated to give the value of x_j at the position of the pin P. In the same way, the value of x_i can be read on a scale lying along the curved line C_2, using as index point the joint A_2 connected to the pin P by a bar of length L_2. Finally, values of the quotient x_k might be read on the circular scale C_3. Instead of pivoting the bar PA_3, of length L_3, to a circular slide, one can constrain the point A_3 to lie on the curve C_3 by a second bar OA_3, also of length R_3, pivoted at the center of this circle. As shown in the figure, the index point has been transferred to this second bar in an obvious way.

The shortcomings of this particular device are obvious: the use of a curved slide, and the nonlinearity of the x_i- and x_k-scales. To improve it one should devise a more satisfactory way to guide the point A_2 along the curve C_2, and should linearize the x_i- and x_k-scale readings by transformer linkages, such as harmonic transformers or three-bar linkages.

How this can be accomplished is illustrated in Fig. 8·16, which shows the first linkage multiplier so designed as to be operable through a domain including positive and negative values of all variables. The point A_2 is constrained to follow the curve C_2 of Fig. 8·15 by placing it on an extension of the central bar of a three-bar linkage $\alpha\beta\gamma\delta$. (The required design technique is indicated in Sec. 10·4.) Motion of A_2 along C_2 produces a

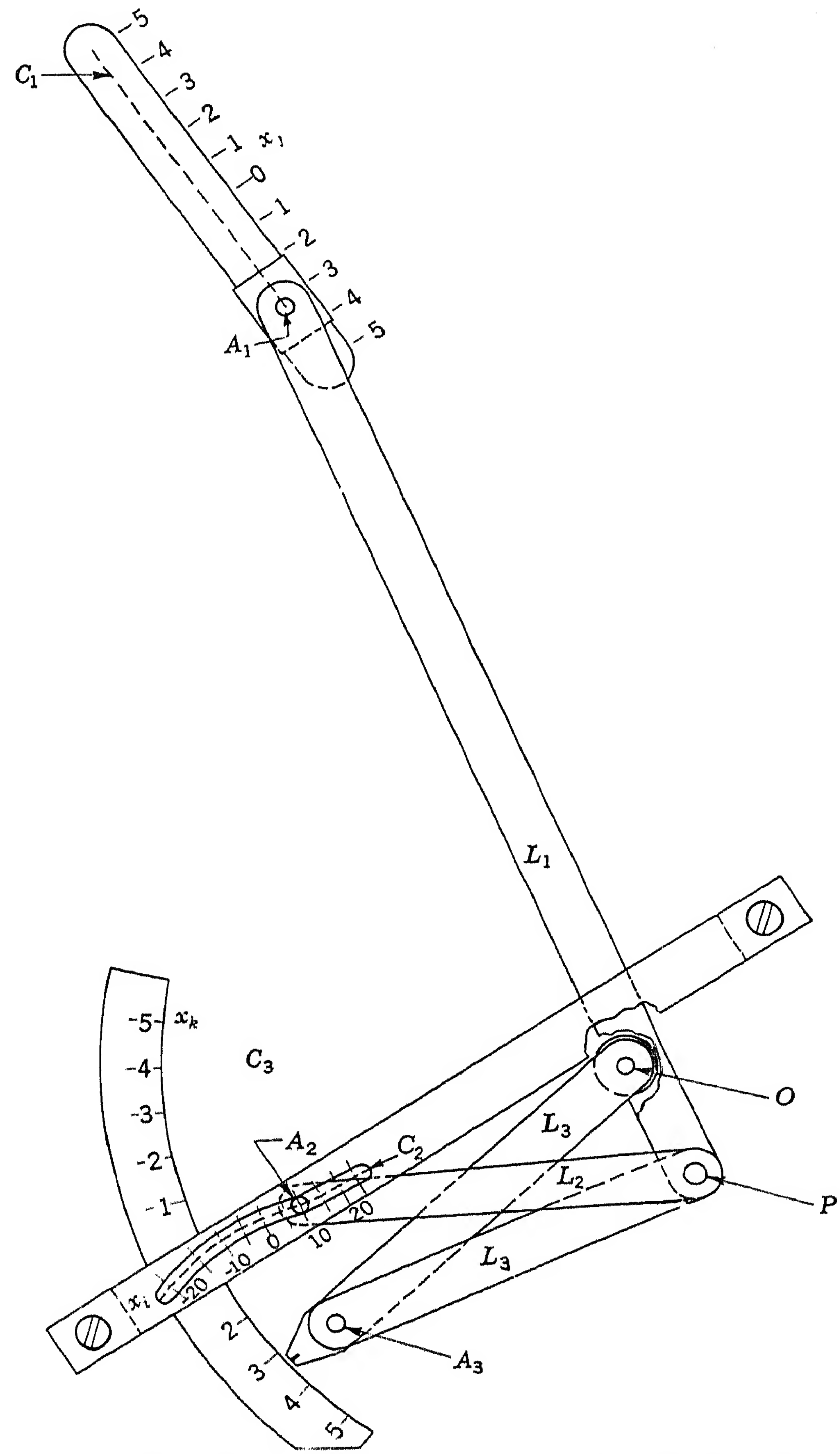

FIG. 8·15.—Mechanization of the grid structure of Fig. 8·14.

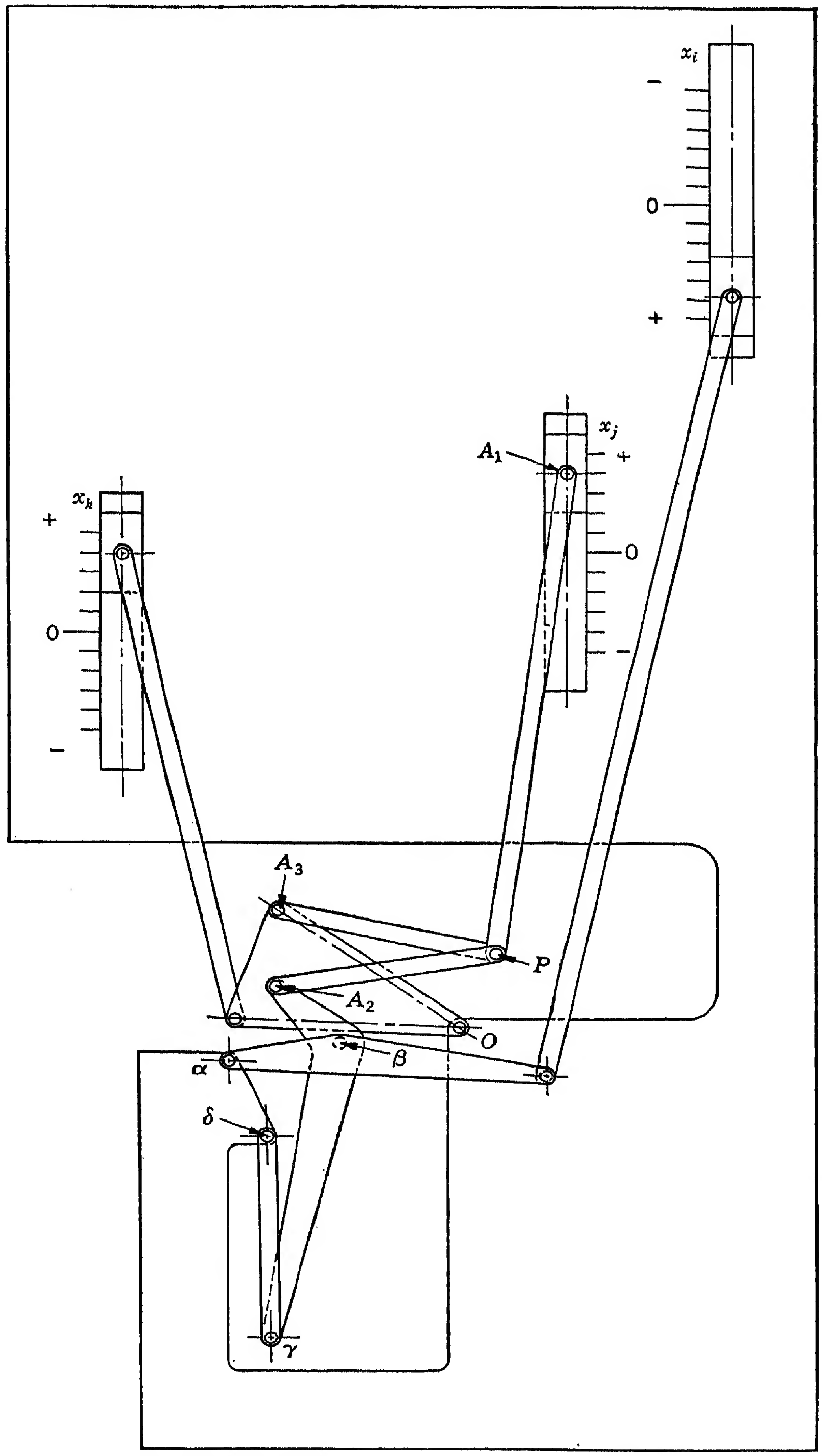

FIG. 8·16.—Linear mechanization of $x_i = x_j x_k$.

corresponding rotation of the bar $\alpha\beta$ of the three-bar linkage; a nonideal harmonic transformer converts this rotation into linearized readings on the x_i-scale. To linearize the x_k-scale the rotation of the bar OA_3 has likewise been converted into linear motion of a slide by means of a nonideal harmonic transformer.

This design of a practical linkage multiplier has thus been arrived at in three steps:

1. Topological transformation of a multiplier grid structure into a convenient form.
2. Design of a simple device for mechanizing this grid structure.
3. Conversion of the design to a more satisfactory form, by applying constraints in a different way and linearizing the scale readings.

An important fourth step is the final adjustment of linkage dimensions. These steps are by no means unique, and one can design a great variety of linkage multipliers. For instance, it is possible to find other transformations of the multiplier grid structure in which the curve C_2 becomes a circle or a straight line, and the design of a linkage constraint for the point A_2 becomes trivial. To accomplish this one needs a thorough understanding of the techniques to be discussed in the next chapter.

CHAPTER 9

BAR-LINKAGE MULTIPLIERS

A technique for designing bar-linkage multipliers will be developed in this chapter, both for its intrinsic interest and as an example of a general technique. The problem of mechanizing any other functional relation with ideal grid structure is essentially the same, as regards the design of the grid generator; differences arise only in the details of transformer linkage design, which will need no discussion here.

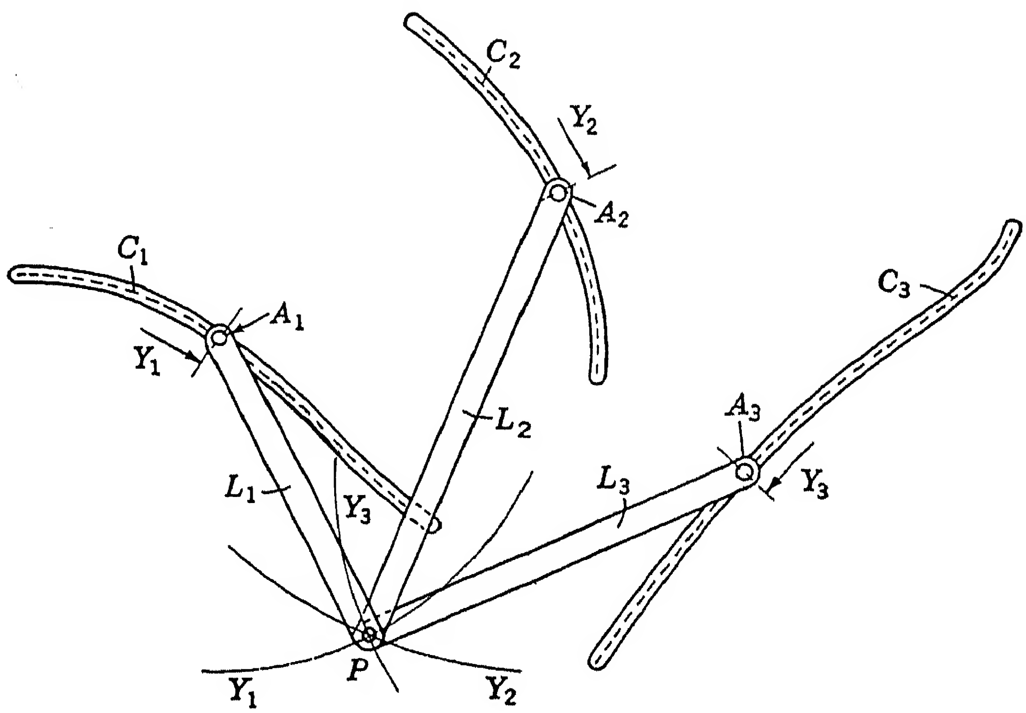

FIG. 9·1.—Star grid generator.

9·1. The Star Grid Generator.—The grid generator considered throughout this and the following chapter will be the "star grid generator" or "star linkage" illustrated in Fig. 9·1. The general principles to be explained can be applied to other grid generators, but the detailed constructions will of course require modification. The reader will recognize that in the case of the star grid generator these constructions are particularly simple; this simplicity and the satisfactory mechanical properties of this device give it a special usefulness in practice.

The star linkage consists of three links, L_1, L_2, L_3, joined together at one end by a common joint P. The lengths of these links we shall also denote by L_1, L_2, L_3. At their far ends are free joints A_1, A_2, A_3, which are in some manner guided along three curves C_1, C_2, C_3. Input and output parameters, Y_1, Y_2, Y_3 can be read at these joints on arbitrarily

graduated scales lying along these curves. The linkage establishes between these parameters a relation

$$Y_3 = G(Y_1, Y_2) \tag{1}$$

which characterizes its behavior as a grid generator.

It is at once clear that any functional relation that can be generated by a star linkage can also be represented by an intersection nomogram consisting of three families of circles, of radii L_1, L_2, L_3, respectively, representing constant values of the parameters Y_1, Y_2, Y_3. In fact, the linkage could be used in drawing this nomogram. If the joint A_1 is fixed at the point Y_1 on the C_1-scale, the joint P can then be made to describe the Y_1-circle on the nomogram; circles corresponding to definite values of Y_2 and Y_3 can similarly be traced out by fixing the joints A_2 and A_3, respectively. Each circle on the nomogram thus represents a corresponding point on one of the three scales. To each configuration of the linkage there corresponds a point on the nomogram at which three circles intersect; corresponding scale readings and nomogram points indicate the same triplet of values of the parameters, Y_1, Y_2, Y_3, satisfying Eq. (1).

It follows that any functional relation that can be generated by a star linkage must have a grid structure that consists of three families of circles with fixed radii, or can be brought into such a form by the general topological transformation, Eq. (8·51).

The grid structure of a star grid generator may be almost ideal over a wide range of parameter values, or strongly nonideal, depending on the link lengths and the choice of curves C_1, C_2, C_3; it is thus useful in mechanizing functions with either ideal or nonideal grid structure. In the present chapter we shall be interested only in designing star grid generators with nearly ideal grid structure.

9·2. A Method for the Design of Star Grid Generators with Almost Ideal Grid Structure.—It will be instructive to examine the grid structure of the star linkage shown in Fig. 9·1. This can be done graphically as illustrated in Fig. 9·2. We choose the center S of the grid structure, and mark the corresponding positions of the joints A_1, A_2, A_3, on the three scales with the values of r, s, t, for this center, 0, 0, 0. About these points we draw circles $C_1^{(0)}$, $C_2^{(0)}$, $C_3^{(0)}$, with radii L_1, L_2, L_3; these intersect at S. Let us choose $C_3^{(0)}$ as the contour B in the grid structure, thus assigning to Y_3 the role of x_k in Sec. 8·3. Near the point $t = 0$ on the Y_3-scale we select another point to correspond to $t = 1$. About this we describe a circle $C_3^{(1)}$, of radius L_3, to serve as the contour C of the grid structure. Between the contours $C_3^{(0)}$ and $C_3^{(1)}$ we can now construct a step structure consisting of arcs of radius L_1, centering on curve C_1, and arcs of radius L_2, centering on curve C_2. Beginning at S we can follow the circle $C_1^{(0)}$ to its intersection with the curve $C_3^{(1)}$. This intersection

corresponds to the indices $r = 0$, $t = 1$; in order to satisfy the relation

$$r + s = t \tag{2}$$

it must also be assigned the index $s = 1$. (All three indices are indicated in Fig. 9·2, though any two of them would be sufficient for identification.) At a distance L_2 from this point there must lie the point $s = 1$ on the curve C_2. About the point $s = 1$ we describe the circle $C_2^{(1)}$, which intersects the contour $B = C_3^{(0)}$ at a point with the indices $s = 1$, $t = 0$; the other

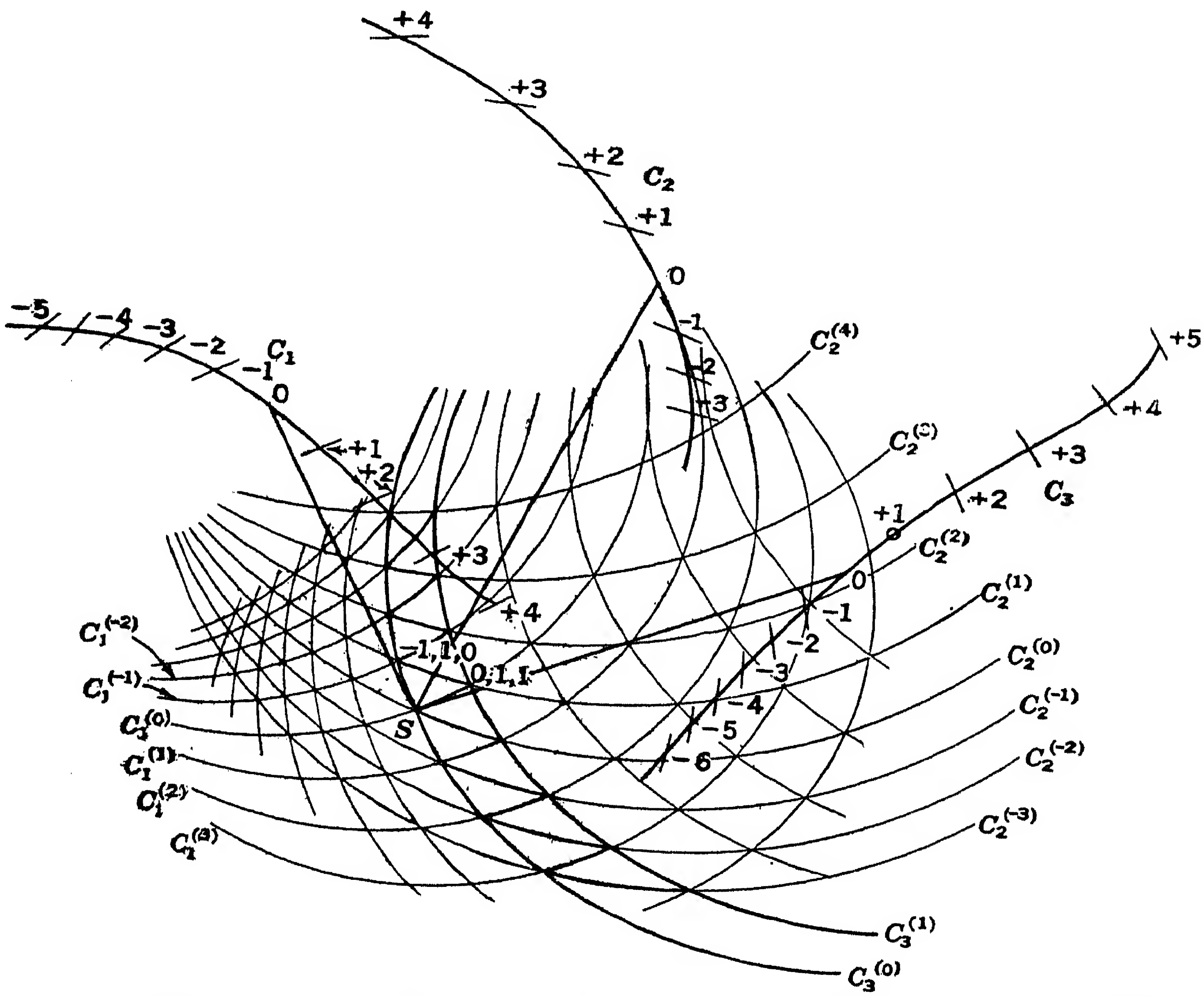

FIG. 9·2.—Grid structure of a given star linkage. The arms of the linkage are shown with the common joint at the center of the grid structure.

index must be $r = -1$. At a distance L_1 from this intersection there must then lie the point $r = -1$ on curve C_1. By continuing this process we can build up a step structure between the chosen contours, and establish on the curves C_1 and C_2 the sequence of points corresponding to integral values of the indices r and s. The families of circles $C_1^{(r)}$ and $C_2^{(s)}$ about these points form the basic grid of the grid structure. All this follows uniquely from our choice of the center $S = (0, 0, 0)$ and the point $t = 1$ on C_3.

If the grid structure of this grid generator were ideal, all intersections of the grid with $r + s = t$ would lie on a circle $C_3^{(t)}$ with radius L_3 and center on the curve C_3. Actually, as shown in Fig. 9·2, it is possible to construct circles $C_3^{(t)}$ that pass very nearly, though not exactly, through these intersections. (Note, for instance, the divergences in the upper right-hand corner of the grid structure.) For practical purposes the grid structure may be considered as ideal over the greater part of the domain illustrated. Within this domain it will mechanize the relation

$$x_3 = x_1 + x_2, \tag{3}$$

if the scale calibration is that established by this construction, or any other relation with ideal grid structure, if the scales are properly transformed. Figure 9·2 shows very clearly the system of curvilinear triangles which is the distinguishing mark of ideal grid structure. So nearly ideal a grid structure is by no means characteristic of star linkages. This particular linkage has been expressly designed to have an almost ideal grid structure, by a method which will now be described in detail.

Our problem is essentially that of constructing three families of circles, $C_1^{(r)}$, $C_2^{(s)}$, $C_3^{(t)}$ (with radii L_1, L_2, L_3, respectively) which intersect to form a triangular structure such as that shown in Fig. 9·2. We begin by choosing arbitrarily six points in a plane. Three of these, $A_1^{(1)}$, $A_1^{(0)}$, $A_1^{(-1)}$, will serve as the points $r = 1, 0, -1$, on the curve C_1 of the completed linkage; they should lie on a line of moderate curvature, with roughly equal spacings, but can otherwise be chosen at will (cf. Fig. 9·3). The other three points, $A_3^{(1)}$, $A_3^{(0)}$, $A_3^{(-1)}$, are to serve as the points $t = 1, 0, -1$, on the curve C_3, and should be chosen subject to similar conditions. About the points $A_1^{(1)}$, $A_1^{(0)}$, $A_1^{(-1)}$, construct circles $C_1^{(1)}$, $C_1^{(0)}$, $C_1^{(-1)}$, with arbitrary radius L_1; similarly construct about the points $A_3^{(1)}$, $A_3^{(0)}$, $A_3^{(-1)}$, the circles $C_3^{(1)}$, $C_3^{(0)}$, $C_3^{(-1)}$, with radius L_3. Since these circles are to form the basis of the grid structure, L_3 should be so large that each C_3-circle intersects each circle $C_1^{(r)}$ in two well-separated points. The intersections of the circles will then fall into groups of nine, well separated in the plane. One of these groups will lie near the center of the grid structure, whereas the other will lie outside the region in which it is almost ideal; it is for this reason that the two groups of intersections should not be close to each other.

Choosing one of the two sets of intersections, we label each intersection with the corresponding indices r, s, t: $(-1, 0, -1)$, $(-1, 1, 0)$, $(-1, 2, 1)$, $(0, -1, -1)$, $(0, 0, 0)$, $(0, 1, 1)$, $(1, -2, -1)$, $(1, -1, 0)$, $(1, 0, 1)$. [The second index is in each case chosen to satisfy Eq. (2).] These nine grid intersections have been chosen with a high degree of arbitrariness; our problem is now to build the grid structure about this nucleus, maintaining its ideal character so far as possible by appropriate choice of the available design constants.

The three intersections $(-1, 0, -1)$, $(0, 0, 0)$, $(1, 0, 1)$ must all lie on the circle $C_2^{(0)}$. By constructing this circle we can establish its radius, L_2, and its center, the point $A_2^{(0)}$ on the curve C_2. The known points, $(-1, 1, 0)$ and $(0, 1, 1)$, and the known radius L_2 then serve to determine

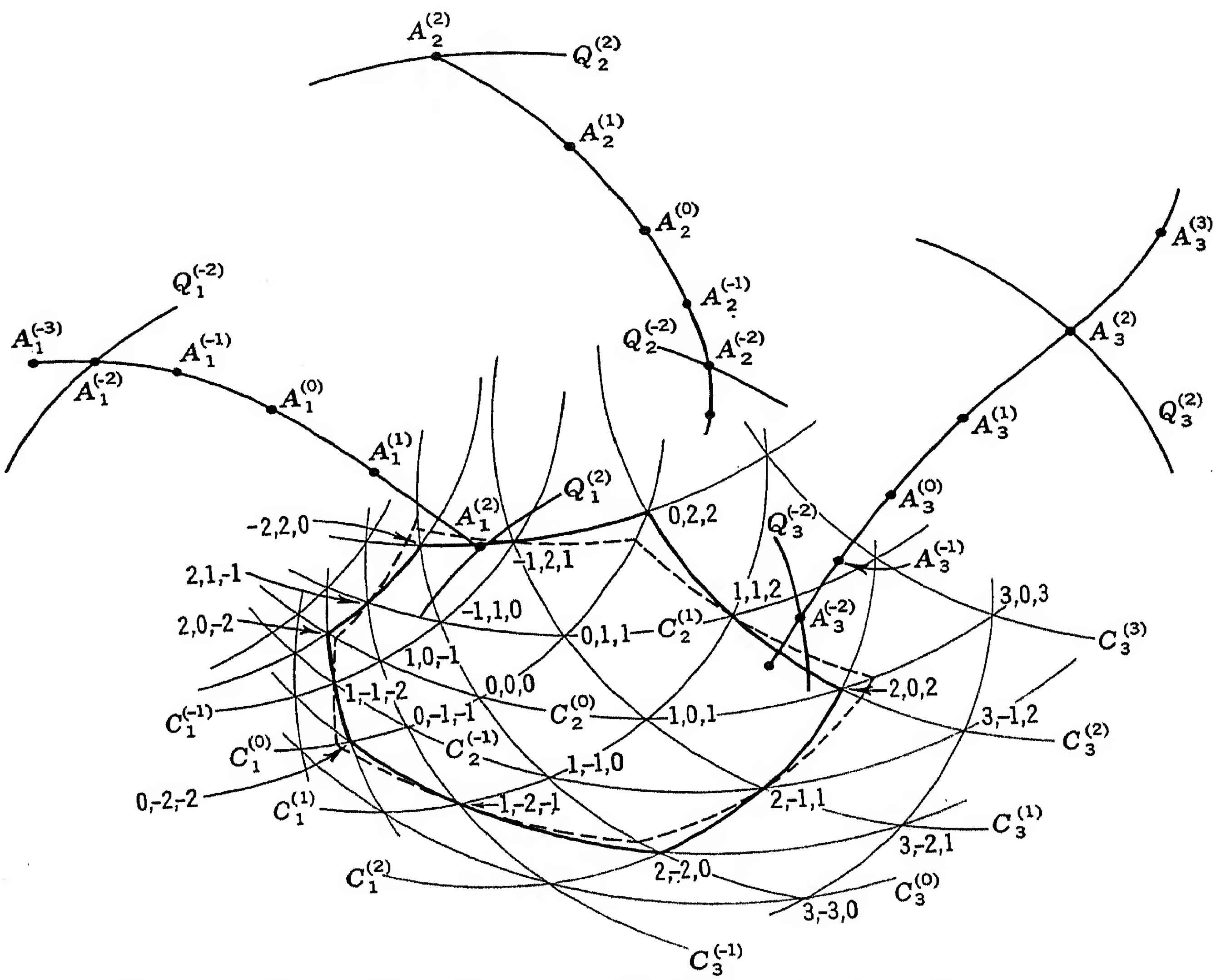

FIG. 9·3.—Construction of a star linkage with nearly ideal grid structure.

the circle $C_2^{(1)}$, with center $A_2^{(1)}$; similarly the points $(0, -1, -1)$ and $(1, -1, 0)$ determine the circle $C_2^{(-1)}$ with center $A_2^{(-1)}$. These new circles fix four additional grid intersections: $(-2, 1, -1)$, $(2, -1, 1)$, $(1, 1, 2)$, and $(-1, -1, -2)$.

There are now determined the three link lengths, L_1, L_2, L_3, and three points on each of the curves C_1, C_2, C_3. By passing smooth curves through these points we can set up a star linkage with a nearly ideal grid structure in the neighborhood of the center $S = (0, 0, 0)$. To improve the accuracy of this construction, and to extend the domain of nearly ideal grid structure, it is necessary to determine other points on these curves. We now know that the point $A_2^{(2)}$ must lie on a circle $Q_2^{(2)}$ of radius L_2 with its center at $(-1, 2, 1)$, and that the point $A_2^{(-2)}$ lies on circle $Q_2^{(-2)}$, with

the same radius and center at (1, −2, −1). Similarly $A_1^{(2)}$ and $A_1^{(-2)}$ lie on circles of radius L_1 about centers (2, −1, 1) and (−2, 1, −1), respectively, and $A_3^{(2)}$ and $A_3^{(-2)}$ lie on circles of radius L_3 about centers (1, 1, 2) and (−1, −1, −2). No further information is to be extracted from the known points of the grid.

Now let us make a tentative choice of the point (−2, 2, 0), on the known circle $C_3^{(0)}$. Together with the known point (−1, 2, 1) this determines the circle $C_2^{(2)}$ and its center $A_2^{(2)}$; $C_2^{(2)}$, in turn, completes the determination of the grid intersection (0, 2, 2). By extension of this process, a tentative choice of the point (−2, 2, 0) leads to equally tentative determinations of other elements of the grid, according to the following scheme:

$$
\begin{array}{ll}
(-2, 2, 0) + (-1, 2, 1) \rightarrow A_2^{(2)}, & C_2^{(2)} \rightarrow (0, 2, 2),\\
(0, 2, 2) + (1, 1, 2) \rightarrow A_3^{(2)}, & C_3^{(2)} \rightarrow (2, 0, 2),\\
(2, 0, 2) + (2, -1, 1) \rightarrow A_1^{(2)}, & C_1^{(2)} \rightarrow (2, -2, 0),\\
(2, -2, 0) + (1, -2, -1) \rightarrow A_2^{(-2)}, & C_2^{(-2)} \rightarrow (0, -2, -2),\\
(0, -2, -2) + (-1, -1, -2) \rightarrow A_3^{(-2)}, & C_3^{(-2)} \rightarrow (-2, 0, -2),\\
(-2, 0, -2) + (-2, 1, -1) \rightarrow A_1^{(-2)}, & C_1^{(-2)} \rightarrow (-2, 2, 0).
\end{array}
$$

Thus we arrive finally at a construction for the point (−2, 2, 0), with which the whole process was started. This construction will, in general, lead back to the tentatively chosen initial point only if that choice was made correctly. For example, an incorrect choice of the point (−2, 2, 0) leads to construction of the dashed grid lines of Fig. 9·3. The curvilinear hexagon, traced out in the clockwise direction, fails to close. A second choice of the initial point leads to a different error in closing; interpolation finally leads to a correct choice and the construction shown in bold lines. There are thus determined two additional points on each of the curves C_1, C_2, C_3, and six additional circles in the grid structure.

These six new circles fix additional grid intersections—enough of them, in fact, to determine immediately two more points on each of C_1, C_2, C_3: $A_1^{(3)}$, $A_1^{(-3)}$, $A_2^{(3)}$, $A_2^{(-3)}$, $A_3^{(3)}$, $A_3^{(-3)}$. For example, the intersection of $C_2^{(-2)}$ and $C_3^{(1)}$ determines (3, −2, 1), and that of $C_2^{(-1)}$ and $C_3^{(2)}$ determines (3, −1, 2); these points, in the lower right-hand corner of Fig. 9·3, in turn determine $A_1^{(3)}$ and $C_1^{(3)}$. It is at this point that the flexibility in the design becomes insufficient to permit construction of an exactly ideal grid structure: these new circles should pass through certain triple intersections, but the construction does not assure that they will do so. For instance, the circles $C_1^{(+3)}$, $C_2^{(-3)}$, and $C_3^{(0)}$ should pass through a common point, (3, −3, 0); in Fig. 9·3 it can be seen that they pass very nearly but not exactly through the same point. A similar failure occurs at (3, 0, 3); perfect triple intersections at these points can be obtained only by changing the original arbitrary assumptions. In the present case this would hardly

be worth while, as the linkage already determined has effectively ideal grid structure in a very large domain.

9·3. Grid Generators for Multiplication.—The example of the preceding section should make it clear that it is a simple and straightforward task to design a star grid generator with almost ideal grid structure over a large domain. From a practical point of view this is only a beginning in the work of designing a satisfactory star grid generator for multiplication. Other aspects of this problem will now be indicated.

Like any other grid generator with ideal grid structure in an extended domain, the star linkage of the preceding section can be used in designing a multiplier. Calibration of the scales in terms of the variables

$$z_1 = kr, \qquad z_2 = ks, \qquad z_3 = kt \tag{5}$$

will convert it into an adder with very simple structure, mechanizing the relation

$$z_1 + z_2 = z_3 \tag{6}$$

throughout a domain within which each variable may be either positive or negative. Recalibration in terms of variables x_1, x_2, x_3, determined by

$$\log_{10} x_1 = z_1, \qquad \log_{10} x_2 = z_2, \qquad \log_{10} x_3 = z_3, \tag{7}$$

will convert it into a multiplier mechanizing

$$x_1 x_2 = x_3 \tag{8}$$

throughout a domain in which all variables are positive.

The most obvious disadvantage of such a multiplier is its use of curved slides. A more generally useful device could be designed if the curves C_1, C_2, C_3 were of simple, mechanically desirable forms; elaboration of the star linkage into a multiplier like that of Fig. 8·15 or Fig. 8·16 would then follow the lines indicated in Sec. 8·7. One can in fact bring the curves C_1, C_2, C_3 into desirable forms by making appropriate changes in those elements of the design that were arbitrarily chosen in Sec. 9·2. A satisfactory method for doing this will be indicated in Sec. 9·5, where it can be illustrated in connection with a problem having additional features of interest.

Multipliers designed in this way do not permit change in sign of any factor. If x_1, for instance, is to pass through 0, then z_1 and r must pass through the corresponding value $-\infty$. To accomplish this in a mechanism with finite travel one must have a z_1-scale of finite length; the sequence of points $A_1^{(r)}$ must approach a point of condensation as $r \to -\infty$. Even when one has assured the existence of such a point of condensation, corresponding to $x_1 = 0$, it will be necessary to face the problem of extending the scale into the region of negative x_1.

Such points of condensation have their equivalents in the grid structure of the relation

$$x_1 = \frac{x_3}{x_2}, \tag{9}$$

an alternative form of Eq. (8). In Fig. 9·4 this grid structure is developed about the center $x_2 = x_3 = 1$, with the line $x_1 = 1.25$ chosen as the contour C. The step structure between the contours B and C approaches the origin in an infinite number of steps; the successively added lines of the rectangular grid will tend to fill out the domain $x_2 > 0$, $x_3 > 0$, but will never extend outside this region. The grid is of course ideal, and includes the contours $x_1 = (1.25)^r$, with r taking on all integral values; as $r \to \infty$ these contours approach the horizontal axis, and as $r \to -\infty$ they approach the vertical axis.

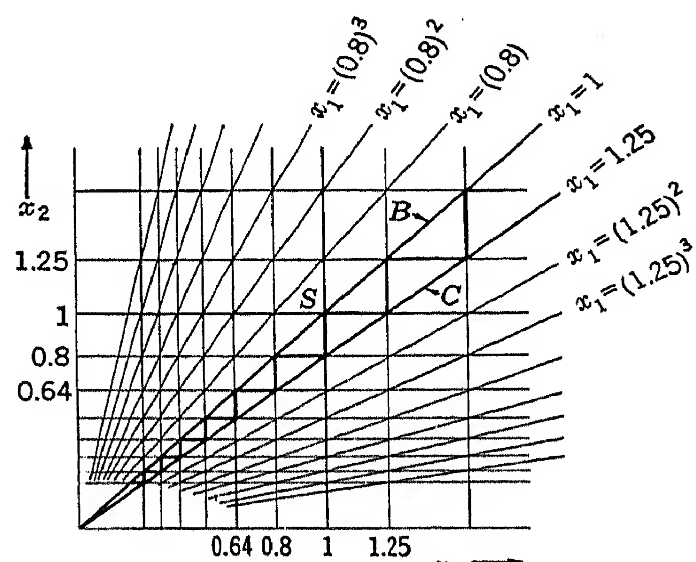

Fig. 9·4.—Grid structure of $x_1 = x_3/x_2$.

To obtain grid structures for this relation in all four quadrants, one must use a separate center for the grid structure in each quadrant. If these four points are chosen in similar positions in the four quadrants, symmetrical with respect to the two axes, and if corresponding contours C are used, then the four grid structures will approach the coordinate axes symmetrically. They will then appear to flow smoothly into each other in crossing these axes, and the whole figure will take on the appearance of a single grid structure (Fig. 9·5). It is important, however, to remember that this result is obtained artificially, and that the coordinate axes are lines of condensation in the grid structure.

A topological transformation of Fig. 9·5 that would carry the three families of straight lines into three families of circles of constant radius would convert it into the ideal grid structure of a star linkage. To each circle of this grid structure there would correspond an integral value of r, s, or t, and a calibration point on one of the scales; to the circles obtained by transformation of the coordinate axes there would correspond points of condensation of the scale calibrations. Such a star linkage would thus have the characteristics to be demanded in a grid generator for a multiplier that must allow change of sign in the variables.

We shall now use this idea as a guide in designing a very satisfactory star grid generator for multiplication.

9·4. A Topological Transformation of the Grid Structure of a Multiplier.—Let us attempt to transform the grid structure of Fig. 9·5 (cartesian coordinates x_2, x_3) into an ideal grid structure in which each of the three families of straight lines in the original structure is represented by a family of congruent circles (cartesian coordinates y_2, y_3).

First, let us consider the family of lines of constant x_1. In the original grid structure all these lines intersect at a common point O. Such a property will not be changed by a topological transformation; in the

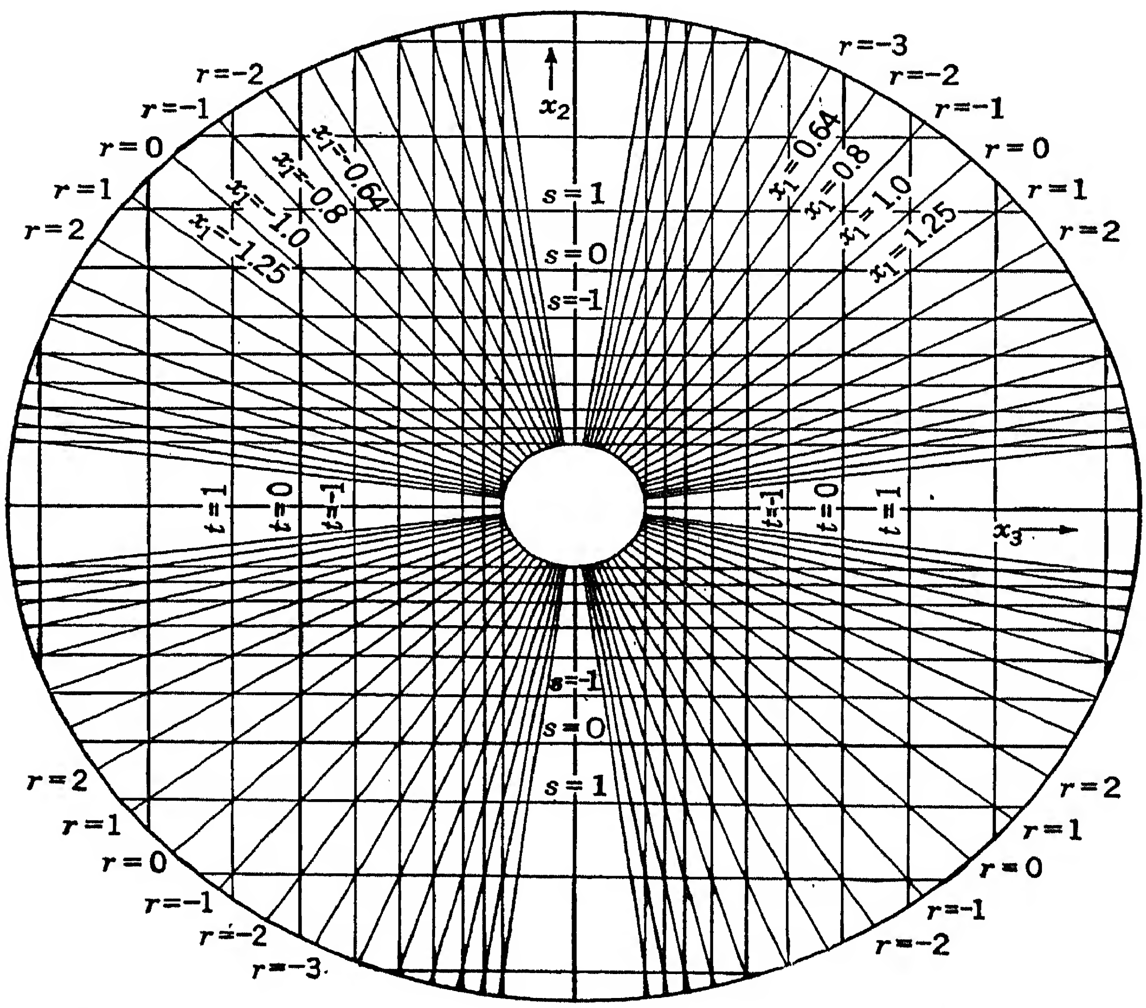

FIG. 9·5.—Grid structure of a multiplier or divider permitting changes in sign of the variables.

transformed grid structure the corresponding family of circles of radius L_1 must all intersect at a common point O'. (See Fig. 9·6.) It follows that the centers of these circles must all lie on a circular arc ab with radius L_1 and center at O'. The radius L_1 can be chosen at will, as the problem is independent of the scale of construction; it is usually convenient to take L_1 as the unit of length.

The relation between a given straight line of the original grid structure and the circle into which it is transformed may be established by examining the topological transformation in the neighborhood of the

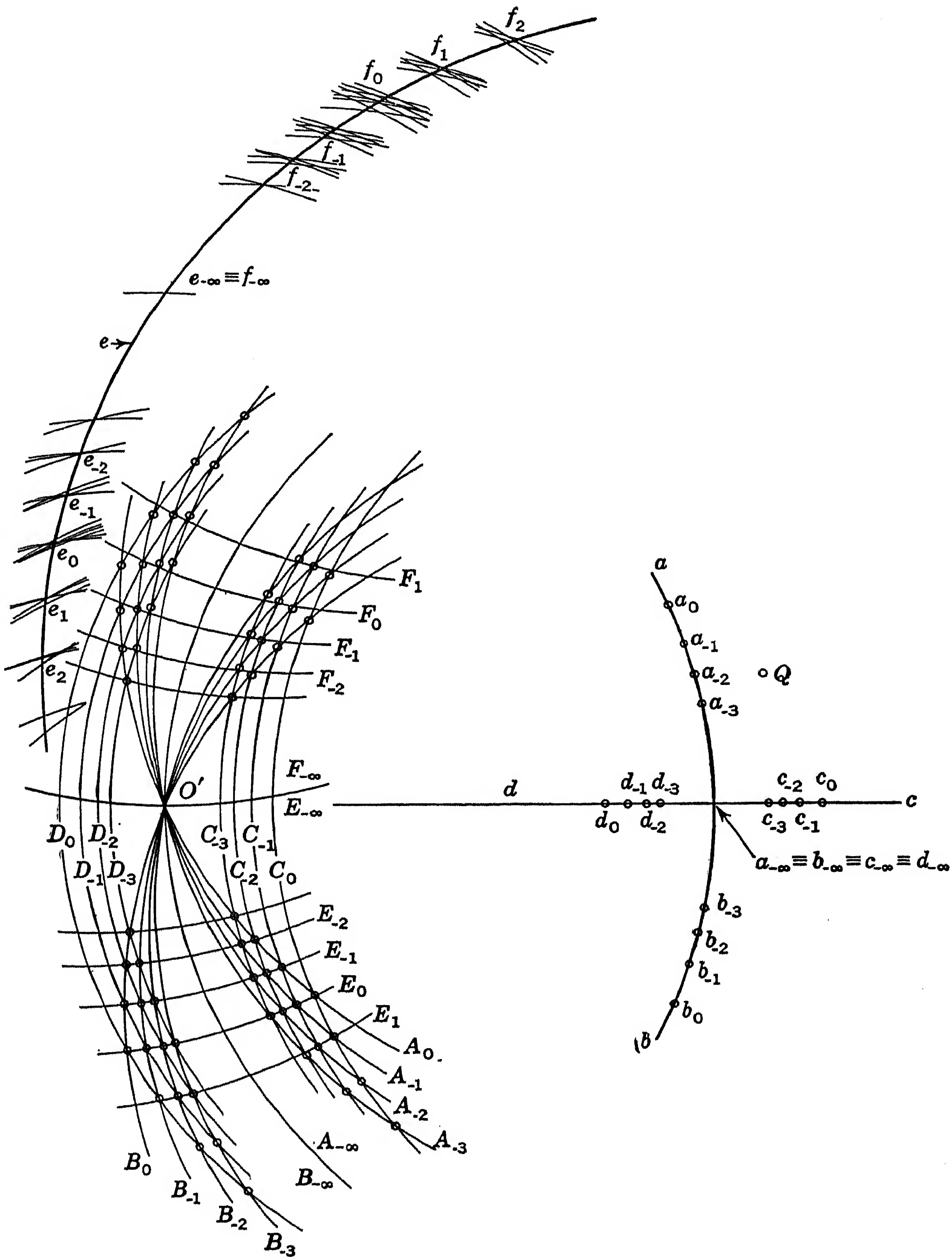

FIG. 9·6.—First topological transformation of the grid structure of a multiplier.

origin O. In its general form this transformation is

$$\left.\begin{aligned} x_2 &= x_2(y_2, y_3), \\ x_3 &= x_3(y_2, y_3). \end{aligned}\right\} \tag{10}$$

In the neighborhood of O, where all variables can be treated as small quantities, this reduces to

$$\left.\begin{aligned} x_2 &= c_{22}y_2 + c_{23}y_3, \\ x_3 &= c_{32}y_2 + c_{33}y_3, \end{aligned}\right\} \tag{11}$$

on neglect of small quantities of the second order (This, of course, is valid only if O is not a singular point of the transformation.) Let us assume that the *transformed grid structure is symmetrical with respect to the horizontal axis*, in the neighborhood of the origin. Then we must have

$$c_{23} = c_{32} = 0, \tag{12}$$

and

$$\frac{x_3}{x_2} = \frac{c_{33}}{c_{22}}\frac{y_3}{y_2}, \tag{13}$$

in the immediate neighborhood of O. In other words, a line of slope x_1 at the origin O of the original grid structure is transformed into a curve through the origin O' with slope changed by the constant factor (c_{33}/c_{22}). Since the slopes of the successive x_1-contours in Fig. 9·5 change in a geometric progression, the slopes at O' of the corresponding circles must also change in geometric progression, and by the same ratio (1.25). This is true also of the slopes of the radii from the origin O' to the centers of these circles, which are the negative reciprocals of the slopes of the circles themselves. Choosing arbitrarily a value of c_{33}/c_{22}, we can then construct, in the transformed grid structure, circles corresponding to each of the lines of constant x_1 in the original grid structure. In Fig. 9·6 there are indicated four of these circles (A_0, A_{-1}, A_{-2}, A_{-3}) with centers above the horizontal axis at points a_0, a_{-1}, a_{-2}, a_{-3}; the distinguishing subscripts are the r values of the original grid lines, which lie in the second and fourth quadrants of Fig. 9·5. The corresponding lines in the first and third quadrants transform into the circles B_0, B_{-1}, B_{-2}, B_{-3}, with centers b_0, b_{-1}, b_{-2}, b_{-3}, which are the mirror images of a_0, a_{-1}, a_{-2}, a_{-3}, in the horizontal axis. The sequence of points a_0, a_{-1}, a_{-2}, . . . , which lies in the domain of positive x_1, has a point of condensation $a_{-\infty}$ on the horizontal axis; an extension of the x_1-scale into the domain of negative x_1 is provided by the symmetrically placed sequence b_0, b_{-1}, . . . , which has the same point of condensation. This point is of course the center of the circle into which the vertical axis of the original grid structure is transformed.

Consideration of this family of circles will make it clear that there exists no topological transformation of the type under discussion which maps the whole of the (x_2, x_3)-plane onto the (y_2, y_3)-plane. The original contours of constant x_1 intersect only at the origin and at infinity, but the circles into which we are attempting to transform them may intersect anywhere in the (y_2, y_3)-plane, if arbitrarily large values of r or x_1 are admitted. We can at best hope to establish a topological transformation that carries a *portion* of the original grid structure (certainly one within which the magnitude of x_1 is limited) into a grid structure consisting of arcs of circles. This is quite sufficient for our purposes, since $r = -\infty$, $x_1 = 0$, are not excluded from the domain of the transformation.

Now let us consider the family of circles of constant x_3. Since the original lines $x_3 = c$ were symmetrical with respect to the horizontal axis, it is natural to give the transformed circles similar symmetry; their centers must lie on the horizontal axis cd. The vertical axis $x_3 = 0$ is already known to be transformed into a circle of radius L_1, with center at $A_{-\infty}$. It follows that this second family of circles must have the same radius as the first: $L_3 = L_1$. Since the lines $x_3 = x_3^{(t)}$ converge on $x_3 = 0$ as $t \longrightarrow -\infty$, the point $a_{-\infty}$ must be a point of condensation on the x_3-scale, as well as on the x_1-scale. The lines of the original grid intersect the x_3-axis at $x_3^{(t)}$; the transformed circles must intersect the y_3-axis at points determined by

$$x_3^{(t)} = x_3(0, y_3^{(t)}), \tag{14}$$

or, in the immediate neighborhood of O', by

$$x_3^{(t)} = c_{33}y_3^{(t)}. \tag{15}$$

The values of $x_3^{(t)}$ go to zero in a geometrical progression (ratio 1.25) as $t \longrightarrow -\infty$. It follows that the sequence of values $y_3^{(t)}$ approaches zero, and the centers of the x_3 circles approach $a_{-\infty}$, in a similar progression as $t \longrightarrow -\infty$. As a first attempt to find a transformation of the desired character, let us assume that this geometrical progression is exact, rather than an approximation valid only in the neighborhood of O'; that is, we assume that Eq. (15) is valid for all t. Then, after choosing arbitrarily a value of c_{33}, we can construct the circle corresponding to any x_3-line of the original grid structure. In Fig. 9·6 there are shown eight of these circles, with centers c_0, c_{-1}, c_{-2}, c_{-3}, and d_0, d_{-1}, d_{-2}, d_{-3}. (The subscript is the index t.) The c's lie in the domain of positive x_3, and have a condensation point at $x_3 = 0$; the d's provide, somewhat artificially, an extension of the scale into the domain of negative x_3.

The assumptions made up to this point [transformation of the x_1- and x_3-contours into families of circles symmetrical to the horizontal axis, validity of Eq. (15), and special values of c_{22} and c_{33}] determine two

families of intersecting circles, and thereby determine completely the nature of the topological transformation. It remains to be seen whether this transformation has the desired character—whether the x_2-contours are also transformed into a family of circles with common radius L_2. It is immediately evident that this is not the case. In Fig. 9·6 there appear 64 points of intersection of the x_1- and x_3-contours, distinguished by small circles. These are the transformed positions of the intersections in the original grid, and through them must pass the transformed contours of constant x_2. It will be observed that the intersections in the lower half of the grid lie on curves that are concave upward, whereas those in the upper half lie in curves (not shown) that are concave downward. By the symmetry of the construction, the straight line $x_2 = 0$ must be transformed, not into a circle, but into the straight line $y_2 = 0$; the radii of curvature of the other x_2-contours increase as they approach this limiting straight line. The transformed ideal grid structure is not that of a star linkage; indeed it is evident that if such a grid structure exists it must be an unsymmetrical one. We can, however, approximate this grid structure by the nonideal grid structure of a star linkage, replacing the system of x_2-contours of the ideal grid structure by a system of approximating circles of the same radius. This "approximately ideal" grid structure, which does have the other characteristics that we desire, will later be made much more nearly ideal by readjustment of the design constants.

It is possible to pass circles very nearly through all the intersections in the lower half plane of Fig. 9·6, by choosing a mean value L_2 for the radius of curvature and locating the centers of the circles in the upper half plane. This will establish the general position of x_2-scale, and will make it necessary to pass through the intersections of the upper half plane circular arcs that are concave upward; the fit there cannot be very good, and we must split the errors of construction as well as possible.

The best way to do this is to construct a circle through one set of intersections in order to establish a radius L_2. (In Fig. 9·6, E_0 is the circle in question, and the radius chosen is just equal to L_1 and L_3.) With this radius, we construct arcs about each of the known grid intersections. If the grid structure under construction were to be ideal, the arcs characterized by a given value of $s = t - r$ would all intersect in a common point. This is not the case here; instead of points of intersection there exist more or less diffuse regions of intersection, within which we can locate the centers of the grid circles with some degree of arbitrariness. This arbitrariness can be used to good advantage. If a simple mechanization of the grid structure is to be possible, the x_2-scale must lie in a simple curve, preferably a straight line or a circle. In the present case, the regions of intersection lie roughly on a circle. In particular, the circular arc e, with center at Q, passes nicely through all regions of inter-

section except for three at the extreme ends. This circle will be taken as the x_2-scale on this scale, and as near to the centers of the regions of intersection as is possible we choose the centers e_1, e_0, e_{-1}, . . . of the grid structure circles E_1, E_0, E_{-1}, . . . in the lower half plane, and the centers f_1, f_0, f_{-1}, . . . , of the grid structure circles F_1, F_0, F_{-1}, . . . , in the upper half plane. The grid structure circles must converge on a

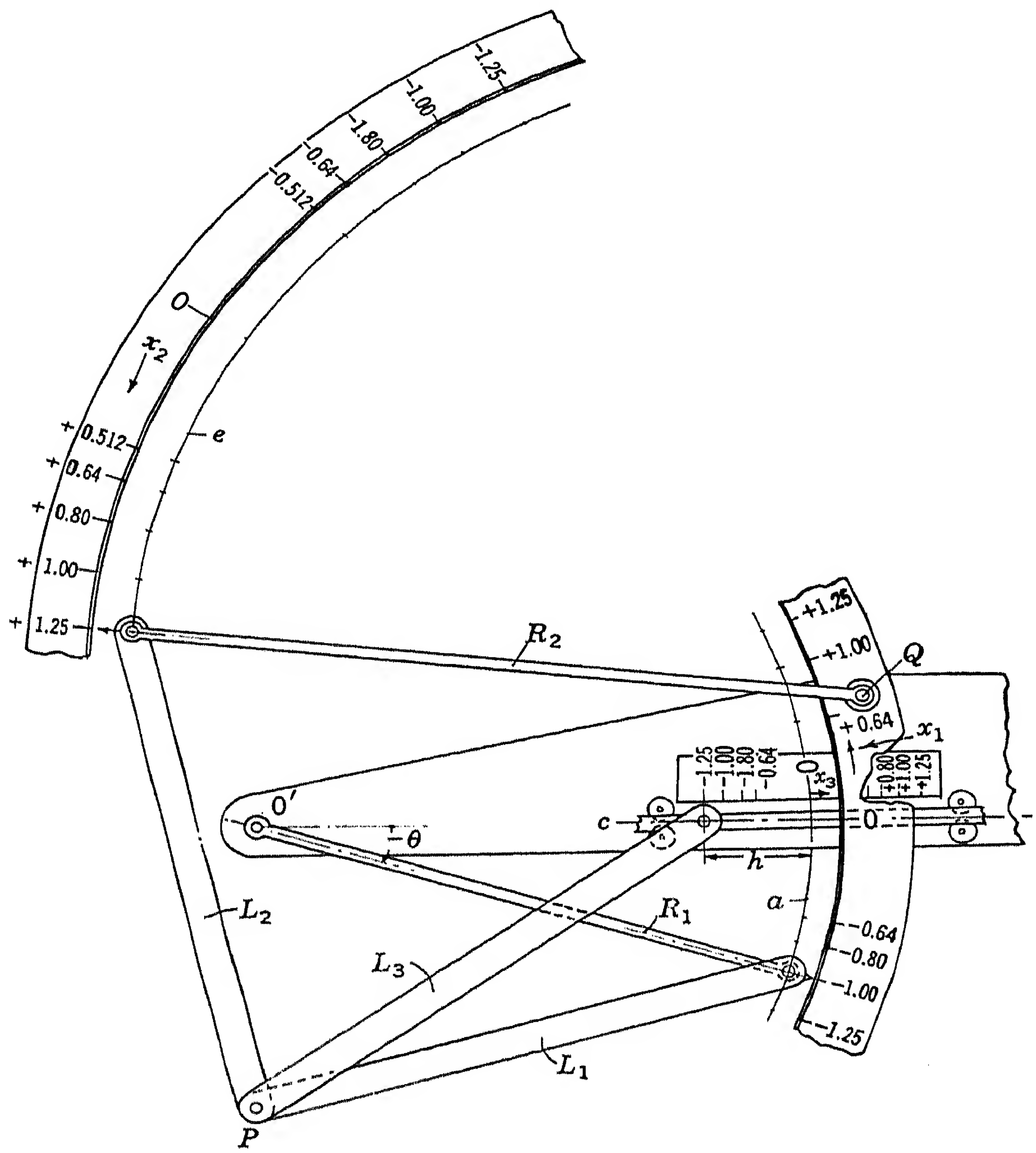

FIG. 9·7.—First approximate multiplier.

circle $E_{-\infty} = F_{-\infty}$ through the origin O'. The center of the circle $E_{-\infty}$ is $e_{-\infty} \equiv f_{-\infty}$, the point of condensation of the point sequence e_s in the positive domain of x_2, and of the point sequence f_s in the negative domain, as $s \to -\infty$; it is the zero point on the x_2-scale. This completes the determination of the constants of the star linkage.

The grid structure of Fig. 9·6 is mechanized by the approximate multiplier sketched in Fig. 9·7. This consists of a star grid generator

with arms L_1, L_2, L_3, meeting at a common joint P. The free end of L_1 is forced to move along a circle a with center O', and the free end of L_2 along a circle e with center Q, by arms R_1 and R_2, respectively; the free end of L_3 moves in a straight slide c. It follows from the theory of the transformation that the lengths of L_1, L_3, and R_1 must be equal; L_2 also has this length, but only accidentally. To use this device as a multiplier, the scales must be calibrated in terms of the variables x_1, x_2, x_3, related to the indices r, s t, by Eqs. (5) and (7). The scale points of Fig. 9·6 thus occur for values of x_1, x_2, x_3, which change in geometric progression; these are the scale points shown in Fig. 9·7. One can easily show that

$$x_1 = K_1 \tan \theta, \tag{16}$$
$$x_3 = K_3 h. \tag{17}$$

Calibrations on the x_2-scale follow (though not uniquely, since the multiplier is not exact) from the relation $x_3 = x_1x_2$.

The reader should sketch this mechanism for $x_1 = 0$ and for $x_2 = 0$, in order to see why in these cases the value of x_3 is necessarily zero. He will also be able to show by simple geometry why the multiplication is almost exact for small values of x_1 and x_2.

9·5. Improvement of the Star Grid Generator for Multiplication.—The errors in the multiplier of Fig. 9·7 appear very clearly in its grid structure, in which many of the triple intersections characteristic of ideal grid structure have disintegrated into small triangles. To improve this design we must change one or more of the families of grid circles in such a way as to reduce the size of these triangles. This can be done by a method that is useful whether the function to be mechanized has ideal or nonideal grid structure.

Let us examine the possibility of improving the grid structure of Fig. 9·6 by changing the family of circles CD, while keeping fixed the families AB and EF. In Fig. 9·8 there are shown eight of the circles AB and 10 of the circles EF, defining 80 points of intersection through which circles CD should pass. It has already been noted that the circles CD must have the same radius as the circles AB; to improve the grid structure we can change only the positions of their centers. Let us attempt to do this by the method of the preceding section, drawing arcs of radius L_3 about the 80 intersections of the grid. As before, the arcs with a common index t do not intersect in a common point, as they must if an ideal grid structure is to be obtained. Instead, we observe an interesting and characteristic phenomenon: arcs with centers in the same quadrant of the grid structure intersect nicely in a series of points that define a curved x_3-scale—but a different scale for each quadrant. This is due to the fact that the four quadrants of the original grid structure are actually independent, and have been associated with each other in a

symmetrical, but essentially artificial, manner. In Fig. 9·8 the points corresponding to positive x_2 have been marked with small circles, the others with dots.

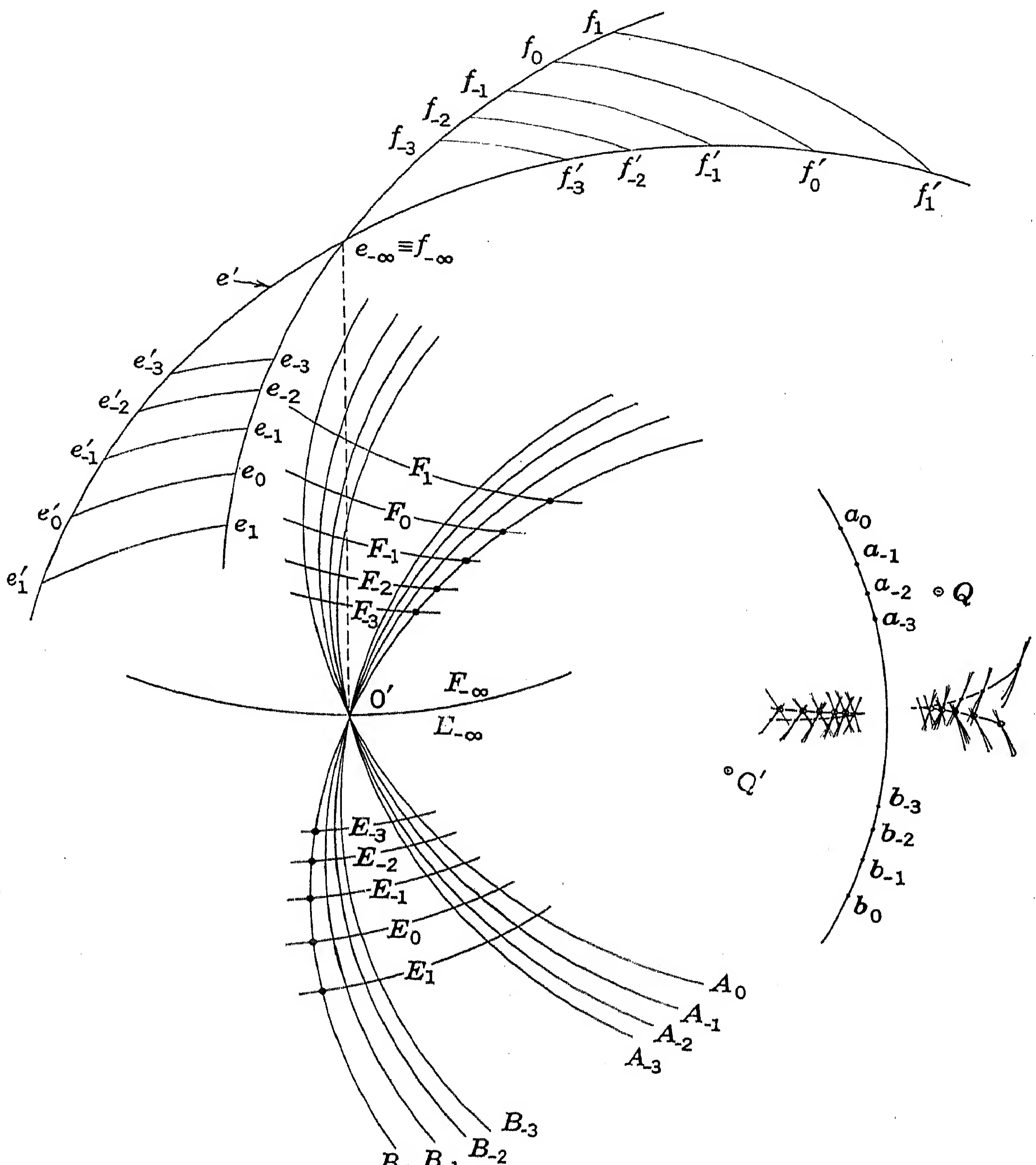

FIG. 9·8.—First step in redesigning the multiplier grid structure.

It is evident that we can add circles CD to produce a grid structure that is nearly ideal in various pairs of quadrants—those with $x_2 > 0$, or with $x_2 < 0$, or $x_1 > 0$, or $x_1 < 0$—but that it will then be far from ideal in the other pair of quadrants. To state it differently, we can

combine the scale segments of Fig. 9·8 in several ways to form an x_3-scale, obtaining a multiplier that will be very accurate so long as one of the factors has a particular sign, but much less accurate when it has the other sign. On the other hand, the difference between the diverging scale segments is too great to permit a satisfactory compromise; no choice of form for the x_3-scale can make the grid structure nearly ideal in all quadrants. *To obtain an ideal grid structure the circles AB and EF must be so chosen that the diverging x_3-scale segments coalesce to form a single x_3-scale.* This method of stating the problem reduces it to an especially convenient form, which can be solved by alternately adjusting the circles AB and EF. We shall choose to change first the family of circles EF.

In varying the grid structure there are two important principles to be observed:

1. The grid structure should not be given more than one degree of freedom at a time.
2. The grid structure should not be excessively sensitive to changes in the varied parameters. This can often be assured by changing parameters in such a way that certain elements of the grid structure remain unchanged.

For example, to improve the grid structure of Fig. 9·8 let us rearrange the circles EF without changing their common radius. Let us maintain the circular form of the x_2-scale, but rotate it about the point $e_{-\infty} \equiv f_{-\infty}$, thus keeping unchanged the circle $E_{-\infty} \equiv F_{-\infty}$. This rotation gives the one degree of freedom that we desire in the problem, according to Principle 1; we must therefore remove all freedom in the calibration of the scale. By Principle 2, the rule for this calibration must be such that the grid structure changes only slowly with rotation of the x_2-scale; we shall therefore demand that it keep unchanged the grid intersections marked with bold dots in Fig. 9·8.

Let rotation of the x_2-scale, e, about the point $e_{-\infty}$ carry it into the position e' (Fig. 9·8). The calibration points e'_s, f'_s on this new scale must lie at distance L_2 from the corresponding fixed grid intersections, and are easily constructed. The new system of grid circles $E'F'$ can then be drawn, and finally, by constructing arcs about the new grid intersections, the new set of x_3-scale segments. Thus the whole construction does have one degree of freedom, and it is easy to study the effect on the form of the x_3-scale segments of rotating the x_2-scale. Trial will show that rotation of the scale in a clockwise direction brings closer together the two x_3-scale segments to the right of $a_{-\infty}$; by an interpolation or extrapolation one finds a rotation of e which makes the separation of these scale segments very small. This is the rotation shown in Fig. 9·8, the tentatively chosen

rotation having been omitted as of little interest. The new scale and the new circles $E'F'$ are shown in Fig. 9·9, together with the new form of the x_3-scale construction. The improvement in the agreement of the x_3-scale segments on the right is very striking, but adjustment of the circles AB will be required to improve the agreement on the left.

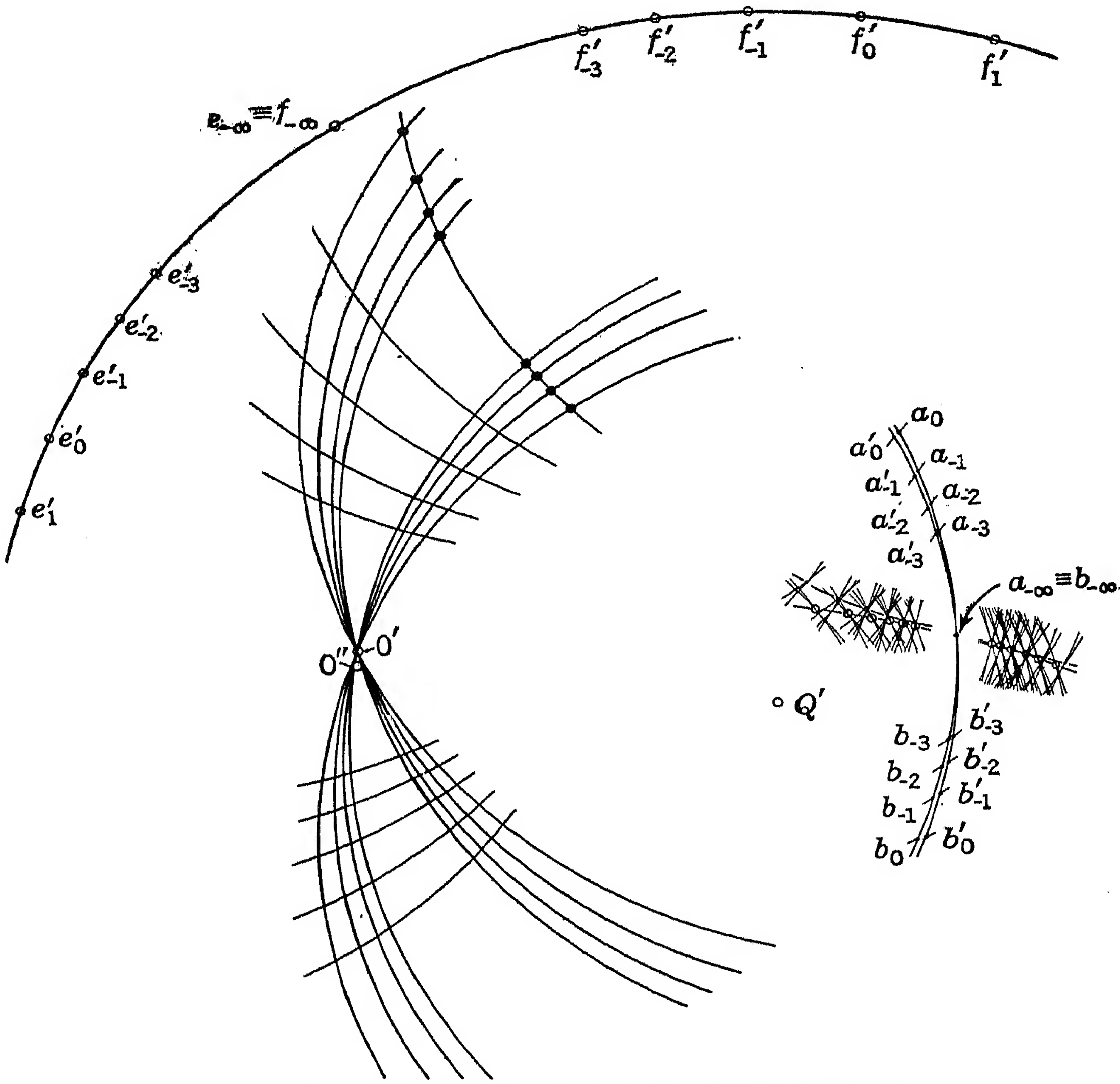

FIG. 9·9.—Second step in redesigning the multiplier grid structure.

To improve the grid structure further let us rearrange the circles AB without changing their radii. To do this we shall keep fixed the form of the x_1-scale, ab, while rotating it about the point $a_{-\infty}$. Calibrations on the new scale will be held at a fixed distance L_1 from the grid intersections indicated by bold dots in Fig. 9·9. With these changes we must make one other change, which has no parallel in the step previously described. Rotation of the x_1-scale will move its center from O' to O''.

The new circles AB will all intersect at this point, through which there must also pass the convergence limit of the circles EF, $E_{-\infty}$. It is therefore necessary to keep L_2 always equal to the distance from $e_{-\infty}$ to O'' as the x_1 scale is rotated. We have then to consider a simultaneous variation of both the circles AB and EF, but it is a variation with one degree of freedom which offers no difficulties.

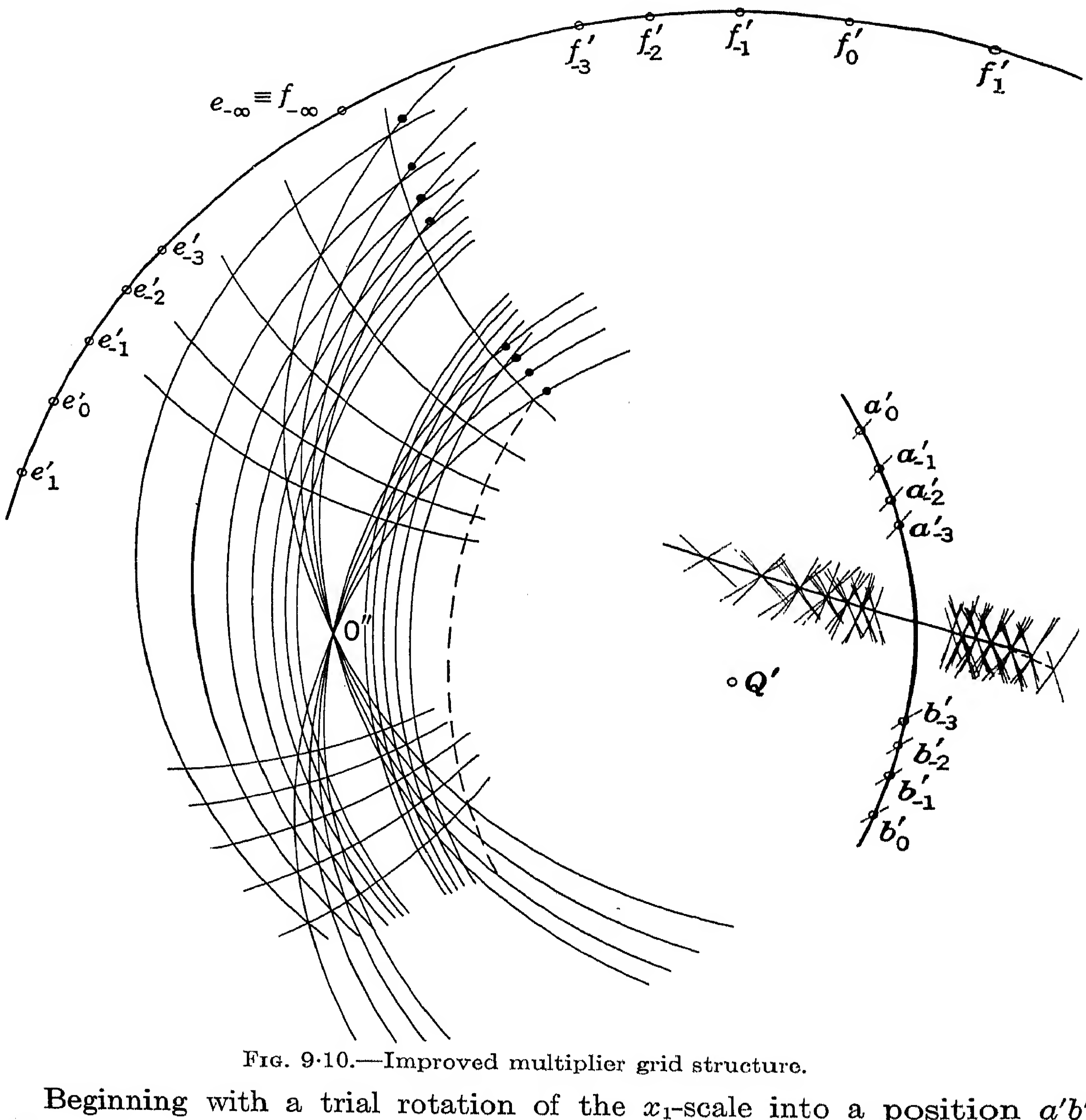

FIG. 9·10.—Improved multiplier grid structure.

Beginning with a trial rotation of the x_1-scale into a position $a'b'$ (Fig. 9·9), one can establish calibration points a'_r, b'_r by drawing arcs about the chosen points of the original grid. The AB circles can then be constructed, the new L_2 determined, and the EF circles constructed. Finally, the new x_3-scale segments can be established, and the best angular position for the x_1-scale determined by an interpolation or

extrapolation. In Fig. 9·10 this construction is shown for an x_1-scale determined by such an interpolation.[1] The four x_3-scale segments do not

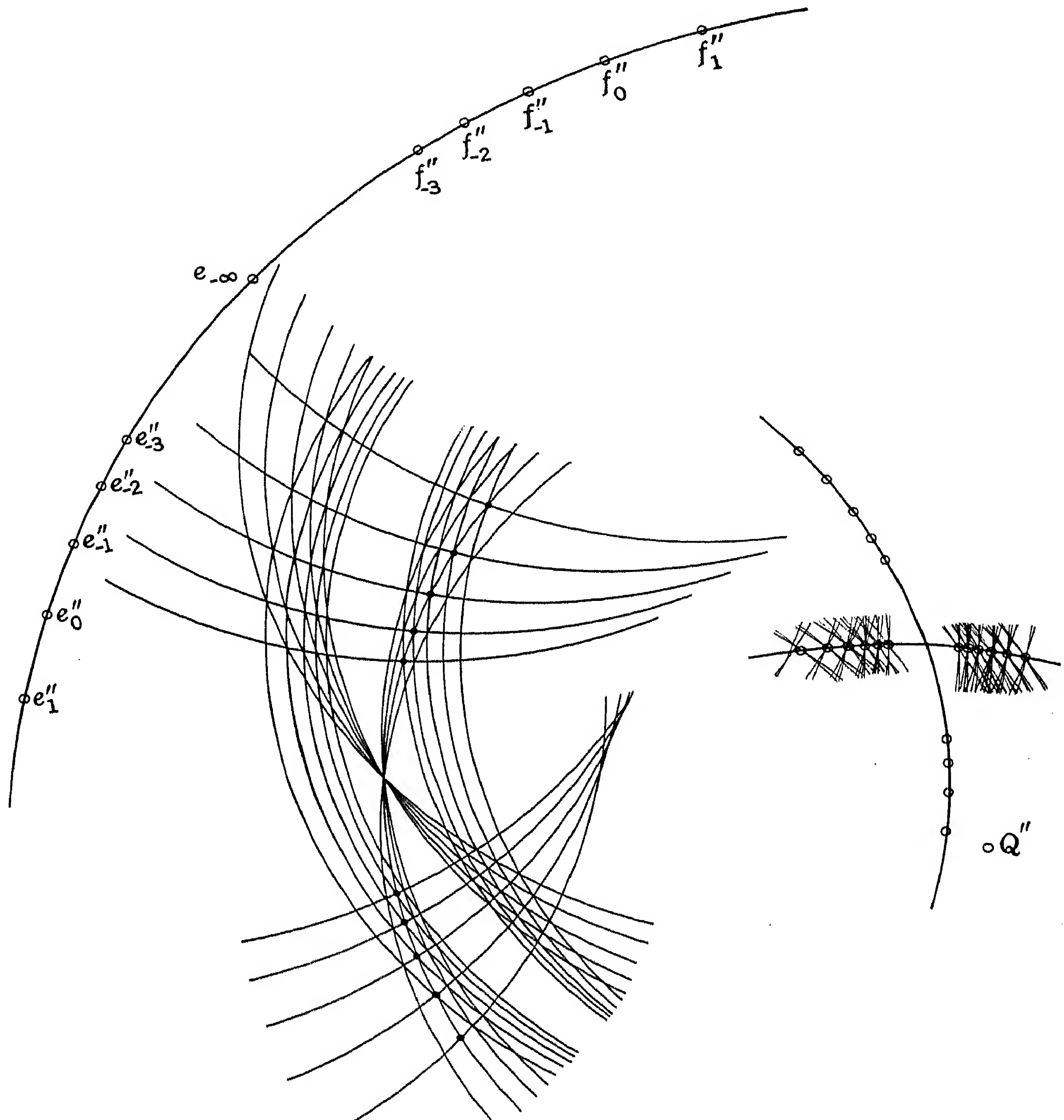

FIG. 9·11.—Multiplier grid structure with circular x_3-scale.

merge exactly, but the groups of arcs make acceptably sharp intersections, through which a straight line can be laid by a small sacrifice in the fit at the extreme right end of the scale. The circles *CD* constructed about

[1] It will be observed that, because of the change in L_2, all grid intersections have been shifted, even those used in constructing the new x_1-scale. (Old positions are shown by bold dots in Fig. 9·10.) This is not a matter of importance; all that is required of the construction is that it shall not shift the grid structure too violently.

points on this rectified x_3-scale are shown in Fig. 9·10. In view of the small number of steps required, the result can be considered very satisfactory: the grid structure is so nearly ideal over a wide domain that analytical methods can be employed for its further improvement.

It is evident that the grid structure of Fig. 9·10 is not the only possible solution of our original problem. The grid structure of Fig. 9·8 could

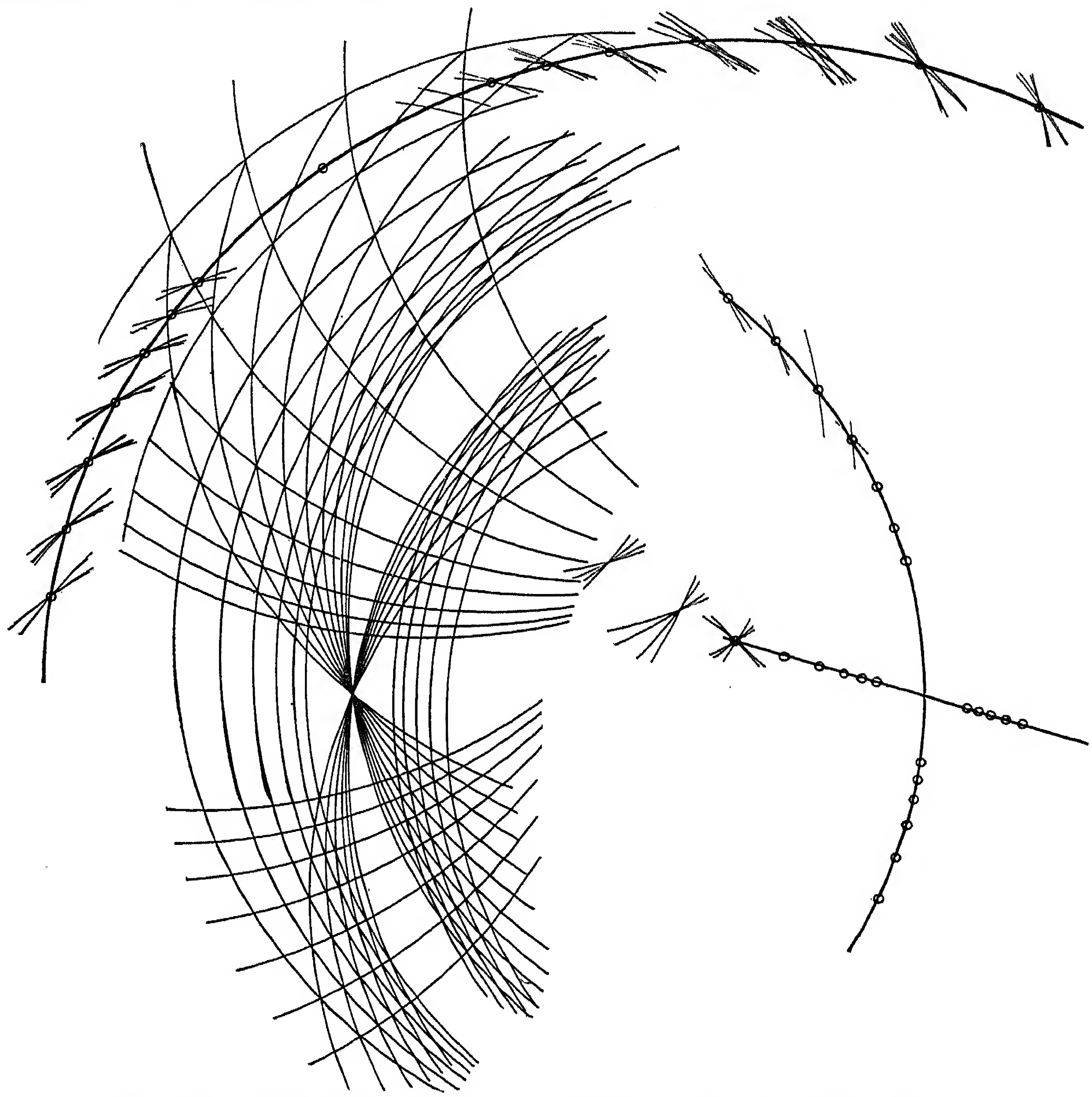

FIG. 9·12.—Multiplier grid structure ideal through a very large domain.

have been varied in many ways other than those described above to obtain even larger domains of nearly ideal grid structure, and different forms of the scales. Indeed, this method is as useful for control of the form and extent of scales as it is for the improvement of grid structures. For instance, the linear x_3-scale of Fig. 9·10 is easily converted into the circular arc shown in Fig. 9·11. This form was obtained by rearranging the circles $E'F'$, this time by increasing the radius of the x_2-scale, while

keeping fixed the points $e'_{-\infty}$ and e'_{-1}. New scale calibrations were so chosen as to keep fixed the grid intersections indicated by bold dots in Fig. 9·11. This figure shows also the new family of circles EF, and the resulting circular form of the x_3-scale; the curvature of this can be changed at will by choosing a new center Q'' for the x_2-scale. A more elaborate series of variations leads to the grid structure shown in Fig. 9·12, with nearly straight scale. The outstanding characteristic of this grid structure is the large domain within which it remains effectively ideal.

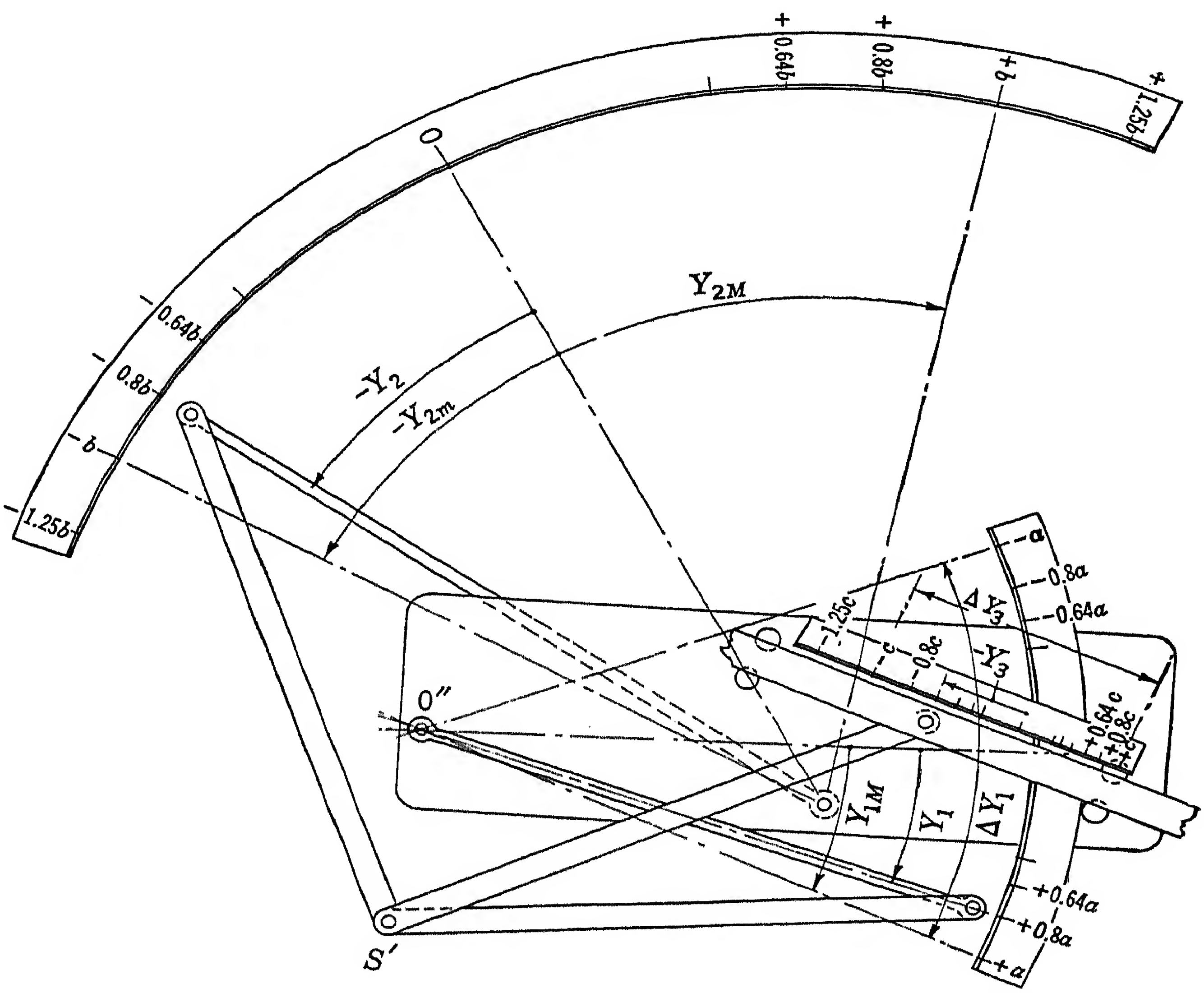

FIG. 9·13.—Improved multiplier, with the grid structure shown in Fig. 9·10.

9·6. Design of Transformer Linkages.—The grid structure of Fig. 9·10 suggests the design for a multiplier shown in Fig. 9·13. The structure of this multiplier is the same as that of Fig. 9·7; increased accuracy has been obtained by changes in the dimensions, but the number and relations of the elements remain unchanged. The ranges of the variables can be changed with some freedom: the readings on the x_1-, x_2-, and x_3-scales can be changed by factors a, b, and c, respectively, provided only that

$$ab = c. \tag{18}$$

Such a multiplier, with nonuniform scales, is of limited interest; the real importance of this device lies in the possibility of using it to drive a computer. In such an application it may be regarded as an ideal grid generator and used together with transformer linkages in the *linear* mechanization of the relations

$$x_3 = x_1x_2, \tag{19}$$
$$x_3 = f_1(x_1)f_2(x_2), \tag{20}$$

or indeed of any functional relation with ideal grid structure. If a linear mechanization of Eq. (19) is required, the function of the transformer linkages may be regarded as that of replacing the nonuniform scales of Fig. 9·13 by uniform scales; in other cases the transformer linkages serve also as function generators.

Let us consider first the problem of designing a multiplier with uniform scales. To describe the configuration of the grid generator we may use internal parameters Y_1, Y_2, Y_3, defined in Fig. 9·13. The scales shown in the figure establish a nonlinear relation of the variables x to the parameters Y,

$$x_r = (x_r|Y_r) \cdot Y_r, \qquad r = 1, 2, 3, \tag{21}$$

which can be determined, for instance, by measurement of the figure. We wish now to establish the same relation between the parameters Y and the variables x as indicated on *uniform* scales. We introduce transformer linkages which present new terminals, described by external parameters X_1, X_2, X_3. These external parameters are related to the internal parameters by the linkage equations

$$X_r = (X_r|Y_r) \cdot Y_r, \qquad r = 1, 2, 3, \tag{22}$$

and to the variables x_1, x_2, x_3, by linear relations,

$$x_r = x_r^{(0)} + K_r(X_r - X_r^{(0)}), \tag{23}$$

which may be symbolized by

$$x_r = (x_r||X_r) \cdot X_r. \tag{24}$$

Our problem is to find linkages such that the linkage operators satisfy the relations

$$(x_r|Y_r) = (x_r||X_r) \cdot (X_r|Y_r), \qquad r = 1, 2, 3. \tag{25}$$

This problem takes on a completely familiar form when it is expressed in terms of homogeneous parameters and variables: θ_1, θ_2, θ_3, corresponding to Y_1, Y_2, Y_3; H_1, H_2, H_3, corresponding to X_1, X_2, X_3; h_1, h_2, h_3, corresponding to x_1, x_2, x_3. In terms of homogeneous parameters and variables a linear transformation reduces to the identical transformation, and Eq. (25) reduces to

$$(h_r|\theta_r) = (H_r|\theta_r). \tag{26}$$

Our problem is thus to find linkages with operators $(H_r|\theta_r)$ having the known form of $(h_r|\theta_r)$, subject to the condition that the input parameters Y_r have a given character—that they are, for instance, angular parameters with a specified angular range. This is exactly the type of problem discussed in Chaps. 4 to 6.

As an example of the use of the same grid generator in linearly mechanizing another functional relation with ideal grid structure, we may consider the problem of mechanizing Eq. (20) with linear scales in x_1, x_2, x_3.

TABLE 9·1.—CHARACTERISTICS OF THE SCALES OF FIG. 9·13

x_1/a	Y_1, degrees	h_1	θ_1
−1.000	−22.3	0.000	0.000
−0.800	−17.6	0.100	0.106
−0.640	−14.0	0.180	0.187
−0.512	−11.1	0.244	0.252
0.000	0.0	0.500	0.502
0.512	11.1	0.756	0.752
0.640	13.9	0.820	0.815
0.800	17.4	0.900	0.894
1.000	22.1	1.000	1.000
x_2/b	Y_2, degrees	h_2	θ_2
−1.000	−33.7	0.000	0.000
−0.800	−27.8	0.100	0.071
−0.640	−22.6	0.180	0.132
−0.512	−19.9	0.244	0.165
0.000	0.0	0.500	0.403
0.512	19.9	0.756	0.642
0.640	25.2	0.820	0.705
0.800	32.1	0.900	0.787
1.000	49.9	1.000	1.000
x_3/c	Y_3	h_3	θ_3
−1.000	−0.264	0.000	0.000
−0.800	−0.198	0.100	0.148
−0.640	−0.148	0.180	0.260
−0.512	−0.112	0.244	0.341
0.000	0.000	0.500	0.592
0.512	0.098	0.756	0.811
0.640	0.120	0.820	0.861
0.800	0.147	0.900	0.921
1.000	0.182	1.000	1.000

The quantities to be multiplied are

$$\left.\begin{aligned} z_1 &= f_1(x_1), \\ z_2 &= f_2(x_2). \end{aligned}\right\} \tag{27}$$

The x_1- and x_2-scales of Fig. 9·13 are then to be interpreted as scales of z_1 and z_2; the relation of x_1 to Y_1 and x_2 to Y_2 follows from the observed relations of z_1 to Y_1 and z_2 to Y_2, together with Eqs. (27). Except for this difference of detail in establishing the form of the operators $(x_r|Y_r)$, the procedure of the preceding paragraph applies without change. The completed mechanism may be of exactly the same type as the multiplier

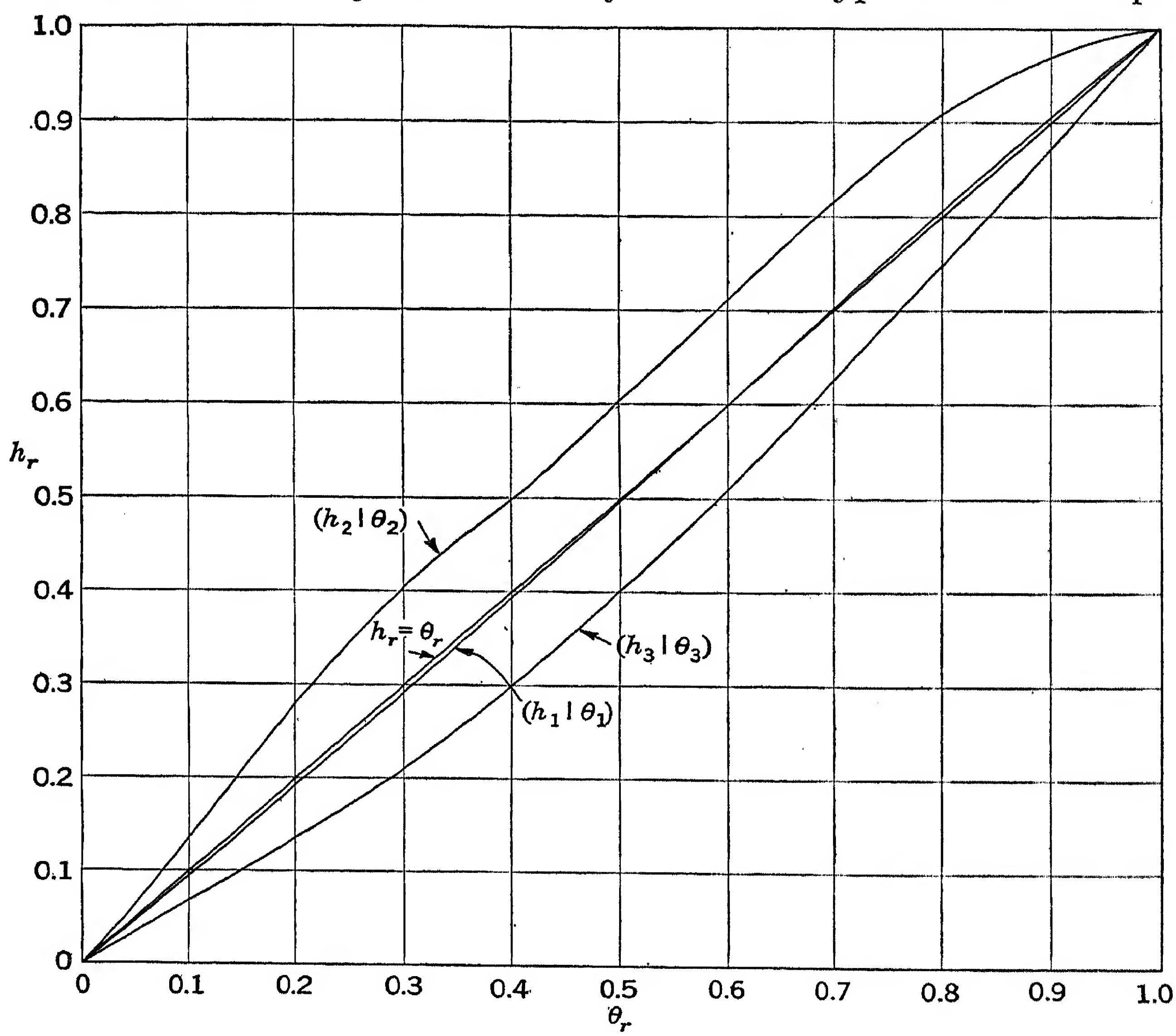

FIG. 9·14.—Operators $(h_r|\theta_r)$ for the multiplier, Fig. 9·13.

itself, or of even simpler form. It is, indeed, one of the important virtues of bar-linkage generators of functions of two independent variables that their complexity does not necessarily increase with the complexity of the analytic form of the function, as its does with conventional computers. This fact will appear most clearly in the next chapter.

As an example of the form of the linearizing operators, we may consider those needed for the multiplier in Fig. 9·13, if the ranges of motion

are to be those indicated in that figure. Table 9·1 shows the value of each variable at the indicated points of calibration, the corresponding value of the associated parameter, andthe homogeneous variables h and θ at each point. The operators $(h_r|\theta_r)$ are plotted in Fig. 9·14. It will be noted that the operator $(h_2|\theta_2)$ shows an appreciable discontinuity in slope when $h_2 = 0.5$. This is due to the still imperfect match between the four quadrants of the transformed nomogram.

The type of linkage used for each transformer will depend both on the nature of the function and on the type of output terminal desired. In

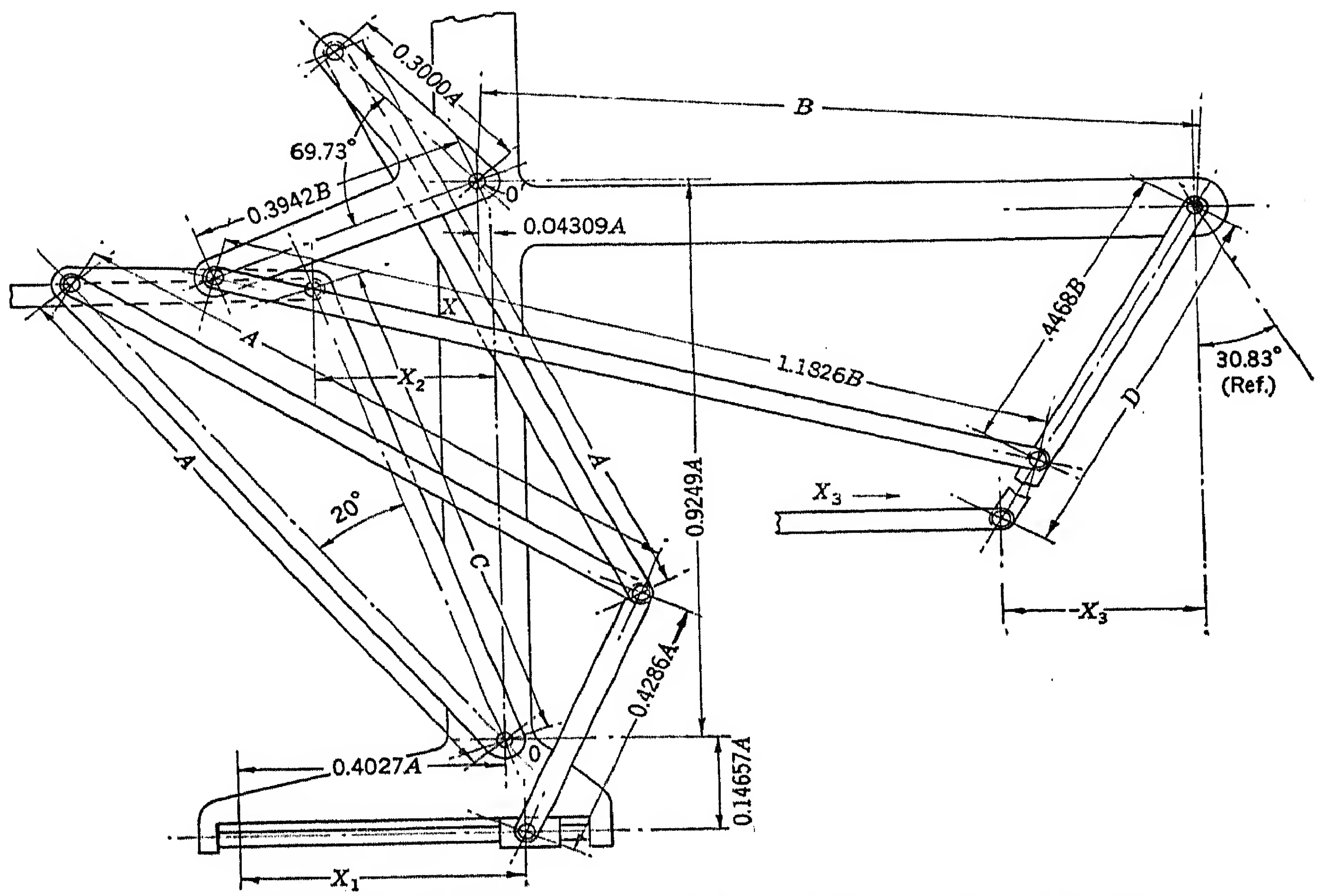

FIG. 9·15.—Multiplier permitting change in sign of only one factor.

general it will be found that the linkages discussed in Chaps. 4 to 6 offer all the flexibility required. Examples are provided by Fig. 8·16, which has already been explained, and by Fig. 9·15. The latter figure shows a multiplier designed to permit change in sign of x_2, but not x_1. The central joint of the star grid generator appears a little below the center of the figure. The bars have their other ends guided along a horizontal straight line, which serves as the x_1-scale, and along circles with centers O, O', respectively. Rotation of the end of one bar about O is transformed into horizontal slide motion proportional to x_2 by an ideal harmonic transformer; rotation of the end of the third bar about O' is transformed into a parallel slide motion proportional to x_3 by a combination of a three-bar linkage and an ideal harmonic transformer. The design

involves four dimensional constants subject to arbitrary choice: A, which determines the scale of the grid generator and the length of the x_1-scale; B, which determines the scale of the three-bar linkage; C and D, which determine the lengths of the x_2- and x_3-scales, respectively. If X_1, X_2, X_3 are displacements measured in the same units, the linkage generates the relation

$$\frac{X_3}{D} = 3.0909\,\frac{X_1}{A}\,\frac{X_2}{C}. \tag{28}$$

The first steps in designing transformer linkages will involve the use of tabular or graphical methods. A graphical presentation of the operators, as in Fig. 9·14, will make it possible to read off values of the operators for evenly spaced values of θ_r, when these are required. [As a rule one should disregard irregularities in the linearizing operators, such as are shown by $(h_2|\theta_2)$ in the example above; the operators should be replaced by smoothly varying approximations.] Such graphical interpolations are not necessary when the geometric method is to be used in designing a three-bar linkage. One then needs to use a geometric series of values of one of the variables involved—such as are provided in Table 9·1 in the case of the variables x_1, x_2, x_3. To apply the geometric method directly to the entries in such a table one would require an overlay constructed for the same geometric ratio (here $g = 1.25$). The overlay would also need to be extended in both directions from the zero line by addition of a new series of lines with spacing [cf. Eq. (5·92)]

$$Y^{(t+1)} - Y^{(t)} = -\alpha g^t, \qquad t = 0, 1, \cdot \cdot \cdot . \tag{29}$$

The details of this extension of the geometric method will present no difficulty to the reader.

To minimize the accumulation of errors in designing transformer linkages, the following procedure is often useful. When two of the transformers have been designed, a graphical recalibration of the third of the original scales can be carried through before its linearizing transformer is designed. For example, let new uniform scales for x_1 and x_2 be constructed and accepted as exact. On these scales lay down geometric series of points

$$\begin{aligned} x_{1\pm}^{(r)} &= \pm C_1 g^r, \\ x_{2\pm}^{(s)} &= \pm C_2 g^s. \end{aligned} \tag{30}$$

Next, construct corresponding calibration points on the original nonuniform x_1- and x_2-scales, using the known constants of the transformer linkages. Then, using the known constants of the grid generator, construct the points $x_{3\pm}^{(r,s)}$ on the original x_3-scale that correspond to $x_1 = x_{1\pm}^{(r)}$ and $x_2 = x_{2\pm}^{(s)}$, for various choices of r and s. If the grid generator were exactly ideal, and the transformer linkages were without structural error,

all the points with

$$r + s = t \tag{31}$$

would fall together on two points of the x_3-scale, corresponding to

$$x_{3\pm}^{(t)} = \pm C_1 C_2 g^t. \tag{32}$$

Actually there will be some scattering of these points, and it will be necessary to choose mean positions for the new calibration points $x_{3\pm}^{(t)}$ on the x_3-scale. This method of constructing the x_3-scale introduces a partial correction for all design errors committed up to this point; it remains only to design the transformer linkage for the x_3-terminal.

9·7. Analytic Adjustment of Linkage Multiplier Constants.—Final adjustment of the constants of a multiplier can be carried out by analytic methods similar to those described in Chap. 7. From the point of view of theory, the present problem differs from the earlier one principally in the necessity for controlling the structural error in a two-dimensional, rather than a one-dimensional, domain. From a practical point of view, the large number of adjustable constants makes a complete treatment of the problem tedious, but assures high accuracy in the result if enough care is taken. The present section will describe a straightforward application of analytic methods to the final adjustment of linkage constants; the next section will indicate some associated or alternative techniques used by the author. The reader should be warned that the practical importance of this part of the design procedure, and the labor required, are out of proportion to the brief discussion that can be devoted to it in this volume.

If the combination of star grid generator and transformer linkages were an exact linear multiplier, it would generate a relation

$$RX_3 = X_1 X_2 \tag{33}$$

between external parameters X_1, X_2, X_3, at least within a domain

$$X_{1m} \leqq X_1 \leqq X_{1M}, \qquad X_{2m} \leqq X_2 \leqq X_{2M}, \qquad X_{3m} \leqq X_3 \leqq X_{3M}. \tag{34}$$

Here R is a constant, and the parameters are so defined that $X_1 = 0$ when $x_1 = 0$, etc. Because of structural errors in the mechanism it will actually generate a relation that can be written as

$$RX_3 = X_1 X_2 + \delta(X_1, X_2). \tag{35}$$

The last small term is the structural-error function of the mechanism, which must be brought within specified tolerances by adjustment of the linkage constants.

In the case of a multiplier it is convenient to gauge the error of the mechanism by the structural-error function. The effort in the calculation can be decreased by computing the error function for spectral values of

X_1 and X_2 which form geometric progressions in the two halves of each input scale:

$$\left.\begin{aligned} X_1^{(r)+} &= X_1^{(0)}\cdot g^r, \\ X_1^{(r)-} &= -X_1^{(0)}\cdot g^r, \end{aligned}\right\} r = \cdots, -2, -1, 0, 1, 2, \cdots, \tag{36a}$$

$$\left.\begin{aligned} X_2^{(s)+} &= X_2^{(0)}\cdot g^s, \\ X_2^{(s)-} &= -X_2^{(0)}\cdot g^s, \end{aligned}\right\} s = \cdots, -2, -1, 0, 1, 2, \cdots. \tag{36b}$$

If the multiplier were exact, the corresponding spectral values of X_3 would form similar geometric progressions in either half of the output scale:

$$\begin{aligned} RX_3^{(r+s)+} &= X_1^{(0)}X_2^{(0)}g^{r+s} = RX_3^{(0)}g^{r+s}, \\ RX_3^{(r+s)-} &= -X_1^{(0)}X_2^{(0)}g^{r+s} = -RX_3^{(0)}g^{r+s}. \end{aligned} \tag{37}$$

The spectral values of X_3 in either half of the scale would then depend only on the value of $r + s$ for the corresponding spectral values of X_1 and X_2. With the actual multiplier we have instead

$$RX_3^{(r\pm,s\pm)} = X_1^{(r)\pm}X_2^{(s)\pm} + \delta(X_1^{(r)\pm}, X_2^{(s)\pm}); \tag{38}$$

the spectral values of X_3 do fall into groups according to the value of $r + s$, but they are scattered about the ideal value for the group, $X_3^{(0)}g^{r+s}$, with errors given by the structural-error function $\delta(X_1^{(r)\pm}, X_2^{(s)\pm})$.

The spectral values of the structural-error function are conveniently arranged as a matrix—or, more properly, as an assembly of four infinite matrices. To simplify the notation we shall write

$$\delta(X_1^{(r)\pm}, X_2^{(s)\pm}) = E_{r,s}^{\pm\pm}. \tag{39}$$

With value of X_1 increasing upward, values of X_2 increasing to the right, the matrix takes the following form:

$$\mathsf{E} = \left(\begin{array}{ccc:c:ccc} E_{1,1}^{+-} & E_{1,0}^{+-} & E_{1,-1}^{+-} & E_{1,-\infty}^{+\pm} & E_{1,-1}^{++} & E_{1,0}^{++} & E_{1,1}^{++} \\ E_{0,1}^{+-} & E_{0,0}^{+-} & E_{0,-1}^{+-} & E_{0,-\infty}^{+\pm} & E_{0,-1}^{++} & E_{0,0}^{++} & E_{0,1}^{++} \\ E_{-1,1}^{+-} & E_{-1,0}^{+-} & E_{-1,-1}^{+-} & E_{-1,-\infty}^{+\pm} & E_{-1,-1}^{++} & E_{-1,0}^{++} & E_{-1,1}^{++} \\ \hdashline E_{-\infty,1}^{\pm-} & E_{-\infty,0}^{\pm-} & E_{-\infty,-1}^{\pm-} & E_{-\infty,-\infty}^{\pm\pm} & E_{-\infty,-1}^{\pm+} & E_{-\infty,0}^{\pm+} & E_{-\infty,1}^{\pm+} \\ \hdashline E_{-1,1}^{--} & E_{-1,0}^{--} & E_{-1,-1}^{--} & E_{-1,-\infty}^{-\pm} & E_{-1,-1}^{-+} & E_{-1,0}^{-+} & E_{-1,1}^{-+} \\ E_{0,1}^{--} & E_{0,0}^{--} & E_{0,-1}^{--} & E_{0,-\infty}^{-\pm} & E_{0,-1}^{-+} & E_{0,0}^{-+} & E_{0,1}^{-+} \\ E_{1,1}^{--} & E_{1,0}^{--} & E_{1,-1}^{--} & E_{1,-\infty}^{-\pm} & E_{1,-1}^{-+} & E_{1,0}^{-+} & E_{1,1}^{-+} \end{array}\right) \tag{40}$$

Each row or column of dots represents an infinite number of rows or columns of spectral values of X_1 as $r \to \pm\infty$, in the case of rows, or of X_2 as $s \to \pm\infty$, in the case of columns. It is, fortunately, not necessary to give detailed consideration to these parts of the matrix. In the graphical process of constructing an ideal grid structure it was sufficient to consider grid lines with small positive and negative values of r and s, and

the circles of convergence, $r = -\infty$, $s = -\infty$; the same restrictions on r and s can be made in the present discussion, and for the same reasons.

If the grid structure is ideal at $X_1 = X_2 = 0$—and it should be kept so throughout the work—the output parameter X_3 will be independent of X_1 when $X_2 = 0$, and independent of X_2 when $X_1 = 0$. All entries in the central cross of the matrix (40) will then have the same value, $E^{\pm\pm}_{-\infty,-\infty}$.

The elements of the structural-error matrix are functions of all structural constants of the multiplier: the dimensions of the star grid generator and the transformer linkages, the origins from which the parameters X_1, X_2, and X_3 are measured, and the constant R of Eq. (38). Let the independent constants be n in number: $g_1, g_2, \ldots g_n$. A small variation Δg_i of the constant g_i will change the matrix element $E^{\pm\pm}_{r,s}$ by an amount $\dfrac{\partial E^{\pm\pm}_{r,s}}{\partial g_i} \cdot \Delta g_i$. It will then modify the matrix E by adding to it Δg_i times the infinite matrix

$$\mathsf{G}_i = \left(\frac{\partial E^{\pm\pm}_{r,s}}{\partial g_i}\right). \tag{41}$$

If small variations are made in all the constants g_i, the structural-error matrix will become, to terms of the first order in the Δg_i,

$$\mathsf{E} + \delta\mathsf{E} = \mathsf{E} + \sum_i \mathsf{G}_i \Delta g_i. \tag{42}$$

The problem is then to determine the form of the matrices G_i and to choose *small* (cf. Sec. 9·3) values for the Δg_i which make the final structural-error matrix $\mathsf{E} + \delta\mathsf{E}$ as small as possible—or at least, to reduce the errors in certain regions of this matrix until they meet specified tolerances.

The labor involved in solution of this problem is considerable, and the work must be arranged with care. It is necessary to consider only the portion of the matrix that corresponds to the domain of action of the multiplier. The central cross of the matrix must be included, but the calculations need not be extended to large negative values of r and s, particularly if variations of the constants are restricted to those that maintain the accuracy of the multiplication for $X_1 = 0$ and $X_2 = 0$. Analytic determination of the derivatives $(\partial E^{\pm\pm}_{r,s})/(\partial g_i)$ is advantageously replaced by large-scale graphical constructions to determine the matrices

$$\left(\frac{\partial E^{\pm\pm}_{r,s}}{\partial g_i}\right) \Delta g_i = \mathsf{G}_i \Delta g_i \tag{43}$$

for small changes Δg_i in each parameter; these matrices can be used directly in the calculations, or converted into the matrices G_i, as desired.

The matrices associated with changes in constants of the terminal linkages have simple forms. Variation in a constant g_i of the output transformer linkage produces a change in X_3 which depends only on X_3; consequently the corresponding matrix G_i has identical entries along each line of constant X_3. These are lines of constant $r + s$: diagonals parallel to the principal diagonals in the lower-left and upper-right quadrants (positive X_3), and diagonals perpendicular to these in the upper-left and lower-right quadrants (negative X_3). All entries in the central cross of the matrix will be identical. A matrix G_i associated with a constant g_i of the X_1-transformer linkage has entries which in each row are proportional to X_2; if g_i is a constant of the X_2-transformer linkage, G_i has entries which in each column are proportional to X_1. In either case, the entries in the central cross will vanish if the changes in the transformer linkages do not affect the accuracy of the multiplication for $X_1 = 0$ and $X_2 = 0$.

In varying the dimensional constants of the star grid generator one should follow the principles discussed in Sec. 9·5; one should make changes with one degree of freedom which maintain the invariance of properly chosen elements of the grid structure, and particularly the exact performance of the multiplier for $X_1 = 0$ and $X_2 = 0$. Such changes can of course be described by a single parameter g_i, which may be termed a "restricted parameter." It would be extremely difficult to compute by analytic methods the matrices G_i associated with restricted parameters; the graphical construction is quite practicable if the work is done on a sufficiently large scale. The entries in the central cross of these matrices are all zero.

It remains to make a linear combination of the matrices E and G_i, $i = 1, 2, \cdots n$, that will have all elements as small as possible within the domain of interest. Following the ideas of Sec. 7·3, one can make n preselected elements of the residual-error matrix vanish exactly. (The solution will of course be spurious if large Δg_i are required.) One can also apply the method of least squares (Sec. 7·6). The author prefers to build up the required linear combination in a succession of steps, in which there are formed linear combinations of the G_i that can be used to reduce the elements in one or another of several regions of the error matrix E without introducing new errors elsewhere. For simplicity, let us divide the domain of interest into two regions, A and B. By laying out the matrices G_i, one can see how to make a number of linear combinations of these which are small in some part of region A. By linear combinations of the resulting matrices one can build up combinations of the G_i which are small throughout region A but large in region B; these can be used to reduce the elements of the error matrix in region B without introducing new errors in region A. Similarly, one

can build up other linear combinations of the G_i which can be used to reduce the errors in region A without introducing new errors in region B. The problem has thus been divided into two simpler and essentially independent problems: that of reducing the error in region A, and that of reducing the error in region B. If these problems are not simple enough to be solved by inspection, each region can again be subdivided, and the process of forming new linear combinations carried through as before. The method requires some flexibility of approach, and the designer will profit from experience. The author finds it a completely satisfactory method.

9·8. Alternative Method for Gauging the Error of a Grid Generator.— It is usually satisfactory to carry out the final analytic adjustment of dimensional constants for the grid generator and transformer linkages separately. This greatly simplifies the calculations by reducing the number of dimensional constants that must be varied simultaneously.

In adjusting the constants of a grid generator it is convenient to use an alternative method for gauging the errors in the almost ideal grid structure. We have noted that, in an ideal grid structure, systems of contours of constant x_1, x_2, x_3 meet in exact triple intersections, whereas in a nonideal grid structure these nodal points of the grid disintegrate into little triangles. To make a star grid generator ideal one would have to make these triangles vanish throughout the domain of interest. The linear dimensions of these triangles have the essential characteristics required of a gauge of the error in the grid structure: they change proportionally to small changes in the dimensional constants of the grid generator, and vanish when the error vanishes. Since they are especially easy to determine by graphical construction, it is very convenient to use them directly as gauging quantities in the final adjustment of linkage constants.

The star grid generator is intended to establish a relation

$$Rx_3 = x_1x_2 \tag{44}$$

between variables x_1, x_2, x_3, read on associated scales which are in general nonuniform. Without attempting to control the uniformity of the scales, we shall attempt to make this relation as exact as possible by varying the constants of the grid generator and the calibration of the scales. As in Sec. 9·7, we choose spectral values of the variables which form geometric progressions:

$$\left.\begin{aligned} x_1^{(r)\pm} &= \pm x_1^{(0)} g^r, \\ x_2^{(s)\pm} &= \pm x_2^{(0)} g^s, \\ x_3^{(t)\pm} &= \pm \frac{x_1^{(0)} x_2^{(0)}}{R}\, g^t. \end{aligned}\right\} r,\ s,\ t = \cdots,\ -2,\ -1,\ 0,\ 1,\ 2,\ \cdots. \tag{45}$$

First, we may construct the x_1- and x_2-contours in the domain of interest. The intersections in the resulting curvilinear grid can be labeled with the index pair $(r\pm, s\pm)$. Next we construct the x_3-contours specified by Eq. (45). These will not, in general, pass through the intersections of the original grid, but will serve to complete small triangles with one vertex at each intersection. Let the side of the $(r\pm, s\pm)$-triangle opposite the $(r\pm, s\pm)$-intersection have length $L_{r,s}^{\pm\pm}$, taken as positive if the x_3-contour passes the intersection on the side of increasing x_3, negative if it passes on the other side. The deviation of the grid structure from the ideal can then be represented by a matrix

$$\mathsf{L} = [L_{r,s}^{\pm\pm}], \tag{46}$$

identical in structure with the matrix of Eq. (40), except that the quantities $E_{r,s}^{\pm\pm}$ are replaced by the quantities $L_{r,s}^{\pm\pm}$.

A change Δg_i in a restricted parameter g_i of the grid generator will change the grid structure; the lengths $L_{r,s}^{\pm\pm}$ will become, to terms of the first order,

$$L_{r,s}^{\pm\pm} + \delta L_{r,s}^{\pm\pm} = L_{r,s}^{\pm\pm} + \frac{\partial L_{r,s}^{\pm\pm}}{\partial g_i} \Delta g_i. \tag{47}$$

The quantities $\delta L_{r,s}^{\pm\pm}$ can be graphically determined for some small Δg_i; it is then a simple matter to write down the matrix

$$\mathsf{H}_i = \left[\frac{\partial L_{r,s}^{\pm\pm}}{\partial g_i}\right], \tag{48}$$

which corresponds to the matrix G_i of Sec. 9·7.

If each of the restricted parameters of the grid structure is changed by a small amount, the matrix of triangle dimensions will become, to terms of the first order,

$$\mathsf{L} + \delta\mathsf{L} = \mathsf{L} + \sum_i \mathsf{H}_i \Delta g_i. \tag{49}$$

To make the grid structure ideal one would like to choose values of the Δg_i (necessarily "small") that make the matrix $\mathsf{L} + \delta\mathsf{L}$ vanish identically. Determination of the Δg_i can then proceed as described in the preceding section, except that one will not in general attach the same relative importance to reduction of the various quantities $L_{r,s}^{\pm\pm}$ as to reduction of the corresponding output errors $E_{r,s}^{\pm\pm}$; what weighting factor is to be applied will be obvious from inspection of the grid structure.

When the scales associated with the grid generator have been determined, it will remain to design the transformer linkages and to adjust their constants as described in Chap. 7. Finally, the performance of the complete mechanism must be determined by exact calculation. The procedure described in this section was applied in designing the multiplier

illustrated in Fig. 9·15. The residual errors are shown in Table 9·2, which gives $x_3 - x_1x_2$ for a series of values of x_1 and x_2, when the constants A, C, D of Eq. (28) are so chosen that the generated relation should be $x_3 = x_1x_2$.

TABLE 9·2.—STRUCTURAL ERROR $x_3 - x_1x_2$ IN MULTIPLIER, FIG. 9·15

x_2 \ x_1	0.000	0.401	0.511	0.660	0.802	1.000
1.000	0.00195	−0.00230	−0.00060	0.00460	−0.00308	0.00790
0.797	0.00195	0.00230	0.00080	−0.00140	−0.00269	0.00080
0.637	0.00195	0.00390	0.00240	0.00006	−0.00250	−0.00250
0.511	0.00195	0.00429	0.00289	0.00070	−0.00230	−0.00390
0.409	0.00195	0.00400	0.00281	0.00070	−0.00220	−0.00410
0.000	0.00195	0.00195	0.00195	0.00195	0.00195	0.00195
−0.409	0.00195	0.00400	0.00320	0.00099	−0.00201	−0.00339
−0.511	0.00195	0.00441	0.00330	0.00150	−0.00250	−0.00330
−0.637	0.00195	0.00419	0.00300	0.00039	−0.00310	0.00039
−0.797	0.00195	0.00330	0.00179	−0.00090	−0.00330	0.00250
−1.000	0.00195	−0.00029	−0.00179	−0.00330	−0.00320	0.00460

CHAPTER 10

BAR-LINKAGE FUNCTION GENERATORS WITH TWO DEGREES OF FREEDOM

The preceding chapter has described a technique for the design of bar-linkage multipliers—a technique which is also applicable in the case of generators of arbitrary functions with ideal grid structure. The present chapter will describe and illustrate a parallel technique for the design of bar linkages that generate a given function with nonideal grid structure. As in the preceding discussion, attention will be restricted to the use of the star grid generator.

10·1. Summary of the Design Procedure.—In designing a star grid generator for a multiplier, we began by considering an intersection nomogram for the given function,

$$x_3 = x_1x_2, \tag{1}$$

in the form of an ideal grid structure. We would have liked to carry out a topological transformation of this into an equivalent nomogram in which each family of lines would be a family of identical circles. The transformed nomogram would necessarily retain the ideal grid structure of the original one; the corresponding star linkage would then be an ideal grid generator. We saw that such a transformation can not be found, but, guided by this idea, we succeeded in laying out three families of identical circles which had nearly the desired characteristics within a restricted region. Then, using graphical methods in adjusting the constants of the corresponding star linkage, we were able to make the grid structure take on more and more nearly the desired ideal form.

The same line of thought can be followed in designing a star grid generator for an arbitrary function. Differences in the procedure arise principally from the fact that in improving the initial grid structure we cannot concentrate simply on making it ideal, but must at each step take account of the special function that is to be mechanized.

To design a star grid generator for a given function of two independent variables,

$$x_3 = f(x_1, x_2), \tag{2}$$

we first represent it by an intersection nomogram consisting of three families of lines;

$$x_1 = x_1^{(r)}, \tag{3a}$$
$$x_2 = x_2^{(s)}, \tag{3b}$$
$$x_3 = x_3^{(t)}. \tag{3c}$$

We desire to apply to this nomogram a topological transformation that will transform each family of curves into a family of circles of constant radius:

1. Circles $C_1^{(r)}$ of radius L_1, centers $A_1^{(r)}$, on the line of centers C_1.
2. Circles $C_2^{(s)}$ of radius L_2, centers $A_2^{(s)}$, on the line of centers C_2.
3. Circles $C_3^{(t)}$ of radius L_3, centers $A_3^{(t)}$, on the line of centers C_3.

If we can find such a transformed nomogram it will be equivalent to the original one, and from it we shall be able to determine the constants of the desired star grid generator: link lengths L_1, L_2, L_3; guiding curves C_1, C_2, C_3; scales with the $x_1^{(r)}$-, $x_2^{(s)}$-, $x_3^{(t)}$-calibrations at points $A_1^{(r)}$, $A_2^{(s)}$, $A_3^{(t)}$, respectively.

In seeking such a transformation we can be guided by the special characteristics, and especially the singularities, of the original nomogram. Under a topological transformation, intersections transform into intersections and points of tangency into points of tangency; these features of the original nomogram must then appear in the transformed nomogram. If all lines of constant x_1 intersect at one point of the original nomogram, then all circles $C_1^{(r)}$ of the transformed nomogram must also intersect in a similar manner. If a line $x_1 = x_1^{(r)}$ is tangent to the line $x_2 = x_2^{(s)}$ where $x_3 = x_3^{(t)}$, then the circles $C_1^{(r)}$ and $C_2^{(s)}$ must be tangent to each other at a point on the circle $C_3^{(t)}$.

As a first step, we lay down tentative transforms of two of the original families of lines, let us say the x_1- and x_2-contours. These will be families of circles that have the invariant characteristics of the original x_1- and x_2-contours, at least within the domain of mechanization; to each will be assigned a tentative value of x_1 or x_2, with due regard for all invariant characteristics of the original assignment. The tentative choice of these transforms is sufficient to determine the form of a tentative topological transformation and a corresponding new form of the third family of curves; to determine these curves we have only to plot, in the curvilinear coordinate system formed by the x_1- and x_2-circles, the curves $x_3 = x_3^{(t)}$ as given by Eq. (2). If this tentative transformation should be the desired one, these x_3-contours will then be circles with the same radius. Of course, we cannot expect so fortunate a result. Usually, however, we can see how to rearrange or renumber the x_1- and x_2-circles so as to make the x_3-contours roughly circular. We thus obtain a transformation of the original nomogram in which two of the families of contours have the desired circular form, and the third family has approximately the desired character. On replacing the third family of curves by a system of approximating circles with the same radius, we

can now convert it into the grid structure of a star linkage which generates, at least approximately, the given function.

It remains to modify this star linkage in such a way as to increase the precision with which it generates the given function, and at the same time to bring its scales into some convenient form, preferably circular. This can usually be accomplished by a method of successive approximations. Accepting the x_2- and x_3-circles, $C_2^{(s)}$ and $C_3^{(t)}$, as determined above, we can replot the contours $x_1 = x_1^{(r)}$ as defined by Eq. (2). These will be nearly circular; they can be approximated by a new system of circles $C_1^{(r)}$, which can often be so chosen that the line of centers has a simple and convenient form. The resulting star-linkage nomogram is usually more accurate than the first approximate nomogram, and more conveniently mechanized. Next, accepting the $C_1^{(r)}$- and $C_3^{(t)}$-circles thus obtained, we can replot the contours $x_2 = x_2^{(s)}$ and replace them by a new set of circles $C_2^{(s)}$, and so on. There is no guarantee that this method will converge on a satisfactory solution of the problem; if it does not, the process must be begun again with a drastically different initial structure.

An alternative method for improving the grid generator will be illustrated in Sec. 10·3.

When a graphical method is no longer adequate for the further improvement of the grid structure, analytical methods can be brought into play. These, again, are essentially the same as those used in the design of multipliers. The grid generator, considered either separately or in combination with transformer linkages, generates a relation between the x_1-, x_2-, x_3-scale readings which may be written as

$$x_3 = f(x_1, x_2) + \delta(x_1, x_2). \tag{4}$$

The structural error $\delta(x_1, x_2)$ is a function of all dimensions of the mechanism, as well as of x_1 and x_2. It can be evaluated for spectral values $x_1^{(r)}$ and $x_2^{(s)}$ of these latter variables and brought within specified tolerances by the methods described in Sec. 9·9. There is, however, no advantage in making a special choice of the spectra $x_1^{(r)}$ and $x_2^{(s)}$, except as this may be indicated by singularities or invariants of the given function.

10·2. Example: First Approximate Mechanization of the Ballistic Function in Vacuum.—As an example, we shall design a star grid generator for the ballistic function in vacuum. The elevation angle x_3 of a gun that is to send a projectile through a point at ground range x_1, relative altitude x_2, may be obtained by solving

$$x_1 \sin x_3 \cos x_3 - x_2 \cos^2 x_3 = \frac{g}{v^2} x_1^2, \tag{5}$$

where v is the initial velocity of the shell and g is the acceleration of gravity. We shall take x_1 and x_2 as input variables in the linkage and generate the required elevation of the gun, x_3, as the output variable. For simplicity in the calculation we shall take $v = 500$ m/sec and $g = 10$ m/sec.[2] The parabolic trajectories of the shells then have the forms shown in Fig. 10·1.

It will be noted that for each target position within the bounding envelope there are two possible values of x_3. The larger value of x_3 corresponds to a high trajectory, which becomes tangent to the envelope of the trajectories before the target is reached. The smaller value of x_3 gives a lower trajectory, with shorter time of flight to the target; the shell reaches the target before it reaches the envelope of trajectories.

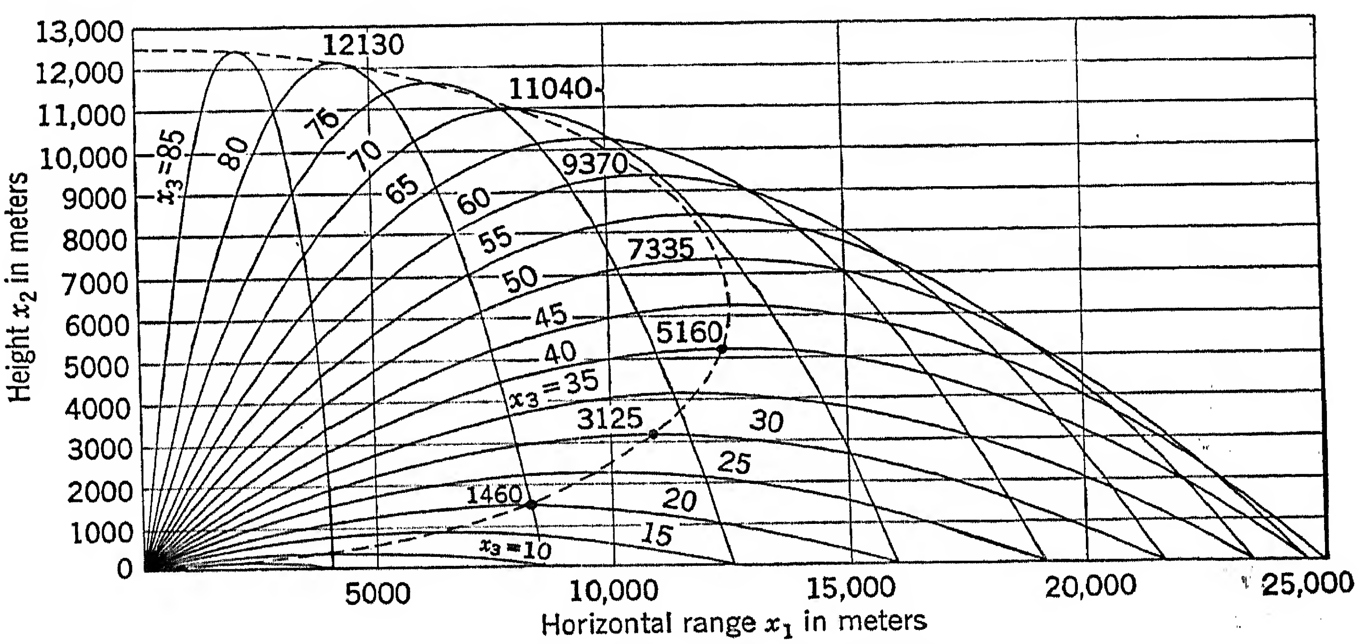

FIG. 10·1.—Trajectories of shells in vacuum. The dashed ellipse is the locus of maximum altitudes. These altitudes are indicated for some of the trajectories.

We shall be interested only in the smaller of the two possible values of x_3 and, correspondingly, only in the portions of the trajectories between the origin and the envelope. We shall also exclude from consideration the region of very small slant range, in the neighborhood of the singular point $x_1 = x_2 = 0$, where x_3 is not defined.

It is to be emphasized that the present example is intended only to illustrate a general technique and does not necessarily constitute the best solution of the stated problem. Equation (5), which is of relatively simple analytic form, can be mechanized by a net of standard computing mechanisms. Such a device will be less desirable mechanically than a bar-linkage function generator, but it will be much easier to design and free from structural errors. These advantages of a computing net are lost in the case of real ballistic functions, which offer no greater difficulties in bar-linkage design than does the present problem. In such

cases however, the usual practice is to separate the function to be generated into two parts, one of simple analytical form, to be generated by a computing net, and the other a residue, to be generated by a bar linkage. The resulting problem in bar-linkage design will then usually be less difficult than that here considered, and the complete solution can be given much greater accuracy. The present example, nevertheless, offers a number of interesting points for discussion.

Since the trajectories in Fig. 10·1 are contours of constant x_3, the figure is actually an intersection nomogram that could serve for the solution of Eq. (5). We shall take it as the starting point of the design process and attempt to find a topological transformation that will transform the parabolas into a family of identical circles, the horizontal lines into a second family of identical circles, and the vertical lines into a third.

Determination of the x_3-scale.—The most difficult stage of the work is always the beginning; every possible clue must be used as a guide. We observe first that all the parabolas intersect in a common point, $x_1 = x_2 = 0$. If the desired transformation exists, it must carry these parabolas into a family of circles, of radius L_3, which also intersect in a common point, the origin of the transformed nomogram. The centers of these circles must then lie on a circle of radius L_3 about the origin; this is the x_3-scale, thus determined as to form and position, but having no known calibration points. One calibration point can of course be chosen at will, without loss of generality. We therefore begin construction of the transformed nomogram, Fig. 10·2, by drawing the x_3-scale and the circle $x_3 = 0$ with arbitrarily chosen radius L_3; the calibration point $x_3 = 0$ on the x_3-scale has been chosen to lie directly below the origin.

Next we observe in Fig. 10·1 that the contour $x_2 = 0$ is tangent to the trajectory $x_3 = 0$ at the origin and lies above it everywhere else. The transformed circle $x_2 = 0$ must then be tangent to the transformed circle $x_3 = 0$ at the origin; in Fig. 10·2 its center must lie directly above or directly below the origin. Comparison with Fig. 10·1 suggests that its center should lie below the origin, and that its radius, L_2, should be greater than L_3. It has been so drawn in Fig. 10·2. The choice of L_2, which has been made arbitrarily, can be changed at will if the design procedure should fail to progress satisfactorily. This choice of the circle $x_2 = 0$ also fixes the point $x_2 = 0$ on the x_2-scale at a distance L_2 below the origin.

Guided by the distribution of intersections of the trajectories $x_3 = x_3^{(i)}$ with the horizontal line $x_2 = 0$, we are now in a position to make a tentative calibration of the x_3-scale. It is a familiar fact that projectiles shot in vacuum at elevation angles x_3 and $90° - x_3$ will have the same

horizontal range; for instance, the parabolas $x_3 = 40°$ and $x_3 = 50°$ of Fig. 10·1 intersect on the line $x_2 = 0$. The trajectory $x_3 = 45°$ gives the greatest horizontal range. The transformed circle $x_3 = 45°$ in Fig. 10·2 must then intersect the circle $x_2 = 0$ at the greatest possible distance from the origin—a distance equal to the diameter of the x_3-circles. This intersection point, S in Fig. 10·2, can be determined by use of a compass. The midpoint of the diameter OS lies on the x_3 scale at the calibration point $x_3 = 45°$; calibration points for $x_3 < 45°$ will lie below this point, calibration points for $x_3 > 45°$, above it.

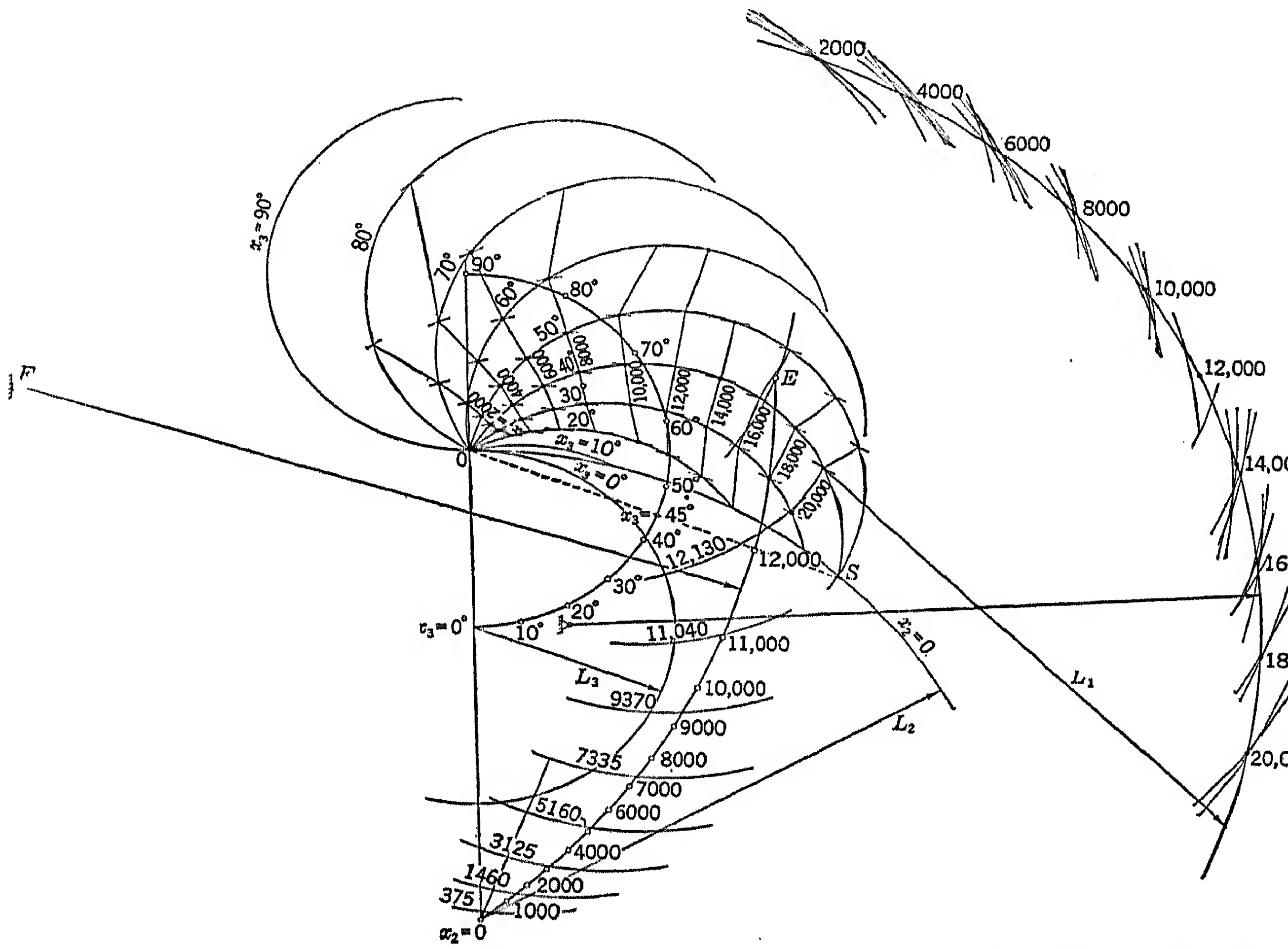

FIG. 10·2.—Construction of tentative scales in mechanization of the ballistic function in vacuum.

We shall now choose other calibration points on the x_3-scale, such that the circles $x_3 = x_3^{(i)}$ and $x_3 = 90° - x_3^{(i)}$ intersect the circle $x_2 = 0$ at the same point. Specifically, having chosen calibration points for $x_3 = 10°, 20°, 30°, 40°$, which interpolate between the known points $x_3 = 0°$ and $x_3 = 45°$, we shall construct the corresponding circles of the transformed nomogram. Through the intersection of each such circle with the line $x_2 = 0$, and the origin, we shall construct a circle of radius L_3. These circles correspond to $x_3 = 80°, 70°, 60°, 50°$, respectively; their centers are the desired calibration points on the x_3-scale. In proceeding thus, we are guided by properties of descending portions of the

parabolic trajectories with $x_3 > 45°$, which have no immediate relevance to the chosen problem. The relations that we have established are thus useful guides in the preliminary calibration of the x_3-scale, but they need not be maintained throughout later developments.

First of all, we note that the circle $x_3 = 90°$, like the associated circle $x_3 = 0°$, must be tangent to the circle $x_2 = 0$; its center must lie directly above the origin. The x_3-scale must then extend through an arc of 180°. Since the scale from $x_3 = 0°$ to $x_3 = 45°$ covers less than 90° of this arc, the spacing between consecutive x_3-calibrations must, on the average, increase with x_3; we can reasonably assume that this increase continues smoothly throughout the length of the scale. We shall therefore choose calibration points $x_3 = 10°, 20°, 30°, 40°$, which have gradually increasing separations and which lead to the determination of points $x_3 = 50°, 60°, 70°, 80°$, with separations that fall into the same smoothly increasing sequence. Such points are easily found; they are shown in Fig. 10·2, together with the associated circles of radius L_3.

Determination of the x_2-scale.—Thus far we have established only the point $x_2 = 0$ on the x_2-scale. As our principal clue in the further construction of this scale we have the points of tangency of the x_2- and x_3-contours. In Fig. 10·1 the horizontal line $x_2 = 375$ is tangent to the parabola $x_3 = 10°$ at its vertex; the transformed circle $x_2 = 375$ in Fig. 10·2 should similarly be tangent to the transformed circle $x_3 = 10°$. The circle $x_3 = 10°$ has already been determined, but we know only the radius of the circle $x_2 = 375$; its center—the point $x_2 = 375$ on the x_2-scale—may lie anywhere on a circle of radius $L_2 - L_3$, with its center at the point $x_3 = 10°$. An arc of this circle near the point $x_2 = 0$ is shown in Fig. 10·2. Similarly, the scale points $x_2 = 1460, 3125, 5160, 7335, 9370, 11040, 12130, 12500$, must lie on circles of radius $L_2 - L_3$ about centers on the x_3-scale, at the points $x_3 = 20°, 30°, 40°, 50°, 60°, 70°, 80°, 90°$, respectively. Arcs of these circles also appear in Fig. 10·2.

There is another clue to the nature of the x_2-scale, but it is relatively unreliable. It is well known that the points of maximum x_2 on the trajectories lie on an ellipse (the dashed curve of Fig. 10·1). These maxima occur at first close to the origin 0; their x_1-coordinates increase with x_3, and then decrease to 0 as x_3 goes to 90°. Now, the transformed nomogram under construction bears some similarity to the original one, Fig. 10·1, in which x_2 increases from bottom to top, x_1 from left to right. In view of this we may expect the points of tangency between the transformed x_2- and x_3-circles to move at first toward the right, as x_3 increases, and then as far as possible to the left. If this is to be the case, the x_2-scale must then rise to the right of the origin, with its upper end E, corresponding to $x_2 = 12500$, at about the same level as the scale point $x_3 = 90°$. Figure 10·2 shows such a choice of E.

A preliminary choice of the x_2-scale can now be made. For mechanical reasons it has been constructed in Fig. 10·2 as a circular arc—a tentative choice that can be modified at any time. The calibrations on this scale are determined by its intersections with the arcs already constructed. For later use, calibration points have been interpolated for evenly spaced values of x_2: 1000, 2000, 3000, . . . 12000. These are easily and accurately determined by plotting on cross-section paper a smooth curve of distance along the x_2-scale against the value of x_2, using the known calibration points, and reading off the distances corresponding to the chosen values of x_2.

This completes the determination of our tentative topological transformation. Contours of constant x_2 can be drawn in at will, but are omitted from Fig. 10·2.

Determination of the x_1-scale.—We have next to construct contours of constant x_1 in the transformed nomogram. This is conveniently done using computed values of x_2 for a series of values of x_1 and x_3, as given in Table 10·1. Only values within our restricted domain of interest are tabulated.

TABLE 10·1.—VALUES OF x_2 COMPUTED BY USE OF EQ. (5)

x_3 \ x_1	2000	4000	6000	8000	10000	12000	14000	16000	18000	20000
80°	8650	12050								
70°	4830	8250	10300	11030	10350					
60°	3150	5650	7500	8700	9350	9250				
50°	2150	4000	5400	6450	7100	7330	7200	6700	5750	4500
40°	1550	2800	3800	4550	5000	5150	5050	4700	4050	3150
30°	1150	1900	2500	2900	3100	3100	2830	2400	1730	850
20°	650	1100	1350	1450	1350	1100	600	0		
10°	280	375	300	75						

To construct the curve $x_1 = 2000$ we refer to the first column of Table 10·1. We construct arcs of radius L_2 with centers at the points $x_2 = 8650$, 4830, 3150, 2150, 1550, 1150, 650, 280, intersecting, respectively, the circles $x_3 = 80°, 70°, 60°, 50°, 40°, 30°, 20°, 10°$. The points of intersection lie on the curve $x_1 = 2000$. In the same way we can determine points on the other contours of constant x_2, as shown in Fig. 10·2. Because of irregularities in the x_2- and x_3-scales, these points do not lie on smooth curves, but on rather irregular ones; they have been connected by straight lines in Fig. 10·2, merely to bring out their relations.

It would have been very gratifying if the contours of constant x_1 had turned out to be circles of constant radius L_1. The actual result is not bad, for a first trial, since the curves do resemble arcs of circles. The radii of these circles are not exactly equal, but it is not difficult to select an average radius L_1.

We have now to construct the x_1-scale. About each of the established points of the contour $x_1 = 2000$ we construct arcs of radius L_1. These intersect near the upper margin of Fig. 10·2 and thus determine roughly the position of the point $x_1 = 2000$ on the x_1-scale. Similar constructions are shown for the established points of the other x_1-contours. The intersections are rather diffuse; the form of the x_1-scale is not determined very precisely. Fortunately, the most diffuse intersections occur for the least critical part of the x_1-scale, the center. For these values of x_1, the x_2- and x_3-contours are very nearly tangent to each other, and the computed value of x_3 is very insensitive to the value of x_1. For instance, let us consider a case in which the central pivot of the star linkage is at a point of tangency of the x_2- and x_3-contours. As long as x_2 is fixed, any displacement of the x_1-input—whether along or perpendicular to the scale—can move the star pivot only along the x_2-circle and thus produce at most a second-order change in x_3. We have, therefore, to attach little importance to the diffuseness of the intersection in the central part of the x_1-scale: we can adjust the position of that part of the scale and its calibration points with relative freedom. The reason for this is also apparent on inspection of Fig. 10·1; for values of x_1 near 12000, a change in x_1 with constant x_2 carries one very nearly along a trajectory with constant x_3. (The steeply descending trajectories we have already excluded from consideration.)

It is evident that the x_1-scale will be nearly circular; in Fig. 10·2 it has been given an accurately circular form. It then becomes clear that the calibrations in x_1 will be almost equally spaced. This fact suggests that an exactly even scale in x_1 should be laid down—a procedure that has been followed in Fig. 10·2. We have thus given to the x_1-scale a particularly simple form, which we can hope to maintain through later stages of the development.

10·3. Example: Improving the Mechanization of the Ballistic Function in Vacuum.—In following the method described in Sec. 10·1 for the improvement of our preliminary mechanization of the ballistic function, we can accept the x_1- and x_3-scales already defined and reconstruct the x_2-scale. It should now be sufficiently clear how this work would proceed. We shall therefore apply another useful technique to this problem.

Let us accept the very convenient x_1-scale of Fig. 10·2 and the established values of L_1, L_2, and L_3. Instead of prescribing the x_2-scale directly, we shall keep unchanged the contour $x_3 = 40°$, and shall require that the new linkage give an exact solution of the problem whenever $x_3 = 40°$. This requirement will completely define the x_2-scale for all values of x_2 less than 5160. For instance, we can locate the scale point $x_2 = 1000$ in the following manner. From the original nomogram we read that when $x_3 = 40°$ and $x_2 = 1000$, x_1 may be 1300 or 23300. About

the points $x_1 = 1300$ and $x_1 = 23300$ on the x_1-scale we draw circular arcs of radius L_1, intersecting the contour $x_3 = 40°$ at points A and B (Fig. 10·3). These points must both lie on the contour $x_2 = 1000$; we therefore construct about them arcs of radius L_2, and locate the scale point $x_2 = 1000$ at their intersection. The scale points $x_2 = 2000, 3000, 4000, 5000$, can be determined similarly by the use of the data in Columns 1 and 2 of Table 10·2.

TABLE 10·2.—VALUES OF x_1 COMPUTED BY EQ. (5)

x_2 \ x_3	40°	50°	60°	70°	80°
1000	1300 23320				
2000	2700 21900				
3000	4350 20250	2850			
4000	6450 18150	4000	2600	1600	800
5000	10000 14500	5300	3400	2100	1000
6000		7000 17600	4350	2600	1240
7000		9600 14950	5400	3160	1500
8000			6700 14950	3850	1800
9000			8650 12950	4600	2100
10000				5600 10450	2480
11000				7600 8400	2950
12000					3850

The scale points thus established lie on a circular arc with center Q_2 (Fig. 10·3) and are equidistant to within the accuracy of the construction. We shall therefore complete the x_2-scale by extending it as a circular arc, with equidistant scale divisions up to $x_2 = 12000$.

It remains to reconstruct the contours of constant x_3 and the x_3-scale. Points on the contours $x_3 = 10°, 20°, 30°$ are conveniently located by the use of the data in the last three rows of Table 10·1; they lie at the intersections of arcs of radius L_1 and L_2 about corresponding points on the x_1- and x_2-scales, respectively. Points on the contours $x_3 = 50°, 60°, 70°, 80°$ can be located similarly by the use of data given in Table 10·2. All these points are shown in Fig. 10·3 as small circles. Through them we can pass circles of radius L_3, with errors that are appreciable only at the outer extremity of a few of the arcs. The centers of these circles lie on a nonuniform x_3-scale that is only roughly circular.

The fact that the x_1- and x_2-scales are even and circular makes this solution of the problem attractive, even though the x_3-scale is of the most general type. No transformer linkages will be required for the inputs; it remains to design a single bar linkage that will both guide the x_3-point of the star linkage over the present noncircular x_3-scale and provide an output motion linear in x_3. How this can be done will be shown in Sec. 10·4. Figure 10·4 shows a schematic layout of the linkage in its present state,

with a curved slide for the output terminal. The elevation scale is restricted to the range $10° < x_3 < 80°$, which alone would be important if the mechanized ballistics had practical significance. This function generator has a very small error for slant ranges greater than 2000 m, except for a few points close to the envelope of trajectories. (The solution near $x_1 = x_2 = 0$ is poor because no attempt was made to force the contours

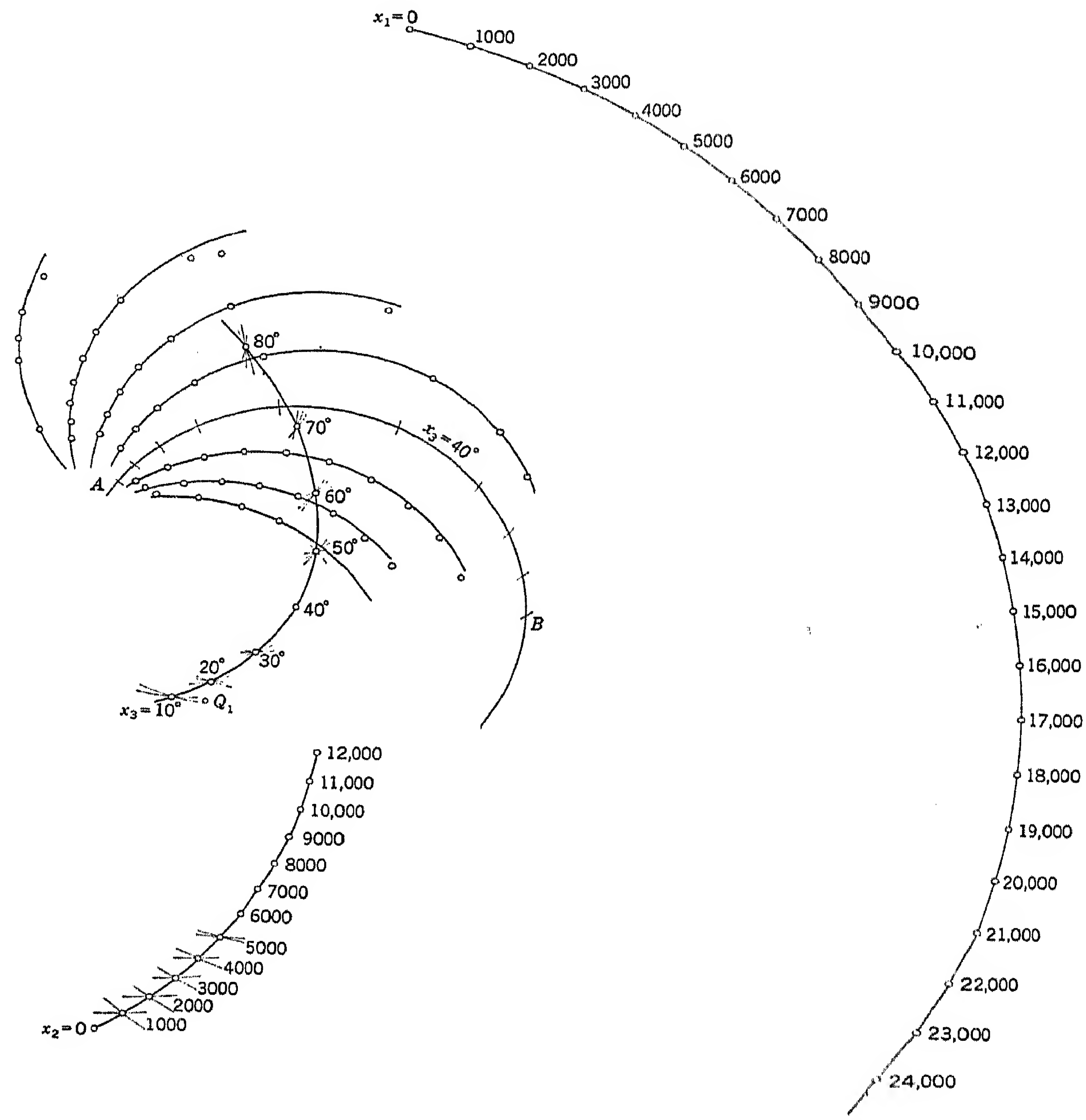

FIG. 10·3.—Construction of improved scales for mechanization of the ballistic function in vacuum.

of constant x_3 to intersect at a single point.) This design could be improved somewhat by graphical methods, without sacrificing the simple forms of the x_1- and x_2-scales; still further improvement could be obtained by applying analytic methods. In practice, however, maximum accuracy could be obtained by reformulation of the problem, introduction of new variables, and use of the bar linkage to mechanize a function of more suitable character.

10·4. Curve Tracing and Transformer Linkages for Noncircular Scales.—Practical application of a grid generator with a nonuniformly curved scale requires solution of two problems:

1. Design of a constraint for the grid-generator terminal that is more satisfactory than a curved slide.
2. Design of a transformer linkage to provide a satisfactory external terminal, usually with an even scale.

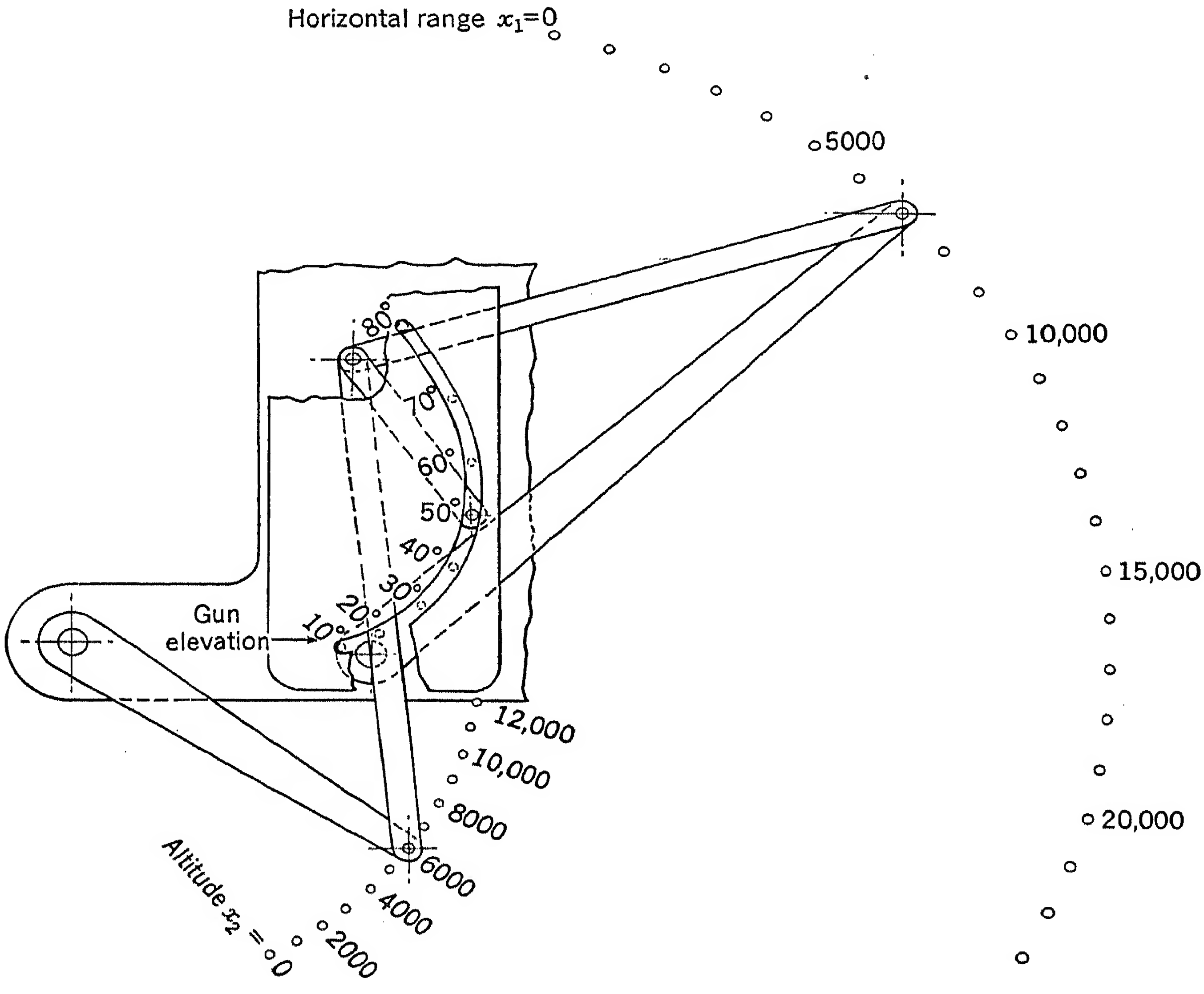

FIG. 10·4.—Schematic layout of ballistic computer.

These problems can often be solved simultaneously by a device such as that sketched in Fig. 10·5, in which the terminal T of the grid generator is pivoted to and guided by a rigid extension QTR of the central link of a three-bar linkage $PQRS$. One of the cranks of this linkage may itself serve as the terminal of the transformer, as shown in Fig. 10·5, or a harmonic transformer may be added to give a slide terminal, as in the multiplier of Fig. 8·16. We shall consider here the first and simpler alternative; the procedure is easily extended to the second case by use of the ideas presented in Chap. 8.

Let us consider that the rigid triangle QTR of Fig. 10·5 consists of rigid bars. The device may then be divided into two parts:

1. A transformer linkage, consisting of the link TR and the crank RS. When the joint T is guided along the scale AB, these elements serve to transform readings on the uneven scale AB into identical readings on the even circular scale CD.
2. A constraint linkage, consisting of the crank PQ and the links QR and QT. This, together with the elements of the transformer linkage, guides the joint T along the scale AB.

In designing such a linkage these parts are considered separately, and in the order listed.

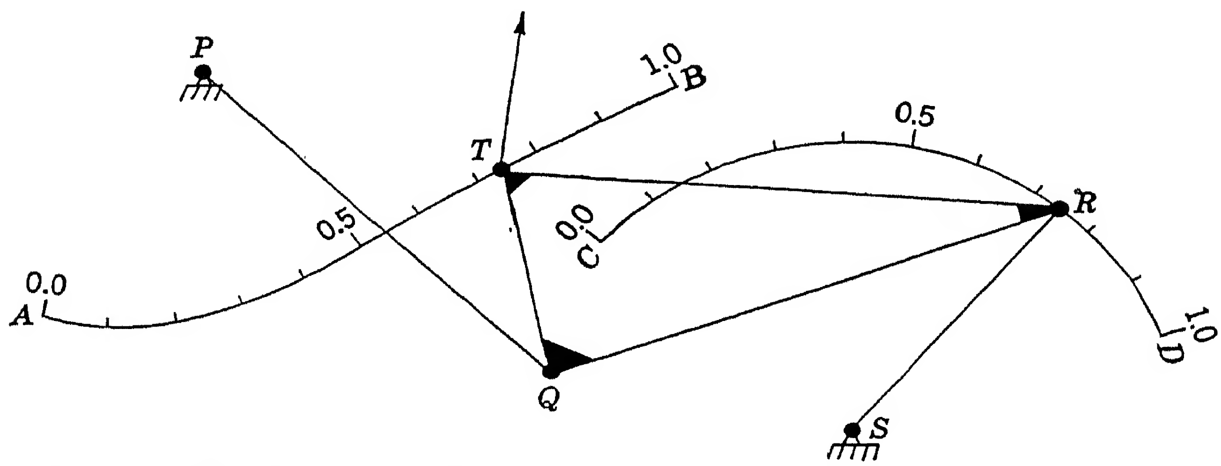

FIG. 10·5.—Linkage transformer from an uneven noncircular scale AB to an even circular scale CD. The joint T will follow AB without further constraint.

The Transformer Linkage.—The transformer linkage can be designed by application of the geometric method for three-bar-linkage design, as described in Chap. 5.

To understand how this can be done without any significant change in the procedure, we may consider the three-bar linkage from a point of view not previously emphasized. A three-bar linkage can be used to generate a relation between an input variable x_1, which can be read on a uniform scale associated with the input crank, and an output variable x_2, which can be read on a uniform scale associated with the output crank. Now, a nonlinear mechanization of the same relation can be obtained by use of the output crank alone; the uniform x_2-scale may be supplemented by a nonuniform x_1-scale, and the output crank used simply as a pointer to indicate corresponding values of x_1 and x_2. The function of the input crank and connecting link in the three-bar linkage is, then, that of transforming this circular but nonuniform scale of x_1 into a uniform circular input scale. It will be observed that the geometric method of three-bar-linkage design can be understood from this point of view; it will be noted also that the circular form of the output scale plays no essential

role in the procedure. This method can be applied, then, whenever it is desired to carry out a transformation between a circular scale and another scale of arbitrary form. (Interchange in the roles of terminals as input and output does not affect the procedure.) For example, it can be used in the design of highly nonideal harmonic transformers, in which one scale is linear, as well as in the present case, where one scale may have arbitrary form.

To design the transformer linkage one can then proceed as follows:

1. Choose a spectrum of values of the variable (for example, x) with differences that change in geometric progression, with ratio g:

$$x^{(r)} = x^{(0)} + \frac{g^r - 1}{g - 1} \cdot \delta. \tag{6}$$

2. Construct the given scale AB, and on it lay down the points corresponding to these spectral values of $x^{(r)}$. These points correspond to the point $P^{(0)}$, $P^{(1)}$, . . . $P^{(n)}$, of Fig. 5·21.
3. About the points $P^{(r)}$ construct circles $C^{(r)}$ with radius $B_2 = \overline{TR}$. This completes a chart corresponding to Fig. 5·21.
4. Over this chart move the characteristic overlay of the geometric method, Fig. 5·23, constructed for the chosen value of g. If it is possible to find a position of this chart (face up or face down) in which successive circles $C^{(0)}$, $C^{(1)}$, $C^{(2)}$, . . . pass through the intersections of an overlay circle with successive radial lines, the required constants of the transformer linkage can be read off at once. The position of the pivot S is the center of the overlay. The circular scale CD must coincide with the overlay circle on which the fit was found; the calibration points on this scale corresponding to the chosen spectrum $x^{(r)}$ lie at the intersection with this circle of the circles $C^{(r)}$. The length of the connecting link TR corresponds to the arbitrarily chosen length B_2.
5. If necessary, try a succession of values of B_2 in order to find that which gives the best fit.

Figure 10·6 shows a transformer linkage, thus designed, for the x_3-scale of Fig. 10·4.

The Constraint Linkage.—The possible paths of the joint T in linkages of this type are the three-bar curves discussed, from a more mathematical point of view, by Roberts, Cayley, and Hippisley.[1] Even as restricted by the choice of the elements TR and RS of the transformer linkage, this

[1] S. Roberts, "On Three-Bar Motion in Plane Space," *Proc. Math. Soc., Lond.*, **7**, 14 (1875).

A. Cayley, "On Three-bar Motion," *Proc. Math. Soc., Lond.*, **7**, 136 (1875).

R. L. Hippisley, "A New Method of Describing a Three-bar Curve," *Proc. Math. Soc., Lond.*, **18**, 136 (1918).

is a large family of curves, with which a great variety of curves AB can be fitted accurately.

A simple graphical method suffices for the design of these linkages. We wish to choose lengths for the bars TQ and QR such that when the points T and R move over their respective scales the point Q will describe a circle. If we then constrain Q to move on this circle, by means of the crank PQ, and R to move on the circle R, by means of the crank SR, the joint T will be constrained to move along the scale AB, as desired. We therefore prepare a chart that shows the scales AB and CD in their proper relation. Over this chart we place a transparent overlay on which is marked a line of length B_2, representing the bar TR. If we now

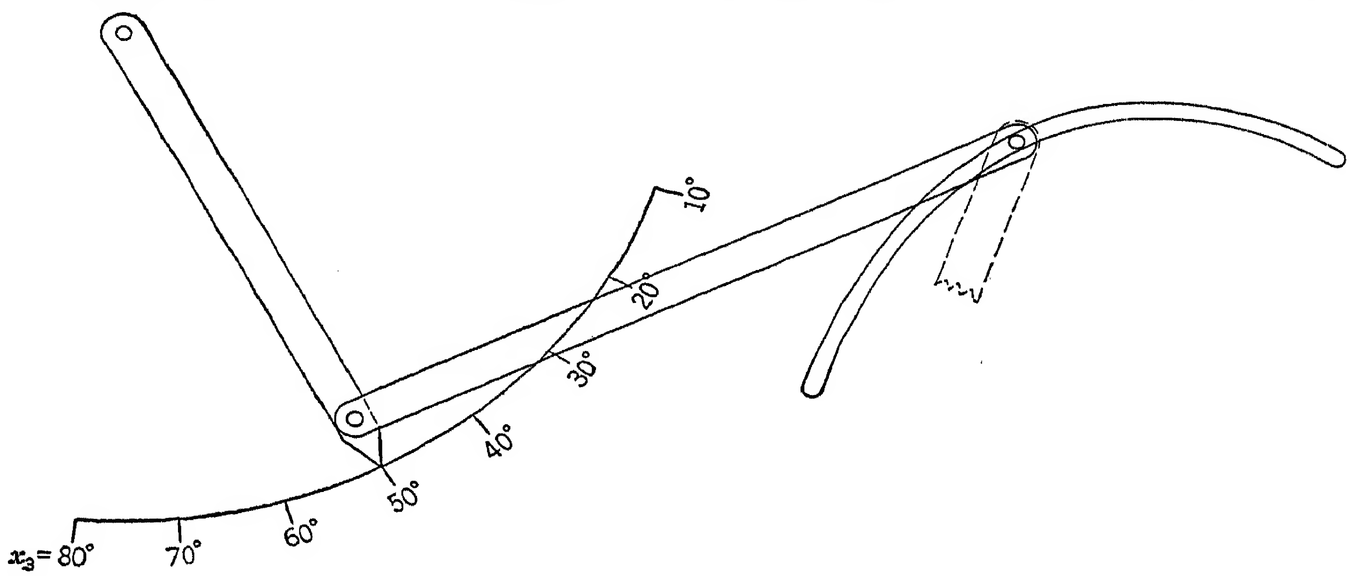

FIG. 10·6.—Transformer linkage for the x_3-scale of Fig. 10·4.

move the ends T and R of this bar along their respective scales, the other points of the overlay will have the motions of points rigidly attached to the bar TR. The path traversed by any point of the overlay can quickly be laid out on the chart. Comparison of a number of these paths will usually call attention to a region on the overlay—in addition to that near the point R—that traverses a nearly circular path. Comparison of the paths of a few points of this region will then suffice for the location on the overlay of the point Q that has the most nearly circular path. The length of the bars TQ and QR can then be measured on the overlay; the pivot P will be located at the center of the circular path, and PQ will have a length equal to its radius. This will complete the determination of the linkage constants—to the accuracy possible by graphical methods.

Figure 10·7 shows, for the example of the preceding sections, the paths of a number of points of the overlay. Since the point T moves over a roughly circular path AB, it was to be expected that a very nearly circular path, QQ', would be found near by—that the bar length TQ would be small. A sketch of the completed transformer-and-constraint linkage for this example is shown in Fig. 10·8.

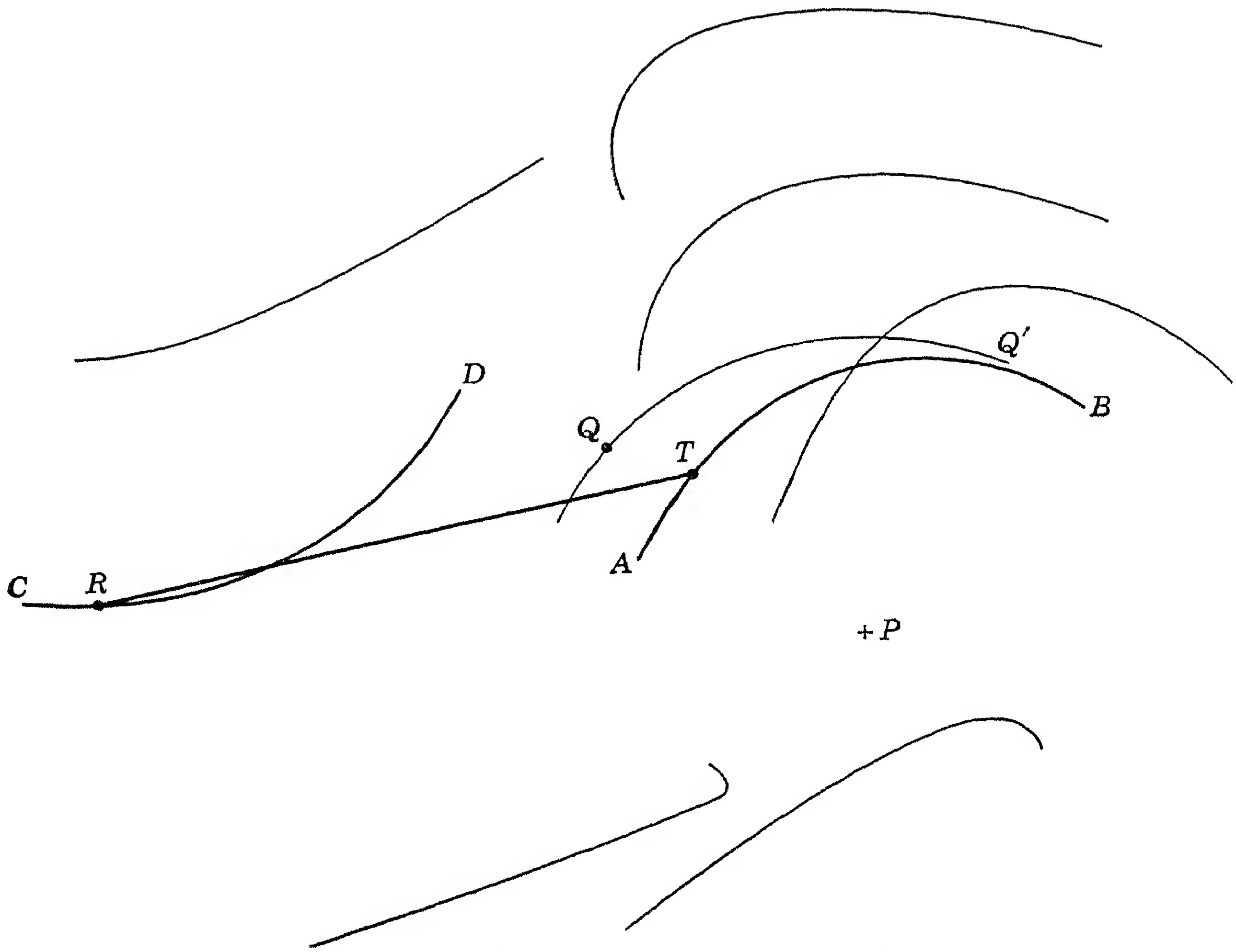

FIG. 10·7.—Paths of points rigidly attached to the bar TR, as its ends move along scales AB and CD. The point P is the center of the circular path QQ'. The scales are the same as in Fig. 10·6.

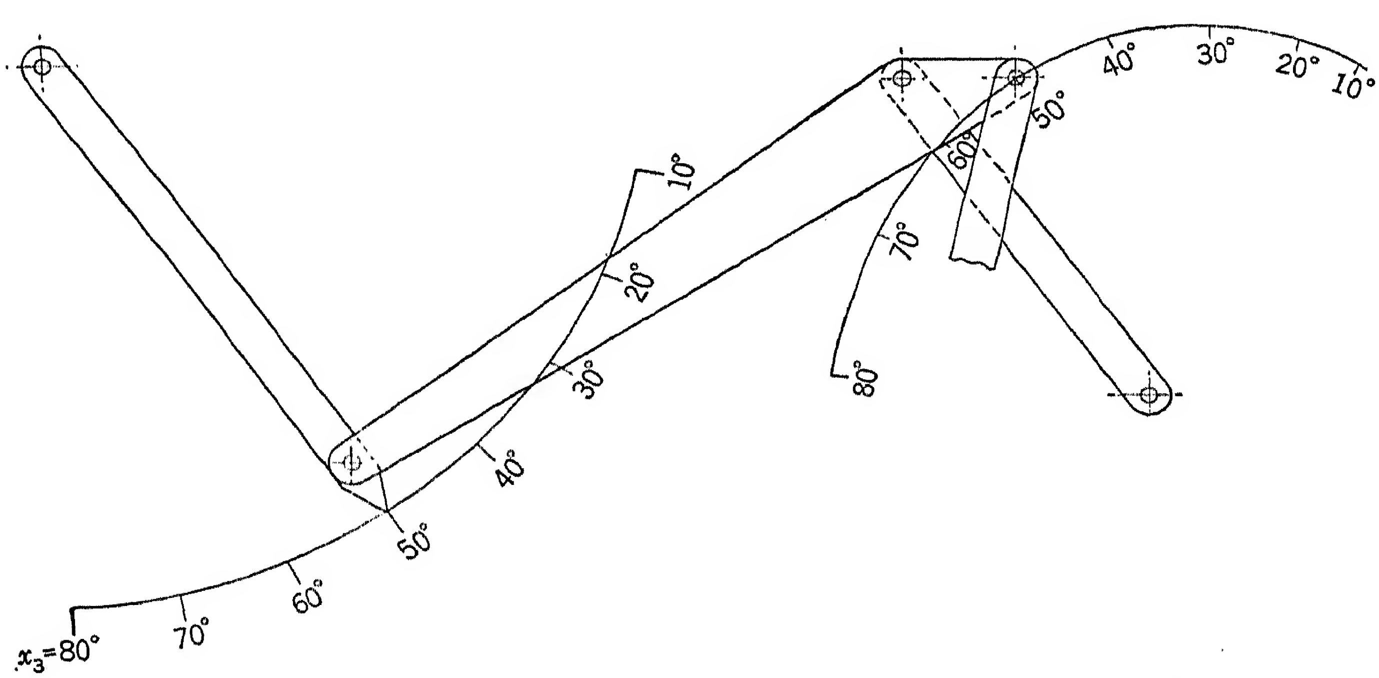

FIG. 10·8.—Complete transformer-and-constraint linkage for x_3-scale of Fig. 10·4.

APPENDIX A

TABLES OF HARMONIC TRANSFORMER FUNCTIONS

An extended discussion of the structure and use of these tables will be found in Secs. 4·3 to 4·7.

A·1. Table A·1. H_k **as a Function of** θ_i.—Each unit of this table may be read in two ways, according to the following schemes:

	X_{im} X_{iM}	g	
θ_i	H_k	H_k^*	$1 - \theta_i$

$1 - \theta_i$	H_k^*	H_k	θ_i
	g	X_{im} X_{iM}	

The defining relations are

$$H_k = \frac{\sin (X_{im} + \theta_i \Delta X_i) - (\sin X_i)_{\min}}{(\sin X_i)_{\max} - (\sin X_i)_{\min}}, \tag{4·12}$$

$$H_k^* = \frac{\cos (X_{im} + \theta_i \Delta X_i) - (\cos X_i)_{\min}}{(\cos X_i)_{\max} - (\cos X_i)_{\min}}, \tag{4·42}$$

$$g = \frac{(\cos X_i)_{\max} - (\cos X_i)_{\min}}{(\sin X_i)_{\max} - (\sin X_i)_{\min}}, \tag{4·31}$$

where max and min indicate, respectively, the maximum and minimum values of the function in question, when

$$X_{im} \leqq X_i \leqq X_{iM} = X_{im} + \Delta X_i.$$

A·2. Table A·2. θ_i **as a Function of** H_k.—In each column are tabulated values of θ_i corresponding to equally spaced values of H_k, for the values of X_{im} and X_{iM} shown at the top of the column. Only those values of X_{im} and X_{iM} are included for which θ_i is a single-valued function of H_k.

TABLE A·1.—H_k AS A FUNCTION OF θ_i

$\Delta x_i = 40°$

θ_i	−65° −25°	1.0000			−60° −20°	0.8391			−55° −15°	0.7002			−50° −10°	0.5774			−45° −5°	0.4663	
0.0	0.0000	0.0000	1.0	0.0	0.0000	0.0000	1.0	0.0	0.0000	0.0000	1.0	0.0	0.0000	0.0000	1.0	0.0	0.0000	0.0000	1.0
0.1	0.0655	0.1286	0.9	0.1	0.0706	0.1346	0.9	0.1	0.0750	0.1421	0.9	0.1	0.0788	0.1517	0.9	0.1	0.0823	0.1647	0.9
0.2	0.1398	0.2523	0.8	0.2	0.1489	0.2630	0.8	0.2	0.1567	0.2763	0.8	0.2	0.1636	0.2934	0.8	0.2	0.1698	0.3166	0.8
0.3	0.2226	0.3705	0.7	0.3	0.2345	0.3847	0.7	0.3	0.2448	0.4021	0.7	0.3	0.2539	0.4246	0.7	0.3	0.2621	0.4551	0.7
0.4	0.3134	0.4826	0.6	0.4	0.3270	0.4989	0.6	0.4	0.3388	0.5188	0.6	0.4	0.3492	0.5446	0.6	0.4	0.3586	0.5795	0.6
0.5	0.4118	0.5882	0.5	0.5	0.4260	0.6051	0.5	0.5	0.4383	0.6259	0.5	0.5	0.4491	0.6527	0.5	0.5	0.4589	0.6891	0.5
0.6	0.5174	0.6866	0.4	0.6	0.5310	0.7028	0.4	0.6	0.5427	0.7228	0.4	0.6	0.5531	0.7485	0.4	0.6	0.5625	0.7834	0.4
0.7	0.6295	0.7774	0.3	0.7	0.6414	0.7916	0.3	0.7	0.6517	0.8090	0.3	0.7	0.6608	0.8315	0.3	0.7	0.6690	0.8620	0.3
0.8	0.7477	0.8602	0.2	0.8	0.7568	0.8710	0.2	0.8	0.7646	0.8842	0.2	0.8	0.7715	0.9013	0.2	0.8	0.7777	0.9245	0.2
0.9	0.8714	0.9345	0.1	0.9	0.8765	0.9405	0.1	0.9	0.8809	0.9480	0.1	0.9	0.8848	0.9576	0.1	0.9	0.8883	0.9706	0.1
1.0	1.0000	1.0000	0.0	1.0	1.0000	1.0000	0.0	1.0	1.0000	1.0000	0.0	1.0	1.0000	1.0000	0.0	1.0	1.0000	1.0000	0.0
	1.0000	115° 155°			1.1918	110° 150°			1.4282	105° 145°			1.7321	100° 140°			2.1445	95° 135°	

θ_i	−40° 0°	0.3640			−35° 5°	0.2737			−30° 10°	0.1989			−25° 15°	0.1375			−20° 20°	0.0882	
0.0	0.0000	0.0000	1.0	0.0	0.0000	0.0000	1.0	0.0	0.0000	0.0000	1.0	0.0	0.0000	0.0000	1.0	0.0	0.0000	0.0000	1.0
0.1	0.0857	0.1837	0.9	0.1	0.0886	0.2102	0.9	0.1	0.0915	0.2445	0.9	0.1	0.0943	0.2911	0.9	0.1	0.0970	0.3577	0.9
0.2	0.1757	0.3505	0.8	0.2	0.1810	0.3973	0.8	0.2	0.1861	0.4564	0.8	0.2	0.1911	0.5336	0.8	0.2	0.1961	0.6377	0.8
0.3	0.2697	0.4997	0.7	0.3	0.2767	0.5604	0.7	0.3	0.2835	0.6347	0.7	0.3	0.2901	0.7264	0.7	0.3	0.2965	0.8387	0.7
0.4	0.3673	0.6305	0.6	0.4	0.3754	0.6988	0.6	0.4	0.3831	0.7783	0.6	0.4	0.3906	0.8686	0.6	0.4	0.3980	0.9595	0.6
0.5	0.4680	0.7422	0.5	0.5	0.4764	0.8116	0.5	0.5	0.4845	0.8866	0.5	0.5	0.4923	0.9593	0.5	0.5	0.5000	1.0000	0.5
0.6	0.5712	0.8344	0.4	0.6	0.5793	0.8984	0.4	0.6	0.5871	0.9591	0.4	0.6	0.5946	0.9984	0.4	0.6	0.6020	0.9595	0.4
0.7	0.6766	0.9066	0.3	0.7	0.6836	0.9588	0.3	0.7	0.6904	0.9954	0.3	0.7	0.6970	0.9854	0.3	0.7	0.7035	0.8387	0.3
0.8	0.7835	0.9584	0.2	0.8	0.7889	0.9924	0.2	0.8	0.7940	0.9954	0.2	0.8	0.7990	0.9205	0.2	0.8	0.8039	0.6377	0.2
0.9	0.8915	0.9896	0.1	0.9	0.8945	0.9992	0.1	0.9	0.8974	0.9591	0.1	0.9	0.9002	0.8039	0.1	0.9	0.9030	0.3577	0.1
1.0	1.0000	1.0000	0.0	1.0	1.0000	0.9789	0.0	1.0	1.0000	0.8866	0.0	1.0	1.0000	0.6364	0.0	1.0	1.0000	0.0000	0.0
	2.7475	90° 130°			3.6535	85° 125°			5.0282	80° 120°			7.2732	75° 115°			11.3426	70° 110°	

TABLE A·1.—H_k AS A FUNCTION OF θ_i — (*Cont.*)

$\Delta X_i = 40°$

θ_i	−20° 20°	0.0882			−15° 25°	0.1375			−10° 30°	0.1989			−5° 35°	0.2737			0° 40°	0.3640	
0.0	0.0000	0.0000	1.0	0.0	0.0000	0.6364	1.0	0.0	0.0000	0.8866	1.0	0.0	0.0000	0.9789	1.0	0.0	0.0000	1.0000	1.0
0.1	0.0970	0.3577	0.9	0.1	0.0998	0.8039	0.9	0.1	0.1026	0.9591	0.9	0.1	0.1055	0.9992	0.9	0.1	0.1085	0.9896	0.9
0.2	0.1961	0.6377	0.8	0.2	0.2010	0.9205	0.8	0.2	0.2060	0.9954	0.8	0.2	0.2111	0.9924	0.8	0.2	0.2165	0.9584	0.8
0.3	0.2965	0.8387	0.7	0.3	0.3030	0.9854	0.7	0.3	0.3096	0.9954	0.7	0.3	0.3164	0.9588	0.7	0.3	0.3234	0.9066	0.7
0.4	0.3980	0.9595	0.6	0.4	0.4054	0.9984	0.6	0.4	0.4129	0.9591	0.6	0.4	0.4207	0.8984	0.6	0.4	0.4288	0.8344	0.6
0.5	0.5000	1.0000	0.5	0.5	0.5077	0.9593	0.5	0.5	0.5155	0.8866	0.5	0.5	0.5236	0.8116	0.5	0.5	0.5320	0.7422	0.5
0.6	0.6020	0.9595	0.4	0.6	0.6094	0.8686	0.4	0.6	0.6169	0.7783	0.4	0.6	0.6246	0.6988	0.4	0.6	0.6327	0.6305	0.4
0.7	0.7035	0.8387	0.3	0.7	0.7099	0.7264	0.3	0.7	0.7165	0.6347	0.3	0.7	0.7233	0.5604	0.3	0.7	0.7303	0.4997	0.3
0.8	0.8039	0.6377	0.2	0.8	0.8089	0.5336	0.2	0.8	0.8139	0.4564	0.2	0.8	0.8190	0.3973	0.2	0.8	0.8243	0.3505	0.2
0.9	0.9030	0.3577	0.1	0.9	0.9057	0.2911	0.1	0.9	0.9085	0.2445	0.1	0.9	0.9114	0.2102	0.1	0.9	0.9143	0.1837	0.1
1.0	1.0000	0.0000	0.0	1.0	1.0000	0.0000	0.0	1.0	1.0000	0.0000	0.0	1.0	1.0000	0.0000	0.0	1.0	1.0000	0.0000	0.0
	11.3426	70° 110°			7.2732	65° 105°			5.0282	60° 100°			3.6535	55° 95°			2.7475	50° 90°	

θ_i	5° 45°	0.4663			10° 50°	0.5774			15° 55°	0.7002			20° 60°	0.8391			25° 65°	1.0000	
0.0	0.0000	1.0000	1.0	0.0	0.0000	1.0000	1.0	0.0	0.0000	1.0000	1.0	0.0	0.0000	1.0000	1.0	0.0	0.0000	1.0000	1.0
0.1	0.1117	0.9706	0.9	0.1	0.1152	0.9576	0.9	0.1	0.1191	0.9480	0.9	0.1	0.1235	0.9405	0.9	0.1	0.1286	0.9345	0.9
0.2	0.2223	0.9245	0.8	0.2	0.2285	0.9013	0.8	0.2	0.2354	0.8842	0.8	0.2	0.2432	0.8710	0.8	0.2	0.2523	0.8602	0.8
0.3	0.3310	0.8620	0.7	0.3	0.3392	0.8315	0.7	0.3	0.3483	0.8090	0.7	0.3	0.3586	0.7916	0.7	0.3	0.3705	0.7774	0.7
0.4	0.4375	0.7834	0.6	0.4	0.4469	0.7485	0.6	0.4	0.4573	0.7228	0.6	0.4	0.4690	0.7028	0.6	0.4	0.4826	0.6866	0.6
0.5	0.5411	0.6891	0.5	0.5	0.5509	0.6527	0.5	0.5	0.5617	0.6259	0.5	0.5	0.5740	0.6051	0.5	0.5	0.5882	0.5882	0.5
0.6	0.6414	0.5795	0.4	0.6	0.6508	0.5446	0.4	0.6	0.6612	0.5188	0.4	0.6	0.6730	0.4989	0.4	0.6	0.6866	0.4826	0.4
0.7	0.7379	0.4551	0.3	0.7	0.7461	0.4246	0.3	0.7	0.7552	0.4021	0.3	0.7	0.7655	0.3847	0.3	0.7	0.7774	0.3705	0.3
0.8	0.8302	0.3166	0.2	0.8	0.8364	0.2934	0.2	0.8	0.8433	0.2763	0.2	0.8	0.8511	0.2630	0.2	0.8	0.8602	0.2523	0.2
0.9	0.9177	0.1647	0.1	0.9	0.9212	0.1517	0.1	0.9	0.9250	0.1421	0.1	0.9	0.9294	0.1346	0.1	0.9	0.9345	0.1286	0.1
1.0	1.0000	0.0000	0.0	1.0	1.0000	0.0000	0.0	1.0	1.0000	0.0000	0.0	1.0	1.0000	0.0000	0.0	1.0	1.0000	0.0000	0.0
	2.1445	45° 85°			1.7321	40° 80°			1.4282	35° 75°			1.1918	30° 70°			1.0000	25° 65°	

TABLE A·1.—H_k AS A FUNCTION OF θ_i — (Cont.)

$\Delta X_i = 50°$

θ_i	−70° −20°	1.0000			−65° −15°	0.8391			−60° −10°	0.7002			−55° −5°	0.5774			−50° 0°	0.4663	
0.0	0.0000	0.0000	1.0	0.0	0.0000	0.0000	1.0	0.0	0.0000	0.0000	1.0	0.0	0.0000	0.0000	1.0	0.0	0.0000	0.0000	1.0
0.1	0.0559	0.1349	0.9	0.1	0.0622	0.1424	0.9	0.1	0.0677	0.1518	0.9	0.1	0.0726	0.1638	0.9	0.1	0.0769	0.1801	0.9
0.2	0.1232	0.2643	0.8	0.2	0.1346	0.2779	0.8	0.2	0.1444	0.2945	0.8	0.2	0.1531	0.3160	0.8	0.2	0.1609	0.3450	0.8
0.3	0.2017	0.3874	0.7	0.3	0.2166	0.4052	0.7	0.3	0.2295	0.4272	0.7	0.3	0.2409	0.4554	0.7	0.3	0.2512	0.4937	0.7
0.4	0.2905	0.5032	0.6	0.4	0.3076	0.5236	0.6	0.4	0.3224	0.5488	0.6	0.4	0.3355	0.5811	0.6	0.4	0.3473	0.6250	0.6
0.5	0.3891	0.6109	0.5	0.5	0.4070	0.6321	0.5	0.5	0.4224	0.6583	0.5	0.5	0.4360	0.6920	0.5	0.5	0.4483	0.7377	0.5
0.6	0.4968	0.7095	0.4	0.6	0.5139	0.7298	0.4	0.6	0.5287	0.7550	0.4	0.6	0.5417	0.7873	0.4	0.6	0.5535	0.8312	0.4
0.7	0.6126	0.7983	0.3	0.7	0.6275	0.8161	0.3	0.7	0.6404	0.8381	0.3	0.7	0.6518	0.8663	0.3	0.7	0.6621	0.9046	0.3
0.8	0.7357	0.8768	0.2	0.8	0.7470	0.8903	0.2	0.8	0.7568	0.9069	0.2	0.8	0.7655	0.9284	0.2	0.8	0.7733	0.9575	0.2
0.9	0.8651	0.9441	0.1	0.9	0.8715	0.9517	0.1	0.9	0.8770	0.9611	0.1	0.9	0.8818	0.9731	0.1	0.9	0.8862	0.9893	0.1
1.0	1.0000	1.0000	0.0	1.0	1.0000	1.0000	0.0	1.0	1.0000	1.0000	0.0	1.0	1.0000	1.0000	0.0	1.0	1.0000	1.0000	0.0
	1.0000	110° 160°			1.1918	105° 155°			1.4282	100° 150°			1.7321	95° 145°			2.1445	90° 140°	

θ_i	−45° 5°	0.3688			−40° 10°	0.2866			−35° 15°	0.2173			−30° 20°	0.1591			−25° 25°	0.1109	
0.0	0.0000	0.0000	1.0	0.0	0.0000	0.0000	1.0	0.0	0.0000	0.0000	1.0	0.0	0.0000	0.0000	1.0	0.0	0.0000	0.0000	1.0
0.1	0.0810	0.2012	0.9	0.1	0.0848	0.2270	0.9	0.1	0.0884	0.2592	0.9	0.1	0.0919	0.3007	0.9	0.1	0.0954	0.3563	0.9
0.2	0.1681	0.3825	0.8	0.2	0.1749	0.4274	0.8	0.2	0.1814	0.4819	0.8	0.2	0.1876	0.5498	0.8	0.2	0.1938	0.6364	0.8
0.3	0.2608	0.5426	0.7	0.3	0.2697	0.5995	0.7	0.3	0.2782	0.6665	0.7	0.3	0.2864	0.7457	0.7	0.3	0.2946	0.8379	0.7
0.4	0.3582	0.6801	0.6	0.4	0.3684	0.7422	0.6	0.4	0.3781	0.8116	0.6	0.4	0.3876	0.8866	0.6	0.4	0.3969	0.9593	0.6
0.5	0.4597	0.7941	0.5	0.5	0.4703	0.8544	0.5	0.5	0.4805	0.9160	0.5	0.5	0.4903	0.9716	0.5	0.5	0.5000	1.0000	0.5
0.6	0.5644	0.8837	0.4	0.6	0.5746	0.9351	0.4	0.6	0.5844	0.9789	0.4	0.6	0.5938	1.0000	0.4	0.6	0.6031	0.9593	0.4
0.7	0.6716	0.9481	0.3	0.7	0.6806	0.9837	0.3	0.7	0.6891	1.0000	0.3	0.7	0.6973	0.9716	0.3	0.7	0.7054	0.8379	0.3
0.8	0.7805	0.9870	0.2	0.8	0.7873	1.0000	0.2	0.8	0.7938	0.9789	0.2	0.8	0.8000	0.8866	0.2	0.8	0.8062	0.6364	0.2
0.9	0.8903	1.0000	0.1	0.9	0.8941	0.9837	0.1	0.9	0.8977	0.9160	0.1	0.9	0.9012	0.7457	0.1	0.9	0.9046	0.3563	0.1
1.0	1.0000	0.9870	0.0	1.0	1.0000	0.9351	0.0	1.0	1.0000	0.8116	0.0	1.0	1.0000	0.5498	0.0	1.0	1.0000	0.0000	0.0
	2.7118	85° 135°			3.4897	80° 130°			4.6027	75° 125°			6.2849	70° 120°			9.0214	65° 115°	

TABLE A·1.—H_k AS A FUNCTION OF θ_i — (*Cont.*)

$\Delta X_i = 50°$

θ_i	−25° 25°	0.1109			−20° 30°	0.1591			−15° 35°	0.2173			−10° 40°	0.2866			−5° 45°	0.3688	
0.0	0.0000	0.0000	1.0	0.0	0.0000	0.5498	1.0	0.0	0.0000	0.8116	1.0	0.0	0.0000	0.9351	1.0	0.0	0.0000	0.9870	1.0
0.1	0.0954	0.3563	0.9	0.1	0.0988	0.7457	0.9	0.1	0.1023	0.9160	0.9	0.1	0.1059	0.9837	0.9	0.1	0.1097	1.0000	0.9
0.2	0.1938	0.6364	0.8	0.2	0.2000	0.8866	0.8	0.2	0.2062	0.9789	0.8	0.2	0.2127	1.0000	0.8	0.2	0.2195	0.9870	0.8
0.3	0.2946	0.8379	0.7	0.3	0.3027	0.9716	0.7	0.3	0.3109	1.0000	0.7	0.3	0.3194	0.9837	0.7	0.3	0.3284	0.9481	0.7
0.4	0.3969	0.9593	0.6	0.4	0.4062	1.0000	0.6	0.4	0.4156	0.9789	0.6	0.4	0.4254	0.9351	0.6	0.4	0.4356	0.8837	0.6
0.5	0.5000	1.0000	0.5	0.5	0.5097	0.9716	0.5	0.5	0.5195	0.9160	0.5	0.5	0.5297	0.8544	0.5	0.5	0.5403	0.7941	0.5
0.6	0.6031	0.9593	0.4	0.6	0.6124	0.8866	0.4	0.6	0.6219	0.8116	0.4	0.6	0.6316	0.7422	0.4	0.6	0.6418	0.6801	0.4
0.7	0.7054	0.8379	0.3	0.7	0.7136	0.7457	0.3	0.7	0.7218	0.6665	0.3	0.7	0.7303	0.5995	0.3	0.7	0.7392	0.5426	0.3
0.8	0.8062	0.6364	0.2	0.8	0.8124	0.5498	0.2	0.8	0.8186	0.4819	0.2	0.8	0.8251	0.4274	0.2	0.8	0.8319	0.3825	0.2
0.9	0.9046	0.3563	0.1	0.9	0.9081	0.3007	0.1	0.9	0.9116	0.2592	0.1	0.9	0.9152	0.2270	0.1	0.9	0.9190	0.2012	0.1
1.0	1.0000	0.0000	0.0	1.0	1.0000	0.0000	0.0	1.0	1.0000	0.0000	0.0	1.0	1.0000	0.0000	0.0	1.0	1.0000	0.0000	0.0
	9.0214	65° 115°			6.2849	60° 110°			4.6027	55° 105°			3.4897	50° 100°			2.7118	45° 95°	

θ_i	0° 50°	0.4663			5° 55°	0.5774			10° 60°	0.7002			15° 65°	0.8391			20° 70°	1.0000	
0.0	0.0000	1.0000	1.0	0.0	0.0000	1.0000	1.0	0.0	0.0000	1.0000	1.0	0.0	0.0000	1.0000	1.0	0.0	0.0000	1.0000	1.0
0.1	0.1138	0.9893	0.9	0.1	0.1182	0.9731	0.9	0.1	0.1230	0.9611	0.9	0.1	0.1285	0.9517	0.9	0.1	0.1349	0.9441	0.9
0.2	0.2267	0.9575	0.8	0.2	0.2345	0.9284	0.8	0.2	0.2432	0.9069	0.8	0.2	0.2530	0.8903	0.8	0.2	0.2643	0.8768	0.8
0.3	0.3379	0.9046	0.7	0.3	0.3482	0.8663	0.7	0.3	0.3596	0.8381	0.7	0.3	0.3725	0.8161	0.7	0.3	0.3874	0.7983	0.7
0.4	0.4465	0.8312	0.6	0.4	0.4583	0.7873	0.6	0.4	0.4713	0.7550	0.6	0.4	0.4861	0.7298	0.6	0.4	0.5032	0.7095	0.6
0.5	0.5517	0.7377	0.5	0.5	0.5640	0.6920	0.5	0.5	0.5776	0.6583	0.5	0.5	0.5930	0.6321	0.5	0.5	0.6109	0.6109	0.5
0.6	0.6527	0.6250	0.4	0.6	0.6645	0.5811	0.4	0.6	0.6776	0.5488	0.4	0.6	0.6924	0.5236	0 4	0.6	0.7095	0.5032	0.4
0.7	0.7488	0.4937	0.3	0.7	0.7591	0.4554	0.3	0.7	0.7705	0.4272	0.3	0.7	0.7834	0.4052	0.3	0.7	0.7983	0.3874	0.3
0.8	0.8391	0.3450	0.2	0.8	0.8469	0.3160	0.2	0.8	0.8556	0.2945	0.2	0.8	0.8654	0.2779	0.2	0.8	0.8768	0.2643	0.2
0.9	0.9231	0.1801	0.1	0.9	0.9274	0.1638	0.1	0.9	0.9323	0.1518	0.1	0.9	0.9378	0.1424	0.1	0.9	0.9441	0.1349	0.1
1.0	1.0000	0.0000	0.0	1.0	1.0000	0.0000	0.0	1.0	1.0000	0.0000	0.0	1.0	1.0000	0.0000	0.0	1.0	1.0000	0.0000	0.0
	2.1445	40° 90°			1.7321	35° 85°			1.4282	30° 80°			1.1918	25° 75°			1.0000	20° 70°	

TABLE A·1.—H_k AS A FUNCTION OF θ_i — (*Cont.*)

$\Delta X_i = 60°$

θ_i	−75° −15°	1.0000	
0.0	0.0000	0.0000	1.0
0.1	0.0457	0.1408	0.9
0.2	0.1060	0.2760	0.8
0.3	0.1800	0.4042	0.7
0.4	0.2670	0.5240	0.6
0.5	0.3660	0.6340	0.5
0.6	0.4760	0.7330	0.4
0.7	0.5958	0.8200	0.3
0.8	0.7240	0.8940	0.2
0.9	0.8592	0.9543	0.1
1.0	1.0000	1.0000	0.0
	1.0000	105° 165°	

	−70° −10°	0.8391	
0.0	0.0000	0.0000	1.0
0.1	0.0534	0.1499	0.9
0.2	0.1196	0.2923	0.8
0.3	0.1980	0.4257	0.7
0.4	0.2877	0.5486	0.6
0.5	0.3876	0.6597	0.5
0.6	0.4967	0.7577	0.4
0.7	0.6138	0.8415	0.3
0.8	0.7377	0.9103	0.2
0.9	0.8669	0.9634	0.1
1.0	1.0000	1.0000	0.0
	1.1918	100° 160°	

	−65° −5°	0.7002	
0.0	0.0000	0.0000	1.0
0.1	0.0600	0.1611	0.9
0.2	0.1314	0.3124	0.8
0.3	0.2136	0.4522	0.7
0.4	0.3055	0.5790	0.6
0.5	0.4062	0.6913	0.5
0.6	0.5146	0.7880	0.4
0.7	0.6294	0.8680	0.3
0.8	0.7495	0.9305	0.2
0.9	0.8735	0.9746	0.1
1.0	1.0000	1.0000	0.0
	1.4282	95° 155°	

	−60° 0°	0.5774	
0.0	0.0000	0.0000	1.0
0.1	0.0658	0.1756	0.9
0.2	0.1419	0.3383	0.8
0.3	0.2274	0.4863	0.7
0.4	0.3213	0.6180	0.6
0.5	0.4227	0.7321	0.5
0.6	0.5303	0.8271	0.4
0.7	0.6432	0.9021	0.3
0.8	0.7599	0.9563	0.2
0.9	0.8793	0.9890	0.1
1.0	1.0000	1.0000	0.0
	1.7321	90° 150°	

	−55° 5°	0.4705	
0.0	0.0000	0.0000	1.0
0.1	0.0711	0.1934	0.9
0.2	0.1513	0.3700	0.8
0.3	0.2398	0.5278	0.7
0.4	0.3355	0.6650	0.6
0.5	0.4375	0.7803	0.5
0.6	0.5446	0.8722	0.4
0.7	0.6556	0.9399	0.3
0.8	0.7694	0.9825	0.2
0.9	0.8846	0.9997	0.1
1.0	1.0000	0.9911	0.0
	2.1254	85° 145°	

θ_i	−50° 10°	0.3801	
0.0	0.0000	0.0000	1.0
0.1	0.0760	0.2143	0.9
0.2	0.1600	0.4065	0.8
0.3	0.2513	0.5746	0.7
0.4	0.3487	0.7167	0.6
0.5	0.4512	0.8312	0.5
0.6	0.5578	0.9169	0.4
0.7	0.6671	0.9728	0.3
0.8	0.7781	0.9983	0.2
0.9	0.8894	0.9932	0.1
1.0	1.0000	0.9575	0.0
	2.6306	80° 140°	

	−45° 15°	0.3032	
0.0	0.0000	0.0000	1.0
0.1	0.0805	0.2391	0.9
0.2	0.1682	0.4492	0.8
0.3	0.2620	0.6279	0.7
0.4	0.3610	0.7732	0.6
0.5	0.4641	0.8837	0.5
0.6	0.5701	0.9580	0.4
0.7	0.6779	0.9953	0.3
0.8	0.7862	0.9953	0.2
0.9	0.8940	0.9580	0.1
1.0	1.0000	0.8837	0.0
	3.2979	75° 135°	

	−40° 20°	0.2376	
0.0	0.0000	0.0000	1.0
0.1	0.0849	0.2693	0.9
0.2	0.1760	0.4997	0.8
0.3	0.2723	0.6887	0.7
0.4	0.3728	0.8344	0.6
0.5	0.4764	0.9351	0.5
0.6	0.5819	0.9896	0.4
0.7	0.6881	0.9974	0.3
0.8	0.7940	0.9584	0.2
0.9	0.8984	0.8731	0.1
1.0	1.0000	0.7422	0.0
	4.2094	70° 130°	

	−35° 25°	0.1815	
0.0	0.0000	0.0000	1.0
0.1	0.0891	0.3067	0.9
0.2	0.1836	0.5604	0.8
0.3	0.2823	0.7584	0.7
0.4	0.3842	0.8984	0.6
0.5	0.4883	0.9789	0.5
0.6	0.5933	0.9992	0.4
0.7	0.6981	0.9588	0.3
0.8	0.8016	0.8583	0.2
0.9	0.9026	0.6988	0.1
1.0	1.0000	0.4819	0.0
	5.5085	65° 125°	

	−30° 30°	0.1340	
0.0	0.0000	0.0000	1.0
0.1	0.0933	0.3547	0.9
0.2	0.1910	0.6347	0.8
0.3	0.2921	0.8369	0.7
0.4	0.3955	0.9591	0.6
0.5	0.5000	1.0000	0.5
0.6	0.6045	0.9591	0.4
0.7	0.7079	0.8369	0.3
0.8	0.8090	0.6347	0.2
0.9	0.9067	0.3547	0.1
1.0	1.0000	0.0000	0.0
	7.4641	60° 120°	

TABLE A·1.—H_k AS A FUNCTION OF θ_i — (*Cont.*)

$\Delta X_i = 60°$

θ_i	−30° 30°	0.1340			−25° 35°	0.1815			−20° 40°	0.2376			−15° 45°	0.3032			−10° 50°	0.3801	
0.0	0.0000	0.0000	1.0	0.0	0.0000	0.4819	1.0	0.0	0.0000	0.7422	1.0	0.0	0.0000	0.8837	1.0	0.0	0.0000	0.9575	1.0
0.1	0.0933	0.3547	0.9	0.1	0.0974	0.6988	0.9	0.1	0.1016	0.8731	0.9	0.1	0.1060	0.9580	0.9	0.1	0.1106	0.9932	0.9
0.2	0.1910	0.6347	0.8	0.2	0.1984	0.8583	0.8	0.2	0.2060	0.9584	0.8	0.2	0.2138	0.9953	0.8	0.2	0.2219	0.9983	0.8
0.3	0.2921	0.8369	0.7	0.3	0.3019	0.9588	0.7	0.3	0.3119	0.9974	0.7	0.3	0.3221	0.9953	0.7	0.3	0.3329	0.9728	0.7
0.4	0.3955	0.9591	0.6	0.4	0.4067	0.9992	0.6	0.4	0.4181	0.9896	0.6	0.4	0.4299	0.9580	0.6	0.4	0.4422	0.9169	0.6
0.5	0.5000	1.0000	0.5	0.5	0.5117	0.9789	0.5	0.5	0.5236	0.9351	0.5	0.5	0.5359	0.8837	0.5	0.5	0.5488	0.8312	0.5
0.6	0.6045	0.9591	0.4	0.6	0.6158	0.8984	0.4	0.6	0.6272	0.8344	0.4	0.6	0.6390	0.7732	0.4	0.6	0.6513	0.7167	0.4
0.7	0.7079	0.8369	0.3	0.7	0.7177	0.7584	0.3	0.7	0.7277	0.6887	0.3	0.7	0.7380	0.6279	0.3	0.7	0.7487	0.5746	0.3
0.8	0.8090	0.6347	0.2	0.8	0.8164	0.5604	0.2	0.8	0.8240	0.4997	0.2	0.8	0.8318	0.4492	0.2	0.8	0.8400	0.4065	0.2
0.9	0.9067	0.3547	0.1	0.9	0.9109	0.3067	0.1	0.9	0.9151	0.2693	0.1	0.9	0.9195	0.2391	0.1	0.9	0.9240	0.2143	0.1
1.0	1.0000	0.0000	0.0	1.0	1.0000	0.0000	0.0	1.0	1.0000	0.0000	0.0	1.0	1.0000	0.0000	0.0	1.0	1.0000	0.0000	0.0
	7.4641	60° 120°			5.5085	55° 115°			4.2094	50° 110°			3.2979	45° 105°			2.6306	40° 100°	

θ_i	−5° 55°	0.4705			0° 60°	0.5774			5° 65°	0.7002			10° 70°	0.8391			15° 75°	1.0000	
0.0	0.0000	0.9911	1.0	0.0	0.0000	1.0000	1.0	0.0	0.0000	1.0000	1.0	0.0	0.0000	1.0000	1.0	0.0	0.0000	1.0000	1.0
0.1	0.1154	0.9997	0.9	0.1	0.1207	0.9890	0.9	0.1	0.1265	0.9746	0.9	0.1	0.1331	0.9634	0.9	0.1	0.1408	0.9543	0.9
0.2	0.2306	0.9825	0.8	0.2	0.2401	0.9563	0.8	0.2	0.2505	0.9305	0.8	0.2	0.2623	0.9103	0.8	0.2	0.2760	0.8940	0.8
0.3	0.3444	0.9399	0.7	0.3	0.3568	0.9021	0.7	0.3	0.3706	0.8680	0.7	0.3	0.3862	0.8415	0.7	0.3	0.4042	0.8200	0.7
0.4	0.4554	0.8722	0.6	0.4	0.4697	0.8271	0.6	0.4	0.4854	0.7880	0.6	0.4	0.5033	0.7577	0.6	0.4	0.5240	0.7330	0.6
0.5	0.5625	0.7803	0.5	0.5	0.5773	0.7321	0.5	0.5	0.5938	0.6913	0.5	0.5	0.6124	0.6597	0.5	0.5	0.6340	0.6340	0.5
0.6	0.6645	0.6650	0.4	0.6	0.6787	0.6180	0.4	0.6	0.6945	0.5790	0.4	0.6	0.7123	0.5486	0.4	0.6	0.7330	0.5240	0.4
0.7	0.7602	0.5278	0.3	0.7	0.7726	0.4863	0.3	0.7	0.7864	0.4522	0.3	0.7	0.8020	0.4257	0.3	0.7	0.8200	0.4042	0.3
0.8	0.8487	0.3700	0.2	0.8	0.8581	0.3383	0.2	0.8	0.8686	0.3124	0.2	0.8	0.8804	0.2923	0.2	0.8	0.8940	0.2760	0.2
0.9	0.9289	0.1934	0.1	0.9	0.9342	0.1756	0.1	0.9	0.9400	0.1611	0.1	0.9	0.9466	0.1499	0.1	0.9	0.9543	0.1408	0.1
1.0	1.0000	0.0000	0.0	1.0	1.0000	0.0000	0.0	1.0	1.0000	0.0000	0.0	1.0	1.0000	0.0000	0.0	1.0	1.0000	0.0000	0.0
	2.1254	35° 95°			1.7321	30° 90°			1.4282	25° 85°			1.1918	20° 80°			1.0000	15° 75°	

TABLE A·1.—H_k AS A FUNCTION OF θ_i — (*Cont.*)

$\Delta X_i = 70°$

θ_i	−80° −10°	1.0000			−75° −5°	0.8391			−70° 0°	0.7002			−65° 5°	0.5812			−60° 10°	0.4809	
0.0	0.0000	0.0000	1.0	0.0	0.0000	0.0000	1.0	0.0	0.0000	0.0000	1.0	0.0	0.0000	0.0000	1.0	0.0	0.0000	0.0000	1.0
0.1	0.0352	0.1464	0.9	0.1	0.0441	0.1570	0.9	0.1	0.0518	0.1702	0.9	0.1	0.0586	0.1858	0.9	0.1	0.0648	0.2036	0.9
0.2	0.0878	0.2874	0.8	0.2	0.1039	0.3065	0.8	0.2	0.1178	0.3301	0.8	0.2	0.1300	0.3580	0.8	0.2	0.1411	0.3893	0.8
0.3	0.1574	0.4209	0.7	0.3	0.1786	0.4461	0.7	0.3	0.1968	0.4773	0.7	0.3	0.2130	0.5139	0.7	0.3	0.2277	0.5543	0.7
0.4	0.2426	0.5449	0.6	0.4	0.2669	0.5739	0.6	0.4	0.2879	0.6096	0.6	0.4	0.3065	0.6513	0.6	0.4	0.3233	0.6961	0.6
0.5	0.3424	0.6576	0.5	0.5	0.3677	0.6879	0.5	0.5	0.3896	0.7251	0.5	0.5	0.4090	0.7680	0.5	0.5	0.4265	0.8126	0.5
0.6	0.4551	0.7574	0.4	0.6	0.4794	0.7864	0.4	0.6	0.5004	0.8221	0.4	0.6	0.5190	0.8623	0.4	0.6	0.5358	0.9021	0.4
0.7	0.5791	0.8426	0.3	0.7	0.6003	0.8679	0.3	0.7	0.6186	0.8991	0.3	0.7	0.6348	0.9329	0.3	0.7	0.6494	0.9633	0.3
0.8	0.7126	0.9122	0.2	0.8	0.7287	0.9313	0.2	0.8	0.7426	0.9549	0.2	0.8	0.7548	0.9787	0.2	0.8	0.7659	0.9951	0.2
0.9	0.8536	0.9648	0.1	0.9	0.8626	0.9755	0.1	0.9	0.8703	0.9887	0.1	0.9	0.8771	0.9989	0.1	0.9	0.8833	0.9973	0.1
1.0	1.0000	1.0000	0.0	1.0	1.0000	1.0000	0.0	1.0	1.0000	1.0000	0.0	1.0	1.0000	0.9934	0.0	1.0	1.0000	0.9696	0.0
	1.0000	100° 170°			1.1918	95° 165°			1.4282	90° 160°			1.7206	85° 155°			2.0794	80° 150°	

θ_i	−55° 15°	0.3956			−50° 20°	0.3224			−45° 25°	0.2593			−40° 30°	0.2047			−35° 35°	0.1577	
0.0	0.0000	0.0000	1.0	0.0	0.0000	0.0000	1.0	0.0	0.0000	0.0000	1.0	0.0	0.0000	0.0000	1.0	0.0	0.0000	0.0000	1.0
0.1	0.0705	0.2241	0.9	0.1	0.0758	0.2479	0.9	0.1	0.0810	0.2762	0.9	0.1	0.0859	0.3104	0.9	0.1	0.0908	0.3528	0.9
0.2	0.1513	0.4248	0.8	0.2	0.1609	0.4654	0.8	0.2	0.1700	0.5123	0.8	0.2	0.1789	0.5674	0.8	0.2	0.1876	0.6327	0.8
0.3	0.2412	0.5991	0.7	0.3	0.2538	0.6490	0.7	0.3	0.2659	0.7048	0.7	0.3	0.2776	0.7671	0.7	0.3	0.2891	0.8358	0.7
0.4	0.3388	0.7444	0.6	0.4	0.3533	0.7961	0.6	0.4	0.3671	0.8508	0.6	0.4	0.3805	0.9066	0.6	0.4	0.3938	0.9588	0.6
0.5	0.4426	0.8586	0.5	0.5	0.4578	0.9046	0.5	0.5	0.4722	0.9481	0.5	0.5	0.4862	0.9837	0.5	0.5	0.5000	1.0000	0.5
0.6	0.5512	0.9399	0.4	0.6	0.5657	0.9728	0.4	0.6	0.5796	0.9953	0.4	0.6	0.5930	0.9974	0.4	0.6	0.6062	0.9588	0.4
0.7	0.6629	0.9871	0.3	0.7	0.6756	0.9996	0.3	0.7	0.6877	0.9917	0.3	0.7	0.6994	0.9474	0.3	0.7	0.7109	0.8358	0.3
0.8	0.7761	0.9996	0.2	0.8	0.7857	0.9847	0.2	0.8	0.7948	0.9373	0.2	0.8	0.8037	0.8344	0.2	0.8	0.8124	0.6327	0.2
0.9	0.8890	0.9772	0.1	0.9	0.8944	0.9282	0.1	0.9	0.8994	0.8329	0.1	0.9	0.9044	0.6602	0.1	0.9	0.9092	0.3528	0.1
1.0	1.0000	0.9201	0.0	1.0	1.0000	0.8312	0.0	1.0	1.0000	0.6801	0.0	1.0	1.0000	0.4272	0.0	1.0	1.0000	0.0000	0.0
	2.5279	75° 145°			3.1020	70° 140°			3.8571	65° 135°			4.8846	60° 130°			6.3432	55° 125°	

TABLE A·1.—H_k AS A FUNCTION OF θ_i — (*Cont.*)

$\Delta X_i = 70°$

θ_i	−35° 35°	0.1577			−30° 40°	0.2047			−25° 45°	0.2593			−20° 50°	0.3224			−15° 55°	0.3956	
0.0	0.0000	0.0000	1.0	0.0	0.0000	0.4274	1.0	0.0	0.0000	0.6801	1.0	0.0	0.0000	0.8312	1.0	0.0	0.0000	0.9201	1.0
0.1	0.0908	0.3528	0.9	0.1	0.0956	0.6602	0.9	0.1	0.1006	0.8329	0.9	0.1	0.1056	0.9282	0.9	0.1	0.1110	0.9772	0.9
0.2	0.1876	0.6327	0.8	0.2	0.1963	0.8344	0.8	0.2	0.2052	0.9373	0.8	0.2	0.2143	0.9847	0.8	0.2	0.2239	0.9996	0.8
0.3	0.2891	0.8358	0.7	0.3	0.3006	0.9474	0.7	0.3	0.3123	0.9917	0.7	0.3	0.3244	0.9996	0.7	0.3	0.3371	0.9871	0.7
0.4	0.3938	0.9588	0.6	0.4	0.4070	0.9974	0.6	0.4	0.4204	0.9953	0.6	0.4	0.4343	0.9728	0.6	0.4	0.4488	0.9399	0.6
0.5	0.5000	1.0000	0.5	0.5	0.5138	0.9837	0.5	0.5	0.5278	0.9481	0.5	0.5	0.5422	0.9046	0.5	0.5	0.5574	0.8586	0.5
0.6	0.6062	0.9588	0.4	0.6	0.6195	0.9066	0.4	0.6	0.6329	0.8508	0.4	0.6	0.6467	0.7961	0.4	0.6	0.6612	0.7444	0.4
0.7	0.7109	0.8358	0.3	0.7	0.7224	0.7671	0.3	0.7	0.7341	0.7408	0.3	0.7	0.7462	0.6490	0.3	0.7	0.7588	0.5991	0.3
0.8	0.8124	0.6327	0.2	0.8	0.8211	0.5674	0.2	0.8	0.8300	0.5123	0.2	0.8	0.8391	0.4654	0.2	0.8	0.8487	0.4248	0.2
0.9	0.9092	0.3528	0.1	0.9	0.9141	0.3104	0.1	0.9	0.9190	0.2762	0.1	0.9	0.9242	0.2479	0.1	0.9	0.9295	0.2241	0.1
1.0	1.0000	0.0000	0.0	1.0	1.0000	0.0000	0.0	1.0	1.0000	0.0000	0.0	1.0	1.0000	0.0000	0.0	1.0	1.0000	0.0000	0.0
	6.3432	55° 125°			4.8846	50° 120°			3.8571	45° 115°			3.1020	40° 110°			2.5279	35° 105°	

θ_i	−10° 60°	0.4809			−5° 65°	0.5812			0° 70°	0.7002			5° 75°	0.8391			10° 80°	1.0000	
0.0	0.0000	0.9696	1.0	0.0	0.0000	0.9934	1.0	0.0	0.0000	1.0000	1.0	0.0	0.0000	1.0000	1.0	0.0	0.0000	1.0000	1.0
0.1	0.1167	0.9973	0.9	0.1	0.1229	0.9989	0.9	0.1	0.1297	0.9887	0.9	0.1	0.1374	0.9755	0.9	0.1	0.1464	0.9648	0.9
0.2	0.2341	0.9951	0.8	0.2	0.2452	0.9787	0.8	0.2	0.2574	0.9549	0.8	0.2	0.2713	0.9313	0.8	0.2	0.2874	0.9122	0.8
0.3	0.3506	0.9633	0.7	0.3	0.3652	0.9329	0.7	0.3	0.3814	0.8991	0.7	0.3	0.3997	0.8679	0.7	0.3	0.4209	0.8426	0.7
0.4	0.4642	0.9021	0.6	0.4	0.4810	0.8623	0.6	0.4	0.4996	0.8221	0.6	0.4	0.5206	0.7864	0.6	0.4	0.5449	0.7574	0.6
0.5	0.5735	0.8126	0.5	0.5	0.5910	0.7680	0.5	0.5	0.6104	0.7251	0.5	0.5	0.6323	0.6879	0.5	0.5	0.6576	0.6576	0.5
0.6	0.6767	0.6961	0.4	0.6	0.6935	0.6513	0.4	0.6	0.7121	0.6096	0.4	0.6	0.7331	0.5739	0.4	0.6	0.7574	0.5449	0.4
0.7	0.7723	0.5543	0.3	0.7	0.7870	0.5139	0.3	0.7	0.8032	0.4773	0.3	0.7	0.8214	0.4461	0.3	0.7	0.8426	0.4209	0.3
0.8	0.8589	0.3893	0.2	0.8	0.8700	0.3580	0.2	0.8	0.8822	0.3301	0.2	0.8	0.8961	0.3065	0.2	0.8	0.9122	0.2874	0.2
0.9	0.9352	0.2036	0.1	0.9	0.9414	0.1858	0.1	0.9	0.9482	0.1702	0.1	0.9	0.9559	0.1570	0.1	0.9	0.9648	0.1464	0.1
1.0	1.0000	0.0000	0.0	1.0	1.0000	0.0000	0.0	1.0	1.0000	0.0000	0.0	1.0	1.0000	0.0000	0.0	1.0	1.0000	0.0000	0.0
	2.0794	30° 100°			1.7206	25° 95°			1.4282	20° 90°			1.1918	15° 85°			1.0000	10° 80°	

TABLE A·1.—H_k AS A FUNCTION OF θ_i — (*Cont.*)

$\Delta X_i = 80°$

θ_i	−85°				−80°				−75°				−70°				−65°		
	−5°	1.0000			0°	0.8391			5°	0.7038			10°	0.5910			15°	0.4956	
0.0	0.0000	0.0000	1.0	0.0	0.0000	0.0000	1.0	0.0	0.0000	0.0000	1.0	0.0	0.0000	0.0000	1.0	0.0	0.0000	0.0000	1.0
0.1	0.0240	0.1516	0.9	0.1	0.0342	0.1638	0.9	0.1	0.0431	0.1780	0.9	0.1	0.0510	0.1937	0.9	0.1	0.0581	0.2113	0.9
0.2	0.0689	0.2984	0.8	0.2	0.0874	0.3203	0.8	0.2	0.1033	0.3457	0.8	0.2	0.1174	0.3735	0.8	0.2	0.1301	0.4043	0.8
0.3	0.1337	0.4374	0.7	0.3	0.1582	0.4666	0.7	0.3	0.1793	0.4999	0.7	0.3	0.1979	0.5359	0.7	0.3	0.2148	0.5752	0.7
0.4	0.2173	0.5662	0.6	0.4	0.2454	0.5996	0.6	0.4	0.2696	0.6375	0.6	0.4	0.2910	0.6778	0.6	0.4	0.3104	0.7206	0.6
0.5	0.3180	0.6820	0.5	0.5	0.3473	0.7169	0.5	0.5	0.3726	0.7560	0.5	0.5	0.3949	0.7964	0.5	0.5	0.4151	0.8377	0.5
0.6	0.4338	0.7827	0.4	0.6	0.4619	0.8161	0.4	0.6	0.4861	0.8530	0.4	0.6	0.5076	0.8893	0.4	0.6	0.5269	0.9243	0.4
0.7	0.5626	0.8663	0.3	0.7	0.5870	0.8954	0.3	0.7	0.6081	0.9265	0.3	0.7	0.6267	0.9549	0.3	0.7	0.6436	0.9787	0.3
0.8	0.7016	0.9311	0.2	0.8	0.7201	0.9531	0.2	0.8	0.7360	0.9752	0.2	0.8	0.7501	0.9917	0.2	0.8	0.7629	0.9997	0.2
0.9	0.8484	0.9760	0.1	0.9	0.8587	0.9882	0.1	0.9	0.8675	0.9982	0.1	0.9	0.8754	0.9991	0.1	0.9	0.8825	0.9871	0.1
1.0	1.0000	1.0000	0.0	1.0	1.0000	1.0000	0.0	1.0	1.0000	0.9949	0.0	1.0	1.0000	0.9769	0.0	1.0	1.0000	0.9410	0.0
		95°				90°				85°				80°				75°	
	1.0000	175°			1.1918	170°			1.4208	165°			1.6921	160°			2.0180	155°	

θ_i	−60°				−55°				−50°				−45°				−40°		
	20°	0.4139			25°	0.3434			30°	0.2822			35°	0.2287			40°	0.1820	
0.0	0.0000	0.0000	1.0	0.0	0.0000	0.0000	1.0	0.0	0.0000	0.0000	1.0	0.0	0.0000	0.0000	1.0	0.0	0.0000	0.0000	1.0
0.1	0.0646	0.2313	0.9	0.1	0.0707	0.2543	0.9	0.1	0.0766	0.2809	0.9	0.1	0.0822	0.3125	0.9	0.1	0.0878	0.3505	0.9
0.2	0.1420	0.4387	0.8	0.2	0.1529	0.4774	0.8	0.2	0.1634	0.5214	0.8	0.2	0.1736	0.5719	0.8	0.2	0.1836	0.6305	0.8
0.3	0.2303	0.6180	0.7	0.3	0.2449	0.6650	0.7	0.3	0.2588	0.7167	0.7	0.3	0.2723	0.7732	0.7	0.3	0.2856	0.8344	0.7
0.4	0.3283	0.7659	0.6	0.4	0.3450	0.8136	0.6	0.4	0.3610	0.8630	0.6	0.4	0.3765	0.9125	0.6	0.4	0.3918	0.9584	0.6
0.5	0.4338	0.8794	0.5	0.5	0.4512	0.9201	0.5	0.5	0.4679	0.9575	0.5	0.5	0.4841	0.9870	0.5	0.5	0.5000	1.0000	0.5
0.6	0.5448	0.9563	0.4	0.6	0.5615	0.9825	0.4	0.6	0.5775	0.9983	0.4	0.6	0.5930	0.9953	0.4	0.6	0.6083	0.9584	0.4
0.7	0.6591	0.9951	0.3	0.7	0.6737	0.9997	0.3	0.7	0.6876	0.9847	0.3	0.7	0.7011	0.9373	0.3	0.7	0.7144	0.8344	0.3
0.8	0.7746	0.9951	0.2	0.8	0.7856	0.9711	0.2	0.8	0.7962	0.9169	0.2	0.8	0.8064	0.8140	0.2	0.8	0.8164	0.6305	0.2
0.9	0 8890	0.9563	0.1	0.9	0.8951	0.8975	0.1	0.9	0.9010	0.7961	0.1	0.9	0.9066	0.6279	0.1	0.9	0.9122	0.3505	0.1
1.0	1.0000	0.8794	0.0	1.0	1.0000	0.7803	0.0	1.0	1.0000	0.6250	0.0	1.0	1.0000	0.3825	0.0	1.0	1.0000	0.0000	0.0
		70°				65°				60°				55°				50°	
	2.4161	150°			2.9121	145°			3.5442	140°			4.3725	135°			5.4950	130°	

TABLE A·1.—H_k AS A FUNCTION OF θ_i — (*Cont.*)

$\Delta X_i = 80°$

θ_i	−40° 40°	0.1820			−35° 45°	0.2287			−30° 50°	0.2822			−25° 55°	0.3434			−20° 60°	0.4139	
0.0	0.0000	0.0000	1.0	0.0	0.0000	0.3825	1.0	0.0	0.0000	0.6250	1.0	0.0	0.0000	0.7803	1.0	0.0	0.0000	0.8794	1.0
0.1	0.0878	0.3505	0.9	0.1	0.0934	0.6279	0.9	0.1	0.0990	0.7961	0.9	0.1	0.1049	0.8975	0.9	0.1	0.1110	0.9563	0.9
0.2	0.1836	0.6305	0.8	0.2	0.1936	0.8140	0.8	0.2	0.2038	0.9169	0.8	0.2	0.2144	0.9711	0.8	0.2	0.2254	0.9951	0.8
0.3	0.2856	0.8344	0.7	0.3	0.2989	0.9373	0.7	0.3	0.3124	0.9847	0.7	0.3	0.3263	0.9997	0.7	0.3	0.3409	0.9951	0.7
0.4	0.3918	0.9584	0.6	0.4	0.4070	0.9953	0.6	0.4	0.4225	0.9983	0.6	0.4	0.4385	0.9825	0.6	0.4	0.4552	0.9563	0.6
0.5	0.5000	1.0000	0.5	0.5	0.5159	0.9870	0.5	0.5	0.5321	0.9575	0.5	0.5	0.5488	0.9201	0.5	0.5	0.5662	0.8794	0.5
0.6	0.6083	0.9584	0.4	0.6	0.6235	0.9125	0.4	0.6	0.6390	0.8630	0.4	0.6	0.6550	0.8136	0.4	0.6	0.6717	0.7659	0.4
0.7	0.7144	0.8344	0.3	0.7	0.7277	0.7732	0.3	0.7	0.7412	0.7167	0.3	0.7	0.7551	0.6650	0.3	0.7	0.7697	0.6180	0.3
0.8	0.8164	0.6305	0.2	0.8	0.8264	0.5719	0.2	0.8	0.8366	0.5214	0.2	0.8	0.8471	0.4774	0.2	0.8	0.8580	0.4387	0.2
0.9	0.9122	0.3505	0.1	0.9	0.9178	0.3125	0.1	0.9	0.9234	0.2809	0.1	0.9	0.9293	0.2543	0.1	0.9	0.9354	0.2313	0.1
1.0	1.0000	0.0000	0.0	1.0	1.0000	0.0000	0.0	1.0	1.0000	0.0000	0.0	1.0	1.0000	0.0000	0.0	1.0	1.0000	0.0000	0.0
	5.4950	50° 130°			4.3725	45° 125°			3.5442	40° 120°			2.9121	35° 115°			2.4161	30° 110°	

θ_i	−15° 65°	0.4956			−10° 70°	0.5910			−5° 75°	0.7038			0° 80°	0.8391			5° 85°	1.0000	
0.0	0.0000	0.9410	1.0	0.0	0.0000	0.9769	1.0	0.0	0.0000	0.9949	1.0	0.0	0.0000	1.0000	1.0	0.0	0.0000	1.0000	1.0
0.1	0.1175	0.9871	0.9	0.1	0.1246	0.9991	0.9	0.1	0.1325	0.9982	0.9	0.1	0.1413	0.9882	0.9	0.1	0.1516	0.9760	0.9
0.2	0.2371	0.9997	0.8	0.2	0.2499	0.9917	0.8	0.2	0.2640	0.9752	0.8	0.2	0.2799	0.9531	0.8	0.2	0.2984	0.9311	0.8
0.3	0.3564	0.9787	0.7	0.3	0.3733	0.9549	0.7	0.3	0.3919	0.9265	0.7	0.3	0.4130	0.8954	0.7	0.3	0.4374	0.8663	0.7
0.4	0.4731	0.9243	0.6	0.4	0.4924	0.8893	0.6	0.4	0.5139	0.8530	0.6	0.4	0.5381	0.8161	0.6	0.4	0.5662	0.7827	0.6
0.5	0.5849	0.8377	0.5	0.5	0.6051	0.7964	0.5	0.5	0.6274	0.7560	0.5	0.5	0.6527	0.7169	0.5	0.5	0.6820	0.6820	0.5
0.6	0.6896	0.7206	0.4	0.6	0.7090	0.6778	0.4	0.6	0.7304	0.6375	0.4	0.6	0.7546	0.5996	0.4	0.6	0.7827	0.5662	0.4
0.7	0.7852	0.5752	0.3	0.7	0.8021	0.5359	0.3	0.7	0.8207	0.4999	0.3	0.7	0.8418	0.4666	0.3	0.7	0.8663	0.4374	0.3
0.8	0.8699	0.4043	0.2	0.8	0.8826	0.3735	0.2	0.8	0.8967	0.3457	0.2	0.8	0.9126	0.3203	0.2	0.8	0.9311	0.2984	0.2
0.9	0.9419	0.2113	0.1	0.9	0.9490	0.1937	0.1	0.9	0.9569	0.1780	0.1	0.9	0.9658	0.1638	0.1	0.9	0.9760	0.1516	0.1
1.0	1.0000	0.0000	0.0	1.0	1.0000	0.0000	0.0	1.0	1.0000	0.0000	0.0	1.0	1.0000	0.0000	0.0	1.0	1.0000	0.0000	0.0
	2.0180	25° 105°			1.6921	20° 100°			1.4208	15° 95°			1.1918	10° 90°			1.0000	5° 85°	

TABLE A·1.—H_k AS A FUNCTION OF θ_i — (Cont.)

$\Delta X_i = 90°$

θ_i	−90° 0°	1.0000			−85° 5°	0.8426			−80° 10°	0.7133			−75° 15°	0.6052			−70° 20°	0.5134	
0.0	0.0000	0.0000	1.0	0.0	0.0000	0.0000	1.0	0.0	0.0000	0.0000	1.0	0.0	0.0000	0.0000	1.0	0.0	0.0000	0.0000	1.0
0.1	0.0123	0.1564	0.9	0.1	0.0239	0.1695	0.9	0.1	0.0339	0.1838	0.9	0.1	0.0428	0.1996	0.9	0.1	0.0508	0.2170	0.9
0.2	0.0489	0.3090	0.8	0.2	0.0699	0.3326	0.8	0.2	0.0879	0.3580	0.8	0.2	0.1038	0.3856	0.8	0.2	0.1183	0.4159	0.8
0.3	0.1090	0.4540	0.7	0.3	0.1368	0.4850	0.7	0.3	0.1607	0.5181	0.7	0.3	0.1819	0.5536	0.7	0.3	0.2010	0.5917	0.7
0.4	0.1910	0.5878	0.6	0.4	0.2229	0.6232	0.6	0.4	0.2505	0.6604	0.6	0.4	0.2748	0.6993	0.6	0.4	0.2969	0.7402	0.6
0.5	0.2929	0.7071	0.5	0.5	0.3262	0.7437	0.5	0.5	0.3550	0.7811	0.5	0.5	0.3804	0.8192	0.5	0.5	0.4034	0.8576	0.5
0.6	0.4122	0.8090	0.4	0.6	0.4441	0.8435	0.4	0.6	0.4717	0.8775	0.4	0.6	0.4961	0.9104	0.4	0.6	0.5181	0.9411	0.4
0.7	0.5460	0.8910	0.3	0.7	0.5738	0.9202	0.3	0.7	0.5977	0.9471	0.3	0.7	0.6189	0.9705	0.3	0.7	0.6381	0.9887	0.3
0.8	0.6910	0.9511	0.2	0.8	0.7119	0.9719	0.2	0.8	0.7300	0.9882	0.2	0.8	0.7459	0.9982	0.2	0.8	0.7604	0.9991	0.2
0.9	0.8436	0.9877	0.1	0.9	0.8552	0.9973	0.1	0.9	0.8652	0.9998	0.1	0.9	0.8740	0.9926	0.1	0.9	0.8820	0.9721	0.1
1.0	1.0000	1.0000	0.0	1.0	1.0000	0.9958	0.0	1.0	1.0000	0.9816	0.0	1.0	1.0000	0.9540	0.0	1.0	1.0000	0.9083	0.0
	1.0000	90° 180°			1.1868	85° 175°			1.4019	80° 170°			1.6524	75° 165°			1.9480	70° 160°	

θ_i	−65° 25°	0.4345			−60° 30°	0.3660			−55° 35°	0.3062			−50° 40°	0.2536			−45° 45°	0.2071	
0.0	0.0000	0.0000	1.0	0.0	0.0000	0.0000	1.0	0.0	0.0000	0.0000	1.0	0.0	0.0000	0.0000	1.0	0.0	0.0000	0.0000	1.0
0.1	0.0581	0.2365	0.9	0.1	0.0651	0.2586	0.9	0.1	0.0717	0.2839	0.9	0.1	0.0781	0.3133	0.9	0.1	0.0844	0.3479	0.9
0.2	0.1316	0.4492	0.8	0.2	0.1441	0.4863	0.8	0.2	0.1560	0.5278	0.8	0.2	0.1676	0.5746	0.8	0.2	0.1790	0.6279	0.8
0.3	0.2187	0.6328	0.7	0.3	0.2353	0.6773	0.7	0.3	0.2511	0.7255	0.7	0.3	0.2664	0.7774	0.7	0.3	0.2815	0.8329	0.7
0.4	0.3172	0.7828	0.6	0.4	0.3362	0.8271	0.6	0.4	0.3544	0.8722	0.6	0.4	0.3720	0.9169	0.6	0.4	0.3894	0.9580	0.6
0.5	0.4246	0.8955	0.5	0.5	0.4445	0.9319	0.5	0.5	0.4635	0.9644	0.5	0.5	0.4819	0.9893	0.5	0.5	0.5000	1.0000	0.5
0.6	0.5384	0.9682	0.4	0.6	0.5575	0.9890	0.4	0.6	0.5756	0.9997	0.4	0.6	0.5933	0.9932	0.4	0.6	0.6106	0.9580	0.4
0.7	0.6557	0.9989	0.3	0.7	0.6723	0.9973	0.3	0.7	0.6881	0.9772	0.3	0.7	0.7034	0.9282	0.3	0.7	0.7185	0.8329	0.3
0.8	0.7737	0.9871	0.2	0.8	0.7862	0.9563	0.2	0.8	0.7981	0.8975	0.2	0.8	0.8096	0.7961	0.2	0.8	0.8210	0.6279	0.2
0.9	0.8894	0.9329	0.1	0.9	0.8963	0.8672	0.1	0.9	0.9029	0.7627	0.1	0.9	0.9093	0.6002	0.1	0.9	0.9156	0.3479	0.1
1.0	1.0000	0.8377	0.0	1.0	1.0000	0.7321	0.0	1.0	1.0000	0.5759	0.0	1.0	1.0000	0.3450	0.0	1.0	1.0000	0.0000	0.0
	2.3016	65° 155°			2.7321	60° 150°			3.2661	55° 145°			3.9440	50° 140°			4.8284	45° 135°	

TABLE A·1.—H_k AS A FUNCTION OF θ_i — (Cont.)

$\Delta X_i = 90°$

θ_i	−45° 45°	0.2071	
0.0	0.0000	0.0000	1.0
0.1	0.0844	0.3479	0.9
0.2	0.1790	0.6279	0.8
0.3	0.2815	0.8329	0.7
0.4	0.3894	0.9580	0.6
0.5	0.5000	1.0000	0.5
0.6	0.6106	0.9580	0.4
0.7	0.7185	0.8329	0.3
0.8	0.8210	0.6279	0.2
0.9	0.9156	0.3479	0.1
1.0	1.0000	0.0000	0.0
	4.8284	45° 135°	

	−40° 50°	0.2536	
0.0	0.0000	0.3450	1.0
0.1	0.0907	0.6002	0.9
0.2	0.1904	0.7961	0.8
0.3	0.2966	0.9282	0.7
0.4	0.4067	0.9932	0.6
0.5	0.5181	0.9893	0.5
0.6	0.6280	0.9169	0.4
0.7	0.7336	0.7774	0.3
0.8	0.8324	0.5746	0.2
0.9	0.9219	0.3133	0.1
1.0	1.0000	0.0000	0.0
	3.9440	40° 130°	

	−35° 55°	0.3062	
0.0	0.0000	0.5759	1.0
0.1	0.0971	0.7627	0.9
0.2	0.2019	0.8975	0.8
0.3	0.3119	0.9772	0.7
0.4	0.4244	0.9997	0.6
0.5	0.5365	0.9644	0.5
0.6	0.6456	0.8722	0.4
0.7	0.7489	0.7255	0.3
0.8	0.8440	0.5278	0.2
0.9	0.9283	0.2839	0.1
1.0	1.0000	0.0000	0.0
	3.2661	35° 125°	

	−30° 60°	0.3660	
0.0	0.0000	0.7321	1.0
0.1	0.1037	0.8672	0.9
0.2	0.2138	0.9563	0.8
0.3	0.3277	0.9973	0.7
0.4	0.4425	0.9890	0.6
0.5	0.5555	0.9319	0.5
0.6	0.6638	0.8271	0.4
0.7	0.7647	0.6773	0.3
0.8	0.8559	0.4863	0.2
0.9	0.9349	0.2586	0.1
1.0	1.0000	0.0000	0.0
	2.7321	30° 120°	

	−25° 65°	0.4345	
0.0	0.0000	0.8377	1.0
0.1	0.1106	0.9329	0.9
0.2	0.2263	0.9871	0.8
0.3	0.3443	0.9989	0.7
0.4	0.4616	0.9682	0.6
0.5	0.5754	0.8955	0.5
0.6	0.6828	0.7828	0.4
0.7	0.7813	0.6328	0.3
0.8	0.8684	0.4492	0.2
0.9	0.9419	0.2365	0.1
1.0	1.0000	0.0000	0.0
	2.3016	25° 115°	

θ_i	−20° 70°	0.5134	
0.0	0.0000	0.9083	1.0
0.1	0.1180	0.9721	0.9
0.2	0.2396	0.9991	0.8
0.3	0.3619	0.9887	0.7
0.4	0.4819	0.9411	0.6
0.5	0.5966	0.8576	0.5
0.6	0.7031	0.7402	0.4
0.7	0.7990	0.5917	0.3
0.8	0.8817	0.4159	0.2
0.9	0.9492	0.2170	0.1
1.0	1.0000	0.0000	0.0
	1.9480	20° 110°	

	−15° 75°	0.6052	
0.0	0.0000	0.9540	1.0
0.1	0.1260	0.9926	0.9
0.2	0.2541	0.9982	0.8
0.3	0.3811	0.9705	0.7
0.4	0.5039	0.9104	0.6
0.5	0.6196	0.8192	0.5
0.6	0.7252	0.6993	0.4
0.7	0.8181	0.5536	0.3
0.8	0.8962	0.3856	0.2
0.9	0.9572	0.1996	0.1
1.0	1.0000	0.0000	0.0
	1.6524	15° 105°	

	−10° 80°	0.7133	
0.0	0.0000	0.9816	1.0
0.1	0.1348	0.9998	0.9
0.2	0.2700	0.9882	0.8
0.3	0.4023	0.9471	0.7
0.4	0.5283	0.8775	0.6
0.5	0.6450	0.7811	0.5
0.6	0.7495	0.6604	0.4
0.7	0.8393	0.5181	0.3
0.8	0.9121	0.3580	0.2
0.9	0.9661	0.1838	0.1
1.0	1.0000	0.0000	0.0
	1.4019	10° 100°	

	−5° 85°	0.8426	
0.0	0.0000	0.9958	1.0
0.1	0.1448	0.9973	0.9
0.2	0.2881	0.9719	0.8
0.3	0.4262	0.9202	0.7
0.4	0.5559	0.8435	0.6
0.5	0.6738	0.7437	0.5
0.6	0.7771	0.6232	0.4
0.7	0.8632	0.4850	0.3
0.8	0.9301	0.3326	0.2
0.9	0.9761	0.1695	0.1
1.0	1.0000	0.0000	0.0
	1.1868	5° 95°	

	0° 90°	1.0000	
0.0	0.0000	1.0000	1.0
0.1	0.1564	0.9877	0.9
0.2	0.3090	0.9511	0.8
0.3	0.4540	0.8910	0.7
0.4	0.5878	0.8090	0.6
0.5	0.7071	0.7071	0.5
0.6	0.8090	0.5878	0.4
0.7	0.8910	0.4540	0.3
0.8	0.9511	0.3090	0.2
0.9	0.9877	0.1564	0.1
1.0	1.0000	0.0000	0.0
	1.0000	0° 90°	

TABLE A·1.—H_k AS A FUNCTION OF θ_i — (*Cont.*)

$\Delta X_i = 100°$

θ_i	−95° 5°	1.0000			−90° 10°	0.8520			−85° 15°	0.7274			−80° 20°	0.6228			−75° 25°	0.5338	
0.0	0.0035	0.0000	1.0	0.0	0.0000	0.0000	1.0	0.0	0.0000	0.0000	1.0	0.0	0.0000	0.0000	1.0	0.0	0.0000	0.0000	1.0
0.1	0.0035	0.1603	0.9	0.1	0.0130	0.1736	0.9	0.1	0.0241	0.1881	0.9	0.1	0.0340	0.2038	0.9	0.1	0.0429	0.2210	0.9
0.2	0.0313	0.3182	0.8	0.2	0.0514	0.3420	0.8	0.2	0.0716	0.3675	0.8	0.2	0.0895	0.3949	0.8	0.2	0.1057	0.4247	0.8
0.3	0.0862	0.4689	0.7	0.3	0.1142	0.5000	0.7	0.3	0.1411	0.5329	0.7	0.3	0.1649	0.5677	0.7	0.3	0.1864	0.6048	0.7
0.4	0.1663	0.6078	0.6	0.4	0.1994	0.6428	0.6	0.4	0.2303	0.6791	0.6	0.4	0.2578	0.7169	0.6	0.4	0.2826	0.7560	0.6
0.5	0.2694	0.7306	0.5	0.5	0.3044	0.7660	0.5	0.5	0.3367	0.8019	0.5	0.5	0.3654	0.8379	0.5	0.5	0.3913	0.8736	0.5
0.6	0.3922	0.8337	0.4	0.6	0.4260	0.8660	0.4	0.6	0.4570	0.8974	0.4	0.6	0.4844	0.9270	0.4	0.6	0.5092	0.9540	0.4
0.7	0.5311	0.9138	0.3	0.7	0.5606	0.9397	0.3	0.7	0.5875	0.9627	0.3	0.7	0.6114	0.9816	0.3	0.7	0.6329	0.9949	0.3
0.8	0.6818	0.9687	0.2	0.8	0.7041	0.9848	0.2	0.8	0.7243	0.9958	0.2	0.8	0.7422	1.0000	0.2	0.8	0.7584	0.9949	0.2
0.9	0.8397	0.9965	0.1	0.9	0.8520	1.0000	0.1	0.9	0.8632	0.9958	0.1	0.9	0.8731	0.9816	0.1	0.9	0.8820	0.9540	0.1
1.0	1.0000	0.9965	0.0	1.0	1.0000	0.9848	0.0	1.0	1.0000	0.9627	0.0	1.0	1.0000	0.9270	0.0	1.0	1.0000	0.8736	0.0
	1.0000	85° 185°			1.1737	80° 180°			1.3748	75° 175°			1.6057	70° 170°			1.8734	65° 165°	

θ_i	−70° 30°	0.4570			−65° 35°	0.3902			−60° 40°	0.3314			−55° 45°	0.2794			−50° 50°	0.2332	
0.0	0.0000	0.0000	1.0	0.0	0.0000	0.0000	1.0	0.0	0.0000	0.0000	1.0	0.0	0.0000	0.0000	1.0	0.0	0.0000	0.0000	1.0
0.1	0.0512	0.2401	0.9	0.1	0.0589	0.2615	0.9	0.1	0.0663	0.2856	0.9	0.1	0.0734	0.3131	0.9	0.1	0.0804	0.3450	0.9
0.2	0.1206	0.4571	0.8	0.2	0.1346	0.4927	0.8	0.2	0.1480	0.5321	0.8	0.2	0.1609	0.5759	0.8	0.2	0.1736	0.6250	0.8
0.3	0.2062	0.6444	0.7	0.3	0.2248	0.6868	0.7	0.3	0.2426	0.7321	0.7	0.3	0.2598	0.7803	0.7	0.3	0.2768	0.8312	0.7
0.4	0.3054	0.7964	0.6	0.4	0.3268	0.8377	0.6	0.4	0.3473	0.8794	0.6	0.4	0.3671	0.9201	0.6	0.4	0.3867	0.9575	0.6
0.5	0.4151	0.9083	0.5	0.5	0.4375	0.9410	0.5	0.5	0.4589	0.9696	0.5	0.5	0.4796	0.9911	0.5	0.5	0.5000	1.0000	0.5
0.6	0.5321	0.9769	0.4	0.6	0.5535	0.9934	0.4	0.6	0.5740	1.0000	0.4	0.6	0.5938	0.9911	0.4	0.6	0.6134	0.9575	0.4
0.7	0.6527	1.0000	0.3	0.7	0.6713	0.9934	0.3	0.7	0.6891	0.9696	0.3	0.7	0.7063	0.9201	0.3	0.7	0.7232	0.8312	0.3
0.8	0.7733	0.9769	0.2	0.8	0.7873	0.9410	0.2	0.8	0.8007	0.8794	0.2	0.8	0.8136	0.7803	0.2	0.8	0.8264	0.6250	0.2
0.9	0.8903	0.9083	0.1	0.9	0.8980	0.8377	0.1	0.9	0.9054	0.7321	0.1	0.9	0.9125	0.5759	0.1	0.9	0.9196	0.3450	0.1
1.0	1.0000	0.7964	0.0	1.0	1.0000	0.6868	0.0	1.0	1.0000	0.5321	0.0	1.0	1.0000	0.3131	0.0	1.0	1.0000	0.0000	0.0
	2.1881	60° 160°			2.5631	55° 155°			3.0176	50° 150°			3.5792	45° 145°			4.2890	40° 140°	

TABLE A·1.—H_k AS A FUNCTION OF θ_i — (*Cont.*)

$\Delta X_i = 100°$

θ_i	−50° 50°	0.2332	
0.0	0.0000	0.0000	1.0
0.1	0.0804	0.3450	0.9
0.2	0.1736	0.6250	0.8
0.3	0.2768	0.8312	0.7
0.4	0.3867	0.9575	0.6
0.5	0.5000	1.0000	0.5
0.6	0.6134	0.9575	0.4
0.7	0.7232	0.8312	0.3
0.8	0.8264	0.6250	0.2
0.9	0.9196	0.3450	0.1
1.0	1.0000	0.0000	0.0
	4.2890	40° 140°	

	−45° 55°	0.2794	
0.0	0.0000	0.3131	1.0
0.1	0.0875	0.5759	0.9
0.2	0.1864	0.7803	0.8
0.3	0.2937	0.9201	0.7
0.4	0.4062	0.9911	0.6
0.5	0.5204	0.9911	0.5
0.6	0.6329	0.9201	0.4
0.7	0.7402	0.7803	0.3
0.8	0.8391	0.5759	0.2
0.9	0.9266	0.3131	0.1
1.0	1.0000	0.0000	0.0
	3.5792	35° 135°	

	−40° 60°	0.3314	
0.0	0.0000	0.5321	1.0
0.1	0.0946	0.7321	0.9
0.2	0.1993	0.8794	0.8
0.3	0.3109	0.9696	0.7
0.4	0.4260	1.0000	0.6
0.5	0.5411	0.9696	0.5
0.6	0.6527	0.8794	0.4
0.7	0.7574	0.7321	0.3
0.8	0.8520	0.5321	0.2
0.9	0.9337	0.2856	0.1
1.0	1.0000	0.0000	0.0
	3.0176	30° 130°	

	−35° 65°	0.3902	
0.0	0.0000	0.6868	1.0
0.1	0.1020	0.8377	0.9
0.2	0.2127	0.9410	0.8
0.3	0.3287	0.9934	0.7
0.4	0.4465	0.9934	0.6
0.5	0.5625	0.9410	0.5
0.6	0.6732	0.8377	0.4
0.7	0.7752	0.6868	0.3
0.8	0.8654	0.4927	0.2
0.9	0.9411	0.2615	0.1
1.0	1.0000	0.0000	0.0
	2.5631	25° 125°	

	−30° 70°	0.4570	
0.0	0.0000	0.7964	1.0
0.1	0.1097	0.9083	0.9
0.2	0.2267	0.9769	0.8
0.3	0.3473	1.0000	0.7
0.4	0.4679	0.9769	0.6
0.5	0.5849	0.9083	0.5
0.6	0.6946	0.7964	0.4
0.7	0.7938	0.6444	0.3
0.8	0.8794	0.4571	0.2
0.9	0.9488	0.2401	0.1
1.0	1.0000	0.0000	0.0
	2.1881	20° 120°	

θ_i	−25° 75°	0.5338	
0.0	0.0000	0.8736	1.0
0.1	0.1180	0.9540	0.9
0.2	0.2416	0.9949	0.8
0.3	0.3671	0.9949	0.7
0.4	0.4908	0.9540	0.6
0.5	0.6087	0.8736	0.5
0.6	0.7174	0.7560	0.4
0.7	0.8136	0.6048	0.3
0.8	0.8943	0.4247	0.2
0.9	0.9571	0.2210	0.1
1.0	1.0000	0.0000	0.0
	1.8734	15° 115°	

	−20° 80°	0.6228	
0.0	0.0000	0.9270	1.0
0.1	0.1269	0.9816	0.9
0.2	0.2578	1.0000	0.8
0.3	0.3886	0.9816	0.7
0.4	0.5156	0.9270	0.6
0.5	0.6346	0.8379	0.5
0.6	0.7422	0.7169	0.4
0.7	0.8351	0.5677	0.3
0.8	0.9105	0.3949	0.2
0.9	0.9660	0.2038	0.1
1.0	1.0000	0.0000	0.0
	1.6057	10° 110°	

	−15° 85°	0.7274	
0.0	0.0000	0.9627	1.0
0.1	0.1368	0.9958	0.9
0.2	0.2757	0.9958	0.8
0.3	0.4125	0.9627	0.7
0.4	0.5430	0.8974	0.6
0.5	0.6633	0.8019	0.5
0.6	0.7697	0.6791	0.4
0.7	0.8589	0.5329	0.3
0.8	0.9284	0.3675	0.2
0.9	0.9759	0.1881	0.1
1.0	1.0000	0.0000	0.0
	1.3748	5° 105°	

	−10° 90°	0.8520	
0.0	0.0000	0.9848	1.0
0.1	0.1480	1.0000	0.9
0.2	0.2959	0.9848	0.8
0.3	0.4394	0.9397	0.7
0.4	0.5740	0.8660	0.6
0.5	0.6956	0.7660	0.5
0.6	0.8006	0.6428	0.4
0.7	0.8858	0.5000	0.3
0.8	0.9486	0.3420	0.2
0.9	0.9870	0.1736	0.1
1.0	1.0000	0.0000	0.0
	1.1737	0° 100°	

	−5° 95°	1.0000	
0.0	0.0000	0.9965	1.0
0.1	0.1603	0.9965	0.9
0.2	0.3182	0.9687	0.8
0.3	0.4689	0.9138	0.7
0.4	0.6078	0.8337	0.6
0.5	0.7306	0.7306	0.5
0.6	0.8337	0.6078	0.4
0.7	0.9138	0.4689	0.3
0.8	0.9687	0.3182	0.2
0.9	0.9965	0.1603	0.1
1.0	0.9965	0.0000	0.0
	1.0000	−5° 95°	

Table A·1.—H_k as a Function of θ_i — (*Cont.*)

$\Delta X_i = 110°$

θ_i	−100° 10°	1.0000			−95° 15°	0.8636			−90° 20°	0.7452			−85° 25°	0.6434			−80° 30°	0.5565	
0.0	0.0129	0.0000	1.0	0.0	0.0030	0.0000	1.0	0.0	0.0000	0.0000	1.0	0.0	0.0000	0.0000	1.0	0.0	0.0000	0.0000	1.0
0.1	0.0001	0.1628	0.9	0.1	0.0044	0.1763	0.9	0.1	0.0137	0.1908	0.9	0.1	0.0246	0.2065	0.9	0.1	0.0344	0.2235	0.9
0.2	0.0186	0.3251	0.8	0.2	0.0347	0.3491	0.8	0.2	0.0543	0.3746	0.8	0.2	0.0741	0.4019	0.8	0.2	0.0921	0.4311	0.8
0.3	0.0677	0.4809	0.7	0.3	0.0930	0.5120	0.7	0.3	0.1202	0.5446	0.7	0.3	0.1467	0.5790	0.7	0.3	0.1707	0.6152	0.7
0.4	0.1457	0.6244	0.6	0.4	0.1770	0.6590	0.6	0.4	0.2091	0.6947	0.6	0.4	0.2397	0.7313	0.6	0.4	0.2674	0.7689	0.6
0.5	0.2496	0.7504	0.5	0.5	0.2838	0.7848	0.5	0.5	0.3178	0.8192	0.5	0.5	0.3497	0.8532	0.5	0.5	0.3786	0.8866	0.5
0.6	0.3756	0.8543	0.4	0.6	0.4093	0.8847	0.4	0.6	0.4421	0.9136	0.4	0.6	0.4726	0.9403	0.4	0.6	0.5003	0.9641	0.4
0.7	0.5191	0.9323	0.3	0.7	0.5489	0.9550	0.3	0.7	0.5775	0.9744	0.3	0.7	0.6040	0.9893	0.3	0.7	0.6280	0.9983	0.3
0.8	0.6749	0.9814	0.2	0.8	0.6976	0.9931	0.2	0.8	0.7191	0.9994	0.2	0.8	0.7390	0.9985	0.2	0.8	0.7570	0.9882	0.2
0.9	0.8372	0.9999	0.1	0.9	0.8498	0.9978	0.1	0.9	0.8617	0.9877	0.1	0.9	0.8726	0.9675	0.1	0.9	0.8825	0.9341	0.1
1.0	1.0000	0.9871	0.0	1.0	1.0000	0.9687	0.0	1.0	1.0000	0.9397	0.0	1.0	1.0000	0.8974	0.0	1.0	1.0000	0.8379	0.0
	1.0000	80° 190°			1.1579	75° 185°			1.3420	70° 180°			1.5543	65° 175°			1.7968	60° 170°	

θ_i	−75° 35°	0.4814			−70° 40°	0.4158			−65° 45°	0.3579			−60° 50°	0.3064			−55° 55°	0.2603	
0.0	0.0000	0.0000	1.0	0.0	0.0000	0.0000	1.0	0.0	0.0000	0.0000	1.0	0.0	0.0000	0.0000	1.0	0.0	0.0000	0.0000	1.0
0.1	0.0436	0.2422	0.9	0.1	0.0522	0.2630	0.9	0.1	0.0603	0.2861	0.9	0.1	0.0682	0.3121	0.9	0.1	0.0760	0.3418	0.9
0.2	0.1087	0.4628	0.8	0.2	0.1242	0.4971	0.8	0.2	0.1390	0.5347	0.8	0.2	0.1534	0.5760	0.8	0.2	0.1676	0.6217	0.8
0.3	0.1928	0.6534	0.7	0.3	0.2135	0.6940	0.7	0.3	0.2333	0.7368	0.7	0.3	0.2525	0.7820	0.7	0.3	0.2713	0.8292	0.7
0.4	0.2929	0.8073	0.6	0.4	0.3168	0.8462	0.6	0.4	0.3396	0.8850	0.6	0.4	0.3617	0.9225	0.6	0.4	0.3835	0.9569	0.6
0.5	0.4053	0.9186	0.5	0.5	0.4302	0.9482	0.5	0.5	0.4541	0.9737	0.5	0.5	0.4772	0.9924	0.5	0.5	0.5000	1.0000	0.5
0.6	0.5258	0.9834	0.4	0.6	0.5497	0.9963	0.4	0.6	0.5726	0.9997	0.4	0.6	0.5947	0.9890	0.4	0.6	0.6165	0.9569	0.4
0.7	0.6501	0.9992	0.3	0.7	0.6708	0.9887	0.3	0.7	0.6906	0.9622	0.3	0.7	0.7098	0.9126	0.3	0.7	0.7287	0.8292	0.3
0.8	0.7735	0.9654	0.2	0.8	0.7891	0.9256	0.2	0.8	0.8039	0.8623	0.2	0.8	0.8183	0.7659	0.2	0.8	0.8324	0.6217	0.2
0.9	0.8916	0.8834	0.1	0.9	0.9002	0.8094	0.1	0.9	0.9083	0.7039	0.1	0.9	0.9162	0.5543	0.1	0.9	0.9240	0.3418	0.1
1.0	1.0000	0.7560	0.0	1.0	1.0000	0.6444	0.0	1.0	1.0000	0.4927	0.0	1.0	1.0000	0.2856	0.0	1.0	1.0000	0.0000	0.0
	2.0771	55° 165°			2.4051	50° 160°			2.7944	45° 155°			3.2641	40° 150°			3.8420	35° 145°	

TABLE A-1.—H_k AS A FUNCTION OF θ_i — (*Cont.*)

$\Delta X_i = 110°$

θ_i	−55° 55°	0.2603	
0.0	0.0000	0.0000	1.0
0.1	0.0760	0.3418	0.9
0.2	0.1676	0.6217	0.8
0.3	0.2713	0.8292	0.7
0.4	0.3835	0.9569	0.6
0.5	0.5000	1.0000	0.5
0.6	0.6165	0.9569	0.4
0.7	0.7287	0.8292	0.3
0.8	0.8324	0.6217	0.2
0.9	0.9240	0.3418	0.1
1.0	1.0000	0.0000	0.0
	3.8420	35° 145°	

	−50° 60°	0.3064	
0.0	0.0000	0.2856	1.0
0.1	0.0838	0.5543	0.9
0.2	0.1817	0.7659	0.8
0.3	0.2902	0.9126	0.7
0.4	0.4053	0.9890	0.6
0.5	0.5228	0.9924	0.5
0.6	0.6383	0.9225	0.4
0.7	0.7475	0.7820	0.3
0.8	0.8466	0.5760	0.2
0.9	0.9318	0.3121	0.1
1.0	1.0000	0.0000	0.0
	3.2641	30° 140°	

	−45° 65°	0.3579	
0.0	0.0000	0.4927	1.0
0.1	0.0917	0.7039	0.9
0.2	0.1961	0.8623	0.8
0.3	0.3094	0.9622	0.7
0.4	0.4274	0.9997	0.6
0.5	0.5459	0.9737	0.5
0.6	0.6604	0.8850	0.4
0.7	0.7667	0.7368	0.3
0.8	0.8610	0.5347	0.2
0.9	0.9397	0.2861	0.1
1.0	1.0000	0.0000	0.0
	2.7944	25° 135°	

	−40° 70°	0.4158	
0.0	0.0000	0.6444	1.0
0.1	0.0998	0.8094	0.9
0.2	0.2109	0.9256	0.8
0.3	0.3292	0.9887	0.7
0.4	0.4503	0.9963	0.6
0.5	0.5698	0.9482	0.5
0.6	0.6832	0.8462	0.4
0.7	0.7865	0.6940	0.3
0.8	0.8758	0.4971	0.2
0.9	0.9478	0.2630	0.1
1.0	1.0000	0.0000	0.0
	2.4051	20° 130°	

	−35° 75°	0.4814	
0.0	0.0000	0.7560	1.0
0.1	0.1084	0.8834	0.9
0.2	0.2265	0.9654	0.8
0.3	0.3499	0.9992	0.7
0.4	0.4742	0.9834	0.6
0.5	0.5947	0.9186	0.5
0.6	0.7071	0.8073	0.4
0.7	0.8072	0.6534	0.3
0.8	0.8913	0.4628	0.2
0.9	0.9564	0.2422	0.1
1.0	1.0000	0.0000	0.0
	2.0771	15° 125°	

θ_i	−30° 80°	0.5565	
0.0	0.0000	0.8379	1.0
0.1	0.1175	0.9341	0.9
0.2	0.2430	0.9882	0.8
0.3	0.3720	0.9983	0.7
0.4	0.4997	0.9641	0.6
0.5	0.6214	0.8866	0.5
0.6	0.7326	0.7689	0.4
0.7	0.8293	0.6152	0.3
0.8	0.9079	0.4311	0.2
0.9	0.9656	0.2235	0.1
1.0	1.0000	0.0000	0.0
	1.7968	10° 120°	

	−25° 85°	0.6434	
0.0	0.0000	0.8974	1.0
0.1	0.1274	0.9675	0.9
0.2	0.2610	0.9985	0.8
0.3	0.3960	0.9893	0.7
0.4	0.5274	0.9403	0.6
0.5	0.6503	0.8532	0.5
0.6	0.7603	0.7313	0.4
0.7	0.8533	0.5790	0.3
0.8	0.9259	0.4019	0.2
0.9	0.9754	0.2065	0.1
1.0	1.0000	0.0000	0.0
	1.5543	5° 115°	

	−20° 90°	0.7452	
0.0	0.0000	0.9397	1.0
0.1	0.1383	0.9877	0.9
0.2	0.2809	0.9994	0.8
0.3	0.4225	0.9744	0.7
0.4	0.5579	0.9136	0.6
0.5	0.6822	0.8192	0.5
0.6	0.7909	0.6947	0.4
0.7	0.8798	0.5446	0.3
0.8	0.9457	0.3746	0.2
0.9	0.9863	0.1908	0.1
1.0	1.0000	0.0000	0.0
	1.3420	0° 110°	

	−15° 95°	0.8636	
0.0	0.0000	0.9687	1.0
0.1	0.1502	0.9978	0.9
0.2	0.3024	0.9931	0.8
0.3	0.4511	0.9550	0.7
0.4	0.5907	0.8847	0.6
0.5	0.7162	0.7848	0.5
0.6	0.8230	0.6590	0.4
0.7	0.9070	0.5120	0.3
0.8	0.9653	0.3491	0.2
0.9	0.9956	0.1763	0.1
1.0	0.9970	0.0000	0.0
	1.1579	−5° 105°	

	−10° 100°	1.0000	
0.0	0.0000	0.9871	1.0
0.1	0.1628	0.9999	0.9
0.2	0.3251	0.9814	0.8
0.3	0.4809	0.9323	0.7
0.4	0.6244	0.8543	0.6
0.5	0.7504	0.7504	0.5
0.6	0.8543	0.6244	0.4
0.7	0.9323	0.4809	0.3
0.8	0.9814	0.3251	0.2
0.9	0.9999	0.1628	0.1
1.0	0.9871	0.0000	0.0
	1.0000	−10° 100°	

TABLE A·1.—H_k AS A FUNCTION OF θ_i — (*Cont.*)

$\Delta X_i = 120°$

θ_i	−105° 15°	1.0000			−100° 20°	0.8745			−95° 25°	0.7642			−90° 30°	0.6667			−85° 35°	0.5815	
0.0	0.0271	0.0000	1.0	0.0	0.0113	0.0000	1.0	0.0	0.0027	0.0000	1.0	0.0	0.0000	0.0000	1.0	1.0	0.0000	0.0000	1.0
0.1	0.0011	0.1640	0.9	0.1	0.0005	0.1777	0.9	0.1	0.0052	0.1923	0.9	0.1	0.0146	0.2079	0.9	0.1	0.0254	0.2248	0.9
0.2	0.0098	0.3299	0.8	0.2	0.0221	0.3541	0.8	0.2	0.0383	0.3796	0.8	0.2	0.0576	0.4067	0.8	0.2	0.0774	0.4356	0.8
0.3	0.0528	0.4903	0.7	0.3	0.0754	0.5215	0.7	0.3	0.1004	0.5539	0.7	0.3	0.1273	0.5878	0.7	0.3	0.1538	0.6232	0.7
0.4	0.1282	0.6383	0.6	0.4	0.1580	0.6725	0.6	0.4	0.1888	0.7075	0.6	0.4	0.2206	0.7431	0.6	0.4	0.2512	0.7794	0.6
0.5	0.2327	0.7673	0.5	0.5	0.2362	0.8007	0.5	0.5	0.2997	0.8336	0.5	0.5	0.3333	0.8660	0.5	0.5	0.3654	0.8974	0.5
0.6	0.3617	0.8718	0.4	0.6	0.3953	0.9003	0.4	0.6	0.4283	0.9269	0.4	0.6	0.4606	0.9511	0.4	0.6	0.4913	0.9719	0.4
0.7	0.5097	0.9472	0.3	0.7	0.5398	0.9670	0.3	0.7	0.5688	0.9831	0.3	0.7	0.5970	0.9945	0.3	0.7	0.6235	0.9998	0.3
0.8	0.6701	0.9902	0.2	0.8	0.6932	0.9979	0.2	0.8	0.7152	0.9999	0.2	0.8	0.7364	0.9945	0.2	0.8	0.7562	0.9799	0.2
0.9	0.8360	0.9989	0.1	0.9	0.8488	0.9917	0.1	0.9	0.8611	0.9764	0.1	0.9	0.8727	0.9511	0.1	0.9	0.8835	0.9129	0.1
1.0	1.0000	0.9729	0.0	1.0	1.0000	0.9486	0.0	1.0	1.0000	0.9138	0.0	1.0	1.0000	0.8660	0.0	1.0	1.0000	0.8019	0.0
	1.0000	75° 195°			1.1435	70° 190°			1.3086	65° 185°			1.5000	60° 180°			1.7197	55° 175°	

θ_i	−80° 40°	0.5077			−75° 45°	0.4430			−70° 50°	0.3858			−65° 55°	0.3346			−60° 60°	0.2887	
0.0	0.0000	0.0000	1.0	0.0	0.0000	0.0000	1.0	0.0	0.0000	0.0000	1.0	0.0	0.0000	0.0000	1.0	0.0	0.0000	0.0000	1.0
0.1	0.0354	0.2432	0.9	0.1	0.0448	0.2633	0.9	0.1	0.0537	0.2856	0.9	0.1	0.0624	0.3104	0.9	0.1	0.0710	0.3383	0.9
0.2	0.0957	0.4666	0.8	0.2	0.1128	0.4999	0.8	0.2	0.1292	0.5359	0.8	0.2	0.1450	0.5752	0.8	0.2	0.1606	0.6180	0.8
0.3	0.1783	0.6604	0.7	0.3	0.2012	0.6993	0.7	0.3	0.2231	0.7402	0.7	0.3	0.2443	0.7828	0.7	0.3	0.2652	0.8271	0.7
0.4	0.2795	0.8161	0.6	0.4	0.3060	0.8530	0.6	0.4	0.3313	0.8893	0.6	0.4	0.3558	0.9243	0.6	0.4	0.3800	0.9563	0.6
0.5	0.3949	0.9270	0.5	0.5	0.4226	0.9540	0.5	0.5	0.4491	0.9769	0.5	0.5	0.4747	0.9934	0.5	0.5	0.5000	1.0000	0.5
0.6	0.5196	0.9882	0.4	0.6	0.5461	0.9982	0.4	0.6	0.5714	0.9991	0.4	0.6	0.5959	0.9871	0.4	0.6	0.6200	0.9563	0.4
0.7	0.6479	0.9970	0.3	0.7	0.6708	0.9834	0.3	0.7	0.6927	0.9549	0.3	0.7	0.7139	0.9056	0.3	0.7	0.7348	0.8271	0.3
0.8	0.7744	0.9531	0.2	0.8	0.7916	0.9104	0.2	0.8	0.8079	0.8462	0.2	0.8	0.8238	0.7526	0.2	0.8	0.8394	0.6180	0.2
0.9	0.8935	0.8584	0.1	0.9	0.9029	0.7823	0.1	0.9	0.9118	0.6778	0.1	0.9	0.9205	0.5347	0.1	0.9	0.9290	0.3383	0.1
1.0	1.0000	0.7169	0.0	1.0	1.0000	0.6048	0.0	1.0	1.0000	0.4571	0.0	1.0	1.0000	0.2615	0.0	1.0	1.0000	0.0000	0.0
	1.9696	50° 170°			2.2573	45° 165°			2.5924	40° 160°			2.9884	35° 155°			3.4641	30° 150°	

TABLE A·1.—H_k AS A FUNCTION OF θ_i — (*Cont.*)

$\Delta X_i = 120°$

θ_i	−60° 60°	0.2887			−55° 65°	0.3346			−50° 70°	0.3858			−45° 75°	0.4430			−40° 80°	0.5077	
0.0	0.0000	0.0000	1.0	0.0	0.0000	0.2615	1.0	0.0	0.0000	0.4571	1.0	0.0	0.0000	0.6048	1.0	0.0	0.0000	0.7169	1.0
0.1	0.0710	0.3383	0.9	0.1	0.0795	0.5347	0.9	0.1	0.0882	0.6778	0.9	0.1	0.0971	0.7823	0.9	0.1	0.1065	0.8584	0.9
0.2	0.1606	0.6180	0.8	0.2	0.1762	0.7526	0.8	0.2	0.1921	0.8462	0.8	0.2	0.2084	0.9104	0.8	0.2	0.2256	0.9531	0.8
0.3	0.2652	0.8271	0.7	0.3	0.2861	0.9056	0.7	0.3	0.3073	0.9549	0.7	0.3	0.3292	0.9834	0.7	0.3	0.3521	0.9970	0.7
0.4	0.3800	0.9563	0.6	0.4	0.4041	0.9871	0.6	0.4	0.4286	0.9991	0.6	0.4	0.4539	0.9982	0.6	0.4	0.4804	0.9882	0.6
0.5	0.5000	1.0000	0.5	0.5	0.5253	0.9934	0.5	0.5	0.5509	0.9769	0.5	0.5	0.5774	0.9540	0.5	0.5	0.6051	0.9270	0.5
0.6	0.6200	0.9563	0.4	0.6	0.6442	0.9243	0.4	0.6	0.6687	0.8893	0.4	0.6	0.6940	0.8530	0.4	0.6	0.7205	0.8161	0.4
0.7	0.7348	0.8271	0.3	0.7	0.7557	0.7828	0.3	0.7	0.7769	0.7402	0.3	0.7	0.7988	0.6993	0.3	0.7	0.8217	0.6604	0.3
0.8	0.8394	0.6180	0.2	0.8	0.8550	0.5752	0.2	0.8	0.8708	0.5359	0.2	0.8	0.8872	0.4999	0.2	0.8	0.9043	0.4666	0.2
0.9	0.9290	0.3383	0.1	0.9	0.9376	0.3104	0.1	0.9	0.9463	0.2856	0.1	0.9	0.9552	0.2633	0.1	0.9	0.9646	0.2432	0.1
1.0	1.0000	0.0000	0.0	1.0	1.0000	0.0000	0.0	1.0	1.0000	0.0000	0.0	1.0	1.0000	0.0000	0.0	1.0	1.0000	0.0000	0.0
	3.4641	30° 150°			2.9884	25° 145°			2.5924	20° 140°			2.2573	15° 135°			1.9696	10° 130°	

θ_i	−35° 85°	0.5815			−30° 90°	0.6667			−25° 95°	0.7642			−20° 100°	0.8745			−15° 105°	1.0000	
0.0	0.0000	0.8019	1.0	0.0	0.0000	0.8660	1.0	0.0	0.0000	0.9138	1.0	0.0	0.0000	0.9486	1.0	0.0	0.0000	0.9729	1.0
0.1	0.1165	0.9129	0.9	0.1	0.1273	0.9511	0.9	0.1	0.1389	0.9764	0.9	0.1	0.1512	0.9917	0.9	0.1	0.1640	0.9989	0.9
0.2	0.2438	0.9799	0.8	0.2	0.2636	0.9945	0.8	0.2	0.2848	0.9999	0.8	0.2	0.3068	0.9979	0.8	0.2	0.3299	0.9902	0.8
0.3	0.3765	0.9998	0.7	0.3	0.4030	0.9945	0.7	0.3	0.4312	0.9831	0.7	0.3	0.4602	0.9670	0.7	0.3	0.4903	0.9472	0.7
0.4	0.5087	0.9719	0.6	0.4	0.5394	0.9511	0.6	0.4	0.5717	0.9269	0.6	0.4	0.6047	0.9003	0.6	0.4	0.6383	0.8718	0.6
0.5	0.6346	0.8974	0.5	0.5	0.6667	0.8660	0.5	0.5	0.7003	0.8336	0.5	0.5	0.7338	0.8007	0.5	0.5	0.7673	0.7673	0.5
0.6	0.7488	0.7794	0.4	0.6	0.7794	0.7431	0.4	0.6	0.8112	0.7075	0.4	0.6	0.8420	0.6725	0.4	0.6	0.8718	0.6383	0.4
0.7	0.8462	0.6232	0.3	0.7	0.8727	0.5878	0.3	0.7	0.8996	0.5539	0.3	0.7	0.9246	0.5215	0.3	0.7	0.9472	0.4903	0.3
0.8	0.9226	0.4356	0.2	0.8	0.9424	0.4067	0.2	0.8	0.9617	0.3796	0.2	0.8	0.9779	0.3541	0.2	0.8	0.9902	0.3299	0.2
0.9	0.9746	0.2248	0.1	0.9	0.9854	0.2079	0.1	0.9	0.9948	0.1923	0.1	0.9	0.9995	0.1777	0.1	0.9	0.9989	0.1640	0.1
1.0	1.0000	0.0000	0.0	1.0	1.0000	0.0000	0.0	1.0	0.9973	0.0000	0.0	1.0	0.9887	0.0000	0.0	1.0	0.9729	0.0000	0.0
	1.7197	5° 125°			1.5000	0° 120°			1.3086	−5° 115°			1.1435	−10° 110°			1.0000	−15° 105°	

TABLE A·1.—H_k AS A FUNCTION OF θ_i — (*Cont.*)

$\Delta X_i = 130°$

θ_i	−110° 20°	1.0000			−105° 25°	0.8849			−100° 30°	0.7824			−95° 35°	0.6909			−90° 40°	0.6087	
0.0	0.0449	0.0000	1.0	0.0	0.0239	0.0000	1.0	0.0	0.0101	0.0000	1.0	0.0	0.0024	0.0000	1.0	0.0	0.0000	0.0000	1.0
0.1	0.0055	0.1640	0.9	0.1	0.0004	0.1779	0.9	0.1	0.0009	0.1926	0.9	0.1	0.0062	0.2082	0.9	0.1	0.0156	0.2250	0.9
0.2	0.0041	0.3327	0.8	0.2	0.0129	0.3572	0.8	0.2	0.0258	0.3828	0.8	0.2	0.0422	0.4098	0.8	0.2	0.0616	0.4384	0.8
0.3	0.0406	0.4975	0.7	0.3	0.0608	0.5287	0.7	0.3	0.0836	0.5610	0.7	0.3	0.1086	0.5945	0.7	0.3	0.1356	0.6293	0.7
0.4	0.1132	0.6497	0.6	0.4	0.1415	0.6837	0.6	0.4	0.1712	0.7181	0.6	0.4	0.2021	0.7529	0.6	0.4	0.2340	0.7880	0.6
0.5	0.2182	0.7818	0.5	0.5	0.2511	0.8141	0.5	0.5	0.2843	0.8459	0.5	0.5	0.3178	0.8768	0.5	0.5	0.3515	0.9063	0.5
0.6	0.3503	0.8868	0.4	0.6	0.3838	0.9134	0.4	0.6	0.4169	0.9380	0.4	0.6	0.4497	0.9598	0.4	0.6	0.4822	0.9782	0.4
0.7	0.5025	0.9594	0.3	0.7	0.5329	0.9764	0.3	0.7	0.5624	0.9895	0.3	0.7	0.5912	0.9978	0.3	0.7	0.6193	0.9998	0.3
0.8	0.6673	0.9959	0.2	0.8	0.6907	0.9999	0.2	0.8	0.7132	0.9979	0.2	0.8	0.7349	0.9887	0.2	0.8	0.7560	0.9703	0.2
0.9	0.8360	0.9945	0.1	0.9	0.8491	0.9826	0.1	0.9	0.8616	0.9628	0.1	0.9	0.8736	0.9330	0.1	0.9	0.8851	0.8910	0.1
1.0	1.0000	0.9551	0.0	1.0	1.0000	0.9256	0.0	1.0	1.0000	0.8858	0.0	1.0	1.0000	0.8337	0.0	1.0	1.0000	0.7660	0.0
	1.0000	70° 200°			1.1301	65° 195°			1.2781	60° 190°			1.4474	55° 185°			1.6428	50° 180°	

θ_i	−85° 45°	0.5359			−80° 50°	0.4720			−75° 55°	0.4152			−70° 60°	0.3644			−65° 65°	0.3185	
0.0	0.0000	0.0000	1.0	0.0	0.0000	0.0000	1.0	0.0	0.0000	0.0000	1.0	0.0	0.0000	0.0000	1.0	0.0	0.0000	0.0000	1.0
0.1	0.0265	0.2430	0.9	0.1	0.0367	0.2627	0.9	0.1	0.0465	0.2842	0.9	0.1	0.0559	0.3079	0.9	0.1	0.0653	0.3343	0.9
0.2	0.0816	0.4687	0.8	0.2	0.1004	0.5012	0.8	0.2	0.1183	0.5360	0.8	0.2	0.1357	0.5735	0.8	0.2	0.1528	0.6140	0.8
0.3	0.1625	0.6655	0.7	0.3	0.1878	0.7032	0.7	0.3	0.2118	0.7423	0.7	0.3	0.2352	0.7829	0.7	0.3	0.2582	0.8247	0.7
0.4	0.2651	0.8233	0.6	0.4	0.2943	0.8584	0.6	0.4	0.3222	0.8927	0.6	0.4	0.3493	0.9256	0.6	0.4	0.3759	0.9556	0.6
0.5	0.3841	0.9339	0.5	0.5	0.4146	0.9588	0.5	0.5	0.4438	0.9795	0.5	0.5	0.4721	0.9942	0.5	0.5	0.5000	1.0000	0.5
0.6	0.5133	0.9918	0.4	0.6	0.5425	0.9993	0.4	0.6	0.5704	0.9982	0.4	0.6	0.5975	0.9852	0.4	0.6	0.6241	0.9556	0.4
0.7	0.6462	0.9940	0.3	0.7	0.6715	0.9778	0.3	0.7	0.6955	0.9477	0.3	0.7	0.7189	0.8991	0.3	0.7	0.7418	0.8247	0.3
0.8	0.7760	0.9403	0.2	0.8	0.7948	0.8954	0.2	0.8	0.8127	0.8308	0.2	0.8	0.8301	0.7402	0.2	0.8	0.8472	0.6140	0.2
0.9	0.8960	0.8335	0.1	0.9	0.9062	0.7563	0.1	0.9	0.9160	0.6534	0.1	0.9	0.9254	0.5167	0.1	0.9	0.9347	0.3343	0.1
1.0	1.0000	0.6791	0.0	1.0	1.0000	0.5677	0.0	1.0	1.0000	0.4247	0.0	1.0	1.0000	0.2401	0.0	1.0	1.0000	0.0000	0.0
	1.8659	45° 175°			2.1188	40° 170°			2.4084	35° 165°			2.7443	30° 160°			3.1394	25° 155°	

TABLE A·1.—H_k AS A FUNCTION OF θ_i — (*Cont.*)

$\Delta X_i = 130°$

θ_i	−65° 65°	0.3185			−60° 70°	0.3644			−55° 75°	0.4152			−50° 80°	0.4720			−45° 85°	0.5359	
0.0	0.0000	0.0000	1.0	0.0	0.0000	0.2401	1.0	0.0	0.0000	0.4247	1.0	0.0	0.0000	0.5677	1.0	0.0	0.0000	0.6791	1.0
0.1	0.0653	0.3343	0.9	0.1	0.0746	0.5167	0.9	0.1	0.0840	0.6534	0.9	0.1	0.0938	0.7563	0.9	0.1	0.1040	0.8335	0.9
0.2	0.1528	0.6140	0.8	0.2	0.1699	0.7402	0.8	0.2	0.1873	0.8308	0.8	0.2	0.2052	0.8954	0.8	0.2	0.2240	0.9403	0.8
0.3	0.2582	0.8247	0.7	0.3	0.2811	0.8991	0.7	0.3	0.3045	0.9477	0.7	0.3	0.3285	0.9778	0.7	0.3	0.3538	0.9940	0.7
0.4	0.3759	0.9556	0.6	0.4	0.4025	0.9852	0.6	0.4	0.4296	0.9982	0.6	0.4	0.4575	0.9993	0.6	0.4	0.4867	0.9918	0.6
0.5	0.5000	1.0000	0.5	0.5	0.5279	0.9942	0.5	0.5	0.5562	0.9795	0.5	0.5	0.5854	0.9588	0.5	0.5	0.6159	0.9339	0.5
0.6	0.6241	0.9556	0.4	0.6	0.6507	0.9256	0.4	0.6	0.6778	0.8927	0.4	0.6	0.7057	0.8584	0.4	0.6	0.7349	0.8233	0.4
0.7	0.7418	0.8247	0.3	0.7	0.7648	0.7829	0.3	0.7	0.7882	0.7423	0.3	0.7	0.8122	0.7032	0.3	0.7	0.8375	0.6655	0.3
0.8	0.8472	0.6140	0.2	0.8	0.8643	0.5735	0.2	0.8	0.8817	0.5360	0.2	0.8	0.8996	0.5012	0.2	0.8	0.9184	0.4687	0.2
0.9	0.9347	0.3343	0.1	0.9	0.9441	0.3079	0.1	0.9	0.9535	0.2842	0.1	0.9	0.9633	0.2627	0.1	0.9	0.9735	0.2430	0.1
1.0	1.0000	0.0000	0.0	1.0	1.0000	0.0000	0.0	1.0	1.0000	0.0000	0.0	1.0	1.0000	0.0000	0.0	1.0	1.0000	0.0000	0.0
	3.1394	25° 155°			2.7443	20° 150°			2.4084	15° 145°			2.1188	10° 140°			1.8659	5° 135°	

θ_i	−40° 90°	0.6087			−35° 95°	0.6909			−30° 100°	0.7824			−25° 105°	0.8849			−20° 110°	1.0000	
0.0	0.0000	0.7660	1.0	0.0	0.0000	0.8337	1.0	0.0	0.0000	0.8858	1.0	0.0	0.0000	0.9256	1.0	0.0	0.0000	0.9551	1.0
0.1	0.1149	0.8910	0.9	0.1	0.1264	0.9330	0.9	0.1	0.1384	0.9628	0.9	0.1	0.1509	0.9826	0.9	0.1	0.1640	0.9945	0.9
0.2	0.2440	0.9703	0.8	0.2	0.2651	0.9887	0.8	0.2	0.2868	0.9979	0.8	0.2	0.3093	0.9999	0.8	0.2	0.3327	0.9959	0.8
0.3	0.3807	0.9998	0.7	0.3	0.4088	0.9978	0.7	0.3	0.4376	0.9895	0.7	0.3	0.4671	0.9764	0.7	0.3	0.4975	0.9594	0.7
0.4	0.5178	0.9782	0.6	0.4	0.5503	0.9598	0.6	0.4	0.5831	0.9380	0.6	0.4	0.6162	0.9134	0.6	0.4	0.6497	0.8868	0.6
0.5	0.6485	0.9063	0.5	0.5	0.6822	0.8768	0.5	0.5	0.7157	0.8459	0.5	0.5	0.7489	0.8141	0.5	0.5	0.7818	0.7818	0.5
0.6	0.7660	0.7880	0.4	0.6	0.7979	0.7529	0.4	0.6	0.8288	0.7181	0.4	0.6	0.8585	0.6837	0.4	0.6	0.8868	0.6497	0.4
0.7	0.8644	0.6293	0.3	0.7	0.8914	0.5945	0.3	0.7	0.9164	0.5610	0.3	0.7	0.9392	0.5287	0.3	0.7	0.9594	0.4975	0.3
0.8	0.9384	0.4384	0.2	0.8	0.9578	0.4098	0.2	0.8	0.9742	0.3828	0.2	0.8	0.9871	0.3572	0.2	0.8	0.9959	0.3327	0.2
0.9	0.9844	0.2250	0.1	0.9	0.9938	0.2082	0.1	0.9	0.9991	0.1926	0.1	0.9	0.9996	0.1779	0.1	0.9	0.9945	0.1640	0.1
1.0	1.0000	0.0000	0.0	1.0	0.9976	0.0000	0.0	1.0	0.9899	0.0000	0.0	1.0	0.9761	0.0000	0.0	1.0	0.9551	0.0000	0.0
	1.6428	0° 130°			1.4474	−5° 125°			1.2781	−10° 120°			1.1301	−15° 115°			1.0000	−20° 110°	

TABLE A·1.—H_k AS A FUNCTION OF θ_i — (*Cont.*)

$\Delta X_i = 140°$

θ_i	−115° 25°	1.0000			−110° 30°	0.8947			−105° 35°	0.8000			−100° 40°	0.7144			−95° 45°	0.6368	
0.0	0.0659	0.0000	1.0	0.0	0.0402	0.0000	1.0	0.0	0.0217	0.0000	1.0	0.0	0.0092	0.0000	1.0	0.0	0.0022	0.0000	1.0
0.1	0.0129	0.1629	0.9	0.1	0.0037	0.1770	0.9	0.1	0.0001	0.1917	0.9	0.1	0.0015	0.2074	0.9	0.1	0.0072	0.2241	0.9
0.2	0.0010	0.3339	0.8	0.2	0.0065	0.3586	0.8	0.2	0.0163	0.3843	0.8	0.2	0.0298	0.4113	0.8	0.2	0.0466	0.4396	0.8
0.3	0.0307	0.5026	0.7	0.3	0.0485	0.5340	0.7	0.3	0.0693	0.5663	0.7	0.3	0.0925	0.5995	0.7	0.3	0.1180	0.6337	0.7
0.4	0.1004	0.6591	0.6	0.4	0.1273	0.6928	0.6	0.4	0.1559	0.7268	0.6	0.4	0.1859	0.7609	0.6	0.4	0.2171	0.7950	0.6
0.5	0.2059	0.7941	0.5	0.5	0.2381	0.8257	0.5	0.5	0.2710	0.8563	0.5	0.5	0.3044	0.8859	0.5	0.5	0.3382	0.9138	0.5
0.6	0.3409	0.8996	0.4	0.6	0.3744	0.9246	0.4	0.6	0.4078	0.9472	0.4	0.6	0.4409	0.9670	0.4	0.6	0.4740	0.9831	0.4
0.7	0.4974	0.9693	0.3	0.7	0.5281	0.9837	0.3	0.7	0.5580	0.9941	0.3	0.7	0.5875	0.9995	0.3	0.7	0.6164	0.9987	0.3
0.8	0.6661	0.9990	0.2	0.8	0.6899	0.9995	0.2	0.8	0.7129	0.9941	0.2	0.8	0.7353	0.9814	0.2	0.8	0.7571	0.9598	0.2
0.9	0.8371	0.9871	0.1	0.9	0.8504	0.9711	0.1	0.9	0.8632	0.9472	0.1	0.9	0.8756	0.9138	0.1	0.9	0.8875	0.8686	0.1
1.0	1.0000	0.9341	0.0	1.0	1.0000	0.9002	0.0	1.0	1.0000	0.8563	0.0	1.0	1.0000	0.8007	0.0	1.0	1.0000	0.7306	0.0
	1.0000	65° 205°			1.1177	60° 200°			1.2500	55° 195°			1.3997	50° 190°			1.5703	45° 185°	

θ_i	−90° 50°	0.5662			−85° 55°	0.5029			−80° 60°	0.4465			−75° 65°	0.3959			−70° 70°	0.3501	
0.0	0.0000	0.0000	1.0	0.0	0.0000	0.0000	1.0	0.0	0.0000	0.0000	1.0	0.0	0.0000	0.0000	1.0	0.0	0.0000	0.0000	1.0
0.1	0.0168	0.2419	0.9	0.1	0.0280	0.2612	0.9	0.1	0.0385	0.2821	0.9	0.1	0.0488	0.3049	0.9	0.1	0.0589	0.3301	0.9
0.2	0.0663	0.4695	0.8	0.2	0.0868	0.5012	0.8	0.2	0.1063	0.5349	0.8	0.2	0.1253	0.5710	0.8	0.2	0.1440	0.6096	0.8
0.3	0.1454	0.6691	0.7	0.3	0.1731	0.7057	0.7	0.3	9.1994	0.7435	0.7	0.3	0.2250	0.7823	0.7	0.3	0.2502	0.8221	0.7
0.4	0.2496	0.8290	0.6	0.4	0.2817	0.8626	0.6	0.4	0.3123	0.8954	0.6	0.4	0.3420	0.9265	0.6	0.4	0.3713	0.9549	0.6
0.5	0.3726	0.9397	0.5	0.5	0.4062	0.9627	0.5	0.5	0.4383	0.9816	0.5	0.5	0.4694	0.9949	0.5	0.5	0.5000	1.0000	0.5
0.6	0.5070	0.9945	0.4	0.6	0.5392	0.9998	0.4	0.6	0.5698	0.9970	0.4	0.6	0.5995	0.9834	0.4	0.6	0.6287	0.9549	0.4
0.7	0.6450	0.9903	0.3	0.7	0.6727	0.9719	0.3	0.7	0.6990	0.9408	0.3	0.7	0.7246	0.8927	0.3	0.7	0.7498	0.8221	0.3
0.8	0.7784	0.9272	0.2	0.8	0.7989	0.8806	0.2	0.8	0.8184	0.8161	0.2	0.8	0.8374	0.7283	0.2	0.8	0.8560	0.6096	0.2
0.9	0.8991	0.8090	0.1	0.9	0.9102	0.7313	0.1	0.9	0.9207	0.6305	0.1	0.9	0.9310	0.4999	0.1	0.9	0.9411	0.3301	0.1
1.0	1.0000	0.6428	0.0	1.0	1.0000	0.5329	0.0	1.0	1.0000	0.3949	0.0	1.0	1.0000	0.2210	0.0	1.0	1.0000	0.0000	0.0
	1.7660	40° 180°			1.9887	35° 175°			2.2398	30° 170°			2.5260	25° 165°			2.8563	20° 160°	

TABLE A·1.—H_k AS A FUNCTION OF θ_i — (*Cont.*)

$\Delta X_i = 140°$

θ_i	−70° 70°	0.3501			−65° 75°	0.3959			−60° 80°	0.4465			−55° 85°	0.5029			−50° 90°	0.5662	
0.0	0.0000	0.0000	1.0	0.0	0.0000	0.2210	1.0	0.0	0.0000	0.3949	1.0	0.0	0.0000	0.5329	1.0	0.0	0.0000	0.6428	1.0
0.1	0.0589	0.3301	0.9	0.1	0.0690	0.4999	0.9	0.1	0.0793	0.6305	0.9	0.1	0.0898	0.7313	0.9	0.1	0.1009	0.8090	0.9
0.2	0.1440	0.6096	0.8	0.2	0.1626	0.7283	0.8	0.2	0.1816	0.8161	0.8	0.2	0.2011	0.8806	0.8	0.2	0.2216	0.9272	0.8
0.3	0.2502	0.8221	0.7	0.3	0.2754	0.8927	0.7	0.3	0.3010	0.9408	0.7	0.3	0.3273	0.9719	0.7	0.3	0.3550	0.9903	0.7
0.4	0.3713	0.9549	0.6	0.4	0.4005	0.9834	0.6	0.4	0.4302	0.9970	0.6	0.4	0.4608	0.9998	0.6	0.4	0.4930	0.9945	0.6
0.5	0.5000	1.0000	0.5	0.5	0.5306	0.9949	0.5	0.5	0.5617	0.9816	0.5	0.5	0.5938	0.9627	0.5	0.5	0.6274	0.9397	0.5
0.6	0.6287	0.9549	0.4	0.6	0.6580	0.9265	0.4	0.6	0.6877	0.8954	0.4	0.6	0.7183	0.8626	0.4	0.6	0.7504	0.8290	0.4
0.7	0.7498	0.8221	0.3	0.7	0.7750	0.7823	0.3	0.7	0.8006	0.7435	0.3	0.7	0.8269	0.7057	0.3	0.7	0.8546	0.6691	0.3
0.8	0.8560	0.6096	0.2	0.8	0.8747	0.5710	0.2	0.8	0.8937	0.5349	0.2	0.8	0.9132	0.5012	0.2	0.8	0.9337	0.4695	0.2
0.9	0.9411	0.3301	0.1	0.9	0.9512	0.3049	0.1	0.9	0.9615	0.2821	0.1	0.9	0.9720	0.2612	0.1	0.9	0.9832	0.2419	0.1
1.0	1.0000	0.0000	0.0	1.0	1.0000	0.0000	0.0	1.0	1.0000	0.0000	0.0	1.0	1.0000	0.0000	0.0	1.0	1.0000	0.0000	0.0
	2.8563	20° 160°			2.5260	15° 155°			2.2398	10° 150°			1.9887	5° 145°			1.7660	0° 140°	

θ_i	−45° 95°	0.6368			−40° 100°	0.7144			−35° 105°	0.8000			−30° 110°	0.8947			−25° 115°	1.0000	
0.0	0.0000	0.7306	1.0	0.0	0.0000	0.8007	1.0	0.0	0.0000	0.8563	1.0	0.0	0.0000	0.9002	1.0	0.0	0.0000	0.9341	1.0
0.1	0.1125	0.8686	0.9	0.1	0.1244	0.9138	0.9	0.1	0.1368	0.9472	0.9	0.1	0.1496	0.9711	0.9	0.1	0.1629	0.9871	0.9
0.2	0.2429	0.9598	0.8	0.2	0.2647	0.9814	0.8	0.2	0.2871	0.9941	0.8	0.2	0.3101	0.9995	0.8	0.2	0.3339	0.9990	0.8
0.3	0.3836	0.9987	0.7	0.3	0.4125	0.9995	0.7	0.3	0.4420	0.9941	0.7	0.3	0.4719	0.9837	0.7	0.3	0.5026	0.9693	0.7
0.4	0.5260	0.9831	0.6	0.4	0.5591	0.9670	0.6	0.4	0.5922	0.9472	0.6	0.4	0.6256	0.9246	0.6	0.4	0.6591	0.8996	0.6
0.5	0.6618	0.9138	0.5	0.5	0.6956	0.8859	0.5	0.5	0.7290	0.8563	0.5	0.5	0.7619	0.8257	0.5	0.5	0.7941	0.7941	0.5
0.6	0.7829	0.7950	0.4	0.6	0.8141	0.7609	0.4	0.6	0.8441	0.7268	0.4	0.6	0.8727	0.6928	0.4	0.6	0.8996	0.6591	0.4
0.7	0.8820	0.6337	0.3	0.7	0.9075	0.5995	0.3	0.7	0.9307	0.5663	0.3	0.7	0.9515	0.5340	0.3	0.7	0.9693	0.5026	0.3
0.8	0.9534	0.4396	0.2	0.8	0.9702	0.4113	0.2	0.8	0.9837	0.3843	0.2	0.8	0.9935	0.3586	0.2	0.8	0.9990	0.3339	0.2
0.9	0.9928	0.2241	0.1	0.9	0.9985	0.2074	0.1	0.9	0.9999	0.1917	0.1	0.9	0.9963	0.1770	0.1	0.9	0.9871	0.1629	0.1
1.0	0.9978	0.0000	0.0	1.0	0.9908	0.0000	0.0	1.0	0.9783	0.0000	0.0	1.0	0.9598	0.0000	0.0	1.0	0.9341	0.0000	0.0
	1.5703	−5° 135°			1.3997	−10° 130°			1.2500	−15° 125°			1.1177	−20° 120°			1.0000	−25° 115°	

TABLE A·2.—θ_i AS A FUNCTION OF H_k

$\Delta X_i = 40°$

H_k	$X_{im} = -90°$ $X_{iM} = -50°$	$-85°$ $-45°$	$-80°$ $-40°$	$-75°$ $-35°$	$-70°$ $-30°$	$-65°$ $-25°$	$-60°$ $-20°$	$-55°$ $-15°$	$-50°$ $-10°$	$-45°$ $-5°$
0.0	0.0000	0.0000	0.0000	0.0000	0.0000	0.0000	0.0000	0.0000	0.0000	0.0000
0.1	0.3104	0.2424	0.2021	0.1769	0.1600	0.1478	0.1387	0.1315	0.1256	0.1206
0.2	0.4399	0.3805	0.3398	0.3111	0.2899	0.2736	0.2607	0.2500	0.2410	0.2332
0.3	0.5398	0.4892	0.4523	0.4245	0.4030	0.3858	0.3715	0.3595	0.3490	0.3398
0.4	0.6246	0.5822	0.5501	0.5251	0.5050	0.4884	0.4743	0.4622	0.4514	0.4417
0.5	0.6998	0.6652	0.6383	0.6167	0.5990	0.5840	0.5710	0.5596	0.5494	0.5400
0.6	0.7682	0.7410	0.7194	0.7018	0.6870	0.6742	0.6630	0.6530	0.6439	0.6355
0.7	0.8314	0.8114	0.7952	0.7817	0.7702	0.7602	0.7513	0.7432	0.7357	0.7287
0.8	0.8906	0.8775	0.8667	0.8576	0.8497	0.8428	0.8365	0.8308	0.8254	0.8202
0.9	0.9467	0.9402	0.9348	0.9302	0.9262	0.9225	0.9192	0.9162	0.9133	0.9106
1.0	1.0000	1.0000	1.0000	1.0000	1.0000	1.0000	1.0000	1.0000	1.0000	1.0000

H_k	$X_{im} = -40°$ $X_{iM} = 0°$	$-35°$ $5°$	$-30°$ $10°$	$-25°$ $15°$	$-20°$ $20°$	$-15°$ $25°$	$-10°$ $30°$	$-5°$ $35°$	$0°$ $40°$	$5°$ $45°$
0.0	0.0000	0.0000	0.0000	0.0000	0.0000	0.0000	0.0000	0.0000	0.0000	0.0000
0.1	0.1164	0.1126	0.1091	0.1060	0.1030	0.1002	0.0975	0.0948	0.0921	0.0894
0.2	0.2264	0.2201	0.2144	0.2090	0.2040	0.1990	0.1942	0.1894	0.1846	0.1798
0.3	0.3315	0.3238	0.3167	0.3099	0.3034	0.2970	0.2908	0.2844	0.2780	0.2713
0.4	0.4328	0.4246	0.4168	0.4093	0.4020	0.3947	0.3874	0.3801	0.3725	0.3645
0.5	0.5313	0.5231	0.5152	0.5076	0.5000	0.4924	0.4848	0.4769	0.4687	0.4600
0.6	0.6275	0.6199	0.6126	0.6053	0.5980	0.5907	0.5832	0.5754	0.5672	0.5583
0.7	0.7220	0.7156	0.7092	0.7030	0.6966	0.6901	0.6833	0.6762	0.6685	0.6602
0.8	0.8154	0.8106	0.8058	0.8010	0.7960	0.7910	0.7856	0.7799	0.7736	0.7668
0.9	0.9079	0.9052	0.9025	0.8998	0.8970	0.8940	0.8909	0.8874	0.8836	0.8794
1.0	1.0000	1.0000	1.0000	1.0000	1.0000	1.0000	1.0000	1.0000	1.0000	1.0000

H_k	$X_{im} = 10°$ $X_{iM} = 50°$	$15°$ $55°$	$20°$ $60°$	$25°$ $65°$	$30°$ $70°$	$35°$ $75°$	$40°$ $80°$	$45°$ $85°$	$50°$ $90°$
0.0	0.0000	0.0000	0.0000	0.0000	0.0000	0.0000	0.0000	0.0000	0.0000
0.1	0.0867	0.0838	0.0808	0.0775	0.0738	0.0698	0.0652	0.0598	0.0533
0.2	0.1746	0.1692	0.1635	0.1572	0.1503	0.1424	0.1333	0.1225	0.1094
0.3	0.2643	0.2568	0.2487	0.2398	0.2298	0.2183	0.2048	0.1886	0.1686
0.4	0.3561	0.3470	0.3370	0.3258	0.3130	0.2982	0.2806	0.2590	0.2318
0.5	0.4506	0.4404	0.4290	0.4160	0.4010	0.3833	0.3617	0.3348	0.3002
0.6	0.5486	0.5378	0.5257	0.5116	0.4950	0.4749	0.4499	0.4178	0.3754
0.7	0.6510	0.6405	0.6285	0.6142	0.5970	0.5755	0.5477	0.5108	0.4602
0.8	0.7590	0.7500	0.7393	0.7264	0.7101	0.6889	0.6602	0.6195	0.5601
0.9	0.8744	0.8685	0.8613	0.8522	0.8400	0.8231	0.7979	0.7576	0.6896
1.0	1.0000	1.0000	1.0000	1.0000	1.0000	1.0000	1.0000	1.0000	1.0000

TABLE A·2.—θ_i AS A FUNCTION OF H_k — (*Cont.*)

$\Delta X_i = 50°$

H_k	$X_{im} = -90°$ $X_{iM} = -40°$	$-85°$ $-35°$	$-80°$ $-30°$	$-75°$ $-25°$	$-70°$ $-20°$	$-65°$ $-15°$	$-60°$ $-10°$	$-55°$ $-5°$	$-50°$ $0°$
0.0	0.0000	0.0000	0.0000	0.0000	0.0000	0.0000	0.0000	0.0000	0.0000
0.1	0.3072	0.2492	0.2111	0.1855	0.1673	0.1539	0.1435	0.1352	0.1283
0.2	0.4358	0.3853	0.3479	0.3198	0.2980	0.2806	0.2664	0.2544	0.2441
0.3	0.5354	0.4922	0.4585	0.4318	0.4100	0.3919	0.3766	0.3632	0.3515
0.4	0.6201	0.5839	0.5546	0.5306	0.5105	0.4932	0.4782	0.4648	0.4527
0.5	0.6955	0.6658	0.6413	0.6206	0.6029	0.5874	0.5736	0.5611	0.5493
0.6	0.7643	0.7409	0.7212	0.7043	0.6895	0.6763	0.6644	0.6534	0.6431
0.7	0.8283	0.8109	0.7960	0.7831	0.7716	0.7612	0.7516	0.7427	0.7343
0.8	0.8884	0.8769	0.8669	0.8582	0.8503	0.8430	0.8363	0.8339	0.8237
0.9	0.9455	0.9397	0.9347	0.9303	0.9262	0.9224	0.9189	0.9154	0.9121
1.0	1.0000	1.0000	1.0000	1.0000	1.0000	1.0000	1.0000	1.0000	1.0000

H_k	$X_{im} = -45°$ $X_{iM} = 5°$	$-40°$ $10°$	$-35°$ $15°$	$-30°$ $20°$	$-25°$ $25°$	$-20°$ $30°$	$-15°$ $35°$	$-10°$ $40°$	$-5°$ $45°$
0.0	0.0000	0.0000	0.0000	0.0000	0.0000	0.0000	0.0000	0.0000	0.0000
0.1	0.1224	0.1173	0.1127	0.1086	0.1048	0.1012	0.0978	0.0944	0.0911
0.2	0.2350	0.2269	0.2195	0.2127	0.2062	0.2000	0.1940	0.1881	0.1822
0.3	0.3408	0.3311	0.3221	0.3135	0.3054	0.2974	0.2896	0.2818	0.2738
0.4	0.4416	0.4313	0.4215	0.4122	0.4030	0.3940	0.3850	0.3759	0.3666
0.5	0.5388	0.5287	0.5189	0.5094	0.5000	0.4906	0.4811	0.4713	0.4612
0.6	0.6334	0.6241	0.6150	0.6060	0.5970	0.5878	0.5785	0.5687	0.5584
0.7	0.7262	0.7182	0.7104	0.7026	0.6946	0.6865	0.6779	0.6689	0.6592
0.8	0.8178	0.8119	0.8060	0.8000	0.7938	0.7873	0.7805	0.7731	0.7650
0.9	0.9089	0.9056	0.9022	0.8988	0.8952	0.8914	0.8873	0.8827	0.8776
1.0	1.0000	1.0000	1.0000	1.0000	1.0000	1.0000	1.0000	1.0000	1.0000

H_k	$X_{im} = 0°$ $X_{iM} = 50°$	$5°$ $55°$	$10°$ $60°$	$15°$ $65°$	$20°$ $70°$	$25°$ $75°$	$30°$ $80°$	$35°$ $85°$	$40°$ $90°$
0.0	0.0000	0.0000	0.0000	0.0000	0.0000	0.0000	0.0000	0.0000	0.0000
0.1	0.0879	0.0846	0.0811	0.0776	0.0738	0.0697	0.0653	0.0603	0.0545
0.2	0.1763	0.1661	0.1637	0.1570	0.1497	0.1418	0.1331	0.1231	0.1116
0.3	0.2657	0.2573	0.2484	0.2388	0.2284	0.2169	0.2040	0.1891	0.1717
0.4	0.3569	0.3466	0.3356	0.3237	0.3105	0.2957	0.2788	0.2591	0.2357
0.5	0.4504	0.4389	0.4264	0.4126	0.3971	0.3794	0.3587	0.3342	0.3045
0.6	0.5473	0.5352	0.5218	0.5068	0.4895	0.4694	0.4454	0.4161	0.3799
0.7	0.6485	0.6368	0.6234	0.6081	0.5900	0.5682	0.5415	0.5078	0.4646
0.8	0.7559	0.7456	0.7336	0.7194	0.7020	0.6802	0.6521	0.6147	0.5642
0.9	0.8717	0.8648	0.8565	0.8461	0.8327	0.8145	0.7889	0.7508	0.6928
1.0	1.0000	1.0000	1.0000	1.0000	1.0000	1.0000	1.0000	1.0000	1.0000

TABLE A-2.—θ_i AS A FUNCTION OF H_k — (*Cont.*)

$\Delta X_i = 60°$

H_k	$X_{im} = -90°$ $X_{iM} = -30°$	$-85°$ $-25°$	$-80°$ $-20°$	$-75°$ $-15°$	$-70°$ $-10°$	$-65°$ $-5°$	$-60°$ $0°$	$-55°$ $5°$	$-50°$ $10°$
0.0	0.0000	0.0000	0.0000	0.0000	0.0000	0.0000	0.0000	0.0000	0.0000
0.1	0.3032	0.2524	0.2166	0.1910	0.1722	0.1579	0.1465	0.1373	0.1295
0.2	0.4307	0.3863	0.3517	0.3243	0.3024	0.2843	0.2691	0.2561	0.2447
0.3	0.5298	0.4917	0.4605	0.4347	0.4129	0.3943	0.3780	0.3637	0.3507
0.4	0.6145	0.5823	0.5551	0.5319	0.5118	0.4941	0.4782	0.4638	0.4506
0.5	0.6902	0.6635	0.6406	0.6206	0.6029	0.5869	0.5723	0.5588	0.5462
0.6	0.7595	0.7384	0.7199	0.7034	0.6885	0.6749	0.6622	0.6503	0.6389
0.7	0.8243	0.8085	0.7944	0.7817	0.7701	0.7592	0.7490	0.7392	0.7297
0.8	0.8855	0.8750	0.8655	0.8568	0.8487	0.8411	0.8338	0.8267	0.8197
0.9	0.9439	0.9386	0.9338	0.9293	0.9251	0.9211	0.9172	0.9133	0.9095
1.0	1.0000	1.0000	1.0000	1.0000	1.0000	1.0000	1.0000	1.0000	1.0000

H_k	$X_{im} = -45°$ $X_{iM} = 15°$	$-40°$ $20°$	$-35°$ $25°$	$-30°$ $30°$	$-25°$ $35°$	$-20°$ $40°$	$-15°$ $45°$	$-10°$ $50°$	$-5°$ $55°$
0.0	0.0000	0.0000	0.0000	0.0000	0.0000	0.0000	0.0000	0.0000	0.0000
0.1	0.1229	0.1170	0.1118	0.1070	0.1026	0.0984	0.0944	0.0905	0.0867
0.2	0.2346	0.2254	0.2169	0.2090	0.2015	0.1943	0.1873	0.1803	0.1733
0.3	0.3389	0.3279	0.3176	0.3077	0.2982	0.2888	0.2796	0.2703	0.2608
0.4	0.4382	0.4265	0.4153	0.4044	0.3936	0.3829	0.3721	0.3611	0.3497
0.5	0.5341	0.5225	0.5112	0.5000	0.4888	0.4775	0.4659	0.4538	0.4412
0.6	0.6279	0.6171	0.6064	0.5957	0.5847	0.5735	0.5618	0.5494	0.5362
0.7	0.7204	0.7112	0.7018	0.6923	0.6824	0.6721	0.6611	0.6493	0.6363
0.8	0.8127	0.8057	0.7985	0.7910	0.7831	0.7746	0.7654	0.7553	0.7439
0.9	0.9056	0.9016	0.8974	0.8930	0.8882	0.8830	0.8771	0.8705	0.8627
1.0	1.0000	1.0000	1.0000	1.0000	1.0000	1.0000	1.0000	1.0000	1.0000

H_k	$X_{im} = 0°$ $X_{iM} = 60°$	$5°$ $65°$	$10°$ $70°$	$15°$ $75°$	$20°$ $80°$	$25°$ $85°$	$30°$ $90°$
0.0	0.0000	0.0000	0.0000	0.0000	0.0000	0.0000	0.0000
0.1	0.0828	0.0789	0.0749	0.0707	0.0662	0.0614	0.0561
0.2	0.1662	0.1589	0.1513	0.1432	0.1345	0.1250	0.1145
0.3	0.2510	0.2408	0.2299	0.2183	0.2056	0.1915	0.1757
0.4	0.3378	0.3251	0.3115	0.2966	0.2801	0.2616	0.2405
0.5	0.4277	0.4131	0.3971	0.3794	0.3594	0.3365	0.3098
0.6	0.5218	0.5059	0.4882	0.4681	0.4449	0.4177	0.3855
0.7	0.6220	0.6057	0.5871	0.5653	0.5395	0.5083	0.4702
0.8	0.7309	0.7157	0.6976	0.6757	0.6483	0.6137	0.5693
0.9	0.8535	0.8421	0.8278	0.8090	0.7834	0.7476	0.6968
1.0	1.0000	1.0000	1.0000	1.0000	1.0000	1.0000	1.0000

TABLE A·2.—θ_i AS A FUNCTION OF H_k — (*Cont.*)

$\Delta X_i = 70°$

H_k	$X_{im} = -90°$ $X_{iM} = -20°$	$-85°$ $-15°$	$-80°$ $-10°$	$-75°$ $-5°$	$-70°$ $0°$	$-65°$ $5°$	$-60°$ $10°$	$-55°$ $15°$
0.0	0.0000	0.0000	0.0000	0.0000	0.0000	0.0000	0.0000	0.0000
0.1	0.2986	0.2530	0.2193	0.1942	0.1750	0.1600	0.1479	0.1379
0.2	0.4247	0.3847	0.3522	0.3257	0.3037	0.2851	0.2692	0.2553
0.3	0.5231	0.4885	0.4592	0.4341	0.4124	0.3934	0.3764	0.3611
0.4	0.6077	0.5782	0.5525	0.5299	0.5097	0.4915	0.4749	0.4596
0.5	0.6836	0.6591	0.6372	0.6175	0.5997	0.5832	0.5678	0.5533
0.6	0.7537	0.7339	0.7161	0.6997	0.6846	0.6704	0.6569	0.6439
0.7	0.8194	0.8045	0.7908	0.7781	0.7661	0.7547	0.7437	0.7328
0.8	0.8819	0.8718	0.8625	0.8537	0.8453	0.8371	0.8291	0.8211
0.9	0.9419	0.9368	0.9320	0.9274	0.9230	0.9186	0.9142	0.9098
1.0	1.0000	1.0000	1.0000	1.0000	1.0000	1.0000	1.0000	1.0000

H_k	$X_{im} = -50°$ $X_{iM} = 20°$	$-45°$ $25°$	$-40°$ $30°$	$-35°$ $35°$	$-30°$ $40°$	$-25°$ $45°$	$-20°$ $50°$	$-15°$ $55°$
0.0	0.0000	0.0000	0.0000	0.0000	0.0000	0.0000	0.0000	0.0000
0.1	0.1294	0.1221	0.1156	0.1098	0.1045	0.0995	0.0947	0.0902
0.2	0.2430	0.2320	0.2218	0.2124	0.2036	0.1951	0.1869	0.1789
0.3	0.3472	0.3342	0.3221	0.3105	0.2994	0.2886	0.2778	0.2672
0.4	0.4452	0.4316	0.4186	0.4059	0.3935	0.3811	0.3687	0.3561
0.5	0.5394	0.5260	0.5129	0.5000	0.4871	0.4740	0.4606	0.4467
0.6	0.6313	0.6189	0.6065	0.5941	0.5814	0.5684	0.5548	0.5404
0.7	0.7222	0.7114	0.7006	0.6895	0.6779	0.6658	0.6528	0.6389
0.8	0.8131	0.8049	0.7964	0.7876	0.7782	0.7680	0.7570	0.7447
0.9	0.9053	0.9005	0.8955	0.8902	0.8844	0.8779	0.8706	0.8621
1.0	1.0000	1.0000	1.0000	1.0000	1.0000	1.0000	1.0000	1.0000

H_k	$X_{im} = -10°$ $X_{iM} = 60°$	$-5°$ $65°$	$0°$ $70°$	$5°$ $75°$	$10°$ $80°$	$15°$ $85°$	$20°$ $90°$
0.0	0.0000	0.0000	0.0000	0.0000	0.0000	0.0000	0.0000
0.1	0.0858	0.0814	0.0770	0.0726	0.0680	0.0632	0.0581
0.2	0.1709	0.1629	0.1547	0.1463	0.1375	0.1282	0.1181
0.3	0.2563	0.2453	0.2339	0.2219	0.2092	0.1955	0.1806
0.4	0.3431	0.3296	0.3154	0.3003	0.2839	0.2661	0.2463
0.5	0.4322	0.4168	0.4003	0.3825	0.3628	0.3409	0.3164
0.6	0.5251	0.5085	0.4903	0.4701	0.4475	0.4218	0.3923
0.7	0.6236	0.6066	0.5876	0.5659	0.5408	0.5115	0.4769
0.8	0.7308	0.7149	0.6963	0.6743	0.6478	0.6153	0.5753
0.9	0.8521	0.8400	0.8250	0.8058	0.7807	0.7470	0.7014
1.0	1.0000	1.0000	1.0000	1.0000	1.0000	1.0000	1.0000

TABLE A-2.—θ_i AS A FUNCTION OF H_k — (*Cont.*)

$\Delta X_i = 80°$

H_k	$X_{im} = -90°$ $X_{iM} = -10°$	$-85°$ $-5°$	$-80°$ $0°$	$-75°$ $5°$	$-70°$ $10°$	$-65°$ $15°$	$-60°$ $20°$	$-55°$ $25°$
0.0	0.0000	0.0000	0.0000	0.0000	0.0000	0.0000	0.0000	0.0000
0.1	0.2932	0.2517	0.2198	0.1952	0.1759	0.1604	0.1478	0.1372
0.2	0.4176	0.3809	0.3502	0.3244	0.3024	0.2835	0.2670	0.2524
0.3	0.5154	0.4832	0.4552	0.4307	0.4090	0.3896	0.3720	0.3559
0.4	0.5997	0.5720	0.5472	0.5250	0.5047	0.4860	0.4686	0.4524
0.5	0.6758	0.6525	0.6313	0.6117	0.5935	0.5764	0.5601	0.5446
0.6	0.7465	0.7276	0.7100	0.6936	0.6779	0.6630	0.6485	0.6344
0.7	0.8133	0.7988	0.7852	0.7722	0.7596	0.7474	0.7354	0.7234
0.8	0.8774	0.8675	0.8580	0.8488	0.8399	0.8310	0.8220	0.8130
0.9	0.9394	0.9343	0.9294	0.9245	0.9197	0.9148	0.9098	0.9046
1.0	1.0000	1.0000	1.0000	1.0000	1.0000	1.0000	1.0000	1.0000

H_k	$X_{im} = -50°$ $X_{iM} = 30°$	$-45°$ $35°$	$-40°$ $40°$	$-35°$ $45°$	$-30°$ $50°$	$-25°$ $55°$	$-20°$ $60°$	$-15°$ $65°$
0.0	0.0000	0.0000	0.0000	0.0000	0.0000	0.0000	0.0000	0.0000
0.1	0.1281	0.1202	0.1132	0.1068	0.1009	0.0954	0.0902	0.0852
0.2	0.2393	0.2274	0.2164	0.2062	0.1964	0.1870	0.1780	0.1690
0.3	0.3410	0.3270	0.3138	0.3010	0.2887	0.2766	0.2646	0.2526
0.4	0.4369	0.4221	0.4077	0.3936	0.3796	0.3656	0.3515	0.3370
0.5	0.5294	0.5145	0.5000	0.4855	0.4706	0.4554	0.4399	0.4236
0.6	0.6204	0.6064	0.5923	0.5779	0.5631	0.5476	0.5314	0.5140
0.7	0.7113	0.6990	0.6862	0.6730	0.6590	0.6441	0.6280	0.6104
0.8	0.8036	0.7938	0.7836	0.7726	0.7607	0.7476	0.7330	0.7165
0.9	0.8991	0.8932	0.8868	0.8798	0.8719	0.8628	0.8522	0.8396
1.0	1.0000	1.0000	1.0000	1.0000	1.0000	1.0000	1.0000	1.0000

H_k	$X_{im} = -10°$ $X_{iM} = 70°$	$-5°$ $75°$	$0°$ $80°$	$5°$ $85°$	$10°$ $90°$
0.0	0.0000	0.0000	0.0000	0.0000	0.0000
0.1	0.0803	0.0755	0.0706	0.0657	0.0606
0.2	0.1601	0.1512	0.1420	0.1325	0.1226
0.3	0.2404	0.2278	0.2148	0.2012	0.1867
0.4	0.3221	0.3064	0.2900	0.2724	0.2535
0.5	0.4065	0.3883	0.3687	0.3475	0.3242
0.6	0.4953	0.4750	0.4528	0.4280	0.4003
0.7	0.5910	0.5693	0.5448	0.5168	0.4846
0.8	0.6976	0.6756	0.6498	0.6191	0.5824
0.9	0.8241	0.8048	0.7802	0.7483	0.7068
1.0	1.0000	1.0000	1.0000	1.0000	1.0000

TABLE A·2.—θ_i AS A FUNCTION OF H_k — (*Cont.*)

$\Delta X_i = 90°$

H_k	$X_{im} = -90°$ $X_{iM} = 0°$	−85° 5°	−80° 10°	−75° 15°	−70° 20°	−65° 25°	−60° 30°	−55° 35°	−50° 40°	−45° 45°
0.0	0.0000	0.0000	0.0000	0.0000	0.0000	0.0000	0.0000	0.0000	0.0000	0.0000
0.1	0.2871	0.2488	0.2185	0.1944	0.1751	0.1593	0.1462	0.1352	0.1256	0.1172
0.2	0.4097	0.3754	0.3460	0.3207	0.2988	0.2797	0.2627	0.2475	0.2337	0.2211
0.3	0.5064	0.4760	0.4490	0.4249	0.4031	0.3833	0.3651	0.3482	0.3324	0.3174
0.4	0.5903	0.5639	0.5397	0.5175	0.4969	0.4777	0.4596	0.4423	0.4257	0.4097
0.5	0.6667	0.6441	0.6230	0.6033	0.5846	0.5667	0.5495	0.5328	0.5163	0.5000
0.6	0.7380	0.7194	0.7018	0.6849	0.6685	0.6527	0.6371	0.6216	0.6061	0.5903
0.7	0.8060	0.7916	0.7776	0.7641	0.7507	0.7375	0.7242	0.7107	0.6969	0.6826
0.8	0.8718	0.8618	0.8519	0.8422	0.8324	0.8225	0.8123	0.8018	0.7907	0.7789
0.9	0.9362	0.9310	0.9257	0.9204	0.9150	0.9094	0.9034	0.8971	0.8903	0.8828
1.0	1.0000	1.0000	1.0000	1.0000	1.0000	1.0000	1.0000	1.0000	1.0000	1.0000

H_k	$X_{im} = -40°$ $X_{iM} = 50°$	−35° 55°	−30° 60°	−25° 65°	−20° 70°	−15° 75°	−10° 80°	−5° 85°	0° 90°
0.0	0.0000	0.0000	0.0000	0.0000	0.0000	0.0000	0.0000	0.0000	0.0000
0.1	0.1097	0.1029	0.0966	0.0906	0.0850	0.0796	0.0743	0.0690	0.0638
0.2	0.2093	0.1982	0.1877	0.1775	0.1676	0.1578	0.1481	0.1382	0.1282
0.3	0.3031	0.2893	0.2758	0.2625	0.2493	0.2359	0.2224	0.2084	0.1940
0.4	0.3939	0.3784	0.3629	0.3473	0.3315	0.3151	0.2982	0.2806	0.2620
0.5	0.4837	0.4672	0.4505	0.4333	0.4154	0.3967	0.3770	0.3559	0.3333
0.6	0.5743	0.5577	0.5404	0.5223	0.5031	0.4825	0.4603	0.4361	0.4097
0.7	0.6676	0.6518	0.6349	0.6167	0.5969	0.5751	0.5510	0.5240	0.4936
0.8	0.7663	0.7525	0.7373	0.7203	0.7012	0.6793	0.6540	0.6246	0.5903
0.9	0.8744	0.8648	0.8538	0.8407	0.8249	0.8056	0.7815	0.7512	0.7129
1.0	1.0000	1.0000	1.0000	1.0000	1.0000	1.0000	1.0000	1.0000	1.0000

$\Delta X_i = 100°$

H_k	$X_{im} = -90°$ $X_{iM} = 10°$	−85° 15°	−80° 20°	−75° 25°	−70° 30°	−65° 35°	−60° 40°	−55° 45°	−50° 50°
0.0	0.0000	0.0000	0.0000	0.0000	0.0000	0.0000	0.0000	0.0000	0.0000
0.1	0.2804	0.2446	0.2156	0.1920	0.1728	0.1568	0.1434	0.1320	0.1221
0.2	0.4007	0.3682	0.3399	0.3151	0.2933	0.2739	0.2565	0.2408	0.2264
0.3	0.4962	0.4671	0.4407	0.4168	0.3948	0.3746	0.3558	0.3382	0.3216
0.4	0.5796	0.5538	0.5300	0.5076	0.4866	0.4667	0.4478	0.4296	0.4119
0.5	0.6559	0.6337	0.6125	0.5924	0.5730	0.5542	0.5359	0.5179	0.5000
0.6	0.7279	0.7093	0.6912	0.6737	0.6565	0.6395	0.6225	0.6054	0.5881
0.7	0.7972	0.7824	0.7679	0.7535	0.7390	0.7245	0.7096	0.6943	0.6784
0.8	0.8650	0.8545	0.8440	0.8333	0.8224	0.8111	0.7994	0.7869	0.7736
0.9	0.9323	0.9266	0.9208	0.9148	0.9086	0.9019	0.8947	0.8868	0.8779
1.0	1.0000	1.0000	1.0000	1.0000	1.0000	1.0000	1.0000	1.0000	1.0000

TABLE A·2.—θ_i AS A FUNCTION OF H_k — (Cont.)

$\Delta X_i = 100°$

H_k	$X_{im} = -45°$ $X_{iM} = 55°$	$-40°$ $60°$	$-35°$ $65°$	$-30°$ $70°$	$-25°$ $75°$	$-20°$ $80°$	$-15°$ $85°$	$-10°$ $90°$
0.0	0.0000	0.0000	0.0000	0.0000	0.0000	0.0000	0.0000	0.0000
0.1	0.1132	0.1053	0.0981	0.0914	0.0852	0.0792	0.0734	0.0677
0.2	0.2131	0.2006	0.1889	0.1776	0.1667	0.1560	0.1455	0.1350
0.3	0.3057	0.2904	0.2755	0.2610	0.2465	0.2321	0.2176	0.2028
0.4	0.3946	0.3775	0.3605	0.3435	0.3263	0.3088	0.2907	0.2721
0.5	0.4821	0.4641	0.4458	0.4270	0.4076	0.3875	0.3663	0.3441
0.6	0.5704	0.5522	0.5333	0.5134	0.4924	0.4700	0.4462	0.4204
0.7	0.6618	0.6442	0.6254	0.6052	0.5832	0.5593	0.5329	0.5038
0.8	0.7592	0.7435	0.7261	0.7067	0.6849	0.6601	0.6318	0.5993
0.9	0.8680	0.8566	0.8432	0.8272	0.8080	0.7844	0.7554	0.7196
1.0	1.0000	1.0000	1.0000	1.0000	1.0000	1.0000	1.0000	1.0000

$\Delta X_i = 110°$

H_k	$X_{im} = -90°$ $X_{iM} = 20°$	$-85°$ $25°$	$-80°$ $30°$	$-75°$ $35°$	$-70°$ $40°$	$-65°$ $45°$	$-60°$ $50°$	$-55°$ $55°$
0.0	0.0000	0.0000	0.0000	0.0000	0.0000	0.0000	0.0000	0.0000
0.1	0.2730	0.2392	0.2113	0.1883	0.1692	0.1531	0.1395	0.1278
0.2	0.3907	0.3597	0.3322	0.3077	0.2859	0.2663	0.2486	0.2324
0.3	0.4847	0.4565	0.4305	0.4066	0.3845	0.3638	0.3444	0.3261
0.4	0.5673	0.5420	0.5181	0.4955	0.4740	0.4534	0.4336	0.4143
0.5	0.6436	0.6212	0.5998	0.5790	0.5588	0.5390	0.5194	0.5000
0.6	0.7161	0.6970	0.6783	0.6598	0.6415	0.6231	0.6046	0.5857
0.7	0.7866	0.7712	0.7557	0.7401	0.7243	0.7081	0.6913	0.6739
0.8	0.8566	0.8453	0.8338	0.8219	0.8095	0.7964	0.7826	0.7676
0.9	0.9272	0.9210	0.9144	0.9074	0.8998	0.8916	0.8825	0.8722
1.0	1.0000	1.0000	1.0000	1.0000	1.0000	1.0000	1.0000	1.0000

H_k	$X_{im} = -50°$ $X_{iM} = 60°$	$-45°$ $65°$	$-40°$ $70°$	$-35°$ $75°$	$-30°$ $80°$	$-25°$ $85°$	$-20°$ $90°$
0.0	0.0000	0.0000	0.0000	0.0000	0.0000	0.0000	0.0000
0.1	0.1175	0.1084	0.1002	0.0926	0.0856	0.0790	0.0728
0.2	0.2174	0.2036	0.1905	0.1781	0.1662	0.1547	0.1434
0.3	0.3087	0.2919	0.2757	0.2599	0.2443	0.2288	0.2134
0.4	0.3954	0.3769	0.3585	0.3402	0.3217	0.3030	0.2839
0.5	0.4806	0.4610	0.4412	0.4210	0.4002	0.3788	0.3564
0.6	0.5664	0.5466	0.5260	0.5045	0.4819	0.4580	0.4327
0.7	0.6556	0.6362	0.6155	0.5934	0.5695	0.5435	0.5153
0.8	0.7514	0.7337	0.7141	0.6923	0.6678	0.6403	0.6093
0.9	0.8605	0.8469	0.8308	0.8117	0.7887	0.7608	0.7270
1.0	1.0000	1.0000	1.0000	1.0000	1.0000	1.0000	1.0000

TABLE A·2.—θ_i AS A FUNCTION OF H_k — (*Cont.*)

$\Delta X_i = 120°$

H_k	$X_{im} = -90°$ $X_{iM} = 30°$	$-85°$ $35°$	$-80°$ $40°$	$-75°$ $45°$	$-70°$ $50°$	$-65°$ $55°$	$-60°$ $60°$
0.0	0.0000	0.0000	0.0000	0.0000	0.0000	0.0000	0.0000
0.1	0.2649	0.2329	0.2059	0.1833	0.1644	0.1483	0.1346
0.2	0.3798	0.3498	0.3230	0.2988	0.2770	0.2572	0.2391
0.3	0.4719	0.4443	0.4186	0.3946	0.3722	0.3511	0.3311
0.4	0.5535	0.5283	0.5042	0.4812	0.4590	0.4376	0.4169
0.5	0.6294	0.6067	0.5846	0.5630	0.5418	0.5208	0.5000
0.6	0.7022	0.6824	0.6627	0.6431	0.6234	0.6034	0.5831
0.7	0.7739	0.7574	0.7407	0.7237	0.7061	0.6879	0.6689
0.8	0.8461	0.8337	0.8208	0.8072	0.7929	0.7775	0.7609
0.9	0.9207	0.9135	0.9057	0.8973	0.8879	0.8774	0.8654
1.0	1.0000	1.0000	1.0000	1.0000	1.0000	1.0000	1.0000

H_k	$X_{im} = -55°$ $X_{iM} = 65°$	$-50°$ $70°$	$-45°$ $75°$	$-40°$ $80°$	$-35°$ $85°$	$-30°$ $90°$
0.0	0.0000	0.0000	0.0000	0.0000	0.0000	0.0000
0.1	0.1226	0.1121	0.1027	0.0943	0.0865	0.0793
0.2	0.2225	0.2071	0.1928	0.1792	0.1663	0.1539
0.3	0.3121	0.2939	0.2763	0.2593	0.2426	0.2261
0.4	0.3966	0.3766	0.3569	0.3373	0.3176	0.2978
0.5	0.4792	0.4582	0.4370	0.4154	0.3933	0.3706
0.6	0.5624	0.5410	0.5188	0.4958	0.4717	0.4465
0.7	0.6489	0.6278	0.6054	0.5814	0.5557	0.5281
0.8	0.7428	0.7230	0.7012	0.6770	0.6502	0.6202
0.9	0.8517	0.8356	0.8167	0.7941	0.7671	0.7351
1.0	1.0000	1.0000	1.0000	1.0000	1.0000	1.0000

$\Delta X_i = 130°$

H_k	$X_{im} = -90°$ $X_{iM} = 40°$	$-85°$ $45°$	$-80°$ $50°$	$-75°$ $55°$	$-70°$ $60°$	$-65°$ $65°$
0.0	0.0000	0.0000	0.0000	0.0000	0.0000	0.0000
0.1	0.2562	0.2256	0.1995	0.1774	0.1586	0.1425
0.2	0.3678	0.3388	0.3124	0.2884	0.2666	0.2466
0.3	0.4579	0.4306	0.4049	0.3808	0.3580	0.3365
0.4	0.5381	0.5128	0.4882	0.4647	0.4419	0.4197
0.5	0.6132	0.5899	0.5671	0.5446	0.5222	0.5000
0.6	0.6860	0.6652	0.6444	0.6233	0.6020	0.5803
0.7	0.7586	0.7408	0.7226	0.7037	0.6841	0.6635
0.8	0.8332	0.8192	0.8044	0.7886	0.7717	0.7534
0.9	0.9122	0.9036	0.8940	0.8834	0.8713	0.8575
1.0	1.0000	1.0000	1.0000	1.0000	1.0000	1.0000

TABLE A·2.—θ_i AS A FUNCTION OF H_k — (*Cont.*)

$\Delta X_i = 130°$

H_k	$X_{im} = -60°$ $X_{iM} = 70°$	$-55°$ $75°$	$-50°$ $80°$	$-45°$ $85°$	$-40°$ $90°$
0.0	0.0000	0.0000	0.0000	0.0000	0.0000
0.1	0.1287	0.1166	0.1060	0.0964	0.0878
0.2	0.2283	0.2114	0.1956	0.1808	0.1668
0.3	0.3159	0.2963	0.2774	0.2592	0.2414
0.4	0.3980	0.3767	0.3556	0.3348	0.3140
0.5	0.4778	0.4554	0.4329	0.4101	0.3868
0.6	0.5581	0.5353	0.5118	0.4872	0.4619
0.7	0.6420	0.6192	0.5951	0.5694	0.5421
0.8	0.7334	0.7116	0.6876	0.6612	0.6322
0.9	0.8414	0.8226	0.8005	0.7744	0.7438
1.0	1.0000	1.0000	1.0000	1.0000	1.0000

$\Delta X_i = 140°$

H_k	$X_{im} = -90°$ $X_{iM} = 50°$	$-85°$ $55°$	$-80°$ $60°$	$-75°$ $65°$	$-70°$ $70°$
0.0	0.0000	0.0000	0.0000	0.0000	0.0000
0.1	0.2470	0.2174	0.1921	0.1704	0.1518
0.2	0.3550	0.3265	0.3005	0.2767	0.2549
0.3	0.4425	0.4154	0.3897	0.3654	0.3423
0.4	0.5209	0.4952	0.4704	0.4462	0.4226
0.5	0.5949	0.5708	0.5471	0.5235	0.5000
0.6	0.6673	0.6452	0.6230	0.6004	0.5774
0.7	0.7405	0.7210	0.7008	0.6797	0.6577
0.8	0.8170	0.8010	0.7838	0.7652	0.7451
0.9	0.9008	0.8901	0.8780	0.8641	0.8482
1.0	1.0000	1.0000	1.0000	1.0000	1.0000

H_k	$X_{im} = -65°$ $X_{iM} = 75°$	$-60°$ $80°$	$-55°$ $85°$	$-50°$ $90°$
0.0	0.0000	0.0000	0.0000	0.0000
0.1	0.1359	0.1220	0.1099	0.0992
0.2	0.2348	0.2162	0.1990	0.1830
0.3	0.3203	0.2992	0.2790	0.2595
0.4	0.3996	0.3770	0.3548	0.3327
0.5	0.4765	0.4529	0.4292	0.4051
0.6	0.5538	0.5296	0.5048	0.4791
0.7	0.6346	0.6103	0.5846	0.5575
0.8	0.7233	0.6995	0.6735	0.6450
0.9	0.8296	0.8079	0.7826	0.7530
1.0	1.0000	1.0000	1.0000	1.0000

APPENDIX B

PROPERTIES OF THE THREE-BAR-LINKAGE NOMOGRAM

This appendix includes a mathematical discussion of the contours of the three-bar-linkage nomogram, and a table of curve coordinates for use in the construction of a nomogram suitable for accurate work. The nomogram itself appears as Fig. B·1, in a folder in the back of the book.

B·1. Contours of Constant b.—In the (p, η)-plane the contours of constant b are given by Eq. (5·44):

$$\eta = \cos^{-1} (\cosh p - \tfrac{1}{2}e^{2b-p}). \tag{1}$$

Since the function $\cos^{-1} x$ is multiple valued, η is a multiple-valued function of p, for any given b. If (p, η) is a point on the contour of constant b, so is $(p, \pm\eta \pm 2k\pi)$, for any integral value of k. When $b > 0$, these points all fall on a single continuous contour; when $b < 0$, the contour consists of a system of isolated closed curves. In any case the complete contour has an infinite set of horizontal axes of symmetry:

$$\eta = k\pi, \qquad k = 0, \pm 1, \pm 2, \cdots. \tag{2}$$

Other symmetry properties depend upon the sign of b.

Contours for $b < 0$ have a vertical axis of symmetry. When $b < 0$,

$$1 - e^{2b} > 0, \tag{3}$$

and one can define a real constant T by

$$T = -\tfrac{1}{2} \ln (1 - e^{2b}), \tag{4a}$$

$$e^{-2T} = 1 - e^{2b}. \tag{4b}$$

In terms of the parameter T, Eq. (1) becomes

$$\eta = \cos^{-1} [e^{-T} \cosh (p + T)]. \tag{5}$$

Thus $\eta(p, b)$ is unchanged by change of sign of $p + T$; the contour is symmetric to reflection in the vertical line

$$p = -T = \tfrac{1}{2} \ln (1 - e^{2b}). \tag{6}$$

The contours of constant $b > 0$ have no vertical axis of symmetry; the above argument does not apply because T as defined by Eq. (4) is no longer real. One can, however, define a real parameter t by the relation

$$e^{-2t} = e^{2b} - 1. \tag{7}$$

In terms of the parameter t, Eq. (1) becomes

$$\eta = \cos^{-1} [e^{-t} \sinh (p + t)]. \tag{8}$$

Change in sign of $(p + t)$ changes the sign of the argument on the right; η can then be replaced by $(2k + 1)\pi - \eta$, where $k = 0, \pm 1, \pm 2, \cdots$. It follows that the contours of constant $b > 0$ have an infinite sequence of centers of symmetry at

$$\left.\begin{aligned} p_k &= -t = \tfrac{1}{2} \ln (e^{2b} - 1), \\ \eta_k &= (k + \tfrac{1}{2})\pi, \qquad k = 0, \pm 1, \pm 2, \cdots . \end{aligned}\right\} \tag{9}$$

The limiting contour, $b = 0$, has no vertical axis or center of symmetry except at infinity. Its equation is

$$\eta = \cos^{-1} (\tfrac{1}{2}e^{p}). \tag{10}$$

This curve intersects the axis $\eta = 0$ at $p = \ln 2$, and has no points for which $p > \ln 2$. It has horizontal asymptotes

$$\eta = (k + \tfrac{1}{2})\pi, \qquad k = 0 \pm 1, \pm 2, \cdots . \tag{11}$$

B·2. Contours of Constant X.—To study the contours of constant X it is necessary to eliminate b from Eq. (1) and Eq. (5·45):

$$p = \tfrac{1}{2} \ln (2 \cos X + 2 \cosh b) + \tfrac{1}{2}\mathrm{b}. \tag{12}$$

These equations may be rewritten in an interesting and symmetrical form:

$$2 \cos \eta = e^{p} + e^{-p}(1 - e^{2b}), \tag{13}$$

$$-2 \cos X = e^{b} + e^{-b}(1 - e^{2p}). \tag{14}$$

Substitution into Eq. (14) of e^b, as given by Eq. (13), leads to the relation

$$\cos X = \frac{e^{p} \cos \eta - 1}{(1 + e^{2p} - 2e^{p} \cos \eta)^{1/2}}. \tag{15}$$

An equivalent but simpler relation,

$$\cot X = \frac{\cos \eta - e^{-p}}{\sin \eta}, \qquad (\sin \eta \sin X > 0) \tag{16}$$

follows from this by trigonometric rearrangement.

For the analysis at hand it is convenient to rewrite Eq. (16) as

$$\sin X \cos \eta - \sin \eta \cos X = \sin Xe^{-p}, \tag{17}$$

or

$$\sin (X - \eta) = \sin Xe^{-p}, \qquad (\sin \eta \sin X > 0). \tag{18}$$

As noted, only that portion of this curve is to be considered for which $\sin \eta$ has the same sign as $\sin X$.

Let $0 < X_0 < 180°$. The contour for which $X = X_0$ must lie only in the region for which $\sin \eta$, like $\sin X_0$, is positive. This contour is then

$$\sin (X_0 - \eta) = \sin X_0 e^{-p}, \qquad (\sin \eta > 0). \tag{19}$$

On the other hand, the contour $X = X_0 - 180°$ must lie only in the region for which $\sin \eta$, like $\sin (X_0 - 180°)$, is negative; it is the contour

$$\sin (X_0 - 180° - \eta) = \sin (X_0 - 180°) e^{-p}, \qquad \sin \eta < 0 \tag{20a}$$

or

$$\sin (X_0 - \eta) = \sin X_0 e^{-p}, \qquad (\sin \eta < 0). \tag{20b}$$

These two contours join smoothly at the origin, forming a continuous curve which approaches the horizontal asymptotes $\eta = X_0$ and

$$\eta = X_0 - 180°$$

as $p \to \infty$.

Since $\sin X_0 > 0$, we may write the complete curve for any X_0 as

$$\sin (X_0 - \eta) = e^{-(p - \ln \sin X_0)}. \tag{21}$$

This is the curve

$$\cos \eta = e^{-p}, \tag{22}$$

translated upward by

$$\Delta\eta = X_0 - 90°, \tag{23}$$

and to the left by

$$\Delta p = -\ln \sin X_0. \tag{24}$$

Thus, all of the curves defined by Eq. (21) have the same form, whatever the value of X_0. Equation (22) gives directly the form of the curve for $X_0 = 90°$, consisting of the contours $X = 90°$ and $X = -90°$.

It will be noted that Eq. (22) differs from Eq. (10) only by a reflection in a vertical line and a translation parallel to the p-axis. It follows that the two contours $X = X_0$ and $X = X_0 - 180°$ form (for any $0 < X_0 < 180°$) a curve of the same form as the contour $b = 0$ reflected in a vertical line.

B·3. Explanation of Table B·1.—Table B·1 gives the coordinates in the (p, η)-plane of the intersection of the contours of constant b and the contours of constant X, for

$$X = 0°, 5°, 10°, \cdots, \quad 180°,$$
$$\mu b = -0.50, -0.49, \cdots, \quad 0.49, 0.50.$$

Reading the coordinate pairs from associated vertical columns, one can plot any contour of constant b; reading them from a single row, one can plot any contour of constant X.

TABLE B·1.—COORDINATES OF POINTS ON THE THREE-BAR-LINKAGE NOMOGRAM

$\mu b =$	−0.50		−0.49		−0.48		−0.47		−0.46		−0.45	
X, degrees	$\mu p + 10$	η, degrees	$\mu p + 10$	η, degrees	$\mu p + 10$	η, degrees	$\mu p + 10$	η, degrees	$\mu p + 10$	η, degrees	$\mu p + 10$	η, degrees
0	10.1193	0.00	10.1218	0.00	10.1242	0.00	10.1267	0.00	10.1293	0.00	10.1319	0.00
5	10.1190	1.20	10.1215	1.22	10.1239	1.24	10.1264	1.26	10.1290	1.29	10.1316	1.31
10	10.1181	2.40	10.1206	2.44	10.1230	2.48	10.1245	2.53	10.1280	2.57	10.1306	2.61
15	10.1167	3.59	10.1191	3.65	10.1215	3.72	10.1239	3.78	10.1264	3.85	10.1290	3.91
20	10.1145	4.77	10.1169	4.85	10.1193	4.94	10.1217	5.02	10.1242	5.11	10.1268	5.20
25	10.1118	5.93	10.1141	6.04	10.1165	6.14	10.1189	6.25	10.1214	6.36	10.1239	6.47
30	10.1084	7.08	10.1107	7.20	10.1131	7.33	10.1155	7.46	10.1179	7.59	10.1203	7.73
35	10.1045	8.20	10.1067	8.35	10.1091	8.50	10.1114	8.65	10.1138	8.80	10.1161	8.96
40	10.1000	9.29	10.1021	9.46	10.1044	9.64	10.1067	9.81	10.1090	9.99	10.1113	10.17
45	10.0948	10.36	10.0969	10.55	10.0991	10.74	10.1013	10.94	10.1035	11.14	10.1058	11.34
50	10.0890	11.38	10.0910	11.60	10.0931	11.81	10.0953	12.03	10.0974	12.25	10.0996	12.48
55	10.0826	12.37	10.0845	12.60	10.0865	12.84	10.0886	13.08	10.0907	13.33	10.0928	13.58
60	10.0756	13.30	10.0774	13.56	10.0793	13.82	10.0812	14.09	10.0833	14.35	10.0852	14.63
65	10.0680	14.19	10.0697	14.47	10.0714	14.75	10.0732	15.04	10.0752	15.33	10.0770	15.62
70	10.0597	15.01	10.0613	15.31	10.0629	15.62	10.0646	15.93	10.0664	16.24	10.0681	16.56
75	10.0508	15.77	10.0523	16.09	10.0538	16.42	10.0553	16.75	10.0569	17.08	10.0585	17.43
80	10.0413	16.45	10.0427	16.79	10.0440	17.14	10.0454	17.49	10.0468	17.85	10.0483	18.22
85	10.0313	17.04	10.0324	17.41	10.0336	17.78	10.0348	18.15	10.0360	18.54	10.0373	18.93
90	10.0207	17.55	10.0216	17.93	10.0226	18.32	10.0236	18.72	10.0246	19.12	10.0257	19.54
95	10.0095	17.95	10.0102	18.35	10.0110	18.76	10.0118	19.18	10.0126	19.60	10.0134	20.04
100	9.9978	18.24	9.9983	18.66	9.9988	19.09	9.9994	19.52	10.0000	19.97	10.0005	20.42
105	9.9857	18.40	9.9859	18.84	9.9861	19.29	9.9864	19.74	9.9868	20.20	9.9870	20.68
110	9.9732	18.43	9.9731	18.88	9.9730	19.34	9.9730	19.81	9.9730	20.29	9.9730	20.78
115	9.9603	18.30	9.9599	18.76	9.9595	19.24	9.9591	19.72	9.9588	20.21	9.9586	20.72
120	9.9471	18.02	9.9463	18.49	9.9456	18.97	9.9449	19.46	9.9442	19.96	9.9435	20.48
125	9.9338	17.56	9.9327	18.03	9.9316	18.51	9.9305	19.01	9.9294	19.52	9.9283	20.05
130	9.9206	16.91	9.9191	17.38	9.9176	17.86	9.9160	18.36	9.9145	18.87	9.9130	19.40
135	9.9074	16.07	9.9055	16.53	9.9036	17.00	9.9016	17.49	9.8997	17.99	9.8976	18.52
140	9.8946	15.02	9.8923	15.46	9.8899	15.92	9.8875	16.39	9.8851	16.88	9.8826	17.39
145	9.8824	13.75	9.8797	14.17	9.8768	14.61	9.8740	15.06	9.8711	15.52	9.8680	16.01
150	9.8711	12.28	9.8679	12.67	9.8646	13.07	9.8613	13.48	9.8579	13.92	9.8543	14.37
155	9.8609	10.61	9.8572	10.95	9.8535	11.31	9.8498	11.68	9.8459	12.06	9.8418	12.46
160	9.8520	8.75	9.8480	9.04	9.8438	9.34	9.8397	9.65	9.8354	9.98	9.8309	10.32
165	9.8447	6.72	9.8404	6.95	9.8360	7.18	9.8315	7.43	9.8269	7.68	9.8219	7.95
170	9.8394	4.56	9.8348	4.71	9.8302	4.88	9.8254	5.05	9.8206	5.22	9.8152	5.41
175	9.8360	2.30	9.8314	2.38	9.8266	2.47	9.8218	2.55	9.8166	2.64	9.8110	2.74
180	9.8349	0.00	9.8302	0.00	9.8253	0.00	9.8203	0.00	9.8151	0.00	9.8097	0.00

TABLE B·1.—COORDINATES OF POINTS ON THE THREE-BAR-LINKAGE NOMOGRAM — (*Cont.*)

μb =	−0.44		−0.43		−0.42		−0.41		−0.40		−0.39	
X, degrees	$\mu p + 10$	η, degrees	$\mu p + 10$	η, degrees	$\mu p + 10$	η, degrees	$\mu p + 10$	η, degrees	$\mu p + 10$	η, degrees	$\mu p + 10$	η, degrees
0	10.1345	0.00	10.1372	0.00	10.1399	0.00	10.1427	0.00	10.1455	0.00	10.1484	0.00
5	10.1342	1.33	10.1369	1.35	10.1396	1.38	10.1424	1.40	10.1452	1.42	10.1481	1.45
10	10.1332	2.66	10.1359	2.70	10.1386	2.75	10.1414	2.80	10.1442	2.84	10.1471	2.89
15	10.1316	3.98	10.1343	4.05	10.1370	4.12	10.1397	4.19	10.1425	4.26	10.1454	4.33
20	10.1294	5.29	10.1320	5.38	10.1347	5.47	10.1374	5.57	10.1401	5.66	10.1430	5.75
25	10.1264	6.59	10.1290	6.70	10.1317	6.81	10.1344	6.93	10.1371	7.05	10.1399	7.17
30	10.1228	7.86	10.1254	8.00	10.1280	8.14	10.1307	8.28	10.1334	8.42	10.1361	8.56
35	10.1186	9.12	10.1211	9.28	10.1237	9.44	10.1263	9.60	10.1290	9.77	10.1316	9.94
40	10.1137	10.35	10.1162	10.53	10.1187	10.72	10.1212	10.90	10.1238	11.09	10.1264	11.29
45	10.1081	11.55	10.1105	11.75	10.1130	11.96	10.1154	12.17	10.1180	12.39	10.1205	12.61
50	10.1019	12.71	10.1042	12.94	10.1066	13.17	10.1090	13.41	10.1115	13.65	10.1139	13.89
55	10.0949	13.83	10.0972	14.08	10.0994	14.34	10.1018	14.60	10.1042	14.87	10.1065	15.14
60	10.0873	14.90	10.0894	15.18	10.0916	15.46	10.0939	15.75	10.0961	16.04	10.0984	16.34
65	10.0791	15.92	10.0810	16.23	10.0831	16.53	10.0852	16.85	10.0873	17.16	10.0895	17.48
70	10.0701	16.88	10.0719	17.21	10.0738	17.54	10.0758	17.88	10.0778	18.22	10.0800	18.57
75	10.0603	17.77	10.0620	18.13	10.0638	18.53	10.0656	18.85	10.0675	19.22	10.0695	19.59
80	10.0499	18.59	10.0514	18.97	10.0531	19.35	10.0547	19.74	10.0564	20.14	10.0583	20.54
85	10.0387	19.32	10.0401	19.72	10.0416	20.13	10.0430	20.55	10.0446	20.97	10.0463	21.40
90	10.0269	19.95	10.0281	20.38	10.0293	20.82	10.0306	21.26	10.0320	21.71	10.0334	22.16
95	10.0144	20.48	10.0154	20.93	10.0162	21.39	10.0174	21.86	10.0185	22.34	10.0197	22.82
100	10.0012	20.89	10.0020	21.36	10.0027	21.84	10.0035	22.34	10.0043	22.84	10.0053	23.35
105	9.9874	21.16	9.9879	21.66	9.9884	22.16	9.9888	22.68	9.9894	23.21	9.9900	23.74
110	9.9731	21.28	9.9732	21.80	9.9734	22.33	9.9735	22.87	9.9738	23.42	9.9740	23.98
115	9.9582	21.24	9.9580	21.77	9.9578	22.32	9.9576	22.88	9.9575	23.45	9.9573	24.04
120	9.9429	21.02	9.9423	21.56	9.9417	22.12	9.9411	22.70	9.9405	23.29	9.9400	23.90
125	9.9273	20.59	9.9263	21.15	9.9252	21.72	9.9241	22.31	9.9231	22.91	9.9222	23.53
130	9.9115	19.94	9.9100	20.50	9.9084	21.08	9.9069	21.67	9.9054	22.29	9.9039	22.92
135	9.8956	19.06	9.8936	19.61	9.8915	20.19	9.8895	20.78	9.8875	21.39	9.8854	22.03
140	9.8801	17.92	9.8775	18.46	9.8749	19.02	9.8723	19.61	9.8697	20.21	9.8670	20.84
145	9.8650	16.51	9.8619	17.03	9.8588	17.57	9.8555	18.14	9.8522	18.72	9.8489	19.32
150	9.8508	14.83	9.8471	15.32	9.8435	15.82	9.8395	16.35	9.8356	16.90	9.8316	17.47
155	9.8378	12.88	9.8335	13.32	9.8293	13.77	9.8247	14.25	9.8202	14.75	9.8155	15.27
160	9.8263	10.67	9.8215	11.05	9.8165	11.44	9.8117	11.85	9.8066	12.27	9.8012	12.72
165	9.8169	8.24	9.8118	8.53	9.8064	8.84	9.8009	9.16	9.7953	9.50	9.7894	9.86
170	9.8100	5.60	9.8045	5.81	9.7990	6.02	9.7928	6.25	9.7867	6.49	9.7802	6.74
175	9.8056	2.84	9.8000	2.94	9.7943	3.05	9.7877	3.17	9.7814	3.29	9.7747	3.42
180	9.8041	0.00	9.7983	0.00	9.7923	0.00	9.7860	0.00	9.7795	0.00	9.7728	0.00

TABLE B·1.—COORDINATES OF POINTS ON THE THREE-BAR-LINKAGE NOMOGRAM — (*Cont.*)

$\mu b =$	−0.38		−0.37		−0.36		−0.35		−0.34		−0.33	
X, degrees	$\mu p + 10$	η, degrees	$\mu p + 10$	η, degrees	$\mu p + 10$	η, degrees	$\mu p + 10$	η, degrees	$\mu p + 10$	η, degrees	$\mu p + 10$	η, degrees
0	10.1513	0.00	10.1543	0.00	10.1573	0.00	10.1604	0.00	10.1635	0.00	10.1667	0.00
5	10.1509	1.47	10.1540	1.49	10.1570	1.52	10.1601	1.54	10.1631	1.57	10.1662	1.59
10	10.1499	2.94	10.1529	2.99	10.1559	3.03	10.1590	3.08	10.1621	3.13	10.1652	3.18
15	10.1482	4.40	10.1511	4.47	10.1541	4.54	10.1572	4.62	10.1603	4.69	10.1634	4.77
20	10.1458	5.85	10.1486	5.95	10.1517	6.04	10.1547	6.14	10.1578	6.24	10.1609	6.34
25	10.1427	7.29	10.1455	7.41	10.1485	7.53	10.1515	7.65	10.1546	7.78	10.1577	7.90
30	10.1389	8.71	10.1417	8.85	10.1446	9.00	10.1476	9.15	10.1506	9.30	10.1537	9.45
35	10.1344	10.11	10.1371	10.28	10.1400	10.45	10.1429	10.62	10.1459	10.80	10.1489	10.98
40	10.1292	11.48	10.1318	11.68	10.1347	11.87	10.1375	12.07	10.1405	12.28	10.1434	12.48
45	10.1232	12.83	10.1258	13.05	10.1286	13.27	10.1314	13.50	10.1343	13.73	10.1371	13.96
50	10.1165	14.14	10.1191	14.38	10.1217	14.63	10.1245	14.89	10.1273	15.14	10.1301	15.40
55	10.1090	15.41	10.1116	15.68	10.1141	15.96	10.1168	16.24	10.1194	16.52	10.1222	16.81
60	10.1008	16.63	10.1032	16.93	10.1057	17.24	10.1082	17.55	10.1108	17.86	10.1135	18.17
65	10.0918	17.81	10.0941	18.14	10.0965	18.47	10.0989	18.81	10.1014	19.15	10.1040	19.49
70	10.0820	18.92	10.0842	19.28	10.0865	19.64	10.0888	20.01	10.0912	20.38	10.0936	20.75
75	10.0714	19.97	10.0734	20.36	10.0756	20.75	10.0778	21.14	10.0800	21.54	10.0823	21.95
80	10.0600	20.95	10.0620	21.36	10.0639	21.78	10.0659	22.21	10.0680	22.64	10.0701	23.08
85	10.0478	21.84	10.0495	22.28	10.0513	22.73	10.0531	23.19	10.0550	23.65	10.0570	24.12
90	10.0348	22.63	10.0363	23.10	10.0379	23.58	10.0395	24.07	10.0412	24.56	10.0429	25.07
95	10.0209	23.31	10.0222	23.82	10.0235	24.33	10.0249	24.84	10.0264	25.37	10.0279	25.91
100	10.0062	23.87	10.0072	24.40	10.0083	24.94	10.0094	25.50	10.0106	26.06	10.0119	26.63
105	9.9907	24.29	9.9914	24.85	9.9922	25.42	9.9930	26.01	9.9939	26.60	9.9949	27.20
110	9.9744	24.55	9.9748	25.14	9.9752	25.74	9.9757	26.35	9.9763	26.98	9.9769	27.62
115	9.9573	24.64	9.9573	25.25	9.9574	25.88	9.9575	26.52	9.9576	27.18	9.9578	27.85
120	9.9395	24.52	9.9391	25.15	9.9387	25.81	9.9384	26.48	9.9380	27.16	9.9378	27.87
125	9.9212	24.17	9.9202	24.83	9.9194	25.50	9.9186	26.19	9.9177	26.91	9.9170	27.64
130	9.9024	23.57	9.9009	24.24	9.8995	24.93	9.8981	25.64	9.8967	26.37	9.8953	27.13
135	9.8834	22.68	9.8813	23.36	9.8792	24.06	9.8771	24.78	9.8751	25.53	9.8730	26.30
140	9.8642	21.49	9.8615	22.16	9.8588	22.86	9.8560	23.58	9.8532	24.33	9.8505	25.10
145	9.8454	19.96	9.8421	20.61	9.8386	21.29	9.8350	22.00	9.8314	22.74	9.8279	23.50
150	9.8274	18.07	9.8233	18.69	9.8190	19.34	9.8147	20.01	9.8102	20.72	9.8057	21.46
155	9.8107	15.81	9.8057	16.38	9.8007	16.97	9.7955	17.60	9.7902	18.25	9.7847	18.94
160	9.7958	13.19	9.7899	13.69	9.7842	14.20	9.7781	14.75	9.7719	15.33	9.7655	15.93
165	9.7831	10.24	9.7768	10.64	9.7703	11.05	9.7637	11.49	9.7566	11.96	9.7493	12.45
170	9.7737	7.00	9.7669	7.28	9.7598	7.57	9.7526	7.88	9.7450	8.21	9.7370	8.56
175	9.7678	3.56	9.7606	3.70	9.7532	3.85	9.7455	4.01	9.7375	4.18	9.7285	4.37
180	9.7658	0.00	9.7585	0.00	9.7509	0.00	9.7430	0.00	9.7347	0.00	9.7261	0.00

TABLE B·1.—COORDINATES OF POINTS ON THE THREE-BAR-LINKAGE NOMOGRAM — (*Cont.*)

μb =	−0.32		−0.31		−0.30		−0.29		−0.28		−0.27	
X, degrees	$\mu p + 10$	η, degrees	$\mu p + 10$	η, degrees	$\mu p + 10$	η, degrees	$\mu p + 10$	η, degrees	$\mu p + 10$	η, degrees	$\mu p + 10$	η, degrees
0	10.1699	0.00	10.1731	0.00	10.1764	0.00	10.1798	0.00	10.1832	0.00	10.1867	0.00
5	10.1695	1.62	10.1728	1.64	10.1760	1.67	10.1795	1.69	10.1829	1.72	10.1863	1.75
10	10.1684	3.23	10.1716	3.28	10.1749	3.34	10.1784	3.39	10.1818	3.44	10.1852	3.49
15	10.1666	4.84	10.1698	4.92	10.1731	5.00	10.1764	5.07	10.1799	5.15	10.1833	5.23
20	10.1641	6.44	10.1673	6.54	10.1705	6.65	10.1738	6.75	10.1772	6.85	10.1806	6.96
25	10.1608	8.03	10.1640	8.16	10.1672	8.29	10.1705	8.42	10.1738	8.55	10.1772	8.68
30	10.1568	9.60	10.1599	9.76	10.1632	9.91	10.1664	10.07	10.1697	10.23	10.1730	10.39
35	10.1520	11.16	10.1551	11.34	10.1582	11.52	10.1615	11.70	10.1647	11.89	10.1680	12.07
40	10.1464	12.69	10.1495	12.89	10.1526	13.10	10.1557	13.32	10.1590	13.53	10.1623	13.74
45	10.1401	14.19	10.1431	14.43	10.1462	14.66	10.1493	14.90	10.1525	15.14	10.1557	15.39
50	10.1330	15.66	10.1359	15.93	10.1389	16.19	10.1420	16.46	10.1451	16.73	10.1482	17.01
55	10.1250	17.10	10.1279	17.39	10.1308	17.69	10.1338	17.98	10.1368	18.28	10.1399	18.59
60	10.1162	18.49	10.1190	18.82	10.1218	19.14	10.1247	19.47	10.1277	19.80	10.1307	20.13
65	10.1066	19.84	10.1093	20.19	10.1120	20.55	10.1148	20.91	10.1177	21.27	10.1206	21.64
70	10.0961	21.13	10.0987	21.51	10.1013	21.90	10.1039	22.29	10.1067	22.69	10.1095	23.09
75	10.0847	22.36	10.0871	22.78	10.0896	23.20	10.0921	23.62	10.0947	24.05	10.0975	24.49
80	10.0723	23.52	10.0746	23.97	10.0769	24.42	10.0794	24.88	10.0818	25.35	10.0844	25.82
85	10.0590	24.59	10.0611	25.08	10.0633	25.57	10.0656	26.06	10.0678	26.56	10.0703	27.07
90	10.0447	25.58	10.0468	26.09	10.0487	26.62	10.0507	27.15	10.0528	27.69	10.0550	28.24
95	10.0295	26.45	10.0312	27.01	10.0329	27.57	10.0347	28.14	10.0366	28.72	10.0386	29.30
100	10.0132	27.21	10.0147	27.80	10.0161	28.40	10.0177	29.01	10.0193	29.62	10.0211	30.25
105	9.9959	27.82	9.9970	28.45	9.9982	29.09	9.9995	29.74	10.0008	30.40	10.0023	31.07
110	9.9775	28.27	9.9783	28.94	9.9792	29.61	9.9801	30.30	9.9811	31.01	9.9822	31.72
115	9.9581	28.54	9.9585	29.24	9.9589	29.95	9.9594	30.69	9.9600	31.43	9.9607	32.20
120	9.9376	28.59	9.9376	29.32	9.9375	30.08	9.9376	30.85	9.9377	31.64	9.9379	32.45
125	9.9163	28.39	9.9157	29.16	9.9151	29.95	9.9146	30.76	9.9142	31.59	9.9138	32.45
130	9.8941	27.90	9.8929	28.70	9.8916	29.53	9.8905	30.37	9.8894	31.24	9.8884	32.14
135	9.8711	27.09	9.8691	27.91	9.8672	28.76	9.8653	29.64	9.8635	30.54	9.8617	31.48
140	9.8477	25.91	9.8449	26.74	9.8421	27.61	9.8394	28.50	9.8367	29.43	9.8341	30.39
145	9.8242	24.30	9.8205	25.13	9.8168	26.00	9.8131	26.90	9.8094	27.83	9.8057	28.81
150	9.8011	22.23	9.7964	23.04	9.7917	23.88	9.7869	24.77	9.7820	25.69	9.7771	26.66
155	9.7791	19.66	9.7734	20.42	9.7675	21.21	9.7615	22.05	9.7553	22.93	9.7492	23.85
160	9.7589	16.57	9.7522	17.24	9.7452	17.95	9.7379	18.71	9.7305	19.50	9.7230	20.34
165	9.7418	12.97	9.7339	13.53	9.7260	14.11	9.7175	14.74	9.7088	15.40	9.6998	16.11
170	9.7286	8.93	9.7198	9.33	9.7109	9.75	9.7015	10.20	9.6917	10.68	9.6817	11.19
175	9.7200	4.56	9.7113	4.76	9.7010	4.99	9.6913	5.22	9.6804	5.48	9.6696	5.75
180	9.7172	0.00	9.7078	0.00	9.6979	0.00	9.6877	0.00	9.6769	0.00	9.6656	0.00

TABLE B·1.—COORDINATES OF POINTS ON THE THREE-BAR-LINKAGE NOMOGRAM — (*Cont.*)

μb =	−0.26		−0.25		−0.24		−0.23		−0.22		−0.21	
X, degrees	$\mu p + 10$	η, degrees	$\mu p + 10$	η, degrees	$\mu p + 10$	η, degrees	$\mu p + 10$	η, degrees	$\mu p + 10$	η, degrees	$\mu p + 10$	η, degrees
0	10.1902	0.00	10.1938	0.00	10.1974	0.00	10.2011	0.00	10.2048	0.00	10.2086	0.00
5	10.1898	1.77	10.1935	1.80	10.1970	1.83	10.2006	1.85	10.2045	1.88	10.2082	1.91
10	10.1886	3.54	10.1923	3.60	10.1959	3.65	10.1995	3.70	10.2033	3.76	10.2071	3.81
15	10.1868	5.31	10.1903	5.39	10.1940	5.47	10.1976	5.55	10.2013	5.63	10.2051	5.71
20	10.1841	7.07	10.1876	7.17	10.1912	7.28	10.1949	7.39	10.1985	7.50	10.2023	7.61
25	10.1807	8.81	10.1842	8.95	10.1878	9.08	10.1914	9.22	10.1951	9.35	10.1988	9.49
30	10.1765	10.55	10.1800	10.71	10.1835	10.87	10.1871	11.03	10.1908	11.20	10.1944	11.36
35	10.1715	12.26	10.1749	12.45	10.1784	12.64	10.1819	12.84	10.1856	13.03	10.1892	13.22
40	10.1656	13.96	10.1690	14.18	10.1725	14.40	10.1760	14.62	10.1796	14.84	10.1832	15.07
45	10.1590	15.63	10.1623	15.88	10.1657	16.13	10.1692	16.38	10.1728	16.63	10.1763	16.89
50	10.1515	17.28	10.1547	17.56	10.1581	17.84	10.1615	18.12	10.1650	18.40	10.1686	18.69
55	10.1430	18.89	10.1463	19.20	10.1496	19.51	10.1529	19.83	10.1563	20.14	10.1598	20.46
60	10.1338	20.47	10.1370	20.81	10.1401	21.16	10.1434	21.50	10.1467	21.85	10.1502	22.20
65	10.1236	22.01	10.1267	22.38	10.1298	22.76	10.1329	23.14	10.1362	23.52	10.1396	23.91
70	10.1124	23.49	10.1154	23.90	10.1184	24.31	10.1215	24.73	10.1246	25.15	10.1279	25.57
75	10.1002	24.93	10.1031	25.37	10.1060	25.82	10.1091	26.26	10.1120	26.73	10.1151	27.19
80	10.0870	26.29	10.0897	26.77	10.0925	27.26	10.0954	27.75	10.0983	28.24	10.1013	28.74
85	10.0727	27.58	10.0753	28.10	10.0779	28.63	10.0806	29.16	10.0834	29.70	10.0862	30.24
90	10.0573	28.79	10.0597	29.35	10.0621	29.92	10.0646	30.49	10.0673	31.07	10.0700	31.66
95	10.0407	29.90	10.0428	30.50	10.0451	31.11	10.0474	31.73	10.0498	32.36	10.0524	32.99
100	10.0229	30.89	10.0248	31.54	10.0268	32.19	10.0289	32.86	10.0311	33.53	10.0334	34.22
105	10.0037	31.75	10.0054	32.44	10.0071	33.15	10.0089	33.86	10.0108	34.59	10.0128	35.31
110	9.9833	32.45	9.9846	33.20	9.9860	33.95	9.9875	34.72	9.9891	35.50	9.9908	36.29
115	9.9615	32.97	9.9624	33.76	9.9634	34.57	9.9645	35.39	9.9657	36.23	9.9670	37.08
120	9.9383	33.27	9.9386	34.12	9.9392	34.98	9.9398	35.86	9.9406	36.75	9.9414	37.67
125	9.9136	33.32	9.9135	34.21	9.9134	35.13	9.9135	36.07	9.9137	37.03	9.9140	38.01
130	9.8875	33.06	9.8867	34.00	9.8859	34.98	9.8854	35.97	9.8849	36.99	9.8846	38.04
135	9.8600	32.44	9.8584	33.43	9.8569	34.45	9.8555	35.51	9.8542	36.59	9.8530	37.71
140	9.8314	31.39	9.8288	32.42	9.8264	33.48	9.8240	34.59	9.8217	35.73	9.8195	36.91
145	9.8020	29.82	9.7983	30.88	9.7946	31.98	9.7911	33.12	9.7876	34.31	9.7841	35.55
150	9.7722	27.67	9.7671	28.73	9.7622	29.84	9.7571	31.00	9.7523	32.21	9.7472	33.49
155	9.7428	24.83	9.7364	25.86	9.7298	26.94	9.7231	28.09	9.7165	29.29	9.7096	30.57
160	9.7150	21.24	9.7069	22.19	9.6986	23.20	9.6901	24.27	9.6815	25.41	9.6725	26.63
165	9.6906	16.86	9.6808	17.67	9.6707	18.54	9.6603	19.46	9.6495	20.46	9.6383	21.53
170	9.6708	11.75	9.6599	12.34	9.6480	12.99	9.6359	13.68	9.6231	14.43	9.6097	15.25
175	9.6582	6.04	9.6459	6.36	9.6333	6.70	9.6197	7.08	9.6052	7.49	9.5905	7.93
180	9.6537	0.00	9.6411	0.00	9.6279	0.00	9.6140	0.00	9.5993	0.00	9.5837	0.00

TABLE B·1.—COORDINATES OF POINTS ON THE THREE-BAR-LINKAGE NOMOGRAM — (*Cont.*)

μb =	−0.20		−0.19		−0.18		−0.17		−0.16		−0.15	
X, degrees	$\mu p + 10$	η, degrees	$\mu p + 10$	η, degrees	$\mu p + 10$	η, degrees	$\mu p + 10$	η, degrees	$\mu p + 10$	η, degrees	$\mu p + 10$	η, degrees
0	10.2124	0.00	10.2163	0.00	10.2203	0.00	10.2243	0.00	10.2284	0.00	10.2325	0.00
5	10.2121	1.93	10.2160	1.96	10.2199	1.99	10.2238	2.02	10.2280	2.04	10.2320	2.07
10	10.2109	3.87	10.2147	3.92	10.2189	3.98	10.2227	4.03	10.2268	4.09	10.2309	4.14
15	10.2089	5.79	10.2128	5.88	10.2167	5.96	10.2207	6.04	10.2247	6.13	10.2288	6.21
20	10.2061	7.72	10.2099	7.83	10.2139	7.94	10.2179	8.05	10.2219	8.16	10.2260	8.27
25	10.2026	9.63	10.2065	9.77	10.2103	9.91	10.2143	10.05	10.2183	10.19	10.2224	10.33
30	10.1982	11.53	10.2021	11.70	10.2059	11.87	10.2098	12.04	10.2139	12.21	10.2179	12.38
35	10.1930	13.42	10.1968	13.62	10.2006	13.81	10.2045	14.01	10.2085	14.21	10.2126	14.41
40	10.1869	15.29	10.1907	15.52	10.1945	15.75	10.1984	15.98	10.2023	16.21	10.2064	16.44
45	10.1800	17.15	10.1838	17.41	10.1875	17.66	10.1914	17.92	10.1952	18.19	10.1992	18.45
50	10.1722	18.98	10.1759	19.27	10.1796	19.56	10.1834	19.85	10.1872	20.15	10.1912	20.44
55	10.1634	20.78	10.1670	21.11	10.1707	21.43	10.1744	21.76	10.1783	22.08	10.1821	22.41
60	10.1536	22.56	10.1572	22.91	10.1609	23.27	10.1645	23.63	10.1684	24.00	10.1721	24.36
65	10.1429	24.30	10.1464	24.69	10.1501	25.09	10.1536	25.48	10.1574	25.88	10.1611	26.28
70	10.1312	26.00	10.1346	26.43	10.1381	26.86	10.1416	27.29	10.1453	27.73	10.1490	28.17
75	10.1184	27.65	10.1216	28.12	10.1250	28.59	10.1285	29.07	10.1320	29.54	10.1357	30.02
80	10.1044	29.25	10.1075	29.76	10.1109	30.27	10.1142	30.79	10.1177	31.31	10.1212	31.84
85	10.0892	30.79	10.0922	31.34	10.0954	31.90	10.0986	32.46	10.1020	33.02	10.1054	33.59
90	10.0728	32.25	10.0756	32.85	10.0786	33.45	10.0817	34.06	10.0849	34.68	10.0882	35.30
95	10.0549	33.64	10.0576	34.28	10.0605	34.93	10.0634	35.59	10.0665	36.26	10.0696	36.93
100	10.0358	34.91	10.0382	35.61	10.0409	36.32	10.0436	37.03	10.0465	37.75	10.0494	38.48
105	10.0150	36.07	10.0172	36.82	10.0196	37.59	10.0221	38.36	10.0247	39.15	10.0274	39.94
110	9.9926	37.09	9.9945	37.91	9.9966	38.73	9.9988	39.57	10.0012	40.42	10.0036	41.28
115	9.9684	37.95	9.9700	38.83	9.9718	39.72	9.9736	40.62	9.9757	41.54	9.9778	42.47
120	9.9424	38.60	9.9436	39.55	9.9449	40.51	9.9463	41.49	9.9479	42.49	9.9497	43.50
125	9.9144	39.01	9.9151	40.03	9.9158	41.07	9.9168	42.13	9.9178	43.22	9.9191	44.32
130	9.8843	39.12	9.8843	40.21	9.8844	41.34	9.8847	42.49	9.8851	43.67	9.8859	44.86
135	9.8520	38.85	9.8512	40.03	9.8505	41.24	9.8499	42.49	9.8496	43.76	9.8495	45.07
140	9.8175	38.13	9.8156	39.39	9.8139	40.68	9.8123	42.03	9.8110	43.41	9.8098	44.84
145	9.7808	36.84	9.7776	38.17	9.7746	39.56	9.7717	40.99	9.7691	42.48	9.7666	44.03
150	9.7424	34.82	9.7375	36.22	9.7329	37.67	9.7283	39.20	9.7239	40.79	9.7197	42.46
155	9.7028	31.92	9.6960	33.34	9.6892	34.84	9.6824	36.42	9.6758	38.09	9.6692	39.86
160	9.6634	27.93	9.6542	29.31	9.6448	30.79	9.6352	32.38	9.6257	34.07	9.6160	35.88
165	9.6267	22.69	9.6147	23.94	9.6022	25.30	9.5896	26.76	9.5763	28.36	9.5629	30.09
170	9.5957	16.14	9.5810	17.11	9.5656	18.18	9.5492	19.36	9.5322	20.66	9.5143	22.10
175	9.5746	8.42	9.5579	8.96	9.5400	9.56	9.5208	10.23	9.5005	10.98	9.4789	11.82
180	9.5671	0.00	9.5494	0.00	9.5306	0.00	9.5104	0.00	9.4888	0.00	9.4655	0.00

TABLE B·1.—COORDINATES OF POINTS ON THE THREE-BAR-LINKAGE NOMOGRAM — (*Cont.*)

μb =	−0.14		−0.13		−0.12		−0.11		−0.10		−0.09	
X, degrees	$\mu p + 10$	η, degrees	$\mu p + 10$	η, degrees	$\mu p + 10$	η, degrees	$\mu p + 10$	η, degrees	$\mu p + 10$	η, degrees	$\mu p + 10$	η, degrees
0	10.2367	0.00	10.2409	0.00	10.2452	0.00	10.2495	0.00	10.2539	0.00	10.2584	0.00
5	10.2363	2.10	10.2405	2.13	10.2447	2.16	10.2491	2.19	10.2535	2.21	10.2580	2.24
10	10.2350	4.20	10.2393	4.26	10.2435	4.31	10.2479	4.37	10.2523	4.43	10.2567	4.48
15	10.2330	6.30	10.2372	6.38	10.2415	6.47	10.2458	6.55	10.2503	6.64	10.2547	6.72
20	10.2301	8.39	10.2344	8.50	10.2386	8.61	10.2429	8.73	10.2474	8.84	10.2518	8.96
25	10.2265	10.47	10.2308	10.61	10.2350	10.76	10.2393	10.90	10.2437	11.04	10.2480	11.19
30	10.2220	12.55	10.2262	12.72	10.2305	12.89	10.2347	13.07	10.2391	13.24	10.2435	13.42
35	10.2166	14.62	10.2208	14.82	10.2250	15.02	10.2293	15.23	10.2336	15.43	10.2380	15.63
40	10.2104	16.67	10.2145	16.91	10.2187	17.14	10.2230	17.37	10.2273	17.61	10.2316	17.85
45	10.2032	18.71	10.2073	18.98	10.2115	19.25	10.2158	19.51	10.2200	19.78	10.2244	20.05
50	10.1951	20.74	10.1992	21.04	10.2034	21.34	10.2076	21.64	10.2118	21.94	10.2162	22.24
55	10.1861	22.75	10.1901	23.08	10.1942	23.41	10.1984	23.75	10.2026	24.09	10.2070	24.42
60	10.1761	24.73	10.1800	25.10	10.1840	25.47	10.1882	25.84	10.1924	26.21	10.1967	26.59
65	10.1650	26.69	10.1688	27.09	10.1729	27.50	10.1770	27.91	10.1811	28.32	10.1853	28.74
70	10.1528	28.62	10.1565	29.06	10.1605	29.51	10.1646	29.96	10.1687	30.41	10.1728	30.87
75	10.1394	30.51	10.1431	31.00	10.1470	31.49	10.1510	31.98	10.1550	32.47	10.1592	32.97
80	10.1248	32.36	10.1285	32.89	10.1323	33.43	10.1362	33.97	10.1402	34.51	10.1443	35.05
85	10.1089	34.17	10.1125	34.75	10.1162	35.33	10.1200	35.92	10.1239	36.50	10.1279	37.10
90	10.0916	35.92	10.0951	36.55	10.0987	37.18	10.1024	37.81	10.1062	38.46	10.1101	39.11
95	10.0728	37.61	10.0762	38.29	10.0797	38.98	10.0832	39.67	10.0869	40.37	10.0908	41.07
100	10.0524	39.22	10.0557	39.96	10.0590	40.71	10.0624	41.46	10.0660	42.22	10.0697	42.99
105	10.0303	40.74	10.0334	41.54	10.0364	42.36	10.0397	43.18	10.0431	44.00	10.0467	44.84
110	10.0063	42.14	10.0091	43.02	10.0120	43.91	10.0150	44.80	10.0182	45.70	10.0216	46.61
115	9.9801	43.42	9.9826	44.37	9.9853	45.34	9.9880	46.32	9.9910	47.30	9.9942	48.29
120	9.9516	44.53	9.9538	45.57	9.9561	46.62	9.9586	47.69	9.9612	48.77	9.9642	49.86
125	9.9206	45.44	9.9223	46.57	9.9242	47.73	9.9263	48.90	9.9286	50.08	9.9312	51.28
130	9.8867	46.09	9.8879	47.33	9.8892	48.60	9.8908	49.88	9.8926	51.19	9.8947	52.52
135	9.8496	46.41	9.8500	47.77	9.8507	49.16	9.8516	50.59	9.8528	52.03	9.8543	53.50
140	9.8090	46.30	9.8084	47.80	9.8081	49.34	9.8082	50.91	9.8085	52.52	9.8092	54.16
145	9.7645	45.62	9.7626	47.27	9.7610	48.97	9.7598	50.72	9.7590	52.52	9.7586	54.37
150	9.7157	44.19	9.7121	46.00	9.7088	47.87	9.7059	49.82	9.7034	51.84	9.7014	53.93
155	9.6629	41.72	9.6568	43.67	9.6510	45.73	9.6457	47.89	9.6407	50.16	9.6364	52.53
160	9.6064	37.82	9.5970	39.89	9.5877	42.10	9.5787	44.46	9.5701	46.97	9.5620	49.65
165	9.5490	31.99	9.5349	34.05	9.5207	36.30	9.5064	38.76	9.4921	41.46	9.4782	44.39
170	9.4955	23.70	9.4758	25.49	9.4552	27.51	9.4336	29.78	9.4113	32.35	9.3881	35.28
175	9.4555	12.78	9.4303	13.88	9.4034	15.14	9.3739	16.62	9.3422	18.35	9.3076	20.42
180	9.4402	0.00	9.4128	0.00	9.3828	0.00	9.3498	0.00	9.3132	0.00	9.2722	0.00

TABLE B·1.—COORDINATES OF POINTS ON THE THREE-BAR-LINKAGE NOMOGRAM — (*Cont.*)

μb =	−0.08		−0.07		−0.06		−0.05		−0.04		−0.03	
X, degrees	$\mu p + 10$	η, degrees	$\mu p + 10$	η, degrees	$\mu p + 10$	η, degrees	$\mu p + 10$	η, degrees	$\mu p + 10$	η, degrees	$\mu p + 10$	η, degrees
0	10.2629	0.00	10.2674	0.00	10.2721	0.00	10.2768	0.00	10.2815	0.00	10.2863	0.00
5	10.2625	2.27	10.2670	2.30	10.2717	2.33	10.2764	2.36	10.2811	2.39	10.2860	2.41
10	10.2613	4.54	10.2658	4.60	10.2704	4.66	10.2751	4.71	10.2799	4.77	10.2846	4.83
15	10.2592	6.81	10.2637	6.89	10.2683	7.98	10.2730	7.07	10.2778	7.15	10.2825	7.24
20	10.2563	9.07	10.2608	9.19	10.2654	9.30	10.2701	9.42	10.2748	9.54	10.2797	9.65
25	10.2526	11.33	10.2571	11.48	10.2617	11.62	10.2664	11.77	10.2710	11.92	10.2760	12.06
30	10.2480	13.59	10.2525	13.77	10.2571	13.94	10.2617	14.12	10.2665	14.29	10.2713	14.47
35	10.2425	15.84	10.2470	16.05	10.2516	16.25	10.2562	16.46	10.2610	16.67	10.2657	16.87
40	10.2361	18.09	10.2407	18.32	10.2452	18.56	10.2499	18.80	10.2545	19.04	10.2593	19.28
45	10.2288	20.32	10.2333	20.59	10.2379	20.86	10.2425	21.14	10.2472	21.41	10.2520	21.68
50	10.2205	22.55	10.2250	22.85	10.2296	23.16	10.2342	23.46	10.2389	23.77	10.2437	24.08
55	10.2112	24.76	10.2158	25.10	10.2203	25.44	10.2249	25.79	10.2295	26.13	10.2343	26.47
60	10.2010	26.97	10.2055	27.34	10.2099	27.72	10.2146	28.10	10.2191	28.48	10.2239	28.86
65	10.1897	29.15	10.1941	29.57	10.1985	29.99	10.2031	30.40	10.2077	30.82	10.2124	31.24
70	10.1771	31.32	10.1815	31.78	10.1859	32.24	10.1904	32.69	10.1951	33.16	10.1998	33.61
75	10.1634	33.47	10.1677	33.97	10.1721	34.47	10.1766	34.97	10.1812	35.48	10.1859	35.98
80	10.1484	35.59	10.1527	36.14	10.1570	36.69	10.1615	37.24	10.1661	37.79	10.1708	38.34
85	10.1320	37.69	10.1362	38.29	10.1405	38.89	10.1449	39.49	10.1495	40.08	10.1541	40.69
90	10.1142	39.75	10.1183	40.40	10.1225	41.06	10.1270	41.71	10.1314	42.37	10.1360	43.02
95	10.0947	41.78	10.0988	42.49	10.1029	43.20	10.1073	43.91	10.1117	44.62	10.1163	45.34
100	10.0735	43.76	10.0775	44.53	10.0816	45.30	10.0858	46.08	10.0902	46.86	10.0948	47.64
105	10.0504	45.67	10.0542	46.52	10.0583	47.36	10.0624	48.21	10.0667	49.07	10.0712	49.92
110	10.0252	47.53	10.0289	48.45	10.0328	49.37	10.0368	50.31	10.0410	51.24	10.0454	52.18
115	9.9976	49.30	10.0011	50.31	10.0048	51.32	10.0087	52.34	10.0128	53.37	10.0172	54.40
120	9.9672	50.96	9.9706	52.07	9.9741	53.19	9.9778	54.31	9.9818	55.44	9.9860	56.58
125	9.9340	52.49	9.9370	53.72	9.9403	54.95	9.9438	56.20	9.9476	57.45	9.9517	58.71
130	9.8971	53.86	9.8998	55.22	9.9028	56.59	9.9060	57.97	9.9096	59.36	9.9135	60.77
135	9.8562	55.00	9.8583	56.51	9.8609	58.05	9.8638	59.60	9.8670	61.16	9.8706	62.74
140	9.8103	55.84	9.8119	57.54	9.8138	59.27	9.8162	61.02	9.8190	62.79	9.8223	64.58
145	9.7587	56.26	9.7593	58.19	9.7604	60.16	9.7620	62.17	9.7642	64.20	9.7670	66.25
150	9.7000	56.08	9.6992	58.29	9.6990	60.57	9.6996	62.89	9.7008	65.26	9.7029	67.66
155	9.6326	55.00	9.6297	57.56	9.6275	60.22	9.6263	62.96	9.6261	65.77	9.6269	68.65
160	9.5546	52.40	9.5481	55.48	9.5426	58.64	9.5381	62.02	9.5354	65.37	9.5341	68.92
165	9.4647	47.60	9.4520	51.08	9.4404	54.85	9.4304	58.91	9.4222	63.23	9.4164	67.81
170	9.3645	38.61	9.3408	42.41	9.3174	46.75	9.2951	51.68	9.2749	57.25	9.2581	63.46
175	9.2097	22.93	9.2285	26.00	9.1834	29.84	9.1349	34.71	9.0834	40.99	9.0315	49.16
180	9.2259	0.00	9.1728	0.00	9.1107	0.00	9.0364	0.00	8.9445	0.00	8.8244	0.00

TABLE B·1.—COORDINATES OF POINTS ON THE THREE-BAR-LINKAGE NOMOGRAM — (*Cont.*)

μb =	−0.02		−0.01		0.00		0.01		0.02	
X, degrees	$\mu p + 10$	η, degrees	$\mu p + 10$	η, degrees	$\mu p + 10$	η, degrees	$\mu p + 10$	η, degrees	$\mu p + 10$	η, degrees
0	10.2912	0.00	10.2960	0.00	10.3010	0.00	10.3060	0.00	10.3112	0.00
5	10.2908	2.44	10.2956	2.47	10.3006	2.50	10.3056	2.53	10.3108	2.56
10	10.2895	4.88	10.2944	4.94	10.2994	5.00	10.3044	5.06	10.3095	5.12
15	10.2874	7.33	10.2923	7.41	10.2973	7.50	10.3023	7.59	10.3074	7.67
20	10.2844	9.77	10.2894	9.88	10.2944	10.00	10.2994	10.12	10.3044	10.23
25	10.2808	12.21	10.2857	12.35	10.2906	12.50	10.2957	12.65	10.3008	12.79
30	10.2761	14.65	10.2810	14.82	10.2860	15.00	10.2910	15.18	10.2961	15.35
35	10.2706	17.08	10.2755	17.29	10.2805	17.50	10.2855	17.71	10.2906	17.92
40	10.2641	19.52	10.2691	19.76	10.2740	20.00	10.2791	20.24	10.2841	20.48
45	10.2568	21.95	10.2617	22.23	10.2667	22.50	10.2717	22.77	10.2768	23.05
50	10.2485	24.39	10.2533	24.69	10.2583	25.00	10.2633	25.31	10.2685	25.61
55	10.2391	26.81	10.2440	27.16	10.2490	27.50	10.2540	27.84	10.2591	28.19
60	10.2287	29.24	10.2336	29.62	10.2386	30.00	10.2436	30.38	10.2487	30.76
65	10.2172	31.66	10.2221	32.08	10.2271	32.50	10.2321	32.92	10.2372	33.34
70	10.2046	34.08	10.2094	34.54	10.2144	35.00	10.2194	35.46	10.2246	35.92
75	10.1907	36.49	10.1946	36.99	10.2005	37.50	10.2046	38.01	10.2107	38.51
80	10.1755	38.89	10.1803	39.45	10.1853	40.00	10.1903	40.55	10.1955	41.11
85	10.1589	41.29	10.1637	41.90	10.1687	42.50	10.1737	43.10	10.1789	43.71
90	10.1407	43.68	10.1456	44.34	10.1505	45.00	10.1556	45.66	10.1607	46.32
95	10.1209	46.06	10.1258	46.78	10.1307	47.50	10.1358	48.22	10.1409	48.94
100	10.0994	48.43	10.1042	49.21	10.1091	50.00	10.1142	50.79	10.1194	51.57
105	10.0758	50.78	10.0797	51.64	10.0855	52.50	10.0897	53.36	10.0958	54.22
110	10.0500	53.12	10.0547	54.06	10.0596	55.00	10.0647	55.94	10.0700	56.88
115	10.0216	55.43	10.0264	56.47	10.0313	57.50	10.0364	58.54	10.0416	59.57
120	9.9904	57.72	9.9951	58.86	10.0000	60.00	10.0051	61.14	10.0104	62.28
125	9.9560	59.97	9.9606	61.23	9.9654	62.50	9.9706	63.77	9.9760	65.03
130	9.9177	62.17	9.9221	63.59	9.9270	65.00	9.9321	66.41	9.9377	67.83
135	9.8747	64.32	9.8791	65.91	9.8839	67.50	9.8891	69.09	9.8947	70.68
140	9.8261	66.38	9.8303	68.19	9.8351	70.00	9.8403	71.81	9.8461	73.62
145	9.7705	68.33	9.7745	70.41	9.7792	72.50	9.7845	74.59	9.7905	76.67
150	9.7058	70.09	9.7095	72.54	9.7140	75.00	9.7195	77.46	9.7258	79.91
155	9.6289	71.57	9.6320	74.53	9.6364	77.50	9.6420	80.47	9.6489	83.43
160	9.5344	72.56	9.5367	76.27	9.5407	80.00	9.5467	83.73	9.5544	87.44
165	9.4134	72.58	9.4134	77.50	9.4167	82.50	9.4234	87.50	9.4334	92.42
170	9.2460	70.26	9.2401	77.51	9.2413	85.00	9.2501	92.49	9.2660	99.74
175	8.9841	59.70	8.9503	72.73	8.9407	87.50	8.9603	102.27	9.0041	115.30
180	8.6532	0.00	8.3572	0.00	$-\infty$	90.00	8.3672	180.00	8.6732	180.00

TABLE B·1.—COORDINATES OF POINTS ON THE THREE-BAR-LINKAGE NOMOGRAM — (*Cont.*)

μb =	0.03		0.04		0.05		0.06		0.07		0.08	
X, degrees	$\mu p + 10$	η, degrees	$\mu p + 10$	η, degrees	$\mu p + 10$	η, degrees	$\mu p + 10$	η, degrees	$\mu p + 10$	η, degrees	$\mu p + 10$	η, degrees
0	10.3163	0.00	10.3215	0.00	10.3268	0.00	10.3321	0.00	10.3374	0.00	10.3429	0.00
5	10.3160	2.59	10.3211	2.61	10.3264	2.64	10.3317	2.67	10.3370	2.70	10.3425	2.73
10	10.3146	5.17	10.3199	5.23	10.3251	5.29	10.3304	5.34	10.3358	5.40	10.3413	5.46
15	10.3125	7.76	10.3178	7.85	10.3230	7.93	10.3283	8.02	10.3337	8.11	10.3392	8.19
20	10.3097	10.35	10.3148	10.46	10.3201	10.58	10.3254	10.70	10.3308	10.81	10.3363	10.93
25	10.3060	12.94	10.3110	13.08	10.3164	13.23	10.3217	13.38	10.3271	13.52	10.3326	13.67
30	10.3013	15.53	10.3065	15.71	10.3117	15.88	10.3171	16.06	10.3225	16.23	10.3280	16.41
35	10.2957	18.13	10.3010	18.33	10.3062	18.54	10.3116	18.75	10.3170	18.95	10.3225	19.16
40	10.2893	20.72	10.2945	20.96	10.2999	21.20	10.3052	21.44	10.3107	21.68	10.3161	21.91
45	10.2820	23.32	10.2872	23.59	10.2925	23.86	10.2979	24.14	10.3033	24.41	10.3088	24.68
50	10.2737	25.92	10.2789	26.23	10.2842	26.54	10.2896	26.84	10.2950	27.15	10.3005	27.45
55	10.2643	28.53	10.2695	28.87	10.2749	29.21	10.2803	29.56	10.2858	29.90	10.2912	30.24
60	10.2539	31.14	10.2591	31.52	10.2646	31.90	10.2699	32.28	10.2755	32.66	10.2810	33.03
65	10.2424	33.76	10.2477	34.18	10.2531	34.60	10.2585	35.01	10.2641	35.43	10.2697	35.85
70	10.2298	36.39	10.2351	36.84	10.2404	37.31	10.2459	37.76	10.2515	38.22	10.2571	38.68
75	10.2159	39.02	10.2212	39.52	10.2266	40.03	10.2321	40.53	10.2377	41.03	10.2434	41.53
80	10.2008	41.66	10.2061	42.21	10.2115	42.76	10.2170	43.31	10.2227	43.86	10.2284	44.41
85	10.1841	44.31	10.1895	44.92	10.1949	45.51	10.2005	46.11	10.2062	46.71	10.2120	47.31
90	10.1660	46.98	10.1714	47.63	10.1770	48.29	10.1825	48.94	10.1883	49.60	10.1942	50.25
95	10.1463	49.66	10.1517	50.38	10.1573	51.09	10.1629	51.80	10.1688	52.51	10.1747	53.22
100	10.1248	52.36	10.1302	53.14	10.1358	53.92	10.1416	54.70	10.1475	55.47	10.1535	56.24
105	10.1012	55.08	10.1067	55.93	10.1124	56.79	10.1183	57.64	10.1242	58.48	10.1304	59.33
110	10.0754	57.82	10.0810	58.76	10.0868	59.69	10.0928	60.63	10.0989	61.55	10.1052	62.47
115	10.0472	60.60	10.0528	61.63	10.0587	62.66	10.0648	63.68	10.0711	64.69	10.0776	65.70
120	10.0160	63.42	10.0218	64.56	10.0278	65.69	10.0341	66.81	10.0406	67.93	10.0472	69.04
125	9.9817	66.29	9.9876	67.55	9.9938	68.80	10.0003	70.05	10.0070	71.28	10.0140	72.51
130	9.9435	69.23	9.9496	70.64	9.9560	72.03	9.9628	73.41	9.9698	74.78	9.9771	76.14
135	9.9006	72.26	9.9070	73.84	9.9138	75.40	9.9209	76.95	9.9283	78.49	9.9362	80.00
140	9.8523	75.42	9.8590	77.21	9.8662	78.98	9.8738	80.73	9.8819	82.46	9.8903	84.16
145	9.7970	78.75	9.8042	80.80	9.8120	82.83	9.8204	84.84	9.8293	86.81	9.8387	88.74
150	9.7329	82.34	9.7408	84.74	9.7496	87.11	9.7590	89.43	9.7692	91.71	9.7800	93.92
155	9.6569	86.35	9.6661	89.23	9.6763	92.04	9.6875	94.78	9.6997	97.44	9.7126	100.00
160	9.5641	91.08	9.5754	94.63	9.5881	97.98	9.6026	101.36	9.6181	104.52	9.6346	107.51
165	9.4464	97.19	9.4622	101.77	9.4804	106.09	9.5004	110.15	9.5220	113.92	9.5447	117.40
170	9.2881	106.54	9.3149	112.75	9.3451	118.32	9.3774	123.25	9.4108	127.59	9.4445	131.39
175	9.0615	125.84	9.1234	134.01	9.1849	140.29	9.2434	145.16	9.2985	149.00	9.3497	152.07
180	8.8544	180.00	8.9845	180.00	9.0864	180.00	9.1707	180.00	9.2428	180.00	9.3059	180.00

TABLE B·1.—COORDINATES OF POINTS ON THE THREE-BAR-LINKAGE NOMOGRAM — (*Cont.*)

μb =	0.09		0.10		0.11		0.12		0.13		0.14	
X, degrees	$\mu p + 10$	η, degrees	$\mu p + 10$	η, degrees	$\mu p + 10$	η, degrees	$\mu p + 10$	η, degrees	$\mu p + 10$	η, degrees	$\mu p + 10$	η, degrees
0	10.3484	0.00	10.3539	0.00	10.3595	0.00	10.3652	0.00	10.3709	0.00	10.3767	0.00
5	10.3480	2.76	10.3535	2.79	10.3591	2.81	10.3647	2.84	10.3705	2.87	10.3763	2.90
10	10.3467	5.52	10.3523	5.57	10.3579	5.63	10.3635	5.69	10.3693	5.74	10.3750	5.80
15	10.3447	8.28	10.3503	8.36	10.3558	8.45	10.3615	8.53	10.3672	8.62	10.3730	8.70
20	10.3418	11.04	10.3474	11.16	10.3529	11.27	10.3586	11.39	10.3644	11.50	10.3701	11.61
25	10.3380	13.81	10.3437	13.96	10.3493	14.10	10.3550	14.24	10.3608	14.39	10.3665	14.53
30	10.3335	16.58	10.3391	16.76	10.3447	16.93	10.3505	17.11	10.3562	17.28	10.3620	17.45
35	10.3280	19.37	10.3336	19.57	10.3393	19.77	10.3450	19.98	10.3508	20.18	10.3566	20.38
40	10.3216	22.15	10.3273	22.39	10.3330	22.63	10.3387	22.86	10.3445	23.09	10.3504	23.33
45	10.3144	24.95	10.3200	25.22	10.3258	25.49	10.3315	25.75	10.3373	26.02	10.3432	26.29
50	10.3062	27.76	10.3118	28.06	10.3176	28.36	10.3234	28.66	10.3292	28.96	10.3351	29.26
55	10.2970	30.58	10.3026	30.91	10.3084	31.25	10.3142	31.59	10.3201	31.92	10.3261	32.25
60	10.2867	33.41	10.3924	33.79	10.2982	34.16	10.3040	34.53	10.3100	34.90	10.3161	35.27
65	10.2753	36.26	10.3811	36.68	10.2870	37.09	10.2929	37.50	10.2988	37.91	10.3050	38.31
70	10.2628	39.13	10.2687	39.59	10.2746	40.04	10.2805	40.49	10.2865	40.94	10.2928	41.38
75	10.2492	42.03	10.2550	42.53	10.2610	43.02	10.2670	43.51	10.2731	44.00	10.2794	44.49
80	10.2343	44.95	10.2402	45.49	10.2462	46.03	10.2523	46.57	10.2585	47.11	10.2648	47.64
85	10.2179	47.90	10.2239	48.50	10.2300	49.08	10.2362	49.67	10.2425	50.25	10.2489	50.83
90	10.2001	50.89	10.2062	51.54	10.2124	52.19	10.2187	52.82	10.2251	53.45	10.2316	54.08
95	10.1808	53.93	10.1869	54.63	10.1932	55.33	10.1997	56.02	10.2062	56.71	10.2128	57.39
100	10.1597	57.01	10.1660	57.78	10.1724	58.54	10.1790	59.29	10.1857	60.04	10.1924	60.78
105	10.1367	60.16	10.1431	61.00	10.1497	61.82	10.1564	62.64	10.1634	63.46	10.1703	64.26
110	10.1116	63.39	10.1182	64.30	10.1250	65.20	10.1320	66.09	10.1391	66.98	10.1463	67.86
115	10.0842	66.71	10.0910	67.70	10.0980	68.68	10.1053	69.66	10.1126	70.63	10.1201	71.58
120	10.0542	70.14	10.0612	71.23	10.0686	72.31	10.0761	73.38	10.0838	74.43	10.0916	75.47
125	10.0212	73.72	10.0286	74.92	10.0363	76.10	10.0442	77.27	10.0523	78.43	10.0606	79.56
130	9.9847	77.48	9.9926	78.81	10.0008	80.12	10.0092	81.40	10.0179	82.67	10.0267	83.91
135	9.9443	81.50	9.9528	82.97	9.9616	84.41	9.9707	85.84	9.9800	87.23	9.9896	88.59
140	9.8992	85.84	9.9085	87.48	9.9182	89.09	9.9281	90.66	9.9384	92.20	9.9490	93.70
145	9.8486	90.63	9.8590	92.48	9.8698	94.28	9.8810	96.03	9.8926	97.73	9.9045	99.38
150	9.7914	96.07	9.8034	98.16	9.8159	100.18	9.8288	102.13	9.8421	104.00	9.8557	105.81
155	9.7264	102.47	9.7407	104.84	9.7557	107.11	9.7710	109.27	9.7868	111.33	9.8029	113.28
160	9.6520	110.35	9.6701	113.03	9.6887	115.54	9.7077	117.90	9.7270	120.11	9.7464	122.18
165	9.5682	120.61	9.5921	123.54	9.6164	126.24	9.6407	128.70	9.6649	130.95	9.6890	133.01
170	9.4781	134.72	9.5113	137.65	9.5436	140.22	9.5752	142.49	9.6058	144.51	9.6355	146.30
175	9.3976	154.58	9.4422	156.65	9.4839	158.38	9.5234	159.86	9.5603	161.12	9.5955	162.22
180	9.3622	180.00	9.4132	180.00	9.4598	180.00	9.5028	180.00	9.5428	180.00	9.5802	180.00

TABLE B-1.—COORDINATES OF POINTS ON THE THREE-BAR-LINKAGE NOMOGRAM — (*Cont.*)

μh =	0.15		0.16		0.17		0.18		0.19		0.20	
χ, degrees	$\mu p + 10$	η, degrees	$\mu p + 10$	η, degrees	$\mu p + 10$	η, degrees	$\mu p + 10$	η, degrees	$\mu p + 10$	η, degrees	$\mu p + 10$	η, degrees
0	10.3825	0.00	10.3884	0.00	10.3943	0.00	10.4003	0.00	10.4063	0.00	10.4124	0.00
5	10.3820	2.93	10.3880	2.96	10.3938	2.98	10.3999	3.01	10.4060	3.04	10.4121	3.07
10	10.3809	5.86	10.3868	5.91	10.3927	5.97	10.3989	6.02	10.4047	6.08	10.4109	6.13
15	10.3788	8.79	10.3847	8.87	10.3907	8.96	10.3967	9.04	10.4028	9.12	10.4089	9.21
20	10.3760	11.73	10.3819	11.84	10.3879	11.95	10.3939	12.06	10.3999	12.17	10.4061	12.28
25	10.3724	14.67	10.3783	14.81	10.3843	14.95	10.3903	15.09	10.3965	15.23	10.4026	15.37
30	10.3679	17.62	10.3739	17.79	10.3798	17.96	10.3859	18.13	10.3921	18.30	10.3982	18.47
35	10.3626	20.59	10.3685	20.79	10.3745	20.99	10.3806	21.19	10.3868	21.38	10.3930	21.58
40	10.3564	23.56	10.3623	23.79	10.3684	24.02	10.3745	24.25	10.3807	24.48	10.3869	24.71
45	10.3492	26.55	10.3552	26.81	10.3614	27.08	10.3675	27.34	10.3738	27.59	10.3800	27.85
50	10.3412	29.56	10.3472	29.85	10.3534	30.15	10.3596	30.44	10.3659	30.73	10.3722	31.02
55	10.3321	32.59	10.3383	32.92	10.3444	33.24	10.3507	33.57	10.3570	33.89	10.3634	34.22
60	10.3221	35.64	10.3284	36.00	10.3345	36.37	10.3409	36.73	10.3472	37.09	10.3536	37.44
65	10.3111	38.72	10.3174	39.12	10.3236	39.52	10.3301	39.91	10.3364	40.31	10.3429	40.70
70	10.2990	41.83	10.3053	42.27	10.3116	42.71	10.3181	43.14	10.3246	43.57	10.3312	44.00
75	10.2857	44.98	10.2920	45.46	10.2985	45.93	10.3050	46.41	10.3116	46.88	10.3184	47.35
80	10.2712	48.16	10.2777	48.69	10.2842	49.21	10.2909	49.73	10.2975	50.24	10.3044	50.75
85	10.2554	51.41	10.2620	51.98	10.2686	52.54	10.2754	53.10	10.2822	53.66	10.2892	54.21
90	10.2382	54.70	10.2449	55.32	10.2517	55.94	10.2586	56.55	10.2656	57.15	10.2728	57.75
95	10.2196	58.07	10.2265	58.74	10.2334	59.41	10.2405	60.07	10.2476	60.72	10.2549	61.36
100	10.1994	61.52	10.2065	62.25	10.2136	62.97	10.2209	63.68	10.2282	64.39	10.2358	65.09
105	10.1774	65.06	10.1847	65.85	10.1921	66.64	10.1996	67.41	10.2072	68.18	10.2150	68.93
110	10.1536	68.72	10.1612	69.58	10.1688	70.43	10.1766	71.27	10.1845	72.09	10.1926	72.91
115	10.1278	72.53	10.1357	73.46	10.1436	74.38	10.1518	75.28	10.1600	76.17	10.1684	77.05
120	10.0997	76.50	10.1079	77.51	10.1163	78.51	10.1249	79.49	10.1336	80.45	10.1424	81.40
125	10.0691	80.68	10.0778	81.78	10.0868	82.87	10.0958	83.93	10.0151	84.97	10.1144	85.99
130	10.0359	85.14	10.0451	86.33	10.0547	87.51	10.0644	88.66	10.0743	89.79	10.0843	90.88
135	9.9995	89.93	10.0096	91.24	10.0199	92.51	10.0305	93.76	10.0412	94.97	10.0520	96.15
140	9.9598	95.16	9.9710	96.59	9.9823	97.97	9.9939	99.32	10.0056	100.61	10.0175	101.87
145	9.9166	100.97	9.9201	102.52	9.9417	104.01	9.9546	105.44	9.9676	106.83	9.9808	108.16
150	9.8697	107.54	9.8839	109.21	9.8983	110.80	9.9129	112.33	9.9275	113.78	9.9424	115.18
155	9.8192	115.14	9.8358	116.91	9.8524	118.58	9.8692	120.16	9.8860	121.66	9.9028	123.08
160	9.7660	124.12	9.7857	125.93	9.8052	127.62	9.8248	129.21	9.8442	130.69	9.8634	132.07
165	9.7129	134.91	9.7363	136.64	9.7596	138.24	9.7822	139.70	9.8047	141.06	9.8267	142.31
170	9.6643	147.90	9.6922	149.34	9.7192	150.64	9.7456	151.82	9.7710	152.89	9.7957	153.86
175	9.6289	163.18	9.6605	164.02	9.6908	164.77	9.7200	165.44	9.7479	166.04	9.7746	166.58
180	9.6155	180.00	9.6488	180.00	9.6804	180.00	9.7106	180.00	9.7394	180.00	9.7671	180.00

TABLE B·1.—COORDINATES OF POINTS ON THE THREE-BAR-LINKAGE NOMOGRAM — (*Cont.*)

$\mu b =$	0.21		0.22		0.23		0.24		0.25		0.26	
X, degrees	$\mu p + 10$	η, degrees	$\mu p + 10$	η, degrees	$\mu p + 10$	η, degrees	$\mu p + 10$	η, degrees	$\mu p + 10$	η, degrees	$\mu p + 10$	η, degrees
0	10.4186	0.00	10.4248	0.00	10.4311	0.00	10.4374	0.00	10.4438	0.00	10.4502	0.00
5	10.4182	3.09	10.4245	3.12	10.4306	3.15	10.4370	3.17	10.4435	3.20	10.4498	3.23
10	10.4171	6.19	10.4233	6.24	10.4295	6.30	10.4359	6.35	10.4423	6.40	10.4486	6.46
15	10.4151	9.29	10.4213	9.37	10.4276	9.45	10.4340	9.53	10.4403	9.61	10.4468	9.69
20	10.4123	12.39	10.4185	12.50	10.4249	12.61	10.4312	12.72	10.4376	12.83	10.4441	12.93
25	10.4088	15.51	10.4151	15.65	10.4214	15.78	10.4278	15.92	10.4342	16.05	10.4407	16.19
30	10.4044	18.64	10.4108	18.80	10.4171	18.97	10.4235	19.13	10.4300	19.29	10.4365	19.45
35	10.3992	21.78	10.4056	21.97	10.4119	22.16	10.4184	22.36	10.4249	22.55	10.4315	22.74
40	10.3932	24.93	10.3996	25.16	10.4060	25.38	10.4125	25.60	10.4190	25.82	10.4256	26.04
45	10.3863	28.11	10.3928	28.37	10.3992	28.62	10.4057	28.87	10.4123	29.12	10.4190	29.37
50	10.3786	31.31	10.3850	31.60	10.3915	31.88	10.3981	32.16	10.4047	32.44	10.4115	32.72
55	10.3698	34.54	10.3763	34.86	10.3829	35.17	10.3896	35.49	10.3963	35.80	10.4030	36.11
60	10.3602	37.80	10.3667	38.15	10.3734	38.50	10.3801	38.84	10.3870	39.19	10.3938	39.53
65	10.3496	41.09	10.3562	41.48	10.3629	41.86	10.3698	42.24	10.3767	42.62	10.3836	42.99
70	10.3379	44.43	10.3446	44.85	10.3515	45.27	10.3584	45.69	10.3654	46.10	10.3724	46.51
75	10.3251	47.81	10.3320	48.27	10.3391	48.74	10.3460	49.18	10.3531	49.63	10.3602	50.07
80	10.3113	51.26	10.3183	51.76	10.3254	52.25	10.3325	52.74	10.3397	53.23	10.3470	53.71
85	10.2962	54.76	10.3034	55.30	10.3106	55.84	10.3179	56.37	10.3253	56.90	10.3327	57.42
90	10.2800	58.34	10.2873	58.93	10.2946	59.51	10.3021	60.08	10.3097	60.65	10.3173	61.21
95	10.2624	62.01	10.2698	62.64	10.2774	63.27	10.2851	63.89	10.2929	64.50	10.3007	65.10
100	10.2434	65.78	10.2511	66.47	10.2589	67.14	10.2668	67.81	10.2748	68.46	10.2829	69.11
105	10.2228	69.69	10.2308	70.41	10.2389	71.14	10.2471	71.85	10.2554	72.56	10.2637	73.25
110	10.2008	73.71	10.2091	74.50	10.2175	75.28	10.2260	76.05	10.2346	76.80	10.2433	77.55
115	10.1770	77.92	10.1857	78.77	10.1945	79.61	10.2034	80.43	10.2124	81.24	10.2215	82.03
120	10.1514	82.33	10.1606	83.25	10.1698	84.14	10.1792	85.02	10.1886	85.88	10.1983	86.73
125	10.1240	86.99	10.1337	87.97	10.1435	88.93	10.1534	89.87	10.1635	90.79	10.1736	91.68
130	10.0946	91.96	10.1049	93.01	10.1154	94.03	10.1259	95.02	10.1367	96.00	10.1475	96.94
135	10.0630	97.29	10.0742	98.41	10.0855	99.49	10.0969	100.55	10.1084	101.57	10.1200	102.56
140	10.0295	103.09	10.0417	104.27	10.0540	105.41	10.0664	106.52	10.0788	107.58	10.0914	108.61
145	9.9941	109.45	10.0076	110.69	10.0211	111.88	10.0346	113.02	10.0483	114.12	10.0620	115.18
150	9.9572	116.51	9.9723	117.79	9.9871	119.00	10.0022	120.16	10.0171	121.27	10.0322	122.33
155	9.9196	124.43	9.9365	125.71	9.9531	126.91	9.9698	128.06	9.9864	129.14	10.0028	130.17
160	9.8825	133.37	9.9015	134.59	9.9201	135.73	9.9386	136.80	9.9569	137.81	9.9750	138.76
165	9.8483	143.47	9.8695	144.54	9.8903	145.54	9.9107	146.46	9.9308	147.33	9.9506	148.14
170	9.8197	154.75	9.8431	155.57	9.8659	156.32	9.8880	157.01	9.9099	157.66	9.9308	158.25
175	9.8005	167.07	9.8252	167.51	9.8497	167.92	9.8733	168.30	9.8959	168.64	9.9182	168.96
180	9.7937	180.00	9.8193	180.00	9.8440	180.00	9.8679	180.00	9.8911	180.00	9.9137	180.00

TABLE B·1.—COORDINATES OF POINTS ON THE THREE-BAR-LINKAGE NOMOGRAM — (*Cont.*)

μb =	0.27		0.28		0.29		0.30		0.31		0.32	
X, degrees	$\mu p + 10$	η, degrees	$\mu p + 10$	η, degrees	$\mu p + 10$	η, degrees	$\mu p + 10$	η, degrees	$\mu p + 10$	η, degrees	$\mu p + 10$	η, degrees
0	10.4567	0.00	10.4632	0.00	10.4698	0.00	10.4764	0.00	10.4831	0.00	10.4899	0.00
5	10.4563	3.25	10.4629	3.28	10.4695	3.31	10.4760	3.33	10.4828	3.36	10.4895	3.38
10	10.4552	6.51	10.4618	6.56	10.4684	6.61	10.4749	6.66	10.4816	6.72	10.4884	6.77
15	10.4533	9.77	10.4598	9.85	10.4664	9.93	10.4731	10.00	10.4798	10.08	10.4866	10.16
20	10.4506	13.04	10.4572	13.15	10.4638	13.25	10.4705	13.35	10.4773	13.46	10.4841	13.56
25	10.4472	16.32	10.4538	16.45	10.4605	16.58	10.4672	16.71	10.4740	16.84	10.4808	16.97
30	10.4430	19.61	10.4497	19.77	10.4564	19.93	10.4632	20.09	10.4699	20.24	10.4768	20.40
35	10.4380	22.93	10.4447	23.11	10.4515	23.30	10.4582	23.48	10.4651	23.66	10.4720	23.84
40	10.4323	26.26	10.4390	26.47	10.4457	26.68	10.4526	26.90	10.4595	27.11	10.4664	27.31
45	10.4257	29.61	10.4325	29.86	10.4393	30.10	10.4462	30.34	10.4531	30.57	10.4601	30.81
50	10.4182	32.99	10.4251	33.27	10.4320	33.54	10.4389	33.81	10.4459	34.07	10.4530	34.34
55	10.4099	36.41	10.4168	36.72	10.4238	37.02	10.4308	37.31	10.4379	37.61	10.4450	37.90
60	10.4007	39.87	10.4077	40.20	10.4147	40.53	10.4218	40.86	10.4290	41.18	10.4362	41.51
65	10.3906	43.36	10.3977	43.73	10.4048	44.09	10.4120	44.45	10.4193	44.81	10.4266	45.16
70	10.3795	46.91	10.3867	47.31	10.3939	47.71	10.4013	48.10	10.4087	48.49	10.4161	48.87
75	10.3675	50.51	10.3747	50.95	10.3821	51.38	10.3896	51.80	10.3971	52.22	10.4047	52.64
80	10.3544	54.18	10.3618	54.65	10.3694	55.12	10.3769	55.58	10.3846	56.03	10.3923	56.48
85	10.3403	57.93	10.3478	58.44	10.3556	58.94	10.3633	59.43	10.3711	59.92	10.3790	60.41
90	10.3250	61.76	10.3328	62.31	10.3407	62.85	10.3487	63.38	10.3568	63.91	10.3647	64.42
95	10.3086	65.70	10.3166	66.28	10.3247	66.86	10.3329	67.43	10.3412	67.99	10.3495	68.55
100	10.2911	69.75	10.2993	70.38	10.3077	70.99	10.3161	71.60	10.3247	72.20	10.3332	72.79
105	10.2723	73.93	10.2808	74.60	10.2895	75.26	10.2982	75.91	10.3070	76.55	10.3159	77.18
110	10.2522	78.28	10.2611	78.99	10.2701	79.70	10.2792	80.39	10.2883	81.06	10.2975	81.73
115	10.2307	82.80	10.2400	83.57	10.2494	84.31	10.2589	85.05	10.2685	85.76	10.2781	86.46
120	10.2079	87.55	10.2177	88.36	10.2276	89.15	10.2375	89.92	10.2476	90.68	10.2576	91.41
125	10.1838	92.55	10.1942	93.41	10.2046	94.24	10.2151	95.05	10.2257	95.84	10.2363	96.61
130	10.1584	97.86	10.1694	98.76	10.1805	99.63	10.1916	100.47	10.2029	101.30	10.2141	102.10
135	10.1317	103.52	10.1435	104.46	10.1553	105.36	10.1672	106.24	10.1791	107.09	10.1911	107.91
140	10.1041	109.61	10.1167	110.57	10.1294	111.50	10.1421	112.39	10.1549	113.26	10.1677	114.09
145	10.0757	116.19	10.0894	117.17	10.1031	118.10	10.1168	119.00	10.1305	119.87	10.1442	120.70
150	10.0471	123.34	10.0620	124.31	10.0769	125.23	10.0917	126.12	10.1064	126.96	10.1211	127.77
155	10.0192	131.15	10.0353	132.07	10.0515	132.95	10.0675	133.79	10.0834	134.58	10.0991	135.34
160	9.9930	139.66	10.0105	140.50	10.0179	141.29	10.0452	142.05	10.0622	142.76	10.0789	143.43
165	9.9698	148.89	9.9888	149.60	10.0075	150.26	10.0260	150.89	10.0439	151.47	10.0618	152.03
170	9.9517	158.81	9.9717	159.32	9.9915	159.80	10.0109	160.25	10.0298	160.67	10.0486	161.07
175	9.9396	169.25	9.9604	169.52	9.9813	169.78	10.0010	170.01	10.0213	170.24	10.0400	170.44
180	9.9356	180.00	9.9569	180.00	9.9777	180.00	9.9979	180.00	10.0178	180.00	10.0372	180.00

Table B·1.—Coordinates of Points on the Three-Bar-Linkage Nomogram — (*Cont.*)

$\mu b =$	0.33		0.34		0.35		0.36		0.37		0.38	
X, degrees	$\mu p + 10$	η, degrees	$\mu p + 10$	η, degrees	$\mu p + 10$	η, degrees	$\mu p + 10$	η, degrees	$\mu p + 10$	η, degrees	$\mu p + 10$	η, degrees
0	10.4967	0.00	10.5035	0.00	10.5104	0.00	10.5173	0.00	10.5243	0.00	10.5313	0.00
5	10.4962	3.41	10.5031	3.43	10.5101	3.46	10.5170	3.48	10.5240	3.51	10.5309	3.53
10	10.4952	6.82	10.5021	6.87	10.5090	6.92	10.5159	6.97	10.5229	7.01	10.5299	7.06
15	10.4934	10.23	10.5003	10.31	10.5072	10.38	10.5141	10.46	10.5211	10.53	10.5282	10.60
20	10.4909	13.66	10.4978	13.76	10.5047	13.86	10.5117	13.96	10.5186	14.05	10.5258	14.15
25	10.4877	17.10	10.4946	17.22	10.5015	17.35	10.5085	17.47	10.5155	17.59	10.5227	17.71
30	10.4837	20.55	10.4906	20.70	10.4976	20.85	10.5046	21.00	10.5117	21.15	10.5189	21.29
35	10.4789	24.02	10.4859	24.20	10.4929	24.38	10.5000	24.55	10.5071	24.72	10.5144	24.89
40	10.4734	27.52	10.4805	27.72	10.4875	27.93	10.4947	28.13	10.5018	28.32	10.5092	28.52
45	10.4671	31.04	10.4743	31.27	10.4814	31.50	10.4886	31.73	10.4958	31.95	10.5032	32.17
50	10.4601	34.60	10.4673	34.86	10.4745	35.11	10.4817	35.37	10.4891	35.62	10.4965	35.86
55	10.4522	38.19	10.4594	38.48	10.4668	38.76	10.4741	39.04	10.4816	39.32	10.4890	39.59
60	10.4435	41.83	10.4508	42.14	10.4582	42.45	10.4657	42.76	10.4732	43.07	10.4808	43.37
65	10.4340	45.51	10.4414	45.85	10.4489	46.19	10.4565	46.53	10.4641	46.86	10.4718	47.19
70	10.4236	49.25	10.4312	49.62	10.4388	49.99	10.4465	50.36	10.4542	50.72	10.4620	51.08
75	10.4123	53.05	10.4200	53.46	10.4278	53.86	10.4356	54.25	10.4434	54.64	10.4514	55.03
80	10.4001	56.92	10.4080	57.36	10.4159	57.79	10.4239	58.22	10.4320	58.64	10.4400	59.05
85	10.3870	60.88	10.3950	61.35	10.4031	61.81	10.4113	62.27	10.4195	62.72	10.4278	63.16
90	10.3729	64.93	10.3812	65.44	10.3895	65.93	10.3979	66.42	10.4063	66.90	10.4148	67.37
95	10.3579	69.09	10.3664	69.63	10.3749	70.16	10.3835	70.67	10.3922	71.18	10.4009	71.69
100	10.3419	73.37	10.3506	73.94	10.3594	74.50	10.3683	75.06	10.3772	75.60	10.3862	76.13
105	10.3249	77.80	10.3339	78.40	10.3430	78.99	10.3522	79.58	10.3614	80.15	10.3707	80.71
110	10.3069	82.38	10.3163	83.02	10.3257	83.65	10.3352	84.26	10.3448	84.86	10.3544	85.45
115	10.2878	87.15	10.2976	87.82	10.3075	88.48	10.3174	89.12	10.3272	89.75	10.3373	90.36
120	10.2678	92.13	10.2780	92.84	10.2884	93.52	10.2987	94.19	10.3091	94.85	10.3195	95.48
125	10.2470	97.36	10.2577	98.09	10.2686	98.81	10.2794	99.50	10.2902	100.17	10.3012	100.83
130	10.2253	102.87	10.2367	103.63	10.2481	104.36	10.2595	105.07	10.2709	105.76	10.2824	106.43
135	10.2030	108.70	10.2151	109.47	10.2271	110.22	10.2392	110.94	10.2513	111.64	10.2634	112.32
140	10.1805	114.90	10.1932	115.67	10.2060	116.42	10.2188	117.14	10.2315	117.84	10.2442	118.51
145	10.1579	121.50	10.1714	122.26	10.1850	123.00	10.1986	123.71	10.2121	124.39	10.2254	125.04
150	10.1357	128.54	10.1502	129.28	10.1647	129.99	10.1790	130.66	10.1933	131.31	10.2074	131.93
155	10.1147	136.06	10.1302	136.75	10.1455	137.40	10.1607	138.03	10.1757	138.62	10.1907	139.19
160	10.0955	144.07	10.1119	144.67	10.1281	145.25	10.1442	145.80	10.1599	146.31	10.1758	146.81
165	10.0793	152.55	10.0966	153.04	10.1137	153.51	10.1303	153.95	10.1468	154.36	10.1631	154.76
170	10.0670	161.44	10.0850	161.79	10.1026	162.12	10.1198	162.43	10.1369	162.72	10.1537	163.00
175	10.0585	170.63	10.0775	170.82	10.0955	170.99	10.1132	171.15	10.1306	171.30	10.1478	171.44
180	10.0561	180.00	10.0747	180.00	10.0930	180.00	10.1109	180.00	10.1285	180.00	10.1458	180.00

TABLE B·1.—COORDINATES OF POINTS ON THE THREE-BAR-LINKAGE NOMOGRAM — (*Cont.*)

μb =	0.39		0.40		0.41		0.42		0.43		0.44	
X, degrees	$\mu p + 10$	η, degrees	$\mu p + 10$	η, degrees	$\mu p + 10$	η, degrees	$\mu p + 10$	η, degrees	$\mu p + 10$	η, degrees	$\mu p + 10$	η, degrees
0	10.5384	0.00	10.5455	0.00	10.5527	0.00	10.5599	0.00	10.5672	0.00	10.5745	0.00
5	10.5381	3.55	10.5452	3.58	10.5524	3.60	10.5596	3.62	10.5669	3.65	10.5742	3.67
10	10.5371	7.11	10.5442	7.16	10.5514	7.20	10.5586	7.25	10.5659	7.30	10.5732	7.34
15	10.5354	10.67	10.5425	10.74	10.5497	10.81	10.5570	10.88	10.5643	10.95	10.5716	11.02
20	10.5330	14.25	10.5401	14.34	10.5474	14.43	10.5547	14.53	10.5620	14.62	10.5694	14.71
25	10.5299	17.83	10.5371	17.95	10.5444	18.07	10.5517	18.19	10.5590	18.30	10.5664	18.41
30	10.5261	21.44	10.5334	21.58	10.5407	21.72	10.5480	21.86	10.5554	22.00	10.5628	22.14
35	10.5216	25.06	10.5290	25.23	10.5363	25.40	10.5437	25.56	10.5511	25.72	10.5586	25.88
40	10.5164	28.71	10.5238	28.91	10.5312	29.10	10.5387	29.28	10.5462	29.47	10.5537	29.65
45	10.5105	32.39	10.5180	32.61	10.5254	32.83	10.5330	33.04	10.5405	33.25	10.5481	33.45
50	10.5039	36.11	10.5115	36.35	10.5190	36.59	10.5266	36.83	10.5342	37.06	10.5419	37.29
55	10.4965	39.86	10.5042	40.13	10.5118	40.40	10.5194	40.66	10.5272	40.92	10.5349	41.17
60	10.4884	43.66	10.4961	43.96	10.5039	44.25	10.5116	44.54	10.5194	44.82	10.5273	45.10
65	10.4795	47.52	10.4873	47.84	10.4952	48.15	10.5031	48.47	10.5110	48.77	10.5191	49.08
70	10.4700	51.43	10.4778	51.78	10.4858	52.12	10.4938	52.46	10.5019	52.79	10.5101	53.12
75	10.4595	55.41	10.4675	55.78	10.4756	56.15	10.4838	56.47	10.4920	56.87	10.5003	57.23
80	10.4483	59.46	10.4564	59.86	10.4647	60.26	10.4731	60.65	10.4814	61.03	10.4899	61.41
85	10.4363	63.60	10.4446	64.03	10.4530	64.45	10.4616	64.87	10.4701	65.28	10.4787	65.68
90	10.4234	67.84	10.4320	68.29	10.4406	68.74	10.4493	69.18	10.4581	69.62	10.4669	70.05
95	10.4097	72.18	10.4185	72.66	10.4274	73.14	10.4363	73.61	10.4454	74.07	10.4544	74.52
100	10.3953	76.65	10.4043	77.16	10.4135	77.66	10.4227	78.16	10.4320	78.64	10.4412	79.11
105	10.3800	81.26	10.3894	81.79	10.3988	82.32	10.4084	82.84	10.4179	83.34	10.4274	83.84
110	10.3640	86.02	10.3738	86.58	10.3835	87.13	10.3934	87.67	10.4032	88.20	10.4131	88.72
115	10.3473	90.96	10.3575	91.55	10.3676	92.12	10.3778	92.68	10.3880	93.23	10.3982	93.76
120	10.3300	96.10	10.3405	96.71	10.3511	97.30	10.3617	97.88	10.3723	98.44	10.3829	98.98
125	10.3122	101.47	10.3231	102.09	10.3341	102.69	10.3452	103.28	10.3563	103.85	10.3673	104.41
130	10.2939	107.08	10.3054	107.71	10.3169	108.33	10.3284	108.92	10.3400	109.50	10.3515	110.06
135	10.2754	112.97	10.2875	113.61	10.2995	114.22	10.3115	114.81	10.3236	115.39	10.3356	115.94
140	10.2570	119.16	10.2697	119.79	10.2823	120.39	10.2949	120.98	10.3075	121.54	10.3201	122.08
145	10.2389	125.68	10.2522	126.28	10.2655	126.86	10.2788	127.43	10.2919	127.97	10.3050	128.49
150	10.2216	132.53	10.2356	133.10	10.2495	133.65	10.2635	134.18	10.2771	134.68	10.2908	135.17
155	10.2055	139.73	10.2202	140.25	10.2347	140.75	10.2493	141.23	10.2635	141.68	10.2778	142.12
160	10.1912	147.28	10.2066	147.73	10.2217	148.15	10.2365	148.56	10.2515	148.95	10.2663	149.33
165	10.1794	155.14	10.1953	155.50	10.2109	155.84	10.2264	156.16	10.2418	156.47	10.2569	156.76
170	10.1702	163.26	10.1867	163.51	10.2028	163.75	10.2190	163.98	10.2345	164.19	10.2500	164.40
175	10.1647	171.58	10.1814	171.71	10.1977	171.83	10.2143	171.95	10.2300	172.06	10.2456	172.16
180	10.1628	180.00	10.1795	180.00	10.1960	180.00	10.2123	180.00	10.2283	180.00	10.2441	180.00

TABLE B·1.—COORDINATES OF POINTS ON THE THREE-BAR-LINKAGE NOMOGRAM — (*Cont.*)

μb =	0.45		0.46		0.47		0.48		0.49		0.50	
X, degrees	$\mu p + 10$	η, degrees	$\mu p + 10$	η, degrees	$\mu p + 10$	η, degrees	$\mu p + 10$	η, degrees	$\mu p + 10$	η, degrees	$\mu p + 10$	η, degrees
0	10.5819	0.00	10.5893	0.00	10.5967	0.00	10.6042	0.00	10.6118	0.00	10.6193	0.00
5	10.5816	3.69	10.5890	3.71	10.5964	3.74	10.6039	3.76	10.6115	3.78	10.6190	3.80
10	10.5806	7.39	10.5880	7.43	10.5955	7.47	10.6030	7.52	10.6106	7.56	10.6181	7.60
15	10.5790	11.09	10.5864	11.15	10.5939	11.22	10.6015	11.28	10.6091	11.35	10.6166	11.41
20	10.5768	14.80	10.5842	14.89	10.5917	14.98	10.5993	15.06	10.6069	15.15	10.6145	15.23
25	10.5739	18.53	10.5814	18.64	10.5889	18.75	10.5965	18.86	10.6041	18.96	10.6118	19.07
30	10.5703	22.27	10.5779	22.41	10.5855	22.54	10.5931	22.67	10.6007	22.80	10.6084	22.92
35	10.5661	26.04	10.5738	26.20	10.5814	26.35	10.5891	26.50	10.5967	26.65	10.6045	26.80
40	10.5613	29.83	10.5690	30.01	10.5767	30.19	10.5844	30.36	10.5921	30.54	10.6000	30.71
45	10.5558	33.66	10.5635	33.86	10.5713	34.06	10.5791	34.26	10.5869	34.45	10.5948	34.64
50	10.5496	37.52	10.5574	37.75	10.5653	37.97	10.5731	38.19	10.5810	38.40	10.5890	38.62
55	10.5428	41.42	10.5507	41.67	10.5586	41.92	10.5665	42.16	10.5745	42.40	10.5826	42.63
60	10.5352	45.37	10.5433	45.65	10.5512	45.91	10.5593	46.18	10.5674	46.44	10.5756	46.70
65	10.5270	49.38	10.5352	49.67	10.5432	49.96	10.5514	50.25	10.5597	50.53	10.5680	50.81
70	10.5181	53.44	10.5264	53.76	10.5346	54.07	10.5429	54.38	10.5513	54.69	10.5597	54.99
75	10.5085	57.57	10.5169	57.92	10.5253	58.25	10.5338	58.58	10.5423	58.91	10.5508	59.23
80	10.4983	61 78	10.5068	62.15	10.5154	62.51	10.5240	62.86	10.5327	63.21	10.5413	63.55
85	10.4873	66.07	10.4960	66.46	10.5048	66.85	10.5136	67.22	10.5224	67.59	10.5313	67.96
90	10.4757	70.46	10.4846	70.88	10.4936	71.28	10.5026	71.68	10.5116	72.07	10.5207	72.45
95	10.4634	74.96	10.4726	75.40	10.4818	75.82	10.4910	76.24	10.5002	76.65	10.5095	77.05
100	10.4505	79.58	10.4600	80.03	10.4694	80.48	10.4788	80.91	10.4883	81.34	10.4978	81.76
105	10.4370	84.32	10.4468	84.80	10.4564	85.26	10.4661	85.71	10.4759	86.16	10.4857	86.60
110	10.4230	89.22	10.4330	89.71	10.4430	90.19	10.4530	90.66	10.4631	91.12	10.4732	91.57
115	10.4086	94.28	10.4188	94.79	10.4291	95.28	10.4395	95.76	10.4499	96.24	10.4603	96.70
120	10.3935	99.52	10.4042	100.04	10.4149	100.54	10.4256	101.03	10.4363	101.51	10.4471	101.98
125	10.3783	104.95	10.3894	105.48	10.4005	105.99	10.4116	106.49	10.4227	106.97	10.4338	107.44
130	10.3630	110.60	10.3745	111.13	10.3860	111.64	10.3976	112.14	10.4091	112.62	10.4206	113.09
135	10.3476	116.48	10.3597	117.01	10.3716	117.51	10.3836	118.00	10.3955	118.47	10.4074	118.93
140	10.3326	122.61	10.3451	123.12	10.3575	123.61	10.3699	124.08	10.3823	124.54	10.3946	124.98
145	10.3180	128.99	10.3311	129.48	10.3440	129.94	10.3568	130.39	10.3697	130.83	10.3824	131.25
150	10.3043	135.63	10.3179	136.08	10.3313	136.52	10.3446	136.93	10.3579	137.33	10.3711	137.72
155	10.2918	142.54	10.3059	142.94	10.3198	143.32	10.3335	143.69	10.3472	144.05	10.3609	144.39
160	10.2809	149.68	10.2954	150.02	10.3097	150.35	10.3238	150.66	10.3380	150.96	10.3520	151.25
165	10.2719	157.05	10.2869	157.32	10.3015	157.57	10.3160	157.82	10.3304	158.05	10.3447	158.28
170	10.2652	164.59	10.2806	164.78	10.2954	164.95	10.3102	165.12	10.3248	165.29	10.3394	165.44
175	10.2610	172.26	10.2766	172.36	10.2918	172.45	10.3066	172.53	10.3214	172.62	10.3360	172.70
180	10.2597	180.00	10.2751	180.00	10.2903	180.00	10.3053	180.00	10.3202	180.00	10.3349	180.00

Index

A

B

C

D

E

I

J

K

L

M

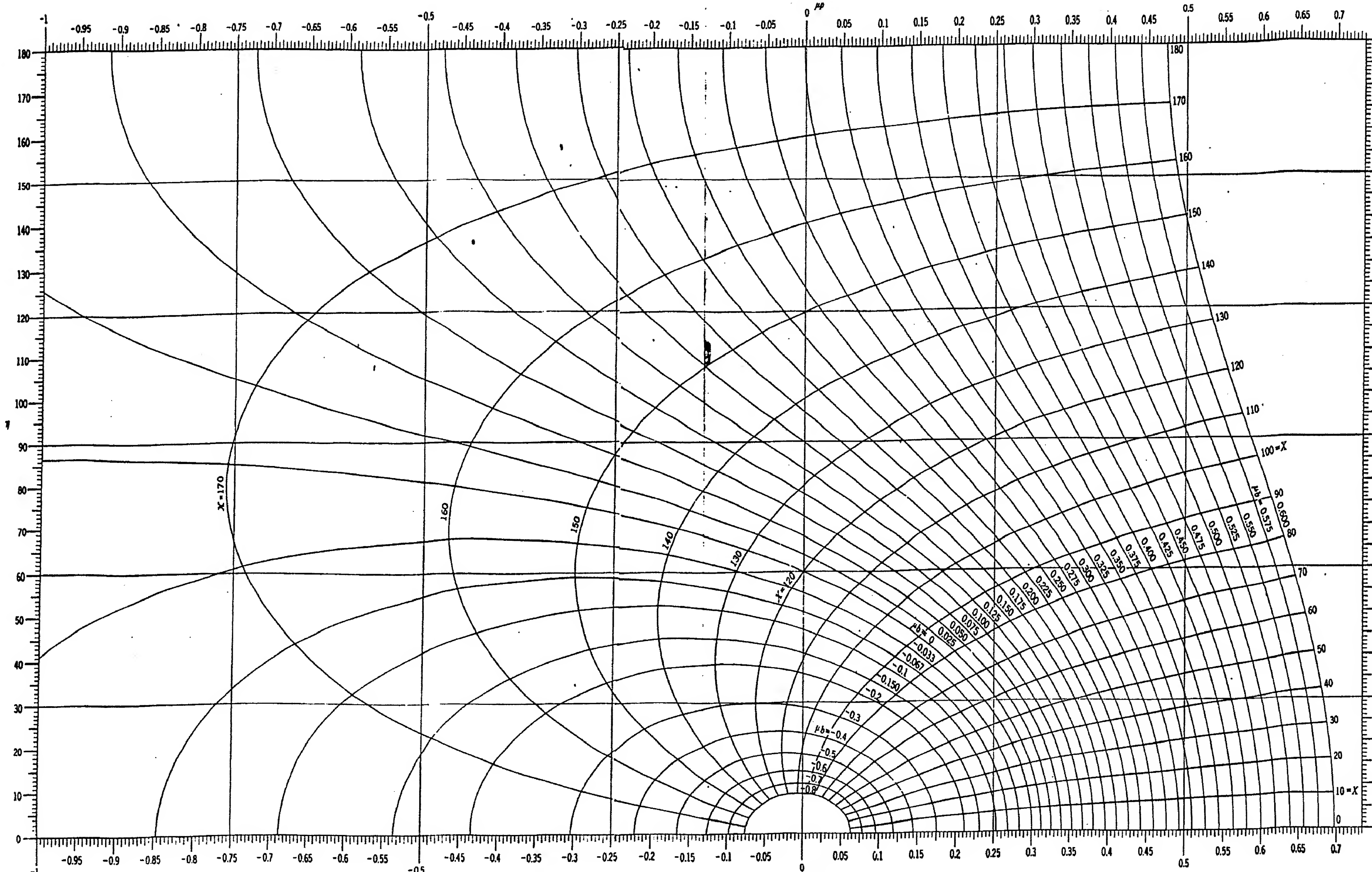

Fig. B-1.—Three-bar-linkage nomogram.